# HIGHLY BRANCHED ISOPRENOID ALKENES FROM DIATOMS:

# A BIOSYNTHETIC AND LIFE CYCLE INVESTIGATION

by

**Guillaume Gabriel Massé**

A thesis submitted to the University of Plymouth in partial fulfilment for the degree of:

**DOCTOR OF PHILOSOPHY**

School of Environmental Sciences

Faculty of Science

**February 2003**

# HIGHLY BRANCHED ISOPRENOID ALKENES FROM DIATOMS:

# A BIOSYNTHETIC AND LIFE CYCLE INVESTIGATION

by

Guillaume Gabriel Massé

## ABSTRACT

In addition to the production of phytol (from chlorophylls) and sterols, a limited number of diatom species are capable of synthesising unusual $C_{25}$ and $C_{30}$ highly branched isoprenoid (HBI) alkenes. At the outset of the current investigation, the structures of most $C_{25}$ and $C_{30}$ HBIs had been identified. Some environmental factors had been shown to control their production, although a detailed understanding of these remained unclear. In addition, the biological functions of the chemicals remained unknown, and the reasons for their production by some species and not by others, was not understood.

Investigations on the distributions of $C_{25}$ and $C_{30}$ HBI alkenes biosynthesised by *Rhizosolenia setigera* demonstrated a dependence on the physiological status of the cells, as measured by the position of this diatom in its life cycle. Thus, while $C_{30}$ HBIs were observed at every stage of the life cycle, $C_{25}$ HBIs were not always present in the cells. Since the synthesis of $C_{25}$ HBIs appears to be stimulated by the onset of auxosporulation (sexual reproduction), an explanation is provided as to why they have rarely been observed in previous studies.

Two novel monocyclic $C_{30}$ alkenes (previously reported in other strains of *Rhizosolenia setigera*), and a novel monocyclic $C_{25}$ alkene were also observed during life cycle experiments. The two $C_{30}$ hydrocarbons structures were subsequently characterised and the potential geochemical relevance of these compounds was highlighted by comparison of their mass spectral and chromatographic properties with those of alkenes reported in sediments and suspended water column particles.

An investigation of terpenoid (including HBI) biosynthesis in the diatoms *Haslea ostrearia*, *Rhizosolenia setigera* and *Pleurosigma intermedium* has been performed. Evidence for species and organelle dependent biosynthetic pathways has been observed. Phytol is synthesised by each species investigated according to the recently discovered methyl-erythritol phosphate (MEP) pathway. This pathway is also involved in the synthesis of $C_{25}$ HBIs in the two species *Haslea ostrearia* and *Pleurosigma intermedium.* In contrast, $C_{25}$ and $C_{30}$ HBIs, and (at least) one monocyclic $C_{30}$ alkene, appear to be made predominantly *via* the mevalonate (MVA) route in the diatom *R. setigera.* Evidence for the contribution of the MVA pathway to the biosynthesis of sterols was found for the diatoms *Rhizosolenia setigera,* and *Pleurosigma intermedium.* In contrast, only contributions from the MEP pathway were found for the biosynthesis of sterols in *Haslea ostrearia.* Preliminary evidence for dynamic interchange between the two pathways has also been observed.

Fractionation of *Rhizosolenia setigera* cells revealed that phytol was present in the chloroplasts, while sterols and HBIs were present in the cytoplasm.

## Table of Contents

**Chapter Four**

**Isoprenoid biosynthesis in three diatom species**

## List of Figures

## List of tables

## ACKNOWLEDGEMENTS

I would like to thank my supervisors, Dr. Simon Belt and Prof. Steve Rowland for their friendship, support, advice and encouragement during the course of this study. I also would like to thank them for their help regarding this manuscript.

I am also indebted to Guy Allard for the good time spent with him in the laboratory. Thanks also for his encouragement, discussions, ideas and friendship.

I would also like to thank the technical staff of the School of Environmental Sciences, University of Plymouth for their expertise and assistance.

The rest of PEGG, past and present, especially Paul S., Paul Mac, Andy and Emma, for their help and friendship.

I also do not forget Dr. Phil Jones and Dr. Pavel Nesterenko for the preparative LC.

Finally, thanks to Jo for her friendship and patience (especially during the long discussions about work with her husband).

Je souhaite remercier tous le membres du Laboratoire de Biologie Marine (Université de Nantes, France) et en particulier Jean-Michel Robert pour avoir mis à ma disposition son savoir et son laboratoire pendant de nombreuses années.

Sans oublier Michel Poulin (pas que pour son petit accent), Philippe T. Delavault et bien sur Alain Barreau du service commun de Microscopie électronique (Université de Nantes, France) pour ses prouesses et les bon moments passés ensemble devant le MEB.

Enfin, un grand merci à Stéphanie pour son amour, sa patience et ses encouragements de tous les instants.

## AUTHOR'S DECLARATION

At no time during the registration for the degree of Doctor of Philosophy has the author been registered for any other University award.

This study was financed with the aid of a research assistantship from the University of Plymouth.

A programme of advanced study was carried out, with relevant scientific seminars and conferences attended at which work was often presented.

**Publications:**

Belt, S.T., Allard, G., **Massé, G.**, Robert, J.-M., and Rowland, S.J. (2000). Important sedimentary sesterterpenoids from the diatom *Pleurosigma intermedium*. *Chemical Communications*, 501-502.

Belt, S.T., Allard, W.G., **Massé, G.**, Robert, J.-M., and Rowland, S.J. (2000). Highly branched isoprenoids (HBIs): Identification of the most common and abundant sedimentary isomers. *Geochimica et Cosmochimica Acta*, **64**: 3839-3851.

Allard, W.G., Belt, S.T., **Massé, G.**, Naumann, R., Robert, J.-M., and Rowland, S.J. (2001). Tetra-unsaturated sesterterpenoids (Haslenes) from *Haslea ostrearia* and related species. *Phytochemistry*, **56**: 795-800.

Belt, S.T., **Massé, G.**, Allard, W.G., Robert, J.-M., and Rowland, S.J. (2001). Identification of a $C_{25}$ highly branched isoprenoid triene in the freshwater diatom *Navicula sclesvicensis*. *Organic Geochemistry*, **32**: 1169-1172.

Belt, S.T., **Massé, G.**, Allard, W.G., Robert, J.-M., and Rowland, S.J. (2001). $C_{25}$ highly branched isoprenoid alkenes in planktonic diatoms of the *Pleurosigma* genus. *Organic Geochemistry*, **32**: 1271-1275.

Belt, S.T., Allard, W.G., Johns, L., König, W.A., **Massé, G.**, Robert, J.-M., and Rowland, S.J. (2001). Variable stereochemistry in highly branched isoprenoids from diatoms. *Chirality*, **13**: 415-419.

Belt, S.T., Allard, W.G., **Massé, G.**, Robert, J.-M., and Rowland, S.J. (2001). Structural characterisation of $C_{30}$ highly branched isoprenoid alkenes (Rhizenes) in the marine diatom *Rhizosolenia setigera*. *Tetrahedron Letters*, **42**: 5583-5585.

**Massé, G.**, Rincé, Y., Cox, E.J., Allard, W.G., Belt, S.T., and Rowland, S.J. (2001). *Haslea salstonica* sp. nov. and *Haslea pseudostrearia* sp. nov. (Bacillariophyceae), two new epibenthic diatoms from the Kingsbridge Estuary, U.K. *Comptes rendus de*

*l'Académie des Sciences, Paris, Sciences de la Vie / Life Sciences*, **324**: 617-626.

**Massé, G.**, Poulin, M., Belt, S.T., Robert, J.-M., Barreau, A., Rincé, Y., and Rowland, S.J. (2001). A simple method for SEM examination of sectionned diatom frustules. *Journal of Microscopy*, **204**: 87-92.

Rowland, S.J., Belt, S.T., Wraige, E.J., **Massé, G.**, Roussakis, C., and Robert, J.-M. (2001). Effects of temperature on polyunsaturation in cytostatic lipids of *Haslea ostrearia*. *Phytochemistry*, **56**: 597-602.

Rowland, S.J., Allard, W.G., Belt, S.T., **Massé, G.**, Robert, J.-M., Blackburn, S., Frampton, D., Revill, A.T., and Volkman, J.K. (2001) Factors influencing the distributions of polyunsaturated terpenoids in the diatom, *Rhizosolenia setigera*. *Phytochemistry*, **58**: 717-728.

Belt, S.T., **Massé, G.**, Allard, W.G., Robert, J.-M., and Rowland, S.J. (2002). Effects of auxosporulation on distributions of $C_{25}$ and $C_{30}$ isoprenoid alkenes in *Rhizosolenia setigera*. *Phytochemistry*, **59**: 141-148.

Poulin, M., **Massé, G.**, Belt, S. T., Delavault, P., Rousseau, F., Robert, J.-M. and Rowland, S. J., (submitted). Morphological, biochemical and molecular evidence for the transfer of *Gyrosigma nipkowii* Meister to the genus *Haslea*, *European Journal of Phycology*.

**Papers Presented**

Michel Poulin, **Guillaume Massé**, Simon T. Belt, Yves Rincé, Jean-Michel Robert, and Steven J. Rowland. The striking case of a sigmoid diatom sharing morphological similarities with *Haslea* species. 16th International Diatom Symposium, 2000 (Athens, Greece).

Yves Rincé, and **Guillaume Massé**, Nouvelles espèces du genre *Haslea*. 19ème Colloque de l'Association des Diatomistes de Langue Francaise, 2000 (Mont-Rigi, Belgium).

Simon T. Belt, W. Guy. Allard, Lesley. Johns, W. A .König, **Guillaume Massé**, Jean-Michel Robert and Steven J. Rowland. Variable stereochemistry in highly branched isoprenoids from diatoms. Symposium on Biological Chirality, 2000 (Szeged, Hungary).

W. Guy Allard, Simon T. Belt, **Guillaume Massé**, Laurence A. Nafie, Steven J. Rowland & Stuart Wakeham. Sedimentary transformations of diatomaceous HBI alkenes. 11th meeting of the European Union of Geosciences, 2001 (Strasbourg, France).

W. Guy Allard, Simon T. Belt, **Guillaume Massé**, Jean-Michel Robert, Laurence A. Nafie and Steven J. Rowland. Cytostatic polyunsaturated alkenes from diatomaceous algae. Natural Products Biology, 2001 (Warwick, U.K).

Simon T. Belt, **Guillaume Massé**, W. Guy Allard and Steven J. Rowland. The effects of auxosporulation on the distributions of $C_{25}$ and $C_{30}$ highly branched isoprenoid (HBI) alkenes in the diatom *Rhizosolenia setigera*. 20th International Meeting on Organic Geochemistry, 2001 (Nancy, France).

**Guillaume Massé**, W. Guy Allard, Simon T. Belt, Jean-Michel Robert, and Steven J. Rowland. New biosynthetic pathways to Highly Branched Isoprenoid (HBI) alkenes in diatoms. 23rd International Symposium on the Chemistry of Natural Products, 2002 (Florence, Italy).

Simon T. Belt, **Guillaume Massé**, and Steven J. Rowland. Biosynthetic studies of di-, sester- and triterpenoids from diatoms. 23rd International Symposium on the Chemistry of Natural Products, 2002 (Florence, Italy).

Michel Poulin, **Guillaume Massé**, Simon T. Belt, Philippe Delavault, Florence Rousseau, Jean-Michel Robert, and Steven J. Rowland. Morphological, biochemical and molecular evidence for the transfer of *Gyrosigma nipkowii* Meister to the genus *Haslea*. 17th International Diatom Symposium, 2002 (Ottawa, Canada).

Michel Poulin, **Guillaume Massé**, Simon T. Belt, Philippe Delavault, Florence Rousseau, Jean-Michel Robert, and Steven J. Rowland. Evidence morphologiques biochimiques et moléculaires pour le transfert de Gyrosigma nipkowii dans le genre Haslea. 21ème Colloque de l'Association des Diatomistes de Langue Française, 2002 (Nantes, France).

Signed.....

Date.....10-3-03.....

## List of common abbreviations

| | |
|---|---|
| DBE | Double Bong Equivalent |
| DOXP | Deoxy-D-Xylulose Phosphate |
| GC-irm-MS | Gas Chromatography-isotope ratio monitoring-Mass Spectrometry |
| GC-MS | Gas Chromatography-Mass Spectrometry |
| Haslenes | $C_{25}$ highly branched isoprenoids |
| HBI | Highly Branched Isoprenoids |
| HPLC | High Performance Liquid Chromatography |
| IEF | Isotopic Enrichment Factor |
| LC | Liquid Chromatography |
| MEP | Methyl-erythritol Phosphate |
| NMR | Nuclear Magnetic Resonance |
| NSL | Non-Saponifiable Lipid |
| Rhizenes | $C_{30}$ highly branched isoprenoids |
| THE | Total Hexane Extract |
| TIC | Total Ion Current |
| TOE | Total Organic Extract |

CHAPTER ONE

# Introduction

This thesis describes an investigation into lipids from diatoms in an attempt to understand the biological controls leading to their production. In particular, the study focuses on the distributions of polyunsaturated alkenes in various species of diatom, the factors that affect these distributions and the biosynthetic mechanisms that are responsible for their formation. The thesis begins with an introduction to diatoms together with an overview of polyunsaturated alkenes in these microorganisms.

## 1.1 Diatoms

Diatoms (Bacillariophyta) are unicellular, eukaryotic algae that require water and light to stimulate their photosynthesis. As a result, they are distributed in virtually all natural waters worldwide. Recent studies, based on a comparison of infrared properties of diatoms and those obtained from interstellar dust (Hoover *et al.*, 1986, 1999), also suggest an extraterrestrial occurrence of these or very similar organisms. Within marine environments on Earth, diatoms exhibit a great diversity (> 30 000 species described), and are considered as one of the most important groups of primary producers in the oceans. Diatom cells contain the same organelles as other photosynthetic eukaryotes (e.g. nucleus, mitochondria, chloroplasts) and are encased by a highly differentiated wall. This wall, consisting of two valves linked by so-called girdle elements, is impregnated with hydrated silica (Figure 1.1) forming the most distinctive structural features of diatoms. Indeed, it is the ultra-structural features of these valves that provide some of the most useful tools in diatom taxonomy (Anonymous, 1975). Diatoms are capable of reproduction by binary fission (asexual reproduction) such that the new valves and girdle elements are formed within the cell (Figure

1.1 c). These new valves are smaller than those of the parent cells, and over time, there is a significant reduction in the average cell size. When the cells reach critical dimensions, their initial size is usually restored *via* sexual reproduction and auxospore formation (Figure 1.2).

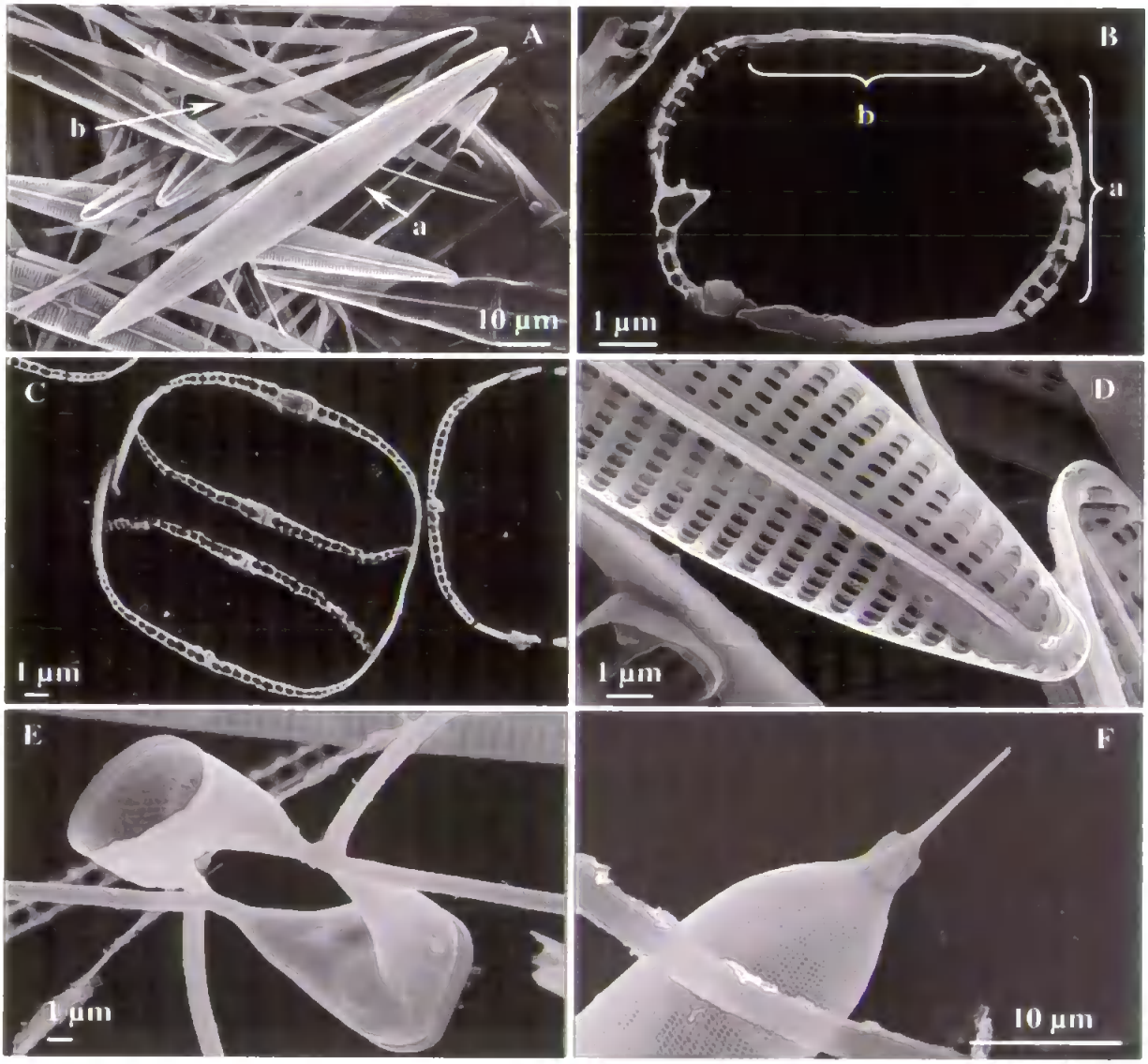


Figure 1.1 Scanning electron micrographs of diatoms. A. *Haslea crucigera*, a: valve, b: girdle element. B. Transapical thin section of *Haslea crucigera*, a: valve, b: girdle elements. C. Transapical thin section of a dividing cell of *Gyrosigma limosum* showing new valves being formed internally. D. Internal view of a strongly silicified valve of the benthic species *Navicula ramosissima*. E, F. External views of lightly silicified valves of planktonic diatoms *Chaetoceros sp.* and *Rhizosolenia cf. styliformis*.

Based on differences of the wall morphology, Round and co-workers (1990) divided the diatoms into three class: Coscinodiscophyceae, Fragillariophyceae and Bacillariophyceae.

Given their widespread occurrence, diatoms also exhibit large differences in their ecology. As a result, diatoms are divided into planktonic and benthic species. Planktonic species live mainly in the water column, while benthic species live in, or near to, the substratum. Due to these ecological differences and necessary adaptations to their habitats, the valves of benthic diatoms are usually strongly silicified, while planktonic diatoms usually exhibit lightly silicified valves to minimise their sinking rates (Figure 1.1).

Figure 1.2 *Rhizosolenia setigera* cells auxosporulating: initial cell formation.

## 1.2 Highly Branched Isoprenoid alkenes: sources and structural features

Lipids are important diatom constituents, representing up to 60% of their dry weight (reviewed by Groth-nard and Robert, 1993). Polar lipids (phospholipids and glycolipids) are usually the most abundant of these, representing up to 90% of the total lipids. Neutral lipids (tri-glycerides, phytol, sterols and hydrocarbons) are usually less abundant. Recently, investigations into the non-saponifiable lipids obtained from laboratory cultures of several diatom species, showed that in addition to the production of phytol (from chlorophylls) and sterols, some species are capable of synthesising unusual $C_{25}$ and $C_{30}$ highly branched isoprenoid (HBI) alkenes (Volkman *et al.*, 1994; Belt *et al.*, 2000a, 2001a,b,c). These HBIs occur in a wide range of sedimentary environments (reviewed by Rowland and Robson, 1990) and since their first discovery in diatom cultures (Volkman *et al.*, 1994), several studies have enabled for the structures of numerous $C_{25}$ and $C_{30}$ HBI isomers to be fully characterised. Indeed, from bulk cultures of the diatom *Haslea ostrearia* (Bory) Simonsen, Belt *et al.* (1996) and Johns *et al.* (1999) characterised the structures of several $C_{25}$ isomers *via* NMR spectroscopy. Later, Wraige *et al.* (1999) excluded the possibility of a bacterial origin of these HBIs (as suggested by Farrington *et al.* (1977), Boehm and Quinn (1978) and Requejo and Quinn (1983)) by reporting the same HBIs in axenic cultures of this species. More recently, several other diatom species belonging to the *Haslea* genus have been reported to be capable of synthesising HBIs (Allard *et al.*, 2001). From large-scale cultures of these three newly identified producers (*Haslea crucigera*, *Haslea salstonica* and *Haslea pseudostrearia*), they determined the structures of new tetra-unsaturated alkenes. Interestingly, all the HBI alkenes found in *Haslea* species share common structural features (Figure 1.4). Indeed, while these hydrocarbons exhibit differences in their degree of unsaturation (2-6 double bonds), all possess the same parent carbon skeleton (Figure 1.3;

Robson and Rowland, 1986). The main characteristic of this acyclic skeleton consists of an alkyl side chain at C7 of the main chain.

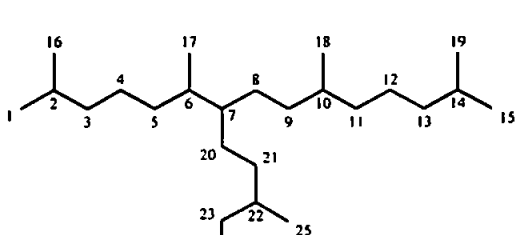


Figure 1.3 Structure and numbering scheme of the parent carbon skeleton of $C_{25}$ HBIs.

In addition, all of these isomers possess a vinyl moiety at C23-C24, a second double bond in either the C5-C6 or C6-C17 positions, and a saturated branch point at C7 (Figure 1.4).

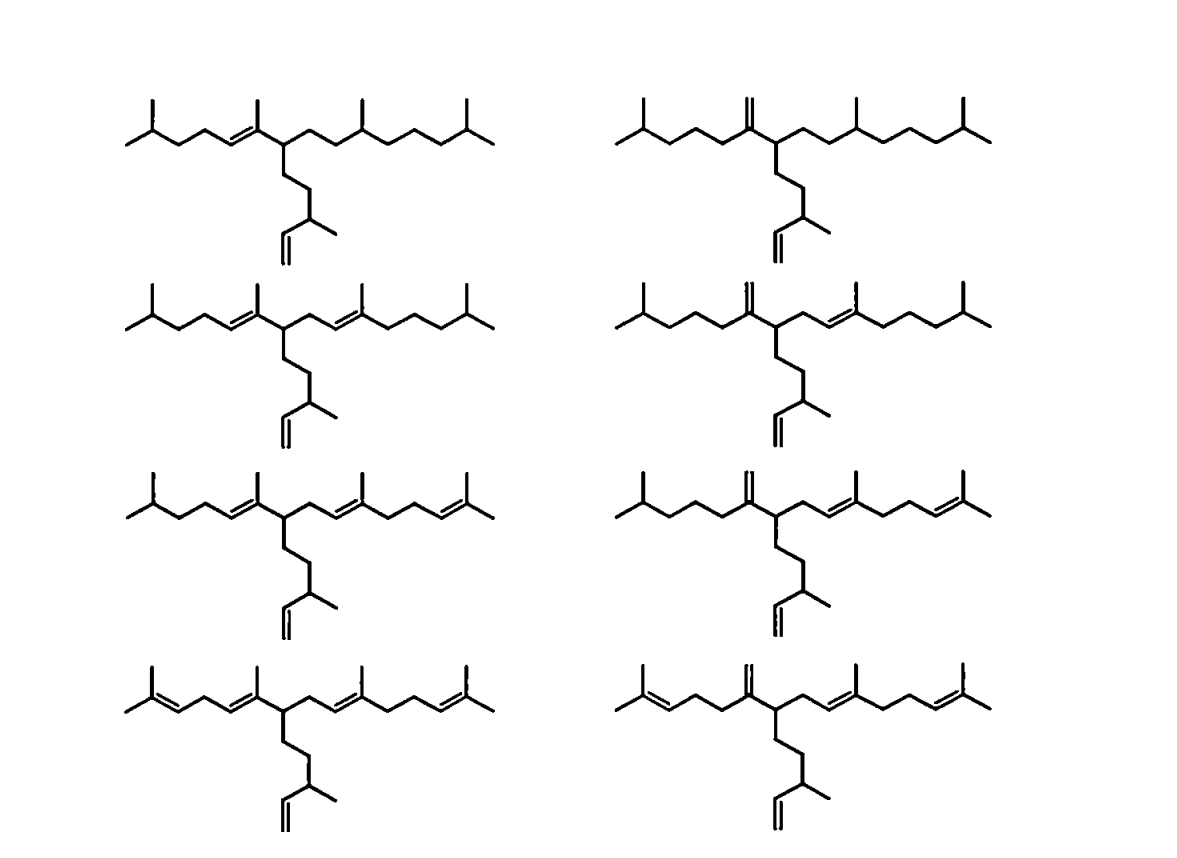

Figure 1.4 Structures of $C_{25}$ HBI alkenes identified from cultures of *Haslea* species.

Most recently, two previously characterised $C_{25}$ HBIs and a new $C_{25}$ isomer (Figure 1.5) were identified in a further *Haslea* species, previously classified as *Gyrosigma nipkowii* (sigmoidal species) and recently transferred into the genus *Haslea* (Belt *et al.*, 2001d; Poulin *et al.*, 2000, 2002, submitted). In contrast to all other $C_{25}$ HBI alkenes from *Haslea* species, two of these compounds were present as diastereoisomers (Figure 1.5). With the discovery of this particular isomer, a geometrical isomerism at position C9-C10 was reported for the first time within the alkenes produced by *Haslea* species.

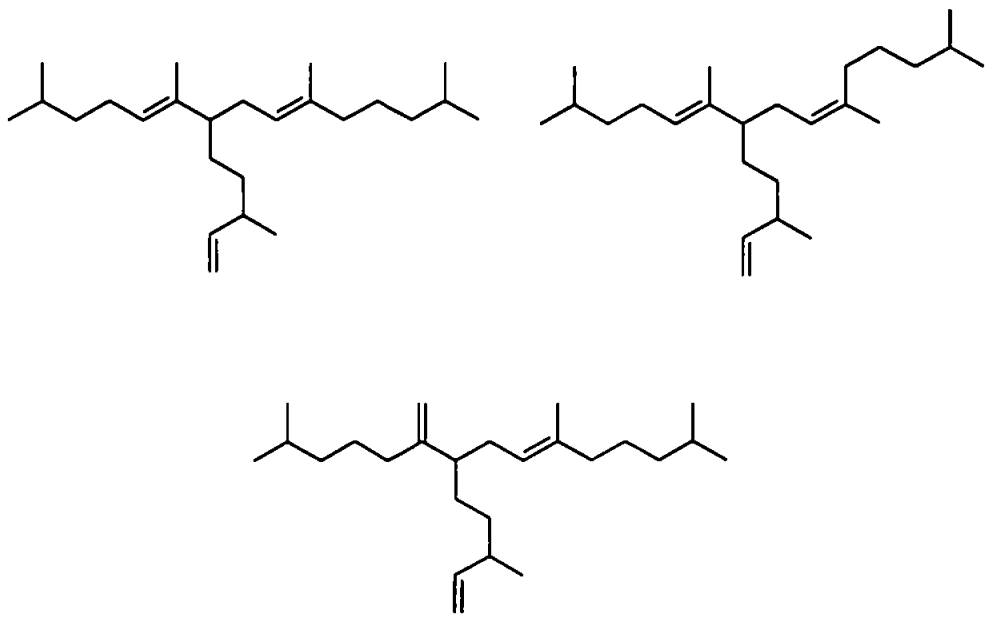

Figure 1.5 Structures of the $C_{25}$ HBIs identified in *Haslea nipkowii*.

An identical isomerism was also reported by Belt *et al.*, (2000a, b), who identified two *Pleurosigma* species (*P. intermedium* and *Pleurosigma sp.*) as sources for the most commonly reported $C_{25}$ HBIs in sediments. From bulk cultures of these diatoms, they elucidated the structures of eight novel $C_{25}$ HBI isomers (Figure 1.6). The structures of these alkenes were found to be isomeric to those found in *Haslea* species. For these isomers, the major branch point at C7 was found to be unsaturated, with a double bond in the C7-C20 position, while the double that was present in either the C5-C6 or C6-C17 positions in HBIs

from *Haslea* species was absent for isomers obtained for *P. intermedium*. In addition, these compounds were found to range in their unsaturation between 3 and 5 (double bonds), while the relative concentrations of both *E* and *Z* isomers (C9-C10) were found to be variable within different *Pleurosigma* cultures (usually *ca* 50% E / 50% Z).

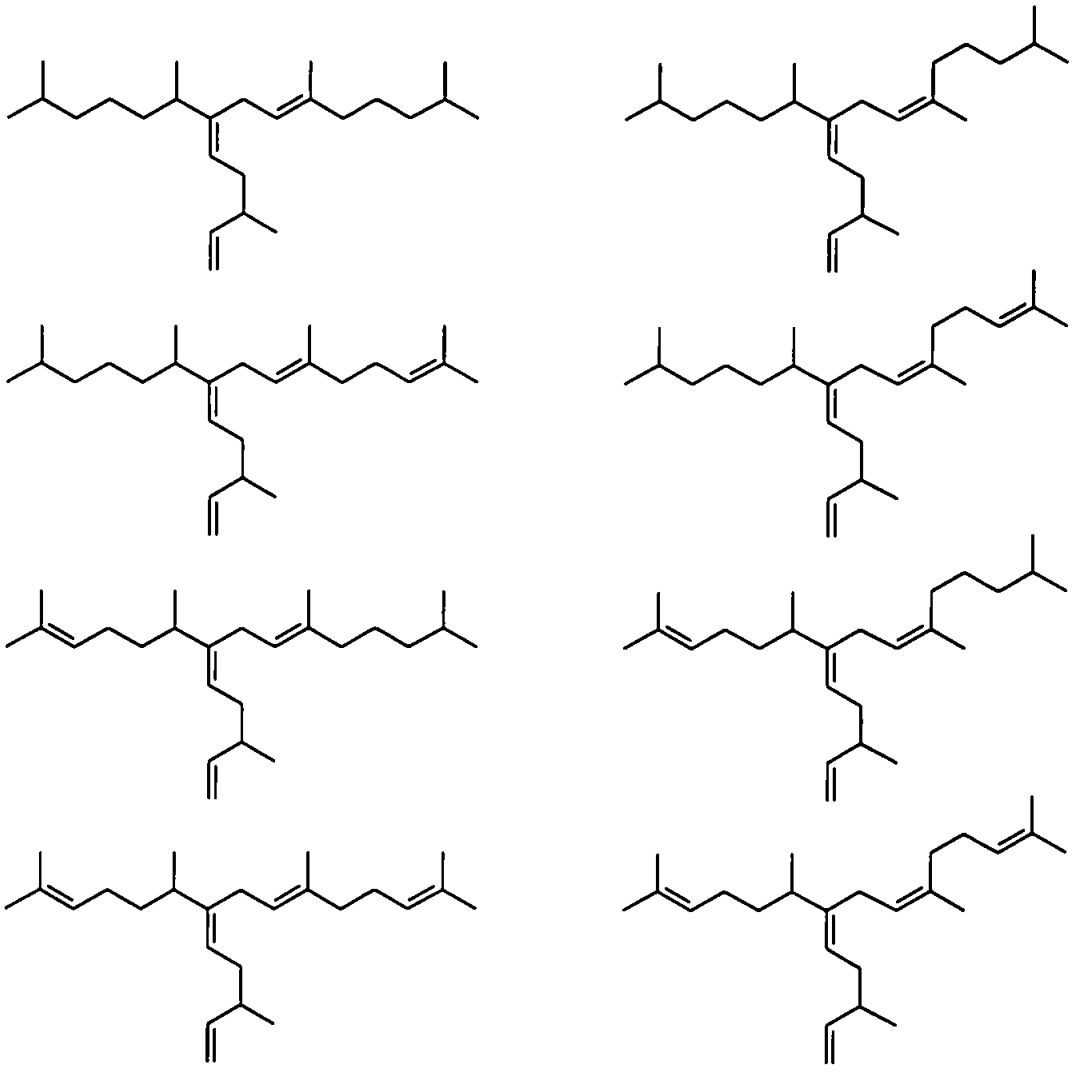

Figure 1.6 Structure of the $C_{25}$ HBIs identified from cultures of *Pleurosigma* species.

Finally, from bulk cultures of the diatom *Rhizosolenia setigera* Brightwell, Belt *et al.* (2001a) elucidated the structures of four $C_{30}$ HBIs (two $C_{30}$ pentaenes and two $C_{30}$ hexaenes) for the first time. Similar structural features to the $C_{25}$ HBIs were observed from these compounds. Consistent with structural features found for HBIs from *P. intermedium*, the

main branch point was located at C7 (Figure 1.7) and found to be unsaturated with a double bond at C7-C25, while geometric isomerism at C9-C10 was also observed.

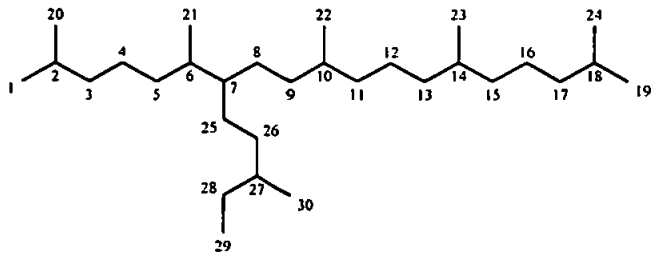


Figure 1.7 Structure of the parent carbon skeleton of $C_{30}$ HBIs.

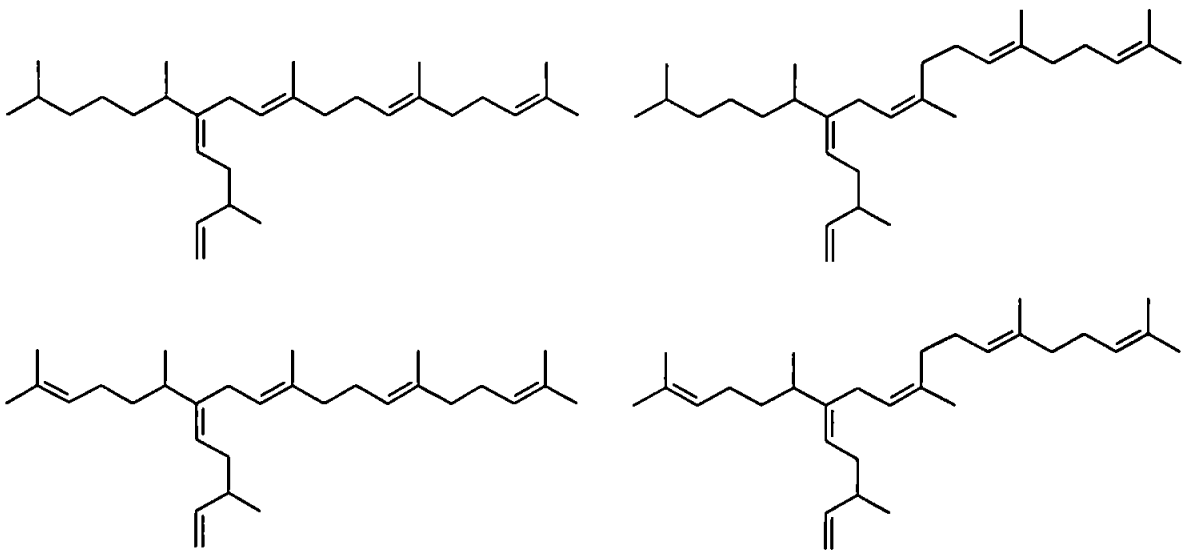

Figure 1.8 Structures of the $C_{30}$ HBIs identified from cultures of *Rhizosolenia setigera*.

### 1.3 Environmental controls on the production of HBIs in diatoms

In addition to the structural characterisation of most $C_{25}$ and $C_{30}$ HBI isomers, the influence of environmental parameters such as salinity (Wraige *et al.*, 1998) and temperature (Rowland *et al.*, 2001a) have also been investigated. While Wraige *et al.* demonstrated that variations in the salinity of the culture media did not affect significantly HBI distributions in *H. ostrearia*, Rowland and co-workers reported a significant effect of the culturing temperature on the distribution of HBIs produced by this species. A low (5°C) culturing temperature increased the saturation of the alkenes ($C_{25:2}$) contained in the cells, while a high (25°C) culturing temperature increased the proportions of the more unsaturated isoprenoids ($C_{25:4}$ - $C_{25:5}$), suggesting that this diatom was sensitive to changes in the environmental conditions and that HBIs may have a significant biological function. In contrast, no clear correlation between changes in the environmental conditions and HBI distributions was detected when similar experiments were performed with the diatom *Pleurosigma intermedium* (Allard *et al.*, unpublished results).

Moreover, while the culture of *Rhizosolenia setigera* investigated by Volkman *et al.* (1994) was found to contain three $C_{30}$ pentaenes and two $C_{30}$ hexaenes with no $C_{25}$ HBIs, Sinninghe Damsté *et al.* showed that a strain of *R. setigera* (CCMP 1330) contained only a single $C_{25}$ pentaene in addition to two novel *n*-alkenes, with no $C_{30}$ homologues (Sinninghe Damsté *et al.*, 1999a,b, 2000). The strain of *R. setigera* (RS-99) isolated from northern France by Belt *et al.* (2001a) contained only four $C_{30}$ HBI isomers (two $C_{30}$ pentaenes and two $C_{30}$ hexaenes) with no $C_{25}$ HBIs. Additionally, Rowland *et al.* (2001b) demonstrated that cells from the same *R. setigera* strain (RS-99) were capable of producing both $C_{25}$ and $C_{30}$ HBI alkenes. Further, these variations were also observed even under well-controlled culturing conditions, indicating that factors other than environmental conditions were also affecting HBI biosynthesis in diatoms.

## 1.4 The present study

At the outset of the present study, it was clear that the likely sources and the structures of most $C_{25}$ and $C_{30}$ HBIs had been identified, and that environmental factors were to some extent controlling their production. However, the controls on variations in their distributions observed during previous studies still remained unclear. In addition, the biological functions of the chemicals remained unknown, although it had been suggested that they may be membrane constituents (Ourisson and Nakatani, 1994; Rowland *et al.*, 2001a). Finally, the reasons for their production by some species and not by others (including very closely related species) was not understood. Therefore, the main aims of this study were to:

(i) investigate the distribution of $C_{25}$ and $C_{30}$ HBI alkenes biosynthesised by *R. setigera* as a function of the position of the diatom in its life cycle.

(ii) search for new HBI producing diatoms in order to understand better the reasons for the occurrence of HBIs in some species and their absence in others.

(iii) perform a comprehensive study of the mechanisms involved in the biosynthesis of HBIs in diatoms.

(iv) examine the intra-cellular compartmentation of isoprenoids in diatoms.

The results of this combined investigation are the main subject of this thesis and are described as follows:

**Chapter 2** describes an examination of (selected) lipid distributions in several species belonging to the *Rhizosolenia* genus and members of closely related genera, together with an investigation of the distributions of $C_{25}$ and $C_{30}$ HBI alkenes biosynthesised by *R. setigera* as a function of its life cycle. As a result, a further species capable of producing both $C_{25}$ and

$C_{30}$ HBI alkenes has been identified and most of the differences in distributions observed in previous studies have been explained. The formation of one new monocyclic $C_{25}$ and two monocyclic $C_{30}$ hydrocarbons have also been observed during a limited phase within the life cycle of *R. setigera*.

**Chapter 3** describes the structural characterisation of these novel monocyclic $C_{30}$ alkenes. The HBI distributions of two *R. setigera* strains were investigated, and sufficient quantities of pure compounds were isolated from bulk cultures of these two strains to allow for the characterisation of their structures *via* GC-MS and NMR spectroscopy.

**Chapter 4** describes the intra-cellular fractionation of *R. setigera* cells in an attempt to understand better the compartmentation and function of isoprenoids in diatoms. In a comprehensive study, the biosynthetic mechanisms involved in terpenoid (including HBIs) formation in the diatoms *Haslea ostrearia*, *Rhizosolenia setigera* and *Pleurosigma intermedium* has been carried out. This has included culturing each species in the presence of pathway-specific inhibitors, together with feeding experiments containing isotopically labelled substrates. Analysis of natural carbon isotope fractionation in these lipids by GC-irm-MS has been used to complement the results from other approaches. Evidence for species and organelle dependent biosynthetic pathways is presented, together with preliminary evidence for dynamic interchange between the two pathways.

(n.b. Individual compounds identified in diatom non-saponifiable fractions are numbered on a chapter-by-chapter basis)

CHAPTER TWO

# HBI distributions in the diatom *Rhizosolenia setigera*: Life cycle effects

## 2.1 Introduction

Since Volkman and co-workers (1994) discovered $C_{30}$ HBIs (rhizenes) in laboratory cultures of the diatom *Rhizosolenia setigera*, several studies have shown that the factors controlling their distribution are not as clear as for the $C_{25}$ HBIs produced by *Haslea ostrearia* and *Pleurosigma intermedium*. The culture of *R. setigera* investigated by Volkman *et al.* (strain CS 62) was found to contain three $C_{30}$ pentaenes ($C_{30:5}$) and two $C_{30}$ hexaenes ($C_{30:6}$) and no $C_{25}$ alkenes were detected (Volkman *et al.*, 1994). Belt and co-workers (2001a) noted a similar, though not identical distribution of $C_{30}$ HBIs (two $C_{30:5}$ and two $C_{30:6}$) in *R. setigera* isolated from northern France (strain RS 99) and elucidated the structures of the $C_{30}$ HBIs for the first time. In contrast, Sinninghe Damsté *et al.* showed that a strain of *R. setigera* isolated from Vineyard Sound, MA, USA (CCMP 1330) contained only a single $C_{25}$ pentaene in addition to two novel *n*-alkenes, with no $C_{30}$ homologues (Sinninghe Damsté *et al.*, 1999a). The structure of the $C_{25:5}$ in this strain was subsequently shown to be that previously found in cultures of *H. ostrearia* (Sinninghe Damsté *et al.*, 1999b).

During the course of our own studies, we have observed both $C_{25}$ and $C_{30}$ HBI alkenes within the same cultures of *R. setigera* together with considerable variations in their distributions (Rowland *et al.*, 2001b). It is of course possible that these differences may be attributable to changes in phenotypic variables employed during the culturing experiments (e.g. light, salinity, temperature, nutrients, etc) or to the use of different strains of diatoms belonging to the same species. Indeed, we have noted some variation in distributions with temperature and salinity, and also with the origin of the diatom strain. Significantly however,

we have also observed variations in distributions under 'controlled' conditions (constant temperature, salinity, light cycle, etc.) using a single strain, indicating that other factors are also important (Rowland *et al.*, 2001b). In addition, Sinninghe Damsté *et al.* (2000) have reported that distributions of the HBI $C_{25:5}$ and $C_{25}$ and $C_{27}$ *n*-alkenes produced by *R. setigera* were quite variable in experiments performed at the same temperature.

One factor worthy of investigation to explain these variations concerns the relationship between the position of the diatom in its life cycle and the variations observed in the HBI distributions. Indeed, significant differences in the dimensions of the cells of RS 99 (northern France) were noticed during consecutive growth cycles. This phenomenon, which occurs as a direct result of cell division (Wimpenny, 1966; Robert, 1978), relates to the fact that the diatom cell content is encased within a silica box or frustule. This exoskeleton is constructed of two almost equal halves (valves), the smaller fitting into the larger like a petri dish. As a result, upon cell division, one of the daughter cells is of the same size as the corresponding parent cell, while the other is smaller by an amount equal to twice the thickness of the frustule (Figure 2.1; Hendey, 1964). Over many generations, the difference in size between initial cells and mother cells is considerable, and the cells reach critical dimensions (Figure 2.2 b, c) such that sexual reproduction, followed by an auxospore formation (Figure 2.2 d, e) is needed to restore their initial size (Figure 2.2 a, c). It is common to observe auxosporulation in laboratory cultures of diatoms, especially centric species such as *Rhizosolenia* species. Many authors have intensively studied this phenomenon, though their investigations have focussed mainly on the factors controlling the auxosporulation and the ultrastructural changes induced (reviewed by Round *et al.*, 1990; Mann *et al.*, 1999). In contrast, very few studies have considered the biochemical implications of such a process, even if several authors assume that auxosporulation has a major impact on the physiological status of the cells. As an example, the concept of "turning or cardinal points in the life cycle

of diatoms" first developed by Geitler (1932) has been amended by Davidovich (1994) proposing that this concept should be first interpreted as "dramatic changes in the physiological and metabolic status of the cell rather than in its size".

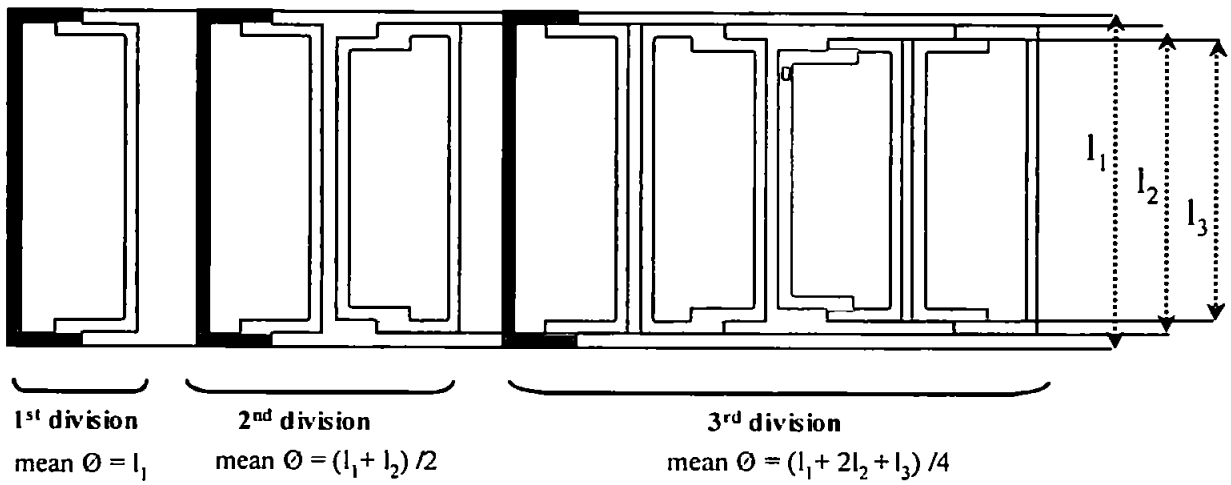


Figure 2.1 Diagrammatic representation of diatom cells, showing the gradual reduction in size of cells through consecutive generations. Redrawn from Hendey (1964).

It was therefore decided to investigate the distribution of $C_{25}$ and $C_{30}$ HBI alkenes biosynthesised by *R. setigera* as a function of the position of the cells through their life cycle. In a preliminary experiment, the effects of auxosporulation only, on the distribution of $C_{25}$ and $C_{30}$ HBI alkenes in *R. setigera* were investigated. Thus, single "daughter" cells were isolated from a culture of the strain RS 99 where an auxosporulation event had recently been observed. In contrast to the HBI distribution of previous cultures of this strain, both $C_{25}$ and $C_{30}$ HBI alkenes were observed within the non-saponifiable fractions obtained from cultures of these daughter cells, indicating that $C_{25}$ biosynthesis may be related to the auxosporulation event. In a second, more extensive set of experiments, the variation in the HBI distribution as a function of the position of the cells through their entire life cycle, including the regeneration of their original size through auxosporulation were measured. Therefore, two *R.*

*setigera* strains were replicated several times over a period of one year and the non-saponifiable lipid fractions obtained from each growth cycle were analysed. The evolution of *R. setigera* through its life cycle was estimated using cell size criteria (Figure 2.10). In addition, given the variability of the HBI distribution within the different *R. setigera* strains, it was first decided to examine the distribution of hydrocarbons in several species belonging to the *Rhizosolenia* genus in addition to members of closely related genera. Therefore, non-saponifiable lipid fractions obtained from six different species of the genus *Rhizosolenia* and closely related genera were examined by GC-MS.

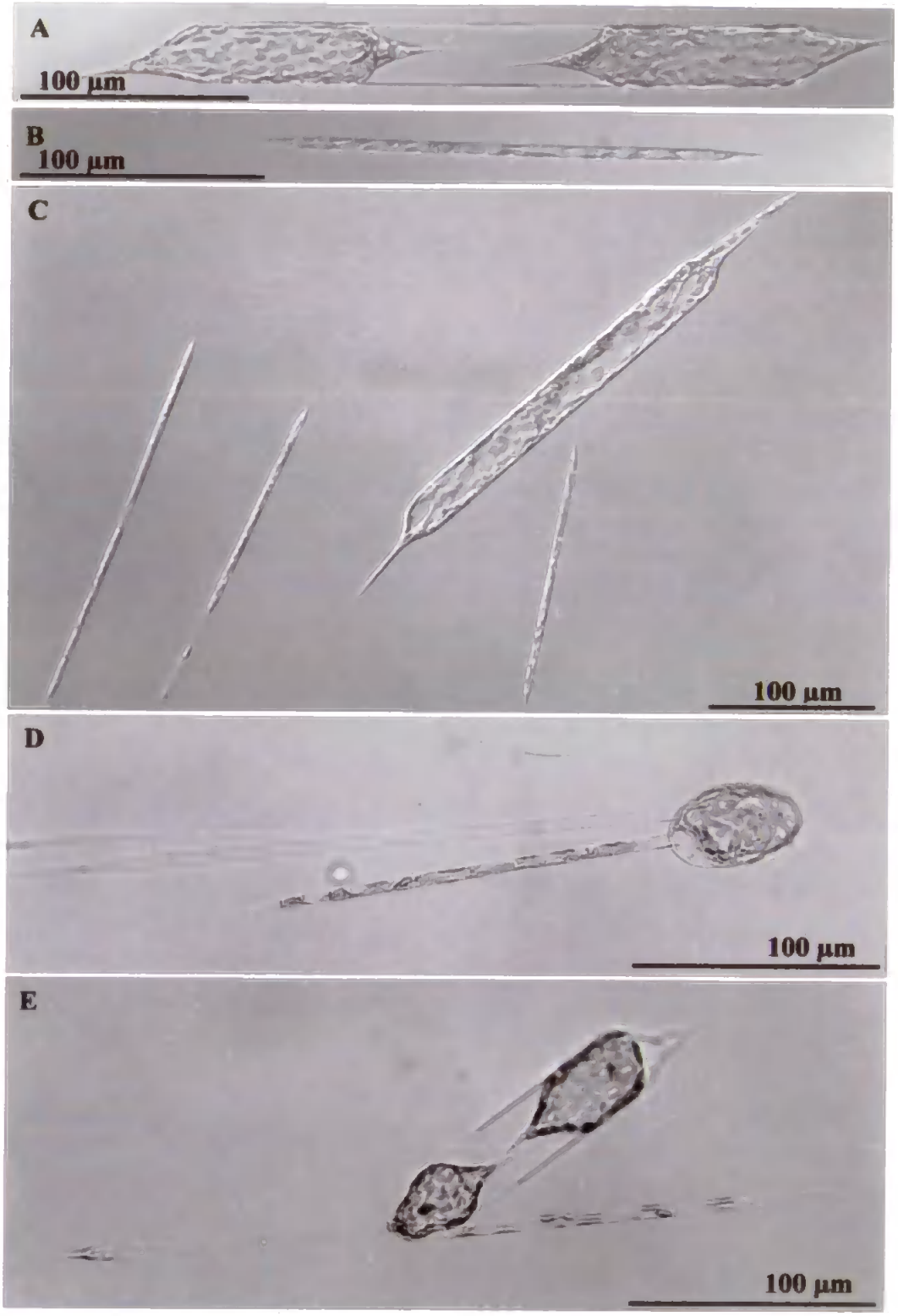


Figure 2.2 Light micrographs of the diatom *Rhizosolenia setigera*. A. Two daughter cells. B. One mother cell. C. Mother and daughter cells. Note the differences in the cell dimensions. D. Auxospore. E. Formation of the initial cell.

## 2.2 Experimental

### *2.2.1 Algal cultures*

*Rhizosolenia pungens* was isolated in May 2000 from the Rance Estuary, Ile et Vilaine (France). *Rhizosolenia robusta* was isolated in July 2000 from surface waters of the Etel River, Morbihan (France). *Urosolenia cf. longiseta* was isolated in June 2001 from surface waters of the freshwater lake from the "Vallée Mabile", Loire-Atlantique (France). *Proboscia indica*, *Guinardia delicatula* and *Guinardia stolterfothii* were isolated in June 2001 from surface waters of the Aber ildut, Finistère (France).

All marine species were grown on F/2 enriched seawater (Guillard, 1975) while the freshwater *Urosolenia* was grown on CHU-10 media (Stein, 1973). Cultures were performed under standard controlled conditions (14°C, 100 µmol photon $cm^{-2}$ $s^{-1}$, 14/10 light/dark cycle) and cells were harvested by filtration at the end of the exponential growing phase.

Cells were quantified by light microscopy, using a Nageotte counting plate. Cell widths were measured by light microscopy using a micrometer (mean values of a hundred measurements). Cell volumes were obtained using a Beckman Coulter multisizer (100 µm orifice tube, 2 ml counted).

### *2.2.2 Life cycle investigations with Rhizosolenia setigera*

**Preliminary experiment: RS-0**

A single cell of the diatom *R. setigera* (RS 99) was isolated from a natural assemblage of the phytoplankton obtained from surface waters of the Etel River, France (25/03/1999) and grown in 250 ml Erlenmeyer flasks containing 150 ml F/2 Guillard medium under standard

controlled conditions. After numerous replications (approx. 1 year), the cells were sufficiently small for auxosporulation to occur. Three different single "daughter" cells were therefore isolated (sub-strains 1-3) and cultured using the same method. At the end of the exponential growing phase, cells were harvested by filtration and stored (-20°C) prior to analysis.

**Experiment 1: RS-1 (Figure 2.3)**

*R. setigera* was isolated from Le Croisic, France (8/8/2000) and grown in 250 ml Erlenmeyer flasks containing 150 ml F/2 Guillard medium under standard controlled conditions. In order to ensure complete equilibration with the culture conditions, cells were replicated several times over a period of one month. After this equilibration period, 150 ml of new F/2 medium was inoculated with a concentration of 100 cell $ml^{-1}$ (cycle 1). At the end of the exponential growing phase (11 days), cells were harvested by filtration, with a sub-sample being used to inoculate a second flask (cycle 2) with the same cell concentration as per cycle 1. This procedure of culturing, harvesting and further inoculation was repeated a further four times to yield a total of six cycles (Figure 2.3). For each cycle, cell counting was performed using light microscopy and cell volumes were determined with a Beckman Coulter-Counter.

**Experiment 2: RS-2**

*R. setigera* (RS 99) was isolated from the Etel River, France (25/03/1999) and cultured using the same general method as described for Experiment 1 with the following exceptions: the cell concentration at the beginning of each cycle was 500 cell $ml^{-1}$ and cells were harvested after 7 days. In addition, single cells were isolated from the strain RS 99 which had been equilibrated in the laboratory for more than one year. As a result, all of the cells were extremely small (*ca* 4 µm width) and believed to be close to the critical size for auxospore

formation and the onset of auxosporulation. The procedure of culturing, harvesting and further inoculation was repeated a further fifty-seven times (*ca* 1 year) to yield a total of fifty-nine cycles.

### *2.2.3 Hydrocarbon analysis*

The extraction of HBIs and their analysis by GC-MS was performed following the general methodology described in Chapter 5.

An internal standard (7-hexylnonadecane, 1.1 μg filter$^{-1}$) was added to each filter prior to extraction in order to quantify the HBI cell concentrations.

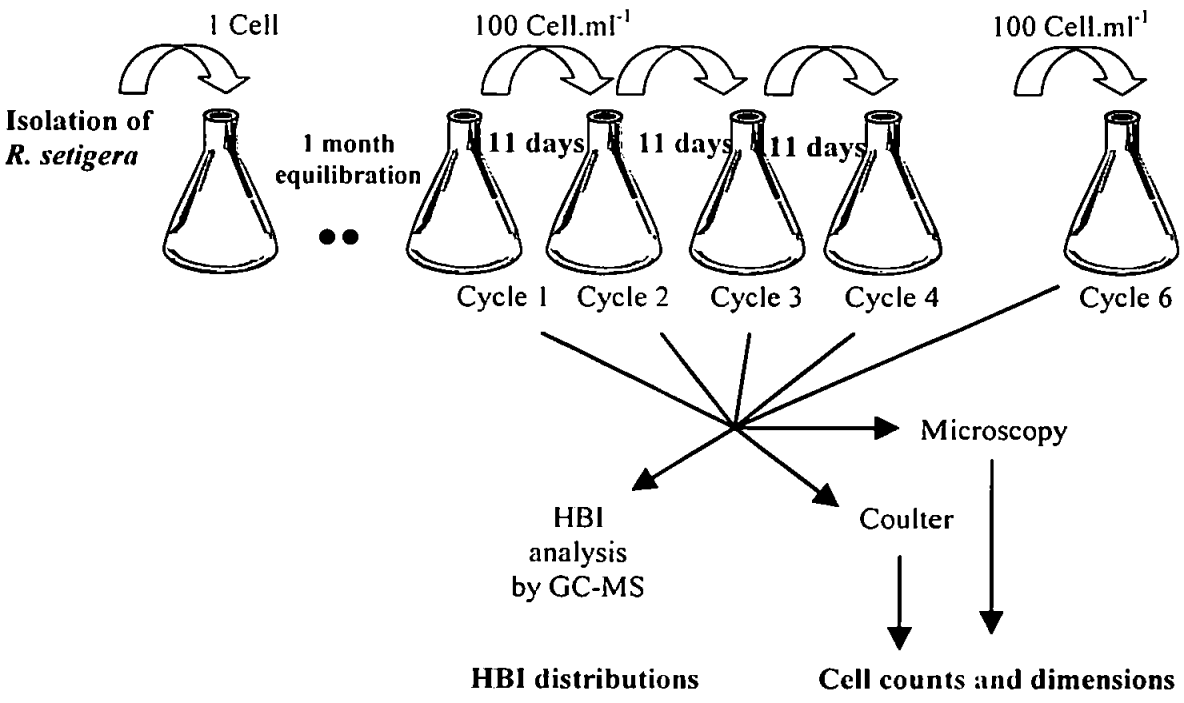


Figure 2.3: Experimental procedure for experiment RS-1.

## 2.3 Results

Figure 2.4 shows the structures of the non-saponifiable lipids identified in these studies.

### *2.3.1 Investigations on the hydrocarbon distribution within Rhizosolenia and related species*

Table 2.1 summarises the results obtained for the analysis of the non-saponifiable lipid (NSL) fractions obtained from small scale cultures of six different *Rhizosolenia* species and related genera.

Analysis of the hydrocarbon fractions obtained from *Rhizosolenia robusta*, *Proboscia indica*, *Guinardia delicatula*, *Guinardia stolterfothii* and *Urosolenia cf. longiseta* (Figure 2.5) revealed that these species produce *n*-$C_{21:6}$ (I, henicosa-3,6,9,12,15,18-hexaene) and phytol (V) but do not produce any HBI alkenes ($C_{25}$ or $C_{30}$ HBIs). In contrast, the NSLs obtained from *Rhizosolenia pungens* exhibited a similar HBI distribution to those observed for the diatom *Rhizosolenia setigera* (with the exception of the strain CCMP 1820 and CCMP 1330). Indeed, a total ion current (TIC) chromatogram of the NSL fraction obtained from a culture of this diatom (Figure 2.6) demonstrated the presence of *n*-$C_{21:6}$ (I), phytol (V), tri, tetra and penta-unsaturated $C_{25}$ HBIs isomers and six $C_{30}$ HBI alkenes (VI-XI).

Table 2.1: Hydrocarbon distribution from six diatom species.

| Species investigated | Phytol V | *n*-$C_{21:6}$ I | HBI Alkenes detected |
|---|---|---|---|
| *Rhizosolenia pungens* | + | + | II-IV, VI-XI |
| *Rhizosolenia robusta* | + | + | - |
| *Proboscia indica* | + | + | - |
| *Guinardia delicatula* | + | + | - |
| *Guinardia stolterfothii* | + | - | - |
| *Urosolenia cf. longiseta* | + | - | - |

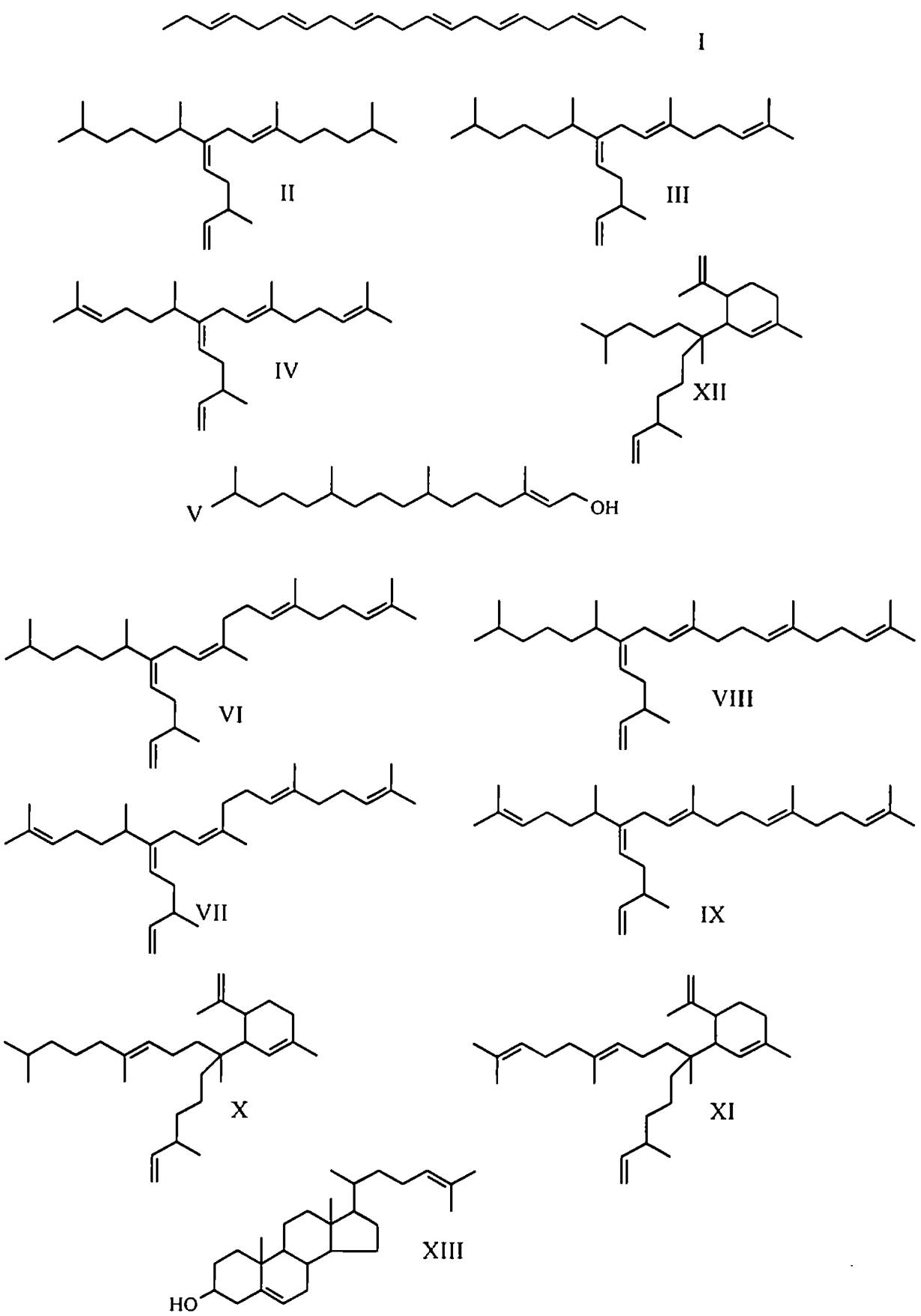


Figure 2.4 Structures of the non-saponifiable lipids identified in these studies.

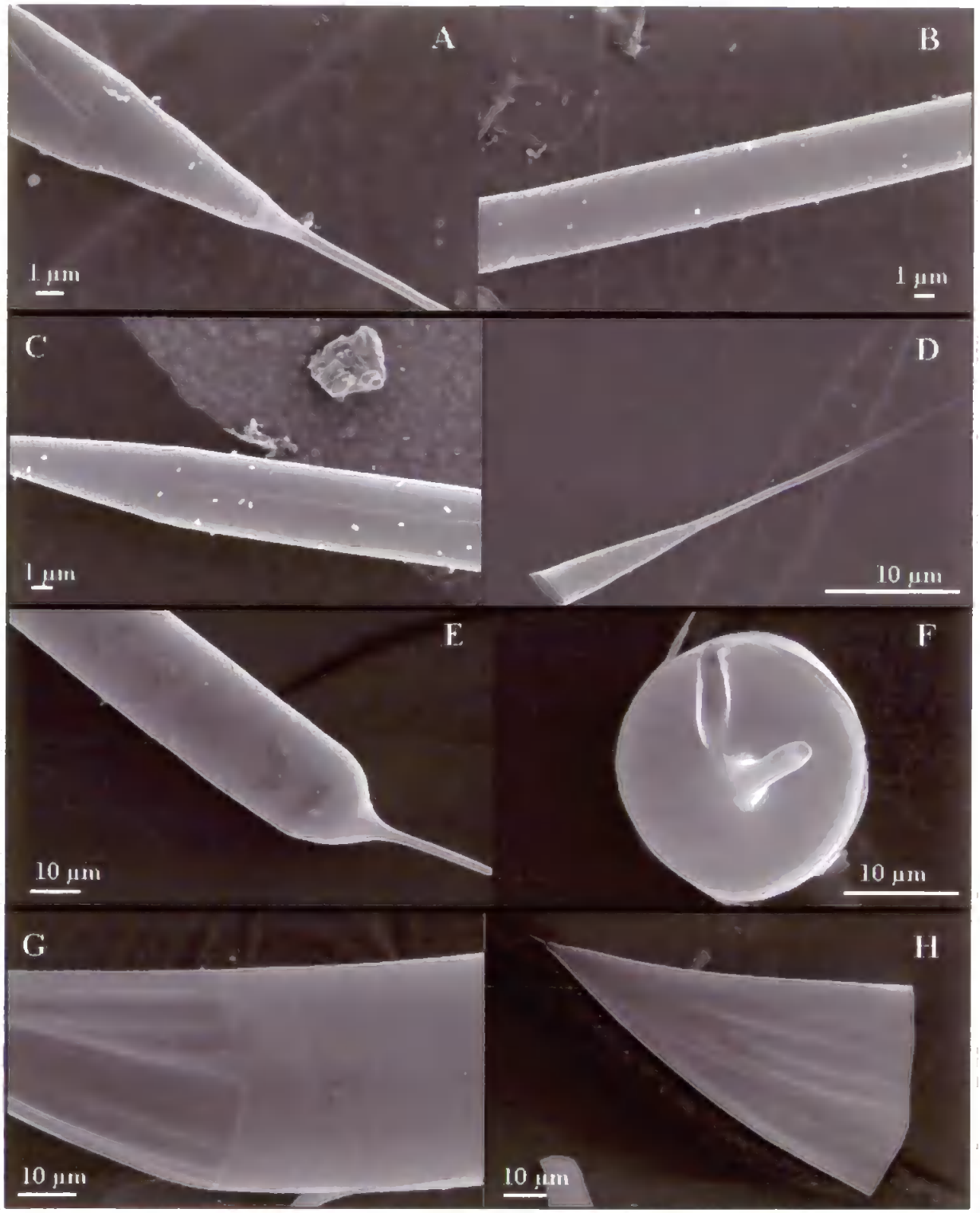


Figure 2.5 Scanning electron micrographs of *Rhizosolenia spp.* and related species. A, B. *Rhizosolenia setigera.* C, D. *Rhizosolenia pungens.* E, F. *Proboscia indica.* G, H. *Rhizosolenia robusta.*

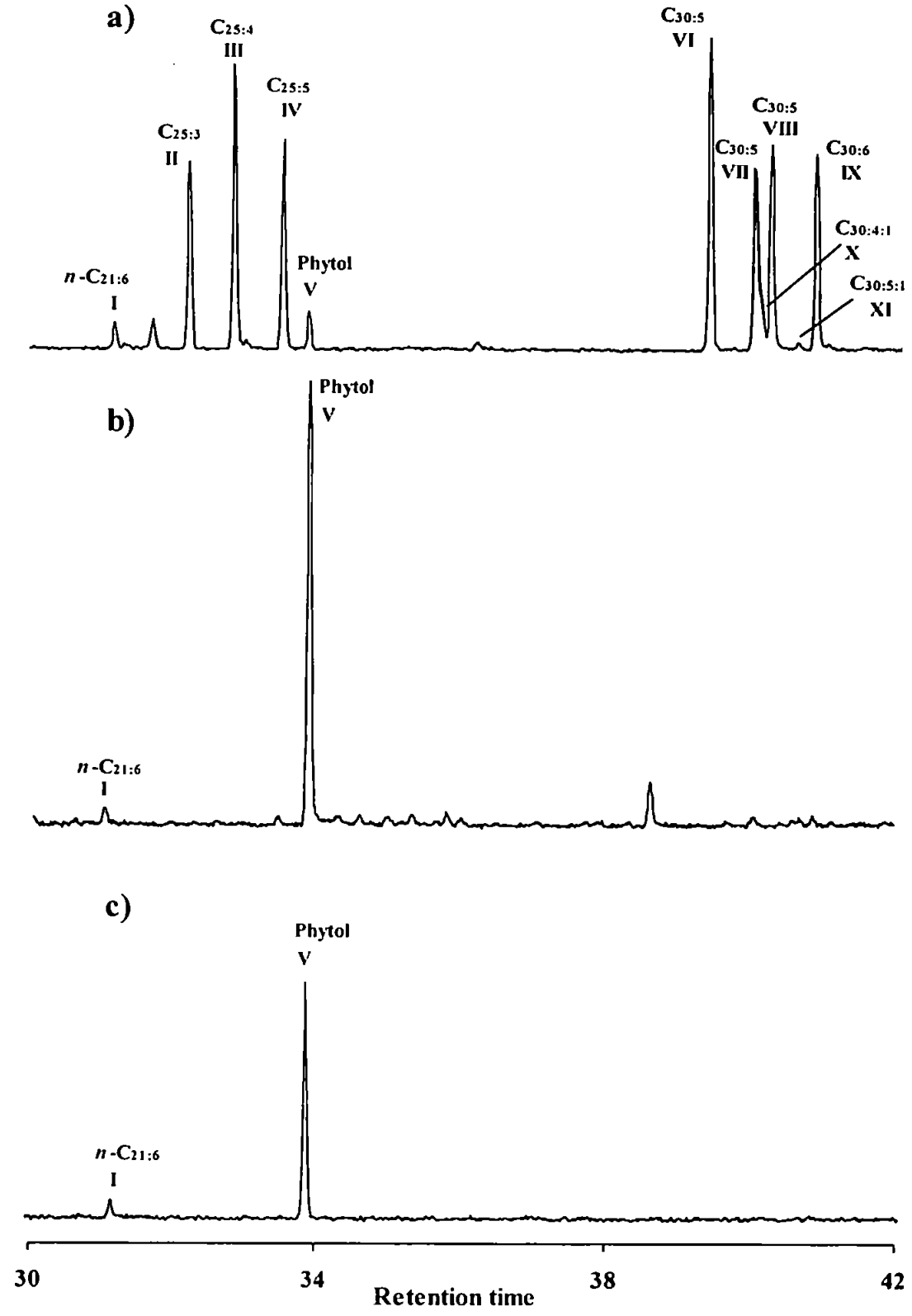


Figure 2.6 Partial TIC chromatograms of the non-saponifiable lipids from cultures of *Rhizosolenia spp.* and related species (a) *Rhizosolenia pungens* (b) *Rhizosolenia robusta* (c) *Proboscia indica.*

2.3.2 *Preliminary experiment:* RS-0

Following extraction and derivatisation, a TIC chromatogram of the non-saponifiable lipid fraction obtained from a culture of the diatom *R. setigera* kept during one year in the laboratory (Figure 2.7 a) demonstrated the presence of *n*-$C_{21:6}$ (I), phytol (V) and four $C_{30}$ HBI (VI-IX) (Rowland *et al.*, 2001a,b), but no $C_{25}$ HBIs alkenes (haslenes) were detected. In addition, the major rhizenes were the pentaene isomers ($C_{30:5}$ / $C_{30:6}$ = 5.4). However, when the non-saponifiable lipid fractions obtained from cultures of the daughter cells were analysed (sub-strains 1-3), some differences were observed (Figure 2.7 b-d). Phytol (V), *n*-$C_{21:6}$ (I) and the $C_{30}$ rhizenes were detected as before, but in addition, the TIC chromatograms revealed the presence of $C_{25}$ HBI isomers. In cultures of the sub-strains 1 and 3 (Figure 2.7 b, d), E isomers of tri and tetra-unsaturated $C_{25}$ HBIs (II and III) were detected, together with small amounts of the related pentaene isomer (IV). In cultures of the sub-strain 2 (Figure 2.7 c), only $C_{25}$ triene and tetraene isomers were detected, with the proportion of tetraene being substantially reduced than for sub-strains 1 and 3.

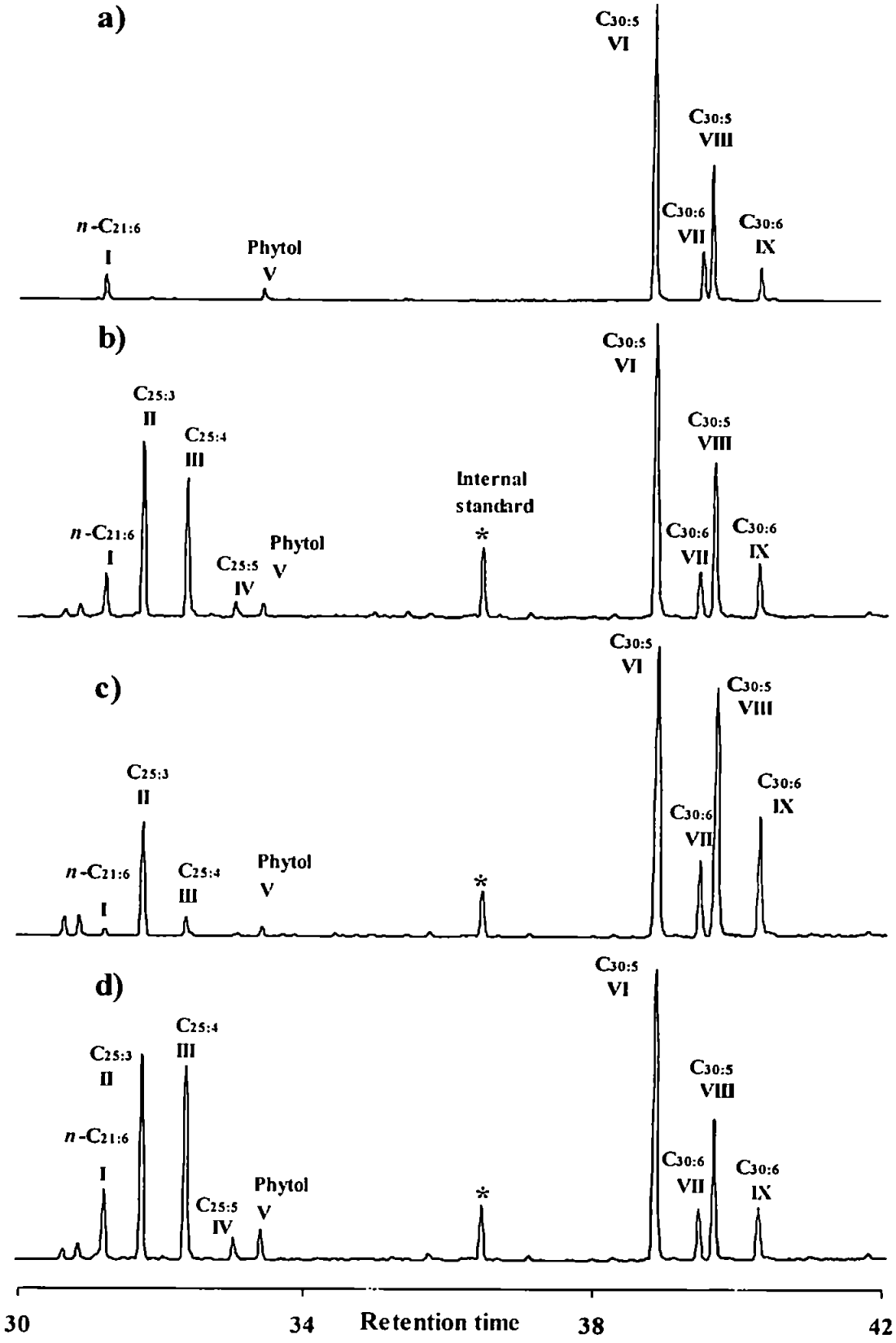


Figure 2.7 Partial TIC chromatograms of the non-saponifiable lipids from cultures of *R. setigera* (a) "mother" cells (b) "daughter" cells 1 (c) "daughter" cells 2 (d) "daughter" cells 3.

2.3.3 *HBI distributions in R. setigera during the post-auxosporulation phase:* RS-1

This experiment was carried out for a total of 6 cycles corresponding (broadly) to a phase distant to that of auxosporulation in the life cycle of the diatom.

Following extraction and derivatisation, TIC chromatograms of the non-saponifiable lipid fractions obtained from each cycle demonstrated the presence of phytol (V), *n*-$C_{21:6}$ (I) and four $C_{30}$ HBI alkenes (VI-IX) as the main identifiable components (Table 2.2). A small amount of $C_{25}$ triene (II) could also be detected in cycle 1 (Figure 2.8). Similar chromatograms were obtained for the following 5 cycles, except that the $C_{25:3}$ observed in cycle 1 could not be detected. For all cycles, the major rhizenes were the pentaene isomers with the pentaene to hexaene ratio remaining essentially constant ($C_{30:5}$ / $C_{30:6}$ = 12 ± 1.4).

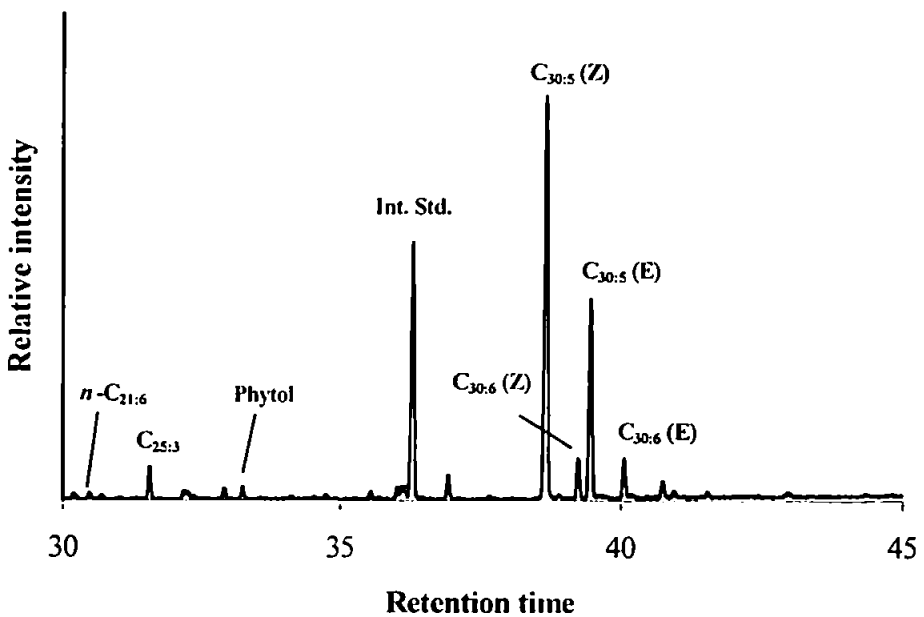


Figure 2.8 Partial TIC chromatogram of a non-saponifiable lipid fraction from RS-1 (cycle 1).

Table 2.2 Cell dimensions and non-saponifiable lipid concentrations obtained from six consecutive cycles (experiment RS-1).

| | Biomass (Cell $ml^{-1}$) | *n*-$C_{21:6}$ (pg $cell^{-1}$) | Phytol (pg $cell^{-1}$) | Total HBI (pg $cell^{-1}$) | Total $C_{25}$ (pg $cell^{-1}$) | Total $C_{30}$ (pg $cell^{-1}$) | $C_{30:5}$ (pg $cell^{-1}$) | $C_{30:6}$ (pg $cell^{-1}$) |
|---|---|---|---|---|---|---|---|---|
| Cycle1 | 11640 | 0.09 | 0.16 | 10.40 | 0.41 | 9.99 | 8.90 | 1.10 |
| Cycle2 | 12400 | 0.00 | 3.74 | 11.70 | 0.00 | 11.70 | 10.67 | 1.03 |
| Cycle3 | 10120 | 0.11 | 0.48 | 9.60 | 0.10 | 9.51 | 8.86 | 0.64 |
| Cycle4 | 9360 | 0.16 | 4.20 | 13.36 | 0.00 | 13.36 | 12.45 | 0.91 |
| Cycle5 | 10720 | 0.12 | 0.09 | 9.33 | 0.02 | 9.31 | 8.65 | 0.66 |
| Cycle6 | 14800 | 0.00 | 2.49 | 10.12 | 0.00 | 10.12 | 9.38 | 0.74 |

| | Mean Width (µm) | Mean volume ($\mu m^3$) | Total HBI (fg $\mu m^{-3}$) | Total $C_{30}$ (fg $\mu m^{-3}$) | $C_{30:5}/C_{30:6}$ |
|---|---|---|---|---|---|
| Cycle1 | 18.71 | 1309 | 7.94 | 7.6 | 8.12 |
| Cycle2 | 18.05 | 1279 | 9.15 | 9.1 | 10.33 |
| Cycle3 | 17.21 | 964 | 9.96 | 9.9 | 13.82 |
| Cycle4 | 16.55 | 1254 | 10.65 | 10.7 | 13.70 |
| Cycle5 | 15.85 | 1151 | 8.11 | 8.1 | 13.12 |
| Cycle6 | 14.98 | 1090 | 9.29 | 9.3 | 12.65 |

*2.3.4 HBI distributions in R. setigera during an entire life cycle: RS-2*

A summary of the data obtained for RS-2 are given in Tables 2.3 and 2.4 (pages 45-48), while Figure 2.9 shows representative partial total ion current chromatograms obtained from several growth cycles.

For this experiment, an inoculum was generated from the strain RS 99. In contrast to RS-1, the cells were believed to be close to the onset of auxosporulation (Figure 2.2 b). Indeed, during the third cycle, auxospores could be detected using light microscopy (Figure 2.2 d). In cycle 3, daughter cells (Figure 2.2 a) represented 14% of the total population, with the proportion increasing (61 %) during cycle 4. By cycles 5 and 6, virtually all cells could be considered to be present as a result of auxosporulation (93 and 100% daughter cells respectively). Cells from a further 53 cycles were harvested to allow for a comparison with the results from RS-1 and to cover an entire life cycle of the diatom. As expected dramatic changes in the cell volume were observed as a result of auxosporulation (Table 2.4, Figure 2.10). Thus, cell volumes were determined for mother (195 ± 15 $\mu m^3$) and daughter (3196 ± 170 $\mu m^3$) cells using a coulter counter (Table 2.4). Between cycles 7 and 51, the cell volumes gradually decreased (3369 to 356 $\mu m^3$) due to consecutive cell division (Figure 2.10). In cycle 35, a few auxospores were detected using microscopy, and the resulting daughter cells were observed in all of the subsequent 24 cycles. However, this phenomenon appeared to be limited and certainly not as dramatic as it appeared in the first auxosporulation stage (cycles 3 to 6) where the whole mother cell population was rapidly replaced by daughter cells. As a result, this new generation represented only a very small proportion (< 0.5%) of the whole population in cycles 36 to 48. During cycle 49, new auxospores were detected, and on this occasion, the resulting daughter cells rapidly replaced the mother cells: In cycle 50, daughter cells represented 4.3% of the total

population, with the proportion increasing during cycle 51 (21%) and 52 (64%). By cycle 53, all cells were present as a result of this second auxosporulation (100% daughter cells). As observed previously, dramatic changes in the cell volume were associated with the auxosporulation (Table 2.4, Figure 2.10). As a comparison, the volume of the mother cells (cycles 48-51) was 364 ± 23 $\mu m^3$, whereas the volume of the daughter cells (cycles 52 to 60) was 6522 ± 439 $\mu m^3$.

When the non-saponifiable lipid fractions for each cycle were analysed quantitatively by GC-MS, some substantial differences in the HBI distributions were observed and these were correlated with the major biological phases of the life cycle (Figure 2.9).

**Pre-auxosporulation 1** (Figure 2.9 a; cycles 1-2): A partial TIC chromatogram from cycle 1 indicated the presence of the same $C_{30:5}$ (VI, VIII) and $C_{30:6}$ (VII, IX) HBI alkenes that were detected in RS-1, although phytol (V) and *n*-$C_{21:6}$ (I) were undetected. In addition, there was a trace amount of the $C_{25}$ triene (II) which was mostly absent in the first experiment (RS-1) and there was a higher concentration of the pair of $C_{30}$ hexaenes compared to the pentaenes. Thus, the $C_{30:5}$ / $C_{30:6}$ ratio was 0.93 which compares with a mean ratio of 12 ± 1.4 in RS-1. Similar observations were made in cycle 2 (Table 2.3).

**Auxosporulation 1** (Figure 2.9 b, c; cycles 3-4): During cycle 3, when auxospores and daughter cells were first detected using light microscopy, the $C_{25:3}$ observed im low concentration in the first two cycles was absent and the $C_{30}$ pentaenes were the dominant isomers ($C_{30:5}$ / $C_{30:6}$ ratio increased sharply to 3.6). In cycle 4, when over 60% of the culture corresponded to daughter cells, the $C_{30:5}$ / $C_{30:6}$ ratio increased further (4.4). In addition, *n*-$C_{21:6}$ (I), the $C_{25}$ triene (II) and phytol (V) were also detected and the total concentration of HBIs (pg $cell^{-1}$) increased significantly during this cycle (Table 2.4).

**Post-auxosporulation 1 – Pre-auxosporulation 2** (Figure 2.9 d-k; cycles 5-49): From cycle 5 to cycle 12, the concentration of the $C_{25}$ triene detected in cycle 4 increased sharply to

reach a maximum of 41 pg cell$^{-1}$ in cycle 12 and then gradually decreased between cycles 13 and 50. In addition, a $C_{25}$ tetraene (III) was detected during cycle 5 while a $C_{25}$ pentaene (IV) was detected in cycle 11. Interestingly, the trends observed for the triene (II) could also be made for both $C_{25:4}$ and $C_{25:5}$ isomers. Thus, their concentrations first increased dramatically (from cycle 11, the tetraene was the most abundant isomer in the cells with a maximum concentration of 107 pg cell$^{-1}$ during cycle 13, whereas the pentaene reached a maximum concentration of 18 pg cell$^{-1}$ during cycle 12) and then gradually decreased between cycles 13-14 and cycle 49. From cycle 42 to cycle 52, only traces of the $C_{25}$ pentaene were detected. Collectively, the total concentration of HBIs ($C_{25}$ and $C_{30}$ HBIs), increased dramatically between cycles 5 and 12 (approximately 10 fold) to reach a maximum of 201 pg cell$^{-1}$ in cycle 12 followed by a gradual decrease until cycle 49. Further, during the phase where the total HBI concentration increased, the $C_{25}$ HBI concentrations increased at a greater rate compared with those for the $C_{30}$ HBIs ($C_{25}$ / $C_{30}$ ratio increased from 0 to 3.8 between cycles 4 and 12, Table 2.3). Additional changes were observed which appeared unrelated to the auxosporulation. For example, small amounts of a further $C_{25}$ triene (XII, *cf.* Chapter 3) and $C_{30}$ tetraene (X, *cf.* Chapter 3) were first detected during cycle 17. The Z isomer of the $C_{30}$ hexaenes (VII) was absent from cycle 18 to cycle 24, apparently replaced by the new $C_{30}$ tetraene (X). From cycle 19, small amounts of a third $C_{30}$ pentaene (XI, *cf.* Chapter 3) were also observed. Finally, the $C_{30:5}$ / $C_{30:6}$ ratio underwent further changes with a gradual reduction between cycles 4 and 17 (4.4 to 1.4) followed by a sharp increase from cycle 18, probably as a result of the absence of the $C_{30}$ hexaene (VII).

**Auxosporulation 2** (cycles 50-52): During cycle 50, a large number of auxospores were detected using light microscopy with subsequent and rapid formation of daughter cells (20% in cycle 51 and 64% during cycle 52). Consistent with the first auxosporulation event, significant changes in the cell lipid contents were observed: phytol, *n*-$C_{21:6}$ and both $C_{25:3}$ and

$C_{25:4}$ concentrations increased sharply from cycle 50. However, on this occasion, no significant changes in the $C_{30}$ unsaturation were observed during the auxosporulation event. Thus the $C_{30:5}/C_{30:6}$ remained unchanged (3.1 ± 0.3).

**Post-auxosporulation 2** (Figure 2.9 l; cycles 53-59): During cycle 53, the $C_{25}$ triene (III) reached a maximum of 25 pg cell$^{-1}$ while the $C_{25}$ pentaene (IV) was detected for the first time since cycle 42. In addition, the $C_{25}$ tetraene and pentaene concentrations increased further until cycle 54 to reach a maximum of 87 and 21 pg cell$^{-1}$, respectively.

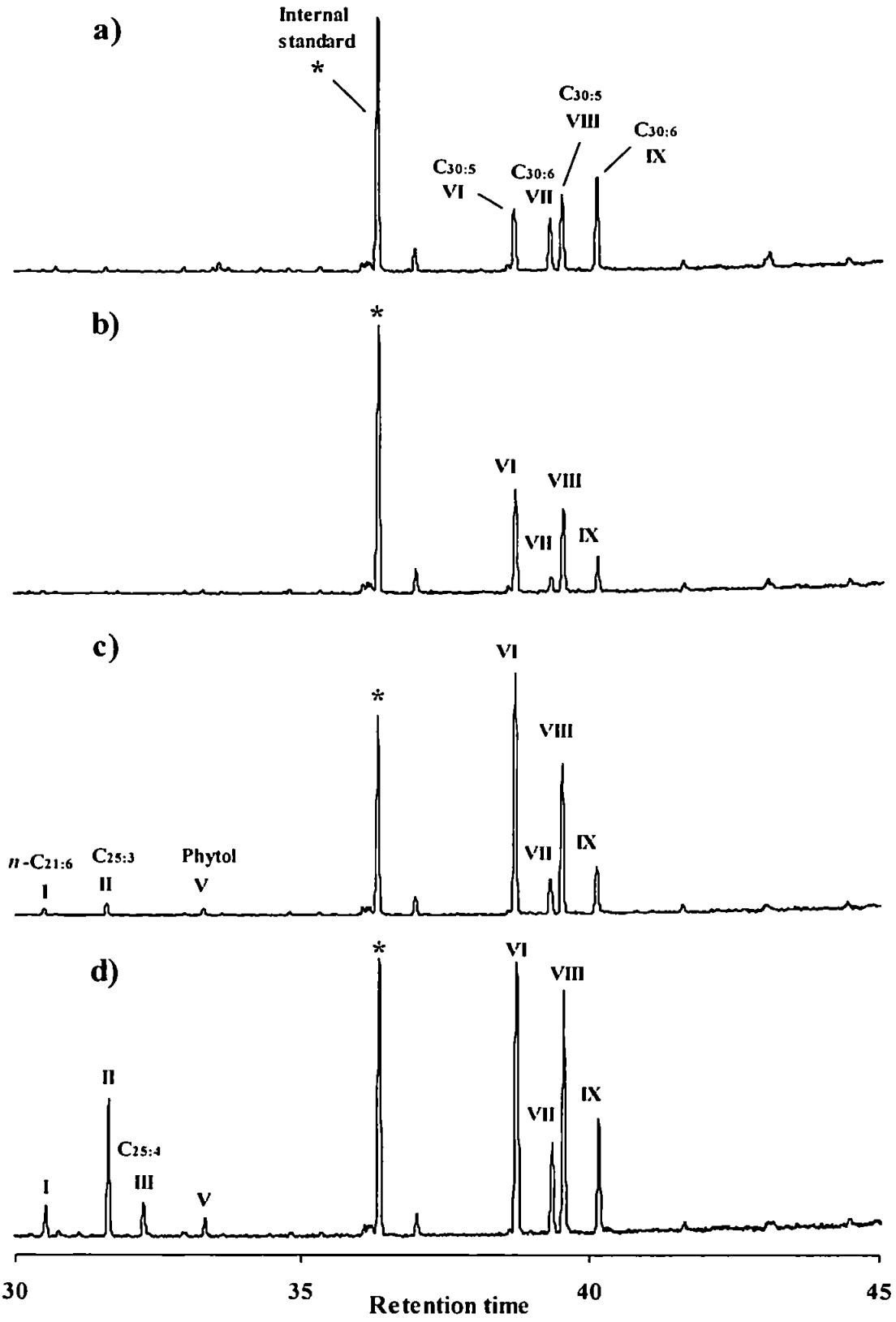


Figure 2.9 Partial TIC chromatograms of the non-saponifiable lipids from cultures of *Rhizosolenia setigera* (a) growth cycle 1, (b) growth cycle 3, (c) growth cycle 4, (d) growth cycle 6.

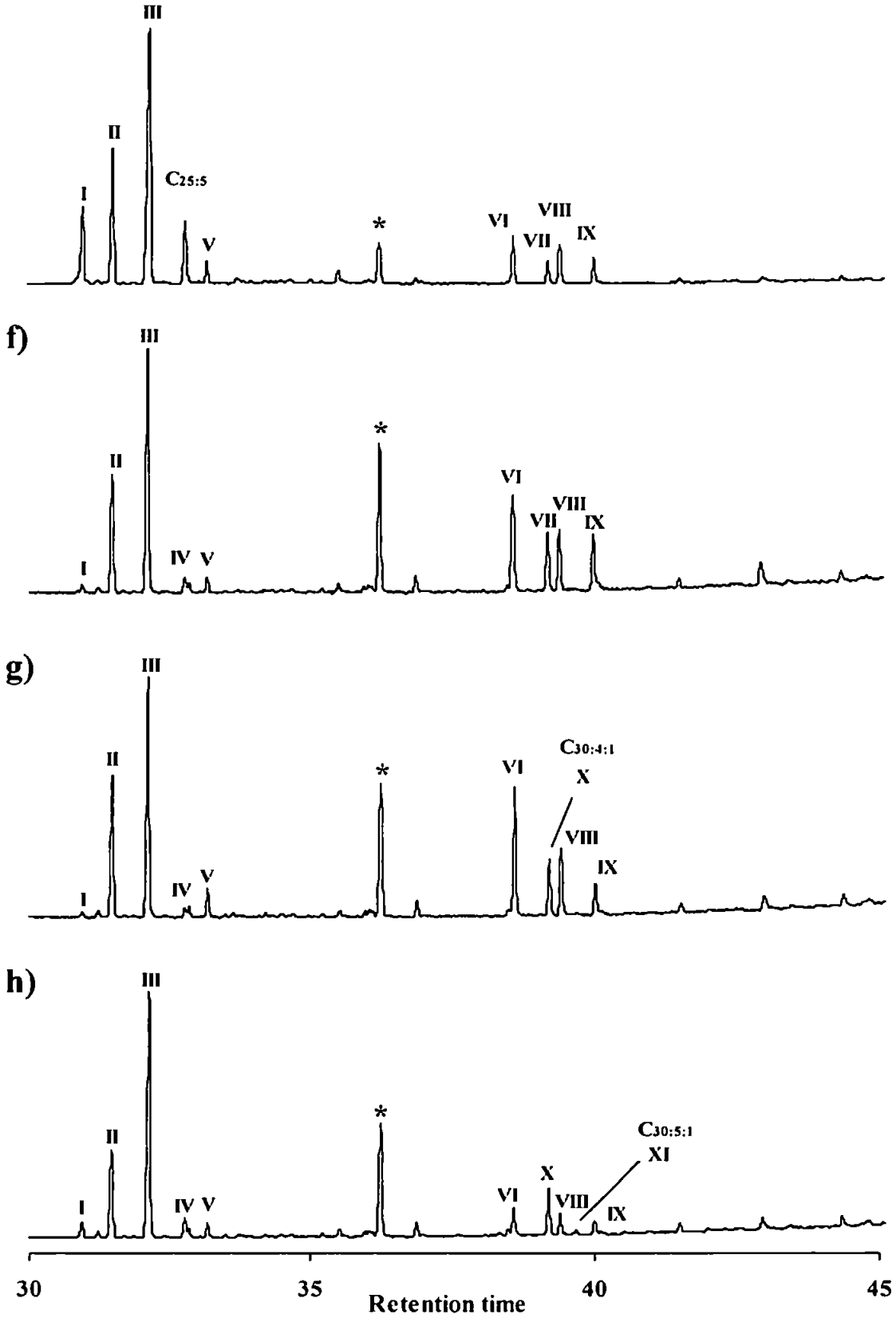


Figure 2.9 (continued) Partial TIC chromatograms of the non-saponifiable lipids from cultures of *R. setigera* (e) growth cycle 12, (f) growth cycle 17, (g) growth cycle 18, (h) growth cycle 23.

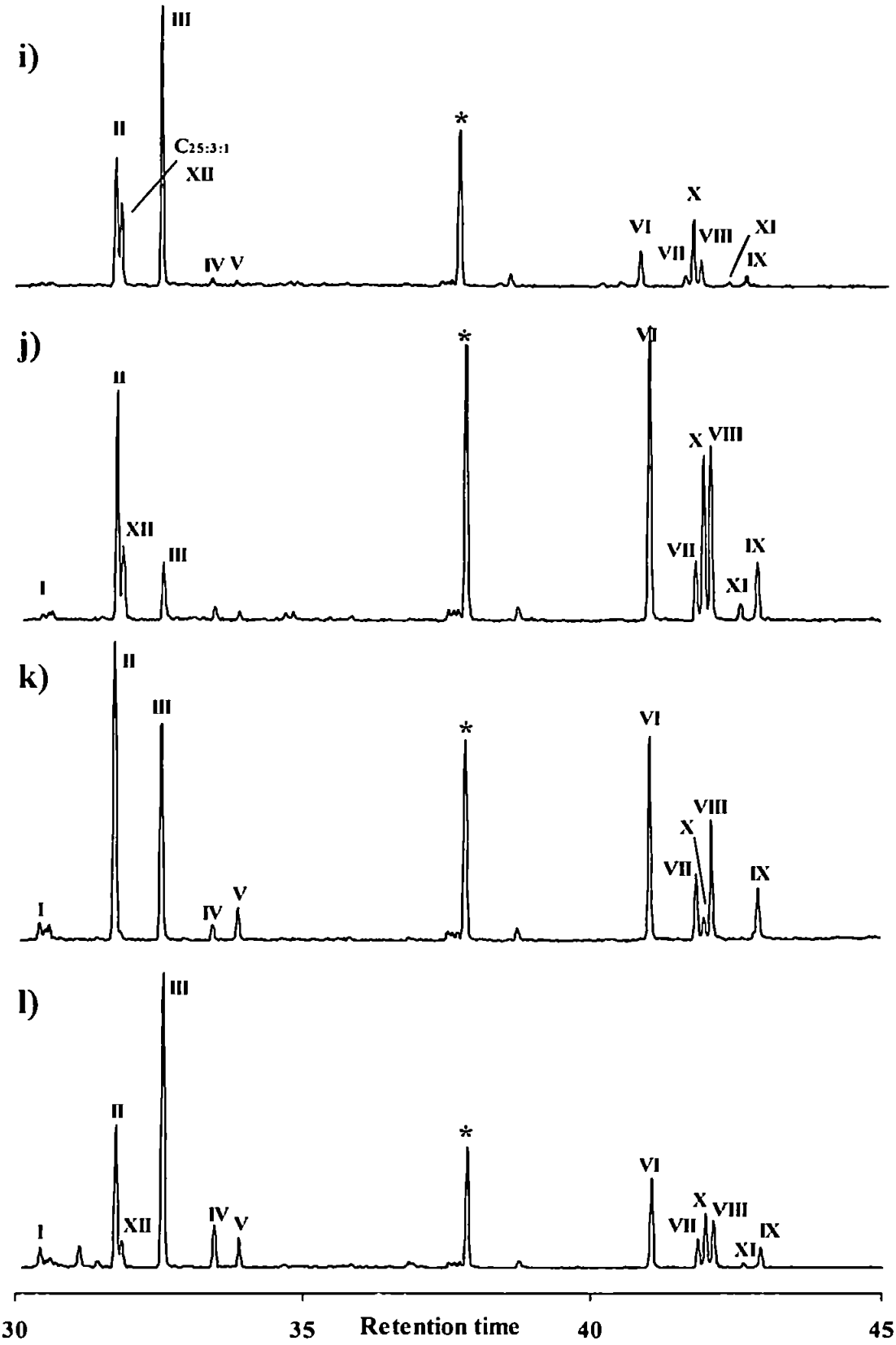


Figure 2.9 (continued) Partial TIC chromatograms of the non-saponifiable lipids from cultures of *R. setigera* (i) growth cycle 32, (j) growth cycle 42, (k) growth cycle 48, (l) growth cycle 53.

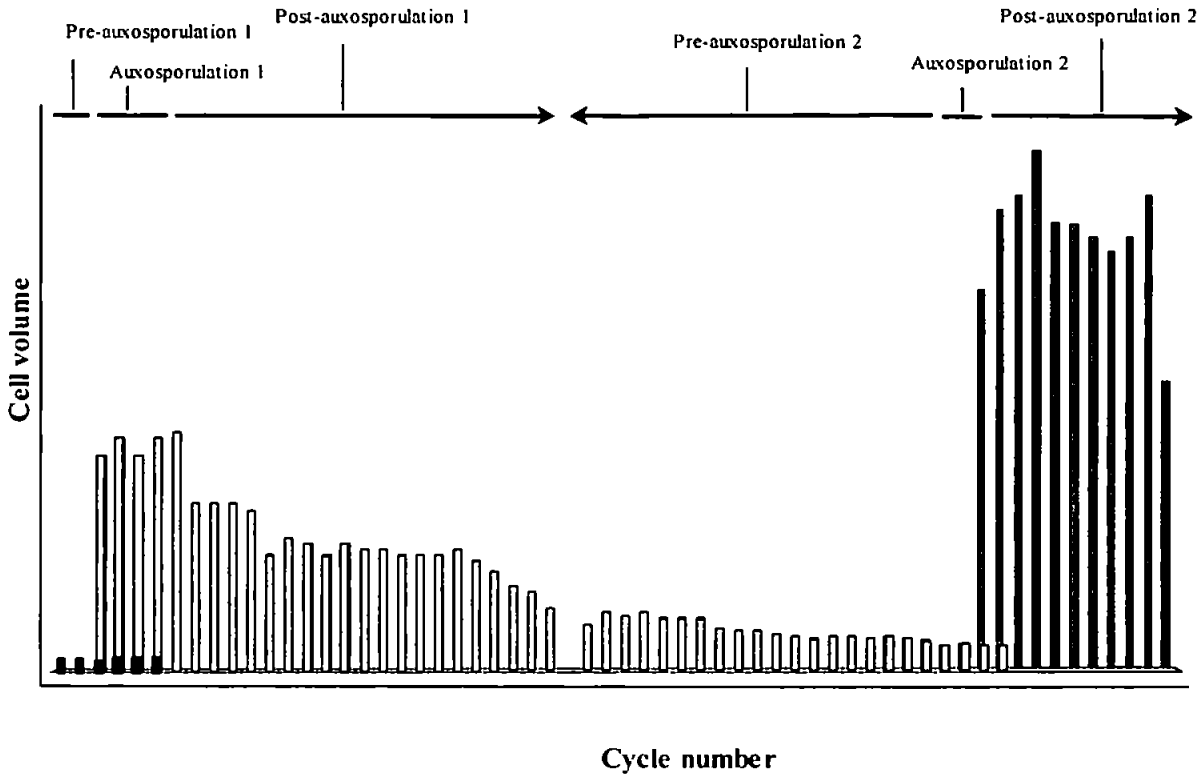


Figure 2.10 Estimation of the position of the diatom through its life cycle in relation with cell size and cycle number.

## 2.4 Discussion

### *2.4.1 Taxonomic comments*

The genus *Rhizosolenia* Brightwell is one of the most important genera of marine phytoplankton (Sundström, 1986). It is widely distributed and sometimes dominates the phytoplankton biomass in highly productive areas of the ocean (Hayward, 1993; Shipe *et al.*, 1999).

Before the revisions of Sundström (1986) and Round *et al.* (1990), this genus was considered as: "an inhomogeneous group of centric diatoms having in common the tubular cell shape

and the valve terminated by a single process or process-like structure". Sundström created the new genera *Proboscia* to separate *Rhizosolenia alata* and *R. indica*, and *Pseudosolenia* to separate *Rhizosolenia calcar-avis* from the other species. He also pointed out the need to create new genera to accommodate species possessing long needle-like processes like *R. pungens* and *R. setigera*, freshwater species such as *R. eriensis* and *R. longiseta* and finally a third genus to separate *R. robusta* from the "true" *Rhizosolenia* species. In addition, Round *et al.* (1990) transferred *R. eriensis* and *R. longiseta* into the new genus *Urosolenia*, and Hasle transferred *R. delicatula* and *R. stolterfothii* into the genus *Guinardia* H. Peragallo. As a result, a large number of the species investigated here, which were formerly placed in the *Rhizosolenia* group, have been transferred into different genera (Figure 2.11). However, the species investigated in this study share several ultrastructural features and even if placed in distinct genera, are still closely related taxa.

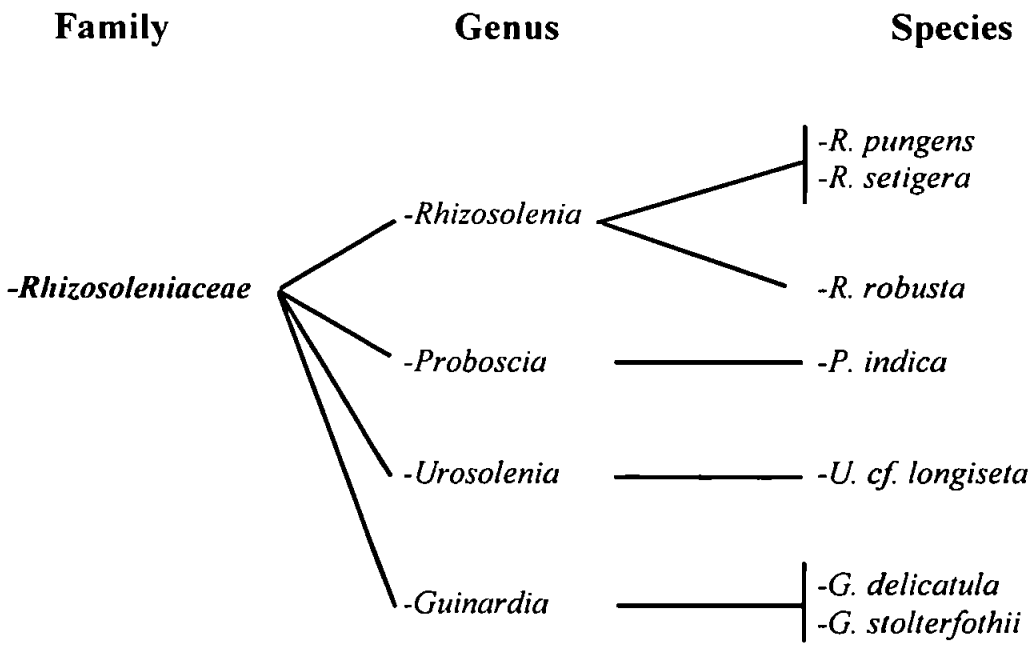


Figure 2.11 Taxonomic relationships between *Rhizosolenia setigera* and related species.

*2.4.2 Variations in HBI distributions between Rhizosolenia and related species*

The non-saponifiable lipid fractions obtained from six species closely related to the genus *Rhizosolenia* have been investigated. Surprisingly, neither HBI alkenes, nor *n*-alkenes were detected in the hydrocarbon fractions from most of these species (Table 2.1). The only diatom, in addition to *R. setigera* which has been found to be capable of synthesising HBI is the diatom *R. pungens*. This may not be too surprising since the ultra-structure of *R. pungens* is almost identical to that of *R setigera*. Similarly, it seems surprising that HBIs were not detected in the related species investigated, although there are other cases where the general trend between morphology and HBI production is not always observed. For example, $C_{25}$ HBIs were absent from cultures of *Pleurosigma angulatum*, *Navicula gracilis*, *N. ramossisima, N. lanceolata* and *N. Phyllepta*, despite their morphological similarities with *Pleurosigma intermedium* and *Navicula sclesviscensis*, two species capable of producing $C_{25}$ HBIs (Belt *et al.*, 2001b).

Given some of the historical difficulties associated with the classification of some *Rhizosolenia* (and closely related genera) species, a more expansive taxonomic and lipid investigation of the *Rhizosolenia* genus may prove helpful in establishing firmer conclusions. Further, well characterised *Rhizosolenia* species, including *R. fallax*, *R. cf. shrubshrolei* as well as *R. cf. hebetata f. semispina* and *Proboscia alata* have been successfully isolated and samples are awaiting analysis.

It seems likely that in culture, the vegetative multiplication phase is more extended than in natural conditions. During experiment RS-2, the cell isolated to create an innoculum for this experiment was very small (*ca* 4 μm width) while the lower threshold of the size ranges recorded in floras is not less than 6-8μm (Hustedt, 1930; Hendey, 1964; Van der Werf and Hulls, 1957-1974). Similar observations were reported by Mann *et al.* (1999) who showed

that cells from the pennate diatom *Sellaphora pupula* can achieve smaller dimensions in culture than those encountered in natural populations. They also noted that for *Sellaphora pupula*, a lower and an upper threshold existed for the sexual reproduction of this diatom, whereas in natural populations, these thresholds did not exist and cells were capable of sexual reproduction at any time. Thus, it seems likely that in natural environments, the cells are in a physiological state where they synthesise both $C_{25}$ and $C_{30}$ HBIs, whereas in culture, it is only the $C_{30}$ HBIs that are always synthesised. Therefore, the fact that $C_{25}$ HBIs are absent during a part of the life cycle of *R. setigera* may be an artefact associated with laboratory culturing. Further, it is probable that these alkenes are always biosynthesised by this diatom in natural conditions. Indeed, the occurrence of both $C_{25}$ and $C_{30}$ HBIs in the non-saponifiable lipid fractions of both *R. pungens* and *R. setigera* (described herein) when they were cultured and analysed immediately following isolation from a natural environment is noteworthy.

### *2.4.3 Variations in HBI distributions in Rhizosolenia setigera as a function of the position of the cells in the life cycle*

When the hydrocarbon fraction obtained from a culture of the diatom *R. setigera* (RS 99) kept during one year in the laboratory was examined by GC-MS, only four $C_{30}$ HBI alkenes (VI-IX) and no $C_{25}$ homologues were detected. However, when the corresponding fractions obtained from cultures of three isolated daughter cells from this strain were analysed, some major differences were observed. Not only were the same $C_{30:5}$ (VI, VIII) and $C_{30:6}$ (VII, IX) HBI alkenes detected, but the TIC chromatograms revealed the presence of $C_{25}$ HBI isomers (II-IV). These observations clearly demonstrated that despite the effects of environmental parameters on HBI biosynthesis (Sinninghe Damsté *et al.*, 2000; Rowland *et al.*, 2001b), the physiological status of the cells must have a major impact on the HBI distribution within the

cells. More importantly, the $C_{25}$ biosynthesis seems to be strongly correlated to a major biological event: auxosporulation. During experiment RS-1, the small amount of $C_{25}$ triene (II) detected during the first growth cycle was absent from the following five cycles. The single cell, when isolated from a natural sample was probably in the middle of the vegetative multiplication phase. As a result, this experiment was probably rather limited in terms of the entire life cycle, taking place a long time after auxosporulation and probably at the end of the phase when $C_{25}$ HBI biosynthesis occurs. To check this hypothesis further, the HBI distribution of *R. setigera* cells was examined during an entire life cycle (experiment RS-2). Therefore, a single cell was isolated from the strain RS 99 which had been equilibrated in the laboratory for more than one year. As a result, all of the cells were extremely small (*ca* 4 µm width) and believed to be close to the critical size for auxospore formation and the onset of auxosporulation. Indeed, during the third cycle, auxospores were detected using light microscopy. As expected, dramatic changes in cell dimensions were observed. During the following 45 cycles, the cell dimensions gradually decreased due to consecutive vegetative multiplication until cycle 49. At this point, when the second auxosporulation occurred, the mean cell volume was 364 ± 23 $\mu m^3$. The volume changes associated with the resulting daughter cells was again dramatic with an increase to a mean volume of 6522 ± 439 $\mu m^3$. Although this is about twice the volume of the daughter cells resulting from the first auxosporulation event, the *relative* enhancement of the cell size (daughter cells vs. mother cells) is consistent with the observations made by Davidovich (1994) on four diatom species, who demonstrated that the size of daughter cells was correlated with the size of mother cells.

The dramatic changes in cell dimensions and concentrations of HBIs (pg $cell^{-1}$) that accompanied auxosporulation phases (cycles 3-4 and cycles 49-51) prompted a consideration of the HBI concentrations on a unit volume basis (1 $\mu m^3$). Using this approach, the total concentration of $C_{30}$ HBIs was found to be reasonably constant with a mean value for the

concentration of $C_{30}$ HBIs per unit volume of 8.0 ± 5.3 fg $\mu m^{-3}$ which compares with that of 9.1 ± 0.9 fg $\mu m^{-3}$ obtained for RS-1. However, while the total $C_{30}$ HBI concentration remained constant, the ratio of the pentaene and hexaene isomers was affected substantially during the period of auxosporulation, with the $C_{30:5}$ / $C_{30:6}$ ratio increasing from 0.9 to 4.4 between cycles 2 and 4. Following the auxosporulation, this ratio underwent a gradual decrease until cycle 17 when the Z isomer of the $C_{30}$ hexaene was apparently replaced by a third $C_{30}$ hydrocarbon (X) with five degrees of unsaturation.

Different changes were observed for the $C_{25}$ HBIs. In contrast to the essential invariance observed for the total $C_{30}$ alkene concentrations, an increase in the concentration of the $C_{25}$ HBIs (especially $C_{25:4}$) with cycle number was observed and this was clearly reflected by an increase in the $C_{25}$ / $C_{30}$ ratio (Figure 2.12). While this trend was initiated by the onset of auxosporulation, the effects taking place during this phase were not as dramatic as those observed for the $C_{30}$ HBIs (*viz.* changes in $C_{30:5}$ / $C_{30:6}$ ratio, *vide infra*). Indeed, consistent changes to the $C_{25}$ HBI concentration took place both during and after auxosporulation, with significant changes taking place in cultures containing only daughter cells, including the observations of the $C_{25}$ tetraene (III) as the major isomer between cycles 11 and 40 (Table 2.3). Consistent with experiments RS-0 and RS-1, RS-2 demonstrated that $C_{25}$ HBI biosynthesis appear to be stimulated by the onset of auxosporulation. The total $C_{25}$ HBI concentration underwent a large increase during the cycles immediately following auxosporulation (cycles 5-12) and then gradually decreased until the next auxosporulation event (Cycles 50-52) when their biosynthesis was again stimulated.

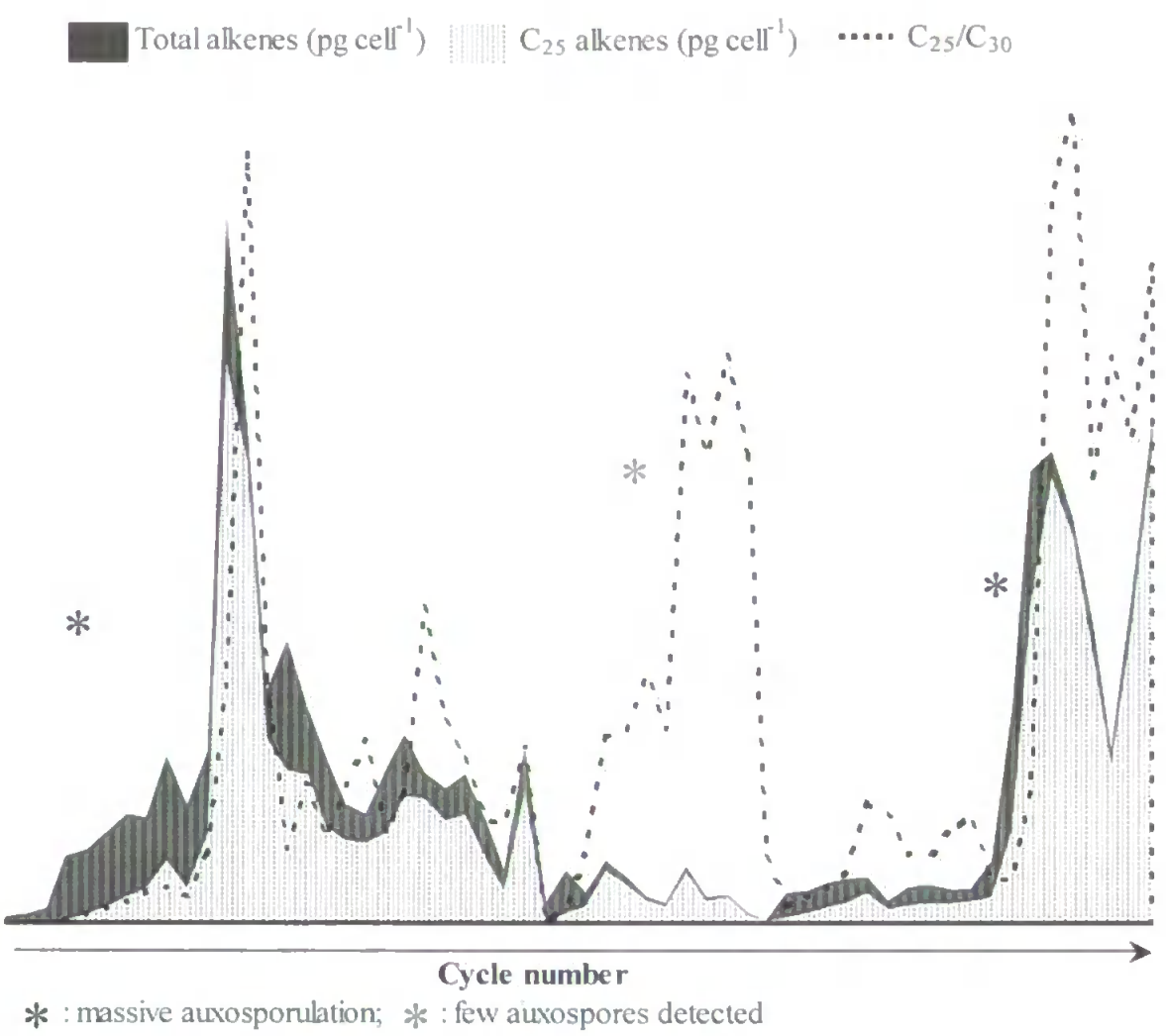


Figure 2.12 Hydrocarbon distribution in *Rhizosolenia setigera* as a function of cell cycle.

When other isoprenoids were considered, it was noted that the concentrations (on a unit cell volume basis) of cholesta-5,24-diene-3β-ol (desmosterol, XIII), the unique sterol present in *R. setigera* (Barrett *et al.*, 1995; Sinninghe Damsté *et al.*, 2000) and of phytol (V) seemed to be strongly correlated with those of the $C_{25}$ alkenes (Tables 2.3, 2.4).

In addition to these variations described for $C_{25}$ and $C_{30}$ HBIs, this detailed life cycle investigation (RS-2) has also provided some insight into the formation of some structurally related mono-cyclic hydrocarbon species comprising both $C_{25}$ and $C_{30}$ homologues. Such species were absent in RS-0 and RS-1 and were again not present during the auxosporulation

events of RS-2. Indeed, it was not until cycle 17 that a $C_{30}$ monocyclic tetraene ($C_{30:4:1}$, X) and a related $C_{25}$ monocyclic triene ($C_{25:3:1}$, XII) were detected. Shortly after, during cycle 19, an additional $C_{30}$ monocyclic pentaene ($C_{30:5:1}$, XI) was detected. Mass spectral properties and retention indices (RI 2548, 2579 $_{HP\text{-}1}$) of the two $C_{30}$ alkenes indicated that they were identical to two hydrocarbons identified in Dabob Bay (Prahl *et al.*, 1980), Puget Sound (Barrick and Hedges, 1981) and Arabian Sea (Allard, 2002) sediment samples, as well as in the hydrocarbon fractions of the diatom *R. setigera* strain CS 389 (Rowland *et al.*, 2001b) and CCMP 1694 (Allard, 2002). In addition, the mass spectrum and retention index (RI 2089 $_{HP\text{-}1}$) of the $C_{25}$ compound indicated that it was identical to that identified in the North West Atlantic (Farrington *et al.*, 1977), Rhode Island Sound (Boehm and Quinn, 1978), Puget Sound (Barrick and Hedges, 1981), as well as in sediment samples obtained from the Arabian Sea, the Cariaco Trench and the Peru upwelling (Allard, 2002). In contrast to the monocyclic $C_{30}$ alkenes, this novel $C_{25}$ hydrocarbon has not been reported previously in diatoms.

These three novel hydrocarbons were subsequently characterised and identified as two monocyclic $C_{30}$ (X, XI) hydrocarbons and a monocyclic $C_{25}$ (XII) hydrocarbon following large scale culture of *Rhizosolenia setigera* (strains RS99 and CCMP 1694), purification by silver ion-HPLC (*cf.* Chapter 3) and analysis by NMR spectroscopy.

## 2.5 Conclusion

This study has demonstrated that distributions of $C_{25}$ and $C_{30}$ HBI alkenes biosynthesised by *R. setigera* are strongly dependent on the position of the diatom in its life cycle, with the most significant changes taking place as a result of auxosporulation. In addition, the formation of related $C_{25}$ and $C_{30}$ hydrocarbon species have been observed to take place well

beyond the period of auxosporulation. These observations (with respect to *R. setigera*) can be summarised as follows:

(1) $C_{30}$ HBIs (rhizenes) are only biosynthesised with five or six degrees of unsaturation, though they are present as mixtures of geometric isomers.

(2) Rhizenes are observed at *every* stage of the life cycle. The total rhizene concentrations (measured on a unit volume basis) remain relatively constant during different stages of the life cycle ($8.0 \pm 5.3$ fg $\mu m^{-3}$), but the degree of unsaturation ($C_{30:5}$ / $C_{30:6}$ ratio) can be highly variable especially during the period of auxosporulation.

(3) Two new monocyclic $C_{30}$ hydrocarbons and one new monocyclic $C_{25}$ hydrocarbon are biosynthesised during a period in its life cycle significantly beyond auxosporulation.

(4) $C_{25}$ HBIs are biosynthesised with between three and five degrees of unsaturation but only as a single (E) geometric isomer.

(5) Unlike the $C_{30}$ HBIs, the $C_{25}$ homologues (haslenes) are not always observed. Their production would appear to be mainly stimulated by the onset of auxosporulation, although their concentrations and unsaturation continue to increase after this phase.

(6) No clear correlation between haslenes and rhizenes in terms of concentration, unsaturation or double bond stereochemistry have been observed during these experiments.

$C_{25}$ and $C_{30}$ HBIs were found in the hydrocarbon fraction obtained from *R. pungens* but not in *R. robusta*, or in any of the other closely related species investigated. Since it is now clear that not all species of the main HBI-producing genera of diatoms are capable of biosynthesising these compounds, a more comprehensive survey of individual species would seem necessary before a completed summary can be made. In addition, while these

investigations have revealed a dependence of HBI distributions on both individual species and life cycle phenomena, an explanation for the differences in the non-saponifiable fractions of the *R. setigera* strains CCMP 1820 and CCMP 1330 noted by Rowland *et al.* (2001b) and Sinninghe Damsté *et al.* (2000) has yet to be found. Given difficulties associated with the classification of some *Rhizosolenia* species, a possible confusion with species exhibiting almost identical morphologies may have occurred during the identification of these two strains. This is in need of further investigation.

Finally, it is likely that the production of $C_{25}$ HBIs (sometimes as the major components of the hydrocarbon fraction) by the diatoms *Rhizosolenia setigera* and *Rhizosolenia pungens*, can clearly contribute toward the sedimentary occurrence of these compounds. Significantly, the $C_{25}$ alkenes synthesised by these species are of the same structural type as the most common and abundant HBIs reported in sediments, and those previously found in other diatoms of the *Pleurosigma* genus (Belt *et al.*, 2000a,b, 2001c). Therefore, it is likely that these diatoms can significantly contribute as a planktonic source of HBIs, especially given their abundance and widespread occurrence (Hendey, 1964; Simonsen, 1974; Hayward, 1993; Shipe *et al.*, 1999). To date, only these two *Rhizosolenia* spp. have been reported as producers of the $C_{30}$ homologues, so their contribution to the sedimentary occurrences of these compounds also seems additionally likely.

Table 2.3 Non-saponifiable lipid concentrations (pg cell$^{-1}$) obtained from fifty-nine consecutive cycles (Cycle 1-30, experiment RS-2).

| | *n*-$C_{21:6}$ I | $C_{25:3}$ II | $C_{25:4}$ III | $C_{25:5}$ IV | Phytol V | $C_{30:5}$ VI + VIII | $C_{30:6}$ VII + IX | $C_{30:4:1}$ X | $C_{30:5:1}$ XI | $C_{25:3:1}$ XII | Desmosterol XIII | $C_{25}/C_{30}$ | $C_{30:5}/C_{30:6}$ |
|---|---|---|---|---|---|---|---|---|---|---|---|---|---|
| Cycle1 | 0.0 | 0.0 | n. d. | n. d. | 0.0 | 0.9 | 1.0 | n. d. | n. d. | n. d. | 0.4 | 0.0 | 0.9 |
| Cycle2 | 0.0 | 0.0 | n. d. | n. d. | 0.0 | 1.0 | 1.2 | n. d. | n. d. | n. d. | 0.4 | 0.0 | 0.8 |
| Cycle3 | 0.0 | 0.0 | n. d. | n. d. | 0.0 | 3.0 | 0.9 | n. d. | n. d. | n. d. | 1.3 | 0.0 | 3.5 |
| Cycle4 | 0.3 | 0.4 | n. d. | n. d. | 0.2 | 14.8 | 3.4 | n. d. | n. d. | n. d. | 7.4 | 0.0 | 4.4 |
| Cycle5 | 0.6 | 2.1 | 0.3 | n. d. | 0.4 | 13.5 | 4.9 | n. d. | n. d. | n. d. | 7.1 | 0.1 | 2.8 |
| Cycle6 | 0.9 | 3.8 | 0.9 | n. d. | 0.5 | 15.0 | 5.9 | n. d. | n. d. | n. d. | 7.0 | 0.2 | 2.5 |
| Cycle7 | 0.7 | 6.0 | 1.4 | n. d. | 1.1 | 18.0 | 5.0 | n. d. | n. d. | n. d. | 20.1 | 0.3 | 3.6 |
| Cycle8 | 0.8 | 5.7 | 3.9 | n. d. | 0.7 | 15.3 | 5.0 | n. d. | n. d. | n. d. | 11.1 | 0.5 | 3.1 |
| Cycle9 | 1.5 | 10.8 | 6.7 | n. d. | 1.2 | 22.2 | 7.8 | n. d. | n. d. | n. d. | 17.6 | 0.6 | 2.8 |
| Cycle10 | 1.0 | 6.1 | 3.4 | n. d. | 0.6 | 17.4 | 6.3 | n. d. | n. d. | n. d. | 9.9 | 0.4 | 2.8 |
| Cycle11 | 1.4 | 11.2 | 13.1 | 0.8 | 1.1 | 15.6 | 7.6 | n. d. | n. d. | n. d. | 14.4 | 1.1 | 2.1 |
| Cycle12 | 4.9 | 41.7 | 99.6 | 18.2 | 6.0 | 26.5 | 15.4 | n. d. | n. d. | n. d. | 89.0 | 3.8 | 1.7 |
| Cycle13 | 1.9 | 12.9 | 107.7 | 11.7 | 5.9 | 6.0 | 4.7 | n. d. | n. d. | n. d. | 92.9 | 12.4 | 1.3 |
| Cycle14 | 1.5 | 7.7 | 40.0 | 4.9 | 1.7 | 8.1 | 5.5 | n. d. | n. d. | n. d. | 32.8 | 3.9 | 1.5 |
| Cycle15 | 1.6 | 17.8 | 23.5 | 2.1 | 1.5 | 22.5 | 14.5 | n. d. | n. d. | n. d. | 31.3 | 1.2 | 1.6 |
| Cycle16 | 1.4 | 11.5 | 28.0 | 2.6 | 1.0 | 10.7 | 8.4 | n. d. | n. d. | n. d. | 26.2 | 2.2 | 1.3 |
| Cycle17 | 1.4 | 8.2 | 17.8 | 1.3 | 1.1 | 11.9 | 8.4 | traces | n. d. | n. d. | 17.3 | 1.3 | 1.4 |
| Cycle18 | 1.1 | 5.0 | 16.6 | 1.5 | 0.8 | 6.3 | 2.2 | 2.2 | n. d. | n. d. | 12.2 | 2.2 | 2.9 |
| Cycle19 | 1.2 | 5.5 | 15.4 | 1.7 | 0.6 | 4.1 | 1.4 | 2.2 | 0.2 | n. d. | 8.0 | 2.9 | 2.8 |
| Cycle20 | 1.6 | 9.5 | 15.4 | 0.6 | 1.7 | 12.4 | 2.3 | 3.4 | 0.1 | n. d. | 15.1 | 1.4 | 5.3 |
| Cycle21 | 2.3 | 11.8 | 23.3 | 0.9 | 1.6 | 10.6 | 2.1 | 4.7 | 0.1 | n. d. | 16.0 | 2.0 | 5.0 |
| Cycle22 | 2.7 | 6.8 | 26.5 | 2.2 | 1.7 | 3.2 | 1.3 | 2.4 | 0.2 | n. d. | 14.5 | 5.0 | 2.5 |
| Cycle23 | 2.3 | 7.5 | 20.3 | 1.5 | 1.1 | 4.0 | 1.2 | 3.6 | 0.4 | n. d. | 9.5 | 3.2 | 3.4 |
| Cycle24 | 1.6 | 8.8 | 20.8 | 1.2 | 1.1 | 6.2 | 1.3 | 3.8 | 0.3 | n. d. | 10.7 | 2.7 | 4.8 |
| Cycle25 | 1.1 | 5.8 | 11.2 | 1.2 | 0.4 | 5.0 | 1.4 | 4.5 | 0.2 | n. d. | 9.0 | 1.7 | 3.6 |
| Cycle26 | 0.5 | 2.5 | 6.2 | 0.5 | 0.4 | 2.9 | 1.5 | 1.5 | 0.0 | n. d. | 4.5 | 1.6 | 1.9 |
| Cycle27 | 2.9 | 11.2 | 24.0 | 1.6 | 2.5 | 6.8 | 1.8 | 4.0 | 0.5 | n. d. | 15.8 | 2.8 | 3.8 |
| Cycle29 | 0.0 | 0.0 | 0.0 | 0.0 | 0.0 | 3.3 | 2.2 | 0.0 | 0.0 | n. d. | 0.0 | 0.0 | 1.5 |
| Cycle30 | 0.0 | 0.9 | 1.7 | 0.4 | 0.3 | 6.2 | 5.8 | 0.0 | 0.0 | n. d. | 2.2 | 0.2 | 1.1 |

n.d. Non detected

Table 2.3 (continued) Non-saponifiable lipid concentrations (pg cell$^{-1}$) obtained from fifty-nine consecutive cycles (Cycle 31-59, experiment RS-2).

| | *n*-$C_{21:6}$ I | $C_{25:3}$ II | $C_{25:4}$ III | $C_{25:5}$ IV | Phytol V | $C_{30:5}$ VI + VIII | $C_{30:6}$ VII + IX | $C_{30:4:1}$ X | $C_{30:5:1}$ XI | $C_{25:3:1}$ XII | Desmosterol XIII | $C_{25}/C_{30}$ | $C_{30:5}/C_{30:6}$ |
|---|---|---|---|---|---|---|---|---|---|---|---|---|---|
| Cycle31 | 0.0 | 1.9 | 2.3 | 0.1 | 0.0 | 2.6 | 1.1 | 0.5 | 0.0 | 0.3 | 1.7 | 1.1 | 2.3 |
| Cycle32 | 0.0 | 3.9 | 8.3 | 0.3 | 0.2 | 2.0 | 0.7 | 2.3 | 0.1 | 2.5 | 2.5 | 3.0 | 2.8 |
| Cycle33 | 0.0 | 2.3 | 6.9 | 0.3 | 0.1 | 1.1 | 0.5 | 1.8 | 0.2 | 1.1 | 1.9 | 3.1 | 2.4 |
| Cycle34 | 0.0 | 1.1 | 4.5 | 0.2 | 0.1 | 0.6 | 0.2 | 0.8 | 0.1 | 0.4 | 1.7 | 4.0 | 3.2 |
| Cycle35 | 0.0 | 0.8 | 3.4 | 0.1 | 0.1 | 0.5 | 0.1 | 0.8 | 0.1 | 0.3 | 1.1 | 3.1 | 3.4 |
| Cycle36 | 0.7 | 2.5 | 10.8 | 1.1 | 0.3 | 0.4 | 0.3 | 0.8 | 0.2 | 0.0 | 3.5 | 8.8 | 1.3 |
| Cycle37 | 0.4 | 1.0 | 4.9 | 0.4 | 0.2 | 0.4 | 0.3 | 0.2 | 0.0 | 0.0 | 2.3 | 7.5 | 1.3 |
| Cycle38 | 0.3 | 1.4 | 5.5 | 0.5 | 0.1 | 0.3 | 0.2 | 0.3 | 0.0 | 0.0 | 2.0 | 9.1 | 1.5 |
| Cycle39 | 0.0 | 0.4 | 2.0 | 0.2 | 0.0 | 0.2 | 0.1 | 0.1 | 0.0 | 0.0 | 0.5 | 7.5 | 2.4 |
| Cycle40 | 0.0 | 0.1 | 0.2 | 0.0 | 0.0 | 0.1 | 0.0 | 0.1 | 0.0 | 0.0 | 0.2 | 1.1 | 4.8 |
| Cycle41 | 0.0 | 1.0 | 0.3 | 0.0 | 0.1 | 4.2 | 0.7 | 2.1 | 0.2 | 0.6 | 1.0 | 0.3 | 6.1 |
| Cycle42 | 0.0 | 1.8 | 0.5 | 0.0 | 0.1 | 4.0 | 1.0 | 1.4 | 0.2 | 0.6 | 1.2 | 0.4 | 3.9 |
| Cycle43 | 0.1 | 2.9 | 0.8 | 0.0 | 0.1 | 4.7 | 1.0 | 1.6 | 0.1 | 0.6 | 1.5 | 0.6 | 4.5 |
| Cycle44 | 0.2 | 3.7 | 1.7 | 0.0 | 0.2 | 4.4 | 1.3 | 1.4 | 0.2 | 0.6 | 3.6 | 0.8 | 3.5 |
| Cycle45 | 0.3 | 4.0 | 4.5 | 0.0 | 0.3 | 2.8 | 1.2 | 0.5 | 0.0 | 0.2 | 2.3 | 1.9 | 2.3 |
| Cycle46 | 0.1 | 1.7 | 2.3 | 0.0 | 0.1 | 1.6 | 0.6 | 0.3 | 0.0 | 0.1 | 1.1 | 1.7 | 2.8 |
| Cycle47 | 0.1 | 3.0 | 2.2 | 0.0 | 0.1 | 3.2 | 1.3 | 0.3 | 0.0 | 0.1 | 1.4 | 1.1 | 2.6 |
| Cycle48 | 0.2 | 3.3 | 2.4 | 0.0 | 0.3 | 3.6 | 1.3 | 0.3 | 0.0 | 0.0 | 2.2 | 1.1 | 2.8 |
| Cycle49 | 0.2 | 2.9 | 2.8 | 0.0 | 0.6 | 2.8 | 1.0 | 0.2 | 0.0 | 0.0 | 2.2 | 1.5 | 2.9 |
| Cycle50 | 0.1 | 2.3 | 3.6 | 0.0 | 0.1 | 2.2 | 0.8 | 0.6 | 0.0 | 0.3 | 1.4 | 1.7 | 2.9 |
| Cycle51 | 0.3 | 3.1 | 3.8 | 0.0 | 0.3 | 6.6 | 1.9 | 2.0 | 0.0 | 0.5 | 4.1 | 0.7 | 3.4 |
| Cycle52 | 0.8 | 12.4 | 12.0 | 0.0 | 0.9 | 21.4 | 6.0 | 9.3 | 0.7 | 2.4 | 9.0 | 0.7 | 3.6 |
| Cycle53 | 3.7 | 25.1 | 54.0 | 7.3 | 4.6 | 23.9 | 8.8 | 9.6 | 0.7 | 4.5 | 24.6 | 2.1 | 2.7 |
| Cycle54 | 3.3 | 15.2 | 87.3 | 21.7 | 5.8 | 4.9 | 2.2 | 3.7 | 0.0 | 3.3 | 21.9 | 11.7 | 2.2 |
| Cycle55 | 3.5 | 10.2 | 77.2 | 20.4 | 4.0 | 2.8 | 1.4 | 3.6 | 0.6 | 3.1 | 22.2 | 13.1 | 2.0 |
| Cycle56 | 3.8 | 7.8 | 54.8 | 12.0 | 1.7 | 4.1 | 1.7 | 4.3 | 0.6 | 2.3 | 11.3 | 7.1 | 2.4 |
| Cycle57 | 1.6 | 3.5 | 32.5 | 7.8 | 3.8 | 1.4 | 0.7 | 2.4 | 0.3 | 1.0 | 16.4 | 9.1 | 1.9 |
| Cycle58 | 5.0 | 8.1 | 60.1 | 13.5 | 3.6 | 4.8 | 1.8 | 3.6 | 0.5 | 2.0 | 16.2 | 7.8 | 2.6 |
| Cycle59 | 10.3 | 14.1 | 94.9 | 21.7 | 5.4 | 5.6 | 2.2 | 4.7 | 0.4 | 4.9 | 27.2 | 10.6 | 2.6 |

Table 2.4 Biomass data, cell dimensions and non-saponifiable lipid concentrations obtained from fifty-nine consecutive cycles (Cycle 1-30, experiment RS-2).

| | Biomass (Cell $ml^{-1}$) | Daughter cell 1 (%) | Mean volume ($\mu m^3$) | Total HBI (pg $cell^{-1}$) | Total $C_{25}$ (pg $cell^{-1}$) | Total $C_{30}$ (pg $cell^{-1}$) | Total Sterol (pg $cell^{-1}$) | Total HBI (fg $\mu m^{-3}$) | Total $C_{25}$ (fg $\mu m^{-3}$) | Total $C_{30}$ (fg $\mu m^{-3}$) | Total Sterol (fg $\mu m^{-3}$) |
|---|---|---|---|---|---|---|---|---|---|---|---|
| Cycle1 | 25440 | 0 | 188.0 | 1.9 | 0.0 | 1.9 | 0.4 | 10.0 | 0.2 | 9.8 | 1.9 |
| Cycle2 | 24320 | 1 | 188.0 | 2.2 | 0.0 | 2.2 | 0.4 | 11.8 | 0.1 | 11.6 | 2.3 |
| Cycle3 | 10560 | 14 | 569.8 | 3.9 | 0.0 | 3.9 | 1.3 | 6.8 | 0.0 | 6.8 | 2.3 |
| Cycle4 | 5800 | 61 | 2092.8 | 18.6 | 0.4 | 18.2 | 7.4 | 8.9 | 0.2 | 8.7 | 3.5 |
| Cycle5 | 6480 | 93 | 2819.5 | 20.7 | 2.4 | 18.3 | 7.1 | 7.3 | 0.9 | 6.5 | 2.5 |
| Cycle6 | 5560 | 100 | 3277.7 | 25.6 | 4.7 | 21.0 | 7.0 | 7.8 | 1.4 | 6.4 | 2.1 |
| Cycle7 | 3070 | 100 | 3369.3 | 30.5 | 7.5 | 23.1 | 20.1 | 9.1 | 2.2 | 6.8 | 6.0 |
| Cycle8 | 4520 | 100 | 2356.4 | 29.9 | 9.6 | 20.3 | 11.1 | 12.7 | 4.1 | 8.6 | 4.7 |
| Cycle9 | 2930 | 100 | 2356.4 | 47.5 | 17.5 | 30.0 | 17.6 | 20.2 | 7.4 | 12.7 | 7.5 |
| Cycle10 | 4140 | 100 | 2356.4 | 33.2 | 9.5 | 23.7 | 9.9 | 14.1 | 4.0 | 10.0 | 4.2 |
| Cycle11 | 3680 | 100 | 2250.9 | 48.4 | 25.1 | 23.2 | 14.4 | 21.5 | 11.2 | 10.3 | 6.4 |
| Cycle12 | 4020 | 100 | 1622.8 | 201.3 | 159.5 | 41.9 | 89.0 | 124.1 | 98.3 | 25.8 | 54.8 |
| Cycle13 | 2120 | 100 | 1875.3 | 142.9 | 132.2 | 10.7 | 92.9 | 76.2 | 70.5 | 5.7 | 49.5 |
| Cycle14 | 4400 | 100 | 1788.4 | 66.1 | 52.6 | 13.6 | 32.8 | 37.0 | 29.4 | 7.6 | 18.3 |
| Cycle15 | 4720 | 100 | 1622.8 | 80.4 | 43.4 | 37.0 | 31.3 | 49.5 | 26.7 | 22.8 | 19.3 |
| Cycle16 | 4480 | 100 | 1788.4 | 61.1 | 42.0 | 19.1 | 26.2 | 34.2 | 23.5 | 10.7 | 14.6 |
| Cycle17 | 4760 | 100 | 1704.3 | 47.5 | 27.2 | 20.3 | 17.3 | 27.9 | 16.0 | 11.9 | 10.1 |
| Cycle18 | 4500 | 100 | 1704.3 | 31.7 | 23.2 | 10.7 | 12.2 | 18.6 | 13.6 | 6.3 | 7.2 |
| Cycle19 | 5560 | 100 | 1622.8 | 28.1 | 22.6 | 7.8 | 8.0 | 17.3 | 13.9 | 4.8 | 4.9 |
| Cycle20 | 5560 | 100 | 1622.8 | 40.2 | 25.5 | 18.3 | 15.1 | 24.8 | 15.7 | 11.2 | 9.3 |
| Cycle21 | 3800 | 100 | 1622.8 | 48.7 | 35.9 | 17.6 | 16.0 | 30.0 | 22.1 | 10.9 | 9.9 |
| Cycle22 | 4440 | 100 | 1704.3 | 40.0 | 35.5 | 7.0 | 14.5 | 23.5 | 20.8 | 4.1 | 8.5 |
| Cycle23 | 5800 | 100 | 1544.0 | 34.4 | 29.3 | 9.2 | 9.5 | 22.3 | 18.9 | 5.9 | 6.2 |
| Cycle24 | 5560 | 100 | 1394.1 | 38.2 | 30.7 | 11.5 | 10.7 | 27.4 | 22.0 | 8.3 | 7.7 |
| Cycle25 | 8040 | 100 | 1185.2 | 24.6 | 18.2 | 11.0 | 9.0 | 20.7 | 15.4 | 9.3 | 7.6 |
| Cycle26 | 6960 | 100 | 1121.4 | 13.5 | 9.1 | 5.8 | 4.5 | 12.0 | 8.2 | 5.2 | 4.0 |
| Cycle27 | 5320 | 100 | 889.0 | 45.4 | 36.8 | 13.1 | 15.8 | 51.0 | 41.4 | 14.7 | 17.7 |
| Cycle29 | 1040 | 100 | 645.0 | 5.6 | 0.0 | 5.6 | 0.0 | 8.7 | 0.0 | 8.7 | 0.0 |
| Cycle30 | 2720 | 100 | 836.5 | 14.9 | 2.9 | 11.9 | 2.2 | 17.8 | 3.5 | 14.3 | 2.7 |

Table 2.4 (continued) Biomass data, cell dimensions and non-saponifiable lipid concentrations obtained from fifty-nine consecutive cycles (Cycle 31-59, experiment RS-2).

| | Biomass (Cell $ml^{-1}$) | Daughter cell 1 (%) | Daughter cell 2 (%) | Mean volume ($\mu m^3$) | Total HBI (pg $cell^{-1}$) | Total $C_{25}$ (pg $cell^{-1}$) | Total $C_{30}$ (pg $cell^{-1}$) | Total Sterol (pg $cell^{-1}$) | Total HBI (fg $\mu m^{-3}$) | Total $C_{25}$ (fg $\mu m^{-3}$) | Total $C_{30}$ (fg $\mu m^{-3}$) | Total Sterol (fg $\mu m^{-3}$) |
|---|---|---|---|---|---|---|---|---|---|---|---|---|
| Cycle31 | 10280 | 100 | 0 | 786.0 | 8.1 | 4.3 | 4.3 | 1.7 | 10.3 | 5.5 | 5.4 | 2.1 |
| Cycle32 | 9120 | 100 | 0 | 836.5 | 15.2 | 12.5 | 5.1 | 2.5 | 18.2 | 15.0 | 6.1 | 3.0 |
| Cycle33 | 11000 | 100 | 0 | 735.6 | 11.1 | 9.5 | 3.5 | 1.9 | 15.1 | 13.0 | 4.7 | 2.6 |
| Cycle34 | 12480 | 100 | 0 | 735.6 | 6.6 | 5.8 | 1.6 | 1.7 | 8.9 | 7.9 | 2.1 | 2.4 |
| Cycle35 | 13360 | 100 | 0 | 735.6 | 5.0 | 4.3 | 1.5 | 1.1 | 6.7 | 5.9 | 2.0 | 1.5 |
| Cycle36 | 11760 | 100 | 0 | 602.7 | 15.0 | 14.3 | 1.6 | 3.5 | 24.9 | 23.8 | 2.7 | 5.9 |
| Cycle37 | 16560 | 100 | 0 | 562.2 | 7.1 | 6.4 | 0.9 | 2.3 | 12.6 | 11.4 | 1.5 | 4.0 |
| Cycle38 | 16400 | 100 | 0 | 562.2 | 7.9 | 7.3 | 0.8 | 2.0 | 14.0 | 13.1 | 1.4 | 3.5 |
| Cycle39 | 17700 | 100 | 0 | 523.6 | 2.8 | 2.5 | 0.3 | 0.5 | 5.3 | 4.8 | 0.6 | 1.0 |
| Cycle40 | 14300 | 100 | 0 | 486.6 | 0.5 | 0.3 | 0.3 | 0.2 | 1.0 | 0.6 | 0.6 | 0.5 |
| Cycle41 | 20300 | 100 | 0 | 451.5 | 6.2 | 1.3 | 7.2 | 1.0 | 13.8 | 2.9 | 15.9 | 2.3 |
| Cycle42 | 19360 | 100 | 0 | 486.6 | 7.3 | 2.3 | 6.6 | 1.2 | 15.0 | 4.7 | 13.6 | 2.5 |
| Cycle43 | 18800 | 100 | 0 | 486.6 | 9.3 | 3.7 | 7.5 | 1.5 | 19.2 | 7.5 | 15.3 | 3.2 |
| Cycle44 | 18000 | 100 | 0 | 451.5 | 11.0 | 5.3 | 7.3 | 3.6 | 24.4 | 11.8 | 16.2 | 8.0 |
| Cycle45 | 19800 | 100 | 0 | 486.6 | 12.5 | 8.5 | 4.5 | 2.3 | 25.7 | 17.5 | 9.3 | 4.7 |
| Cycle46 | 20600 | 100 | 0 | 451.5 | 6.2 | 4.0 | 2.5 | 1.1 | 13.7 | 8.9 | 5.4 | 2.5 |
| Cycle47 | 21800 | 100 | 0 | 418.0 | 9.7 | 5.2 | 4.8 | 1.4 | 23.3 | 12.5 | 11.4 | 3.3 |
| Cycle48 | 21400 | 100 | 0 | 356.2 | 10.5 | 5.7 | 5.1 | 2.2 | 29.6 | 16.0 | 14.4 | 6.1 |
| Cycle49 | 26700 | 99 | 1 | 386.3 | 9.5 | 5.8 | 3.9 | 2.2 | 24.6 | 14.9 | 10.2 | 5.7 |
| Cycle50 | 20700 | 96 | 4 | 574.5 | 9.0 | 5.9 | 3.6 | 1.4 | 15.6 | 10.3 | 6.3 | 2.4 |
| Cycle51 | 15000 | 83 | 17 | 1663.3 | 15.5 | 7.0 | 10.5 | 4.1 | 9.3 | 4.2 | 6.3 | 2.4 |
| Cycle52 | 4000 | 36 | 64 | 4343.4 | 51.8 | 24.4 | 37.4 | 9.0 | 11.9 | 5.6 | 8.6 | 2.1 |
| Cycle53 | 2240 | 0 | 100 | 7439.1 | 119.1 | 86.4 | 43.0 | 24.6 | 16.0 | 11.6 | 5.8 | 3.3 |
| Cycle54 | 2120 | 0 | 100 | 6378.9 | 131.4 | 124.2 | 10.9 | 21.9 | 20.6 | 19.5 | 1.7 | 3.4 |
| Cycle55 | 2320 | 0 | 100 | 6378.9 | 112.0 | 107.8 | 8.5 | 22.2 | 17.6 | 16.9 | 1.3 | 3.5 |
| Cycle56 | 2080 | 0 | 100 | 6181.4 | 80.4 | 74.6 | 10.8 | 11.3 | 13.0 | 12.1 | 1.7 | 1.8 |
| Cycle57 | 2440 | 0 | 100 | 5988.0 | 46.0 | 43.8 | 4.9 | 16.4 | 7.7 | 7.3 | 0.8 | 2.7 |
| Cycle58 | 2440 | 0 | 100 | 6181.4 | 88.2 | 81.6 | 10.7 | 16.2 | 14.3 | 13.2 | 1.7 | 2.6 |
| Cycle59 | 2080 | 0 | 100 | 6786.5 | 138.5 | 130.8 | 12.8 | 27.2 | 20.4 | 19.3 | 1.9 | 4.0 |

CHAPTER THREE

# Identification of novel monocyclic $C_{25}$ and $C_{30}$ hydrocarbons from the diatom *Rhizosolenia setigera*

## 3.1 Introduction

$C_{20}$, $C_{25}$ and $C_{30}$ highly branched isoprenoids (HBIs) are ubiquitous chemicals found in a great diversity of environmental matrices, ranging from recent sediments to ancient oils (reviewed by Rowland and Robson, 1990). In 1994, Volkman *et al.* discovered $C_{25}$ and $C_{30}$ HBIs in laboratory cultures of the diatoms *Haslea ostrearia* and *Rhizosolenia setigera*, respectively, thus confirming that diatoms were the likely sources of these widespread chemicals (Volkman *et al.*, 1994). From bulk cultures of the diatom *Haslea ostrearia*, Belt and co-workers structurally characterized a group of HBIs possessing a $C_{25}$ skeleton with between three and five double bonds (Belt *et al.*, 1996). Later, a single penta-unsaturated $C_{25}$ HBI previously characterized from *Haslea ostrearia* was reported in a culture of *Rhizosolenia setigera* (strain CCMP 1330) isolated from North Atlantic sea-water (Sinninghe Damsté *et al.*, 1999a,b, 2000). Given the widespread occurrence of both *Haslea* (reviewed by Robert, 1983) and *Rhizosolenia* species, it seemed likely that sources of the compounds reported in sediments had been identified. However, differences in mass spectral properties and retention indices were found between HBIs identified in the algae and those found in most sediment and seawater samples, suggesting that the most common and abundant sedimentary isomers may originate from another source; most likely another diatom species or group of species. An investigation into the hydrocarbon distributions of over fifty diatom species led to the identification of several new species capable of biosynthesising $C_{25}$ and $C_{30}$ HBIs. Allard *et al.* (2001) determined the structures of several

new tetra-unsaturated $C_{25}$ HBI alkenes from bulk cultures of the diatom *Haslea crucigera*, a well characterized member of the *Haslea* genus, as well as from cultures of newly characterized members of this group including *Haslea salstonica* and *Haslea pseudostrearia* (Massé *et al.*, 2001). More importantly, from cultures of the diatom *Pleurosigma intermedium*, Belt *et al.* (2000a,b) identified $C_{25}$ HBIs ranging from two to five degrees in their unsaturation whose mass spectral properties and retention indices were in excellent agreement with those commonly reported in sediments. Thus, the widespread occurrence of this diatom (Peragallo, 1890-1891, Hendey, 1964, Simonsen, 1974) along with a subsequent discovery of these HBIs in laboratory cultures of a planktonic member of the genus *Pleurosigma* (Belt *et al.*, 2001c) suggested that this genus was a more likely source of the most common and abundant sedimentary HBIs isomers. The contribution of diatoms to $C_{25}$ HBI production and their occurrence in sedimentary environmental matrices now appears well established.

In their initial report, Volkman *et al.* (1994) identified a group of HBIs possessing a $C_{30}$ skeleton with five or six double bonds in laboratory cultures of *Rhizosolenia setigera*. They found that the hydrocarbon fraction of this diatom contained three $C_{30}$ pentaenes and two $C_{30}$ hexaenes. Recently, Belt and co-workers (2001a), found a similar but not identical distribution in a *Rhizosolenia setigera* strain isolated from the French Atlantic coast (RS 99). In this case, only four $C_{30}$ HBIs (two pentaenes and two hexaenes) were found in the hydrocarbon fraction of laboratory cultures of this diatom. From bulk cultures, they characterized the structures of these four $C_{30}$ HBIs (VI-IX, Figure 3.1, Belt *et al.*, 2001a). At the same time, Rowland *et al.* (2001b) demonstrated that the strain of *R. setigera* originally studied by Volkman and co-workers (CS 389) was able to produce (simultaneously) two $C_{25}$ trienes, three $C_{30}$ pentaenes and three $C_{30}$ hexaenes. The two $C_{25}$ trienes were found to be the same E and Z isomers found in *P. intermedium*, whereas four of the $C_{30}$ HBIs (E and Z

isomers of both $C_{30:5}$ and $C_{30:6}$ HBIs) were found to be identical to those characterized by Belt *et al.* (2001a). During the course of their studies, Rowland *et al.* (2001b) found that the strain RS 99 was also able to produce both $C_{25}$ and $C_{30}$ HBIs, with the $C_{25}$ compounds corresponding to those previously characterized from *P. intermedium*. This indicated that the diatom *R. setigera* could also be considered as a source organism for the most common and abundant sedimentary $C_{25}$ HBIs isomers. In addition to these observations, Rowland *et al.* found that variations of growth temperature were found to affect significantly the HBI distribution in *R. setigera* CS 389, while changes in the HBI distribution of RS 99 were also observed within cultures grown under 'identical' environmental conditions. This suggested that not only were culture conditions responsible for these dramatic variations, but that differences in the physiological status of the algae may also be a contributing factor (*cf.* Chapter 2). Subsequently, during an experiment investigating the effect of the auxosporulation (sexual reproduction) on the distribution of $C_{25}$ and $C_{30}$ HBIs in RS 99, it was shown that $C_{25}$ HBI production is initiated by the onset of auxosporulation. In addition, while the four $C_{30}$ HBIs previously characterized from this diatom were found during its entire life cycle, three previously uncharacterised hydrocarbons (two $C_{30}$ compounds and a $C_{25}$ isomer possessing four degrees of unsaturation) were biosynthesised during the second phase of the life cycle. The mass spectral characteristics and retention indices of the two $C_{30}$ compounds indicated that they contained five and six degrees of unsaturation, and that they were identical to hydrocarbons identified in Dabob Bay (Prahl *et al.*, 1980), Puget Sound (Barrick and Hedges, 1981) and Arabian Sea (Allard, 2002) sediment samples, as well as those found in other strains of *R. setigera* (CS 389; Rowland *et al.*, 2001b and CCMP 1694; Allard, 2002). The mass spectral characteristics and retention index of the new $C_{25}$ hydrocarbon indicated that it was identical to that identified in the North West Atlantic (Farrington *et al.*, 1977), Rhode Island Sound (Boehm and Quinn, 1978), Puget Sound

(Barrick and Hedges, 1981) and Arabian Sea, Cariaco Trench and Peru Up-welling sediment samples (Allard, 2002). In contrast to the $C_{30}$ compounds, this novel $C_{25}$ polyene has not previously been reported in hydrocarbon fractions of any other diatom species.

Given the potential geochemical importance of these three uncharacterised hydrocarbons, it was decided to determine their structures following isolation from bulk cultures of *Rhizosolenia setigera* (CCMP 1694 and RS 99) and subsequent characterisation by GC-MS and NMR spectroscopy.

## 3.2 Experimental

### *3.2.1 Algal cultures*

*Rhizosolenia setigera*, strain RS 99 was isolated from surface waters in Le Croisic, France. An alternative strain, CCMP 1694, isolated from the Gulf of Oman (Arabian sea), was purchased from the Provasoli-Guillard Centre for the Culture of Marine Phytoplankton. RS 99 (2 x 25 L) and CCMP 1694 (300 L) were grown in F/2 enriched sea-water (Guillard, 1975) under controlled conditions (14 °C, 100 μmol photon $m^{-2}$ $s^{-1}$, 14/10 Light/Dark cycle). A second culture of the CCMP 1694 strain was grown using the same general method, except that the growth temperature was 20 °C.

For the three cultures, cells were harvested by centrifugation at the end of the exponential growing phase.

### *3.2.2 Isolation of HBIs*

Following centrifugation, large-scale cultures of *R. setigera* gave concentrated algal pastes which were freeze dried. The resulting pastes were extracted five times by ultra-sonication in

dichloromethane/methanol (50/50 v/v) to yield total organic extracts (TOEs). Solvents were then removed under reduced pressure and the extracts were applied onto an open column containing previously deactivated $SiO_2$ (5% $H_2O$, 30 min) and equilibrated with hexane. Hydrocarbon fractions were eluted with hexane (5 column volumes) and examined by GC-MS. Silver-ion chromatography using a preparative HPLC system (Chromspher 5 Lipid column; hexane/isopropanol, 99:1, 1ml $min^{-1}$) was used to obtain pure compounds in the following amounts: $C_{30}$ (5 DBEs): 10 mg), $C_{30}$ (6 DBEs): 3 mg, $C_{25}$ (4 DBEs): <0.1 mg (DBE – double bond equivalent).

## 3.3 Results

Figure 3.1 shows the structures of hydrocarbons previously identified in the diatom *Rhizosolenia setigera*.

### *3.3.1 Hydrocarbon distribution in Rhizosolenia setigera (strain RS 99) and Rhizosolenia cf. setigera (strain CCMP 1694)*

Analysis of the GC-MS total ion current (TIC) chromatograms of the non-saponifiable lipid fraction from *R. setigera* RS 99 revealed the presence of $C_{25}$ and $C_{30}$ alkenes along with small amounts of *n*-$C_{21:6}$ (I). Figure 3.2 shows a representative partial TIC chromatogram obtained for RS 99. The $C_{25}$ HBI isomers consisted of two trienes (E and Z isomers) previously identified from cultures of *P. intermedium* (II-III; Belt *et al.*, 2000a,b). These two trienes were also accompanied by a small amount of a single $C_{25}$ tetraene. Analysis of the mass spectral characteristics and retention index (RI 2089 $_{HP\text{-}1}$) of this compound suggested that it had not been previously reported in diatoms, though it had been observed in sediments (reviewed by Allard, 2002).

In addition to the $C_{25}$ HBIs, the TIC chromatogram revealed the presence of a suite of four $C_{30}$ HBIs (VI-IX) previously characterised by Belt *et al.* (2001a), together with two additional $C_{30}$ compounds (RI 2548, 2579 $_{HP-1}$) observed previously in strains of *R. setigera* (Volkman *et al.*, 1994, 1998; Rowland *et al.*, 2001b) and sediments (reviewed by Allard, 2002). Although these compounds were structurally uncharacterised, mass spectral data ($M^+$ = 412, 410) indicated that they contained five (RI 2548 $_{HP-1}$) and six (RI 2579 $_{HP-1}$) degrees of unsaturation respectively.

Analysis of GC-MS total ion current (TIC) chromatograms corresponding to non-saponifiable lipid fractions from *R. cf. setigera* CCMP 1694 revealed a similar although not identical hydrocarbon distribution to that found for RS 99 (Figure 3.3). Indeed, *n*-$C_{21:6}$ (I) was detected, together with small amounts of the $C_{25}$ triene (II) and a suite of five $C_{30}$ hydrocarbons. The GC-MS characteristics of three of these compounds corresponded to the three $C_{30}$ HBIs VI, VIII and IX previously observed in the RS 99 strain along with the two additional $C_{30}$ compounds (RI 2548, 2579 $_{HP-1}$). Thus, the non-saponifiable lipid components of both *R. setigera* strains were found to be similar, although a $C_{30}$ hexaene (VII), and the unidentified $C_{25}$ hydrocarbon were not detected in CCMP 1694. In addition, the two novel $C_{30}$ alkenes were the major hydrocarbons present in the non-saponifiable lipid fraction of CCMP 1694, while in RS 99, the four $C_{30}$ HBIs (VI-IX) were the dominant hydrocarbons.

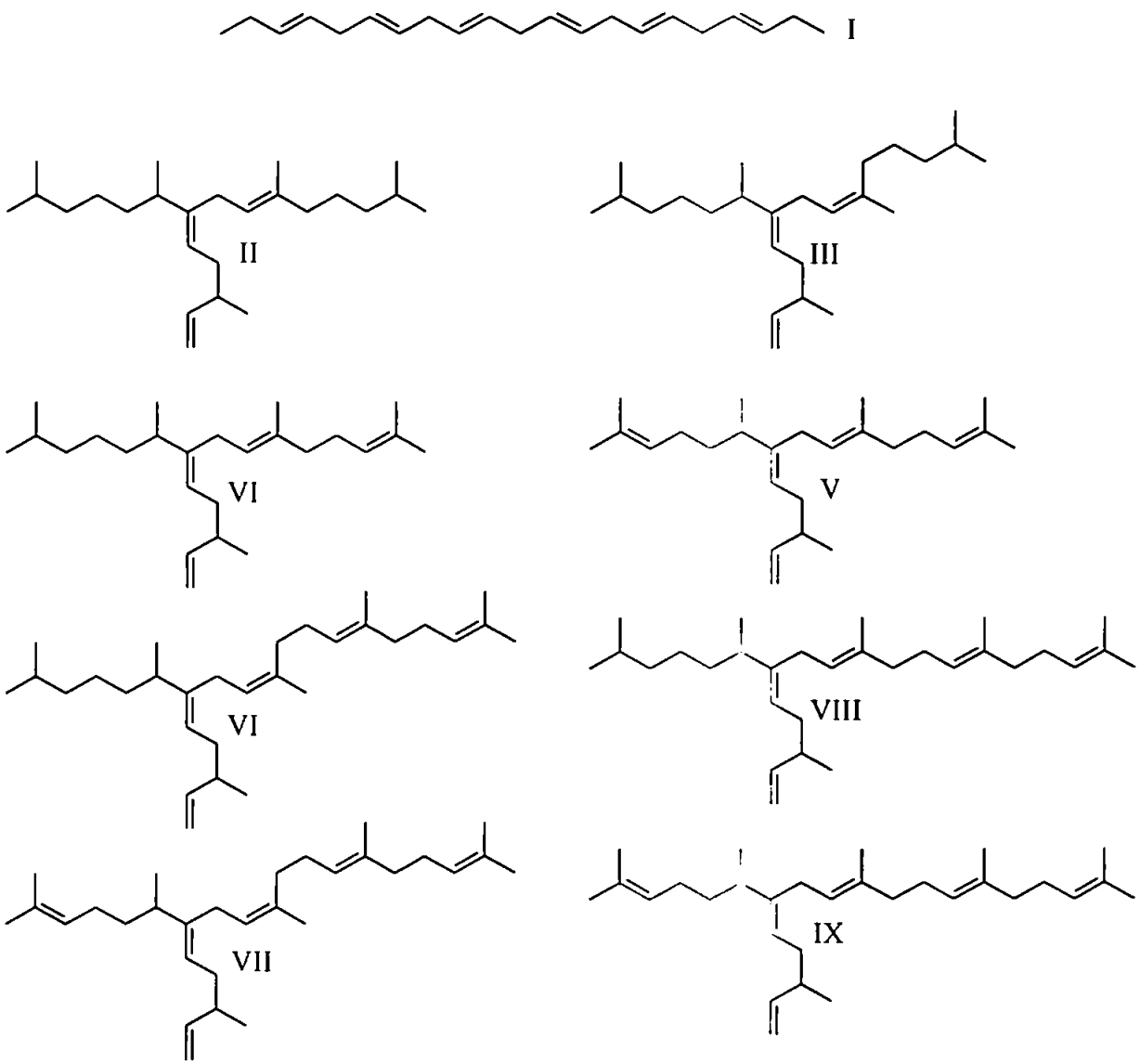


Figure 3.1 Representative structures of hydrocarbons previously identified in cultures of the diatom *Rhizosolenia setigera.*

Surprisingly, the HBI distribution in the second culture of CCMP 1694 (20 °C) remained essentially unchanged from that of the first (14 °C) despite the significant change in the growth temperature.

### *3.3.2 Chromatographic and mass spectral analysis of two novel $C_{30}$ hydrocarbons from CCMP1694*

The mass spectra obtained for the two novel $C_{30}$ alkenes were consistent with compounds containing five ($M^{+\cdot}$ 412; RI $2548_{HP\text{-}1}$) and six ($M^{+}$ 410; RI $2579_{HP\text{-}1}$) degrees of unsaturation or DBEs. As such, the mass spectra obtained for these two compounds were very similar to those obtained for the $C_{30}$ pentaenes and hexanes (VI-IX) characterized by Belt *et al.* (2001a). However, while the mass spectra of the two pentaenes (VI, VIII) exhibited enhanced ions with *m/z* 191 (VIII only), 231, 299 and 357, the mass spectrum of the novel $C_{30}$ compound with 5 DBEs (compound A) exhibited a quite different mass spectrum with ions at *m/z* 231, 259, 274, 299 and 397, and a particularly intense ion at *m/z* 315. The mass spectrum of the related compound with 6 DBEs (compound B) was very similar, with a mass unit difference of 2 for the majority of the ions (Figure 3.4).

Hydrogenation ($PtO_2.2H_2O$/hexane; 10h) of A and B produced a single and common $C_{30}$ hydrocarbon with 2 degrees of unsaturation (Figure 3.5), together with associated with small amounts of a compound with one degree of unsaturation. Hydrogenation of the $C_{30}$ HBIs resulted in the formation of a single alkane ($C_{30:0}$) exhibiting a characteristic fragment ion at *m/z* 308 (Figure 3.5). At this point, it was clear that the carbon skeleton of A and B must be different from the $C_{30}$ HBI pentanes and hexaenes characterised previously. However, since both A and B gave the same compound after hydrogenation, this indicated that they possessed the same parent skeleton.

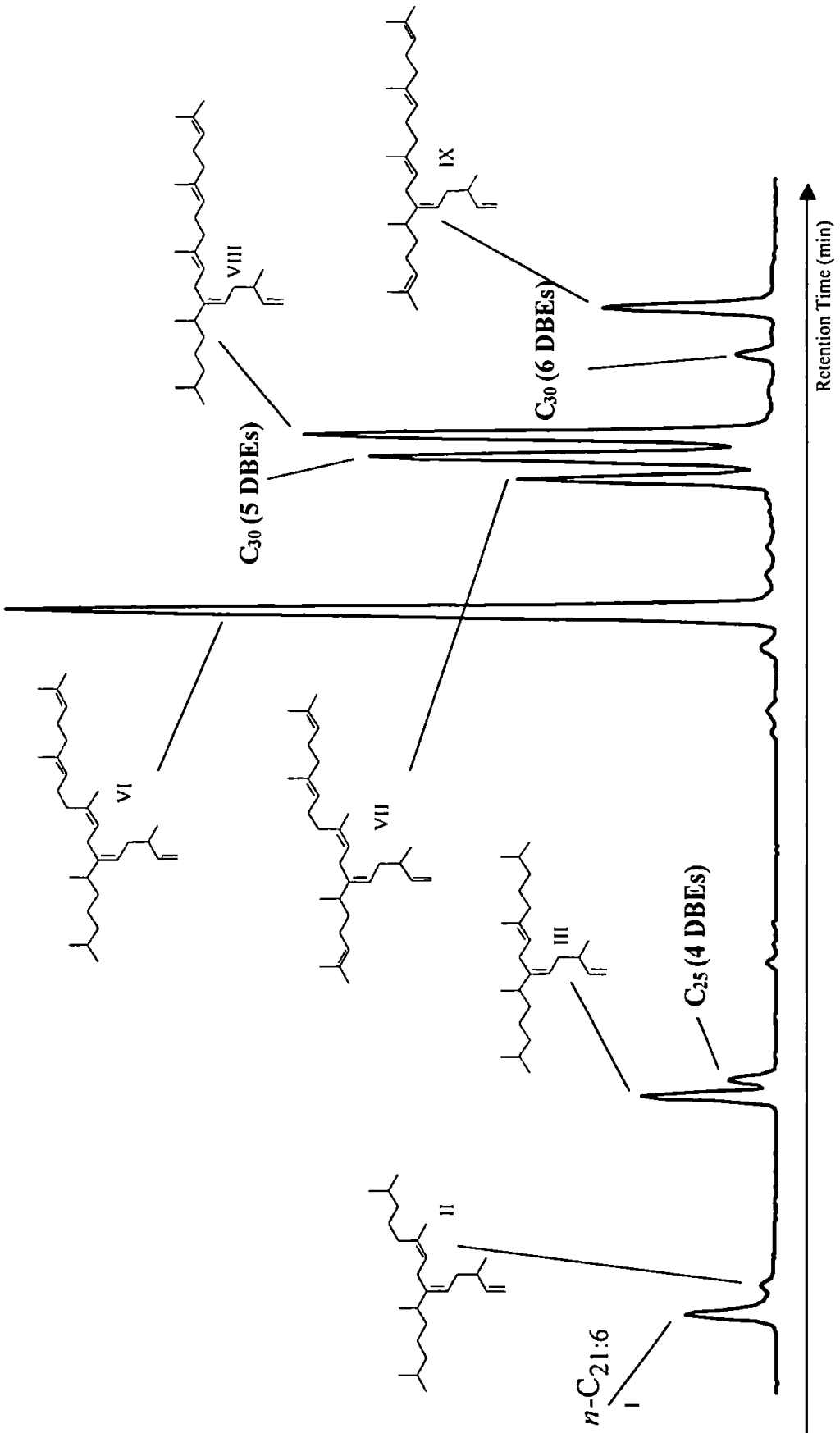


Figure 3.2 Partial TIC chromatograms showing the hydrocarbon distribution in *Rhizosolenia setigera* RS 99.

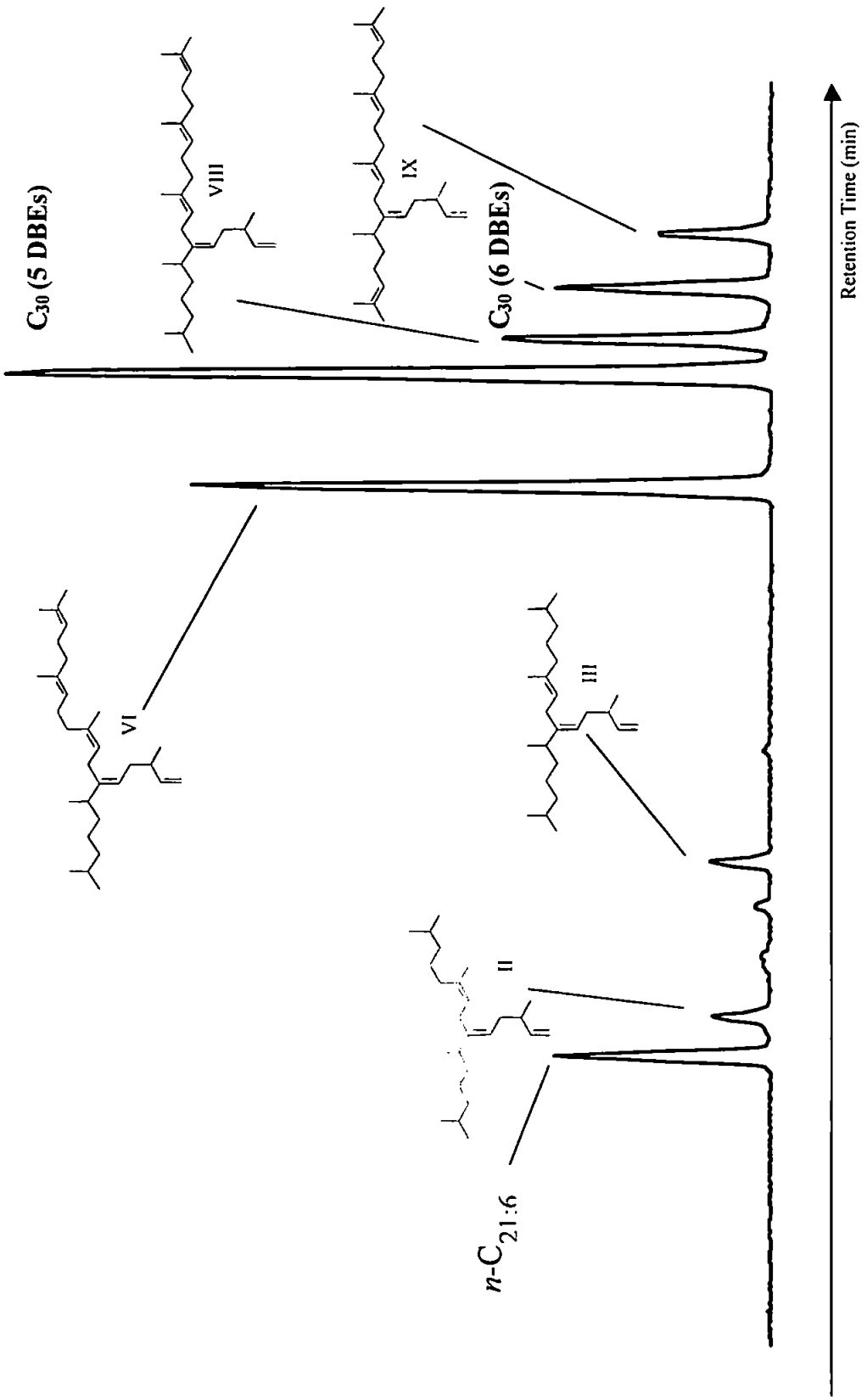


Figure 3.3 Partial TIC chromatograms showing the hydrocarbon distribution in *Rhizosolenia setigera* CCMP 1694.

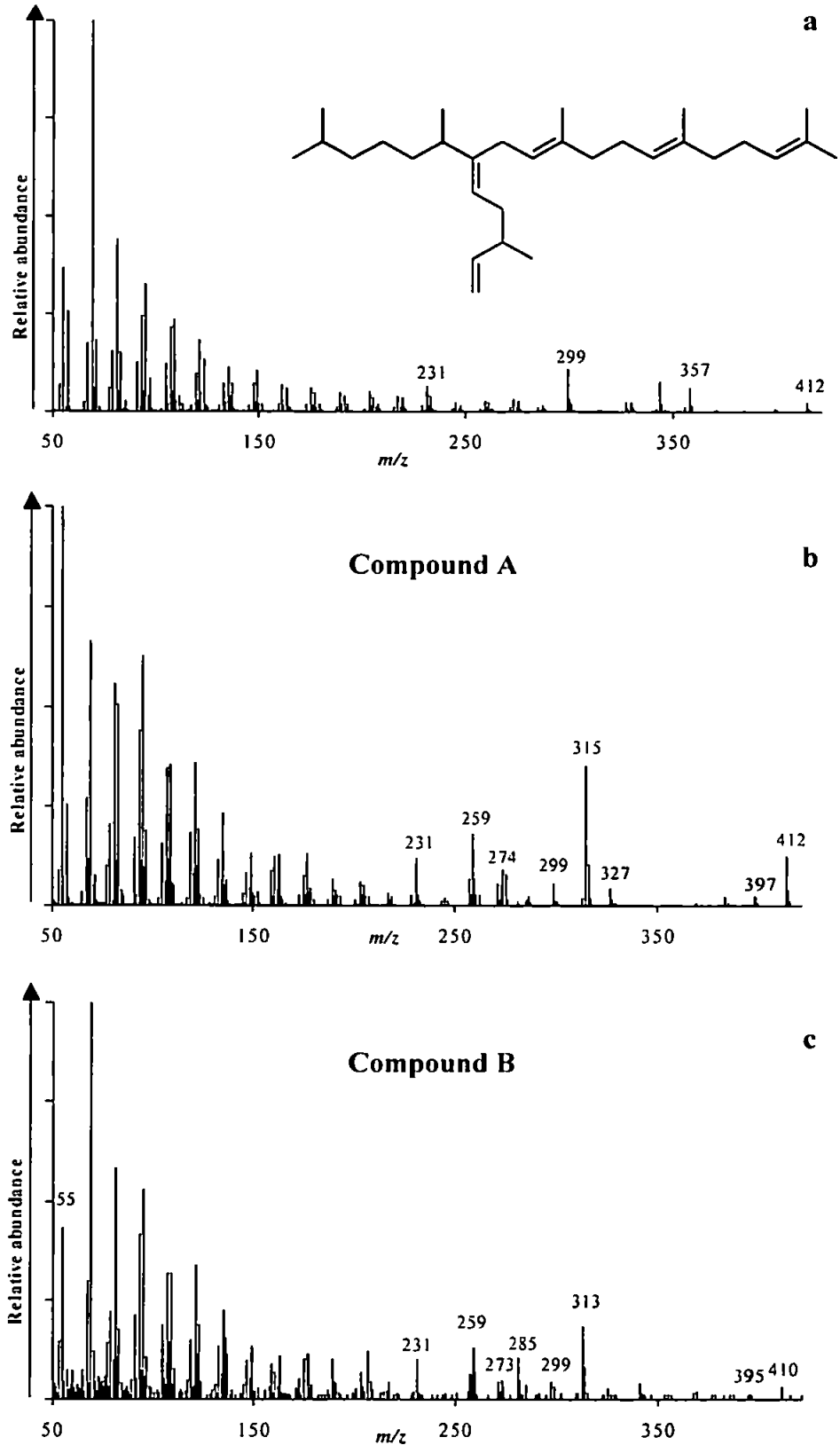


Figure 3.4 Mass spectra of (a) authenticated $C_{30:5}$ (VI), (b) $C_{30}$ (5 DBEs), compound A and (c) $C_{30}$ (6 DBEs), compound B isolated from cultures of the diatom *Rhizosolenia setigera*.

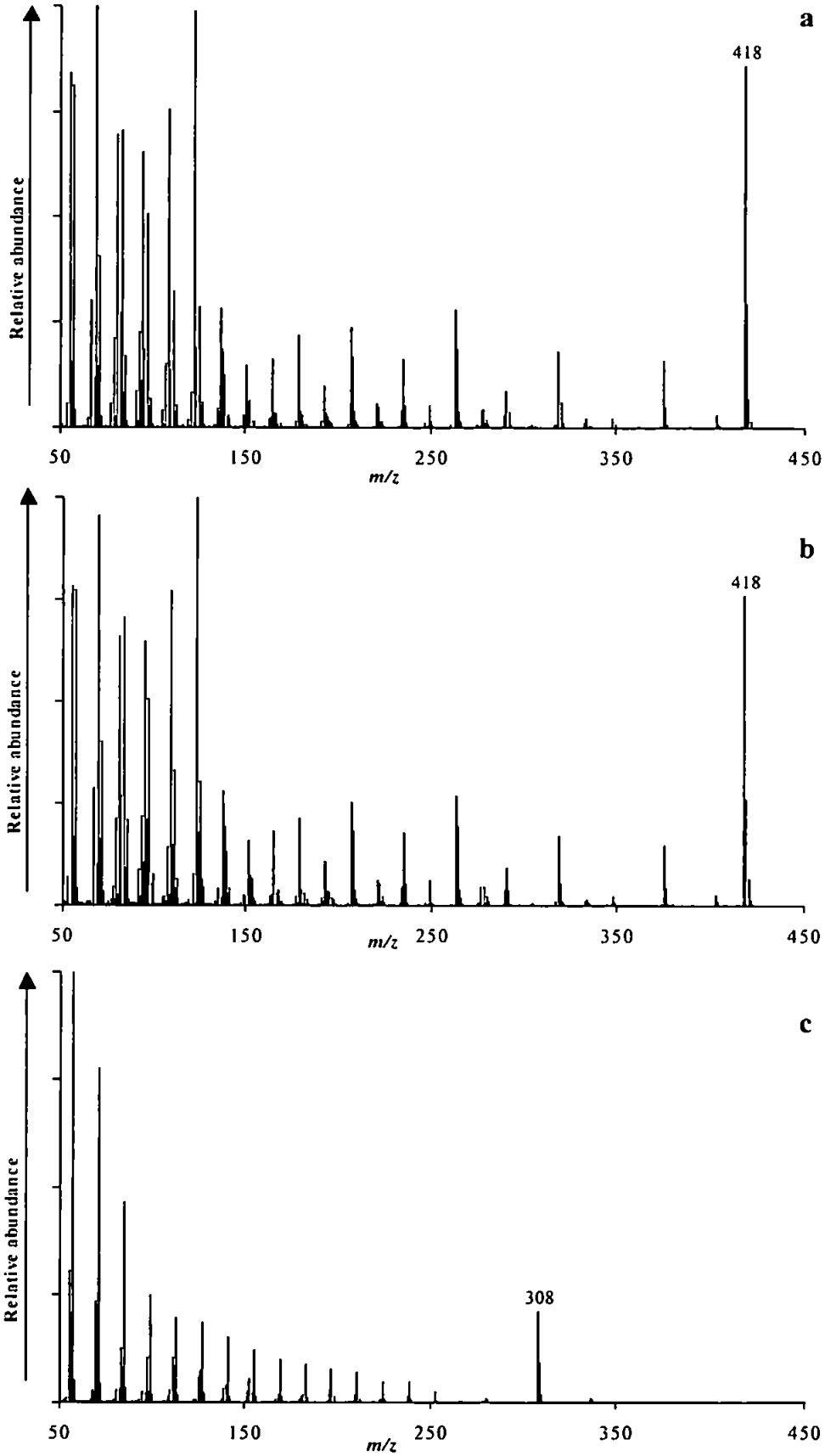


Figure 3.5 Mass spectra of (a) $C_{30}$ (6 DBEs), (b) $C_{30}$ (5 DBEs) and (c) authentic $C_{30:5}$ (VI) after extensive hydrogenation.

Extraction of the ion intensities for *m/z* 418 and 420 from the total ion current chromatogram of the hydrogenation products revealed the presence of an additional $C_{30}$ compound with 1 DBE which co-eluted with the major hydrogenation product. Comparison of the mass spectra of the two compounds with 1 DBE revealed that they were extremely similar. Therefore, it seemed likely that hydrogenation of both A and B initially gave a $C_{30}$ hydrocarbon possessing at least one double bond in a position fairly resistant to hydrogenation. Following exhaustive hydrogenation, this compound would yield a pair of isomers (each with 1 DBE) possessing e.g. axial - equatorial isomerism within a ring system (Allard, 2002).

### *3.3.3 Chromatographic and mass spectral analysis of a novel $C_{25}$ hydrocarbon from RS 99*

Examination of the mass spectrum obtained for the novel $C_{25}$ hydrocarbon (compound C) showed that it contained 4 DBEs ($M^+$ 344; RI $2089_{HP\text{-}1}$). The mass spectrum of compound C was also very similar to those obtained for the $C_{25}$ HBI tetraenes characterised by Belt *et al.* (2000a, b) and to the two novel $C_{30}$ compounds A and B (Figure 3.6). Thus, the mass spectrum of this compound exhibited enhanced ions with *m/z* 231 and 259. Additionally, the mass spectrum of compound C showed relatively intense ions at *m/z* 247, 329 and 344 which are 68/66 mass units lower than the ions *m/z* 315/313, 397/395 and 412/410 exhibited by the mass spectra of A and B (n.b. *m/z* 68 corresponds to a $C_5$ unit containing one double bond and *m/z* 66 corresponds to this $C_5$ unit plus an additional double bond elsewhere in the molecule). This suggested that C is a structural homologue of A and B and that all of these compounds have a mono-cyclic core.

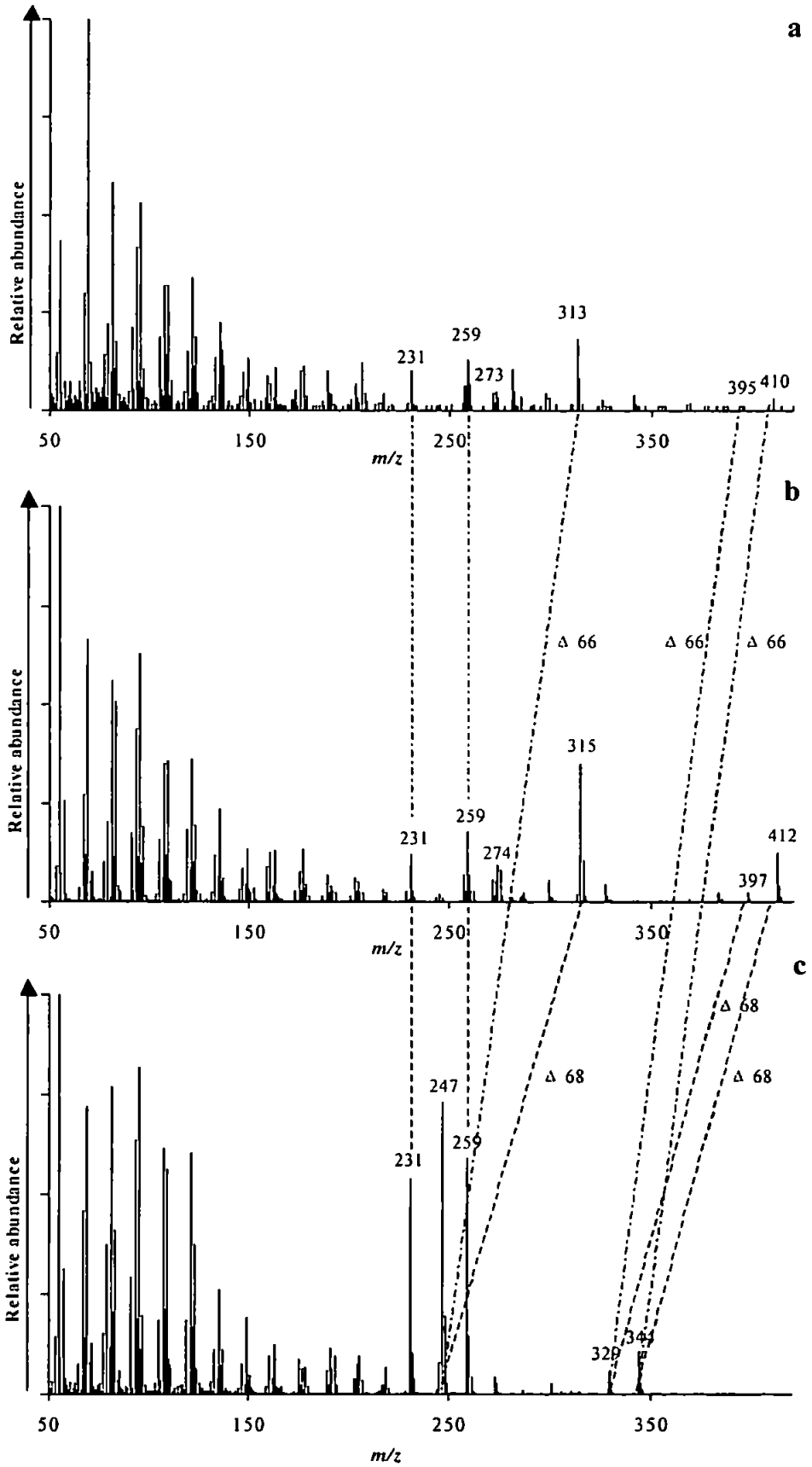


Figure 3.6 Mass spectra of (a) $C_{30}$ (6 DBEs), (b) $C_{30}$ (5 DBEs) and (c) $C_{25}$ (4 DBEs) compounds isolated from cultures of the diatom *Rhizosolenia setigera*.

### *3.3.4 Characterisation of $C_{30:4:1}$ (X) by $^{1}H$ and $^{13}C$ NMR spectroscopy*

Examination of the $^{1}H$ (Table 3.1) and $^{13}C$ (Table 3.2) NMR spectra of compound A (10 mg) isolated from CCMP 1694 revealed the presence of a vinyl moiety (C15 - C16), a structural feature common to virtually all known poly-unsaturated acyclic $C_{25}$ and $C_{30}$ HBIs, an acyclic tri-substituted double bond (C6-C7), a further tri-substituted double bond contained within a ring (C22-C23), a 1,1-disubstituted double bond (C27-C29), a single isopropyl moiety (C1-C2-C17), a quaternary alkyl carbon (C10) and a number of different methyl groups. Individual carbon multiplicities were established using DEPT spectroscopy, while the connections of the various structural sub-units was achieved *via* a combination of COSY, HMQC ($^{1}J_{C-H}$) and HMBC ($^{2,3}J_{C-H}$) 2-D correlations. Using these combined NMR methods, the structure of A was determined as X (Figure 3.7).

### *3.3.5 Characterisation of $C_{30:5:1}$ (XI) by $^{1}H$ and $^{13}C$ NMR spectroscopy*

Examination of the $^{1}H$ (Table 3.3) and $^{13}C$ NMR (Table 3.4) spectra for compound B (6 DBEs) revealed many of the same spectroscopic features encountered for the closely related compound A (X). The only significant difference corresponded to the absence of any resonances associated with an isopropyl moiety, together with new resonances attributable to a terminal tri-substituted double bond. From these differences, the structure of compound B was deduced to be XI (Figure 3.7). $^{1}H$ and $^{13}C$ chemical shift assignments could be made by direct comparison with those made previously for X.

Table 3.1 $^{1}H$ NMR data for the $C_{30:4:1}$ X.

| Chemical shift (ppm ) | Assignment X | Multiplicity (Coupling constant, Integration ) |
|---|---|---|
| 5.68 | 15 | ddd (J = 17, 10, 7 Hz, 1H) |
| 5.08 | 7 | t (J = 7 Hz, 1H) |
| 4.9 | 16, 22 | m (3H) |
| 4.6 | 28 | m (2H) |
| 2.4 | 26 | m (2H) |
| 2.26 | 21 | t (J = 10 Hz, 1H) |
| 1.9 - 2.1 | 5, 8, 14, 24 | m (7H) |
| 1.82, 1.42 | 25 | m (2H) |
| 1.65 | 29 | s (3H) |
| 1.56, 1.57 | 18, 30 | 2 x s (6H) |
| 1.1 - 1.5 | 2, 3, 4, 9, 11, 12, 13 | m (13H) |
| 0.96 | 20 | d (J = 7 Hz, 3H) |
| 0.85 | 1, 17 | d (J = 7 Hz, 6H) |
| 0.79 | 19 | s (3H) |

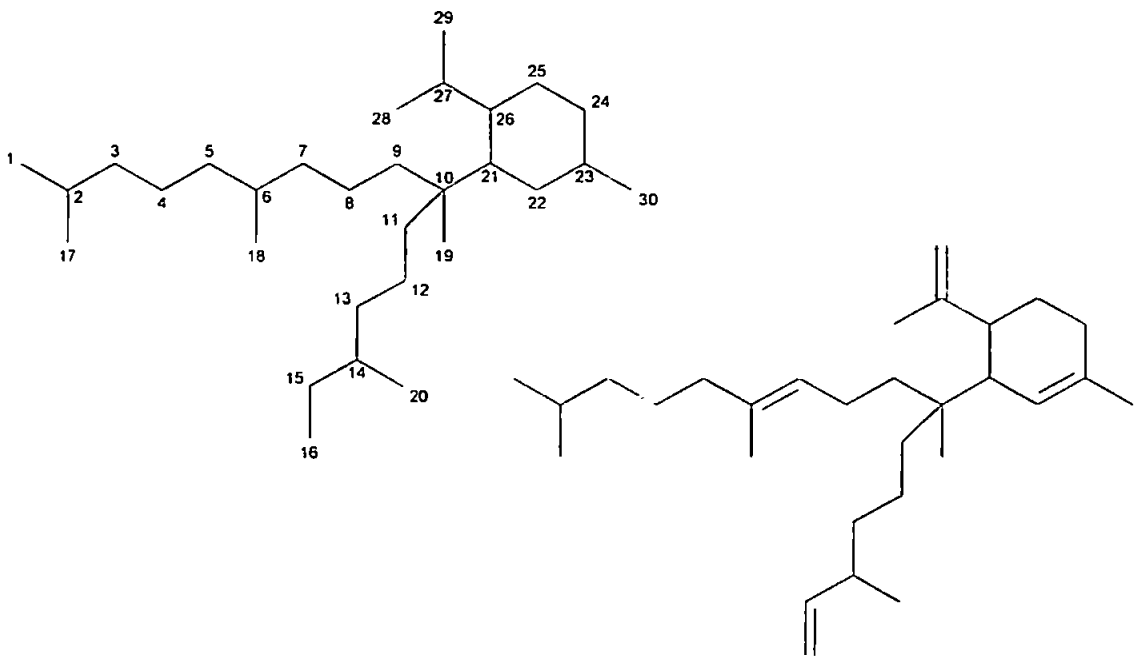

Table 3.2 $^{13}C$ NMR data for the $C_{30:4:1}$ X.

| Chemical shift (ppm) | Multiplicity (DEPT) | Assignment |
|---|---|---|
| 148.13 | C | 27 |
| 145.06 | CH | 15 |
| 136.01 | C | 23 |
| 135.19 | C | 6 |
| 125.99 | CH | 22 |
| 124.13 | CH | 7 |
| 112.27 | $CH_2$ | 16 |
| 109.34 | $CH_2$ | 28 |
| 52.22 | CH | 21 |
| 51.90 | CH | 26 |
| 46.60 | C | 10 |
| 42.56 | $CH_2$ | 11 |
| 40.33 | $CH_2$ | 24 |
| 40.06 | $CH_2$ | 5 |
| 38.80 | $CH_2$ | 3 |
| 38.13 | $CH_2$ | 13 |
| 37.87 | $CH_2$, CH | 9, 14 |
| 28.75 | $CH_2$ | 25 |
| 27.99 | CH | 2 |
| 26.70 | $CH_2$ | 8 |
| 25.88 | $CH_2$ | 4 |
| 22.75 | $CH_3$ | 1, 17 |
| 22.62 | $CH_2$ | 12 |
| 21.06 | $CH_3$ | 19 |
| 20.25 | $CH_3$ | 20 |
| 19.98 | $CH_3$ | 29 |
| 16.66 | $CH_3$ | 30 |
| 16.04 | $CH_3$ | 18 |

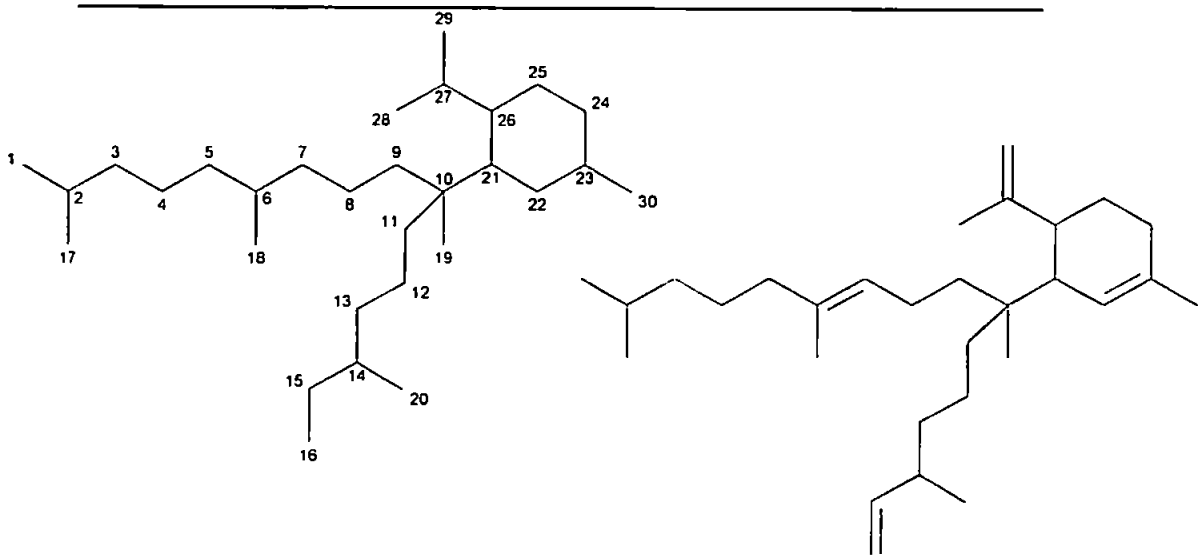

Table 3.3 $^{1}H$ NMR data for the $C_{30:5:1}$ XI.

| Chemical shift (ppm) | Assignment | Multiplicity (Coupling constant, Integration) |
|---|---|---|
| 5.68 | 15 | ddd (J = 17, 10, 7 Hz, 1H) |
| 5.08 | 3, 7 | m (2H) |
| 4.9 | 16, 22 | m (3H) |
| 4.6 | 28 | m (2H) |
| 2.4 | 26 | m (1H) |
| 2.26 | 21 | t (J = 10 Hz, 1H) |
| 1.9 - 2.1 | 4, 5, 8, 14, 24 | m (9H) |
| 1.82, 1.42 | 25 | m (2H) |
| 1.65-1.65 | 1, 17, 18, 29, 30 | 5 x s (15H) |
| 1.1 - 1.5 | 9, 11, 12, 13 | m (8H) |
| 0.96 | 20 | d (J = 7 Hz, 3H) |
| 0.79 | 19 | s (3H) |

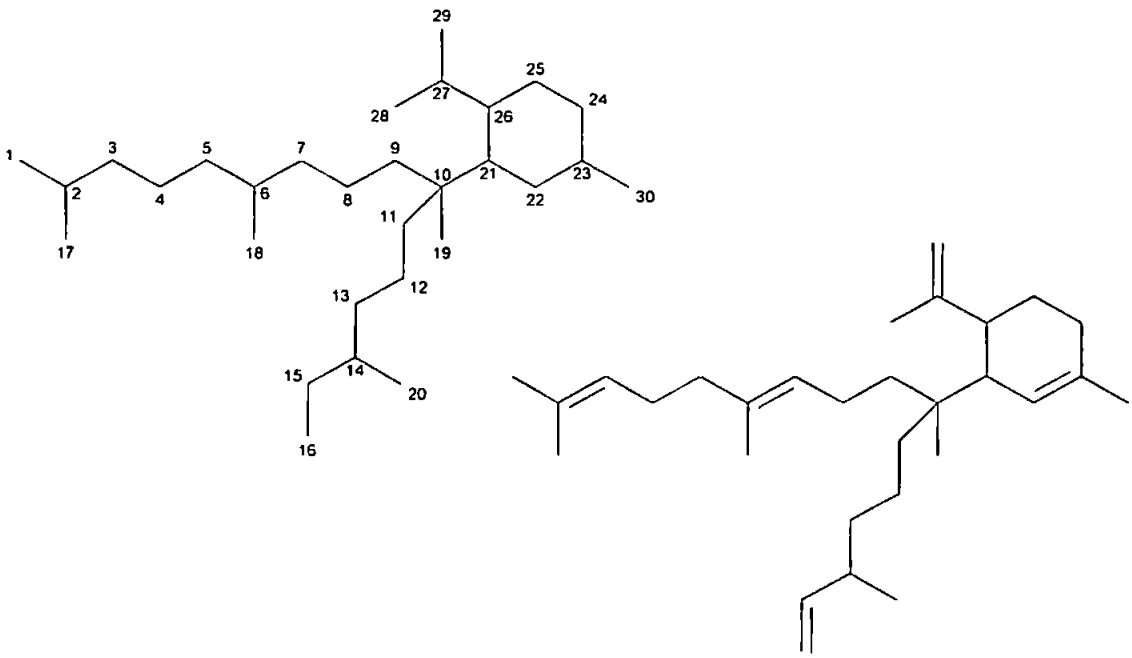

Table 3.4 $^{13}C$ NMR data for the $C_{30:5:1}$ XI.

| Chemical shift (ppm) | Multiplicity (DEPT) | Assignment |
|---|---|---|
| 148.1 | C | 27 |
| 145.1 | CH | 15 |
| 136 | C | 23 |
| 134.8 | C | 6 |
| 131.1 | C | 2 |
| 126 | CH | 22 |
| 124.4, 124.5 | CH | 3, 7 |
| 112.2 | $CH_2$ | 16 |
| 109.3 | $CH_2$ | 28 |
| 52.2 | CH | 21 |
| 51.9 | CH | 26 |
| 46.6 | C | 10 |
| 42.6 | $CH_2$ | 11 |
| 40.3 | $CH_2$ | 24 |
| 39.8 | $CH_2$ | 5 |
| 38.2 | $CH_2$ | 13 |
| 37.8 | $CH_2$, CH | 9, 14 |
| 28.8 | $CH_2$ | 25 |
| 26.9 | $CH_2$ | 4 |
| 26.8 | $CH_2$ | 8 |
| 25.8 | $CH_3$ | 1 |
| 22.6 | $CH_2$ | 12 |
| 21.1 | $CH_3$ | 19 |
| 20.2 | $CH_3$ | 20 |
| 20 | $CH_3$ | 29 |
| 17.8 | $CH_3$ | 17 |
| 16.7 | $CH_3$ | 30 |
| 16.1 | $CH_3$ | 18 |

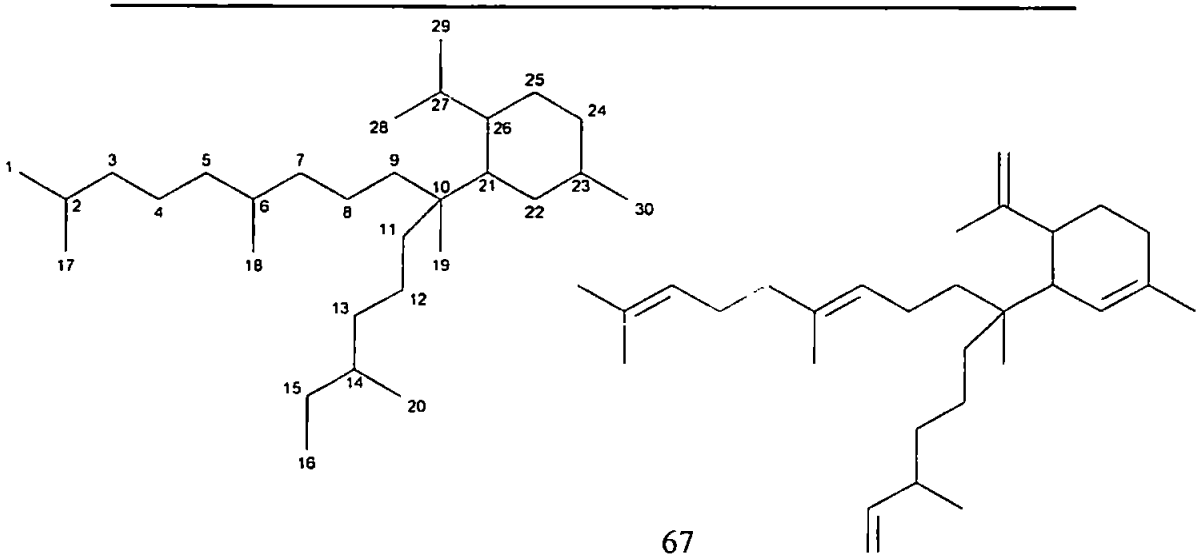

### *3.3.6 Hydrogenation of $C_{30:4:1}$ (X) and analysis by $^{1}H$ and $^{13}C$ NMR spectroscopy*

Partial hydrogenation of X (2.0 mg; $PtO_2.2H_2O$/hexane) yielded a $C_{30}$ hydrocarbon possessing 2 DBEs (MS) in *ca* 95% purity (GC). $^{1}H$ and $^{13}C$ NMR spectral analysis of this compound demonstrated that it possessed a single double bond contained within a six-membered ring (Tables 3.5, 3.6) with all of the other double bonds in X absent. The structure of this compound (XII) is consistent with the partial hydrogenation behaviour of X and XI described previously, since it would be expected to be formed from both of these two polyenes.

Table 3.5 $^{1}H$ NMR data for the $C_{30:1:1}$ XII.

| Chemical shift (ppm) | Assignment | Multiplicity (coupling constant, integration) |
|---|---|---|
| 4.92 | 22 | (J=10, 1H) |
| 2 | 21, 24 | M (3H) |

Table 3.6 $^{13}C$ NMR data for the $C_{30:1:1}$ XII.

| Chemical shift (ppm) | Multiplicity (DEPT) | Assignment |
|---|---|---|
| 135.3 | C | 23 |
| 127.5 | CH | 22 |
| 51.5 | CH | 21 |
| 50.3 | CH | 26 |
| 46.7 | C | 10 |
| 42.8 | $CH_2$ | 9 |
| 40.5 | $CH_2$ | 24 |
| 16.5 | $CH_3$ | 30 |
| 11.5 | $CH_3$ | 16 |

### *3.3.7 Characterisation of $C_{25:3:1}$(XII)*

Insufficient quantities of the related monocyclic $C_{25}$ compound (C) could be obtained for analysis by $^{1}H$ or $^{13}C$ NMR spectroscopy. However, due to the mass spectral similarities between this compound and those of X and XI, the structure of XIII is proposed (Figure 3.7).

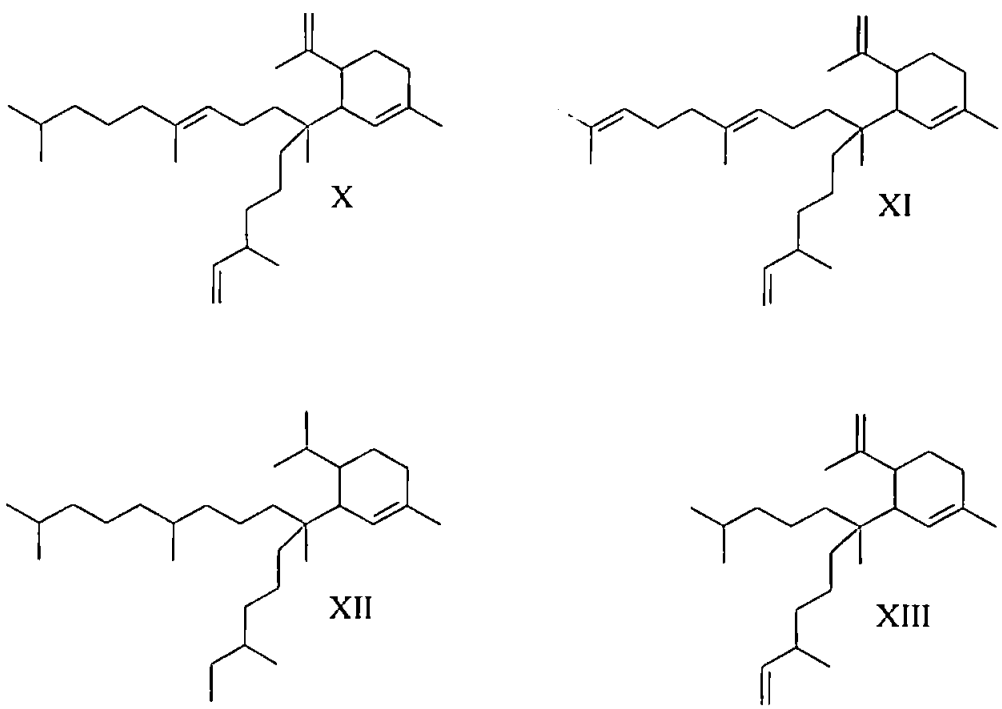


Figure 3.7 Structures of novel monocyclic $C_{30}$ hydrocarbons (X-XII) characterised in this study and proposed structure of a $C_{25}$ analogue (XIII) identified in cultures of the diatom *Rhizosolenia setigera.*

## 3.4 Discussion

### *3.4.1 $C_{25}$ and $C_{30}$ cyclic isoprenoid alkenes: structural relationships with previously characterised HBIs in diatoms*

The results described herein have identified the sources (*Rhizosolenia spp.*) of $C_{25}$ and $C_{30}$ monocyclic isoprenoid alkenes previously reported in sediments and water column particles. The structural characterisation of these novel compounds was achieved using NMR spectroscopy and mass spectrometry. While these novel hydrocarbons possess a vinyl moiety consistent with the majority of $C_{25}$ and $C_{30}$ HBIs identified previously in *Haslea spp.* (Belt *et al.*, 1996; Johns *et al.*, 1999; Wraige *et al.*, 1997, 1999; Allard *et al.* , 2001), *P. intermedium* (Belt *et al.*, 2000a, b) and *R. setigera* (Belt *et al.*, 2001a), they also exhibit such major structural differences, that their biosynthetic relationship with HBIs could be questioned.

Indeed, a main structural feature exhibited by virtually all of the previously characterised acyclic HBIs is a branch point at C7, which is saturated in compounds from *Haslea* species and unsaturated in those synthesised by *Pleurosigma* and *Rhizosolenia* species. As such, $C_{25}$ HBIs are probably derived from the coupling at C6 of a farnesyl-pyrophosphate unit ($C_{15}$) with a geranyl-pyrophosphate unit ($C_{10}$), while $C_{30}$ HBIs would derive from the analogous coupling of two farnesyl-pyrophosphate units (Figure 3.8).

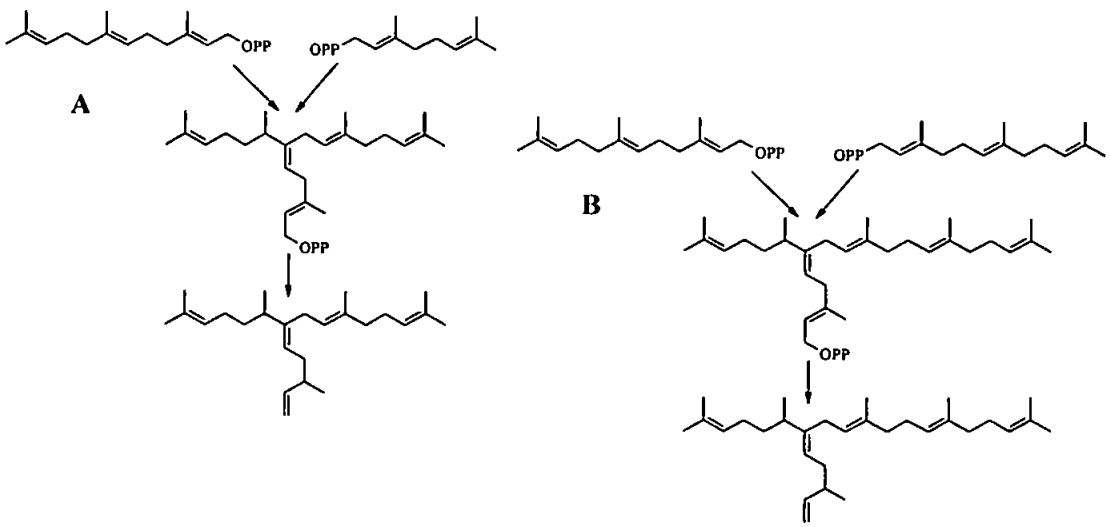


Figure 3.8 Simplified representation corresponding to a hypothetical biosynthetic pathway of $C_{25}$ (A) and $C_{30}$ (B) isoprenoid alkenes.

In contrast, the structures of these novel monocyclic alkenes, suggest that they derive from a coupling at C10 of a geranylgeranyl-pyrophosphate ($C_{20}$) and a geranyl-pyrophosphate ($C_{10}$) followed by a cyclisation (Figure 3.9).

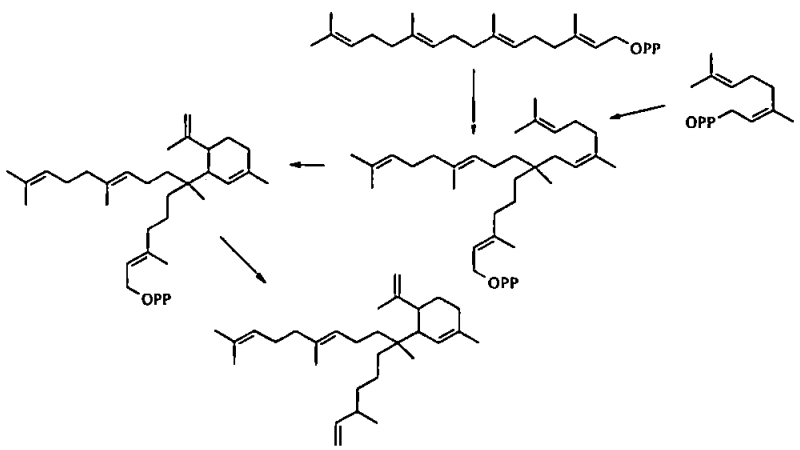


Figure 3.9 Simplified representation of a hypothetical biosynthetic pathway of monocyclic $C_{30}$ isoprenoid alkenes.

*3.4.2 Taxonomical implications*

When Volkman and co-workers (1994) identified $C_{30}$ HBIs in laboratory cultures of the diatom *R. setigera* (strain CS-62), they found that the hydrocarbon fraction of this diatom contained three $C_{30}$ pentaenes and two $C_{30}$ hexaenes. Two of the reported compounds exhibited similar mass spectra and retention indices to $C_{30:4:1}$ and $C_{30:5:1}$ characterised in this study. However, Volkman *et al.* (1994) concluded that all of the hydrocarbons possessed the same acyclic HBI skeleton, even though they reported the presence of two 'monounsaturated alkenes' in the hydrogenation products derived from the mixture of $C_{30}$ hydrocarbons. They reasonably attributed the presence of these monoenes to a residual double bond highly resistant to hydrogenation. However, based on their reported retention indices and mass spectral characteristics, it is clear that these two compounds correspond to the monocyclic $C_{30}$ alkenes characterised in the present study following isolation from two further *R. setigera* strains (CCMP 1694 and RS 99). In addition, Rowland and co-workers (2001b) reported the presence of X and XI in the non-saponifiable lipid fraction obtained from a fourth *R. setigera* strain (CS-389) isolated from the Huon estuary (Australia). It is also apparent that rather like $C_{25}$ HBIs in *R. setigera*, these $C_{30}$ alkenes are not always synthesised by this diatom (*cf.* Chapter 2), and this may explain why they were not detected in earlier investigations of the RS 99 strain (Belt *et al.*, 2001a). To date, CCMP 1330 and CCMP 1820 are the only *R. setigera* strains in which the presence of monocyclic alkenes in the non-saponifiable lipid fraction have not been reported. The possibility exists that these intra-species variations may originate from where they were isolated, and thus relate to evolution of the individual strains. However, since similar hydrocarbon contents were observed for strains isolated from the North-Atlantic, Indian and Pacific Oceans, it is also possible that misidentification of individual strains has taken place, particularly as the taxonomy of the *Rhizosolenia* genus is uncertain (Sundström, 1986).

### *3.4.3 Occurrence of monocyclic $C_{30}$ alkenes in sediments and water-column particles*

The discovery of $C_{25}$ and $C_{30}$ HBI alkenes in cultures of the diatoms *H. ostrearia*, *R. setigera* (Volkman *et al.*, 1994) and *Pleurosigma spp.* (Belt *et al.* 2000a, 2001c) has allowed the structural characterisation of several HBIs previously reported in sediments and other environmental matrices to be determined (Allard, 2002). Prior to these studies, the low concentrations of HBIs in environmental samples meant that their structural characterisation was restricted to the identification of their carbon skeleton and the assignment of their unsaturation indices using mass spectrometry. Within the context of the current study, Prahl *et al.* (1980) reported four $C_{30}$ alkenes (RI 2509, 2563, 2558 and $2590_{SP2100}$) in sediments and sediment trap particles from Dabob Bay, USA. Based on these retention indices and mass spectral characteristics, Allard (2002) identified the compound with RI $2509_{SP2100}$ as the $C_{30}$ pentaene VI and the compound with RI $2558_{SP2100}$ as being the uncharacterised $C_{30}$ 'pentaene' he observed in the hydrocarbon fraction from *R. setigera* CCMP 1694. This second compound has been characterised herein as being the monocyclic $C_{30}$ tetraene (X). Barrick and Hedges (1981) also reported a suite of four $C_{30}$ alkenes in sediments from Puget Sound (USA) exhibiting identical retention indices (RI 2509, 2563, 2558 and $2590_{SP2100}$). Once again, by comparison of their retention indices and mass spectral characteristics with those of authenticated compounds, Allard (2002) identified the compounds with RI 2509 and 2563 to be two $C_{30}$ HBI pentaenes (VI and VII respectively). He also showed that the compounds with retention indices RI 2558 and 2590 corresponded to two $C_{30}$ polyenes observed in CCMP 1694. These have been characterised in the current study and identified as a monocyclic $C_{30}$ tetraene (X) and a monocyclic $C_{30}$ pentaene (XI). Both $C_{30:4:1}$ and $C_{30:5:1}$ can also be assigned to two $C_{30}$ alkenes reported by Osterroht *et al.* (1983). In addition, Allard (2002) found $C_{30:4:1}$ to be the major isomer in samples from sediments and sediment trap particles obtained from the Arabian Sea which had previously been analysed by

Wakeham *et al.* (2002). From these combined observations, the apparent widespread occurrence of these monocyclic $C_{30}$ compounds is now well established. Given its abundance, wide geographical distribution, it is likely that *R. setigera* contributes significantly towards the occurrence of these novel monocyclic alkenes as well as acyclic $C_{25}$ and $C_{30}$ HBIs in sediments and water column particles.

### *3.4.4 Occurrence of a monocyclic $C_{25}$ alkene in sediments, water-column particles and biota*

The mass spectral characteristics and retention index of the $C_{25}$ compound partially characterised herein indicates that it is identical to a $C_{25}$ hydrocarbon identified in the North West Atlantic (Farrington *et al.*, 1977), Rhode Island Sound (Boehm and Quinn, 1978), Puget Sound (Barrick and Hedges, 1981) and Arabian Sea, Cariaco Trench and Peru Up-welling sediment and sediment trap particles (Allard, 2002). Thus, similarly to the monocyclic $C_{30}$ alkenes X and XI, this novel $C_{25}$ hydrocarbon appears to be of widespread occurrence and that its likely source is *R. setigera*.

## 3.5 Conclusion

The structures of two monocyclic $C_{30}$ alkenes (X, XI) have been rigorously characterised by NMR spectroscopy and mass spectrometry, and the source of a structurally related $C_{25}$ homologue has been reported for the first time. The diatoms *R. setigera* and *R. cf. setigera* have been identified as sources for these alkenes. The ecological importance and widespread distribution of *Rhizosolenia* species, probably accounts for the presence of these alkenes in sediments, as well as in water column particles.

CHAPTER FOUR

# Isoprenoid biosynthesis in three diatom species

## 4.1 Introduction

Isoprenoids are numerous (more than 20 000 identified compounds) and ubiquitous chemicals exhibiting a wide diversity of essential biological functions (Ourisson and Nakatani, 1994; Sacchettini and Poulter, 1997). For example, phytol (one of the most abundant organic molecules in nature) serves to anchor chlorophyll, a light-harvesting pigment involved in photosynthesis, whereas carotenoids such as β-carotene are involved in light-protecting activities in plants (Eisenreich *et al.*, 1998). Some other terpenoids (e.g. sterols) play an important role in reinforcing the membranes of all living organisms (Ourisson and Nakatani, 1994; Pozzi *et al.*, 1996). Taxol, derived from the Yew tree (Holmes *et al.*, 1995), exhibits interesting cytostatic activities, and is now widely used in the chemotherapy of many malignant tumours. The great diversity in structure, function and potential pharmaceutical activity of terpenoids has led to a large number of studies on their biosyntheses.

It is now well established that all the isoprenoids are biosynthesised from two $C_5$ precursors, isopentenyl diphosphate (IPP, **7** )and dimethylallyl diphosphate (DMAPP, **8**). For many years, the acetate/mevalonate pathway (Qureshi and Porter, 1981) was considered as the only biosynthetic route leading to IPP and DMAPP (Figure 4.1, A). Briefly, acetoacetyl CoA (**3**) obtained from a condensation of two acetyl CoA units (**2**) yields hydroxy-3-methylglutaryl CoA (**4**) by addition of a third acetyl CoA. Hydroxy-3-methylglutaryl CoA is then reduced to mevalonic acid (**5**), phosphorylated to give 5-pyrophospho-mevalonate (**6**) and finally IPP

(7) after elimination of phosphate and $CO_2$. IPP can be reversibly converted to DMAPP (**8**) by IPP isomerase (McCaskill and Croteau, 1999; Figure 4.2).

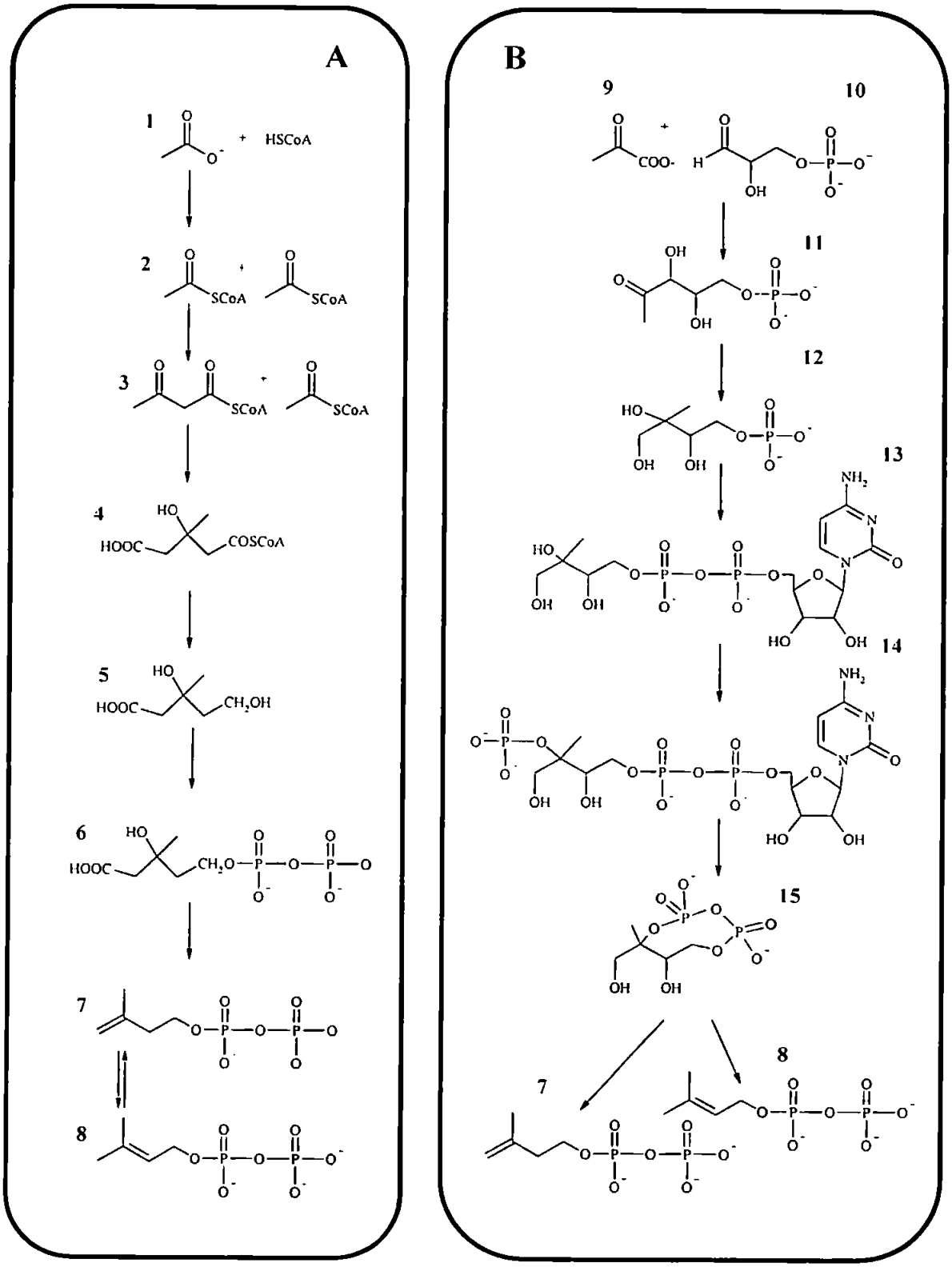


Figure 4.1 Biosynthetic pathways to isopentenyl diphosphate and dimethylallyl diphosphate. A. Acetate-mevalonate pathway. B. Mevalonate independent pathway.

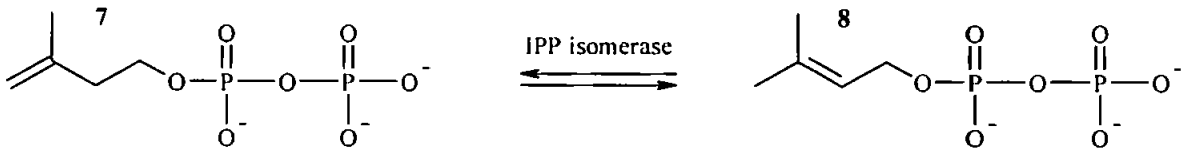


Figure 4.2 Reversible conversion of isopentenyl pyrophosphate to dimethylallyl pyrophosphate by an isomerase.

During several decades, it was universally accepted that IPP and DMAPP were exclusively synthesised from mevalonate *via* this route. However, while several authors (reviewed by Rohmer, 1999) reported efficient incorporation of isotopically labelled mevalonate or acetate into sterols, triterpenoids and sesquiterpenoids (Figure 4.3 A), these precursors were not or very poorly incorporated into chloroplastidic isoprenoids such as carotenoids, diterpenes or monoterpenes. They explained these observations by proposing a lack of permeability of the chloroplast membrane toward these precursors. Flesch and Rohmer (1988) reported labelling patterns inconsistent with the mevalonate pathway in hopanoids from bacteria grown with [1-$^{13}$C] labelled acetate (Figure 4.3 B). They first interpreted these results according to the mevalonate pathway, assuming a compartmentation of the acetate metabolism and a lack of exchange between two distinct acetate pools. However, further experiments performed with the eubacterium *Escherichia coli*, allowed Rohmer *et al.* (1993) to describe a novel mevalonate-independent pathway (MEP) yielding IPP from pyruvate (**9**) and glyceraldehyde-3-phosphate (**10**) with 1-deoxy-D-xylulose 5-phosphate (**11**) and 2-C-methyl-D-erythritol 4-phosphate (MEP, **12**) identified as intermediates (Figure 4.1 B).

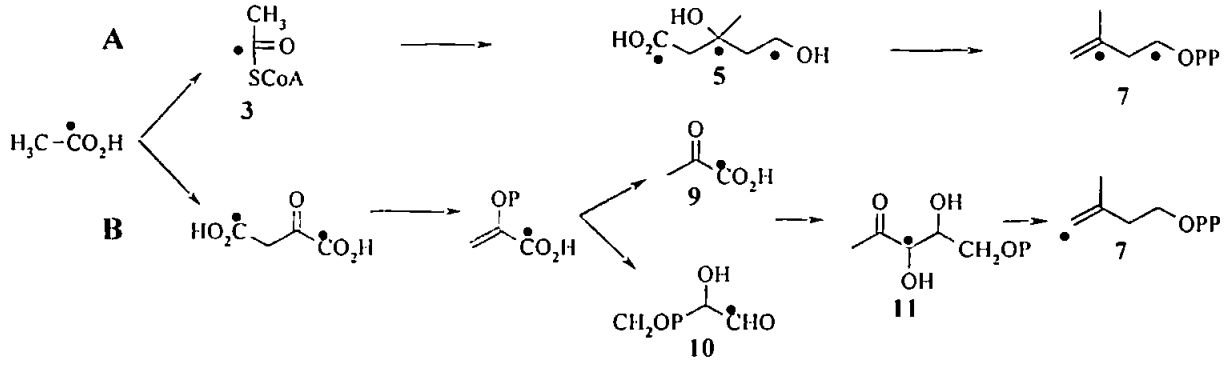


Figure 4.3 Incorporation of [1-$^{13}$C] acetate into isopentenyl pyrophosphate. A. Acetate-mevalonate pathway. B. Acetate metabolism *via* the glyoxylate shunt and incorporation of glyceraldehyde-3-phosphate and pyruvate into IPP *via* the mevalonate independent route.

Since this discovery, many authors have studied the distribution of these two pathways within a large number of organisms by incorporation of $^{13}$C or $^{2}$H labelled precursors (reviewed by Eisenreich *et al.*, 1998; Lichtenthaler, 1999) or using highly specific inhibitors of the individual pathways (Bach and Lichtenthaler, 1982, 1983; Zeidler *et al.*, 1998; Hagen and Grünewald, 2000; Lichtenthaler *et al.*, 2000). A third approach, alternative to precursor-based or inhibitor-based studies has been developed by Jux *et al.* (2001). These authors demonstrated that natural $^{13}$C/$^{12}$C isotope ratios could be used to determine whether the IPP is produced predominantly by the acetate/mevalonate or the methylerythritol phosphate (MEP) pathway. Based on these three approaches, a classification of terpenoid producers according to their biosynthetic pathways has been developed, and it has been established that archaea, certain bacteria, yeasts, fungi, some protozoa and animals use only the mevalonate pathway, while many bacteria, green algae and some protists rely exclusively on the MEP pathway (Eisenreich *et al.*, 2001; Steinbacher *et al.*, 2002; Wilson, 2002). Some algae, streptomycetes, mosses and liverworts, two marine diatoms and higher plants appear to use both pathways in the biosynthesis of isoprenoids. The discovery that the MEP pathway appears to be absent from humans, while several organisms including many human

pathogens, use exclusively this new route for isoprenoid biosynthesis, is providing new perspectives on drug design using enzymes implicated in this pathway as potential targets for chemotherapeutics (Vial, 2000; Wilson, 2002). Indeed, fosmidomycin, a specific inhibitor of 1-deoxy-D-xylulose 5-phosphate reductoisomerase involved in the non-mevalonate pathway (Kuzuyama *et al.*, 1998) has been shown to exhibit *in-vitro* and *in-vivo* activities against multidrug resistant *Plasmodium* strains (Jomaa *et al.*, 1999). Recent findings (Lichtenthaler *et al*, 1997; Lichtenthaler, 1999; Cvejić and Rohmer, 2000; Steinbacher *et al.*, 2002) suggest that the mevalonate pathway seems to be implicated in cytosolic sterol biosynthesis whereas the MEP pathway appears to be involved in the formation of plastidic or apicoplastidic isoprenoids, although the compartmental separation of the two biosynthetic pathways does not appear to be absolute (Nabeta *et al.*, 1995; Lichtenthaler, 1999).

As a group, diatoms exhibit a great diversity (> 30 000 described species) and are considered as one of the most important groups of primary producers in the oceans. Some species are already cultured on a large scale in the aquaculture and cosmetics industries (Brown *et al.*, 1997). Several diatoms have been shown to contain a large number of isoprenoids (Volkman *et al.*, 1994; Barrett *et al.*, 1995; Véron *et al.*, 1998) and as such, they could be considered to be an important reservoir of potentially useful terpenoids. Indeed, in a recent study, Rowland *et al.* (2001a) reported that $C_{25}$ highly branched isoprenoids (HBIs) synthesised by the diatom *Haslea ostrearia* exhibited *in-vitro* activity against melanoma and lung cancer cells. They also reported a dramatic effect of the growth temperature on the biosynthesis of HBIs. A culture of this diatom was grown at 15°C, and was used to inoculate different flasks grown at different temperatures (5, 15, 25°C). The unsaturation of the HBIs increased with the growth temperature, which is the inverse trend to that exhibited by fatty acids esters involved in membrane fluidity processes (Quinn *et al.*, 1989). However, these results suggest that the

diatom is sensitive to environmental conditions and that the modification of the mean unsaturation index of the HBI polyenes suggests that they may have a significant biological function. Ourisson and Nakatani (1994) suggested that these acyclic isoprenoids may be membrane lipids, but as yet, a formal identification of their location and biological function is not known.

Therefore, it appeared important to examine the location and determine the biosynthesis of isoprenoids (including HBIs) in a number of different diatoms, in order to better understand their function. To examine isoprenoid compartmentation in diatoms, *Rhizosolenia setigera* cells were fractionated according to established procedures and their individual terpenoid composition investigated using GC-MS. To achieve the determination of isoprenoid biosynthesis in diatoms, a combined approach was adopted. In a first set of experiments, the diatoms *Haslea ostrearia*, *Pleurosigma intermedium* and *Rhizosolenia setigera* were grown in the presence of specific inhibitors of both pathways (mevinolin and fosmidomycin for the mevalonate and MEP pathways respectively). In a second set of experiments, the same three species were grown in the presence of labelled precursors ($^{13}CO_2$, $^{13}$C-carbonate, [1-$^{13}$C] acetate, [2-$^{13}$C] acetate, $^{2}H_3$ acetate and D-[1-$^{13}$C] glucose) and the extent and nature of incorporation investigated using mass spectrometry and NMR techniques. Finally, in a third set of experiments, these three species were grown under normal laboratory conditions, and the natural $^{13}C/^{12}C$ isotope ratio of individual compounds was investigated using isotope-ratio mass spectrometric techniques.

## 4.2 Experimental

### *4.2.1 Algal cultures*

*Rhizosolenia setigera* (strain RS 99) was isolated in Spring 1999 from surface waters at Le Croisic (France) while *Haslea ostrearia* and *Pleurosigma intermedium* were isolated from microphytobenthic communities in oyster ponds from the Bay of Bourgneuf (France) at the same time of the year (1999). Small-scale cultures were grown in 50 ml culture tubes, 250 ml Erlenmeyer flasks or 2 l round-bottomed flasks, depending on the experimental requirements, whereas large-scale cultures were performed using 25 l glass barrels. Both small and large-scale cultures were performed using F/2 Guillard enriched seawater and grown under controlled conditions (see Chapter 5). During all of the experiments, cells were harvested by filtration at the end of the exponential growing phase.

### *4.2.2 Cell fractionation*

*R. setigera* cells from a 300 l culture were harvested by filtration through a 30 µm gauze at the end of the exponential growing phase, washed in 0.2 µm filtered sea-water and re-suspended in isolation buffer (626 mM sorbitol, 6 mM $Na_2$-EDTA, 5 mM $MgCl_2$, 10 mM KCl, 1 mM $MnCl_2$, 50 mM HEPES-KOH pH 8.0, 1% BSA; Wittpoth *et al.*, 1998) in a volume of 1 ml per 1 L culture. All the following steps were carried out between 0-4°C. The suspension was gently homogenised using a Dounce potter (15 strokes) to break the cells, to yield the crude extract. An aliquot of this crude extract was frozen to obtain the non-saponifiable lipid content of the whole cells. Before purification, the crude extract was re-filtered through a 30 µm gauze to eliminate the large cell debris.

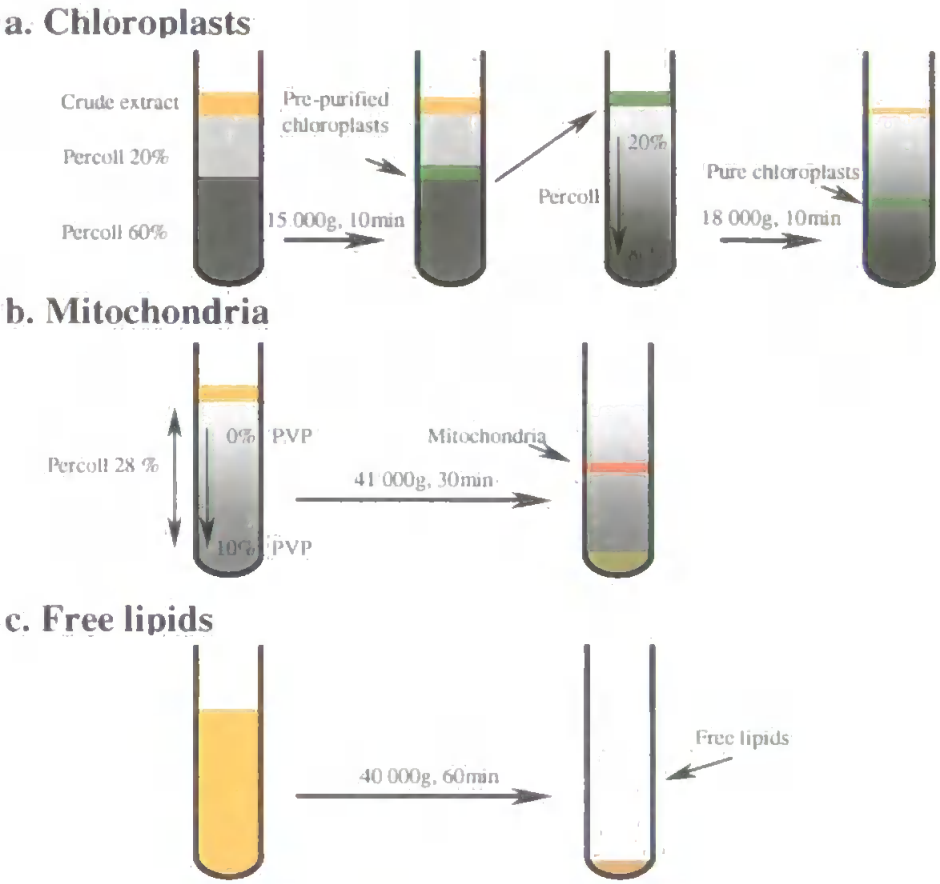


Figure 4.4 Schematic diagram illustrating the fractionation procedures for *R. setigera* cells. a, chloroplasts. b, mitochondria. c, free lipid fraction.

Pure chloroplast fractions were obtained in two steps (Figure 4.4a). The first step consisted of centrifuging (15000 g, 10 min, 4°C) the crude extract through a step gradient of Percoll (20 and 60%) adjusted to iso-osmolarity with sorbitol (final concentration: 626mM). Pre-purified chloroplasts formed a band at the interface between 20 and 60% Percoll bands. This band was collected carefully using a Pasteur pipette, diluted with isolation buffer and re-centrifuged (18000 g, 10 min, 4°C) through a linear Percoll gradient (20-80%). Pure chloroplasts accumulated in a band at approximately 40% Percoll. After removal of the supernatant, this band was carefully collected using a Pasteur pipette and stored at –20°C prior to analysis by GC-MS. Purity and integrity of the chloroplasts were checked using light microscopy.

Mitochondria were purified according to the procedure described by Moore and Proudlove (1987) for pea leaves (Figure 4.4b). Briefly, mitochondria from the *R. setigera* crude extract were isolated by centrifugation (41000 g, 30 min, 4°C) on a linear PVP (polyvinylpyrrolidone)-Percoll gradient (28% of Percoll and 0-10% gradient of PVP).

Free lipids were obtained by differential centrifugation (Figure 4.4c), according to the methodology described by Sullivan (1978). After centrifugation (40000g, 60 min, 4°C) of the crude extract, the supernatant was carefully collected and stored at –20°C prior to analysis.

*4.2.3 Inhibition experiments*

Mevinolin/lovastatin (Figure 4.5 [**2,3**]) is a well known inhibitor of the 3-hydroxy-3-methylglutaryl-coenzyme A reductase, a key enzyme in the acetate/mevalonate pathway (Bach and Lichtenthaler, 1982), whereas fosmidomycin (Figure 4.5 [**1**]) has been demonstrated to be a specific inhibitor of 1-deoxy-D-xylulose 5-phosphate reductoisomerase, an enzyme involved in the non-mevalonate pathway (Kuzuyama *et al.*, 1998; Zeidler *et al.*, 1998).

The three diatom species, *Haslea ostrearia*, *Rhizosolenia setigera* and *Pleurosigma intermedium* were each grown in the presence of increasing concentrations of fosmidomycin or mevinolin in order to investigate their effect on the non-saponifiable lipid content of the cells and their distributions. The three species were grown in 50 ml culturing tubes containing 15 ml of F/2 Guillard's medium under the standard controlled conditions described in Chapter 5. The sodium salt of fosmidomycin was purchased from Molecular Probes (The Netherlands); mevinolin/lovastatin was purchased from Calbiochem-Novabiochem (France).

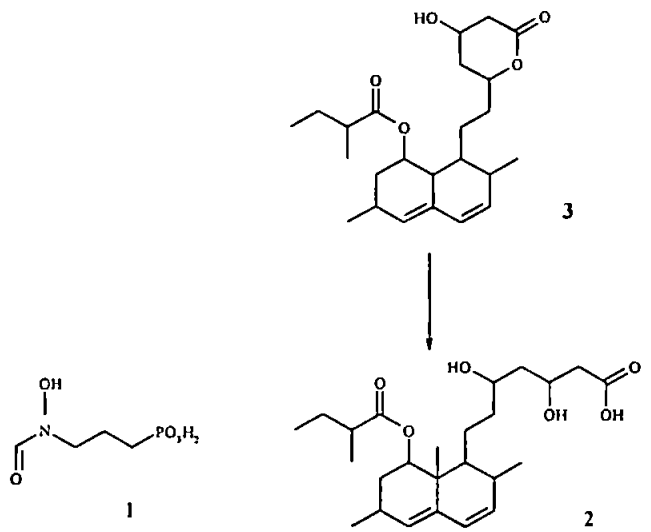


Figure 4.5: Structures of fosmidomycin [**1**] and both active [**2**] and inactive [**3**] forms of mevinolin.

Mevinolin [**3**] required activation prior to being used (Jakobisiak *et al.*, 1991) and was converted to the active form [**2**] by dissolving 10 mg of the lactone [**3**] in 250 µl of 100% ethanol, adding 375 µl of 0.1 M NaOH, heating at 50°C for 2 hr and adjusting to a volume of 5 ml with ultra-pure water. Aliquots of this stock solution were stored at –20°C.

Concentrations of the inhibitors were based on those used in previous investigations (Schindler *et al.*, 1984; Zeidler *et al.*, 1998; Kuzuyama *et al.*, 1998; Hagen and Grünewald, 2000). Cell counts and monitoring of the cultures, together with the extraction, purification and analysis of the HBIs by GC-MS was performed as described in Chapter 5.

### *4.2.4 Isotopic labelling: small scale experiments*

It has now been extensively demonstrated that at least two alternative biosynthetic pathways exist for the formation of IPP, the common precursor of all isoprenoids. While acetate is a direct precursor of the mevalonate pathway (Figure 4.1 A), $CO_2$ is a precursor of the MEP pathway (Figure 4.1 B). Glucose, when metabolised, can be used as a precursor for both

pathways (Figure 4.6). As a result, when using [1-$^{13}$C] glucose, both pathways can be clearly differentiated by the labelling patterns in IPP (Eisenreich *et al.*, 1998; Cvejić and Rohmer, 2000).

It was therefore decided to grow *H. ostrearia, R. setigera* and *P. intermedium* in the presence of isotopically enriched ($^{13}$C) acetate, glucose and $CO_2$ or isotopically enriched ($^{2}$H) acetate. For the three diatom species, $^{13}CO_2$ incorporation experiments were performed in a modified 2 l round bottomed flask (Figure 4.7) in order to avoid any contamination by atmospheric $CO_2$. $CO_2$ was released daily from $Ba^{13}CO_3$ (isotopic abundance 20%) by addition of 2 M $H_2SO_4$ with a syringe. Experiments using sodium [1-$^{13}$C] acetate (20-50% isotopic abundance), sodium [2-$^{13}$C] acetate (20-50% isotopic abundance), $^{2}H_3$ acetate (20% isotopic abundance) and D-[1-$^{13}$C] glucose (20% isotopic abundance) were performed in 250 ml (*R. setigera, P. intermedium*) or 2 l flasks (*H. ostrearia*). The substrates were 20-50% isotopically enriched with $^{13}$C or $^{2}$H in order to follow their incorporation within the different isoprenoids (including HBIs) synthesized by these three diatoms. Sodium [1-$^{13}$C] acetate (99% isotopic abundance), sodium [2-$^{13}$C] acetate (99% isotopic abundance), sodium $^{2}H_3$ acetate (99% isotopic abundance), D-[1-$^{13}$C] glucose (99% isotopic abundance) and $Ba^{13}CO_3$ (99% isotopic abundance) were obtained from Sigma-Aldrich (France).

These experiments, based on externally added precursors, are limited by the fact that the organisms are not studied under natural environmental conditions. Indeed, the administration of precursors at a high concentration may affect the natural balance of the cellular intermediates and have an impact on the metabolic network. During previous studies investigating the biosynthesis of isoprenoids in a green alga (Schwender *et al.*, 1996) or in diatoms (Cvejić and Rohmer, 2000), some experiments were performed with relatively high concentrations of $^{13}$C labelled acetate (1g $l^{-1}$). Compared to the acetate concentrations found

in natural environments, use of such high concentrations is probably unrealistic, and further, high concentrations of acetate may 'disturb' the organisms under study. *Haslea ostrearia*, *Rhizosolenia setigera* and *Pleurosigma intermedium* were therefore grown with different acetate enrichments (0, 500, 1000 mg $l^{-1}$) in order to see if any modifications to the HBI distributions in the cells were induced at high acetate concentrations.

Cell counts, monitoring of the culture, extraction, purification and identification of the isoprenoids was performed as described in Chapter 5. Incorporation (including quantification) of stable isotopes was achieved using GC-MS methods.

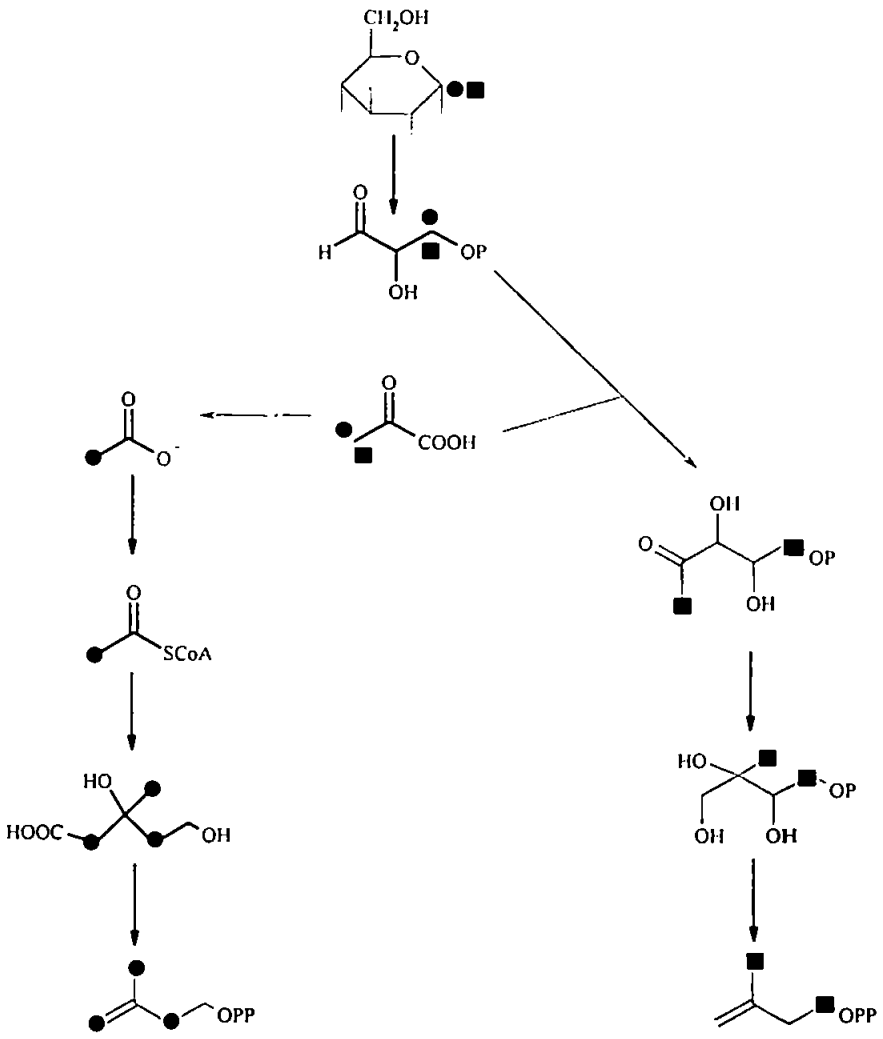


Figure 4.6 Labelling of isopentenyl pyrophosphate from [1-$^{13}$C] glucose *via* the mevalonate pathway (●) or *via* the MEP pathway (■).

Figure 4.7: Purpose-built culturing flask used for $^{13}CO_2$ incorporation experiments.

*4.2.5 Isotopic labelling: large scale experiments*

HBIs are secondary metabolites from a few diatom species and their cellular concentrations are very low within the three species investigated (2-40 pg cell$^{-1}$). In order to obtain sufficient amounts of HBIs to observe the labelling patterns of IPP by NMR spectroscopy (> 0.1 mg), large scale cultures (50 l) were needed. *Rhizosolenia setigera, Pleurosigma intermedium* and *Haslea ostrearia* were therefore grown in the presence of different $^{13}C$ or $^{2}H$-labelled precursors in 2 x 25 l barrels containing F/2 Guillard's medium under standard controlled conditions. Sodium [1-$^{13}C$] acetate (20% or 100% isotopic abundance), sodium [2-$^{13}C$] acetate (20% isotopic abundance) or sodium [$^{2}H_3$] acetate (20% isotopic abundance) were added in order to obtain a final concentration of 250 mg l$^{-1}$. In order to control the availability of carbon from other sources, culture media were bubbled with $CO_2$-free air (15 l h$^{-1}$), and $Na_2CO_3$ (150 or 10 mg l$^{-1}$) was added to provide an inorganic carbon source. Since

it was not feasible to obtain a large-scale culture (100-200 l) using $^{13}CO_2$ released from $Ba^{13}CO_3$, large-scale experiments were performed using $^{13}C$ $Na_2CO_3$. At the end of the exponential growing phase, the cells were harvested by filtration and the resulting algal paste was freeze-dried. Total lipids were then extracted using methanol/dichloromethane (50:50, v/v). Phytol, desmosterol and HBI fractions were then obtained following the methodology described in Chapter 5. Individual isomers from the HBI fraction obtained by open column chromatography were separated by silver-ion ($Ag^+$) chromatography (Chromspher 5 lipid, 250 x 4.6 mm I.D.) under isocratic conditions (hexane-isopropanol; 98.75:1.25 v/v).

*4.2.6 Monitoring of stable isotope incorporation by GC-MS: isotopic enrichment factors*

For stable isotope enrichment experiments, levels of $^2H$ and $^{13}C$ incorporation were estimated using mass spectrometry. In their recent study on the biosynthesis of 2-methyl-3-buten-2-ol (MBO) from pine needles, Zeidler and Lichtenthaler (2001) estimated the degree of isotopic labelling in MBO after incubation of the needles with labelled precursors using a simple ratio of mass spectral peak intensities. However, in contrast to 2-methyl-3-buten-2-ol, the increased molecular masses together with the variable structures of the terpenoids synthesised by the three diatoms studied here, means that such ratios would not allow for an accurate measure of the degree of labelling to be made. Instead, $^{13}C$ or $^2H$ "isotopic enrichment factors" were calculated for each compound according to Equation 4.1, where M, M+1, etc are the values of the molecular ions for various isotopomers, $I_M$ is the intensity of the molecular ion, $I_{M+1}$ is the intensity of the M+1 peak, $I_{M+X}$ is the intensity of the highest mass ion (quantifiable), and n is the number of carbon atoms (for $^{13}C$ labelled substrates) or hydrogen atoms (for $^2H$ labelled substrates) in the molecule. For phytol and sterols, $I_M$ was taken at M-18 in order not to incorporate in the calculation the 3 carbon atoms from the silylating agent. Comparison of $^{13}C$ or $^2H$ isotopic enrichment factors (IEFs) from

compounds obtained from cells cultured in the presence of isotopically labelled precursors with those obtained from control cultures thus revealed the level of $^{13}C$ or $^{2}H$ incorporation within individual compounds. Note, while IEFs calculated for individual compounds could be compared quantitatively, comparisons between different terpenoids are only semi-quantitative owing to variations in atomic composition.

Isotopic Enrichment Factor =

$$\frac{100}{n}\left\{\frac{(M*I_M)+(M+1*I_{M+1})+.....+(M+X*I_{M+X})}{I_M+I_{M+1}+.....+I_{M+X}} - M\right\} \quad \text{(Eqn. 4.1)}$$

*4.2.7 Natural $^{12}C/^{13}C$ isotope ratios, GC-irm-MS*

Analysis of the non-saponifiable lipid fractions obtained from cultures of *R. setigera*, *P. intermedium* and *H. ostrearia* performed under normal growth conditions was achieved using a NERC Varian 3400 gas chromatograph (GC), fitted with a 60 m dimethylpolysiloxane ZB1 Phenomenex column (0.32 mm internal diameter). The eluting compounds were combusted online at 850°C with a catalyst system (Cu/Pt) and the resulting $CO_2$ was transferred into a Delta S isotope-ratio mass spectrometer (Finnigan Mat). The GC oven temperature was programmed from 40-300°C at 10°C $min^{-1}$ and held at the final temperature for 20 minutes. All ratios are given as $\delta^{13}C$ values: $\delta^{13}C$ [‰]= $[(R_{sample}/ R_{standard}) -1 ] \times 10^3$ with R corresponding to the $^{13}C/^{12}C$ ratio of the sample or the standard (Vienna Pee Dee Belemnite). For phytol and sterols, a correction was applied to take into account the contributions from the silylating agent.

*4.2.8 Monitoring of stable isotope incorporation by NMR spectroscopy*

$^{13}C$ NMR spectra of individual compounds were recorded in $CDCl_3$ using a Jeol EX 270 spectrometer equipped with a DELTA station. $^{13}C$ peak assignments of the individual terpenoids were compared with previously published data (Goad and Akihisha, 1997; Arigoni *et al.*, 1997; Belt *et al.*, 1996, 2000a,b, 2001a). Relative $^{13}C$ abundances for individual carbon atoms was calculated by comparison of $^{13}C$ peak intensity between $^{13}C$ labelled and unlabelled material. For each compound analysed, a carbon atom was identified that should show no enrichment from isotopically enriched $^{13}C$ acetate and given a relative intensity of 1.0. Consequently, carbon nuclei exhibiting an enhancement in intensity as a result of site-specific $^{13}C$ incorporation would have relative peak intensity >1.0.

## 4.3 Results

*4.3.1 Non-saponifiable lipids from the diatom Rhizosolenia setigera*

A description of the structures and distributions of the non-saponifiable lipids synthesised from the diatom *R. setigera* can be found elsewhere in this thesis (Chapters 1, 2 and 3). Briefly, analysis of the GC-MS total ion current (TIC) chromatograms of the non-saponifiable lipid fractions from *R. setigera* (RS 99) generally showed the presence of *n*-$C_{21:6}$ (I), phytol (II), desmosterol (cholesta-5,24-diene-3β-ol, III) and four acyclic $C_{30}$ alkenes isomers (IV-VII). During the post-auxosporulation phase, *R. setigera* also synthesises up to three acyclic $C_{25}$ alkenes isomers (VIII-X) along with two monocyclic $C_{30}$ alkenes (XI, XII). Figure 4.8 summarises the structures of all the non-saponifiable lipids identified in this biosynthetic study.

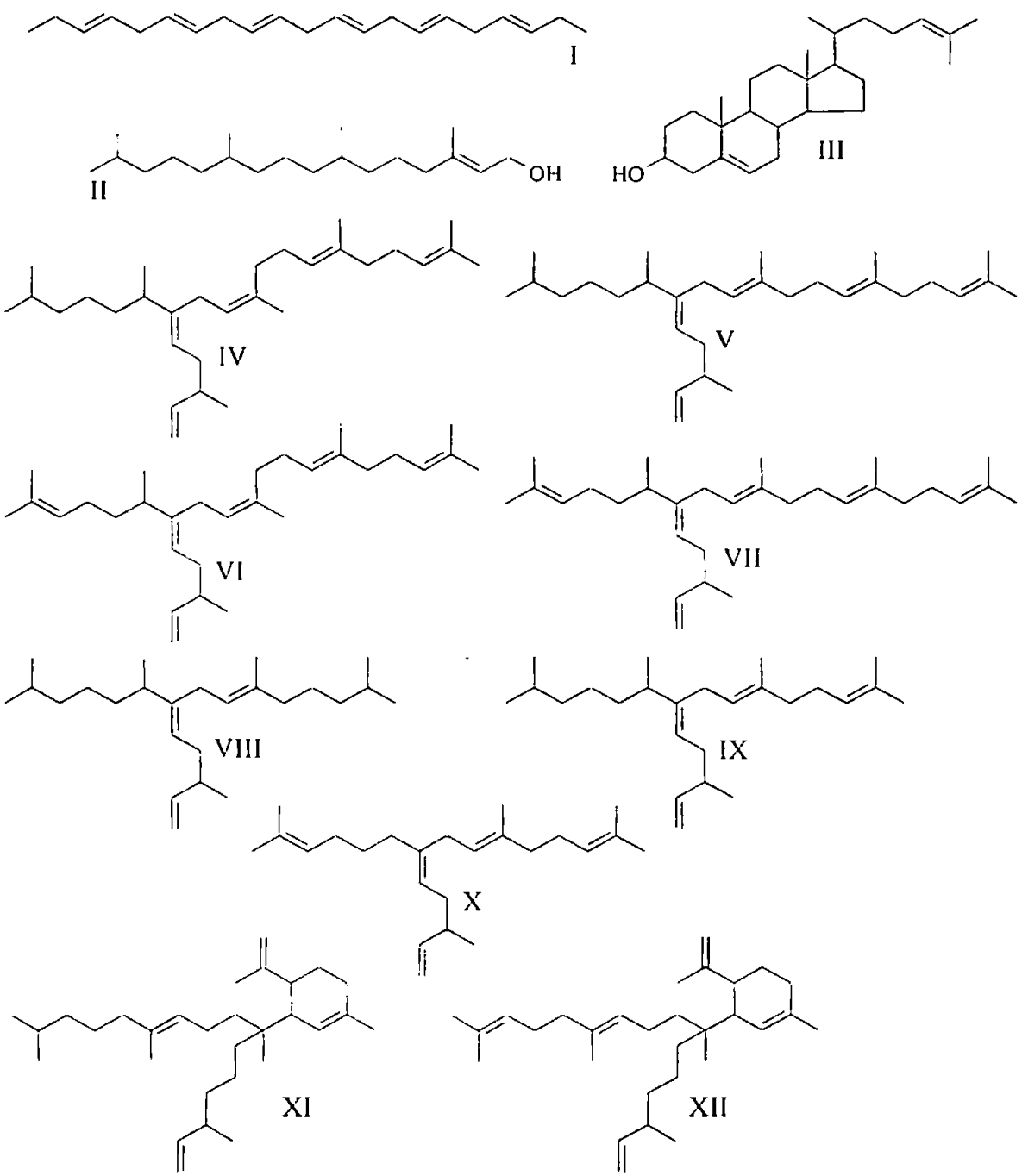


Figure 4.8 Non-saponifiable lipids obtained from various cultures of the diatom *Rhizosolenia setigera*. I: *n*-$C_{21:6}$, II: phytol, III: desmosterol, IV-VII: $C_{30}$ HBIs, VIII-X: $C_{25}$ HBIs, XI: $C_{30:4:1}$, XII: $C_{30:5:1}$.

*4.3.2 Compartmentation of isoprenoids in the diatom Rhizosolenia setigera*

Following differential centrifugation and purification on Percoll-PVP gradients, pure enriched fractions of chloroplasts, free lipids and mitochondria were obtained from a crude extract of the diatom *R. setigera*. GC-MS analysis of the non-saponifiable lipid fraction obtained from the crude extract revealed the presence of *n*-$C_{21:6}$ (I), phytol (II), desmosterol (III) and $C_{30}$ HBIs (IV-VII) along with small amounts of a $C_{25}$ triene (VIII). In the chloroplast fraction, phytol along with small amounts of *n*-$C_{21:6}$ were observed, while only trace amounts of the other isoprenoids were detected. In contrast, in the free lipid fraction, phytol and *n*-$C_{21:6}$ were not detected while large amounts of HBIs and desmosterol were observed. In the mitochondria enriched fraction, all the isoprenoids detected in the crude extract were present. However when the purity of this fraction was checked using light microscopy, a large number of plastids were found, indicating that the purification of this organelle was not completely successful and that the results obtained for this fraction must be interpreted carefully. Table 4.1 summarises the non-saponifiable lipid composition as a percentage of the total non-saponifiable lipid composition of each fraction.

Table 4.1 Non-saponifiable lipid composition (percentage) of fractions obtained from *R. setigera*.

| | Crude extract | Chloroplast | Free lipid | Mitochondria |
|---|---|---|---|---|
| *n*-$C_{21:6}$ | 6.1 | 4.1 | 0.0 | 2.9 |
| Phytol | 38.0 | 81.8 | 0.0 | 25.2 |
| $C_{25:3}$ | 1.0 | 0.0 | 1.5 | 0.8 |
| $C_{25:4}$ | 0.0 | 0.0 | 0.9 | 0.0 |
| $C_{25:5}$ | 0.0 | 0.0 | 0.0 | 0.0 |
| $C_{30:5}$ Z | 12.3 | 3.7 | 29.0 | 18.7 |
| $C_{30:5}$ E | 11.5 | 3.1 | 25.2 | 17.1 |
| $C_{30:6}$ Z | 7.5 | 1.8 | 14.4 | 12.3 |
| $C_{30:6}$ E | 8.7 | 2.0 | 14.3 | 13.0 |
| Desmosterol | 14.9 | 3.6 | 14.8 | 10.1 |
| Total | 100.0 | 100.0 | 100.0 | 100.0 |

In summary, the presence of phytol seems to be essentially restricted to the chloroplast fraction while the HBIs and desmosterol seem to be of cytoplasmic origin.

### *4.3.3 Isoprenoid biosynthesis in the diatom Rhizosolenia setigera*

#### *4.3.3.1 Inhibition experiments*

Since mother cells synthesise predominantly $C_{30}$ HBIs (with very small amounts of $C_{25}$ HBIs) and daughter cells synthesise both $C_{25}$ and $C_{30}$ HBIs in significant proportions (Chapter 2), it was decided to perform inhibition experiments using both cell types, each in the presence of mevinolin or fosmidomycin.

In the presence of mevinolin, the growth of both mother and daughter cells was dramatically retarded with increasing concentration of this inhibitor (Table 4.2, 4.3). Even at a concentration 20 times lower (1μg $ml^{-1}$) than that used for the other species investigated (20 μg $ml^{-1}$), mevinolin strongly inhibited the growth of *R. setigera* (80-90% inhibition). In contrast, the growth of *R. setigera* was significantly less sensitive to the presence of fosmidomycin. Fosmidomycin did not reduce the cell growth of daughter cells up to the limit of concentration used (100 μg $l^{-1}$) and the growth of mother cells was significantly retarded only at high concentrations (75-100 μg $l^{-1}$) of the inhibitor.

For mother cells, and in the presence of both inhibitors, phytol and *n*-$C_{21:6}$ were not sufficiently abundant to be quantified. $C_{30}$ HBIs were significantly depleted from the cells when they were grown in the presence of 0.5 μg $ml^{-1}$ of mevinolin and were absent from cells grown in the presence of 1 μg $ml^{-1}$ of this inhibitor (Figure 4.9). Interestingly, when the cells were cultured without any inhibitor, no traces of any cyclic $C_{30}$ compounds (*cf.* Chapter 3) were observed, while in the presence of 0.5 μg $ml^{-1}$ of mevinolin, the monocyclic tetraene $C_{30:4:1}$ was present in the cells as the major isomer along with lower amounts of the related

pentaene isomer ($C_{30:5:1}$). Finally, the biosynthesis of the major sterol in *R. setigera*, desmosterol, was also dramatically inhibited when the cells were cultured in the presence of mevinolin and like the $C_{30}$ HBIs, was not detected in the cells grown in the presence of 1 μg $ml^{-1}$ of this inhibitor. In contrast, fosmidomycin did not reduce the $C_{30}$ or sterol content of the cells, and indeed, concentrations of these compounds were two to three times greater in the cells grown with 75-100 μg $ml^{-1}$ of fosmidomycin than in the control culture.

In the experiment performed with daughter cells, mevinolin exhibited the same dramatic effect on the cell growth whereas fosmidomycin had no significant effect. No clear changes were observed in the concentrations of *n*-$C_{21:6}$ for either inhibitor, and phytol was not present in sufficient amounts to be quantified satisfactorily. Consistent with the results observed for mother cells, mevinolin dramatically reduced the $C_{30}$ HBI concentration per cell (97% inhibition at 0.75 μg $ml^{-1}$). At a concentration of 1 μg $ml^{-1}$, $C_{30}$ HBIs were not detected. The $C_{25}$ HBIs were also dramatically inhibited (94% of inhibition for a concentration of 0.75 μg $ml^{-1}$). At a concentration of 1μg $ml^{-1}$, neither $C_{25}$ HBIs nor desmosterol were detected (Figure 4.9). However, in contrast to the results observed for mother cells, the synthesis of HBIs ($C_{25}$ and $C_{30}$) and desmosterol appeared to be inhibited by the presence of fosmidomycin, especially at higher concentrations. Thus, each of the concentrations of the HBIs and of desmosterol were observed to reduce with increasing concentrations of the inhibitor.

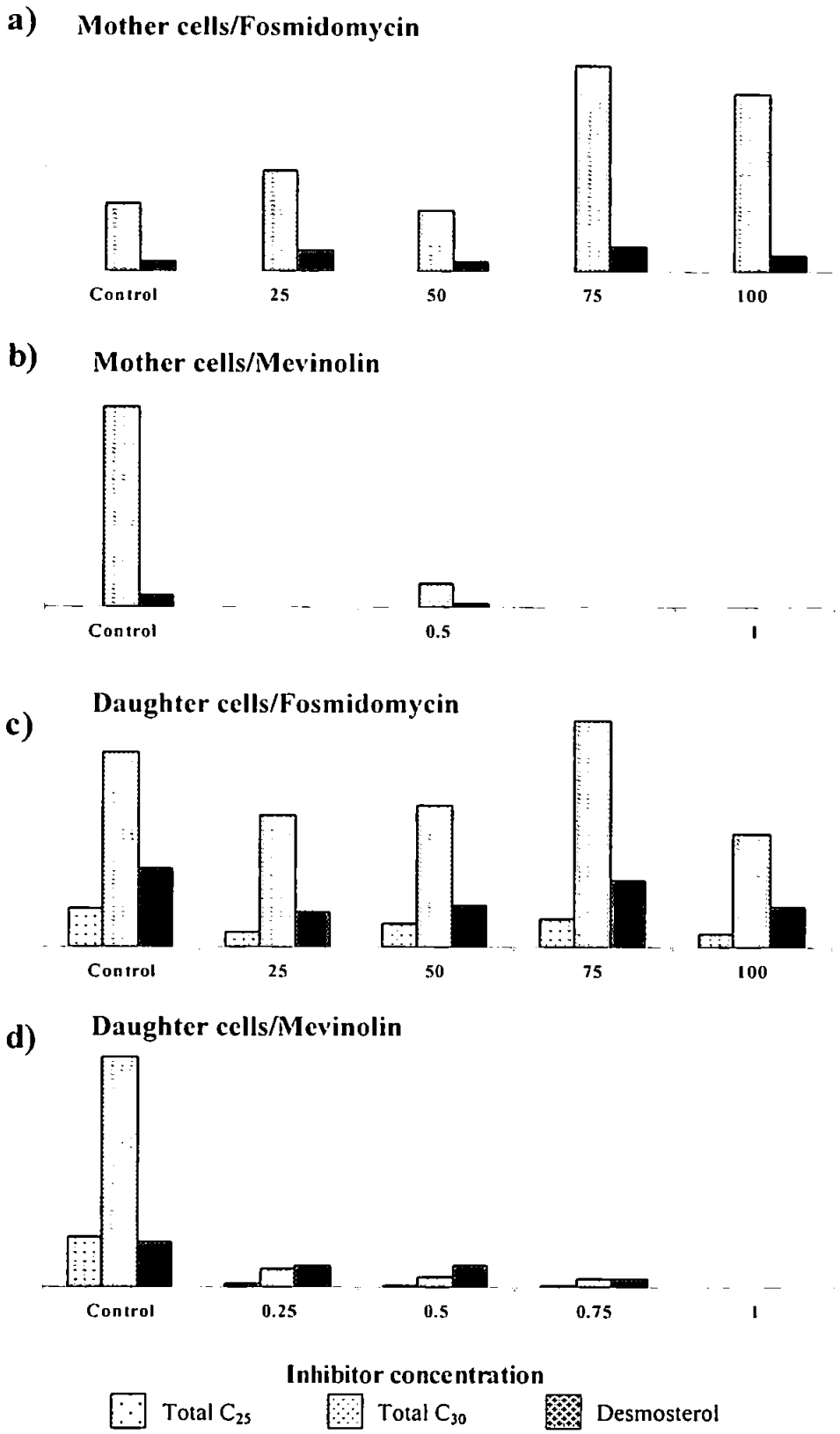


Figure 4.9 Hydrocarbon distribution in *R. setigera* cells at the end of the exponential growing phase in the presence of varying concentrations of pathway-specific inhibitor (μg $ml^{-1}$). (a) "mother" cells, fosmidomycin (b) "mother" cells, mevinolin (c) "daughter" cells, fosmidomycin (d) "daughter" cells, mevinolin.

Table 4.2 Biomass data (cell $ml^{-1}$) and non-saponifiable lipid concentrations (pg $cell^{-1}$) of *Rhizosolenia setigera* cells (mother cells) at the end of the exponential growing phase in the presence of varying concentrations of fosmidomycin and mevinolin (μg $ml^{-1}$).

| | Fosmidomycin | | | | |
|---|---|---|---|---|---|
| | **Control** | **25** | **50** | **75** | **100** |
| Biomass | 66400 | 49200 | 86133 | 14667 | 19467 |
| *n*-$C_{21:6}$ | n/a | n/a | n/a | n/a | n/a |
| Phytol | n/a | n/a | n/a | n/a | n/a |
| $C_{25:3}$ E | n/a | n/a | n/a | n/a | n/a |
| $C_{25:4}$ E | n/a | n/a | n/a | n/a | n/a |
| $C_{25:5}$ E | n/a | n/a | n/a | n/a | n/a |
| $C_{30:5}$ Z | 0.55 | 0.92 | 0.57 | 1.89 | 1.60 |
| $C_{30:5}$ E | 0.57 | 0.82 | 0.52 | 1.46 | 1.16 |
| $C_{30:6}$ Z | 0.37 | 0.62 | 0.35 | 1.52 | 1.42 |
| $C_{30:6}$ E | 0.64 | 0.84 | 0.48 | 1.68 | 1.47 |
| Desmosterol | 0.30 | 0.70 | 0.32 | 0.80 | 0.54 |
| Total $C_{25}$ | n/a | n/a | n/a | n/a | n/a |
| Total $C_{30}$ | 2.13 | 3.20 | 1.92 | 6.56 | 5.64 |

n/a Below limit of detection

| | Mevinolin | | |
|---|---|---|---|
| | **Control** | **0.5** | **1** |
| Biomass | 36133 | 41333 | 4800 |
| *n*-$C_{21:6}$ | n/a | n/a | n/a |
| Phytol | n/a | n/a | n/a |
| $C_{25:3}$ E | n/a | n/a | n/a |
| $C_{25:4}$ E | n/a | n/a | n/a |
| $C_{25:5}$ E | n/a | n/a | n/a |
| $C_{30:5}$ Z | 1.54 | 0.12 | n/a |
| $C_{30:5}$ E | 1.15 | 0.07 | n/a |
| $C_{30:6}$ Z | 0.97 | n/a | n/a |
| $C_{30:6}$ E | 1.09 | 0.05 | n/a |
| $C_{30:4:1}$ | n/a | 0.29 | n/a |
| Desmosterol | 0.28 | 0.09 | n/a |
| Total $C_{25}$ | n/a | n/a | n/a |
| Total $C_{30}$ | 4.75 | 0.54 | n/a |

n/a Below limit of detection

Table 4.3 Biomass data (cell $ml^{-1}$) and non-saponifiable lipid concentrations (pg $cell^{-1}$) of *Rhizosolenia setigera* (daughter cells) cells at the end of the exponential growing phase in the presence of varying concentrations of of fosmidomycin and mevinolin (μg $ml^{-1}$).

| | Fosmidomycin | | | | |
|---|---|---|---|---|---|
| | **Control** | **25** | **50** | **75** | **100** |
| Biomass | 11960 | 12040 | 12680 | 11800 | 11440 |
| *n*-$C_{21:6}$ | 0.24 | 0.27 | 0.31 | 0.49 | 0.24 |
| Phytol | n/a | n/a | n/a | n/a | n/a |
| $C_{25:3}$ E | 1.61 | 0.62 | 0.90 | 1.02 | 0.45 |
| $C_{25:4}$ E | 1.25 | 0.52 | 0.81 | 1.17 | 0.56 |
| $C_{25:5}$ E | 0.21 | n/a | 0.10 | 0.12 | 0.08 |
| $C_{30:5}$ Z | 4.89 | 4.38 | 4.86 | 9.23 | 4.32 |
| $C_{30:5}$ E | 5.32 | 3.87 | 3.93 | 5.80 | 3.06 |
| $C_{30:6}$ Z | 2.02 | 0.89 | 1.04 | 1.29 | 0.66 |
| $C_{30:6}$ E | 3.38 | 1.46 | 1.47 | 1.84 | 1.06 |
| Desmosterol | 6.22 | 2.76 | 3.36 | 5.32 | 3.24 |
| Total $C_{25}$ | 3.07 | 1.14 | 1.82 | 2.31 | 1.10 |
| Total $C_{30}$ | 15.61 | 10.60 | 11.29 | 18.17 | 9.11 |

n/a Below limit of detection

| | Mevinolin | | | | |
|---|---|---|---|---|---|
| | **Control** | **0.25** | **0.50** | **0.75** | **1** |
| Biomass | 2000 | 12600 | 11920 | 3480 | 2200 |
| *n*-$C_{21:6}$ | n/a | 0.11 | 0.10 | 0.46 | n/a |
| Phytol | n/a | n/a | n/a | n/a | n/a |
| $C_{25:3}$ E | 2.23 | 0.29 | 0.16 | n/a | n/a |
| $C_{25:4}$ E | 4.78 | 0.20 | 0.16 | 0.26 | n/a |
| $C_{25:5}$ E | 1.00 | n/a | n/a | n/a | n/a |
| $C_{30:5}$ Z | 13.07 | 1.29 | 0.72 | 0.58 | n/a |
| $C_{30:5}$ E | 10.08 | 1.14 | 0.66 | 0.66 | n/a |
| $C_{30:6}$ Z | 6.01 | 0.06 | n/a | n/a | n/a |
| $C_{30:6}$ E | 7.39 | 0.34 | 0.29 | n/a | n/a |
| Desmosterol | 7.19 | 3.37 | 3.41 | 1.31 | n/a |
| Total $C_{25}$ | 8.01 | 0.49 | 0.32 | 0.26 | n/a |
| Total $C_{30}$ | 36.54 | 2.83 | 1.67 | 1.24 | n/a |

n/a Below limit of detection

In summary, the dramatic inhibition of both $C_{25}$ and $C_{30}$ HBIs along with desmosterol by mevinolin indicates that the involvement of the mevalonate pathway is essential for the biosynthesis of these compounds for both mother and daughter cells of *R. setigera*. In contrast, although the growth of mother cells was strongly inhibited with high concentrations of fosmidomycin, the synthesis of the HBIs and desmosterol were not inhibited at any of the concentrations tested and a moderate increase in their concentrations was observed. This indicates that the non-mevalonate pathway is probably not involved to a significant extent in the biosynthesis of these compounds in mother cells of *R. setigera*. It is also plausible that the synthesis of other lipids was inhibited by fosmidomycin, with consequential over-production of $C_{30}$ HBIs and desmosterol in order to replace them. For the daughter cells, cell growth was not inhibited even with high concentrations of fosmidomycin, but an inhibition of the synthesis of both HBIs and desmosterol at high concentrations of the inhibitor was observed. Since HBI and desmosterol biosynthesis was also inhibited in the presence of mevinolin, it seems likely that both the MEP and mevalonate routes contribute to the biosynthesis of these compounds in daughter cells.

*4.3.3.2 Isotope labelling: small scale experiments*

**Experiments using unlabelled acetate:**

When the diatom *R. setigera* was cultured in the presence of varying concentrations of sodium acetate, the final cell biomass was found to be essentially invariant of acetate concentration, although some modifications in the cell lipid content were observed (Table 4.4). The concentrations (per cell) of all of the HBIs examined increased (approx. 3 fold) in the presence of 0.5 g $l^{-1}$ of added acetate in the culture medium. When the concentration of acetate was increased further (1 g $l^{-1}$), the HBI concentrations (per cell) also showed an enhancement, but it was not as large as that observed for the culture containing 0.5 g $l^{-1}$ of

acetate. Further, while no cyclic $C_{30}$ compounds were detected in the cells cultured in the absence of any added acetate, significant amounts of $C_{30:4:1}$ and $C_{30:5:1}$ were detected when the cells were grown in the presence of this substrate. In contrast to these observations, the concentrations of phytol, desmosterol and *n*-$C_{21:6}$ were not significantly affected by the presence of acetate in the culture medium.

Table 4.4 Biomass data (cell $ml^{-1}$) and non-saponifiable lipid concentrations (pg $cell^{-1}$) in *Rhizosolenia setigera* cells after incubation with varying concentrations of unlabelled acetate (g $l^{-1}$).

| | 0 (Control) | 0.5 | 1 |
|---|---|---|---|
| Biomass | 6000 | 7440 | 6720 |
| *n*-$C_{21:6}$ | 1.07 | 0.92 | 1.27 |
| Phytol | 0.44 | 0.37 | 0.37 |
| $C_{25:3}$ E | 5.42 | 11.01 | 8.11 |
| $C_{25:4}$ E | 12.49 | 16.85 | 16.91 |
| $C_{25:5}$ E | 2.32 | 2.29 | 2.26 |
| $C_{30:5}$ Z | 2.55 | 5.52 | 3.29 |
| $C_{30:5}$ E | 1.55 | 3.42 | 2.17 |
| $C_{30:6}$ Z | 0.68 | 2.12 | 1.16 |
| $C_{30:6}$ E | 1.37 | 2.76 | 2.21 |
| $C_{30:4:1}$ | n/a | 2.87 | 1.12 |
| $C_{30:5:1}$ | n/a | 0.32 | 0.14 |
| Desmosterol | 9.91 | 8.96 | 7.87 |

**Stable isotope incorporation – analysis by mass spectrometry**

When *R. setigera* was cultured (2 l) in the presence of $^{13}CO_2$ (20% isotopic abundance) and unlabelled sodium acetate (1g $l^{-1}$) and the products analysed by mass spectrometry (see section 4.2.6), it could be seen that $^{13}C$ was efficiently incorporated into phytol, all of the $C_{25}$ and $C_{30}$ HBI isomers and desmosterol (Table 4.5). In contrast, phytol appeared not to be labelled with $^{13}C$ when the cells were cultured in the presence of 1-$^{13}C$ acetate (150 ml, 1 g $l^{-1}$, 20% isotopic abundance), but a significant incorporation of $^{13}C$ from labelled acetate was detected for all of the HBIs and desmosterol. In addition, when the cells were grown in the

presence of $^{2}H_3$-acetate, incorporation of deuterium was observed in HBIs and desmosterol, but not in phytol. These results indicated that acetate was utilised by *R. setigera* for the biosynthesis of HBIs and desmosterol but not for the biosynthesis of phytol and that, therefore, the mevalonate pathway was involved in the biosynthesis of the HBIs and desmosterol but not for phytol.

Finally, when the cells were cultured in the presence of D-2-$^{13}$C leucine (150ml, 0.2g $l^{-1}$, 50% isotopic abundance) and D-1-$^{13}$C glucose (150ml, 0.2g $l^{-1}$, 50% isotopic abundance), no incorporation of $^{13}$C was detected in any of the HBIs, desmosterol or phytol.

Table 4.5 Isotopic enrichment factors for non-saponifiable lipids from *Rhizosolenia setigera* after incubation with $^{13}$C and $^{2}$H labelled precursors.

**$^{13}$C labelled precursors**

| | Control | Acetate | [1-$^{13}$C] Acetate | $^{13}CO_2$ | [1-$^{13}$C] Glucose | [2-$^{13}$C] Leucine |
|---|---|---|---|---|---|---|
| Phytol | 1.0 | 1.4 | 1.2 | 6.1 • | 1.4 | n/a |
| $C_{25:3}$ E | 1.1 | 1.3 | 4.5 • | 5.1 • | 1.1 | 1.0 |
| $C_{25:4}$ E | 1.2 | 1.1 | 4.8 • | 5.6 • | 1.0 | 1.0 |
| $C_{25:5}$ E | 1.0 | 1.4 | 4.3 • | 5.5 • | 0.9 | n/a |
| $C_{30:5}$ Z | 0.9 | 0.8 | 3.9 • | 4.9 • | 1.0 | 1.0 |
| $C_{30:5}$ E | 0.9 | 1.0 | 3.9 • | 5.4 • | 0.8 | 0.9 |
| $C_{30:6}$ Z | 1.1 | 0.9 | 4.1 • | 4.7 • | 0.9 | 0.5 |
| $C_{30:6}$ E | 0.9 | 0.9 | 3.9 • | 5.4 • | 1.0 | 0.4 |
| Desmosterol | 1.3 | 1.1 | 4.6 • | 5.5 • | 1.2 | 1.3 |

**$^{2}$H labelled precursors**

| | Control | Acetate | $^{2}H_3$ Acetate |
|---|---|---|---|
| Phytol | 0.5 | 0.7 | 0.6 |
| $C_{25:3}$ E | 0.6 | 0.7 | 3.9 • |
| $C_{25:4}$ E | 0.7 | 0.6 | 4.3 • |
| $C_{25:5}$ E | 0.6 | 0.8 | 4.4 • |
| $C_{30:5}$ Z | 0.5 | 0.4 | 3.7 • |
| $C_{30:5}$ E | 0.5 | 0.6 | 3.5 • |
| $C_{30:6}$ Z | 0.7 | 0.5 | 3.8 • |
| $C_{30:6}$ E | 0.5 | 0.5 | 4.2 • |
| Desmosterol | 0.8 | 0.7 | 3.8 • |

(• Significant incorporation; n/a Below limit of detection)

**Varying concentrations of isotopically labelled acetate and stable isotope incorporation:**

In order to carry out stable isotope incorporation studies on a scale sufficient for analysis of lipids by NMR spectroscopy, a series of preliminary experiments was undertaken to optimise conditions. This was achieved by culturing *R. setigera* in the presence of increasing concentrations of $^{13}$C-labelled acetate, with subsequent measurement of isotopic incorporation into the HBIs, desmosterol and phytol. With the exception of phytol, an increase of the percentage of $^{13}$C incorporated into the other isoprenoids was observed with increasing $^{13}$C-acetate concentration. Consistent with previous observations (Table 4.5), phytol was not labelled by $^{13}$C-acetate at any of the concentrations used (Table 4.6). For the HBIs and desmosterol, the average isotopic enrichment factors for these compounds were approximately 1.4 when a concentration of 0.01 g $l^{-1}$ of acetate was added to the culture medium, 2.3 when a concentration of 0.1 g $l^{-1}$ of acetate was added to the culture medium, and 4.7 when the concentration was increased ten-fold to 1 g $l^{-1}$. These results suggested that in order to obtain sufficient enrichment for analysis by NMR spectroscopy, a concentration of $^{13}$C-acetate in the range 0.25-0.5 g $l^{-1}$ at 50% isotopic enrichment (or equivalent) would probably be required.

Table 4.6 Isotopic enrichment factors for non-saponifiable lipids from *Rhizosolenia setigera* after incubation with varying concentrations of $^{13}C$ labelled acetate (50% isotopic enrichment).

| | [1-$^{13}$C] Acetate 0.01g l$^{-1}$ | [1-$^{13}$C] Acetate 0.1g l$^{-1}$ | [1-$^{13}$C] Acetate 1g l$^{-1}$ |
|---|---|---|---|
| Phytol | 1.1 | 1.1 | 1.2 |
| $C_{25:3}$ E | 1.3 | 2.2 | 4.2 |
| $C_{25:4}$ E | 1.4 | 2.3 | 4.9 |
| $C_{25:5}$ E | 1.5 | 2.6 | 4.6 |
| $C_{30:5}$ Z | 1.4 | 2.0 | 4.8 |
| $C_{30:5}$ E | n/a | n/a | n/a |
| $C_{30:6}$ Z | n/a | n/a | n/a |
| $C_{30:6}$ E | n/a | n/a | n/a |
| Desmosterol | 1.5 | 2.3 | 5.1 |

n/a Below limit of detection

**Inhibition experiment and stable isotope incorporation:**

From the observations made from the pathway-specific blocking experiments together with the small-scale isotope labelling experiments, it appears that in the diatom *Rhizosolenia setigera*, both pathways are contributing to the biosynthesis of non-saponifiable lipids. Phytol seems to be made exclusively *via* the mevalonate-independent pathway, while the contribution of the mevalonate pathway seems to be essential for the biosynthesis of HBIs and desmosterol. Given the difference in the results obtained with mother and daughter cells cultured in the presence of fosmidomycin (Section 4.3.3.1), it appears that, depending on the position of the cells within their life cycle, the mevalonate-independent pathway could also contribute to the biosynthesis of HBIs and sterols in this diatom. To check this hypothesis further, an experiment using both isotopically labelled acetate and fosmidomycin was performed. Tables 4.7 and 4.8 show the hydrocarbon concentrations (pg cell$^{-1}$) and isotopic enrichment factors for these hydrocarbons when *R. setigera* cells were incubated with [1-$^{13}$C] acetate at different isotopic percentages in the presence of increasing concentrations of fosmidomycin.

Consistent with the first set of inhibition experiments performed with daughter cells, fosmidomycin did not significantly reduce the growth of the cells even at relatively high concentration of the inhibitor. However, in contrast to the results observed during the first experiment with daughter cells, the synthesis of $C_{30}$ HBIs was not retarded by the presence of fosmidomycin. Moreover, the concentrations of these compounds were greater in the cells grown in the presence of fosmidomycin than in those from the control culture (*cf.* observations made for mother cells; Section 4.3.3.1). However, the formation of the $C_{25}$ HBIs, desmosterol and phytol were found to be significantly reduced with increasing fosmidomycin concentrations. As a result, the HBI distributions were significantly modified (reflected by the decreasing $C_{25}/C_{30}$ ratio) with increasing fosmidomycin concentrations. Since the two sets of experiments using daughter cells were carried out with differences in the culture conditions (e.g. absence/presence of added acetate), and with cells in (probably) different physiological states, it is difficult to make too many firm comparisons between them. However, what is clear is that there is dynamic use of both biosynthetic pathways in the synthesis of HBIs and desmosterol, and that the partitioning between the two pathways is dependent on the position of *R. setigera* within its life cycle. A more controlled study of this dynamic contribution from the two pathways is clearly worthy of future study.

In terms of isotopic incorporation, $^{13}C$ from the acetate added to the culture medium was not incorporated into phytol in any of the culture conditions tested. Interestingly, for the HBIs and desmosterol, similar and significant $^{13}C$ incorporation was observed at each condition tested indicating that these compounds were made at least in part *via* the mevalonate route. However, the degree of $^{13}C$ incorporation into these compounds also increased when the cells were cultured in the presence of increasing concentrations of fosmidomycin, consistent with a 'switch' to the mevalonate route when the MEP pathway is blocked.

Table 4.7 Biomass (cell $ml^{-1}$) and non-saponifiable lipids concentration (pg $cell^{-1}$) in *Rhizosolenia setigera* cells after incubation with [1-$^{13}$C] acetate and fosmidomycin.

| | 0% [1-$^{13}$C] Acetate | | | | | 20% [1-$^{13}$C] Acetate | | | | | 100% [1-$^{13}$C] Acetate | | | | |
|---|---|---|---|---|---|---|---|---|---|---|---|---|---|---|---|
| | 0 | 25 | 50 | 75 | 100 | 0 | 25 | 50 | 75 | 100 | 0 | 25 | 50 | 75 | 100 |
| Nb. cell $ml^{-1}$ ($x10^3$) | 43.6 | 51.4 | 55.0 | 48.0 | 52.2 | 47.2 | 50.8 | 56.0 | 53.2 | 54.6 | 51.0 | 54.0 | 53.6 | 53.4 | 55.4 |
| Phytol | 0.4 | 0.3 | 0.5 | 0.5 | 0.5 | 0.6 | 0.4 | 0.5 | 0.5 | n/a | 0.5 | 0.5 | n/a | n/a | n/a |
| $C_{25:3}$ E | 3.8 | 4.8 | 2.1 | 3.9 | 3.9 | 8.0 | 7.2 | 3.7 | 4.4 | 4.8 | 8.7 | 10.8 | 5.0 | 5.4 | 4.8 |
| $C_{25:4}$ E | 3.3 | 4.2 | 2.4 | 3.6 | 3.2 | 5.9 | 5.5 | 3.4 | 3.3 | 3.0 | 7.2 | 9.1 | 4.6 | 4.7 | 3.2 |
| $C_{25:5}$ E | 0.7 | 0.9 | 0.5 | 0.8 | 0.7 | 1.6 | 1.4 | 0.9 | 0.6 | 0.5 | 1.5 | 2.1 | 1.3 | 0.9 | 0.8 |
| $C_{30:5}$ Z | 4.9 | 7.2 | 6.7 | 11.8 | 12.2 | 11.1 | 10.3 | 7.6 | 8.4 | 12.1 | 6.1 | 10.7 | 7.6 | 10.7 | 12.2 |
| $C_{30:5}$ E | 6.4 | 6.8 | 6.2 | 10.7 | 11.0 | 12.3 | 9.9 | 6.7 | 8.0 | 10.5 | 7.8 | 10.6 | 6.9 | 9.9 | 11.7 |
| $C_{30:6}$ Z | 2.8 | 4.1 | 3.7 | 6.2 | 6.2 | 6.2 | 6.2 | 5.1 | 4.8 | 5.5 | 4.2 | 7.6 | 4.9 | 5.8 | 5.8 |
| $C_{30:6}$ E | 4.5 | 5.1 | 5.0 | 8.4 | 8.0 | 9.0 | 8.2 | 6.2 | 6.2 | 7.0 | 6.3 | 8.7 | 5.7 | 7.7 | 7.7 |
| Desmosterol | 2.7 | 3.6 | 3.6 | 6.3 | 5.4 | 6.5 | 4.0 | 5.1 | 3.5 | 2.6 | 4.6 | 7.0 | 3.2 | 2.6 | 3.0 |
| Total $C_{25}$ | 7.8 | 9.9 | 5.0 | 8.3 | 7.8 | 15.5 | 14.1 | 8.0 | 8.3 | 8.3 | 17.4 | 22.0 | 10.9 | 11.0 | 8.8 |
| Total $C_{30}$ | 18.6 | 23.2 | 21.6 | 37.1 | 37.4 | 38.6 | 34.6 | 25.6 | 27.4 | 35.1 | 24.4 | 37.6 | 25.1 | 34.1 | 37.4 |
| $C_{25}/C_{30}$ | 0.42 | 0.43 | 0.23 | 0.22 | 0.21 | 0.40 | 0.41 | 0.31 | 0.30 | 0.24 | 0.71 | 0.59 | 0.43 | 0.32 | 0.24 |

n/a Below limit of detection

Table 4.8 Isotopic enrichment factors for non-saponifiable lipids from *Rhizosolenia setigera* cells after incubation with [1-$^{13}$C] acetate and fosmidomycin.

| | 0% [1-$^{13}$C] Acetate | | | | | 20% [1-$^{13}$C] Acetate | | | | | 100% [1-$^{13}$C] Acetate | | | | |
|---|---|---|---|---|---|---|---|---|---|---|---|---|---|---|---|
| | 0 | 25 | 50 | 75 | 100 | 0 | 25 | 50 | 75 | 100 | 0 | 25 | 50 | 75 | 100 |
| Phytol | 1.5 | n/a | n/a | n/a | n/a | n/a | 1.2 | n/a | n/a | n/a | 1.1 | n/a | n/a | n/a | n/a |
| $C_{25:3}$ E | 0.9 | 1.0 | 0.9 | 1.0 | 1.1 | 2.1 | 2.0 | 2.2 | 2.4 | 2.4 | 5.6 | 6.2 | 6.2 | 7.4 | 7.9 |
| $C_{25:4}$ E | n/a | n/a | n/a | n/a | n/a | n/a | n/a | n/a | n/a | n/a | n/a | n/a | n/a | n/a | n/a |
| $C_{25:5}$ E | n/a | n/a | n/a | n/a | n/a | n/a | n/a | n/a | n/a | n/a | n/a | n/a | n/a | n/a | n/a |
| $C_{30:5}$ Z | 0.8 | 1.0 | 1.1 | 1.3 | 1.0 | 1.7 | 2.3 | 2.0 | 2.4 | 2.5 | 4.6 | 4.6 | 5.1 | 6.2 | 7.0 |
| $C_{30:5}$ E | 0.8 | 1.1 | 1.1 | 1.2 | 1.0 | 1.9 | 2.2 | 2.0 | 2.0 | 2.5 | 4.3 | 4.3 | 6.1 | 6.9 | 8.0 |
| $C_{30:6}$ Z | 0.7 | 1.1 | 0.9 | 1.1 | 1.2 | 1.9 | 1.7 | 1.9 | 2.2 | 2.2 | 4.9 | 4.4 | 6.7 | 6.5 | 7.1 |
| $C_{30:6}$ E | 1.0 | 1.3 | 1.7 | 1.1 | 0.7 | 2.0 | 2.1 | 1.7 | 2.1 | 2.2 | 5.0 | 4.7 | 5.5 | 6.5 | 8.3 |
| Desmosterol | 1.1 | 1.2 | 1.2 | 1.1 | 1.0 | 2.1 | 2.2 | 2.4 | 2.1 | 2.2 | 5.7 | 6.0 | 6.4 | 7.2 | 7.1 |

n/a Below limit of detection

*4.3.3.3 Isotope labelling: large scale experiments*

In order to complement the experiments carried out with inhibitors and isotopically enriched substrates (small-scale), large-scale cultures were grown in order to establish the positional incorporation of the various isotopes by analysis of purified lipids by NMR spectroscopy. Since the small-scale experiments had determined those substrates that showed evidence of isotopic incorporation (*viz.* $CO_2$ and acetate), these larger-scale studies were carried out using these precursors only. The resulting labelling patterns in individual lipids (including isomers of HBI alkenes) was achieved using NMR spectroscopy. A summary of these experiments is shown in Table 4.9.

Table 4.9 Large-scale experiments using isotopically labelled substrates in cultures of the diatom *Rhizosolenia setigera.*

| | Control | Experiment 1 | Experiment 2 | Experiment 3 | Experiment 4 | Experiment 5 |
|---|---|---|---|---|---|---|
| Labelled precursor | None | [1-$^{13}$C] Acetate | [1-$^{13}$C] Acetate | $^{13}CO_2$ | [2-$^{13}$C] Acetate | $^{2}H_3$ Acetate |
| Isotopic abudance | Natural | 20% | 99% | 20% | 20% | 20% |
| Acetate | 250 mg $l^{-1}$ | 250 mg $l^{-1}$ | 250 mg $l^{-1}$ | 250 mg $l^{-1}$ | 250 mg $l^{-1}$ | 250 mg $l^{-1}$ |
| $CO_2$ | 10 mg $l^{-1}$ | 10 mg $l^{-1}$ | 10 mg $l^{-1}$ | 150 mg $l^{-1}$ | 10 mg $l^{-1}$ | 10 mg $l^{-1}$ |

**Stable isotope incorporation – analysis by mass spectrometry**

At the end of the exponential growing phase for each large-scale culture, the cells were harvested by filtration and the non-saponifiable lipids analysed using the methodology described in Chapter 5. Identification of individual compounds together with their isotopic enrichment factors was determined by GC-MS (Table 4.10). These results were consistent with those obtained from the small-scale incubation studies. Thus, while the isotopic composition of phytol was not effected by the presence of labelled acetate, $^{2}H$ and $^{13}C$ were significantly incorporated into HBIs and desmosterol isolated from cells cultured in the presence of $^{2}H_3$-acetate and $^{13}C$-acetate, respectively. In contrast, when the cells were

cultured in the presence of $^{13}CO_2$, $^{13}C$ was incorporated into all of the non-saponifiable lipids as expected.

Table 4.10 Isotope enrichment factors for non-saponifiable lipids from *Rhizosolenia setigera* after incubation with labelled ($^{13}C$ or $^{2}H$) precursors (large scale experiments).

| | Experiment 1 [1-$^{13}$C] Acetate | Experiment 2 [1-$^{13}$C] Acetate | Experiment 3 $^{13}CO_2$ | Experiment 4 [2-$^{13}$C] Acetate | Experiment 5 $^{2}H_3$ Acetate |
|---|---|---|---|---|---|
| Phytol | 1.4 | 1.7 | 7.6 | n/a | 0.9 |
| $C_{25:3}$ E | 1.7 | 4.8 | 6.6 | 1.8 | 2.1 |
| $C_{25:4}$ E | n/a | n/a | 7.0 | n/a | 2.3 |
| $C_{25:5}$ E | 1.7 | 4.4 | 6.7 | 2.1 | 2.0 |
| $C_{30:5}$ Z | 1.7 | 4.6 | 6.6 | 1.8 | 1.9 |
| $C_{30:5}$ E | 1.7 | 4.5 | 6.6 | 2.3 | 2.3 |
| $C_{30:6}$ Z | 1.7 | 4.7 | 6.4 | 2.2 | 2.2 |
| $C_{30:6}$ E | n/a | n/a | 6.7 | n/a | n/a |
| Desmosterol | 2.6 | 4.7 | 6.5 | n/a | 2.0 |

n/a Below limit of detection

**Site-specific isotopic incorporation: analysis by NMR spectroscopy**

Following GC-MS analysis of a small aliquot of the total organic extracts obtained from large-scale cultures of *R. setigera*, HBIs, phytol, and desmosterol were isolated using open column chromatographic techniques following the methodology described in Chapter 5. Individual HBI isomers were obtained using silver-ion ($Ag^+$) chromatography techniques on a preparative HPLC system. Figure 4.10 shows a representative chromatogram of a mixture of compounds from *R. setigera* obtained using silver ion chromatography techniques, while Figure 4.11 shows partial GC-MS TIC chromatograms obtained from various sub-fractions (A-G). Table 4.11 summarises the quantities of isolated compounds obtained from the various large-scale experiments.

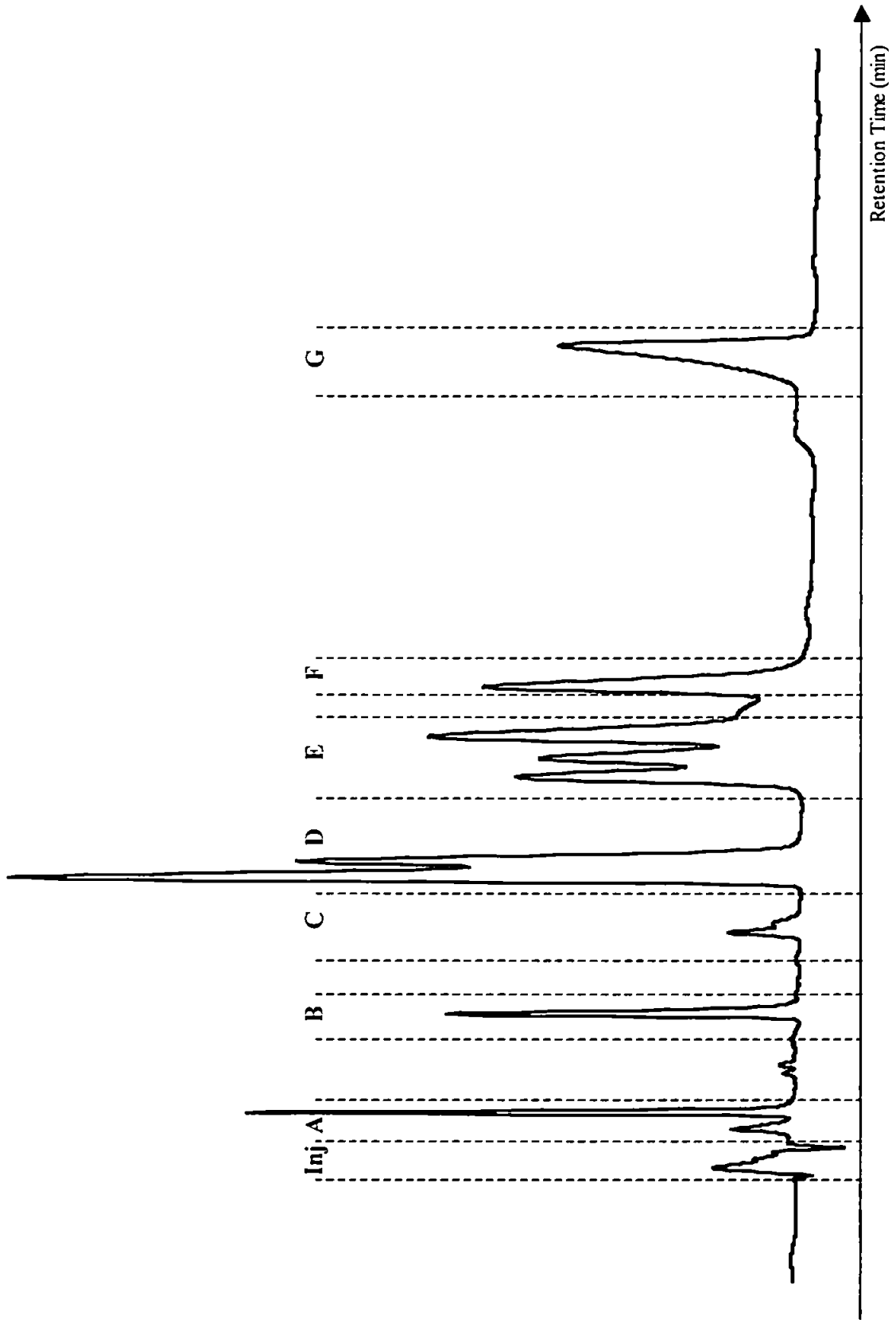


Figure 4.10 Ag-HPLC chromatogram of an hydrocarbon extract of *Rhizosolenia setigera* RS 99. Flow rate, 1 ml min-1, hexane-isopropanol (98.75:1.25, v/v).

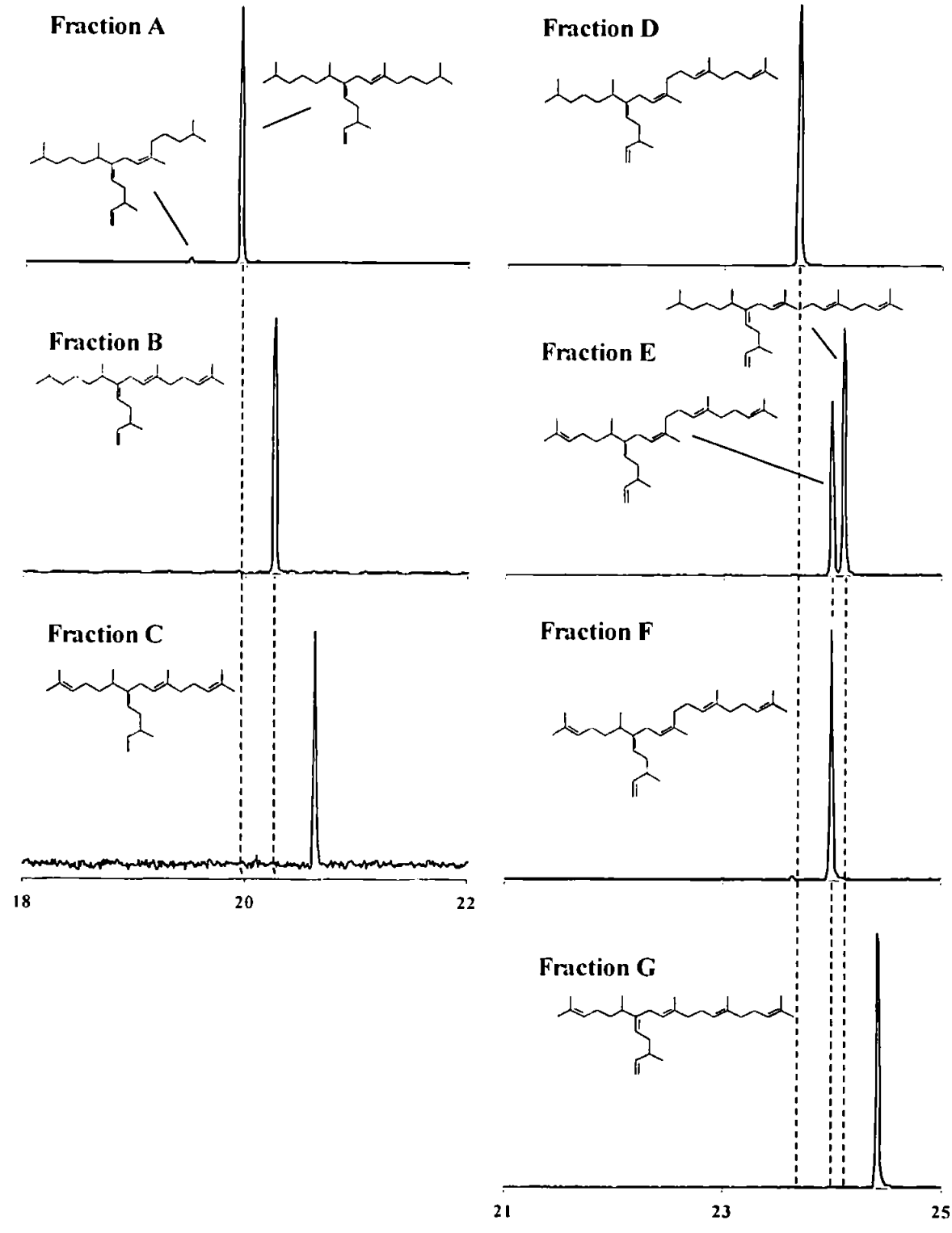


Figure 4.11 Partial TIC chromatograms of fractions A-G obtained from Ag-HPLC of an hydrocarbon fraction from *Rhizosolenia setigera* RS 99.

Table 4.11 Quantities of non-saponifiable lipids (mg) obtained from large-scale cultures of *R. setigera* containing isotopically enriched substrates.

| | Control | Experiment 1 | Experiment 2 | Experiment 3 |
|---|---|---|---|---|
| Phytol | **1.4** | **0.1** | - | **0.8** |
| $C_{25:3}$ E | **1.1** | **0.4** | **0.4** | 0.1 |
| $C_{25:4}$ E | 0.1 | - | 0.1 | 0.1 |
| $C_{30:5}$ Z | **11.1** | **1.3** | **0.7** | **0.8** |
| $C_{30:5}$ E | **3.3** | **0.9** | **0.4** | 0.2 |
| $C_{30:6}$ Z | - | 0.3 | 0.3 | 0.4 |
| $C_{30:6}$ E | - | 0.4 | 0.2 | 0.2 |
| $C_{30:4:1}$ | **10.5** | **0.7** | < 0.1 | - |
| Desmosterol | **9.5** | **5.8** | - | 0.6 |

$^{13}C$ NMR spectra were recorded for the compounds shown in bold in Table 4.11. Relative $^{13}C$ abundances for individual carbon nuclei were determined by comparing the relative intensities of $^{13}C$ peaks from samples obtained from labelled and unlabelled (control) cultures. For $C_{25}$ - $C_{30}$ HBIs and the monocyclic compound $C_{30:4:1}$, C-5 (Figures 4.12, 4.13, 4.15, numbering schemes) was used as an internal reference since this carbon was not expected to be labelled by the $^{13}C$ from the [1-$^{13}C$] acetate in these compounds. In the case of desmosterol, C-1 was used as the internal reference (Figure 4.16, numbering scheme). This approach was also used for the analysis of the non-saponifiable lipids isolated from the cells cultured in the presence of $^{13}C$ enriched $CO_2$. However, since all of the carbon atoms of each molecule were expected to be labelled using this substrate, the spectroscopic comparison between $^{13}C$ labelled and 'unlabelled' compounds was only used to demonstrate whether the labelling was indeed uniform. In these cases, the level of incorporation was estimated using mass-spectrometry techniques.

***Phytol***

Corroborating the observations made from small-scale experiments (Section 4.3.3.2), examination of the $^{13}C$ NMR spectrum and mass spectrum obtained for phytol isolated from *R. setigera* cells grown in the presence of [1-$^{13}C$] labelled acetate revealed that there was no incorporation of $^{13}C$ into this compound. In contrast, phytol was uniformly labelled when the cells were incubated in the presence of $^{13}CO_2$ suggesting that this compound arises directly from $CO_2$, and is probably made exclusively by the mevalonate-independent pathway.

***$C_{30:5}$ (Z, IV)***

The $^{13}C$ NMR spectrum and mass spectrum of the $C_{30}$ pentaene $C_{30:5}$ (Z, IV) revealed that similar to phytol, $^{13}C$ was uniformly incorporated into this compound when *R. setigera* cells were incubated in the presence of $^{13}C$ labelled $CO_2$ (Tables 4.12 and 4.13). However, in contrast to phytol, examination of the $^{13}C$ NMR spectrum obtained for this compound isolated from cells grown in the presence of [1-$^{13}C$] labelled acetate revealed that $^{13}C$ signals corresponding to C-2,4,6,8,10,12,14,16,18,25,27,29 were enhanced in $^{13}C$ relative to the reference carbon (C-5). Averaged enhancement factors were 1.8 and 6.4 for Experiments 1 and 2, respectively, corresponding to 20% and 100% isotope abundance of [1-$^{13}C$] acetate (Table 4.12). These $^{13}C$ enriched carbon atoms correspond to C-1 and C-3 of the (six) IPP precursors that the $C_{30}$ HBIs are made from (Table 4.13). Thus, from these observations, it is now clearly demonstrated that acetate is directly incorporated into $C_{30:5}$ (Z) according to the mevalonate pathway. Figure 4.12 shows the expected / observed labelling pattern for $C_{30:5}$ (Z) obtained from cells cultured in the presence of [1-$^{13}C$] acetate.

Table 4.13 Average $^{13}C$ enhancements of individual IPP carbon atoms within $C_{30:5}$ (Z, IV) HBI isolated from *R. setigera* cells cultured in the presence of various $^{13}C$ labelled substrates.

| Carbon atom of IPP | Control | [1-$^{13}$C] acetate (20%) | [1-$^{13}$C] acetate (100%) | $^{13}CO_2$ (20%) |
|---|---|---|---|---|
| C-1 | 1.1 | **1.9** | **6.9** | 0.9 |
| C-2 | 0.9 | 0.9 | 0.8 | 0.9 |
| C-3 | 0.7 | **1.7** | **5.9** | 0.8 |
| C-4 | 1.0 | 0.9 | 1.0 | 0.9 |
| C-5 | 0.7 | 0.8 | 1.0 | 1.0 |

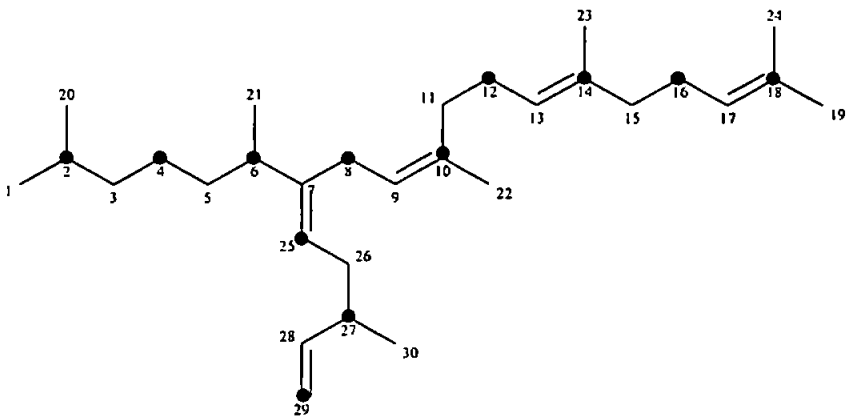


Figure 4.12 Numbering scheme and observed labelling pattern (•) in $C_{30:5}$ (Z, IV) HBI after feeding *R. setigera* cells with [1-$^{13}$C] labelled acetate.

### *$C_{30:5}$ (E, V)*

The $^{13}C$ NMR spectrum of $C_{30:5}$ (E, V) from cells grown in the presence of [1-$^{13}$C] acetate revealed that $^{13}C$ signals corresponding to C-2,4,6,8,10,12,14,16,18,25,27,29 were enhanced with $^{13}C$ by factors of 2.4 and 8.3 for enrichment of 20% and 100% in [1-$^{13}$C] acetate ,respectively (Table 4.14). These observations are entirely consistent with those made for the closely related Z isomer described previously, with enhanced positions corresponding to C-1 and C-3 of IPP (Table 4.15). Thus, from these observations, it is clearly demonstrated that both E and Z isomers of the $C_{30}$ pentaene are biosynthesised using acetate *via* the mevalonate pathway in their biosyntheses.

Table 4.15 Average $^{13}C$ enhancements of individual IPP carbon atoms within $C_{30:5}$ (E, V) HBI isolated from *R. setigera* cells cultured in the presence of [1-$^{13}C$] acetate.

| Carbon atom of IPP | Control | [1-$^{13}C$] acetate (20%) | [1-$^{13}C$] acetate (100%) |
|---|---|---|---|
| C-1 | 1.0 | **2.5** | **9.2** |
| C-2 | 0.8 | 1.1 | 1.2 |
| C-3 | 0.7 | **2.2** | **7.5** |
| C-4 | 1.0 | 1.0 | 1.0 |
| C-5 | 0.9 | 0.8 | 0.9 |

### *$C_{25:3}$ (E, VIII)*

The $^{13}C$ NMR spectrum of the $C_{25}$ triene ($C_{25:3}$ (E, VIII)) revealed that $^{13}C$ signals corresponding to C-2,4,6,8,10,12,14,20,22,24 were enhanced in $^{13}C$ (by factors of 2.0 and 7.8 for cultures containing 20% and 100% [1-$^{13}C$] acetate respectively; Table 4.16). As expected, these carbon atoms correspond to C-1 and C-3 of the (five) IPP precursors from which this compound is made (Table 4.17). Figure 4.13 shows the expected / observed labelling pattern observed for this compound after feeding cells of *R. setigera* with [1-$^{13}C$] acetate.

From these $^{13}C$ NMR spectroscopic measurements, it can be summarised that both $C_{25}$ and $C_{30}$ HBIs in *R. setigera* are biosynthesised (at least in part) *via* the acetate/mevalonate pathway.

Table 4.17 Average $^{13}C$ enhancements of individual IPP carbon atoms within $C_{25:3}$ (E, VIII) HBI isolated from *R. setigera* cells cultured in the presence of [1-$^{13}C$] acetate.

| Carbon atom of IPP | Control | [1-$^{13}C$] acetate 20% of $^{13}C$ | [1-$^{13}C$] acetate 100% of $^{13}C$ |
|---|---|---|---|
| C-1 | 1.1 | **2.0** | **7.3** |
| C-2 | 0.9 | 0.7 | 1.2 |
| C-3 | 0.7 | **2.1** | **8.3** |
| C-4 | 1.1 | 0.9 | 1.0 |
| C-5 | 0.9 | 0.9 | 1.0 |

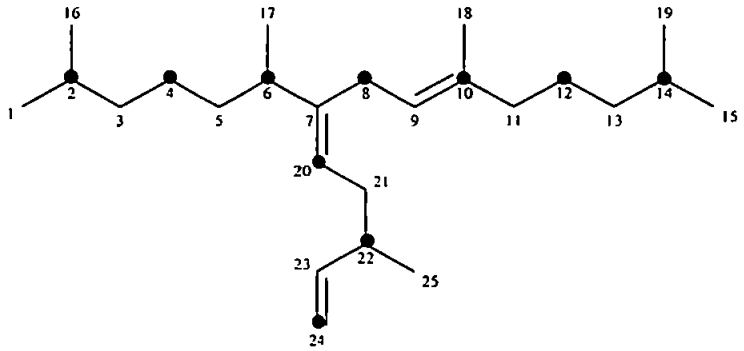


Figure 4.13 Numbering scheme and observed labelling pattern in $C_{25:3}$ (E) after feeding *R. setigera* cells with [1-$^{13}$C] labelled acetate.

### *$C_{30:4:1}$ (XI)*

Fractionation of individual $C_{25}$ and $C_{30}$ HBIs also provided the opportunity to investigate the biosynthesis of one of the monocyclic $C_{30}$ hydrocarbons by NMR spectroscopy. However, owing to the relatively low abundance of this isomer in the majority of cultures, sufficient quantity for analysis by $^{13}$C NMR spectroscopy was only available from the 20% [1-$^{13}$C] enriched acetate experiment. From the $^{13}$C NMR spectrum obtained for this compound, signals from C-2,4,6,8,10,12,14,16,21,23,25,27, corresponding to C-1 and C-3 of the six IPP precursor molecules that give rise to this compound, were enhanced in $^{13}$C, with an average enhancement factor of 1.9; Table 4.19). However, although this average enhancement is similar to that observed found for the acyclic $C_{30}$ pentaenes isolated from the same culture, when the individual IPP units were examined in more detail, it was found that for some of these (IPP-2, 3 and 6, Figure 4.14), the C-3 atom did not show a clear enhancement compared to positions C-2, C-4 and C-5 (Table 4.18, Figure 4.15). In contrast, C-1 for these three IPP units (IPP-2, 3 and 6) exhibited similar $^{13}$C enhancements to the C-1 and C-3 atoms of the other IPP units (IPP-1, 4 and 5). This contrasts with the enhancements observed for the two acyclic $C_{30:5}$ isomers which exhibited extremely uniform labelling for the C-1 and C-3 positions of IPP throughout (Tables 4.12 and 4.13).

Table 4.19 Average $^{13}C$ enhancements of individual IPP carbon atoms within the monocyclic $C_{30}$ hydrocarbon $C_{30:4:1}$ (XI) isolated from *R. setigera* cells cultured in the presence of 20% enriched [1-$^{13}C$] acetate.

| Carbon atom of IPP | Control | [1-$^{13}C$] acetate (20%) |
|---|---|---|
| C-1 | 1.0 | **2.1** |
| C-2 | 1.0 | 1.1 |
| C-3 | 0.5 | **1.7** |
| C-4 | 0.9 | 1.1 |
| C-5 | 0.8 | 1.1 |

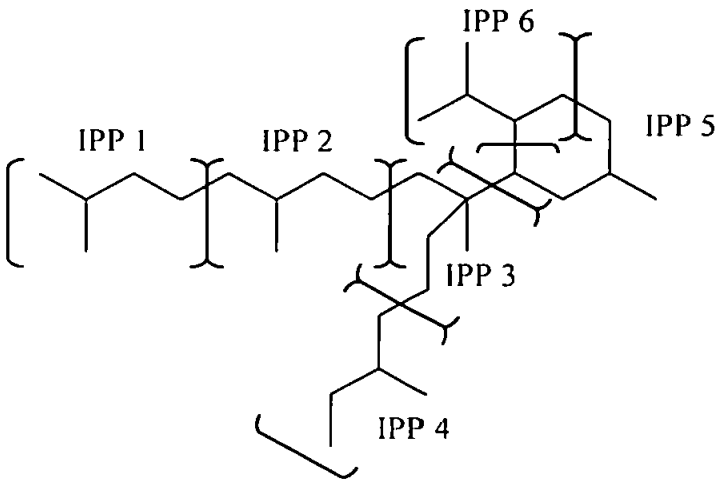


Figure 4.14 Proposed arrangement of six IPP units within $C_{30:4:1}$ (XI).

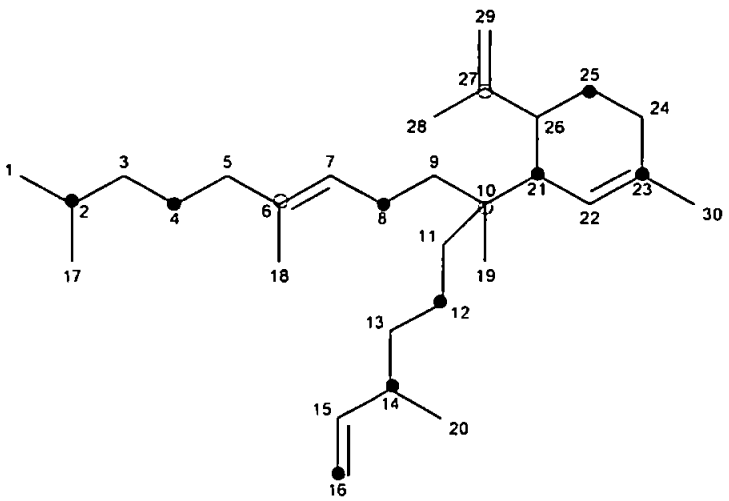


Figure 4.15 Numbering scheme and observed labelling pattern in $C_{30:4:1}$ (XI) after feeding *R. setigera* cells with [1-$^{13}C$] acetate. • clear and significant incorporation of $^{13}C$, o reduced or unclear incorporation of $^{13}C$.

***Desmosterol (III)***

The $^{13}C$ NMR spectrum obtained from desmosterol (III) isolated from *R. setigera* cells cultured in the presence of 20% enriched [1-$^{13}C$] acetate, showed enhanced signals corresponding to C-2,4,6,8,10,11,12,14,16,20,23,25. (Table 4.20) with an average enhancement of 1.6; Table 4.21). However, in a manner similar to that described previously for $C_{30:4:1}$, not all of the IPP units (Figure 4.16) showed a clear enhancement of both C-1 or C-3 positions compared to those for the corresponding C-2, C-4 and C-5 atoms.

Table 4.21 Average $^{13}C$ enhancements of individual IPP carbon atoms within desmosterol (III) isolated from *R. setigera* cells cultured in the presence of 20% enriched [1-$^{13}C$] acetate.

| Carbon atom of IPP | Control | [1-$^{13}C$] acetate (20%) |
|---|---|---|
| C-1 | 1.0 | 1.5 |
| C-2 | 0.7 | 1.0 |
| C-3 | 0.7 | 1.6 |
| C-4 | 0.8 | 1.0 |
| C-5 | 0.8 | 0.8 |

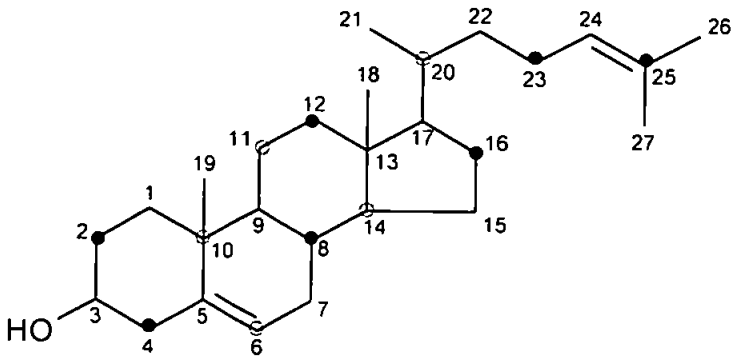


Figure 4.16 Numbering scheme and observed labelling pattern in desmosterol (III) after feeding *R. setigera* cells with [1-$^{13}C$] labelled acetate. ● clear and significant incorporation of $^{13}C$, o reduced or unclear incorporation of $^{13}C$.

Table 4.12 $^{13}C$ NMR data for $C_{30:5}$ (Z, IV) obtained from *R. setigera* grown in the presence of various isotopically labelled substrates.

| Carbon number | Chemical shift (ppm) | Carbon atom of IPP | Control | [1-$^{13}$C] acetate 20% | [1-$^{13}$C] acetate 100% | $^{13}CO_2$ 20% |
|---|---|---|---|---|---|---|
| 28 | 144.7 | 2 | 0.6 | 0.9 | 0.9 | 1.0 |
| 7 | 143.1 | 2 | 0.5 | 0.7 | 0.5 | 0.6 |
| 10 | 135.7 | 3 | 0.5 | 1.3 | 4.7 | 0.6 |
| 14 | 135.1 | 3 | 0.4 | 1.6 | 5.5 | 0.7 |
| 18 | 131.3 | 3 | 0.2 | 1.3 | 5.3 | 0.6 |
| 13 | 124.5 | 2 | 0.9 | 0.9 | 0.9 | 0.9 |
| 17 | 124.3 | 2 | 1.1 | 0.8 | 0.8 | 0.9 |
| 9 | 124.1 | 2 | 1.0 | 1.0 | 1.1 | 1.0 |
| 25 | 122.9 | 1 | 1.2 | 1.8 | 5.7 | 0.8 |
| 29 | 112.2 | 1 | 1.1 | 1.8 | 6.9 | 1.0 |
| 15 | 39.8 | 4 | 1.0 | 0.7 | 0.8 | 0.8 |
| 3 | 39.4 | 2 | 1.2 | 0.8 | 0.9 | 0.9 |
| 27 | 38.3 | 3 | 1.1 | 1.9 | 6.5 | 0.9 |
| 5 | 35.4 | 4 | 1.0 | 1.0 | 1.0 | 1.0 |
| 26 | 34.5 | 4 | 1.3 | 0.8 | 0.9 | 0.9 |
| 6 | 34.4 | 3 | 1.2 | 2.0 | 6.7 | 0.9 |
| 11 | 31.9 | 4 | 1.2 | 0.9 | 0.9 | 0.9 |
| 8 | 29.1 | 1 | 1.1 | 1.7 | 6.8 | 0.7 |
| 2 | 28 | 3 | 0.8 | 1.9 | 6.9 | 0.8 |
| 12 | 26.8 | 1 | 1.2 | 1.8 | 6.2 | 0.8 |
| 16 | 26.7 | 1 | 1.2 | 1.9 | 7.0 | 0.9 |
| 4, 19 | 25.8 | 1, 4 | 0.9 | 1.6* | 4.9* | 0.9 |
| 22 | 23.6 | 5 | 1.0 | 0.8 | 0.9 | 0.9 |
| 1, 20 | 22.7 | 4, 5 | 0.8 | 0.8 | 1.1 | 1.0 |
| 21, 30 | 19.6 | 5, 5 | 0.7 | 0.7 | 1.1 | 1.0 |
| 24 | 17.8 | 5 | 0.5 | 0.8 | 1.1 | 1.0 |
| 23 | 16 | 5 | 0.6 | 0.6 | 0.7 | 0.9 |

* According to the labelling pattern from the mevalonate pathway, only C-4 should be labelled.

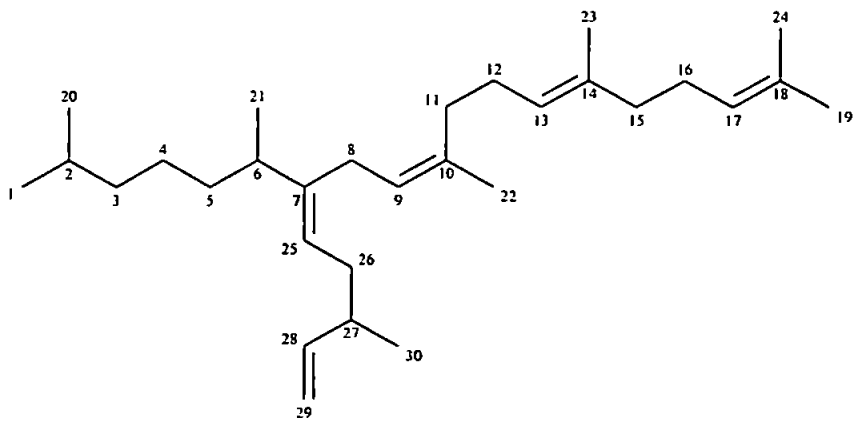

Table 4.14 $^{13}C$ NMR data for $C_{30:5}$ (E, V) obtained from *R. setigera* grown in the presence of [1-$^{13}C$] acetate.

| Carbon number | Chemical shift (ppm) | Carbon atom of IPP | Control | [1-$^{13}C$] acetate 20% | [1-$^{13}C$] acetate 100% |
|---|---|---|---|---|---|
| 28 | 144.7 | 2 | 0.6 | 1.2 | 1.3 |
| 7 | 142.7 | 2 | 0.5 | 1.0 | 1.0 |
| **10** | 135.7 | **3** | 0.5 | **1.9** | **7.1** |
| **14** | 135 | **3** | 0.4 | **2.3** | **6.9** |
| **18** | 131.4 | **3** | 0.3 | **2.0** | **7.7** |
| 13 | 124.5 | 2 | 0.8 | 1.0 | 1.4 |
| 17 | 124.4 | 2 | 1.0 | 1.1 | 1.1 |
| 9 | 123.4 | 2 | 0.8 | 1.1 | 1.2 |
| **25** | 122.8 | **1** | 1.0 | **2.5** | **8.4** |
| **29** | 112.3 | **1** | 1.2 | **2.3** | **7.8** |
| 11 | 39.9 | 4 | 1.1 | 1.2 | 1.1 |
| 15 | 39.8 | 4 | 1.2 | 0.8 | 0.8 |
| 3 | 39.3 | 2 | 1.1 | 1.0 | 1.0 |
| **27** | 38.3 | **3** | 1.0 | **2.2** | **7.9** |
| 5 | 35.4 | 4 | 1.0 | 1.0 | 1.0 |
| 26 | 34.5 | 4 | 1.1 | 1.2 | n/a |
| **6** | 34.4 | **3** | 1.0 | **2.6** | **8.1** |
| **8** | 29.3 | **1** | 0.7 | **2.5** | **9.5** |
| **2** | 28 | **3** | 0.9 | **2.2** | **7.3** |
| **12** | 26.8 | **1** | 1.3 | **2.4** | **8.6** |
| **16** | 26.7 | **1** | 1.3 | **2.5** | **9.5** |
| **4, 19** | 25.8 | **1, 4** | 0.8 | **1.9*** | **6.1*** |
| 1, 20 | 22.7 | 4, 5 | 1.1 | 1.0 | 1.0 |
| 21 | 19.7 | 5 | 1.4 | 0.8 | 1.2 |
| 30 | 19.6 | 5 | 1.2 | 1.0 | 1.1 |
| 24 | 17.8 | 5 | 0.5 | 0.5 | 0.8 |
| 23 | 16 | 5 | 0.6 | 0.8 | 0.7 |
| 22 | 15.9 | 5 | 0.7 | 0.8 | 0.7 |

* According to the labelling pattern from the mevalonate pathway, only C-4 should be labelled.

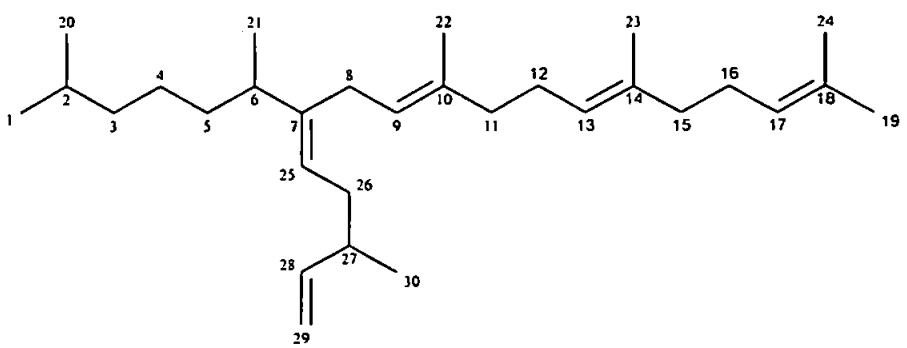

Table 4.16 $^{13}C$ NMR data for $C_{25:3}$ (E, VIII) obtained from *R. setigera* grown in the presence of [1-$^{13}C$] acetate.

| Carbon number | Chemical shift (ppm) | Carbon atom of IPP | Control | [1-$^{13}C$] acetate 20% of $^{13}C$ | [1-$^{13}C$] acetate 100% of $^{13}C$ |
|---|---|---|---|---|---|
| 23 | 144.7 | 2 | 0.7 | 0.5 | 1.2 |
| 7 | 142.8 | 2 | 0.4 | 1.1 | n/a |
| **10** | 136 | **3** | 0.2 | **2.3** | **7.0** |
| 9 | 123.2 | 2 | 1.1 | 0.7 | 1.7 |
| **20** | 122.8 | **1** | 1.2 | **2.0** | **6.2** |
| **24** | 112.2 | **1** | 1.3 | **1.8** | **7.4** |
| 11 | 40.1 | 4 | 1.2 | 0.6 | 1.0 |
| 3 | 39.4 | 2 | 1.2 | 0.9 | 1.0 |
| 13 | 38.8 | 2 | 1.2 | 0.5 | 0.8 |
| **22** | 38.3 | **3** | 0.9 | **1.7** | **8.5** |
| 5 | 35.4 | 4 | 1.0 | 1.0 | 1.0 |
| 21 | 34.5 | 4 | 1.2 | 1.0 | 0.8 |
| **6** | 34.4 | **3** | 1.2 | **2.3** | **7.9** |
| **8** | 29.3 | **1** | 1.0 | **1.7** | **6.5** |
| **2,14** | 28 | **3,3** | 0.7 | **2.0** | **9.0** |
| **12** | 25.9 | **1** | 1.0 | **1.9** | **7.5** |
| **4** | 25.8 | **1** | 1.2 | **2.4** | **9.0** |
| 1,15,16,19 | 22.7 | 4,4,5,5 | 1.1 | 0.8 | 1.0 |
| 17,25 | 19.6 | 5,5 | 0.8 | 1.0 | 1.1 |
| 18 | 15.8 | 5 | 0.7 | 0.8 | 0.6 |

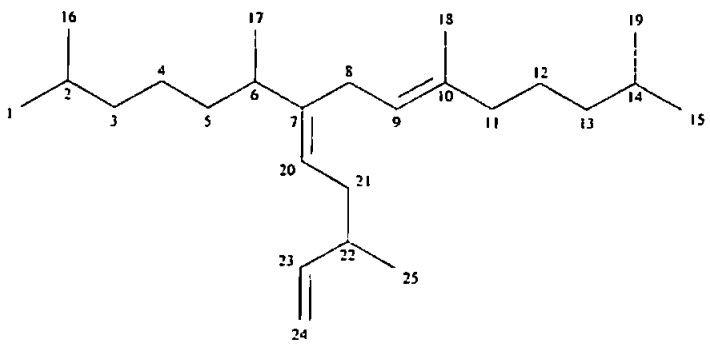

Table 4.18 $^{13}C$ NMR data for $C_{30:4:1}$ (XI) obtained from *R. setigera* grown in the presence of [1-$^{13}C$] acetate.

| Carbon number | Chemical shift (ppm) | Carbon atom of IPP | Control | [1-$^{13}C$] acetate 20% |
|---|---|---|---|---|
| **27** | 148.1 | **3** | 0.4 | **1.4** |
| 15 | 145.1 | 2 | 0.7 | 0.8 |
| **23** | 136.0 | **3** | 0.5 | **1.9** |
| **6** | 135.2 | **3** | 0.3 | **1.5** |
| 22 | 126.0 | 2 | 1.0 | 1.0 |
| 7 | 124.1 | 2 | 0.8 | 1.5 |
| **16** | 112.3 | **1** | 0.9 | **2.4** |
| 28 | 109.3 | 4 | 1.1 | 1.3 |
| **21** | 52.2 | **1** | 1.1 | **1.9** |
| 26 | 51.9 | 2 | 1.2 | 1.1 |
| **10** | 46.6 | **3** | 0.6 | **1.3** |
| 11 | 42.6 | 2 | 1.0 | 1.3 |
| 24 | 40.3 | 4 | 1.1 | 1.2 |
| 5 | 40.1 | 4 | 1.0 | 1.0 |
| 3 | 38.8 | 2 | 1.2 | 1.0 |
| 13 | 38.1 | 4 | 1.0 | 1.1 |
| 9,14 | 37.9 | 4,3 | 0.6 | **1.5*** |
| **25** | 28.8 | **1** | 1.0 | **1.8** |
| **2** | 28.0 | **3** | 0.7 | **1.9** |
| **8** | 26.7 | **1** | 1.2 | **1.7** |
| **4** | 25.9 | **1** | 0.9 | **2.2** |
| 1,17 | 22.8 | 4,5 | 0.8 | 1.3 |
| **12** | 22.6 | **1** | 0.9 | **2.5** |
| 19 | 21.1 | 5 | 0.9 | 1.4 |
| 20 | 20.3 | 5 | 1.0 | 1.2 |
| 29 | 20.0 | 5 | 0.9 | 0.9 |
| 30 | 16.7 | 5 | 0.8 | 0.9 |
| 18 | 16.0 | 5 | 0.6 | 0.9 |

* According to the labelling pattern from the mevalonate pathway, only C-14 should be labelled.

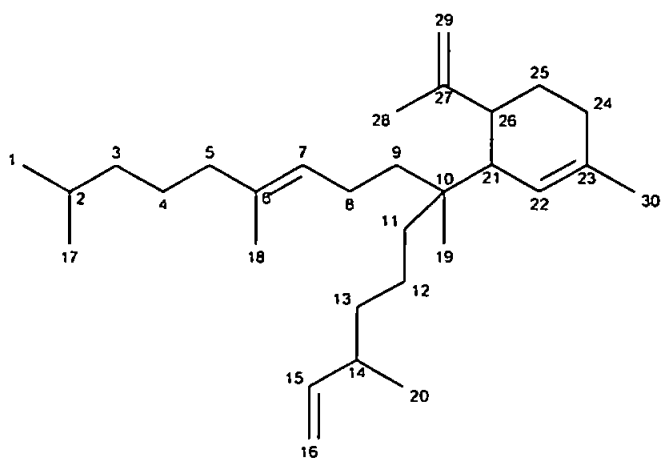

Table 4.20 $^{13}C$ NMR data for desmosterol (III) obtained from *R. setigera* grown in the presence of [1-$^{13}C$] acetate.

| Carbon number | Chemical shift (ppm) | Carbon atom of IPP | Control | [1-$^{13}C$] acetate 20% of $^{13}C$ |
|---|---|---|---|---|
| 5 | 140.8 | 2 | 0.5 | 1.5 |
| **25** | 131.1 | **3** | 0.3 | **2.9** |
| 24 | 125.3 | 2 | 0.8 | 1.3 |
| **6** | 121.8 | **1** | 1.2 | **1.5** |
| 3 | 71.9 | 4 | 1.0 | 1.3 |
| **14** | 56.8 | **3** | 1.1 | **1.5** |
| 17 | 56.1 | 2 | 1.0 | 0.6 |
| 9 | 50.2 | 2 | 1.2 | 0.7 |
| 13 | 42.4 | 2 | 0.6 | 1.3 |
| **4** | 42.3 | **3** | 1.1 | **1.6** |
| **12** | 39.8 | **1** | 0.9 | **2.4** |
| 1 | 37.3 | 4 | 1.1 | 1.1 |
| **10** | 36.6 | **3** | 0.5 | **1.6** |
| 22 | 36.2 | 4 | 0.9 | 0.9 |
| **20** | 35.7 | **3** | 1.1 | **1.2** |
| 7,8 | 31.9 | 4,3 | 0.8 | **1.5*** |
| **2** | 31.7 | **1** | 1.0 | **1.9** |
| **16** | 28.3 | **1** | 1.1 | **1.4** |
| 27 | 25.9 | 4 | 0.9 | 1.1 |
| **23** | 24.8 | **1** | 1.0 | **1.7** |
| 15 | 24.4 | 4 | 0.9 | 0.9 |
| **11** | 21.2 | **1** | 1.2 | **1.3** |
| 19 | 19.5 | 5 | 1.0 | 0.8 |
| 21 | 18.7 | 5 | 1.1 | 0.8 |
| 26 | 17.8 | 5 | 0.6 | 1.1 |
| 18 | 11.9 | ? | 1.0 | 0.8 |

* According to the labelling pattern from the mevalonate pathway, only C-8 should be labelled.

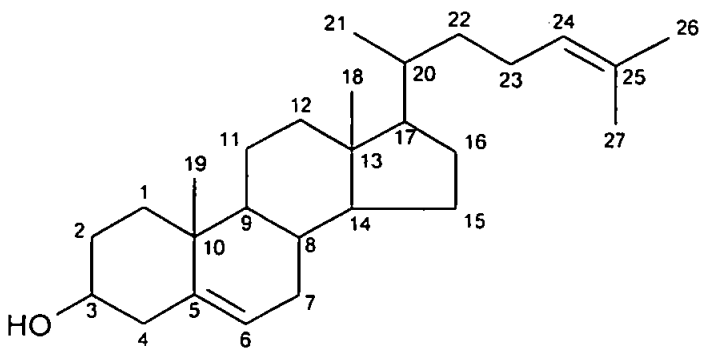

In summary, while the absence of $^{13}C$ incorporation into phytol from labelled acetate was confirmed by mass spectral and NMR analyses, a significant and uniform incorporation of $^{13}C$ from $^{13}CO_2$ (supplied as $Na_2{}^{13}CO_3$) was observed. From these observations, together with those taken from inhibition and small-scale isotopic enrichment experiments, it appears that phytol is made exclusively *via* the non-mevalonate (MEP) pathway. In contrast, NMR analyses on both $C_{25}$ and $C_{30}$ HBIs isolated from *R. setigera* cells cultured in the presence of [1-$^{13}C$] acetate clearly demonstrated a site-specific incorporation of $^{13}C$ according to the mevalonate pathway, consistent with inhibition of these compounds by mevinolin (Section 4.3.3.1). It also appears that acetate is directly incorporated into the major sterol of *R. setigera* (*viz.* desmosterol), together with the dominant monocyclic hydrocarbon ($C_{30:4:1}$), and therefore, the mevalonate pathway is also involved in the biosynthesis of these terpenes.

*4.3.3.4 Analysis of lipids from R. setigera by GC-irm-MS: A preliminary study*

In order to investigate the biosyntheses of the non-saponifiable lipids in *R. setigera* without the potential interferences from isotopically labelled substrates, cells were cultured in natural conditions and in the presence of fosmidomycin (75 μg $ml^{-1}$) with subsequent lipid analysis by GC-irm-MS. The $\delta^{13}C$ value of each non-saponifiable lipid was measured, and to allow for within-run instrument drift, differences between the measured and certified values of the nearest eluting *n*-alkane reference were added to the measured value of each analyte to give a range. The mean within-run variations from the certified values were: ((n=4) *n*-$C_{24}$, 0.7 ± 0.4 ‰; *n*-$C_{27}$, 0.1 ± 0.1 ‰). Unfortunately, phytol was not present in sufficient amounts to allow the $\delta^{13}C$ to be satisfactorily quantified. However, desmosterol and four $C_{30}$ HBIs isomers were present in sufficient amounts to allow for their $\delta^{13}C$ values

to be determined. The $\delta^{13}C$ values obtained for the two $C_{30}$ pentaenes and desmosterol were very similar (–27.2 ‰ and -27.4 ‰ respectively), while a 3 ‰ difference was exhibited by the $C_{30}$ hexaenes (-24.3 ‰). Interestingly, all of these compounds exhibited more negative $\delta^{13}C$ values when they were isolated from cells cultured in the presence of fosmidomycin (Table 4.22).

Table 4.22 $\delta^{13}C$ values of the non-saponifiable lipids obtained from cultures of *R. setigera* grown in natural conditions and in the presence of fosmidomycin (75 μg $ml^{-1}$).

| | A | B | |
|---|---|---|---|
| $\delta^{13}C$ | Control | Fosmidomycin | $\delta^{13}C_B - \delta^{13}C_A$ |
| Phytol | n/a | n/a | n/a |
| $C_{30:5}$ (Z) | -26.6 | -27.5 | -0.9 |
| $C_{30:5}$ (E) | -27.8 | -30.2 | -2.5 |
| $C_{30:6}$ (Z) | -24.1 | -26.0 | -1.9 |
| $C_{30:6}$ (E) | -24.5 | -26.6 | -2.1 |
| Desmosterol* | -27.4 | -27.9 | -0.5 |

* includes a correction factor (+0.63)due to the presence of TMS. Average values from two samples are given.

During the life cycle experiment RS-2 (Section 2.3.4), *Rhizosolenia setigera* cells were cultured in natural conditions, without any added organic carbon source in the culture medium. Following extraction, saponification and derivatisation, the hydrocarbon fractions from cycles 1, 3, 5, 7, 9 and 11 were analysed by GC-irm-MS. The $\delta^{13}C$ value of each non-saponifiable lipid was measured as before. The mean within-run variations from the certified values were : ((n=12) *n*-$C_{24}$, 0.7 ± 0.2 ‰; *n*-$C_{27}$, 0.1 ± 0.6 ‰). Some major differences in the natural $^{13}C/^{12}C$ isotope ratios between individual hydrocarbons as well as between growth cycles were observed (Table 4.23).

In cycles 1, 3, 9 and 11, phytol was not present in sufficient quantities for the $\delta^{13}C$ values to be quantified satisfactorily. In cycles 5 and 7 the $\delta^{13}C$ value of phytol was found to be -

22.6 ‰. In cycles 1 and 3, four $C_{30}$ HBIs and desmosterol were detected (*cf.* Chapter 2). In cycle 1, the $\delta^{13}C$ values of these compounds were found to be -32.5 ‰ and -32.4 ‰ for the $C_{30}$ HBIs (average of the values obtained for the four isomers) and desmosterol, respectively. From cycles 2 to 11, the similarity in the $\delta^{13}C$ values was maintained, but surprisingly, showed a gradual increase (becoming more positive) with increasing cycle number (Figure 4.17). From cycle 5, the $C_{25}$ HBIs were also present in sufficient quantities for their $\delta^{13}C$ values to be quantified satisfactorily. These $\delta^{13}C$ values were again very similar to those exhibited by the $C_{30}$ HBIs and desmosterol, and an increase in these values was also observed with consecutive cycles. One explanation for these findings is that in the early stages of this experiment, both desmosterol and the HBIs are made from the same (or similar) isotopic pool of IPP (pool A), while phytol is biosynthesised from an isotopically distinct pool (pool B). As the life cycle experiment progresses, all of the compounds would appear to be biosynthesised from an increasing contribution from pool B.

Table 4.23 $\delta^{13}C$ values of the non-saponifiable lipids obtained from cultures of *R. setigera* during different phases of its life cycle (RS-2, see chapter 2). Average values from two samples are given.

| $\delta^{13}C$ | Cycle 1 | Cycle 3 | Cycle 5 | Cycle 7 | Cycle 9 | Cycle 11 |
|---|---|---|---|---|---|---|
| Phytol* | n/a | n/a | -22.6 | -22.6 | n/a | n/a |
| $C_{25:3}$ | n/a | n/a | -27.0 | -25.1 | -23.7 | -23.0 |
| $C_{25:4}$ | n/a | n/a | -27.6 | -26.5 | -24.4 | -23.5 |
| $C_{30:5}$ (Z) | -32.7 | -29.4 | -27.8 | -26.2 | -24.1 | -23.7 |
| $C_{30:5}$ (E) | -32.8 | -29.6 | -27.9 | -26.1 | -23.8 | -23.6 |
| $C_{30:6}$ (Z) | -32.6 | -30.9 | -27.6 | -26.1 | -23.3 | -22.7 |
| $C_{30:6}$ (E) | -31.9 | -30.2 | -28.0 | -26.2 | -24.6 | -23.1 |
| Desmosterol* | -32.4 | -30.6 | -28.3 | -27.4 | -26.2 | -25.3 |

* includes correction factors for phytol and desmosterol from TMS (+1.06 for phytol and +0.63 for desmosterol)

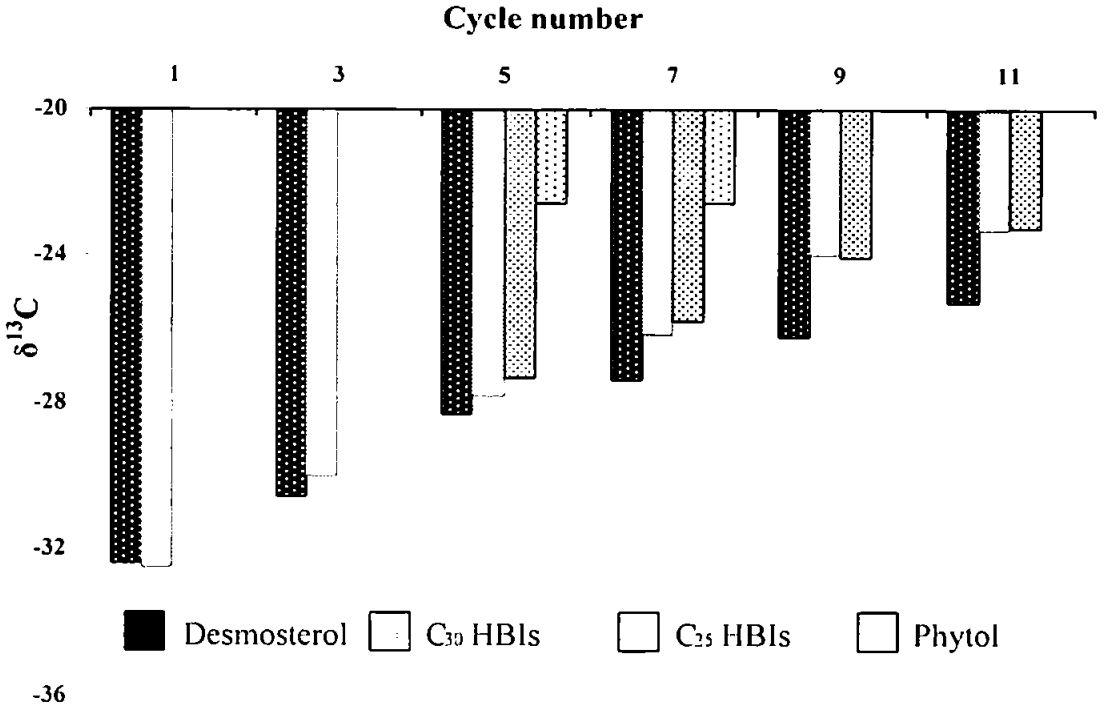


Figure 4.17 Changes in the $\delta^{13}C$ values of the non-saponifiable lipids from *R. setigera* as a function of growth cycle.

*4.3.4 Discussion*

From both pathway-specific inhibition and isotopic labelling experiments, it now seems clear that both MEP and MVA pathways are in operation for the biosynthesis of terpenoids in the diatom *Rhizosolenia setigera.* In the case of phytol, both small and large-scale labelling experiments revealed that this compound was not labelled when either $^{2}H$ or $^{13}C$-labelled acetate were applied to the cells. In contrast, substantial and uniform labelling was observed when the cells were cultured in the presence of $^{13}CO_2$. Similar observations were made by Cvejić and Rohmer (2000) for the diatom *Phaeodactylum tricornutum* who concluded that phytol was biosynthesised by the MEP route. Heintze *et al.* (1990) showed that acetate appeared not to be a suitable precursor for studying the biosynthesis of plastidic isoprenoids. In a later study, Lichtenthaler *et al.* (1997) conclusively demonstrated that in plants, plastidic isoprenoids were synthesized *via* the MEP route and not *via* the MVA pathway, thus

providing an explanation for the absence of labelling from acetate into these isoprenoids. The labelling studies described herein provide indirect evidence for the formation of phytol via the MEP pathway, since even though Harwood (1997) showed that acetate was easily capable of crossing plastidic membranes, and therefore available for fatty acid biosynthesis in plastids, there is still some uncertainty concerning the general availability of acetate for isoprenoid biosynthesis in plastids. Glucose would have been a suitable precursor for more rigorous labelling studies since the MVA and MEP pathways can be clearly differentiated by the observed labelling pattern in isoprenic units after incorporation of [1-$^{13}$C] glucose (Figure 4.6, Rohmer *et al.*, 1993; Eisenreich *et al.*, 1998). However, in agreement with the observations made by Cvejić and Rohmer (2000) with *P. tricornutum*, glucose was not utilized for the biosynthesis of isoprenoids in *R. setigera*. Recently 1-deoxy-D-xylulose 5-phosphate (DOXP) and 2-C-methyl-D-erythritol 4-phosphate (MEP) have been identified as intermediates in the formation of isoprenoids by the mevalonate independent route (Arigoni *et al.*, 1997; Sagner *et al.*, 1998), while the use of isotopically enriched DOXP and MEP have further demonstrated the involvement of the MEP route for terpenoid synthesis (Putra *et al.*, 1998; Charon *et al.*, 1999). As glucose is not metabolised by *R setigera*, experiments involving the presence of e.g. labelled DOXP may prove to be useful to show unambiguously, the participation (exclusive or otherwise) of the MEP pathway in the biosynthesis of phytol in this diatom.

Although there is indirect evidence for the involvement of the MEP route in the biosynthesis of phytol, there is clear and direct evidence for the involvement of the mevalonate pathway in the biosynthesis of other terpenes in *R. setigera*. Thus, very low concentrations of mevinolin, a MVA-specific inhibitor, were required to reduce the cell concentrations of desmosterol, while from isotopic labelling experiments, [1-$^{13}$C] acetate was directly incorporated within this sterol resulting in a site-specific labelling pattern observed by $^{13}$C

NMR spectroscopy again consistent with incorporation *via* the mevalonate pathway. This result is not surprising since numerous studies have shown that these ubiquitous lipids are synthesised *via* the mevalonate pathway (Reviewed by Eisenreich *et al.*, 1998; Lichtenthaler, 1999). $C_{27}$ to $C_{29}$ sterols are common in diatoms, and Cvejić and Rohmer (2000) showed that intact acetate was incorporated into $C_{27}$ and $C_{28}$ sterols from *P. tricornutum* and *Nitzschia ovalis*, suggesting that sterols in diatoms are also synthesised via the MVA pathway. In the experiments carried out by Cvejić and Rohmer (2000), employment of [1-$^{13}$C] acetate (20% isotopic abundance), resulted in an average incorporation of $^{13}$C of 6 ± 1% (*P. tricornutum*) and 12 ± 2% (*N. ovalis*) of $^{13}$C abundance into C-2,4,6,8,10,11,14,16,20,23,25 of epibrassicasterol, a $C_{28}$ sterol. The observations described here for desmosterol from *R. setigera* are similar (identical labelling pattern) except that the average $^{13}$C abundance is significantly lower (2.1%) than that observed by Cvejić and Rohmer (2000). This is probably due to the lower acetate concentration used in the current study (0.25 g $l^{-1}$) compared to that used by Cvejić and Rohmer (1.0 g $l^{-1}$). Inhibition and labelling studies are also consistent with the formation of $C_{25}$ and $C_{30}$ HBIs via the MVA route. Similar to desmosterol, very low concentrations of mevinolin were required to reduce the cell concentrations of these compounds, and from labelling experiments, [1-$^{13}$C] acetate was specifically (and evenly) incorporated within these molecules according to the expected labelling pattern resulting from the mevalonate pathway operation.

Observations from the fractionation of *R. setigera* cells revealed that phytol was located in the chloroplasts while sterols and HBIs were present in the cytoplasm. A large number of studies performed on the formation of mono, di, sester, tri and tetraterpenes in plants show that an apparent division exists for the biosynthesis of these compounds in higher plants (reviewed by Lichtenthaler, 1999). Thus, the mevalonate pathway is located in the cytoplasm contributing to the biosynthesis of sesquiterpenes and triterpenes, while the methyl-erytritol-

phosphate (MEP) pathway is located in the plastids, and accounts for the biosynthesis of monoterpenes, diterpenes and tetraterpenes.

The observations described here are entirely consistent with these previous findings from higher plants. As such, while phytol, found in the chloroplast, is made exclusively by the MEP pathway, $C_{30}$ HBIs along with desmosterol and the monocyclic triterpene $C_{30:4:1}$ are found in the free lipid fraction (cytoplasm) and are made from the mevalonate pathway. Sesterterpenes (including $C_{25}$ HBIs formed via the MVA pathway here) have not been previously investigated.

*4.3.4.1 Dynamic allocation of both pathways, life cycle effects*

In addition to the clear evidence for the involvement of the MVA pathway in the biosynthesis of $C_{25}$ and $C_{30}$ HBIs, $C_{30:4:1}$ and desmosterol in *R. setigera*, results presented in this thesis provide evidence for the contribution from the MEP route to the formation of these compounds. Thus, in experiments using daughter cells, both mevinolin and fosmidomycin reduced the cell concentrations of HBIs and desmosterol, although the inhibition with fosmidomycin was not always observed. When related experiments were carried out using both fosmidomycin and [1-$^{13}$C] acetate, an increase in the incorporation of $^{13}$C in the presence of increasing concentrations of the inhibitor was observed. One explanation for this is that while under normal growth conditions, both the MEP and MVA pathways contribute to the synthesis of these compounds, inhibition of the MEP route results in a compensatory switch to the MVA route. However, this switch is not entirely efficient since reductions in concentrations of the HBIs and desmosterol are also observed.

Evidence for the contribution of both MEP and MVA pathways to the biosynthesis of HBIs and desmosterol in *R. setigera* also came from GC-irm-MS analysis of these lipids obtained from samples from a life cycle experiment. When the $\delta^{13}$C values of individual non-

saponifiable lipids obtained from several consecutive cycles corresponding to different phases of the life cycle were analysed by GC-irm-MS, some major differences between individual compounds were observed as well as between the growth cycles. The $\delta^{13}C$ values of phytol (when present in sufficient amounts for the $\delta^{13}C$ to be satisfactorily quantified) were significantly higher than those obtained for both the HBIs and desmosterol when the cells were close to the auxosporulation or sexual reproductive phase. However, during later phases, the $\delta^{13}C$ values obtained for the HBIs and desmosterol increased and tended towards that of phytol which remained constant.

In a previous study, Jux *et al.* (2001) demonstrated that it is possible to discriminate between the MEP and MVA pathways using $\delta^{13}C$ ratios obtained from GC-irm-MS techniques. Indeed, the thiamine-dependent pyruvate dehydrogenase yielding acetyl CoA from pyruvate in the mevalonate pathway shows a kinetic preference for the formation of the lighter isotopomers, thus producing acetyl CoA that is depleted in $^{13}C$ (Melzer and Schmidt, 1987). In the MEP pathway, the condensation of pyruvate with glyceraldehyde-3-phosphate to yield 1-deoxy-D-xylulose 5-phosphate (DOXP) also involves a thiamine dependant decarboxylation. However, the synthesis of DOXP requires only one decarboxylation, while the formation of mevalonate requires three molecules of acetyl CoA and consequently, three decarboxylations take place. As a result, IPP originating from the mevalonate pathway is significantly depleted in $^{13}C$ compared to that which originates from the MEP route. As a result, $\delta^{13}C$ values for terpenes made predominantly via the MVA route are more negative than for compounds made by the MEP route

Experiments described herein (inhibition and stable isotope incorporation) have shown that in *R. setigera*, phytol is synthesised according to the MEP pathway, while the mevalonate pathway contributes to the synthesis of both HBIs and desmosterol. The significant

differences in the $\delta^{13}C$ values obtained for phytol (-22.6 ‰) and both HBIs (-32.5 ‰) and desmosterol (-32.4 ‰) during the early stages of the life cycle corroborate these observations. However, the progressive increase in the values obtained for both HBIs and desmosterol during cycles 3, 5, 9 and 11, with the values obtained for all compounds in cycle 11 being within experimental error of that of phytol, indicates an increasing participation of the contribution of the MEP pathway toward the synthesis of these isoprenoids. Presumably, this either reflects a modification to the major biosynthetic pathway operating in the endoplasmic reticulum where the HBIs and sterols are finally assembled, or more likely, that there is an increase in the export of chloroplastidic IPP to the cytoplasmic organelle (Chappell, 1995).

*4.3.5 Non-saponifiable lipids from the diatom Haslea ostrearia*

A description of the structures and distributions of the isoprenoids synthesised from the diatom *Haslea ostrearia* can be found elsewhere in this thesis (Chapter 1). Briefly, analysis of the GC-MS total ion current (TIC) chromatograms of the non-saponifiable lipid fraction from *H. ostrearia* usually revealed the presence of *n*-$C_{21:6}$ (I), phytol (II), sitosterol (stigmast-5-ene-3β-ol, XIII) and a number of acyclic $C_{25}$ alkenes (XIV-XXIII). Figure 4.19 summarises the structures of all the non-saponifiable lipids identified in this biosynthetic study. Given intra-species variations in the distributions of $C_{25}$ HBIs from *H. ostrearia*, all of the biosynthetic experiments were performed with the same strain. In addition, while the GC separation of HBIs with different degrees of unsaturation was readily achieved, regioisomers were not sufficiently separated to allow for accurate quantification (Figure 4.18). It was therefore decided to calculate concentrations of $C_{25}$ HBIs as the sum of the contributions from each of the regioisomers for a given degree of unsaturation (i.e. XIV and XV for $C_{25:2}$; XVI and XVII for $C_{25:3}$; XVIII to XXI for $C_{25:4}$; XXII and XXIII for $C_{25:5}$).

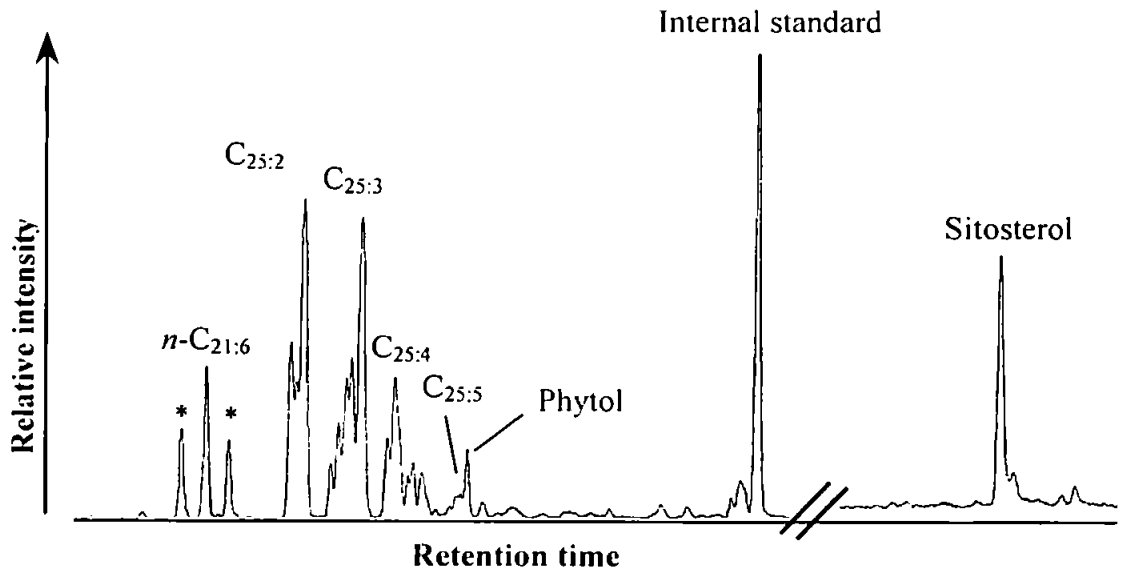


Figure 4.18 Representative partial TIC chromatogram of a non saponifiable lipid fraction from *Haslea ostrearia*. The peaks marked with a * are due to fatty acids.

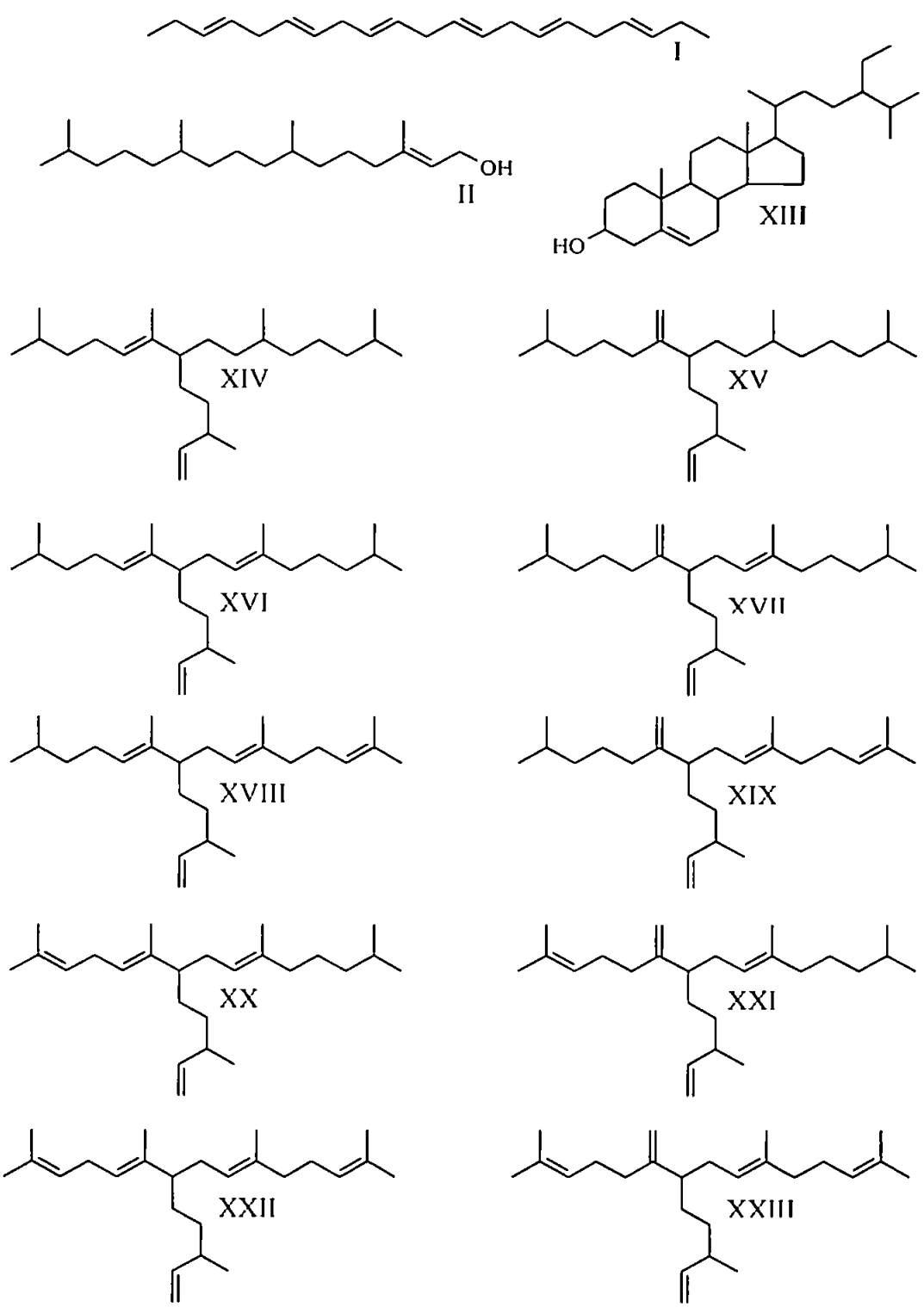


Figure 4.19 Non-saponifiable lipids obtained from various cultures of the diatom *Haslea ostrearia*. I: *n*-$C_{21:6}$, II: phytol, XIII: sitosterol, XIV-XV: $C_{25:2}$, XVI-XVII: $C_{25:3}$, XVIII-XXI: $C_{25:4}$, XXII-XXIII: $C_{25:5}$.

### *4.3.6 Hydrocarbon biosynthesis in the diatom Haslea ostrearia*

#### *4.3.6.1 Inhibition experiments*

When *Haslea ostrearia* was cultured in the presence of mevinolin, the cell growth was found to decrease with increasing concentration of added inhibitor. At the highest concentrations tested (10 and 20 μg $ml^{-1}$), mevinolin significantly reduced the growth rates and the final cell biomass (41-72% growth inhibition). For all of the concentrations tested, the amount of *n*-$C_{21:6}$ (per cell) was found to be essentially invariant and no significant reduction in the $C_{25}$ HBI and sterol content (per cell) was observed. Moreover, at the highest concentration of mevinolin used (20 μg $l^{-1}$), the sterol and $C_{25}$ HBI cell concentrations were higher than in the control culture (Table 4.24, Figure 4.20).

Since mevinolin inhibits the acetate/mevalonate pathway, it almost certainly inhibits the synthesis of essential fatty acids that are involved in membrane structures. Further, if HBIs are functioning as membrane lipids as suggested by Ourisson and Nakatani (1994), it is possible that in the presence of mevinolin, cells of *Haslea ostrearia* are able to synthesise some HBIs in order to replace these other depleted membrane components.

In contrast, when the diatoms were cultured in the presence of fosmidomycin, no inhibition of the cell growth was detected, even at a relatively high concentration of the inhibitor (100 μg $l^{-1}$). However, a dramatic reduction of the cell concentrations of the non-saponifiable lipids was observed. At the highest concentrations used (75 and 100 μg $ml^{-1}$), fosmidomycin significantly reduced the biosynthesis of both *n*-$C_{21:6}$ and phytol (by 32-41% and 73-80%, respectively). The major sterol in *H. ostrearia* (sitosterol) together with the $C_{25}$ HBIs were also reduced in abundance (by 73% and 65% compared to the control). Interestingly, despite the dramatic decrease of all these lipids, only minor modifications in their relative distributions were observed (Table 4.25).

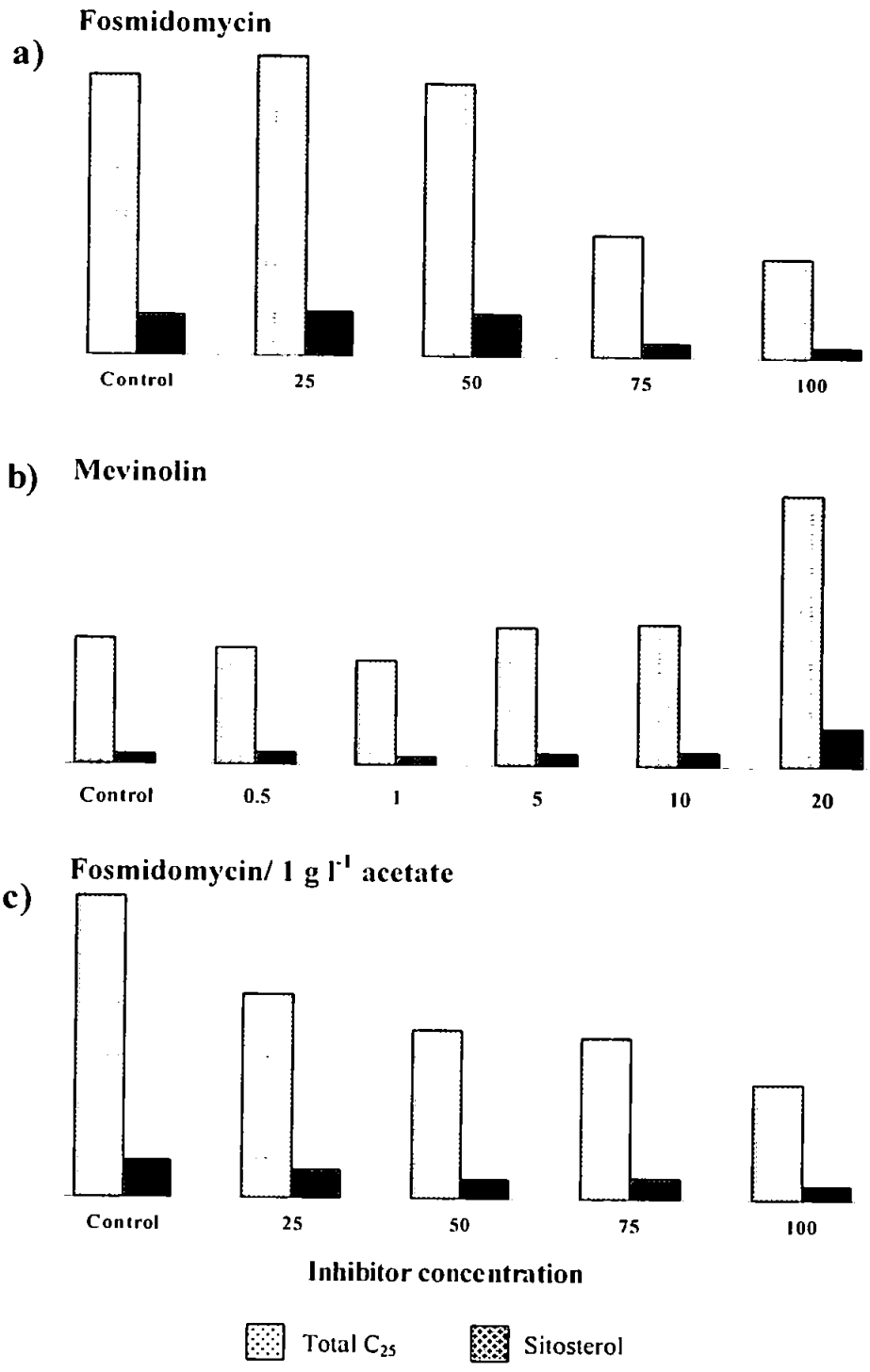


Figure 4.20 Hydrocarbon distribution in *H. ostrearia* cells at the end of the exponential growing phase in the presence of varying concentrations of pathway-specific inhibitor (μg $ml^{-1}$). (a) fosmidomycin (b) mevinolin (c) fosmidomycin, 1 g $l^{-1}$ of acetate.

Table 4.24 Biomass data (cell $ml^{-1}$) and non-saponifiable lipid concentrations (pg $cell^{-1}$) for *Haslea ostrearia* cultured in the presence of increasing concentrations of mevinolin or fosmidomycin (μg $ml^{-1}$).

| | Mevinolin | | | | | |
|---|---|---|---|---|---|---|
| | **Control** | **0.5** | **1** | **5** | **10** | **20** |
| Biomass | 124533 | 122800 | 106800 | 100200 | 74000 | 34600 |
| *n*-$C_{21:6}$ | 0.13 | 0.14 | 0.11 | 0.16 | 0.16 | 0.13 |
| Phytol | 0.03 | 0.04 | n/a | n/a | n/a | n/a |
| $C_{25:2}$ | 0.57 | 0.57 | 0.47 | 0.66 | 0.58 | 0.54 |
| $C_{25:3}$ | 0.43 | 0.39 | 0.38 | 0.51 | 0.62 | 1.69 |
| $C_{25:4}$ | 0.16 | 0.13 | 0.11 | 0.11 | 0.09 | 0.29 |
| $C_{25:5}$ | 0.02 | 0.02 | 0.02 | 0.03 | 0.03 | 0.03 |
| Sitosterol | 0.10 | 0.11 | 0.09 | 0.11 | 0.14 | 0.37 |
| Total $C_{25}$ | 1.18 | 1.10 | 0.98 | 1.30 | 1.33 | 2.55 |

n/a Below limit of detection

| | Fosmidomycin | | | | |
|---|---|---|---|---|---|
| | **Control** | **25** | **50** | **75** | **100** |
| Biomass | 58133 | 60000 | 63600 | 89467 | 70000 |
| *n*-$C_{21:6}$ | 0.37 | 0.40 | 0.47 | 0.25 | 0.22 |
| Phytol | 0.15 | 0.14 | 0.19 | 0.04 | 0.03 |
| $C_{25:2}$ | 1.76 | 2.12 | 2.25 | 0.86 | 0.80 |
| $C_{25:3}$ | 2.13 | 2.13 | 1.91 | 0.99 | 0.76 |
| $C_{25:4}$ | 1.10 | 1.06 | 0.74 | 0.35 | 0.26 |
| $C_{25:5}$ | 0.14 | 0.16 | 0.11 | 0.03 | n/a |
| Sitosterol | 0.75 | 0.81 | 0.78 | 0.25 | 0.20 |
| Total $C_{25}$ | 5.14 | 5.47 | 5.01 | 2.23 | 1.82 |

n/a Below limit of detection

Table 4.25 Non-saponifiable lipid distributions expressed as percentages of the total hydrocarbon content in *Haslea ostrearia* in the presence of increasing concentrations of fosmidomycin (μg $ml^{-1}$).

| | Fosmidomycin | | | | |
|---|---|---|---|---|---|
| | **Control** | **25** | **50** | **75** | **100** |
| *n*-$C_{21:6}$ | 3.2 | 3.3 | 4.1 | 5.0 | 5.4 |
| Phytol | 1.3 | 1.1 | 1.7 | 0.8 | 0.7 |
| $C_{25:2}$ | 15.3 | 17.2 | 19.6 | 17.2 | 19.6 |
| $C_{25:3}$ | 18.5 | 17.3 | 16.7 | 19.8 | 18.6 |
| $C_{25:4}$ | 9.5 | 8.6 | 6.5 | 7.0 | 6.4 |
| $C_{25:5}$ | 1.2 | 1.3 | 1.0 | 0.6 | 0.0 |
| Sitosterol | 6.5 | 6.6 | 6.8 | 5.0 | 4.9 |

These results obtained from inhibition studies suggest that $C_{25}$ HBIs, sitosterol, phytol and *n*-$C_{21:6}$ are synthesised or preferentially synthesised *via* the non-mevalonate pathway. However, as these experiments were performed without any added carbon source, it was then possible that when fosmidomycin was used, the cells were unable to switch toward another pathway as no substrate was available. In order to establish whether this species was capable of switching to the MVA route to synthesis some or all of these lipids when the MEP route was inhibited, a further experiment was performed using fosmidomycin in the presence of added acetate (1g $l^{-1}$; Table 4.26).

Table 4.26 Biomass data (cell $ml^{-1}$) and non-saponifiable lipid concentrations (pg $cell^{-1}$) for *Haslea ostrearia* cultured in the presence of increasing concentrations of fosmidomycin (μg $ml^{-1}$) and acetate (1g $l^{-1}$).

| | Fosmidomycin | | | | |
|---|---|---|---|---|---|
| | **Control** | **25** | **50** | **75** | **100** |
| Biomass | 91467 | 119467 | 99733 | 116000 | 119733 |
| *n*-$C_{21:6}$ | 0.38 | 0.28 | 0.25 | 0.28 | 0.21 |
| Phytol | 0.34 | 0.13 | 0.08 | 0.10 | 0.09 |
| $C_{25:2}$ | 0.62 | 0.52 | 0.34 | 0.45 | 0.15 |
| $C_{25:3}$ | 2.30 | 1.85 | 1.40 | 1.46 | 1.04 |
| $C_{25:4}$ | 2.35 | 1.22 | 1.20 | 0.95 | 0.83 |
| $C_{25:5}$ | 0.26 | 0.15 | 0.15 | 0.10 | 0.10 |
| Sitosterol | 0.70 | 0.52 | 0.37 | 0.40 | 0.27 |
| Total $C_{25}$ | 5.53 | 3.75 | 3.10 | 2.96 | 2.13 |

On this occasion, inhibition of sitosterol, $C_{25}$ HBIs, phytol and *n*-$C_{21:6}$ again occurred and to the same extent as observed for the experiment carried out in the absence of added acetate. This additional result suggests that these lipids are synthesised exclusively *via* the non-mevalonate pathway in the diatom *Haslea ostrearia*, and that the MVA route would appear not to be utilised, even when the MEP route is blocked.

*4.3.6.2 Isotope labelling: small scale experiments*

**Experiments using unlabelled acetate:**

When the diatom *Haslea ostrearia* was cultured in the presence of varying concentrations of sodium acetate, the final cell biomass was found to be essentially invariant of added acetate concentration, although some modifications in the content of the non-saponifiable lipids content was observed (Table 4.27). In the presence of added acetate, the cell concentrations of *n*-$C_{21:6}$, phytol and the $C_{25}$ HBIs showed a significant decrease. This decrease, rather than an increase, is consistent with the biosynthesis of these isoprenoids *via* the non-mevalonate route (as indicated from inhibition experiments) and not from the acetate/mevalonate pathway. Feeding this diatom with acetate probably enhances the heterotrophic growth of the cells, and consequently depletes the $CO_2$ assimilation *via* photosynthesis. The net enhanced production of other metabolites *via* the acetate/mevalonate pathway (e.g. fatty acids) probably then becomes favoured compared to the formation of phytol or the $C_{25}$ HBIs. In addition, no major changes in the HBI distributions were detected when the cells were cultured in the presence of acetate.

Table 4.27 Biomass data (cell $ml^{-1}$) and hydrocarbon concentration (pg $cell^{-1}$) in *Haslea ostrearia* cells after incubation with varying concentrations of unlabelled acetate (g $l^{-1}$).

| | Control | 0.5 | 1 |
|---|---|---|---|
| Biomass | 96000 | 92267 | 97867 |
| *n*-$C_{21:6}$ | 0.45 | 0.20 | 0.19 |
| Phytol | 0.13 | 0.09 | 0.08 |
| $C_{25:2}$ | 0.56 | 0.11 | 0.15 |
| $C_{25:3}$ | 2.08 | 0.69 | 0.79 |
| $C_{25:4}$ | 1.03 | 0.44 | 0.50 |
| $C_{25:5}$ | 0.08 | 0.04 | 0.04 |

**Stable isotope incorporation-analysis by mass spectrometry**

When *H. ostrearia* was cultured in the presence of $^{13}CO_2$ and unlabelled sodium acetate (1g $l^{-1}$), $^{13}C$ was efficiently incorporated within phytol, all of the $C_{25}$ HBI isomers and sitosterol (average isotopic enrichment factor: 6.5% ± 0.6%, Table 4.28). In contrast, phytol was not labelled when the cells were cultured in the presence of either [1-$^{13}C$] or [2-$^{13}C$] acetate, and a relatively small (2.2 and 2.3% for [1-$^{13}C$] and [2-$^{13}C$] acetate, respectively) incorporation of $^{13}C$ from labelled acetate was detected for the $C_{25}$ HBIs and sterols. In addition, when the cells were grown in the presence of [$^{2}H_3$] acetate, no incorporation of deuterium was observed in any of the compounds examined (Table 4.28). Since [$^{2}H_3$] acetate was not utilised directly by the cells, the small incorporation of $^{13}C$ from the labelled acetates detected in both $C_{25}$ and sitosterol was probably due to the catabolism of the acetate into $^{13}CO_2$ prior to incorporation.

Finally, when the cells were cultured in the presence of D-[2-$^{13}C$] leucine, no incorporation of $^{13}C$ was detected in any of the $C_{25}$ HBIs or in the sitosterol, although the isotopic enrichment factor calculate for phytol was found to be relatively high (2.0%) compared to those calculate for phytol in the presence of other isotopically labelled precursors. In the

presence of D-[1-$^{13}$C] glucose (0.2 g $l^{-1}$, 50% isotopic abundance), cells of *H. ostrearia* did not grow at all.

Table 4.28 Isotopic enrichment factors for lipids from *Haslea ostrearia* after incubation with labelled precursors.

**$^{13}$C labelled precursors**

| | Control | Acetate | [1-$^{13}$C] Acetate | [2-$^{13}$C] Acetate | $^{13}CO_2$ | [2-$^{13}$C] Leucine |
|---|---|---|---|---|---|---|
| Phytol | 1.4 | 0.9 | 0.9 | 1.2 | 6.5 • | 2.0 |
| $C_{25:2}$ | 0.8 | 1.1 | 2.4 ° | 2.1 ° | 6.8 • | n/a |
| $C_{25:3}$ | 0.9 | 0.8 | 2.2 ° | 2.2 ° | 7.3 • | 1.2 |
| $C_{25:4}$ | 1.1 | 1.3 | 2.2 ° | 2.5 ° | 6.9 • | 1.2 |
| sitosterol | 1.1 | 1.0 | 2.3 ° | 2.3 ° | 5.9 • | 1.2 |

n/a Below limit of detection

**Deuterium Labelled precursors**

| | Control | Acetate | $^{2}H_3$ Acetate [1] |
|---|---|---|---|
| Phytol | 0.7 | 0.5 | 0.9 |
| $C_{25:2}$ | 0.4 | 0.6 | 0.9 |
| $C_{25:3}$ | 0.5 | 0.4 | 1.0 |
| $C_{25:4}$ | 0.6 | 0.7 | 1.1 |
| sitosterol | 0.7 | 0.6 | 1.0 |

• Significant incorporation, ° small incorporation (possibly *via* degradation of the precursor)

[1] Experiment realised in conditions that differ from control and unlabelled acetate experiment (150 ml cultures for both control and acetate experiments and 25 L culture for $^{2}H_3$ acetate experiment)

In summary, isotopic labelling patterns are consistent with the observations from inhibition experiments which indicate that all the terpenoids synthesised by the diatom *Haslea ostrearia* are made exclusively from the non-mevalonate pathway.

*4.3.6.3 Analysis of lipids from H. ostrearia by GC-irm-MS: A preliminary study*

In order to investigate the biosyntheses of the non-saponifiable lipids in *Haslea ostrearia* without the potential interferences from isotopically labelled substrates, *Haslea ostrearia* cells were cultured under normal conditions and in the presence of mevinolin (10 μg $ml^{-1}$). At the end of the exponential growing phase, cells were harvested by filtration and their non-saponifiable lipids fraction analysed by GC-irm-MS. The $\delta^{13}C$ values of each lipid was measured, and to allow for within-run instrument drift, differences between the measured and certified values of the nearest eluting *n*-alkane reference were added to the measure value of each analyte to give a range. The mean within-run variations from the certified values were: ((n=4) *n*-$C_{19}$, 0.4 ± 0.2 ‰; *n*-$C_{24}$, 0.7 ± 0.7 ‰; *n*-$C_{27}$, 0.3 ± 0.3 ‰). Unfortunately, phytol was not present in sufficient amounts to allow the $\delta^{13}C$ to be satisfactorily quantified. However, the major sterol, sitosterol and two of the $C_{25}$ HBI isomers were present in sufficient amounts to allow their $\delta^{13}C$ values to be determined. The $\delta^{13}C$ value obtained for sitosterol (-22.0 ‰) was much higher than that obtained for desmosterol (-27.4 ‰) from *R. setigera* cultured at the same time and under identical conditions. Even higher $\delta^{13}C$ values were obtained for the dienes (-16.2 ‰) and trienes (-19.4 ‰). Surprisingly, while the $\delta^{13}C$ value obtained for sitosterol obtained from cultures containing mevinolin was very similar to the control, the corresponding $\delta^{13}C$ values for the $C_{25}$ HBIs were slightly more negative (Table 4.29).

Table 4.29 $\delta^{13}C$ values of the non-saponifiable lipids obtained from cultures of *Haslea ostrearia* grown under natural conditions and in the presence of mevinolin (10 μg $ml^{-1}$). Average values from two samples are given.

| $\delta^{13}C$ | Control | Mevinolin |
|---|---|---|
| Phytol* | n/a | n/a |
| $C_{25:2}$ | -16.2 | -17.3 |
| $C_{25:3}$ | -19.4 | -21.0 |
| Sitosterol* | -22.0 | -22.1 |

* includes correction factors for phytol and sitosterol from TMS (+1.06 for phytol and +0.63 for sitosterol), n/a Below limit of detection. Average values from two samples are given.

*4.3.6.4 Influence of light intensity on the biosynthesis of HBIs in the diatom Haslea ostrearia*

Recently, Wildermuth and Fall (1996) demonstrated that the emission of isoprene (a plastidic isoprenoid from poplar leaves synthesised *via* the mevalonate-independent route (Zeidler *et al.*, 1997)) was a light dependent process, providing supporting evidence for the localization of the MEP pathway in plastids (Lichtenthaler, 1999). In order to further check the hypothesis that $C_{25}$ HBIs are made exclusively by the MEP pathway in the diatom *Haslea ostrearia*, cells were cultured in triplicate under different light intensities (10, 50, 100 and 200 μmol photon $m^{-2}$ $s^{-1}$). With the exception of the illumination conditions, all of the other experimental parameters were identical (F/2 enriched sea-water, 14°C, 14/10 light/dark cycle). Cells were harvested by filtration at the end of the exponential growing phase and their HBI content analysed by GC-MS following the methodology described in Chapter 5.

Corroborating the observations of Rowland *et al.* (2001a) for *H. ostrearia* cultured at 15°C, only a single $C_{25}$ triene (XVII) was detected in the cells for all the light conditions

tested. In addition, the HBI cell concentration generally increased with increasing light intensity (Table 4.30).

Table 4.30 Mean $C_{25}$ concentrations (pg $cell^{-1}$) obtained from cultures of *Haslea ostrearia* grown under different light intensities (μmol photon $m^{-2}$ $s^{-1}$).

| Light intensisty | 10 | 50 | 100 | 200 |
|---|---|---|---|---|
| $C_{25:3}$ | 1.56 | 1.41 | 1.63 | 2.17 |
| Standard deviation | 0.20 | 0.15 | 0.51 | 0.54 |

Average values from three samples are given.

This relationship between light intensity employed in the culturing and HBI cell concentration represents partial evidence for a plastidic localization of the HBI biosynthesis, or at least that the IPP units from which they are made, originate in the plastid and for the involvement of the MEP pathway toward their synthesis.

### *4.3.7 Discussion*

The results obtained from the all the experiments performed with the diatom *H. ostrearia*, support the hypothesis that the mevalonate pathway is not contributing to the non-saponifiable lipid biosynthesis in this species and that they are made via the MEP route. Mevinolin was found to have no effect on the cell isoprenoid concentrations, whereas fosmidomycin dramatically retarded their synthesis, even in the presence of acetate. In addition, from labelling experiments, only a small incorporation of $^{13}C$ from labelled acetate was detected in HBIs and sitosterol, while no deuterium was incorporated in these terpenoids when the cells were cultured in the presence of [$^{2}H_3$] acetate. This indicates that acetate is not incorporated directly into isoprenoids, but that the small $^{13}C$ enrichment detected in these compounds was probably incorporated as $^{13}CO_2$ after degradation of the labelled acetates. In

addition, when the cells were cultured in the presence of $^{13}CO_2$, $^{13}C$ was efficiently incorporated into all the isoprenoids present in this diatom. Finally, when examined individually by GC-irm-MS, all of the isoprenoids obtained from this species cultured under natural conditions exhibited high $\delta^{13}C$ values, including sitosterol, a triterpenoid usually made by the mevalonate pathway (Eisenreich, 1998; Lichtenthaler, 1999). The $\delta^{13}C$ were all very similar to those obtained for phytol (made by the MEP pathway) in cells of the diatom *R. setigera* cultured under identical conditions. Further evidence for the non-involvement of the mevalonate pathway to the biosynthesis of isoprenoid in this species was obtained when no significant differences were detected in the $\delta^{13}C$ values of the same compounds extracted from cells cultured in the presence of mevinolin.

Thus, in *H. ostrearia*, and in contrast to what was observed for the diatom *R. setigera*, the non-saponifiable lipids are synthesised exclusively *via* the MEP pathway. Similar conclusions were made by Schwender *et al.* (1996) in the green alga *Scenedesmus obliquus*. However, when they studied the biosynthesis of phytol, plastoquinone, carotenoids (β-carotene, lutein) and sterols (chondrillasterol, 22,23 dihydrochondrillasterol, ergost-7-enol) in this species using $^{13}C$-labelled glucose and acetate, unexpected labelling patterns of isoprenic units were found. Indeed, similarly to what Flesh and Rohmer (1988) observed with *E. coli*, when they cultured the cells in the presence of [1-$^{13}C$] labelled acetate, $^{13}C$ was only found in C-4 of IPP units from phytol and chondrillasterol. They showed that [1-$^{13}C$] acetate was transformed into [1-$^{13}C$] pyruvate and [1-$^{13}C$] glyceraldehyde-3-phosphate (GAP). Condensation of pyruvate and GAP resulted in the loss of the $^{13}C$ from pyruvate and $^{13}C$ from the triose phosphate was incorporated into C-4 of IPP (Figure 4.3 B).

To date no evidence for the operation of this glyoxylate shunt in the diatom *H. ostrearia* has been found. However, this could explain the small incorporation of $^{13}C$ from labelled acetates detected during labelling experiments.

Further experiments using direct precursors of the MEP pathway such as labelled 1-deoxy-D-xylulose and large scale experiments using labelled acetate allowing sufficient quantities of individual isoprenoids to be analysed by NMR spectroscopy techniques are required to unambiguously support the conclusions made from these preliminary investigations.

### *4.3.8 Non-saponifiable lipids from the diatom Pleurosigma intermedium*

A description of the structures and distributions of the isoprenoids synthesised from the diatom *Pleurosigma intermedium* can be found elsewhere in this thesis (Chapter 1). Briefly, analysis of the GC-MS total ion current (TIC) chromatograms of the non-saponifiable lipid fraction from *P. intermedium* generally revealed the presence of *n*-$C_{21:6}$ (I), phytol (II), squalene (XXIV) and at least eight $C_{27}$-$C_{28}$ sterols. For most experiments, four sterols where found in sufficient amounts to be satisfactorily quantified, although only two of these, cholesterol (cholest-5-ene-3β-ol, XXV) and 24-methylenecholesterol (ergosta-5,24-diene-3β-ol, XXVI) were unambiguously identified. In addition, up to six acyclic $C_{25}$ HBI isomers (VIII-X and XXVII-XXIX) could be found in the non-saponifiable lipid fraction of this diatom. Figure 4.21 summarises the structures of all the non-saponifiable lipids identified in this biosynthetic study.

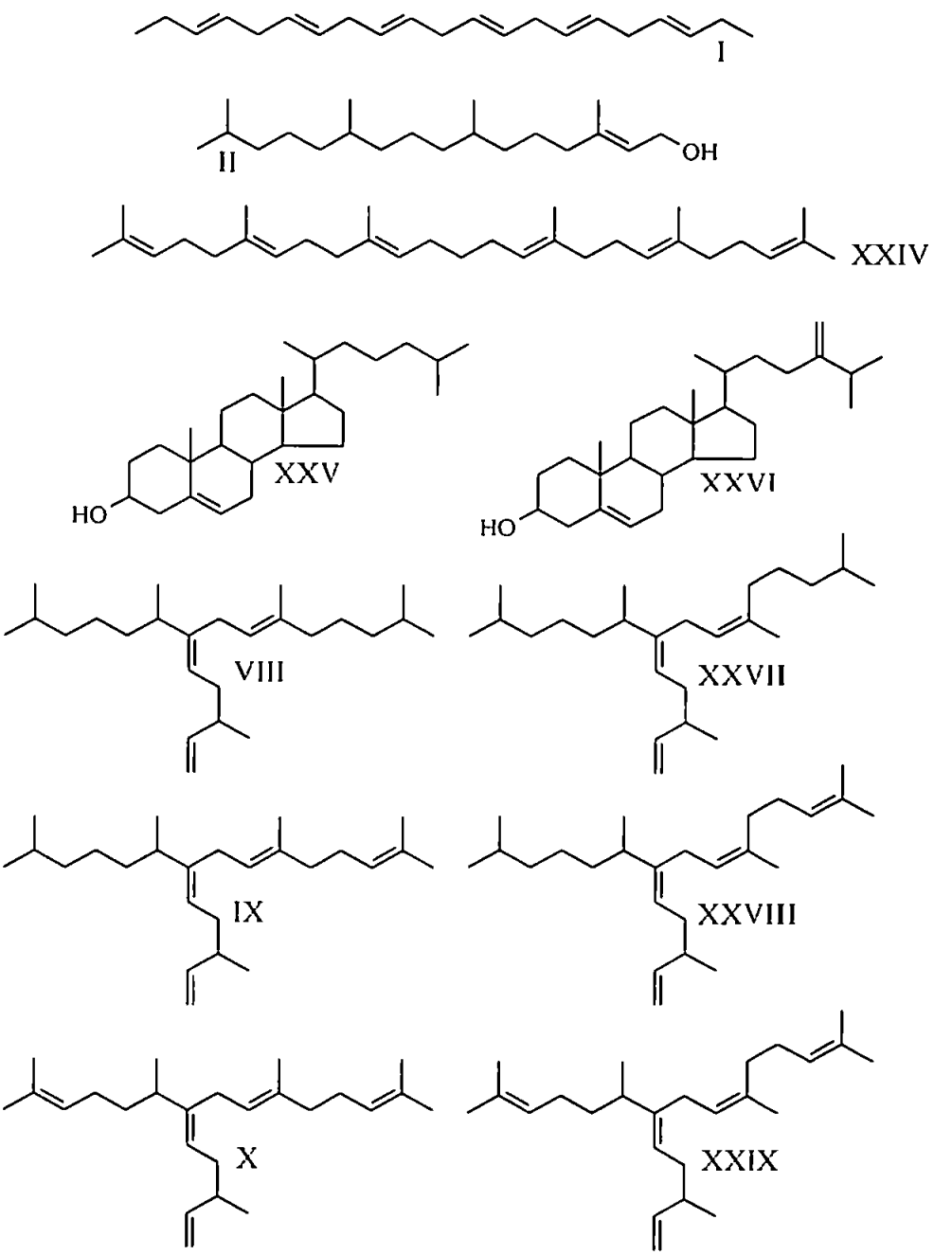


Figure 4.21 Non-saponifiable lipids identified in various cultures of the diatom *Pleurosigma intermedium*. I: *n*-$C_{21:6}$, II: phytol, XXIV: squalene, XXV: cholesterol, XXVI: 24-Methylenecholesterol, VIII: $C_{25:3}$ (E), IX: $C_{25:4}$ (E), X: $C_{25:5}$ (E), XXVII: $C_{25:3}$ (Z), XXVIII: $C_{25:4}$ (Z), XXIX: $C_{25:5}$ (Z).

### *4.3.9 Isoprenoid biosynthesis in the diatom Pleurosigma intermedium*

#### *4.3.9.1 Inhibition experiments*

In contrast to the observations made for *H. ostrearia*, both mevinolin and fosmidomycin were found to reduce the growth of *P. intermedium*, although the inhibition effect from the former was more pronounced (cf. *R. setigera*). Indeed, while at the highest concentrations tested (10 and 20 μg $ml^{-1}$), mevinolin significantly reduced the growth rates and the final cell biomass (35-64% growth inhibition), only 14 and 49% of growth inhibition was observed when the cells were cultured in the presence of 75 and 100 μg $ml^{-1}$ of fosmidomycin. However, mevinolin did not significantly inhibit the biosynthesis of *n*-$C_{21:6}$, phytol, squalene, sterols or the $C_{25}$ HBIs. In fact, the concentrations of *n*-$C_{21:6}$, squalene and sterols showed an increase with increasing mevinolin concentrations, while phytol and $C_{25}$ HBI concentrations were found to be essentially invariant.

In contrast to the observations made for *H. ostrearia*, the phytol concentration remained relatively constant when the cells were cultured in the presence of increasing concentrations of fosmidomycin, even if the *n*-$C_{21:6}$ content was slightly reduced. In addition, the squalene and most of the sterol concentrations increased in the presence of increasing concentrations of fosmidomycin. The total $C_{25}$ HBI cell concentration increased when relatively low concentrations of fosmidomycin were applied to the cells (25 and 50 μg $ml^{-1}$). When higher concentrations were tested, a slight decrease in their concentrations was then observed. However, for the $C_{25}$ HBIs, it is interesting to note that their distributions were dependent on the fosmidomycin concentrations (Table 4.31; Figure 4.22). In the absence of any inhibitor in the culture, the pentaenes (X, XXIX) were the major isomers (65% of the total HBIs in the cells), tetraenes (IX, XXVIII) represented 32% of the total HBIs and only traces of trienes (VIII, XXVII) were detected (3%). When the concentrations of fosmidomycin applied to the

cells was increased (up to 75 μg $ml^{-1}$), the contribution from the pentaenes decreased (from 65 to 17%), while the tetraenes became the major isomers (from 32 to 76%) and the triene contribution increased slightly (from 3 to 8%). At the maximum fosmidomycin concentration used, the contribution from the tetraenes decreased slightly (from 76 to 71%) while the triene concentrations increased further (from 8 to 9%).

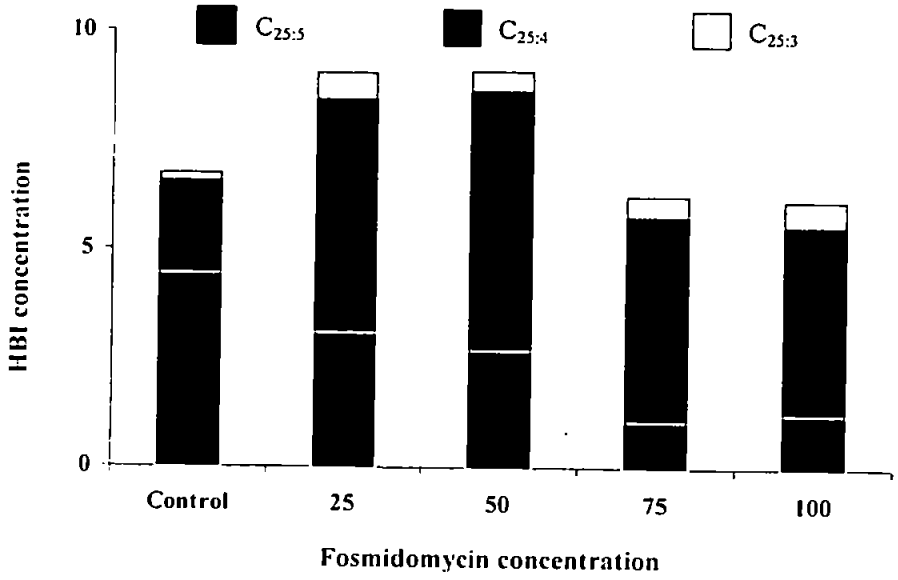


Figure 4.22 $C_{25}$ HBI concentrations (pg $cell^{-1}$) in *Pleurosigma intermedium* cells cultured in the presence of increasing concentrations of fosmidomycin (μg $l^{-1}$).

The apparent failure of either mevinolin or fosmidomycin to cause an inhibition of HBI biosynthesis suggests that either *P. intermedium* is able to switch between pathways to compensate for the presence of an inhibitor, or that mevinolin and/or fosmidomycin inhibit the biosynthesis of other essential compounds required for cell growth before significant inhibition of the HBIs takes place.

An experiment using both fosmidomycin and mevinolin in the same culture of *P. intermedium* was therefore conducted in order to investigate the possibility of a switch between the MVA and MEP pathways for the synthesis of isoprenoids (Table 4.32). HBIs

were still detected in cells in the presence of the highest concentration of both inhibitors (75 and 15 μg $ml^{-1}$ of fosmidomycin and mevinolin) and in greater amounts compared to control cells. Consistent with the first experiment, the biosynthesis of the pentaenes was significantly inhibited when the cells were cultured in the presence of fosmidomycin.

Table 4.31 Biomass data (cell $ml^{-1}$) and non-saponifiable lipid concentrations (pg $cell^{-1}$) of *Pleurosigma intermedium* grown in the presence of mevinolin or fosmidomycin (μg $ml^{-1}$).

| | Mevinolin | | | | | |
|---|---|---|---|---|---|---|
| | **Control** | **0.5** | **1** | **5** | **10** | **20** |
| Biomass | 20440 | 20520 | 20080 | 20160 | 13200 | 7400 |
| *n*-$C_{21:6}$ | 0.27 | 0.42 | 0.31 | 0.36 | 0.31 | 0.60 |
| Phytol | 0.42 | 1.08 | 0.71 | 0.74 | 0.75 | 0.32 |
| $C_{25:3}$ (Z) | n/a | 0.25 | 0.14 | 0.21 | 0.14 | 0.57 |
| $C_{25:4}$ (Z) | 0.85 | 1.66 | 1.32 | 1.64 | 1.15 | 1.57 |
| $C_{25:3}$ (E) | 0.17 | 0.32 | 0.21 | 0.32 | 0.29 | 0.38 |
| $C_{25:5}$ (Z) | 0.51 | 0.81 | 0.52 | 0.66 | 1.07 | 0.76 |
| $C_{25:4}$ (E) | 1.04 | 1.48 | 1.17 | 1.55 | 1.68 | 1.18 |
| $C_{25:5}$ (E) | 0.68 | 0.84 | 0.49 | 0.76 | 1.32 | 0.64 |
| Squalene | 1.24 | 1.72 | 0.94 | 0.57 | 3.22 | 2.79 |
| unidentified $C_{27}$ sterol | 2.42 | 3.24 | 2.93 | 2.75 | 2.67 | 4.61 |
| Cholesterol | 1.50 | 1.51 | 1.51 | 1.79 | 1.27 | 2.82 |
| unidentified $C_{28}$ sterol | 0.44 | 0.66 | 0.54 | 0.55 | 0.35 | 0.74 |
| 24-Methylenecholesterol | 0.28 | 0.34 | 0.27 | 0.37 | 0.17 | 0.23 |
| Total $C_{25}$ | 3.26 | 5.36 | 3.84 | 5.14 | 5.65 | 5.09 |

| | Fosmidomycin | | | | |
|---|---|---|---|---|---|
| | **Control** | **25** | **50** | **75** | **100** |
| Biomass | 30044 | 27378 | 21689 | 25778 | 15289 |
| *n*-$C_{21:6}$ | 1.09 | 1.16 | 1.34 | 1.11 | 0.77 |
| Phytol | 1.27 | 1.91 | 1.29 | 1.28 | 1.46 |
| $C_{25:3}$ (Z) | 0.11 | 0.23 | 0.20 | 0.21 | 0.35 |
| $C_{25:4}$ (Z) | 1.05 | 2.37 | 2.61 | 2.25 | 1.99 |
| $C_{25:3}$ (E) | 0.07 | 0.37 | 0.25 | 0.27 | 0.23 |
| $C_{25:5}$ (Z) | 2.07 | 1.42 | 1.17 | 0.49 | 0.50 |
| $C_{25:4}$ (E) | 1.12 | 3.04 | 3.39 | 2.50 | 2.38 |
| $C_{25:5}$ (E) | 2.34 | 1.64 | 1.50 | 0.55 | 0.72 |
| Squalene | 1.77 | 2.49 | 2.80 | 1.61 | 2.55 |
| unidentified $C_{27}$ sterol | 2.94 | 3.87 | 4.57 | 4.14 | 4.45 |
| Cholesterol | 1.71 | 2.14 | 2.41 | 2.06 | 2.43 |
| unidentified $C_{28}$ sterol | 0.59 | 0.98 | 0.82 | 0.62 | 0.58 |
| 24-Methylenecholesterol | 0.34 | 0.53 | 0.41 | 0.37 | 0.36 |
| Total $C_{25}$ | 6.75 | 9.07 | 9.13 | 6.27 | 6.17 |

Table 4.32 Biomass data (cell $ml^{-1}$) and non-saponifiable lipid concentrations (pg $cell^{-1}$) of *Pleurosigma intermedium* grown in the presence of both mevinolin and fosmidomycin (μg $ml^{-1}$).

| | Fosmidomycin / Mevinolin | | | | |
|---|---|---|---|---|---|
| | **Control** | **0/75** | **7.5/25** | **15/75** | **15/0** |
| Biomass | 3200 | 34900 | 24400 | 6800 | 1320 |
| *n*-$C_{21:6}$ | n/a | 0.82 | 0.22 | 0.58 | n/a |
| Phytol | n/a | 1.97 | 1.13 | 1.01 | n/a |
| $C_{25:3}$ (Z) | n/a. | n/a | n/a | n/a | n/a |
| $C_{25:4}$ (Z) | n/a | 5.05 | 3.31 | 4.25 | 1.89 |
| $C_{25:3}$ (E) | n/a | 0.64 | 0.42 | 0.44 | n/a |
| $C_{25:5}$ (Z) | 2.11 | 0.72 | 0.85 | 4.44 | 2.53 |
| $C_{25:4}$ (E) | 0.96 | 5.81 | 3.50 | 4.67 | 2.66 |
| $C_{25:5}$ (E) | 3.72 | 1.00 | 0.88 | 4.63 | 4.92 |
| Squalene | 9.68 | 4.93 | 1.27 | 3.38 | 15.22 |
| unidentified $C_{27}$ sterol | 7.75 | 12.52 | 9.58 | 20.21 | 20.61 |
| Cholesterol | 11.50 | 6.10 | 5.80 | 13.68 | 28.63 |
| unidentified $C_{28}$ sterol | n/a | 3.31 | 1.40 | 2.45 | n/a |
| 24-Methylenecholesterol | n/a | 1.43 | 0.82 | 1.61 | n/a |
| Total $C_{25}$ | 6.80 | 13.22 | 8.97 | 18.43 | 12.00 |

n/a Below limit of detection

In contrast to the observations made for both *R. setigera* and *Haslea ostrearia*, no clear conclusions concerning the biosynthetic routes used by the diatom *Pleurosigma intermedium* to synthesise isoprenoids, based on these pathway-specific blocking experiments could be made.

*4.3.9.2 Isotope labelling: small scale experiments*

**Experiments using unlabelled acetate:**

When the diatom *Pleurosigma intermedium* was cultured in the presence of varying concentrations of sodium acetate, the final cell biomass was found to be essentially invariant while some modifications in the cell lipid content were observed. Table 4.33 summarise the results obtained for this experiment. The concentration (per cell) of all the lipid examined,

except squalene, apparently increased dramatically (approx. 3 fold) in the presence of 0.5 g $l^{-1}$ of added acetate in the culture medium. In contrast, when the concentration of acetate increased further (1 g $l^{-1}$), the concentration (per cell) of all the lipid examined then slightly decreased. No significant changes in the HBI distributions were detected when the cells were cultured in the presence of acetate.

Table 4.33 Biomass data (cell $ml^{-1}$) and hydrocarbon concentration (pg $cell^{-1}$) in *Pleurosigma intermedium* cells after incubation with varying concentrations of unlabelled acetate (g $l^{-1}$).

| | Control | 0.5 | 1 |
|---|---|---|---|
| Biomass | 8080 | 9400 | 9920 |
| *n*-$C_{21:6}$ | 1.26 | 3.70 | 3.25 |
| Phytol | 2.25 | 6.10 | 4.62 |
| $C_{25:4}$ (Z) | 2.81 | 9.55 | 7.58 |
| $C_{25:5}$ (Z) | 4.36 | 11.21 | 5.71 |
| $C_{25:4}$ (E) | 2.46 | 6.20 | 4.42 |
| $C_{25:5}$ (E) | 2.89 | 5.60 | 2.98 |
| Squalene | 6.64 | 4.38 | 2.22 |

**Stable isotope incorporation – analysis by mass spectrometry**

When *P. intermedium* was cultured in the presence of D-[1-$^{13}$C] glucose or D-[2-$^{13}$C] leucine, no incorporation of $^{13}$C was detected by mass spectrometry in any of the examined non-saponifiable lipids, indicating that neither precursor was metabolised by this species. In contrast, when *P. intermedium* was cultured in the presence of $^{13}CO_2$ (20% enrichment) and unlabelled sodium acetate (1g $l^{-1}$), $^{13}$C was efficiently incorporated within phytol, all of the $C_{25}$ HBI isomers, squalene and the sterols (average isotopic enrichment factor: 4.8% ± 0.8%; Table 4.34). In contrast, a relatively small incorporation of $^{13}$C from [1-$^{13}$C] acetate was detected for phytol and the $C_{25}$ HBIs (average isotopic enrichment factor: 2.4% ± 0.2%), while $^{13}$C was efficiently incorporated within squalene and sterols (average isotopic enrichment factor: 4.2% ± 0.7%). When the cells were grown in the presence of [$^{2}H_3$]

acetate, incorporation of deuterium (measured by MS) was not observed in phytol or in the HBIs (Table 4.34). This indicated that intact [$^2H_3$] acetate was not directly utilised by the cells, and that the small incorporation of $^{13}C$ from [1-$^{13}C$] acetate detected in these compounds, was probably due to partial degradation of this precursor (into $^{13}CO_2$) before incorporation *via* the non-mevalonate pathway. However, deuterium was incorporated into squalene and each of the sterols, indicating that direct incorporation of [$^2H_3$] acetate into these compounds *via* the mevalonate pathway had occurred.

Table 4.34 Isotopic enrichment factors for the non-saponifiable lipids from *Pleurosigma intermedium* after incubation with labelled precursors

**$^{13}C$ labelled precursors**

| | Control | Acetate | [1-$^{13}C$] Acetate | $^{13}CO_2$ | [1-$^{13}C$] Glucose | [2-$^{13}C$] Leucine |
|---|---|---|---|---|---|---|
| Phytol | 1.3 | 1.2 | 2.0 ° | 4.0 • | 1.0 | 1.1 |
| $C_{25:4}$ Z | 1.3 | 1.3 | 2.4 ° | 4.5 • | 1.5 | 0.8 |
| $C_{25:5}$ Z | 1.2 | 1.1 | 2.3 ° | 5.9 • | 1.3 | 1.2 |
| $C_{25:4}$ E | 1.2 | 1.2 | 2.6 ° | 4.4 • | 1.1 | 0.9 |
| $C_{25:5}$ E | 1.3 | 1.1 | 2.5 ° | 5.2 • | 1.3 | 1.0 |
| Squalene | 1.1 | 1.2 | 5.2 • | 6.2 • | 0.8 | 1.2 |
| unidentified $C_{27}$ sterol | 1.1 | 1.1 | 3.7 • | 4.0 • | 1.1 | 1.2 |
| cholesterol | 1.1 | 1.1 | 4.1 • | 4.6 • | 1.2 | 1.2 |
| 24-Methylcholesterol | 1.3 | 1.5 | 3.8 • | 4.4 • | 1.4 | 1.5 |

**Deuterium labelled precursors**

| | Control | Acetate | $^2H_3$ Acetate |
|---|---|---|---|
| Phytol | 0.6 | 0.7 | 0.7 |
| $C_{25:4}$ Z | 0.7 | 0.8 | 0.7 |
| $C_{25:5}$ Z | 0.7 | 0.7 | 0.7 |
| $C_{25:4}$ E | 0.7 | 0.7 | 0.6 |
| $C_{25:5}$ E | 0.8 | 0.7 | 0.7 |
| Squalene | 0.7 | 0.7 | 1.8 • |
| unidentified $C_{27}$ sterol | 0.7 | 0.7 | 2.3 • |
| cholesterol | 0.7 | 0.7 | 2.4 • |
| 24-Methylcholesterol | 0.7 | 0.8 | 2.2 • |

• Significant incorporation, ° small incorporation (possibly *via* degradation of the precursor)

*4.3.9.3 Analysis of lipids from P. intermedium by GC-irm-MS: A preliminary study*

As a third approach to study the biosynthesis of the non-saponifiable lipids in *Pleurosigma intermedium*, cells were cultured under natural conditions, or in the presence of mevinolin (10 μg $ml^{-1}$) or fosmidomycin (75 μg $ml^{-1}$), followed by analysis of these lipids by GC-irm-MS. The $\delta^{13}C$ values of each non-saponifiable lipid was measured, and to allow for within-run instrument drift, differences between the measured and certified values of the nearest eluting *n*-alkane reference were added to the measure value of each analyte to give a range. The mean within run variations from the certified values were: ((n=6) *n*-$C_{24}$, 0.7 ± 0.7 ‰; *n*-$C_{27}$, 0.8 ± 0.8 ‰). Phytol was not present in sufficient quantities from cells cultured under natural conditions to allow for the $\delta^{13}C$ values to be measured satisfactorily. However, in the inhibition experiments, squalene, two $C_{27}$ sterols and four $C_{25}$ HBI isomers were present in sufficient amounts to allow their $\delta^{13}C$ values to be determined. The $\delta^{13}C$ values obtained for squalene, cholesterol and a further unidentified sterol were -23.1 ‰, -24.1 ‰ and -23.8 ‰, respectively. The two sterol values were more positive than that obtained for desmosterol from *R. setigera* cultured at the same time and under identical conditions (-27.4 ‰) but more negative than that obtained for sitosterol from *H. ostrearia* (-22.0 ‰). In addition, large differences were observed in the $\delta^{13}C$ values obtained for the $C_{25}$ HBIs. A 4.6 ‰ difference was observed between two tetraene geometric isomers -18.5 ‰ and -23.1 ‰ for IX and XXVIII respectively) while a 5.9 ‰ difference was observed between two pentaene diastereoisomers (-26.2 ‰ and -20.3 ‰ for X and XXIX, respectively). Consistent with the observations made for *R. setigera*, all the compounds obtained from the cells cultured in the presence of mevinolin exhibited more positive $\delta^{13}C$ values than those obtained from the control (Table 4.35). In the presence of fosmidomycin, these values increased even further.

Table 4.35 $\delta^{13}C$ values of the non-saponifiable lipids obtained from cultures of *P. intermedium* grown in natural conditions and in the presence of mevinolin (10 μg $ml^{-1}$) or fosmidomycin (75 μg $ml^{-1}$).

| $\delta^{13}C$ | Control | Mevinolin | Fosmidomycin |
|---|---|---|---|
| Phytol* | n/a | -23.6 | -21.5 |
| $C_{25:4}$ (Z) | -23.1 | -19.7 | -17.5 |
| $C_{25:3}$ (E) | n/a | -19.6 | -20.5 |
| $C_{25:5}$ (Z) | -20.3 | -19.3 | -17.2 |
| $C_{25:4}$ (E) | -18.5 | -18.2 | -17.9 |
| $C_{25:5}$ (E) | -26.2 | -20.8 | -21.6 |
| Squalene | -23.1 | -19.7 | -19.8 |
| unidentified $C_{27}$ sterol* | -23.5 | -21.5 | -18.7 |
| Cholesterol* | -24.1 | -23.5 | -19.3 |

* includes correction factors for phytol and sterols from TMS (+1.06 for phytol and +0.63 for both sterols), n/a Below limit of detection. Average values from two samples are given.

### *4.3.10 Discussion*

The results obtained from these experiments performed with the diatom *P. intermedium*, support the hypothesis that both mevalonate and MEP pathways contribute to the biosynthesis of terpenoids in this species. Unfortunately, the observations made from the inhibition experiments do not allow for any definite conclusions to be made concerning the individual biosynthetic routes used by this species. Thus, while inhibition of cell growth was clear in the case of mevinolin, there was no inhibition of the isoprenoid concentrations in the cells. Similar observations were made with fosmidomycin for most of the isoprenoids. Phytol, *n*-$C_{21:6}$, squalene and sterol concentrations were not significantly effected by the presence of fosmidomycin, although the distribution of the individual $C_{25}$ HBI isomers was altered. The reasons for this are, as yet, unclear.

From isotopic labelling experiments, only a small incorporation of $^{13}C$ from [1-$^{13}C$] acetate was detected in HBIs and phytol, while a significant $^{13}C$ incorporation was detected for squalene and sterols. However, deuterium was incorporated into squalene and sterols, but not

into phytol and the HBIs, when the cells were cultured in the presence of [$^2H_3$] acetate indicating that acetate is directly incorporated into triterpenoids, but not into phytol (a diterpenoid) or the $C_{25}$ HBIs (sterterpenoids). $^{13}C$ incorporation into the latter compounds probably occurs *via* $^{13}CO_2$ after degradation of [1-$^{13}C$] acetate. When *P. intermedium* was cultured in the presence of $^{13}CO_2$, $^{13}C$ was efficiently incorporated into all the isoprenoids present in this diatom. Surprisingly, when examined individually by GC-irm-MS, no clear differences between the $\delta^{13}C$ values obtained for the triterpenes and the $C_{25}$ HBIs were observed. Even more surprising are the results obtained for these compounds isolated from cells cultured in the presence of inhibitors. Indeed, when either mevinolin or fosmidomycin was present in the culture, the $\delta^{13}C$ values of all the isoprenoids are substantially more positive. Further experiments are required before the observations made from these preliminary investigations can be fully understood.

### 4.4 Conclusion

The biosynthesis of non-saponifiable lipids in the three diatoms *Rhizosolenia setigera*, *Haslea ostrearia* and *Pleurosigma intermedium* have been investigated using pathway-specific inhibition methods, stable isotope incorporation experiments and analysis of natural isotopic fractionation. The early steps of terpenoid biosynthesis have been investigated in the three diatom species *Rhizosolenia setigera*, *Haslea ostrearia* and *Pleurosigma intermedium*. The studies described herein demonstrate that in these three diatoms, terpenes are biosynthesised by both the MEP and MVA pathways. The distribution of the two pathways is dependent on the individual species, the lipid type, and in the cases of $C_{25}$ and $C_{30}$ HBI alkenes, the isomeric form. In *R. setigera* and *P. intermedium*, sterols are made according to the mevalonate pathway, while in *Haslea ostrearia*, the MEP route is the main contributor to their biosynthesis. In all three diatoms,

phytol is made exclusively via the MEP pathway. These observations are entirely consistent with previous findings from diatoms, green algae and higher plants (Eisenreich *et al.*, 1998; Lichtenthaler, 1999; Cvejic and Rohmer, 2000). Indeed, similar to what was observed for *P. intermedium* and *R. setigera*, Cvejić and Rohmer (2000) demonstrated that in two diatom species (*Phaeodactylum tricornutum* and *Nitzschia alba*), sterols were synthesised according to the mevalonate pathway, while phytol was made exclusively *via* the MEP route. In contrast, the observations made for *H. ostrearia*, are more consistent with those made previously from green algae, in which the mevalonate pathway is absent.

Concerning HBI alkenes, it is clear that the mevalonate pathway is involved in the biosynthesis of $C_{25}$ and $C_{30}$ HBIs in *R. setigera*. Additionally, evidence for a contribution from the non-mevalonate pathway to these compounds also exists, and that the level of this contribution appears to be related to the physiological status of the cells.

In the case of *P. intermedium*, there is no evidence for the formation of $C_{25}$ HBIs *via* the mevalonate route, despite these compounds having the same isomeric structures as those found in *R. setigera*. The same is true for the $C_{25}$ HBIs biosynthesised by *H. ostrearia*, which are regioisomers of those found in *R. setigera* and *P. intermedium*. *For P. intermedium* (isotopic incorporation) and *H. ostrearia* (isotopic incorporation and inhibition studies), these (preliminary) experiments indicate that their $C_{25}$ HBIs are made *via* the MEP route only.

Finally, observations from the fractionation of *R. setigera* cells were consistent with previous findings from higher plants concerning phytol and desmosterol, and provided information on the localisation of HBIs in the cells. As a result, it is now unambiguously demonstrated that HBIs are present neither in the outer and inner membranes nor in the stroma of chloroplasts and that these alkenes are present in the free-lipid fraction (i.e. Cytoplasm). However, since a limited number of the cell organelles were successfully

isolated (only pure chloroplasts and free lipids fractions were obtained), it is still possible that these lipids could be also localised in the plasma membranes or in other cellular organelles (e.g. mitochondria, endoplasmic reticulum). In addition, since the mevalonate pathway appears to proceed in the cytosol while the MEP is localised in the chloroplast, the inter-species differences observed for the biosynthesis of $C_{25}$ and $C_{30}$ HBIs in diatoms, may also reflect differences in their compartmentation. Therefore, further fractionation experiments preformed on *R. setigera* as well as other diatoms are required to obtain additional information as to their location, and consequently, concerning their physiological purpose.

Table 4.36 Biosynthetic pathways and location of isoprenoids in *Rhizosolenia setigera*, *Haslea ostrearia* and *Pleurosigma intermedium*.

| Species | Phytol | Highly branched isoprenoids | | Sterols |
|---|---|---|---|---|
| | | Haslenes | Rhizenes | |
| *Rhizosolenia setigera* | MEP | MVA + MEP | MVA + MEP | MVA |
| *Haslea ostrearia* | MEP | MEP | - | MEP |
| *Pleurosigma intermedium* | MEP | MEP | - | MVA |
| Location (*R. setigera*) | Chloroplasts | Cytoplasm | Cytoplasm | Cytoplasm |

# CHAPTER FIVE

## Experimental Details

### 5.1 General Procedures

Glassware was cleaned in Decon-90, rinsed in distilled/Millipore-grade water, oven-dried (150°C; overnight) and finally, when needed, rinsed with an appropriate solvent (e.g. hexane) immediately before use. All chemicals used for preparing the diatom culture media were analytical-grade and plant cell culture-tested whereas all solvents were HPLC-grade (Rathburn) and found to be of adequate purity.

Whatman GFF glass fibre filters were used to harvest small scale cultures and when required preliminarily oven dried (450°C, 4 h) to remove traces of organic impurities.

Silica gel (BDH; 60-120 mesh) was used as the stationary phase for open column chromatography. The silica was solvent extracted (Soxhlet; dichloromethane; 24 h), activated by heating (180°C; 24 h) and deactivated immediately before use by shaking (40 min) with the appropriate quantity of Millipore grade water (5%).

Anhydrous sodium sulphate, silver sand and cotton wool were all solvent extracted with dichloromethane before use to remove trace organic impurities.

### 5.2 Sampling methodology

Diatoms were collected from various locations, including both benthic and planktonic compartments from marine and freshwater environments. Benthic diatoms were collected at low tide with a sterile syringe from the uppermost 1 cm of mud or sediment surface.

Planktonic diatoms were collected using a 75 µm plankton net. Samples were preserved in the dark in a cool box prior to analysis in the laboratory.

### 5.3 Species identification, light microscopy, scanning electron microscopy

Individual species were identified using a combination of light (LM) and scanning electron microscopy (SEM) techniques (Olympus Provis, JEOL 6400F). Benthic cells and some strongly silicified planktonic diatoms were prepared following Hendey's methodology (1974) and then rinsed with distilled water. A portion of the cleaned cells was mounted in Hyrax for further LM observations and a second portion dried onto aluminium stubs and coated with gold/palladium for SEM (JEOL 6400F). For the very delicate species such as *Rhizosolenia spp.*, a special methodology was required to dry the sample: cleaned cells were dehydrated using an alcohol bath series and dried using critical point techniques (Beninger *et al.*, 1995).

### 5.4 Diatom isolation and general culturing conditions

In the laboratory, single cells were isolated under the microscope and transferred by pipette onto 6 ml cell culturing plates previously filled with sterile F/2 enriched seawater or CHU-10 enriched freshwater (Guillard, 1975; Stein, 1973). Table 5.1 summarises the chemical composition of both F/2 and CHU-10 media. Cells were grown under controlled conditions (14°C, 100 µmol photon $m^{-2} s^{-1}$, 14/10 light/dark cycle) in a culture room (Figure 5.1). After 8-12 days, cells were transferred onto a 250 ml Erlenmeyer flask containing 150 ml of F/2 or CHU-10 medium.

When bulk cultures were required, cells from a 250 ml Erlenmeyer flask were transferred to a 4 l flask containing 2 l of medium and subsequently to a 25 l barrel containing 22 l of medium. This barrel was then used as an innoculum for 300 or 450 l tanks (Figure 5.2). Bulk

cultures were grown under natural (greenhouse) or controlled conditions (culture room) depending on the experimental requirements:

- Greenhouse : natural conditions (variable temperature and light intensity)
- Culture room : controlled conditions (constant temperature and constant light intensity)

Table 5.1 Chemical composition F/2 and CHU-10 culture media.

| Element | CHU-10 Final concentration (mg $l^{-1}$) | F/2 Final concentration (mg $l^{-1}$) |
|---|---|---|
| | Filtered freshwater | Filtered sea-water |
| $NO_3^-$ | $Ca(NO_3)_2.4H_2O$; 57.56 | $NaNO_3$; 75.00 |
| $PO_4^{3-}$ | $K_2HPO_4$; 10.00 | $NaH_2PO_4.H_2O$; 5.00 |
| $SiO_3^{2-}$ | $Na_2SiO_3.9H_2O$; 58.00 | $Na_2SiO_3.9H_2O$; 30.00 |
| $CO_3^{2-}$ | $Na_2CO_3$; 20.00 | - |
| $Mg^{2+}$ | $MgSO_4.7H_2O$; 25.00 | - |
| $Fe^{3+}$ | $FeCl_3.6H_2O/Na_2EDTA$; 3.15/4.36 | $FeCl_3.6H_2O/Na_2EDTA$; 3.15/4.36 |
| $Cu^{2+}$ | - | $CuSO_4.5H_2O$; 9.80 x10E$^{-3}$ |
| $Zn^{2+}$ | - | $ZnSO_4.7H_2O$; 22.00 x10E$^{-3}$ |
| $Co^{2+}$ | - | $CoCl_2.6H_2O$; 10.00 x10E$^{-3}$ |
| $Mn^{2+}$ | - | $MnCl_2.4H_2O$; 180.00 x10E$^{-3}$ |
| **Thiamine HCl** | 200.00 x10E$^{-3}$ | 200.00 x10E$^{-3}$ |
| **Cyanocobalamin** | 1.00 x10E$^{-3}$ | 1.00 x10E$^{-3}$ |
| **Biotin** | 1.00x10E$^{-3}$ | 1.00x10E$^{-3}$ |

### 5.5 Cell harvesting

A growth curve of a diatom batch culture can be represented diagrammatically and divided into three phases (Figure. 5.3):

- The lag phase, where recently transferred cells adapt themselves to the new conditions.

- The exponential growing phase, where cells are actively dividing themselves (the most productive period of growth).

- The stationary phase, where the cell density is so high that there is a mutual shading diminishing the photosynthetic efficiency (Myers, 1962), and where nutrient ($NO_3^-$, $PO_4^{3-}$, $SiO_3^{2-}$) concentration can be limiting (Robert, 1983).

Figure 5.1 Small scale cultures of various diatom species under controlled conditions.

Figure 5.2 Bulk cultures of a planktonic diatom (left) and of a benthic diatom (right).

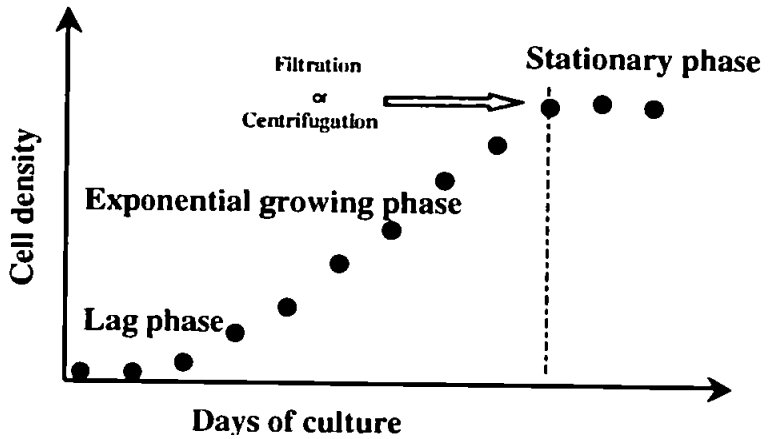

Figure 5.3: Typical growing curve of a diatom culture.

In order to determine the physiological status of the cultures, cells were quantified daily using a Nageotte counting plate. HBI analysis was carried out on cells harvested at the end of the exponential growing phase. For small scale cultures, cells were harvested by filtration using Whatman GFF glass fibre filters whereas for large scale cultures, cells were harvested by continuous flow centrifugation (Cepa patberg) and freeze dried prior to extraction.

### 5.6 Hydrocarbon extraction from small scale algal cultures

Each filter was extracted three times with hexane to yield total hexane extracts (THEs). After the removal of the solvent under a stream of nitrogen gas, the THEs were saponified with 5% KOH in methanol/water (80/20) at 80°C for 30 min to remove triglyceride esters of fatty acids. The non-saponifiable lipids (NSL) were then re-extracted into hexane and dried over anhydrous $Na_2SO_4$. Prior to analyses by GC-MS, the hexane was removed from samples under a stream of nitrogen and the NSL fractions were silylated (BSTFA:TMCS 99:1; 50 µl) at 70°C for 30 min. When required for the quantification of HBI cell content, an internal standard (7-hexylnonadecane; 1.1 µg $filter^{-1}$) was added prior to the extraction of the filters with hexane.

### 5.7 Isoprenoid extraction from large scale algal cultures

Centrifuged large scale diatom cultures gave a concentrated algal paste which was then freeze dried. The paste was then extracted five times using dichloromethane/methanol (50:50, v/v,) to yield a total organic extract (TOE). Solvents were then removed under reduced pressure and the extract obtained was kept frozen (-20°C) before purification.

### 5.8 Isolation and purification of isoprenoids

Isolation and purification of phytol, sterols and HBIs from the TOEs was achieved using a combination of open column chromatography (5% deactivated $SiO_2$/ hexane) techniques and preparative high pressure chromatography techniques (Chromspher 5 lipid column).

For open columns, the size varied depending on the amount of material to be separated, with a typical ratio of 50:1 $SiO_2$:TOE (w/w). The hydrocarbon fraction was obtained from the TOE after application onto the column and elution with hexane (5 column volumes), sterols and phytol were eluted using a series of solvents of increasing polarity (typically dichloromethane, acetone and methanol). Table 5.2 summarises the isoprenoid composition of each fraction obtained.

The hydrocarbons obtained in the hexane fraction were analysed directly by GC-MS. Dichloromethane, acetone and methanol fractions were saponified with 5% KOH in methanol/water (80/20) at 80°C for 30 min to remove triglyceride esters of fatty acids, re-extracted with hexane and sylilated (BSTFA:TMCS 99:1; 70°C, 30 min.) before analysis by GC-MS and combined where appropriate (i.e. both dichloromethane and acetone fractions could contain phytol and sterols).

Table 5.2 Isoprenoid composition of the fractions obtained by open column chromatography (5% deactivated $SiO_2$)

| Fraction | Components |
|---|---|
| Hexane | *n*-$C_{21:6}$, HBIs, Squalene |
| DCM | Phytol, Sterols |
| Acetone | Phytol, Sterols |
| Methanol | Phytol |

Phytol and sterols were separated on a smaller silica column eluted with dichloromethane and acetone respectively. Table 5.3 summarises the amount of eluent necessary for the isolation of phytol and sterols.

Table 5.3 Elution volumes (in column volume equivalents) required for the isolation of phytol and sterols by open column chromatography (5% deactivated $SiO_2$).

| Eluent | Eluent volume | Components |
|---|---|---|
| DCM | 1-3 | - |
| DCM | 3-5 | Phytol |
| DCM | 5-9 | Phytol, Sterols |
| Acetone | 1-3 | Sterols |
| Acetone | 3-6 | - |

Individual lipids from the hydrocarbon fraction obtained by open column chromatography were separated by silver-ion chromatography (Chromspher 5 lipid, 250X4.6 mm I.D.) under isocratic conditions. A Hewlett Packard 5010 HPLC system coupled to a Hewlett Packard diode array detector was used. The fractions were collected manually and the isocratic mobile phase was composed of hexane with a mixture of hexane-isopropanol (75:25, v/v), the percentage of each solvent being determined by the composition of the fraction to purify. When the hydrocarbon fraction contained both $C_{25}$ and $C_{30}$ HBI isomers, a preliminary fractionation using open column chromatography (5% deactivated $SiO_2$) was necessary prior

to the separation by silver-ion chromatography to allow sufficient resolution for the isolation of individual isomers. (e.g. Hydrocarbon fractions obtained from the diatom *Rhizosolenia setigera* could contain both $C_{25}$ and $C_{30}$ HBIs )

### 5.9 Microscale hydrogenation

Hydrogen gas was bubbled through a solution of the HBI extract dissolved in hexane (5 ml) in the presence of the hydrogenation catalyst ($PtO_2.2H_2O$; 0.1 g). Aliquots were removed at regular intervals to monitor the hydrogenation progress by GC-MS. Following hydrogenation, samples were filtered through a glass Pasteur pipette containing anhydrous sodium sulphate, and the solvent was removed under nitrogen prior to storage.

### 5.10 Gas chromatography-mass spectrometry

A Hewlett-Packard 5890 Series II gas chromatograph (GC), fitted with a 12 m fused silica HP-1 column (0.2 mm internal diameter) and coupled to a 5970 Series Mass Selective Detector (MSD) was used to perform gas chromatography-mass spectrometry (GC-MS) analyses. The GC oven temperature was programmed from 40-300°C at 5°C $min^{-1}$ and held at the final temperature for 10 minutes. Operating conditions for the mass spectrometer were 250°C for the ion source temperature and 70eV for the ionisation energy. Spectra (50-500 Daltons) were collected using Hewlett Packard MS-Chemstation software.

Identification of individual compounds was achieved by comparison of retention indices and mass spectra with authentic standards.

### 5.11 Nuclear magnetic resonance spectroscopy

NMR analysis of purified HBIs (typically 0.1 – 20 mg) was performed using a JEOL EX-270 FT-NMR spectrometer. 1-D ($^{1}H$, $^{13}C$ and DEPT) and 2-D (COSY, HMQC, HMBC) were all recorded in $CDCl_3$ using residual $CHCl_3$ (7.24 ppm) and $^{13}CDCl_3$ (77.0 ppm) as references. Data were collected using JEOL Delta software.

# CHAPTER SIX

## Conclusions and Future Work

The main objective of this study was to understand better the controls on the production of terpenoids by diatoms, with a particular emphasis on highly branched isoprenoid alkenes (HBIs). Since the discovery of these alkenes in cultures of the two diatom species *Haslea ostrearia* and *Rhizosolenia setigera*, the structures of numerous $C_{25}$ and $C_{30}$ HBI alkenes have been determined, including those commonly found in the geosphere (Figure 6.1). At the outset of the present study, the structures of a total of twenty-six different HBI alkenes had been established by various spectroscopic methods. However, despite the analysis by the author of more than fifty diatom species, only a very limited number have been found to be producers of $C_{25}$ or $C_{30}$ HBIs (Table 6.1). The reasons for their production by some species and not by others (including very closely related species) remain unclear. Further, although it has been suggested that these acyclic isoprenoids may be membrane constituents (Ourisson and Nakatani, 1994; Rowland *et al.*, 2001a), their true biological function remains to be verified.

In addition, while previous investigations had demonstrated that environmental factors such as temperature are capable of controlling the HBI biosynthesis of $C_{25}$ HBIs in the diatom *Haslea ostrearia*, other studies had shown that the factors controlling the distributions of the related $C_{25}$ and $C_{30}$ HBI alkenes in the diatom *Rhizosolenia setigera* remained unclear. Therefore, a study on the biological controls on isoprenoid (including HBIs) production in diatoms was proposed in order to understand better their biological function. To this end, the specific objectives of this study were:

(i) To investigate the distribution of HBI alkenes biosynthesised by *R. setigera* as a function of its physiological status.

(ii) To determine the biosynthetic pathways responsible for isoprenoid formation in a number of different diatoms.

(iii) To examine the distribution of isoprenoids within various organelles of diatoms.

(iv) To continue the characterisation of $C_{25}$ and $C_{30}$ HBIs (and related hydrocarbons) in diatoms.

In order to meet these objectives, the author needed to:

1. Isolate a range of diatoms from the natural environment.

2. Obtain single species of diatoms from assemblages and identify them using light and electron microscopic techniques.

3. Culture individual species of diatoms under a range of controlled experimental conditions.

4. Extract, purify, identify and quantify a suite of terpenoid lipids in diatoms using LC, GC, GC-MS, GC-irm-MS and NMR spectroscopy.

5. Characterise the physiological status of one species of diatom (*R. setigera*) using microscopy methods.

6. Fractionate individual diatom organelles using centrifugation methods.

The results of this study are presented and discussed in Chapters 2-4. This final chapter provides a summary of the results and a brief discussion of their significance.

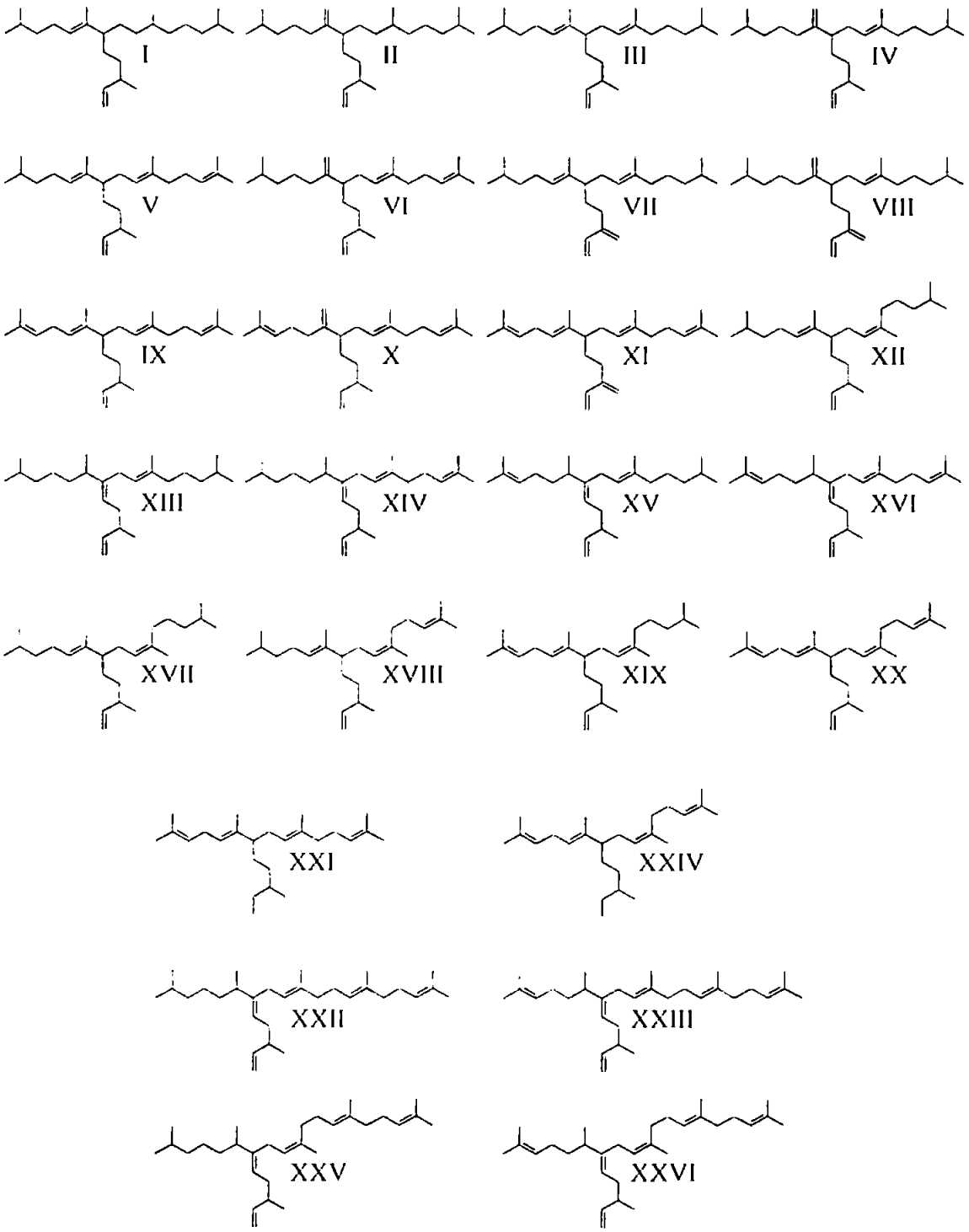


Figure 6.1 Structures of $C_{25}$ and $C_{30}$ HBI alkenes identified previously in cultured diatoms.

Table 6.1 A summary of all the diatom species investigated for the presence of HBI alkenes. The names of HBI-producing species are highlighted in bold.

| Species name | Ecology | HBI structures |
|---|---|---|
| ***Haslea ostrearia*** | Marine / Benthic | I-XI |
| ***Haslea crucigera*** | Marine / Benthic | VI, X |
| ***Haslea salstonica*** | Marine / Benthic | VI |
| ***Haslea pseudostrearia*** | Marine / Benthic | V, X |
| ***Haslea nipkowii*** | Marine / Benthic | III, IV, XII |
| *Haslea wawrikae* | Marine / Planktonic | |
| ***Pleurosigma intermedium*** | Marine / Benthic | XIII-XX |
| *Pleurosigma angulatum* | Marine / Benthic | |
| ***Pleurosigma planktonicum*** | Marine / Planktonic | XXI, XXIV |
| ***Pleurosigma sp.*** | Marine / Planktonic | XIV-XVI, XVIII-XX |
| *Gyrosigma limosum* | Marine / Benthic | |
| *Gyrosigma fasciola* | Marine / Benthic | |
| *Gyrosigma sp.* | Marine / Benthic | |
| *Gyrosigma sp.* | Freshwater / Benthic | |
| *Navicula ramosissima* | Marine / Benthic | |
| *Navicula phyllepta* | Marine / Benthic | |
| *Navicula sp.* | Marine / Benthic | |
| ***Navicula sclesvicensis*** | Freshwater / Benthic | XIII |
| *Navicula gracilis* | Freshwater / Benthic | |
| *Navicula lanceolata* | Freshwater / Benthic | |
| *Amphora hyalina* | Marine / Benthic | |
| *Amphora sp.* | Marine / Benthic | |
| *Stauroneis glacialis* | Marine / Benthic | |
| *Stauroneis constricta* | Marine / Benthic | |
| *Nitzschia alexandrina* | Marine / Benthic | |
| *Nitzschia closterium* | Marine / Benthic | |
| *Entomoneis paludosa* | Marine / Benthic | |
| *Entomoneis alata* | Marine / Benthic | |
| *Grammatophora marina* | Marine / Planktonic | |
| *Synedra tabulata* | Freshwater / Benthic | |
| *Tabellaria fenestrata* | Freshwater / Benthic | |
| *Cymbella sp.* | Freshwater / Benthic | |
| *Asterionella formosa* | Freshwater / Planktonic | |
| ***Rhizosolenia setigera*** | Marine / Planktonic | XIII-XVII, XXII, XXIII, XXV, XXVI |
| ***Rhizosolenia pungens*** | Marine / Planktonic | XIII-XVI, XXII, XXIII, XXV, XXVI |
| *Rhizosolenia robusta* | Marine / Planktonic | |
| *Guinardia delicatula* | Marine / Planktonic | |
| *Guinardia solstherfothii* | Marine / Planktonic | |
| *Proboscia indica* | Marine / Planktonic | |
| *Dytilum brightwellii* | Marine / Planktonic | |
| *Odontella sinensis* | Marine / Planktonic | |
| *Eucampia zodiacus* | Marine / Planktonic | |
| *Chaetoceros spp.* | Marine / Planktonic | |
| *Skeletonema costatum* | Marine / Planktonic | |
| *Coscinodiscus sp.* | Marine / Planktonic | |
| *Thalassiosira sp.* | Marine / Planktonic | |
| *Urosolenia cf. longiseta* | Freshwater / Planktonic | |
| *Achanthoceras zachariasi* | Freshwater / Planktonic | |
| *Melosira italica* | Freshwater / Planktonic | |

The first aim of this study was to attempt to identify the factors determining the variations in distributions of HBI alkenes in the diatom *R. setigera,* since in contrast to the diatom *H. ostrearia*, considerable variations in the distributions of HBIs in *R. setigera* were observed within different strains of this species, as well as from strains cultured under apparently 'identical' conditions. At the outset of this investigation, six different species of the genus *Rhizosolenia* and closely related genera were examined for HBIs using GC-MS (Chapter 2). As a result, an additional diatom species (*Rhizosolenia pungens*) was found capable of producing both $C_{25}$ and $C_{30}$ HBIs, and their distributions were found to be almost identical to those often observed in *R. setigera.* However, in contrast with the genus *Haslea*, HBI production in the genus *Rhizosolenia* appears to be restricted to a limited number of species.

More significantly, this study has revealed that the distributions of $C_{25}$ and $C_{30}$ HBI alkenes in *R. setigera* (strain RS 99) are highly dependent on the physiological status of the cells, as measured by the position of this diatom in its life cycle. Thus, while $C_{30}$ HBIs are observed at every stage of the life cycle, $C_{25}$ HBIs are not always present in the cells. Since their synthesis appears to be stimulated by the onset of auxosporulation (sexual reproduction), this almost certainly explains why they have rarely been observed in previous studies.

In addition, two novel monocyclic $C_{30}$ alkenes previously reported (but not characterised) in other strains of *R. setigera*, and a novel monocyclic $C_{25}$ alkene were observed much later than the auxosporulation event. The two $C_{30}$ hydrocarbons were subsequently characterised and identified as XXVII and XXVIII (Figure 6.2) using mass spectrometry and NMR spectroscopic techniques (Chapter 3). The potential geochemical relevance of these compounds was highlighted by comparison of their mass spectral and chromatographic

properties with those of alkenes reported in sediments and suspended water column particles.

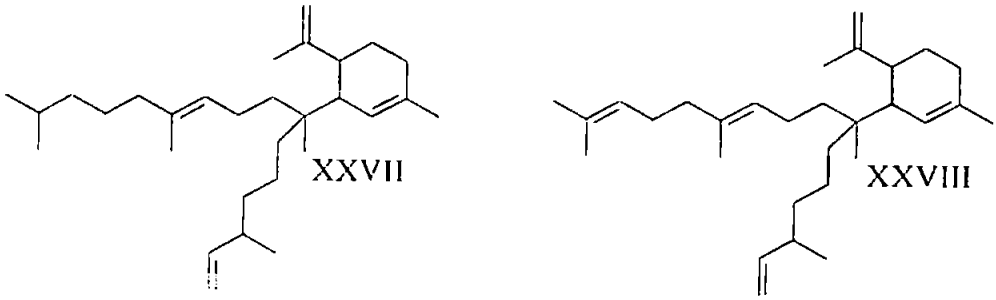


Figure 6.2 Structures of two novel monocyclic $C_{30}$ alkenes characterised in this study.

The second aim of this work was to characterise the biosynthetic pathways leading to isoprenoid formation in the diatoms *Rhizosolenia setigera*, *Haslea ostrearia* and *Pleurosigma intermedium*. Experiments using pathway-specific inhibitors, $^{13}C$ and $^{2}H$ labelled precursors, along with isotope-ratio mass spectrometric techniques (Chapter 4) allowed the biosynthetic routes to the production of several isoprenoids in these three diatom species to be determined. The results of this combined experimental approach has demonstrated that the metabolic pathways involved in the biosynthesis of terpenoids in diatoms is both species and terpene dependent. Indeed, phytol, a chloroplastidic diterpene, is synthesised by each species investigated according to the recently discovered methyl-erythritol phosphate (MEP) pathway. Although this pathway is involved in the synthesis of $C_{25}$ HBIs in the two species *H. ostrearia* and *P. intermedium*, $C_{25}$ and $C_{30}$ HBIs, and the monocyclic $C_{30}$ alkene XXVII, appear to be made predominantly *via* the mevalonate (MVA) route in the diatom *R. setigera*. Similar, though not identical observations were made for the major sterols in these three species. Thus, evidence for the contribution of the MVA pathway

was found for the biosynthesis of desmosterol, a $C_{27}$ sterol synthesised by the diatom *R. setigera,* and for the four sterols produced by *P. intermedium*. In contrast, only contributions from the MEP pathway were found for the biosynthesis of sitosterol, the major ($C_{29}$) sterol found in *H. ostrearia*.

The third aim of this study was to examine the intra-cellular location of isoprenoids (including HBIs) in diatoms. Fractionation of *R. setigera* cells revealed that phytol was present in the chloroplasts as expected, while sterols and HBIs were present in the cytoplasm. These observations are consistent with previous findings from higher plants which have shown that the mevalonate pathway, operating in the cytoplasm, accounts for the biosynthesis of sesquiterpenes and triterpenes, while the MEP pathway, functioning in the chloroplasts, contributes to the biosynthesis of monoterpenes, diterpenes and tetraterpenes.

Despite numerous studies on the biosynthesis of terpenoids, sesterterpenes (including $C_{25}$ HBIs) have not been previously investigated. Since they might be considered to be "intermediate" between diterpenes ($C_{20}$) and triterpenes ($C_{30}$), one may have expected a contribution from both routes to their biosynthesis. In fact, both isotopic labelling and fractionation studies revealed that these compounds were made by (predominantly) a single pathway, although the pathway itself appears to be species dependent.

Further conclusions can also be drawn from this study, with some of these providing the basis for some suggested further work. For example, while life cycle experiments together with investigations on the non-saponifiable lipids obtained from *R. setigera* (and related species) provide an explanation for most of the variations of $C_{25}$ and $C_{30}$ HBI distributions observed between *R. setigera* strains, the differences in HBI composition found in the non-saponifiable fractions of the strains CCMP 1820 and CCMP 1330 noted by Rowland *et al.* (2001b) and Sinninghe Damsté *et al.* (1999a,b, 2000) remain unexplained. Therefore, a more

expansive taxonomic and lipid investigation of the *Rhizosolenia* genus and closely related genera would be of interest, and may prove to be helpful in understanding these variations. Given the ecological importance of this genus (one of the most represented genera in the phytoplankton), and since several *Rhizosolenia* strains were found to synthesise the most common HBIs in sediment and water column particles, this additional study may also confirm the geochemical importance of species belonging to this genus. In addition, through investigation of further diatom species, sources of $C_{20}$ HBIs may be established. To date, source organisms for these compounds have not been identified despite several geochemical reports (reviewed by Rowland and Robson, 1990).

Inhibition and stable isotope incorporation experiments performed herein have provided clear evidence for the contribution of the MVA pathway toward the synthesis of both HBIs and desmosterol in *R. setigera,* and sterols in *P. intermedium*, while evidence for the involvement (exclusive or not) of the MEP route in the biosynthesis of other isoprenoids in the three diatoms studied has been obtained. Since the evidence for the operation of the MEP pathway is not as comprehensive as that obtained for the involvement of the MVA route, further experiments, involving culturing the three diatoms in the presence of labelled deoxy-D-xylulose phosphate or methyl-erythritol phosphate (known intermediates in the MEP pathway) would be valuable in verifying the participation (exclusive or not) of the MEP pathways in the biosynthesis of these lipids. Also, as unique genes associated with each of the two pathways have been identified, the localisation (or not) of such genes should also prove to be informative.

Analysis of natural carbon isotopic fractionation analysis of the non-saponifiable lipids of *R. setigera* obtained from a life cycle experiment (RS-2) using GC-irm-MS, revealed significant differences in the $\delta^{13}C$ values of individual lipids, as well as some intriguing

variations between the growth cycles or different phases of the life cycle (Chapter 4). Significant differences were observed between the $\delta^{13}C$ values of phytol and those obtained for both HBIs and sterols during the pre-auxosporulation phase, while in later phases (post-auxosporulation), the $\delta^{13}C$ values of both HBIs and desmosterol increased significantly and tended toward that of phytol which remained constant. Thus, the HBIs and sterols appear to be made from both pathways, with the partitioning of these two pathways dependent on the physiological status of the cells. Since complementary experiments have shown that phytol is made exclusively *via* the MEP route, these observations provide evidence for an increasing contribution of the MEP pathway toward the biosynthesis of HBIs and sterols during both the auxosporulation and the early post-auxosporulation phases. Arguably, while these observations relate to the most significant period of the diatom's life cycle, a further study, encompassing an entire life cycle, would seem necessary in order for a full appreciation of this partitioning of biosynthetic pathways to be made. This partitioning may also be affected by e.g. photosynthetic rates vs. inorganic carbon uptake, which could also be determined experimentally.

Finally, observations made following the intra-cellular fractionation of *R. setigera* cells were consistent with previous findings from higher plants concerning phytol and desmosterol. Thus, phytol was located in the chloroplasts, while desmosterol was found in the cytoplasm. In addition, the experiments provided information on the localisation of HBIs in cells of *R. setigera* even though only pure plastid and free lipid fractions were obtained. As a result, it has been demonstrated that HBIs are absent from the outer and inner membranes and the stroma of chloroplasts, and that these alkenes are present in the free-lipid fraction. However, it is also still probable that these lipids are constituents of plasma membranes or are localised in other cellular organelles (e.g. mitochondria, endoplasmic reticulum). Therefore, further fractionation experiments performed on diatoms according to established procedures

(Hodges and Mills, 1986; Price *et al.*, 1987; Briskin *et al.*, 1987; Kinne-Saffran and Kinne, 1989; Wiltpoth *et al.*, 1998; Moore and Proudlove, 1987) are required before their function(s) are fully elucidated. Finally, since Takajo *et al.* (2001) have demonstrated that HBI pyrophosphates can spontaneously form vesicles, and as such could be implicated in the formation of primitive membranes, an investigation into the presence of these compounds in diatoms may also help in understanding the biological significance of HBI alkenes.

## References


Allard, W.G. (2002). Sources and structures of commonly occurring Highly Branched Isoprenoid alkenes. PhD dissertation. *University of Plymouth.*

Allard, W.G., Belt, S.T., Massé, G., Naumann, R., Robert, J.-M., and Rowland, S.J. (2001). Tetra-unsaturated sesterterpenoids (Haslenes) from *Haslea ostrearia* and related species. *Phytochemistry*, **56**: 795-800.

Anonymous (1975). Proposals for a standardization of diatom terminology and diagnoses. *Nova Hedwigia. Beih.*, **53**: 323-354.

Arigoni, D., Sagner, S., Latzel, C., Eisenreich, W., Bacher, A., and Zenk, M.H. (1997). Terpenoid biosynthesis from 1-deoxy-D-xylulose in higher plants by intramolecular skeletal rearrangement. *Proceedings of The National Academy of Sciences of The United States of America*, **94**: 10600-10605.

Bach, T.J. and Lichtenthaler, H.K. (1982). Mevinolin: A highly specific inhibitor of microsomal 3-hydroxy-3-methylglutaryl-coenzyme A reductase of radish plants. *Zeitschrift Fur Naturforschung C*, **37**: 46-50.

Bach, T.J. and Lichtenthaler, H.K. (1983). Inhibition by mevinolin of plant growth, sterol formation and pigment accumulation. *Physiologia Plantarum*, **59**: 50-60.

Barrett, S.M., Volkman, J.K., and Dunstan, G.A. (1995). Sterols of 14 species of marine diatoms (Bacillariophyta). *Journal of Phycology*, **31**: 360-369.

Barrick, R.C. and Hedges, J.I. (1981). Hydrocarbon geochemistry of the Puget Sound region - II. Sedimentary diterpenoid, steroid and triterpenoid hydrocarbons. *Geochimica et Cosmochimica Acta,* **45**: 381-392.

Belt, S.T., Cooke, D.A., Robert, J.-M., and Rowland, S.J. (1996). Structural characterisation of widespread polyunsaturated isoprenoid biomarkers: a $C_{25}$ triene, tetraene and pentaene from the diatom *Haslea ostrearia* Simonsen.

*Tetrahedron Letters*, **37**: 4755-4758.

Belt, S.T., Allard, G., Massé, G., Robert, J.-M., and Rowland, S.J. (2000a). Important sedimentary sesterterpenoids from the diatom *Pleurosigma intermedium*. *Chemical Communications*, 501-502.

Belt, S.T., Allard, W.G., Massé, G., Robert, J.-M., and Rowland, S.J. (2000b). Highly branched isoprenoids (HBIs): Identification of the most common and abundant sedimentary isomers. *Geochimica et Cosmochimica Acta*, **64**: 3839-3851.

Belt, S.T., Allard, W.G., Massé, G., Robert, J.-M., and Rowland, S.J. (2001a). Structural characterisation of $C_{30}$ highly branched isoprenoid alkenes (Rhizenes) in the marine diatom *Rhizosolenia setigera*. *Tetrahedron Letters*, **42**: 5583-5585.

Belt, S.T., Massé, G., Allard, W.G., Robert, J.-M., and Rowland, S.J. (2001b). Identification of a $C_{25}$ highly branched isoprenoid triene in the freshwater diatom *Navicula sclesvicensis*. *Organic Geochemistry*, **32**: 1169-1172.

Belt, S.T., Massé, G., Allard, W.G., Robert, J.-M., and Rowland, S.J. (2001c). $C_{25}$ highly branched isoprenoid alkenes in planktonic diatoms of the *Pleurosigma* genus. *Organic Geochemistry*, **32**: 1271-1275.

Belt, S.T., Allard, W.G., Johns, L., König, W.A., Massé, G., Robert, J.-M., and Rowland, S.J. (2001d). Variable stereochemistry in highly branched isoprenoids from diatoms. *Chirality*, **13**: 415-419.

Beninger, P.G., St Jean, S.D., and Poussart, Y. (1995). Labial palps of the blue mussel *Mytilus edulis* (*Bivalvia, Mytilidae*). *Marine Biology*, **123**: 293-303.

Boehm, P.D. and Quinn, J.G. (1978). Benthic hydrocarbons of Rhode Island Sound. *Estuarine and Coastal Marine Science*, **6**: 471-494.

Briskin, D.P., Leonard, R.T., and Hodges, T.K. (1987). Isolation of the Plasma Membrane: Membrane Markers and General Principles. *Methods in Enzymology*, **148**: 542-558.

Brown, M.R., Jeffrey, S.W., Volkman, J.K., and Dunstan, G.A. (1997). Nutritional properties of microalgae for mariculture. *Aquaculture*, **151**: 315-331.

Chappell, J., (1995). Biochemistry and molecular biology of the isoprenoid biosynthetic-pathway in plants. *Annual review of plant physiology and plant molecular biology*, **46**: 521-547.

Charon, L., Hoeffler, J.F., Pale-Grosdemange, C., and Rohmer, M. (1999). Synthesis of [3,5,5,5-H-2(4)]-2-C-methyl-D-erythritol, a substrate designed for the elucidation of the mevalonate independent route for isoprenoid biosynthesis. *Tetrahedron Letters*, **40**: 8369-8373.

Cvejić, J.H. and Rohmer, M. (2000). $CO_2$ as main carbon source for isoprenoid biosynthesis *via* the mevalonate-independent methylerythritol 4-phosphate route in the marine diatoms *Phaeodactylum tricornutum* and *Nitzschia ovalis*. *Phytochemistry*, **53**: 21-28.

Davidovich, N.A. (1994). Factors controlling the size of initial cells in diatoms. *Russian Journal of Plant Physiology*, **41**: 220-224.

Eisenreich, W., Schwarz, M., Cartayrade, A., Arigoni, D., Zenk, M.H., and Bacher, A. (1998). The deoxyxylulose phosphate pathway of terpenoid biosynthesis in plants and microorganisms. *Chemistry & Biology* , **5**: 221-233.

Eisenreich, W., Rohdich, F., and Bacher, A. (2001). Deoxyxylulose phosphate pathway to terpenoids. *Trends in Plant Science*, **6**: 78-84.

Farrington, J.W., Frew, N.M., Gschwend, P.M., and Tripp, B.W. (1977). Hydrocarbons in cores of northwestern Atlantic coastal and continental margin sediments. *Estuarine and Coastal Marine Science*, **5**: 793-808.

Flesch, G. and Rohmer, M. (1988). Prokaryotic hopanoids - The biosynthesis of the bacteriohopane skeleton - Formation of isoprenic units from 2 distinct acetate pools and a novel type of carbon carbon linkage between a triterpene and d-ribose. *European Journal of Biochemistry*, **175**: 405-411.

Geitler, L. (1932). Der Formwechsel der pennaten diatomeen. *Archiv für Protistenkunde*, **78**: 1-226.

Goad, J.L. and Akihisha, T. (1997). Analysis of Sterols. Blackie Academic and Professional, London, 1-431.

Groth-nard C. and Robert, J-M. (1993). Les lipides des diatomées. *Diatom Research*, **8**: 281-308.

Guillard, R.R.L. (1975). Culture of phytoplankton for feeding marine invertebrates. *In* Culture of Marine Invertebrates. Smith, W.L. and Chanley, M.H. [Eds.] Plenum Press, New York, 26-60.

Hagen, C. and Grunewald, K. (2000). Fosmidomycin as an inhibitor of the non-mevalonate terpenoid pathway depresses synthesis of secondary carotenoids in flagellates of the green alga *Haematococcus pluvialis*. *Journal of Applied Botany*, **74**: 137-140.

Harwood, J.L. (1997). Plant lipid metabolism . *In* Plant Biochemistry. Dey, P.M. and Harborne, J.B. [Eds.] Academic Press, London, 244.

Hayward, T.L. (1993). Oceanography - the rise and fall of *Rhizosolenia*. *Nature*, **363**: 675-676.

Heintze, A., Görlach, J., Leuschner, C., Hoppe, P., Hagelstein, P., Schultze-Siebert, D. and Schultz, G. (1990). Plastidic isoprenoid synthesis during chloroplast development. Change from metabolic autonomy to division-of-labour stage. *Plant Physiology*, **93**: 1121-1127.

Hendey, N.I. (1964). An Introductory Account of the Smaller Algae of British Coastal Waters. Part V : Bacillariophyceae (Diatoms). Ministry of Agriculture, Fisheries and Food [ed.], Her Majesty's Stationary Office, London, 1-317.

Hendey, N.I. (1974). The permanganate method for cleaning freshly gathered diatoms. *Microscopy*, **32**: 423-426.

Hodges, T.K. and Mills, D. (1986). Isolation of the Plasma Membrane. *Methods in Enzymology*, **118**: 41-54.

Holmes, F.A., Kudelka, A.P., Kavanagh, J.J., Huber, M.H., Ajani, J.A., and Valero, V. (1995). Current status of clinical-trials with paclitaxel and docetaxel. *Taxane Anticancer Agents*, ACS symposium series **583**: 31-57.

Hoover, R.B., Hoyle, F., Wickramasinghe, N.C., Hoover, M.J., and Al-Mufti, S. (1986). Diatoms on Earth, comets, Europa and in interstellar space. *Earth Moon and Planets*, **35**: 19-45.

Hoover, R.B., Hoyle, F., Wickramasinghe, N.C., Hoover, M.J., and Al-Mufti, S. (1999). Diatoms on Earth, comets, Europa and in interstellar space. *Astrophysics and Space Science*, **268**: 197-224.

Hustedt, F. (1930). Kieselagen. Teil I. *In* Kryptogamen-Flora von Deutschland, Österreich un der Schweiz. Rabenhorst, L. [Ed.], Otto Koeltz Science Publishers, Koenigstein, 1-920.

Jakobisiak, M., Bruno, S., Skierski, J.S., and Darzynkiewicz, Z. (1991). Cell cycle-specific effects of lovastatin. *Proceedings of The National Academy of Sciences of The United States of America*, **88**: 3628-3632.

Johns, L., Wraige, E.J., Belt, S.T., Lewis, C.A., Massé, G., Robert, J.-M., and Rowland, S.J. (1999). Identification of a $C_{25}$ highly branched isoprenoid (HBI) diene in Antarctic sediments, Antarctic sea-ice diatoms and cultured diatoms. *Organic Geochemistry*, **30**: 1471-1475.

Johns, L., Belt, S., Lewis, C.A., Rowland, S., Massé, G., Robert, J.-M., and König, W.A. (2000). Configurations of polyunsaturated sesterterpenoids from the diatom, *Haslea ostrearia*. *Phytochemistry*, **53**: 607-611.

Jomaa, H., Wiesner, J., Sanderbrand, S., Altincicek, B., Weidemeyer, C., Hintz, M., Turbachova, I., Eberl, M., Zeidler, J., Lichtenthaler, H.K., Soldati, D., and Beck, E. (1999). Inhibitors of the nonmevalonate pathway of isoprenoid biosynthesis as

antimalarial drugs. *Science*, **285**: 1573-1576.

Jux, A., Gleixner, G., and Boland, W. (2001). Classification of terpenoids according to the methylerythritolphosphate or the mevalonate pathway with natural C-12/C-13 isotope ratios: Dynamic allocation of resources in induced plants. *Angewandte Chemie-International Edition*, **40**: 2091-2093.

Kinne-Saffran, E. and Kinne, R.K.H. (1989). Membrane Isolation: Strategy, Techniques, Markers. *Methods in Enzymology*, **172**: 3-17.

Kuzuyama, T., Shimizu, T., Takahashi, S., and Seto, H. (1998). Fosmidomycin, a specific inhibitor of 1-deoxy-D-xylulose-5-phosphate reductoisomerase in the non-mevalonate pathway for terpenoid biosynthesis. *Tetrahedron Letters*, **39**: 7913-7916.

Lichtenthaler, H.K. (1999). The 1-deoxy-D-xylulose-5-phosphate pathway of isoprenoid biosynthesis in plants. *Annual Review of Plant Physiology and Plant Molecular Biology*, **50**: 47-65.

Lichtenthaler, H.K., Schwender, J., Disch, A., and Rohmer, M. (1997). Biosynthesis of isoprenoids in higher plant chloroplasts proceeds *via* a mevalonate-independent pathway. *Febs Letters*, **400**: 271-274.

Lichtenthaler, H.K., Zeidler, J., Schwender, J., and Muller, C. (2000). The non-mevalonate isoprenoid biosynthesis of plants as a test system for new herbicides and drugs against pathogenic bacteria and the malaria parasite. *Zeitschrift Fur Naturforschung C*, **55**: 305-313.

Mann, D.G., Chepurnov, V.A., and Droop, S.J.M. (1999). Sexuality, incompatibility, size variation, and preferential polyandry in natural populations and clones of *Sellaphora pupula* (Bacillariophyceae). *Journal of Phycology*, **35**:152-170.

Massé, G., Rincé, Y., Cox, E.J., Allard, W.G., Belt, S.T., and Rowland, S.J. (2001). *Haslea salstonica* sp. nov. and *Haslea pseudostrearia* sp. nov. (Bacillariophyceae), two new epibenthic diatoms from the Kingsbridge Estuary, U.K. *Comptes rendus de l'Académie des Sciences, Paris, Sciences de la Vie /*

*Life Sciences*, **324**: 617-626.

McCaskill, D. and Croteau, R. (1999). Isopentenyl diphosphate is the terminal product of the deoxyxylulose-5-phosphate pathway for terpenoid biosynthesis in plants. *Tetrahedron Letters*, **40**: 653-656.

Melzer, E. and Schmidt, H.L. (1987). Carbon isotope effects on the pyruvate-dehydrogenase reaction and their importance for relative C-13 depletion in lipids. *Journal of Biological Chemistry*, **262**: 8159-8164.

Moore, A.L. and Proudlove, M.O. (1987). Purification of plant-mitochondria on silica sol gradients. *Methods in Enzymology*, **148**: 415-420.

Myers, J. (1962). Laboratory Cultures. *In*: Physiology and Biochemistry of Algae. Lewin, R.A. [ed.], Academic Press, London, 603-613.

Nabeta, K., Kawae, T., Kikuchi, T., Saitoh, T., and Okuyama, H. (1995). Biosynthesis of chlorophyll *a* from C-13-labelled mevalonates and glycine in liverwort. Nonequivalent labelling of phytyl side chain. *Chemical Communications*, 2529-2530.

Osterroht, C., Petrick, G., and Wenck, A. (1983). Seasonal variation of particulate hydrocarbons in relation to biological parameters. *Marine Chemistry*, **14**: 175-194.

Ourisson, G. and Nakatani, Y. (1994). The terpenoid theory of the origin of cellular life: The evolution of terpenoids to cholesterol. *Chemistry & Biology*, **1**: 11-23.

Peragallo, H. (1890-1891). Monographie du genre *Pleurosigma* et des genres alliés. *Le Diatomiste*, **1**: 13.

Poulin, M., Massé, G., Belt, S. T., Rincé, Y., Robert, J.-M. and Rowland, S. J., (2000). A striking case of a sigmoid diatom sharing features with *Gyrosigma* and *Haslea*, *16th International Diatom Symposium*, Athens.

Poulin, M., Massé, G., Belt, S. T., Delavault, P., Rousseau, F., Robert, J.-M. and

Rowland, S. J., (2002). Morphological, biochemical and molecular evidence for the transfer of *Gyrosigma nipkowii* Meister to the genus *Haslea*, *17th International Diatom Symposium*, Ottawa.

Poulin, M., Massé, G., Belt, S. T., Delavault, P., Rousseau, F., Robert, J.-M. and Rowland, S. J., (submitted). Morphological, biochemical and molecular evidence for the transfer of *Gyrosigma nipkowii* Meister to the genus *Haslea*, *European Journal of Phycology*.

Pozzi, G., Birault, V., Werner, B., Dannenmuller, O., Nakatani, Y., Ourisson, G., and Terakawa, S. (1996). Single-chain polyprenyl phosphates form "primitive" membranes. *Angewandte Chemie-International Edition*, **35**: 177-180.

Prahl, F.G., Bennett, J.T., and Carpenter, R. (1980). The early diagenesis of aliphatic hydrocarbons and organic matter in sedimentary particulates from Dabob Bay, Washington. *Geochimica et Cosmochimica Acta*, **44**: 1967-1976.

Price, C.A., Cushman, J.C., Mendiola-Morgenthaler, L.R., and Reardon, E.M. (1987). Isolation of Plastids in Density Gradients of Percoll and Other Silica Sols. *Methods in Enzymology*, **148**: 157-179.

Putra, S.R., Lois, L.M., Campos, N., Boronat, A., and Rohmer, M. (1998). Incorporation of [2,3-C-13(2)]- and [2,4-C-13(2)]-D-1- deoxyxylulose into ubiquinone of *Escherichia coli via* the mevalonate-independent pathway for isoprenoid biosynthesis. *Tetrahedron Letters*, **39**: 23-26.

Quinn, J.G., Joo, F., and Vigh, L. (1989). The role of unsaturated lipids in membrane structure and stability. *Progress in Biophysical and Molecular Biology*, **53**: 71-103.

Qureshi, N. and Porter, J.W. (1981). Conversion of acetyl-coenzyme A to isopentenyl pyrophosphate. *In*: Biosynthesis of Isoprenoid Compounds. Vol. 1. Porter, J.W. and Spurgeon, S.L. [eds.], Wiley, New York, 47-93.

Requejo, A.G. and Quinn, J.G. (1983). Geochemistry of $C_{25}$ and $C_{30}$ biogenic alkenes in sediments of the Narragansett bay estuary. *Geochimica et Cosmochimica*

*Acta*, **47** : 1075-1090.

Robert, J.-M. (1978). Variations biométriques de l'algue *Navicula ostrearia* Bory (diatomée pennée) en culture. *Bulletin de la Société Phycologique de France*, **23**: 38-44.

Robert, J.-M. (1983). Fertilité des eaux des claire ostréicoles et verdissement : utilisation de l'azote par les diatomées dominantes. PhD dissertation. *Université de Nantes*.

Robson, J.N. and Rowland, S.J. (1986). Identification of novel widely distributed sedimentary acyclic sesterterpenoids. *Nature*, **324**: 561-563.

Rohmer, M., Knani, M., Simonin, P., Sutter, B., Sahm, H. (1993). Isoprenoid biosynthesis in bacteria - A novel pathway for the early steps leading to isopentenyl diphosphate. *Biochemical Journal*, **295**: 517-524.

Rohmer, M. (1999). The discovery of a mevalonate-independent pathway for isoprenoid biosynthesis in bacteria, algae and higher plants. *Natural Product Reports*, **16**: 565-574.

Round, F.E., Crawford, R.M., and Mann, D.G. (1990). The Diatoms. Biology and morphology of the genera. Cambridge University Press, Cambridge, 1-747.

Rowland, S.J. and Robson, J.N. (1990). The widespread occurrence of highly branched acyclic $C_{20}$, $C_{25}$ and $C_{30}$ hydrocarbons in recent sediments and biota - a review. *Marine Environmental Research*, **30**: 191-216.

Rowland, S.J., Belt, S.T., Wraige, E.J., Massé, G., Roussakis, C., and Robert, J.-M. (2001a). Effects of temperature on polyunsaturation in cytostatic lipids of *Haslea ostrearia*. *Phytochemistry*, **56**: 597-602.

Rowland, S.J., Allard, W.G., Belt, S.T., Massé, G., Robert, J.-M., Blackburn, S., Frampton, D., Revill, A.T., and Volkman, J.K. (2001b). Factors influencing the distributions of polyunsaturated terpenoids in the diatom, *Rhizosolenia setigera*.

*Phytochemistry*, **58**: 717-728.

Sacchettini, J.C. and Poulter, C.D. (1997). Biochemistry - Creating isoprenoid diversity. *Science*, **277**: 1788-1789.

Sagner, S., Latzel, C., Eisenreich, W., Bacher, A., and Zenk, M.H. (1998). Differential incorporation of 1-deoxy-D-xylulose into monoterpenes and carotenoids in higher plants. *Chemical Communications*, 221-222.

Schindler, S., Bach, T.J., and Lichtenthaler, H.K. (1984). Differential inhibition by mevinolin of prenyllipid accumulation in radish seedlings. *Zeitschrift Fur Naturforschung C*, **40**: 208-214.

Schwender, J., Seemann, M., Lichtenthaler, H.K., and Rohmer, M. (1996). Biosynthesis of isoprenoids (carotenoids, sterols, prenyl side- chains of chlorophylls and plastoquinone) *via* a novel pyruvate/glyceraldehyde 3-phosphate non-mevalonate pathway in the green alga *Scenedesmus obliquus*. *Biochemical Journal*, **316**: 73-80.

Shipe, R.F., Brzezinski, M.A., Pilskaln, C., and Villareal, T.A. (1999). *Rhizosolenia* mats: An overlooked source of silica production in the open sea. *Limnology and Oceanography*, **44**: 1282-1292.

Simonsen, R. (1974). The Diatom Plankton of the Indian Ocean Expedition of R.V. "Meteor". *In* : Forschungsergebnisse, Reihe D. 19. Gebruder Borntraegier, Berlin, 1-66.

Sinninghe Damsté, J.S., Rijpstra, W.I.C., Schouten, S., Peletier, H., van der Maarel, M.J.E.C., and Gieskes, W.W.C. (1999a). A $C_{25}$ highly branched isoprenoid alkene and $C_{25}$ and $C_{27}$ *n*-polyenes in the marine diatom *Rhizosolenia setigera*. *Organic Geochemistry*, **30**: 95-100.

Sinninghe Damsté, J.S., Schouten, S., Rijpstra, W.C., Hopmans, E.C., Peletier, H., Gieskes, W.W.C., and Geenevasen, J.J. (1999b). Structural identification of the $C_{25}$ highly branched isoprenoid pentaene in the marine diatom *Rhizosolenia*

*setigera. Organic Geochemistry,* **30**: 1581-1583.

Sinninghe Damsté, J.S., Schouten, S., Rijpstra, W.I.C., Hopmans, E.C., Peletier, H., Gieskes, W.W.C., Geenevasen, J.A.J. (2000). Novel polyunsaturated *n*-alkenes in the marine diatom *Rhizosolenia setigera. European Journal of Biochemistry,* **267**: 5727-5732.

Stein, J. (1973). Handbook of Phycological methods. Culture methods and growth measurements. Cambridge University Press, New-York, 1-448.

Steinbacher, S., Kaiser, J., Wungsintaweekul, J., Hecht, S., Eisenreich, W., Gerhardt, S., Bacher, A., and Rohdich, F. (2002). Structure of 2C-methyl-D-erythritol-2,4-cyclodiphosphate synthase involved in mevalonate-independent biosynthesis of isoprenoids. *Journal of Molecular Biology,* **316**: 79-88.

Sullivan, C.W. (1978). Isolation and characterization of diatom membranes. *In* Handbook of Phycological Methods. Vol. III. Physiological and Biochemical Methods. Hellebust, J.A. and Craigie, J.S. [Eds.] Cambridge University Press, New-York, 39-55.

Sundström, B.G., (1986). The marine genus *Rhizosolenia*. A new approach to taxonomy. PhD dissertation. *University of Lund*, Sweden.

Takajo, S., Nagano, H., Dannenmuller, O., Ghosh, S., Albrecht, A.M., Nakatani, Y., Ourisson, G. (2001). Membrane properties of sodium 2- and 6-(poly)prenyl-substituted polyprenol phosphates. *New Journal of Chemistry,* **25**: 917-929.

van der Werf, A. and Hulls, H. (1957-1974) Diatomeeënflora van Nederland. Otto Koeltz Science Publishers, Koenigstein, 1-142.

Véron, B., Dauguet, J.C., and Billard, C. (1998). Sterolic biomarkers in marine phytoplankton. II. Free and conjugated sterols of seven species used in mariculture. *Journal of Phycology*, **34**: 273-279.

Vial, H.J. (2000). Isoprenoid biosynthesis and drug targeting in the apicomplexa.

*Parasitology Today*, **16**: 140-141.

Volkman, J.K., Barrett, S.M., and Dunstan, G.A. (1994). $C_{25}$ and $C_{30}$ highly branched isoprenoid alkenes in laboratory cultures of two marine diatoms. *Organic Geochemistry*, **21**: 407-413.

Volkman, J.K., Barrett, S.M., Blackburn, S.I., Mansour, M.P., Sikes, E.L., and Gelin, F. (1998). Microalgal biomarkers: A review of recent research developments. *Organic Geochemistry*, **29**: 1163-1179.

Wakeham, S.G., Peterson, M.L., Hedges, J.I. and Lee, C. (2002). Lipid biomarker fluxes in the Arabian Sea, with a comparison to the equatorial Pacific Ocean Cycle. *Deep Sea Research II*, **49**: 2265-2301.

Wildermuth, M.C. and Fall, R. (1996). Light-dependent isoprene emission - Characterization of a thylakoid-bound isoprene synthase in *Salix discolor* chloroplasts. *Plant Physiology*, **112**: 171-182.

Wilson, R.J.M. (2002). Progress with parasite plastids. *Journal of Molecular Biology*, **319**: 257-274.

Wimpenny, R.S. (1966). The size of diatoms. IV. The cell diameters in *Rhizosolenia styliformis* var. *oceanica*. *Journal of the marine biological Association U. K.*, **46**: 541-546.

Wittpoth, C., Kroth, P.G., Weyrauch, K., Kowallik, K.V., and Strotmann, H. (1998). Functional characterization of isolated plastids from two marine diatoms. *Planta*, **206**: 79-85.

Wraige, E.J., Belt, S.T., Lewis, C.A., Cooke, D.A., Robert, J.-M., Massé, G., and Rowland, S.J. (1997). Variations in structures and distributions of $C_{25}$ highly branched isoprenoid (HBI) alkenes in cultures of the diatom, *Haslea ostrearia* (Simonsen). *Organic Geochemistry*, **27**: 497-505.

Wraige, E.J., Belt, S.T., Massé, G., Robert, J.-M., and Rowland, S.J. (1998). Variations in distributions of $C_{25}$ highly branched isoprenoid (HBI) alkenes in

the diatom, *Haslea ostrearia*: influence of salinity. *Organic Geochemistry,* **28**: 855-859.

Wraige, E.J., Johns, L., Belt, S.T., Massé, G., Robert, J.-M., and Rowland, S. (1999). Highly branched $C_{25}$ isoprenoids in axenic cultures of *Haslea ostrearia*. *Phytochemistry,* **51**: 69-73.

Zeidler, J.G., Lichtenthaler, H.K., May, H.U., and Lichtenthaler, F.W. (1997). Is isoprene emitted by plants synthesized via the novel isopentenyl pyrophosphate pathway? *Zeitschrift Fur Naturforschung C*, **52**: 15-23.

Zeidler, J., Schwender, J., Muller, C., Wiesner, J., Weidemeyer, C., Beck, E., Jomaa, H., and Lichtenthaler, H.K. (1998). Inhibition of the non-mevalonate 1-deoxy-D-xylulose-5-phosphate pathway of plant isoprenoid biosynthesis by fosmidomycin. *Zeitschrift Fur Naturforschung C*, **53**: 980-986.

Zeidler, J. and Lichtenthaler, H.K. (2001). Biosynthesis of 2-methyl-3-buten-2-ol emitted from needles of *Pinus ponderosa* via the non-mevalonate DOXP/MEP pathway of isoprenoid formation. *Planta*, **213**: 323-326.

# APPENDIX

## Other considerations

The present study describes an investigation into organic lipids from diatoms in an attempt to understand the biological controls leading to their production. The experiments performed during this investigation were based on previously published data, and on previous studies to which the author contributed.

Investigation of the lipid content of more than fifty diatom species isolated, identified and cultured by the author led to the identification of several species capable of producing $C_{25}$ or $C_{30}$ HBIs. Among these investigated diatom species, some *Pleurosigma spp.* were found to synthesise the most commonly reported $C_{25}$ HBI isomers in sediments. From large-scale cultures of some of these species, the structures of most $C_{25}$ and $C_{30}$ HBIs were characterised These observations were described in the following publications:

1. Belt, S.T., Allard, G., **Massé, G.**, Robert, J.-M., and Rowland, S.J. (2000). Important sedimentary sesterterpenoids from the diatom *Pleurosigma intermedium*. *Chemical Communications*, 501-502.

2. Belt, S.T., Allard, W.G., **Massé, G.**, Robert, J.-M., and Rowland, S.J. (2000). Highly branched isoprenoids (HBIs): Identification of the most common and abundant sedimentary isomers. *Geochimica et Cosmochimica Acta*, **64**: 3839-3851.

3. Allard, W.G., Belt, S.T., **Massé, G.**, Naumann, R., Robert, J.-M., and Rowland, S.J. (2001). Tetra-unsaturated sesterterpenoids (Haslenes) from *Haslea ostrearia* and related species. *Phytochemistry*, **56**: 795-800.

4. Belt, S.T., **Massé, G.**, Allard, W.G., Robert, J.M., and Rowland, S.J. (2001). Identification of a $C_{25}$ highly branched isoprenoid triene in the freshwater diatom *Navicula sclesvicensis*. *Organic Geochemistry*, **32**: 1169-1172.

5. Belt, S.T., **Massé, G.**, Allard, W.G., Robert, J.-M., and Rowland, S.J. (2001). $C_{25}$ highly branched isoprenoid alkenes in planktonic diatoms of the *Pleurosigma* genus. *Organic Geochemistry*, **32**: 1271-1275.

6. Belt, S.T., Allard, W.G., Johns, L., König, W.A., **Massé, G.**, Robert, J.-M., and Rowland, S.J. (2001). Variable stereochemistry in highly branched isoprenoids from diatoms. *Chirality*, **13**: 415-419.

7. Belt, S.T., Allard, W.G., **Massé, G.**, Robert, J.-M., and Rowland, S.J. (2001). Structural characterisation of $C_{30}$ highly branched isoprenoid alkenes (Rhizenes) in the marine diatom *Rhizosolenia setigera. Tetrahedron Letters*, **42**: 5583-5585.

In addition, this extensive survey of HBI producing species led to the discovery of two new members of the genus *Haslea*, and to the transfer into this group of a sigmoid species previously placed in the genus *Gyrosigma*. For the latter, an improved methodology for the examination of the fine diatom valves structure using scanning electron microscopy was developed by the author. These studies were described in the following publications:

8. **Massé, G.**, Rincé, Y., Cox, E.J., Allard, W.G., Belt, S.T., and Rowland, S.J. (2001). *Haslea salstonica* sp. nov. and *Haslea pseudostrearia* sp. nov. (Bacillariophyceae), two new epibenthic diatoms from the Kingsbridge Estuary, U.K. *Comptes rendus de l'Académie des Sciences, Life Sciences*, **324**: 617-626.

9. **Massé, G.**, Poulin, M., Belt, S.T., Robert, J.-M., Barreau, A., Rincé, Y., and Rowland, S.J. (2001). A simple method for SEM examination of sectionned diatom frustules. *Journal of Microscopy*, **204**: 87-92.

10. Poulin, M., **Massé, G.**, Belt, S. T., Delavault, P., Rousseau, F., Robert, J.-M. and Rowland, S. J., (submitted). Morphological, biochemical and molecular evidence for the transfer of *Gyrosigma nipkowii* Meister to the genus *Haslea*, *European Journal of Phycology*.

Finally, preliminary studies on the biological and environmental controls on the production of HBIs by *Haslea ostrearia* and *Rhizosolenia setigera* have been reported in the following publications, with the author having carried out the majority of the diatom culturing and characterisation work:

11. Rowland, S.J., Belt, S.T., Wraige, E.J., **Massé, G.**, Roussakis, C., and Robert, J.-M. (2001). Effects of temperature on polyunsaturation in cytostatic lipids of *Haslea ostrearia*. *Phytochemistry*, **56**: 597-602.

12. Rowland, S.J., Allard, W.G., Belt, S.T., **Massé, G.**, Robert, J.-M., Blackburn, S., Frampton, D., Revill, A.T., and Volkman, J.K. (2001) Factors influencing the distributions of polyunsaturated terpenoids in the diatom, *Rhizosolenia setigera*. *Phytochemistry*, **58**: 717-728.

13. Belt, S.T., **Massé, G.**, Allard, W.G., Robert, J.-M., and Rowland, S.J. (2001). Effects of auxosporulation on distributions of $C_{25}$ and $C_{30}$ isoprenoid alkenes in *Rhizosolenia setigera*. *Phytochemistry*, **59**: 141-148.

# APPENDIX II

## Monitoring of stable isotope incorporation by GC-MS: isotopic enrichment factors

For stable isotope enrichment experiments, levels of $^{2}H$ and $^{13}C$ incorporation were estimated using mass spectrometry (Section 4.2.6). $^{13}C$ or $^{2}H$ "isotopic enrichment factors" were calculated for each compound according to Equation 4.1, where M, M+1, etc are the values of the molecular ions for various isotopomers, $I_M$ is the intensity of the molecular ion, $I_{M+1}$ is the intensity of the M+1 peak, $I_{M+X}$ is the intensity of the highest mass ion (quantifiable), and n is the number of carbon atoms (for $^{13}C$ labelled substrates) or hydrogen atoms (for $^{2}H$ labelled substrates) in the molecule.

Isotopic Enrichment Factor =

$$\frac{100}{n}\left\{\frac{(M*I_M)+(M+1*I_{M+1})+.....+(M+X*I_{M+X})}{I_M+I_{M+1}+.....+I_{M+X}} - M\right\} \qquad \text{(Eqn. 4.1)}$$

This approach is exemplified using analysis of $C_{25:3}$ (I) obtained from a culture of the diatom *Rhizosolenia setigera* in the presence (A) or in absence (B) of [1-$^{13}C$] labelled acetate

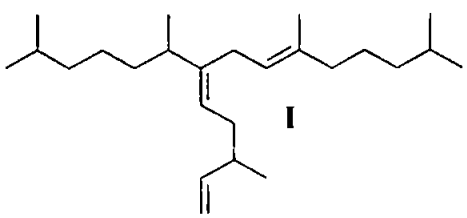

**I**

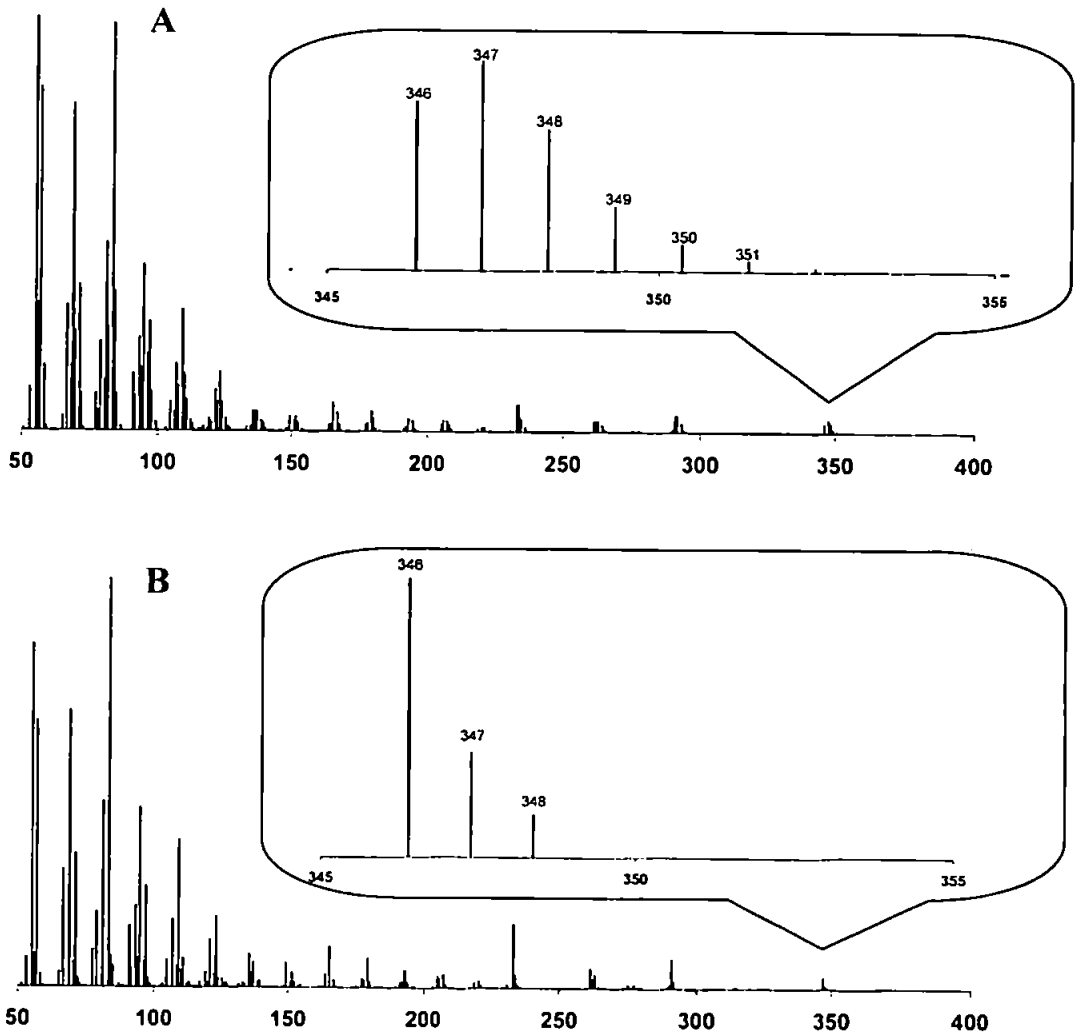


Mass spectra of $C_{25:3}$ (I). A. (I) isolated from cells grown in the presence of [1-$^{13}$C] labelled acetate. B. (I) isolated from cells grown in natural conditions.

| | M | M+1 | M+2 | M+3 | M+4 |
|---|---|---|---|---|---|
| *m/z* | 346 | 347 | 348 | 349 | 350 |
| **A** | 83 | 100 | 63 | 8 | 15 |
| **B** | 100 | 28 | 5 | 0 | 0 |

Molecular weight (MW)of I = 346

$$\text{Average mass of I (AM)} = \frac{(M^* I_M + M{+}1^* I_{M+1} + M{+}2^* I_{M+2} + M{+}3^* I_{M+3} + M{+}4^* I_{M+4})}{(I_M + I_{M+1} + I_{M+2} + I_{M+3} + I_{M+4})}$$

Isotopic Enrichment Factor (IEF)= 100x(AM-MW)/C

| | M | IEF |
|---|---|---|
| A | 347.2 | 4.6 |
| B | 346.3 | 1.1 |

ChemComm

# Important sedimentary sesterterpenoids from the diatom *Pleurosigma intermedium*

Simon T. Belt,*[a] Guy Allard,[a] Guillaume Massé,[ab] Jean-Michel Robert[b] and Steve Rowland[a]

[a] *Petroleum and Environmental Geochemistry Group, Department of Environmental Sciences, University of Plymouth, Drake Circus, Plymouth, UK PL4 8AA. E-mail: sbelt@plymouth.ac.uk*

[b] *ISOMer, Faculté des Sciences et des Techniques, Université de Nantes, 2 Rue de la Houssinière, 44027 Nantes Cedex 3, France*

*Received (in Liverpool, UK) 8th December 1999, Accepted 16th February 2000*

**The new sesterterpenoids (5*E*,8*E*/*Z*)-3,9,13-trimethyl-6-(1,5-dimethylhex-4-enyl)tetradeca-1,5,8,12-tetraene have been isolated from the diatom *Pleurosigma intermedium* and characterised structurally by NMR spectroscopy.**

Highly branched isoprenoid (HBI) $C_{25}$ and $C_{30}$ hydrocarbons are ubiquitous chemicals found in environmental matrices ranging from recent sediments to ancient oils.[1] The parent structures of these geochemicals (**1** and **2**, Fig. 1) were established by synthesis[1,2] during the 1980s, but it was not until 1994, that Volkman *et al.*[3] reported their occurrence in the diatoms *Haslea ostrearia* ($C_{25}$) and *Rhizosolenia setigeru* ($C_{30}$) thus revealing the only known source organisms for these compounds. In our own studies, we have reported on the structures of the compounds in *H. ostrearia*, together with descriptions of some of the controls governing their unsaturation.[4–7] The most common HBIs possess between two and six double bonds, though pentaenes and hexaenes are relatively rare in *H. ostrearia*[5] (*e.g.* structures **3** and **4**, Fig. 1). In a recent report, *Rhizosolenia setigeru* was shown to produce a $C_{25}$ HBI pentaene rather than $C_{30}$ compounds,[8] but to date, no further species or genus of diatoms have been shown to produce this class of widespread organic geochemicals. In terms of stereochemistry, HBIs exist as single geometric isomers in all cases (*E* where appropriate), though they are often reported as mixtures of configurational diastereoisomers.[4,9,10]

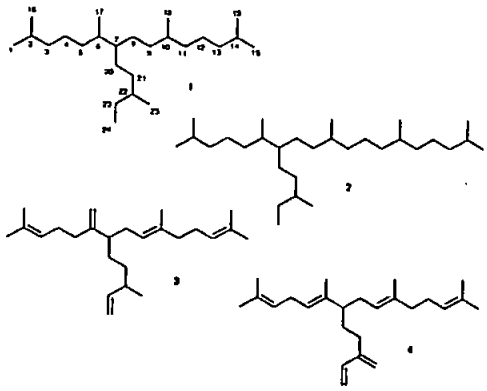

Fig. 1 $C_{25}$ and $C_{30}$ HBI parent structures and typical alkenes.

Here, we report the identification of an entirely different genus of diatom which biosynthesises $C_{25}$ HBIs of a previously unreported structural type, which nonetheless appears to be common in sediments.

*Pleurosigma intermedium* is a benthic diatom measuring *ca.* 130 × 20 μm that is commonly found in estuarine muds. After large scale (400 L) culture of this species (Bay of Bourgneuf, France) followed by harvesting, centrifugation and freeze drying, we isolated a lipid fraction by extraction with hexane. Subsequent saponification (to remove triglyceride esters of fatty acids) and extraction (hexane) yielded a hydrocarbon fraction that was analysed by GC and GC–MS. Analysis of these chromatograms revealed the presence of *n*-$C_{21:5}$, *n*-$C_{21:6}$, squalene and eight compounds possessing related but different properties to previously reported HBIs.[4,5,7] Thus, hydrogenation of this mixture resulted in the formation of a single compound having identical GC–MS characteristics[1] to that of the authentic $C_{25}$ alkane **1**. Following purification by column chromatography ($SiO_2$/hexane) and re-examination by GC–MS, the two major components (> 55%) of the hydrocarbon fraction were assigned as new HBI pentaenes ($C_{25:5}$, $M^+$ 342, RI 2126,2172 $_{HP\text{-}5}$; 2112,2159 $_{HP\text{-}1}$, relative abundance 1.6 : 1). The mass spectra of the two compounds were virtually identical, suggesting that that they were stereoisomers rather than positional isomers. Examination of the $^1H$ and $^{13}C$ NMR spectra† revealed the presence of four trisubstituted alkene moieties, together with a vinyl group, a structural feature common to all known HBIs. For all of these previously reported HBIs, the main branch point is at C-7, probably as the result of a biosynthetic coupling of geranyl and farnesyl type precursors.[9] However, for these new sesterterpenoids isolated from *Pleurosigma intermedium*, C-7 is unsaturated with a double bond between C-7 and C-20 (note: the numbering scheme for NMR assignments is shown for parent alkane **1**). The determination of this double bond position (C7–C20) and of the other trisubstituted double bonds was established using 2-D NMR methods (COSY, HMQC, HMBC) resulting in structures **5** and **6** (Fig. 2), namely 3,9,13-trimethyl-6-(1,5-dimethylhex-4-enyl)tetradeca-1,5,8,12-tetraene. Of particular note is the absence of any $^{13}C$ resonances in the 40–50 ppm region indicative of saturated, branched positions (C-7) observed for all previously reported HBIs.[4–10] Instead, alkenic C-7 resonates at $\delta$ 142.8 and 142.4 for **6** and **5**, respectively. To date, we have not been successful in separating the two $C_{25:5}$ isomers using further chromatography including argentation TLC. However, both spectroscopic ($^{13}C$ NMR) and chromatographic (GC) separations of these compounds are most consistent with the presence of two geometric isomers (C9–C10). The mixed double bond stereochemistry of C9–C10 (and not C7–C20) was determined by careful examination of the NMR data. Specifi-

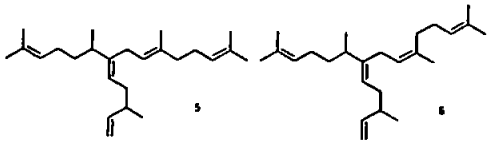

Fig. 2 Structures of $C_{25}$ pentaenes isolated from *Pleurosigma intermedium*.

DOI: 10.1039/a909670a

cally, unique $^1H$ and $^{13}C$ ($CH_3$) resonances at $\delta$ 1.55, 1.69 (H-18) and $\delta$ 15.8, 23.4 (C-18) were observed for **5** and **6** (with **6** being the major isomer). Two further $^{13}C$ resonances for C-11, each of which correlated with the corresponding H-18 protons in the HMBC spectrum were also observed. Since the alternative position for geometric isomerism (C7–C20) does not possess a $CH_3$ substituent, the position of *E*/*Z* isomerism is limited to C9–C10. In order to determine the stereochemistry of the C7–C20 double bond, NOE data were obtained for **5** and **6**. Significantly, NOEs were observed between H-6 and H-20, indicating an *E* configuration. The remaining six HBIs consisted of two trienes ($C_{25:3}$) and four tetraenes ($C_{25:4}$) on the basis of their mass spectra ($M^+$ 346 and 344, respectively), though insufficient quantities of these compounds were present in the culture to allow for comprehensive NMR analysis.

HBIs in general have been proposed as potential biomarkers or palaeoenvironmental indicators.[11] However, to date, the environmental record of these compounds does not correlate well with those compounds structurally characterised from previous large scale cultures of diatoms including *Haslea ostrearia* and *Rhizosolenia setigera*.[4–10] The reason for this may be that HBIs from these two species undergo relatively mild diagenetic reactions (*e.g.* alkene isomerisation) but since the products of laboratory simulations of these processes do not produce the sedimentary isomers,[12] a more attractive explanation is that other diatoms such as *Pleurosigma intermedium* are the producers of many of the common sedimentary HBIs. To address this more fully, we now intend to isolate and characterise all of the HBIs produced by *Pleurosigma intermedium* under different culture conditions and to compare the mass spectra and chromatographic data (retention indices) of these with the numerous geochemical reports.[13] A preliminary investigation of this type indicates that two of the $C_{25}$ pentaenes (RI 2124, 2169 $_{DB-5}$) reported from the Todos os Santos Bay, Brazil,[14] are HBIs **5** and **6**.

We would like to acknowledge the British Council (ALLIANCE program) and the University of Plymouth for funding (G. A. and G. M.).

## Notes and references

† Selected NMR data for **5** and **6** at 270 and 400 MHz for $^1H$ in $CDCl_3$, (numbering shown for parent alkane **1**). $^1H$, COSY: $\delta$ 5.74 (ddd, 1H, *J* 17.5, 10.0, 7.0 Hz, H-23), 5.10 (m, 4H, H-3,9,13,20), 4.93 (m, 2H, H-24), 2.58 (m, 3H, H-6,8), 2.01 (m, 9H, H-4,11,12,21,22), 1.69 (s, 3H, H-18, 6), 1.65 (s, 6H, H-1,15), 1.58 (s, 3H, H-16/19), 1.55 (s, 6H, H-16/19,18, 5), 0.95 (d, 3H, *J* 6.5 Hz, H-25), 0.94, 0.93 (2 × d, 3H, *J* 6.5 Hz, H-17).

$^{13}C$, DEPT, HMQC, HMBC: $\delta$ 144.5 (C-23), 142.8 (C-7, 6), 142.4 (C-7, 5), 135.6 (C-10), 131.4, 131.2, 131.1 (C-2,14), 124.9, 124.4, 123.9, 123.3, 123.0, 122.9, (C-3,9,13,20), 112.1 (C-24), 39.8 (C-11, 5), 38.2 (C-22), 35.2 (C-5), 34.4 (C-21), 33.9 (C-6), 31.8 (C-11, 6) 29.2 (C-8, 5), 28.9 (C-8, 6), 26.7, 26.6, 26.4 (C-4,12), 25.7 (C-1,15), 23.4 (C-18, 6), 19.5 (C-25), 19.4 (C-17), 17.6 (C-16,19), 15.8 (C-18, 5).

1 J. N. Robson and S. J. Rowland, *Nature*, 1986, 324, 561.
2 J. N. Robson and S. J. Rowland, *Tetrahedron Lett.*, 1988, 29, 3837.
3 J. K. Volkman, S. M. Barratt and G. A. Dunstan, *Org. Geochem.*, 1994, 21, 407.
4 S. T. Belt, D. A. Cooke, J.-M. Robert and S. J. Rowland, *Tetrahedron Lett.*, 1996, 37, 4755.
5 E. J. Wraige, S. T. Belt, C. A. Lewis, D. A. Cooke, J.- M. Robert, G. Massé and S. J. Rowland, *Org. Geochem.*, 1997, 27, 497.
6 E. J. Wraige, S. T. Belt, L. Johns, G. Massé, J.-M. Robert and S. J. Rowland, *Org. Geochem.*, 1998, 28, 855.
7 E. J. Wraige, S. T. Belt, L. Johns, G. Massé, J.-M. Robert and S. J. Rowland., *Phytochemistry*, 1999, 15, 69.
8 J. S. Sinninghe Damsté, W. I. C. Rijpstra, S. Schouten, H. Peletier, M. J. E. C. van der Maarel and W. W. C. Gieskes, *Org. Geochem.*, 1999, 30, 95.
9 L. Johns, E. J. Wraige, S. T. Belt, C. A. Lewis, G. Massé, J.-M. Robert and S. J. Rowland, *Org. Geochem.*, 1999, 30, 1471.
10 L. Johns, S. T. Belt, C. A. Lewis, S. J. Rowland, G. Massé, J.-M. Robert and W. König, *Phytochemistry*, 2000, 53, 607.
11 D. A. Yon, G. Ryback and J. R. Maxwell, *Tetrahedron Lett.*, 1982, 23, 2143.
12 S. T. Belt, G. Allard, J. Rintatalo, L. Johns, A. C. T. van Duin and S. J Rowland, *Geochim. Cosmochim. Acta*, 1999, submitted.
13 S. J. Rowland and J. N. Robson , *Mar. Environ. Res.*, 1990, 30, 191.
14 C. Porte, D. Barceló, T. M. Tavares, V. C. Rocha and J. Albaigés, *Arch. Environ. Contam. Toxicol.*, 1990, 19, 263.

*Communication a909670a*

Pergamon

Geochimica et Cosmochimica Acta, Vol. 64, No. 22, pp. 3839–3851, 2000

0016-7037/00 $20.00 + .00

PII S0016-7037(00)00464-6

# Highly branched isoprenoids (HBIs): Identification of the most common and abundant sedimentary isomers

SIMON T. BELT,[1,*] W. GUY ALLARD,[1] GUILLAUME MASSÉ,[1,2] JEAN-MICHEL ROBERT,[2] and STEVEN J. ROWLAND[1,*]

[1]Petroleum and Environmental Geochemistry Group, Department of Environmental Sciences, University of Plymouth, Drake Circus, Plymouth, PL4 8AA, Devon, UK

[2]ISOMer, Faculté des Sciences et des Techniques, Université de Nantes, 2 Rue de la Houssinière, 44027 Nantes Cedex 3, France

(*Received March 6, 2000; accepted in revised form May 12, 2000*)

Abstract—Tri- and tetraunsaturated highly branched isoprenoid (HBI) alkenes are widespread sedimentary geochemicals but few have been isolated from sediments in sufficient quantities for rigorous identification. However, two $C_{25}$ trienes, four $C_{25}$ tetraenes and two $C_{25}$ pentaenes have now been isolated from the diatom *Pleurosigma intermedium* following bulk scale culture, and these have been purified by column chromatography and fully characterised by NMR spectroscopy and mass spectrometry. The compounds have been used to identify the previously unknown, but common and abundant HBIs found previously in many studies of sediments, particles and biota from around the world. These HBIs are structurally different to those reported from other diatoms. For example, unlike HBIs from the diatoms *Haslea ostrearia* and *Rhizosolenia setigera*, the alkenes in *P. intermedium* are unsaturated at the major branch point of the carbon skeleton and *E/Z* isomerism is observed for one of the trisubstituted double bonds. There is no evidence for the presence of configurational diastereoisomerism. The distributions of HBIs in *P. intermedium* (including the *E/Z* ratios) also show a dependence on the growth conditions within the five cultures studied. The positions of the double bonds in the HBIs of *P. intermedium*, and by inference, of the sediments, are consistent with the positions of sulphur incorporation in some of the HBI thiolanes and thiophenes which have been reported previously in some sediments and oils. *Copyright © 2000 Elsevier Science Ltd*

## 1. INTRODUCTION

Since the first reports of $C_{25}$ highly branched isoprenoid (HBI) hydrocarbons in sediments (e.g., Gearing et al., 1976; Farrington et al., 1977) and the determination of the parent carbon skeleton by synthesis (I, see Appendix 1; Robson and Rowland, 1986) many studies have described the occurrence of a large number of different HBI isomers with 0–6 degrees of unsaturation, in a wide range of geochemical settings (reviewed by Rowland and Robson, 1990). When Volkman et al. (1994) reported the presence of several $C_{25}$ HBI alkenes in a culture of the benthic diatom *Haslea ostrearia*, it seemed likely that a source of the sedimentary compounds had been found, though the authors noted that the distributions in the alga were different from those in many sediments and seawater.

Determinations of the structures, including double bond positions and stereochemistry, and in some cases, either the relative or absolute stereochemistries of the asymmetric centres (Johns et al., 2000) of a number of dienes through hexaenes (III-X) from large scale cultures of *H. ostrearia* and recently from the diatom *Rhizosolenia setigera*, have succeeded the initial findings (Belt et al., 1996; Volkman et al., 1998; Wraige et al., 1997; Wraige et al., 1999; Johns et al., 1999; Sinninghe Damsté et al., 1999a;b). Pseudo-homologous $C_{30}$ HBIs have also been found in cultures of *R. setigera* (Volkman et al., 1994), though to date, the structures of these compounds have not been elucidated. From detailed studies on the structures of $C_{25}$ HBIs, it became apparent that there were indeed often discrepancies between the chromatographic (RI) and mass spectral properties of many of the sedimentary isomers and those found in *H. ostrearia* and *R. setigera* (c.f., Volkman et al., 1994). This led us to consider whether the biological HBI distributions were affected by algal growth conditions such as salinity or temperature (Wraige et al., 1997; Wraige et al., 1999) and if HBIs produced by diatoms such as *H. ostrearia* might undergo rapid diagenetic changes in sediments to yield isomeric forms of the biogenic compounds (Belt et al., 2000a). Although both phenotypic and diagenetic variables did alter HBI isomer distributions, there was often still a poor correspondence of the resulting distributions with sedimentary HBIs. For example, whereas HBI dienes and trienes isolated from *H. ostrearia* underwent facile isomerisation and cyclisation reactions under mild acid conditions including Montmorillonite clay, most of the products were not those widely reported in sediments to date (Belt et al., 2000a). This led us to consider the possibility that the common and abundant sedimentary HBI isomers may originate from diatom sources which had not previously been studied.

In the present study, we report the isolation and characterisation by NMR spectroscopy, of six new HBI alkenes from several large scale cultures of the common benthic diatom, *Pleurosigma intermedium*. Possibly *P. intermedium* is a further source of these widespread and often abundant biomarkers, although many diatom species remain to be studied, including both benthic and planktonic members of the genus. Importantly, in contrast to the structures of HBIs characterised previously from diatoms, the chromatographic and mass spectral properties of these compounds show an excellent correlation with those HBIs most commonly reported in sediments (Rowland and Robson, 1990). Thus the common sedimentary isomers have at last been identified.

*Author to whom correspondence should be addressed (s.belt@plymouth.ac.uk).

## 2. EXPERIMENTAL

### 2.1. Isolation of HBI Alkenes

*P. intermedium* was isolated from oyster ponds of the Bay of Bourgneuf (France). Batch cultures of the diatom were grown in Nantes in an outdoor culture facility (9/7–21/7 1999; Culture 1 (PI-1) and 7/9–14/9 1999; Culture 2 (PI-2)) or in an indoor laboratory (21/10–5/11 1999; Culture 3 (PI-3), 11/2–25/2 2000; Culture 4 (PI-4) and 15/2–9/3 2000; Culture 5 (PI-5)). Cultures were grown in seawater obtained from an underground supply in Nantes at constant salinity (31 per mil). Samples were collected during the stationary phase of the growth cycle and filtered to produce a concentrate of algal cells. These were subsequently freeze dried and extracted with hexane (Soxhlet) to produce a total hexane extract (THE). The THE was saponified (KOH/MeOH) to remove triglyceride esters of fatty esters and the non-saponifiable lipids re-extracted into hexane. The hexane extract was further washed with water and then dried ($Na_2SO_4$). Isolation and purification of HBIs was achieved using column chromatography ($SiO_2$/hexane). Fractions from the column chromatography were analysed by GC-MS and combined where appropriate (i.e. HBIs with the same degree of unsaturation). Separation of individual isomers was not achieved using the chromatographic methods used. Fractions suitable for analysis by NMR spectroscopy (>95% (GC)) were obtained from PI-1, PI-2 and PI-3 in the following amounts (mg). PI-1: $C_{25:3}$ (5.6); $C_{25:4}$ (17.0); $C_{25:5}$ (44.0). PI-2: $C_{25:3}$ (29.0); $C_{25:4}$ (46.0); $C_{25:5}$ (39.0). PI-3: $C_{25:3}$ (1.6); $C_{25:4}$ (12.5); $C_{25:5}$ (13.0).

### 2.2. Chromatographic and Spectroscopic Analysis

GC-MS analysis of hexane extracts and of purified HBIs was performed with a Hewlett Packard 5890 Series II gas chromatograph coupled to a Hewlett Packard Mass Selective Detector (5970 series) fitted with a 12 m (0.2 mm i.d.) fused silica column (HP-1 stationary phase). Auto splitless injection and He carrier gas were used. The gas chromatograph oven temperature was programmed from 40–300°C at 5°C $min^{-1}$ and held at the final temperature for 10 min. MS operating conditions were: ion source temperature 250°C and 70 eV ionisation energy. Spectra (50–550 Da) were collected using Chemstation software. GC-MS analysis was also performed using a Finnigan MAT GCQ™ spectrometer incorporating a quadrupole ion trap fitted with a 30 m fused silica (0.25 mm internal diameter) HP-5 column. Auto-splitless injection and He carrier gas was used. The GC temperature programme was as before. The mass spectrometer conditions were: Ion source temperature 200°C and 70 eV ionisation energy. Spectra (50–450 Da) were collected using Finnigan MAT GCQ™ software. NMR analysis of purified HBIs was performed using a JEOL EX-270 FT-NMR spectrometer. 1-D ($^1H$, $^{13}C$ and DEPT), 2-D (COSY, HMQC, HMBC) and difference nOe measurements were all recorded in $CDCl_3$ using residual $CHCl_3$ (7.24 ppm) and $^{13}CDCl_3$ (77.0 ppm) as references.

## 3. CHARACTERISATION OF NEW HBI STRUCTURES

### 3.1. Chromatographic and Mass Spectral Analysis of HBIs

Analysis of GC-MS total ion chromatograms of the non-saponifiable lipid fractions from several cultures of *P. intermedium* typically showed the presence of eight compounds that have chromatographic (RI) and mass spectral properties that are consistent with HBI alkenes. For example, Figure 1 shows examples of partial total ion chromatograms of hydrocarbon fractions obtained from 2 cultures (PI-1 and PI-4) of *P. intermedium*. The presence of *n*-$C_{21:5}$, *n*-$C_{21:6}$ as additional components together with significant variability in HBI distributions can also be noted. Hydrogenation ($H_2/PtO_2.2H_2O$) of aliquots of solutions containing these HBIs resulted in the formation of a compound which co-chromatographed with, and had an identical mass spectrum to that obtained for authentic $C_{25:0}$ (Robson and Rowland, 1986). Thus, the parent carbon skeleton (I) for these eight compounds is verified. Examination of the mass spectral data reveals that this suite of HBIs can be grouped into two trienes ($C_{25:3}$, $M^+$ 346), four tetraenes ($C_{25:4}$, $M^+$ 344) and two pentaenes ($C_{25:5}$, $M^+$ 342). For the trienes and the pentaenes, the fragmentation patterns and ion distributions are extremely similar for each degree of unsaturation (see Figure 2) suggesting the occurrence of geometric or configurational isomers rather than positional isomers. Certainly, there is evidence from previously characterised HBIs that positional isomerisation (for a given degree of unsaturation) results in significant differences in fragmentation pathways and relative ion intensities. For example, HBIs V and VI which have been isolated from cultures of *H. ostrearia* (Belt et al., 1996; Wraige et al., 1997; Wraige et al., 1999), have mass spectra (Fig. 3) that show major differences particularly in the relative intensities of ions with m/z 261, 233 (and different base peaks), despite the similarity in their structures and RIs (2103 and 2106 for V and VI respectively). Similarly, the pseudo-homologous $C_{25}$ pentaenes IX and X isolated from *R. setigera* (IX) and *H. ostrearia* (IX, X), have substantially different mass spectra (Figure 3) despite the minor differences in structure.

In contrast to the trienes and pentaenes, the mass spectra of the four $C_{25}$ tetraenes isolated from *P. intermedium* do have noticeable differences between them though qualitatively they can be grouped into two pairs. Thus, tetraenes with RI 2074 and $2121_{HP\text{-}1}$ (Figure 4) have major fragments at m/z 289 and 177, while the related tetraenes with RI 2078 and $2124_{HP\text{-}1}$ have characteristic ions at m/z 301 and 180. In some cases, there are ions that are common to all 4 tetraenes, though the relative intensities are different and fall into 2 pairs (e.g., m/z 259, 149; Fig. 4). These observations are consistent with the presence of a pair of positional isomers, each of which exists as a pair of geometric isomers. The position of one or more of the double bonds presumably precludes this from occurring with the related trienes and pentaenes (vide infra).

### 3.2. Analysis of HBIs by NMR Spectroscopy

#### *3.2.1. HBI trienes: $C_{25:3}$*

We recently reported the structures of two $C_{25:5}$ HBIs (XI, XII) which were isolated from a single large scale culture of *P. intermedium* and characterised by NMR spectroscopy (Belt et al., 2000b). Structural features for these two pentaenes include (i) a vinyl moiety (C23–C24) common to virtually all other HBIs; (ii) three tri-substituted double bonds (C2–C3, C9–C10, C13–C14); (iii) a tri-substituted double bond at the major HBI branch point (C7–C20); and (iv) the presence of both *E* and *Z* isomers at C9–C10 (see I for numbering scheme). These latter

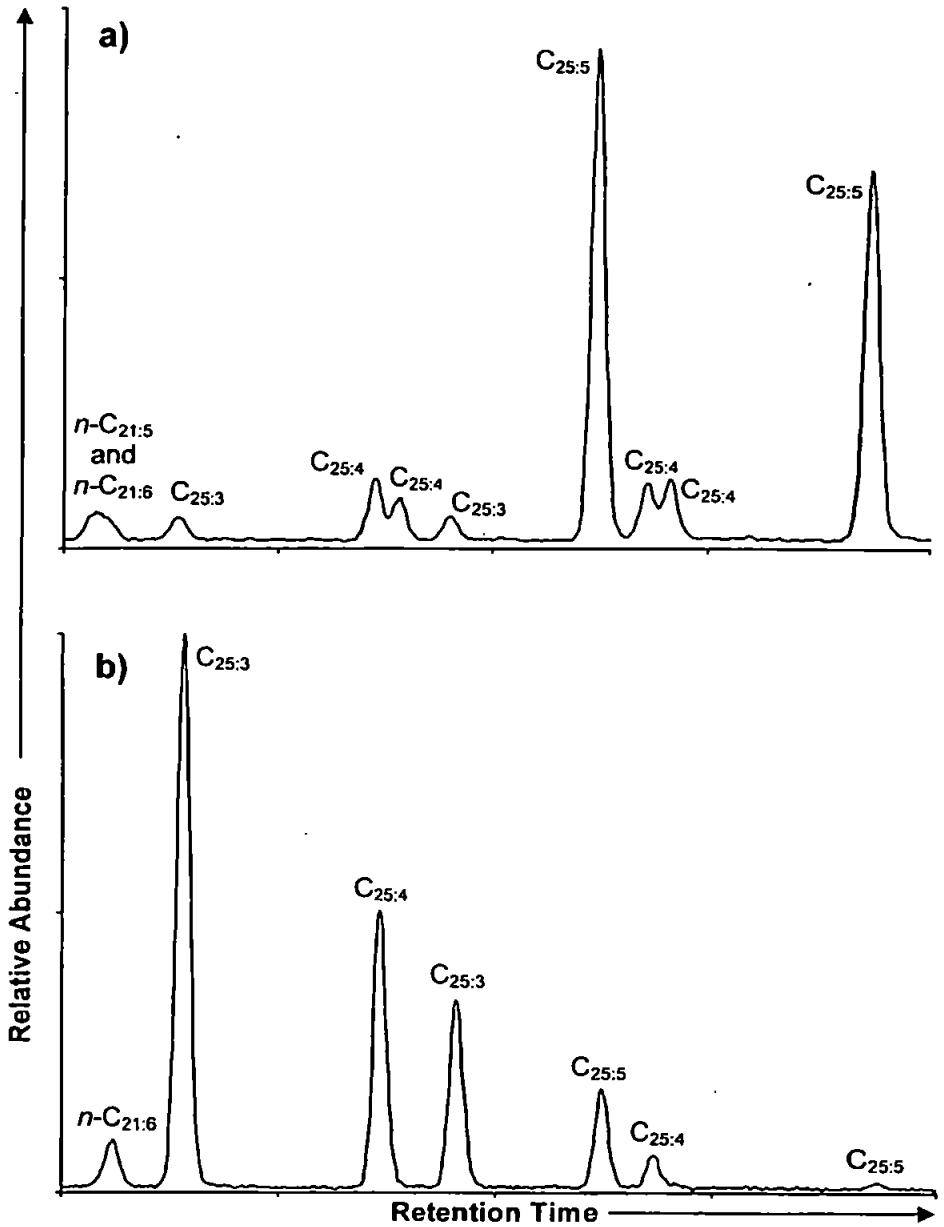


Fig. 1. Partial Total Ion Chromatograms (TICs) of hexane extracts from 2 cultures of *P. intermedium* (a) PI-1 (b) PI-4.

two features have not been previously reported for HBIs isolated from cultures of either *H. ostrearia* (Belt et al., 1996; Johns et al., 1999; Wraige et al., 1997; Wraige et al., 1999) or *R. setigera* (Sinninghe Damsté et al., 1999b). In the current study, we have obtained sufficient quantities of the remaining six HBIs (trienes and tetraenes) for complete characteristion by NMR spectroscopy. Analysis of these NMR spectra has revealed some similar features to those observed for the pentaenes.

The $^{1}H$ and $^{13}C$ NMR spectra of a mixture of the two trienes reveals the presence of a vinyl moiety (C23–C24) together with two trisubstituted double bonds (C9–C10, C7–C20), six allylic (H-6, 11, 21, 22) and two doubly allylic (H-8) protons, twelve $(CH_3)_2CH$ protons (H-1, 15, 16, 19), six $(CH_3)CH$ protons (H-17, 25) and an isolated $CH_3$ group (H-18). Quaternary (DEPT) alkene $^{13}C$ resonances are observed for C-7 for each triene consistent with our observations made previously for XI and XII (Belt et al., 2000b). Geometric isomerism of the

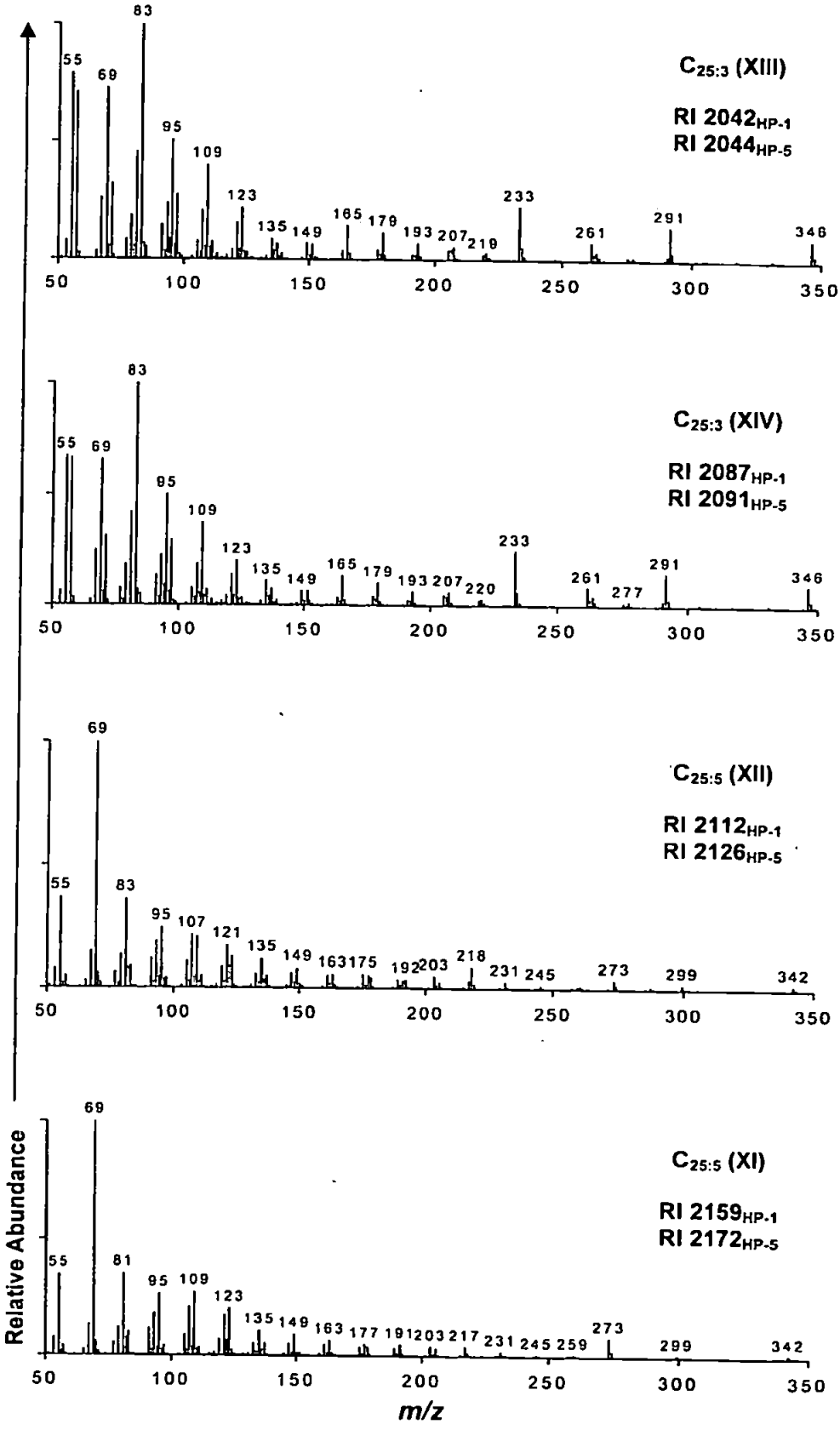


Fig. 2. Mass spectra of HBI trienes ($C_{25:3}$) and pentaenes ($C_{25:5}$) isolated from *P. intermedium*.

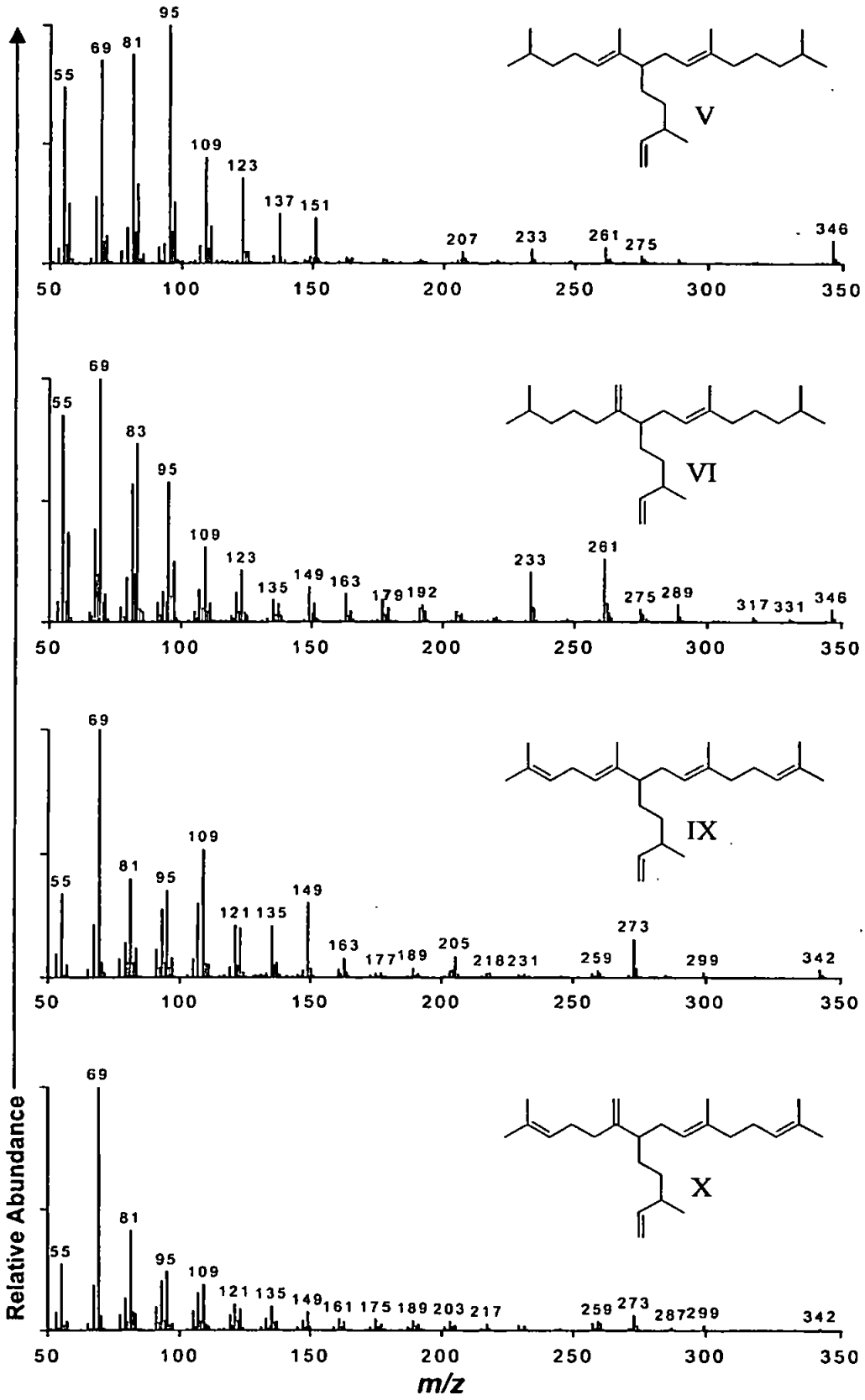


Fig. 3. Mass spectra of HBI trienes ($C_{25:3}$) and pentaenes ($C_{25:5}$) isolated from *H. ostrearia*.

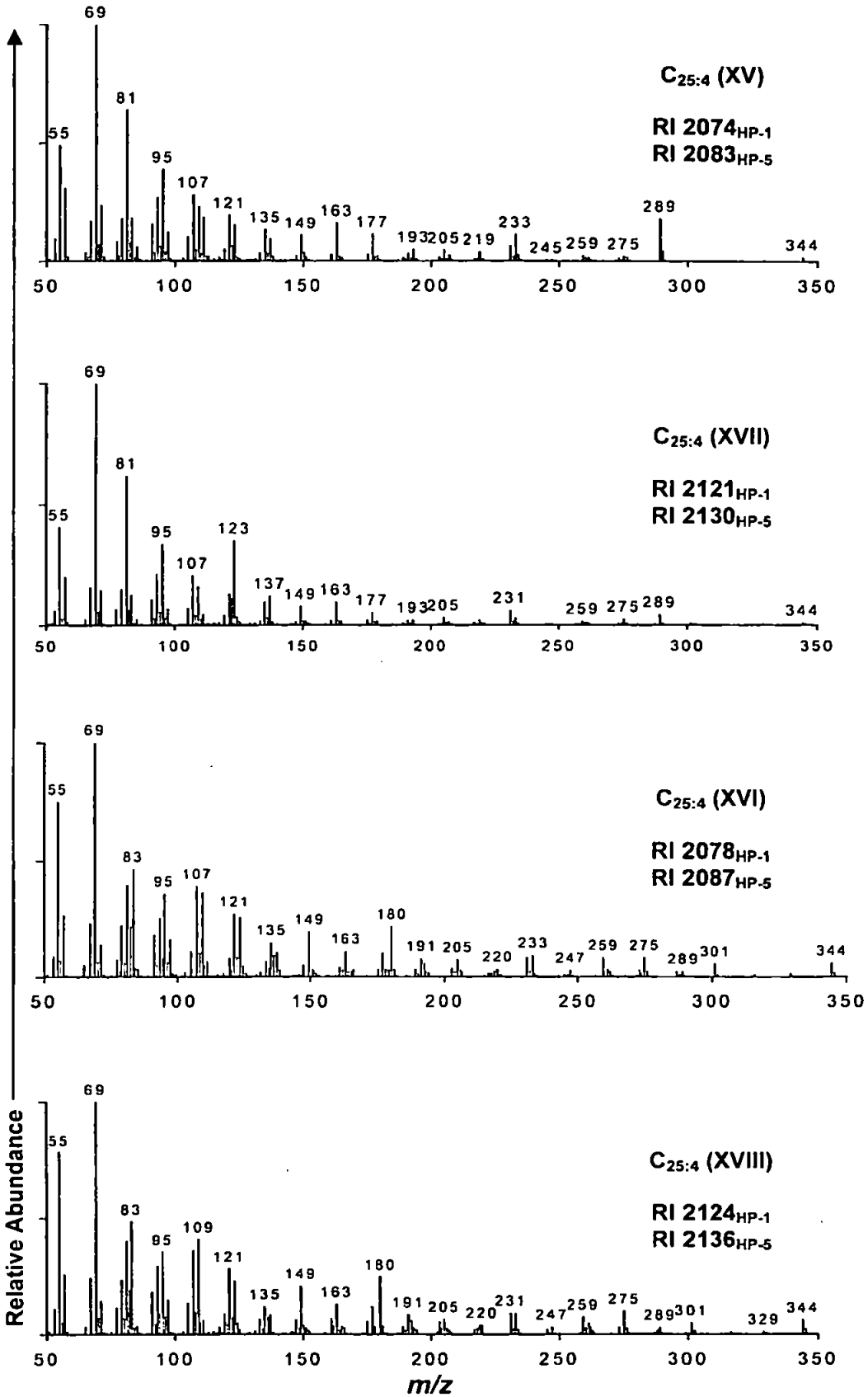


Fig. 4. Mass spectra of HBI tetraenes ($C_{25:4}$) isolated from *P. intermedium*.

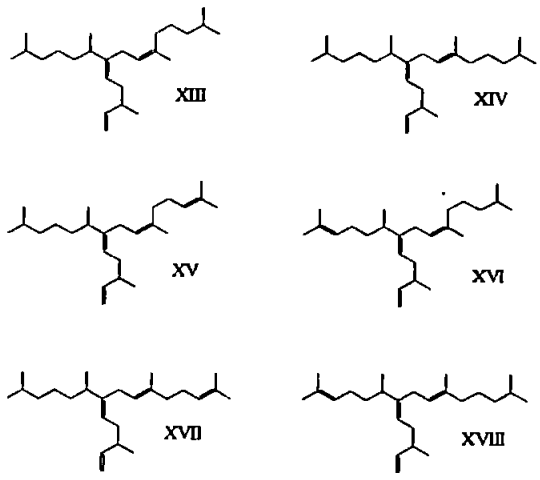


Fig. 5. Structures of HBI trienes ($C_{25:3}$) and tetraenes ($C_{25:4}$) isolated from *P. intermedium*.

C9–C10 double bond has previously been observed for the pentaenes XI and XII (Belt et al., 2000b) and there is further evidence for this type of isomerism associated with XIII and XIV. Thus, the $^1$H NMR spectrum of a mixture of the two trienes reveals two $CH_3$ singlets (H-18) due to the presence of both *E* and *Z* isomers (1.54 and 1.69 ppm respectively). An analogous pair of resonances is observed in the $^{13}$C spectrum (23.5 and 15.7 ppm for XIII and XIV respectively). Comprehensive chemical shift assignments were made using routine 2-D NMR methods ($^1$H-$^1$H, $^{1-3}J_{C-H}$). The structures of the two trienes are therefore established as XIII and XIV (Fig. 5).

Although the characterisation of XIII and XIV is unambiguous and can be achieved using approximately equal concentration mixtures of trienes, assignment of NMR resonances to each individual HBI was achieved by comparison of $^1$H and $^{13}$C NMR data obtained from solutions containing different, but known (GC) relative concentrations of the two isomers (Table 1). The stereochemistry of the C9–C10 double bond for XIII and XIV was determined most conveniently by analysis of the chemical shifts for H/C-18 and C-11 for each compound (Belt et al., 2000b). This in turn enabled the GC elution order of the 2 isomers to be determined (viz. *Z* before *E*).

### 3.2.2. *HBI tetraenes: $C_{25:4}$*

The characterisation of the tetraenes isolated from *P. intermedium* is complicated by the presence of 4 isomeric compounds compared to 2 for the related trienes XIII and XIV. However, the $^1$H and $^{13}$C NMR spectra of mixtures of tetraenes from all 5 cultures exhibit features which can be attributable to double bonds in each of the 3 positions identified for the trienes XIII and XIV (viz. C9–C10, C7–C20 and C23–C24) together with *E/Z* isomerisation at C9–C10. In addition, the $^1$H and $^{13}$C data also demonstrate that all solutions of tetraenes contain an equal number of isopropyl ($(CH_3)_2CH$) and isoprenyl ($(CH_3)_2C=$) moieties irrespective of the composition of the mixture. Therefore, the appearance of 4 tetraenes can be rationalised in terms of 2 structurally isomeric forms, each containing a terminal, trisubstituted double bond at C2–C3 or C13–C14 together with a pair of geometric isomers (C9–C10) for each of these (XV–XVIII).

In order to characterise the compounds individually and to determine their GC elution order, examination was made of solutions containing varying proportions of the different tetraenes in a manner similar to that performed for the trienes XIII and XIV (vide infra). GC and GC-MS analysis of the tetraene fraction from culture 3 (PI-3) shows that the major isomer (RI $2074_{HP\text{-}1}$) is the first GC-eluting compound observed in PI-1, and that 2 of the other 3 tetraenes (RI 2078, $2124_{HP\text{-}1}$) are virtually absent. Examination of the $^1$H and $^{13}$C NMR data for

Table 1. Relative concentrations of HBI trienes ($C_{25:3}$), tetraenes ($C_{25:4}$) and pentaenes ($C_{25:5}$) together with geometric isomer ratios following extractions of HBIs from five bulk cultures of *P. intermedium*.

| HBI | $C_{25:3}$ | $C_{25:3}$ | $C_{25:4}$ | $C_{25:4}$ | $C_{25:4}$ | $C_{25:4}$ | $C_{25:5}$ | $C_{25:5}$ |
|---|---|---|---|---|---|---|---|---|
| RI HP-1 | 2042 | 2087 | 2074 | 2121 | 2078 | 2124 | 2112 | 2159 |
| RI HP-5 | 2044 | 2091 | 2083 | 2130 | 2087 | 2136 | 2126 | 2172 |
| Structure | XIII | XIV | XV | XVII | XVI | XVIII | XII | XI |
| Culture 1 (PI-1) | | | | | | | | |
| Relative amount | 1.0 | 0.78 | 2.0 | 1.8 | 1.3 | 1.8 | 15 | 11 |
| *Z/E* ratio | 1.3 | | 1.1 | | 0.72 | | 1.4 | |
| Culture 2 (PI-2) | | | | | | | | |
| Relative amount | 1.0 | 0.48 | 0.79 | 0.40 | 0.21 | 0.23 | 0.94 | 0.58 |
| *Z/E* ratio | 2.1 | | 2.0 | | 0.91 | | 1.6 | |
| Culture 3 (PI-3) | | | | | | | | |
| Relative amount | 1.0 | 0.3 | 8.0 | 2.3 | — | — | 9.6 | 1.8 |
| *Z/E* ratio | 3.0 | | 3.5 | | — | | 5.3 | |
| Culture 4 (PI-4) | | | | | | | | |
| Relative amount | 1.0 | 0.35 | 0.54 | 0.076 | — | — | 0.18 | 0.023 |
| *Z/E* ratio | 2.9 | | 7.1 | | — | | 7.7 | |
| Culture 5 (PI-5) | | | | | | | | |
| Relative amount | 1.0 | 0.54 | 1.1 | 0.52 | — | — | 0.39 | 0.16 |
| *Z/E* | 1.9 | | 2.1 | | — | | 2.4 | |

this major isomer reveals that the stereochemistry at C9–C10 is Z (1.70 ppm (H-18); 23.5 ppm (C-18); Belt et el., 2000b).

To determine which terminal position of the main carbon chain is unsaturated (C2–C3 or C13–C14) for the major isomer, we have used the dependence of the $^{13}C$ chemical shift for C-10 on the nature of C13–C14 observed for the corresponding trienes (XIII and XIV) and pentaenes (XI and XII) (Belt et al., 2000b). Thus, the $^{13}C$ resonances for C-10 appear at 136.1 and 136.0 ppm for the Z and E isomers XIII and XIV respectively, with the spectral order and chemical shift separation being the same in all cases studied. In contrast, the corresponding resonances for the related pentaenes XI and XII both appear at 135.6 ppm due to co-resonance for the two isomers. Therefore, the chemical shift for C-10 is strongly dependent on whether C13–C14 is saturated (eg trienes XIII and XIV) or unsaturated (e.g., pentaenes XI and XII). Importantly, the C-10 resonances for the tetraene fractions from PI-1 and PI-2 exhibit 3 peaks due to the presence of compounds containing unsaturation at C2–C3 (136.1 and 136.0 ppm) and C13–C14 (135.6 ppm) which verifies that the observations made for the C-10 chemical shift from the trienes (XIII and XIV) and the pentaenes (XI and XII) can be translated to the tetraenes (XV–XVIII). The resonance for the major tetraene isomer from PI-3 appears as a single peak at 135.6 ppm which establishes that C13–C14 must be unsaturated (c.f., pentaenes XI and XII). Since the Z configuration (C9–C10) for this isomer is also known, this compound can be assigned to structure XV (Fig. 5).

The other tetraene component (RI $2121_{HP-1}$) from this culture (PI-3) can be identified as XVII due to the observations of corresponding $^{1}H$ and $^{13}C$ resonances for H/C-18 together with the similarity between the mass spectral data obtained for these two isomers (Fig. 4). Other spectroscopic data for XVII also lends further support for unsaturation at the C13–C14 position. Chemical shifts for C-11 (*E* isomer only) for the previously characterised triene XIV and pentaene XI appear at 40.0 and 39.8 ppm respectively, while spectra of mixtures containing significant concentrations of all four tetraenes (i.e., PI-1 and PI-2) exhibit two resonances coincident with these. This is consistent with the presence of tetraene isomers possessing unsaturation at both C2–C3 and C13–C14 positions. In the case of PI-3 which contains predominantly XV (i.e., Z isomer), there is sufficient quantity of the related *E* isomer to observe a single resonance for C-11 at 39.8 ppm which is most consistent with unsaturation at C13–C14 (c.f. chemical shift of pentaene XI vide infra). Finally, since the $^{13}C$ NMR spectra obtained for mixtures of all 4 tetraenes demonstrate that the remaining 2 isomers (RI 2078, $2124_{HP-1}$) have a double bond in the C2–C3 position, and that for each of the triene, tetraene and pentaene pairs (XIII and XIV, XV and XVII, XI and XII) the GC elution order is Z before *E*, we can infer that tetraenes with RIs 2078 and $2124_{HP-1}$ can be assigned to XVI and XVIII respectively (n.b. the mass spectra for these two compounds are also very similar (Fig. 4) which supports these assignments).

## 4. DISCUSSION

### 4.1. Taxonomy and Distribution of *P. intermedium*

*P. intermedium* is demonstrably a producer of a range of HBI alkenes, as are *H. ostrearia* and *R. setigera* (e.g., Volkman et al., 1994). Whilst the cultures examined herein were not axenic (c.f., Wraige et al., 1999), the quantities of HBIs produced argue against a bacterial source. The taxonomy of *P. intermedium* has been described in detail elsewhere (Peragallo, 1890–1891; Peragallo and Peragallo, 1897–1908; Hendey, 1964; Cardinal et al., 1986; Cardinal et al., 1989). Briefly, it is a benthic alga that belongs to the same Class (Bacillariophyceae) as the other known producers of HBIs (viz *H. ostrearia* and *R. setigera*). However, the taxonomy of *P. intermedium* lies closer to *H. ostrearia* than *R. setigera* since they share the same Order (Pennales) and Family (Naviculaceae) (c.f. Order Centrales for *R. setigera* (Simonsen, 1974)). *P. intermedium* has been reported in UK (Smith, 1853; Hendey, 1964), French (Peragallo, 1890–1891; Peragallo and Peragallo, 1897–1908) and Canadian (Cardinal et al., 1986; Cardinal et al., 1989) coastal sediments and it has also been observed in Arctic regions (Cleve and Grunow, 1880). Peragallo (1890–1891) concludes that *P. intermedium* has a widespread global occurrence. Nichols et al. (1988) described the presence of an unknown *Pleurosigma* species in mixed communities of Antarctic sea-ice diatoms. Interestingly, the hydrocarbons of this mixture contained a $C_{25}$ HBI diene.

### 4.2. Structural Features of HBIs from *P. intermedium*

In this paper, we have described a new source diatom species (*P. intermedium*) for $C_{25}$ HBI trienes and tetraenes and determined the structures of these compounds using NMR spectroscopy and mass spectrometry. We have also presented RI data for these compounds in order to facilitate comparison with other geochemical reports of HBIs. The structures of the 6 new HBIs described here are clearly pseudo-homologous to those reported for the pentaenes from *P. intermedium* described previously (Belt et al., 2000b). In addition, they show similarities but important differences compared to those reported previously from *H. ostrearia* (Belt et al., 1996; Johns et al., 1999; Wraige et al., 1997; Wraige et al., 1999) and *R. setigera* (Sinninghe Damsté et al., 1999b). Thus, while the new trienes from *P. intermedium* (XIII and XIV) have 2 double bonds whose positions are common with trienes from *H. ostrearia* (viz., C9–C10 and C23–C24 positions), the third double bond is located at the C7–C20 position, resulting in an unsaturated branch point (c.f., pentaenes XI and XII, Belt et al., 2000b). This is in contrast to previously reported HBIs from *H. ostrearia* (Belt et al., 1996; Johns et al., 1999; Wraige et al., 1997; Wraige et al., 1999) and *R. setigera* (Sinninghe Damsté et al., 1999b), in which C-7 is saturated ($sp^3$ hybridised). Further similarities are noted for the related tetraenes (XV–XVIII) which contain an additional double bond in either the C2–C3 (XVI and XVIII) or C13–C14 (XV and XVII) positions compared with trienes XIII and XIV. (n.b. only tetraenes with a double bond in the C13–C14 position have been observed to date from *H. ostrearia* (Belt et al., 1996)). A further structural correlation can be made with the previously reported pentaenes XI and XII since these contain double bonds in both C2–C3 and C13–C14 positions (Belt et al., 2000b).

Of additional note are the stereochemical features of these new compounds, which include the presence of both *E* and Z isomers at position C9–C10, with the relative concentrations of these dependent on the cultures from which they have been isolated (Table 1). In contrast, mixtures of related stereoiso-

Table 2. Correlation between HBIs isolated from *P. intermedium* with sedimentary reports. Assignments are made on the basis of both GC (RI) and mass spectral data.

| Reference | This report | | Barrick et al. 1980 | Volkman et al. 1983 | Porte et al. 1990 | Prahl et al. 1980 | Requejo et al. 1984 | Requejo and Quinn 1983; 1985 | Albaiges et al. 1984 | Osterroht et al. 1983 | Shaw et al. 1985 | Voudrias and Smith 1986 | Venkatesan 1988 | Matsueda and Handa 1986[a,b] |
|---|---|---|---|---|---|---|---|---|---|---|---|---|---|---|
| Column phase | HP-1 | HP-5 | SP-2100 | SP-2100 | DB-5 | SP2100 | SE-30 | SE-30 | DB-5 | SP1200 | OV101 | SE-52 | DB-5 | SE-52 |
| Compound | | | | | | | | | | | | | | |
| $C_{25:3}$ XIII | 2042 | 2044 | 2044 | 2044 | 2044 | | | 2044 | | | | | 2046 | 2047 |
| $C_{25:3}$ XIV | 2087 | 2091 | 2090 | 2090 | 2091 | 2090 | 2091 | 2091 | 2091 | 2089 | 2092 | 2091 | | 2092 |
| $C_{25:4}$ XV | 2074 | 2083 | 2078 | 2078 | 2079 | | | | | | | | | 2083 |
| $C_{25:4}$ XVI | 2078 | 2087 | | | 2086 | | | | | | | | | |
| $C_{25:4}$ XVII | 2121 | 2130 | 2124 | 2124 | 2126 | | | | | | | | | |
| $C_{25:4}$ XVIII | 2124 | 2136 | | | 2133 | | | | | | | | | |
| $C_{25:5}$ XII | 2112 | 2126 | | | 2124 | | | | | | | | | |
| $C_{25:5}$ XI | 2159 | 2172 | | | 2169 | | | | | | | | | |

mers due to isomerisation at C7–C20 are not observed. This type of geometric isomerisation has not been reported for HBIs from other diatoms although structural isomerism is common (Belt et al., 1996; Johns et al., 1999; Sinninghe Damsté et al., 1999b; Wraige et al., 1997; Wraige et al., 1999). Further, all 6 newly characterised HBIs have two asymmetric centres at C-6 and C-22 with consequential potential for further stereoisomerism. However, both NMR and chromatographic evidence for XIII–XVIII indicates a fixed configuration at each of these two chiral centres and that each compound exists as a single enantiomer. Thus, each HBI elutes as a single peak from both HP-1 and HP-5 GC stationary phases, while in solution (NMR), there is no doubling of $^{1}H$ or $^{13}C$ resonances, a feature that is common for mixtures of HBI diastereoisomers (Belt et al., 1996). This apparent enantioselectivity in the biosynthesis of HBI by *P. intermedium* is in contrast to that found for many other HBIs, where the presence of congurational diastereoisomerism has been reported (Belt et al., 1996; Wraige et al., 1999). In summary, all HBIs found in *P. intermedium* have double bonds that are common to all 8 compounds characterised (viz., C7–C20, C9–C10 and C23–C24) with the tetraenes (×4) and pentaenes (×2) containing an additional 1 and 2 isoprenyl moieties respectively.

### 4.3. HBIs Found in Sediments, Particles and Biota

Whether *P. intermedium* will prove to be a widespread source of HBIs in the environment remains to be seen. Other species of the genus including planktonic organisms should probably be examined, in addition to related genera of diatoms.

Nonetheless, *P. intermedium* has proved to be a valuable source of a range of novel HBIs as described above and these authenticated compounds now allow us to identify most of the previously unidentified HBIs in sediments, biota and sedimentary particles. Thus, the RI and MS properties for these HBI trienes and tetraenes together with the observation of geometric isomers for each type are all in excellent agreement with the observations and proposals put forward by other authors who have reported HBIs in geochemical samples. Barrick et al. (1980) identified 2 $C_{25}$ HBI trienes and 2 tetraenes in sediments from Puget Sound, USA whose RIs ($C_{25:3}$ 2044, $2090_{SP\text{-}2100}$; $C_{25:4}$ 2078, $2124_{SP\text{-}2100}$) are very similar to those found for XIII, XIV, XV and XVII (Table 2). Further, a comparison of the mass spectra for XIII or XIV with those reported by Barrick et al. (1980) for the Puget Sound trienes shows an excellent correlation between common ions (e.g., m/z 346, 291, 233, 165, 83 and 69) and their relative intensities. A similar correlation can be made between XV or XVII and the two tetraenes reported in the same sediments (Barrick et al., 1980). Thus, the HBIs reported by Barrick et al. (1980) can be identified as being XIII, XIV, XV and XVII. $C_{25}$ HBI trienes and tetraenes have also been reported in sediment traps collected from Puget Sound (Bates et al., 1984) and from neighbouring Washington coastal sediments (Prahl and Carpenter, 1984), though the RI data of the latter were not reported, precluding confirmation of their identities here.

In a later report, Porte et al. (1990) identified $C_{25}$ HBI trienes and tetraenes in bivalves collected from the Todos os Santos Bay (Brazil). The chromatographic and mass spectral properties of these HBIs were very similar to those found by Barrick et al. (1980) for the HBIs found in Puget Sound sediments. In addition, Porte et al. (1990) reported 2 previously unreported tetraenes whose mass spectra were identical to each other yet different from the other pair of tetraenes found in the same bivalves. Comparison of the RIs and mass spectra for the two pairs of tetraenes and the triene pair reported by Porte et al. (1990) with those obtained for the HBIs described here from *P. intermedium* indicates that they are the same compounds. Thus, as a result of the structural, chromatographic and mass spectral characteristion of XIII–XVIII, the proposal by Barrick et al. (1980) and Porte et al. (1990) that HBI trienes and tetraenes may exist as mixtures of geometric isomers has now been verified and, importantly, the positions of the double bonds resulting in the geometric isomerism have been identified.

Porte et al. (1990) also noted that bivalves analysed from the Todos os Santos Bay contained 4 $C_{25}$ pentaenes (Table 2) with 2 of these (RI 2144, $2169_{DB\text{-}5}$) possessing identical mass spectra. On the basis of matching RI and mass spectral data, we propose that 2 of these compounds (RI 2124, $2169_{DB\text{-}5}$) correspond to the HBIs XII and XI (RI 2126, $2172_{HP\text{-}5}$), which are pseudo-homologues of XIII–XVIII (Belt et al., 2000b).

There are a number of other reports of sedimentary HBIs that can reasonably be assigned to those characterised and described

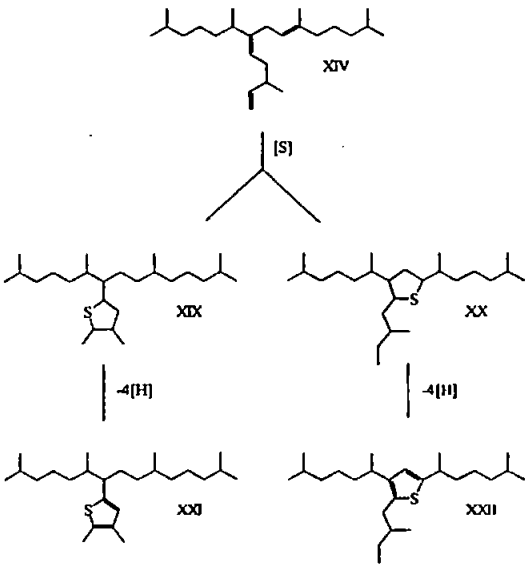


Fig. 6. Potential route for diagenetic incorporation of sulphur into HBI trienes to yield HBI thiolanes and thiophenes (HBITs).

here via combined analyses of GC (RI) and mass spectral data. These assignments are summarised in Table 2.

From our data (Fig. 1; Table 1), it is clear that there is a significant variation in the distributions of the 8 HBIs that are biosynthesised by *P. intermedium* between different cultures. However, since we do not understand the reasons for this variability, we are unable (at present) to make any definitive correlations with sedimentary distributions of these HBIs. It is also apparent that although the HBIs produced by *P. intermedium* are the most commonly reported ones, there are almost certainly other species or genera of diatoms that contribute to global distributions. In particular, the occurrence of HBIs in the water column (Prahl et al., 1980; Osterroht et al., 1983; Volkman et al., 1983; Albaiges et al., 1984; Bates et al., 1984; Matsueda and Handa, 1986a;b) is probably better explained as a result of planktonic production rather than from a benthic source. Significantly, the *Pleurosigma* genus is extremely widespread (van Heurck, 1899) with some of the species being planktonic (Simonsen, 1974; Hendey, 1964). Examples of these include *P. elongatum*, *P. normanii* and *P. aestuarii* and these should receive further attention for HBI biosynthesis in order that a more comprehensive account of HBI sources can be made.

### 4.4. Potential Early Diagenesis of HBIs from *P. intermedium*

In addition to the determination of the structures of common sedimentary HBIs, the compounds described here may provide an insight into the potential sources of diagenetic products of HBIs in sediments. These include sulphurised derivatives of HBIs (viz., HBI thiolanes and thiophenes, HBITs) which have been reported in a variety of geochemical samples (see e.g., Kohnen et al., 1990; Sinninghe Damsté and de Leeuw, 1990; Sinninghe Damsté et al., 1989). Further, it is also known that sulphur-rich macromolecular aggregates are important geochemical sinks for HBI alkenes (Bosch et al., 1998). In the cases of well characterised HBITs (e.g., XIX, XXI–XXII, Fig. 6), the positions of the thiolane and thiophene moieties are in poor agreement with the double bond positions in HBIs from diatoms such as *H. ostrearia* and *R. setigera* (Belt et al., 1996; Johns et al., 1999; Sinninghe Damsté et al., 1999; Wraige et al., 1997; Wraige et al., 1999) and so incorporation of sulphur into these HBI isomers to yield these HBITs seems unlikely. In contrast, the presence of an unsaturated branch point (C7–C20) together with double bonds in the C9–C10 and C23–C24 positions for HBIs XI–XVIII isolated from *P. intermedium*, provides the possibility for sulphur incorporation to yield (Figure 6) HBITs that have been reported and structurally verified (Sinninghe Damsté et al., 1989; Kohnen et al., 1990). Thus, HBI alkenes from *P. intermedium* are realistic precursors to sedimentary HBITs. Laboratory experiments to simulate these transformations will be conducted in the future.

*Acknowledgments*—We would like to thank the British Council for a travel grant (ALLIANCE) and the University of Plymouth for research funds (GA and GM).

*Special handling:* M. C. Kennicutt II

## REFERENCES

Albaiges J., Grimalt J., Bayona J. M., Riseborough R. W., de Lappe B., and Walker II W. (1984) Dissolved, particulate and sedimentary hydrocarbons in a deltaic environment. In *Advances in Organic Geochemistry 1983* (eds. P. A. Schenk, J. W. de Leeuw, and G. W. M. Lijmbach). *Org. Geochem.* 6, 237–248.

Barrick R. C., Hedges J. I., and Peterson M. L. (1980) Hydrocarbon geochemistry of the Puget Sound region—I. Sedimentary acyclic hydrocarbons. *Geochim. Cosmochim. Acta* 44, 1349–1362.

Bates T. S., Hamilton S. E., and Cline J. D. (1984) Vertical transport and sedimentation of hydrocarbons in the central main basin of Puget Sound, Washington. *Environ. Sci. Technol.* 18, 299–305.

Belt S. T., Cooke D. A., Robert J.-M., and Rowland S. J. (1996) Structural characterisation of widespread polyunsturated isoprenoid biomarkers: A $C_{25}$ triene, tetraene and pentaene from the diatom *Haslea ostrearia* Simonsen. *Tetrahedron Lett.* 37, 4755–4758.

Belt S. T., Allard W. G., Rintatalo J., Johns L. A,. van Duin A. C. T., and Rowland S. J. (2000a) Clay and acid catalysed isomerisation and cyclisation reactions of highly branched isoprenoid (HBI) alkenes: Implications for sedimentary reactions and distributions. *Geochim. Cosmochim. Acta* in press.

Belt S. T., Allard G., Massé G., Robert J.-M., and Rowland S. (2000b) Important sedimentary sesterterpenoids from the diatom *Pleurosigma intermedium*. *Chem. Commun.* 501–502.

Bosch H.-J., Sinninghe Damsté J. S., and de Leeuw J. W. (1998) Molecular palaeontology of Eastern Mediterranean sapropels: Evidence for photic zone euxinia. In *Proc. ODP, Sci. Results*, (eds. A. H. F. Robertson, K.-C. Emeis, C. Richter, and A. Camerlenghi) Vol. 160 pp. 285–295. College Station, TX (Ocean Drilling Program).

Cardinal A., Poulin M., and Bérard-Therriault L. (1986) Les diatomées benthiques de substrats durs des eaux marines et saumatres du Quebec. 5. Naviculaceae; les genres *Donkinia, Gyrosigma et Pleurosigma*. *Naturaliste can. Rev. Ecol. Syst.* 113, 167–190.

Cardinal A., Poulin M., and Bérard-Therriault L. (1989) New criteria for species characterisation in the genera *Donkinia, Gyrosigma* and *Pleurosigma* (Naviculaceae, Bacillariophyceae). *Phycologia* 28, 15–27.

Cleve P. T. and Grunow A. (1880) Beiträge zur Kenntniss der arctischen Diatomeen. *K. svenska Vetensk.—Akd. Handl.* 17, 1–121.

Farrington J. W., Frew N. M., Gschwend P. M., and Tripp B. W.

(1977). Hydrocarbons in cores of Northwestern Atlantic Coastal and continental margin sediments. *Estuar. Coast. Mar. Sci.* 5, 793–808.
Gearing P., Newman-Gearing J., Lytle T., and Sever-Lytle J. (1976). Hydrocarbons in 60 northeast Gulf of Mexico shelf sediments: A preliminary survey. *Geochim. Cosmochim. Acta* 40, 1005–1017.
Hendey N. I. (1964) An introductory account of the smaller algae in British coastal waters. V. Bacillariophyceae (Diatoms) In *Fishery Investigations MAFF Series IV*, pp. 241–247. London.
van Heurck H. (1899) Traité des Diatomées. pp. 249–259, Anvers.
Johns L., Wraige E. J., Belt S. T., Lewis C. A., Massé G., Robert J.-M., and Rowland S. J. (1999) Identification of $C_{25}$ highly branched isoprenoid (HBI) dienes in Antarctic sediments, sea-ice diatoms and laboratory cultures of diatoms. *Org. Geochem.* 30, 1471–1475.
Johns L., Belt S. T., Lewis C. A., Rowland S., Massé G., Robert J.-M., and König W. A. (2000) Configurations of polyunsaturated sesterterpenoids from the diatom, *Haslea ostrearia*. *Phytochem.* 53, 607–611.
Kohnen M. E. L., Sinninghe Damsté J. S., Kock van-Dalen A. C., ten Haven H. L., Rullkötter J., and de Leeuw J. W. (1990) Origin and diagenetic transformations of $C_{25}$ and $C_{30}$ highly branched isoprenoid sulphur: Further evidence for the formation of organically bound sulphur during early diagenesis. *Geochim. Cosmochim. Acta* 54, 3053–3063.
Matsueda M. and Handa N. (1986a) Source of organic matter in the sinking particles collected from the Pacific sector of the Antarctic Ocean by sediment trap experiments. *Mem. Natl. Inst. Polar Res.* (spec. issue) 20, 364–379.
Matsueda M. and Handa N. (1986b) Vertical flux of hydrocarbons as measured in sediment traps in the eastern North Pacific Ocean. *Mar. Chem.* 20, 179–182.
Nichols P. D., Volkman J. K., Palmisano A. C., Smith G. A., and White D. C. (1988) Occurrence of an isoprenoid $C_{25}$ diunsaturated alkene and high neutral lipid content in Antarctic sea-ice diatom communities. *J. Phycol.* 24, 90–96.
Osterroht C., Petrick G., and Wenck A. (1983) Seasonal variation of particulate hydrocarbons in relation to biological parameters. *Mar. Chem.* 14, 175–94.
Peragallo H. (1890–1891) Monographie du genre *Pleurosigma* et des genres allies. *Le Diatomiste* 1, 13.
Peragallo H. and Peragallo M. (1897–1908) Diatomées marines de France et des districts maritimes voisins (eds. M. J. Tempère) pp. 156–166. Grez-sur-Loing.
Porte C., Barcelo D., Tavres T.M., Rocha V.C., and Albaiges J. (1990). The use of Mussel Watch and molecular marker concepts in studies of hydrocarbons in a tropical bay. *Arch. Environ. Contam. Toxicol.* 19, 236–274.
Prahl F. G., Bennett T. J., and Carpenter R. (1980) The early diagenesis of aliphatic hydrocarbons and organic matter in sedimentary particles from Dabob Bay, Washington. *Geochim. Cosmochim. Acta* 44, 1967–1976.
Prahl F. G. and Carpenter R. (1984) Hydrocarbons in Washington Coastal sediments. *Estuar. Coast. Shelf Sci.* 18, 703–720.
Requejo A. G. and Quinn J. G. (1983) Geochemistry of $C_{25}$ and $C_{30}$ biogenic alkenes in sediments of the Narragansett Bay estuary. *Geochim. Cosmochim. Acta* 47, 1075–1090.
Requejo A. G., Quinn J. G., Gearing J. N., and Gearing P. J. (1984) $C_{25}$ and $C_{30}$ biogenic alkenes in a sediment core from the upper anoxic basin of the Pettaquamscutt River (Rhode Island, USA). *Org. Geochem.* 7, 1–10.
Requejo A. G. and Quinn J. G. (1985) $C_{25}$ and $C_{30}$ biogenic alkenes in sediments and detritus of a New England salt marsh. *Estuar. Coast. Shelf Sci.* 20, 281–297.
Robson J. N. and Rowland S. J. (1986) Identification of novel widely distributed sedimentary acyclic sesterterpenoids. *Nature* 324, 561–563.
Rowland S. J. and Robson J. N. (1990) The widespread occurrence of highly branched acyclic $C_{20}$, $C_{25}$ and $C_{30}$ hydrocarbons in recent sediments and biota—a review. *Mar. Environ. Res.* 30, 191–216.
Shaw D. G., Hogan T. E., and McIntosh D. J. (1985) Hydrocarbons of the sediments of Port Valdez, Alaska: Consequences of five years permitted discharge. *Estuar. Coast. Shelf Sci.* 21, 131–144.
Simonsen R. (1974) The Diatom plankton of the Indian Ocean expedition of R.V. "Meteor". In *Forschungsergebnisse* (ed. D. Reihe). Vol. 19, pp. 1–66. Gebruder Borntraegier, Berlin.
Sinninghe Damsté J. S. and de Leeuw J. W. (1990) Analysis, structure and geochemical significance of organically-bound sulphur in the geosphere: State of the art and future research. In *Advances of Organic Geochemistry* (eds. B. Durand and F. Behar) *Org. Geochem.* 16, 1077–1101.
Sinninghe Damsté J. S., van Koert E. R., Kock-van Dalen A. C., de Leeuw J. W., and Schenk P. A. (1989) Characterisation of highly branched isoprenoid thiophenes occurring in sediments and immature crude oils. *Org. Geochem.* 15, 555–567.
Sinninghe Damsté J. S., Rijpstra W. I. C., Schouten S., Peletier H., van der Maarel M. J. E. C., and Gieskes W. W. C. (1999a) A $C_{25}$ highly branched isoprenoid alkene and $C_{25}$ and $C_{27}$ *n*-polyenes in the marine diatom *Rhizosolenia setigera*. *Org. Geochem.* 30, 95–100.
Sinninghe Damsté J. S., Schouten S., Rijpstra W. I. C., Hopmans E. C., Peletier H., Gieskes W. W. C., and Geenevasen J. A. J. (1999b) Structural identification of the $C_{25}$ highly branched isoprenoid pentaene in the marine diatom *Rhizosolenia setigera*. *Org. Geochem.* 30, 1581–1583.
Smith W. (1853) A Synopsis of the British Diatomaceae. 1. Taylor and Francis, London. pp. 241–247.
Venkatesan M. I. (1988) Organic geochemistry of marine sediments in the Antarctic region. Marine lipids in McMurdo Sound. *Org. Geochem.* 12, 13–27
Volkman J. K., Farrington J. W., Gagosian R. B., and Wakeham S. G. (1983) Lipid composition of coastal marine sediments from the Peru upwelling region. In *Advances in Organic Geochemistry 1981* (eds. M. Bjoroy et al). pp.228–240. Wiley, Chichester, UK.
Volkman J. K., Barratt S. M., and Dunstan G. A. (1994) $C_{25}$ and $C_{30}$ highly branched isoprenoid alkenes in laboratory cultures of two marine diatoms. *Org. Geochem.* 21, 407–414.
Volkman J. K., Barrett S. M., Blackburn S. I., Mansour M. P., Sikes E. L., and Gelin F. (1998) Microalgal biomarkers: A review of recent research developments. *Org. Geochem.* 29, 1163–1179.
Voudrias E. A. and Smith C. L. (1986) Hydrocarbon pollution from marinas in estuarine sediments. *Estuar. Coast. Shelf Sci.* 22, 271–284.
Wraige E. J., Belt S. T., Lewis C. A., Cooke D. A., Robert J.-M., Massé G., and Rowland S. J. (1997) Variations in structures and distributions of $C_{25}$ highly branched isoprenoid (HBI) alkenes in cultures of the diatom, *Haslea ostrearia* (Simonsen). *Org. Geochem.* 27, 497–505.
Wraige E. J., Johns L., Belt S. T., Massé G., Robert J.-M., and Rowland S. (1999) Highly branched $C_{25}$ isoprenoids in axenic cultures of *Haslea ostrearia*. *Phytochem.* 51, 69–73.

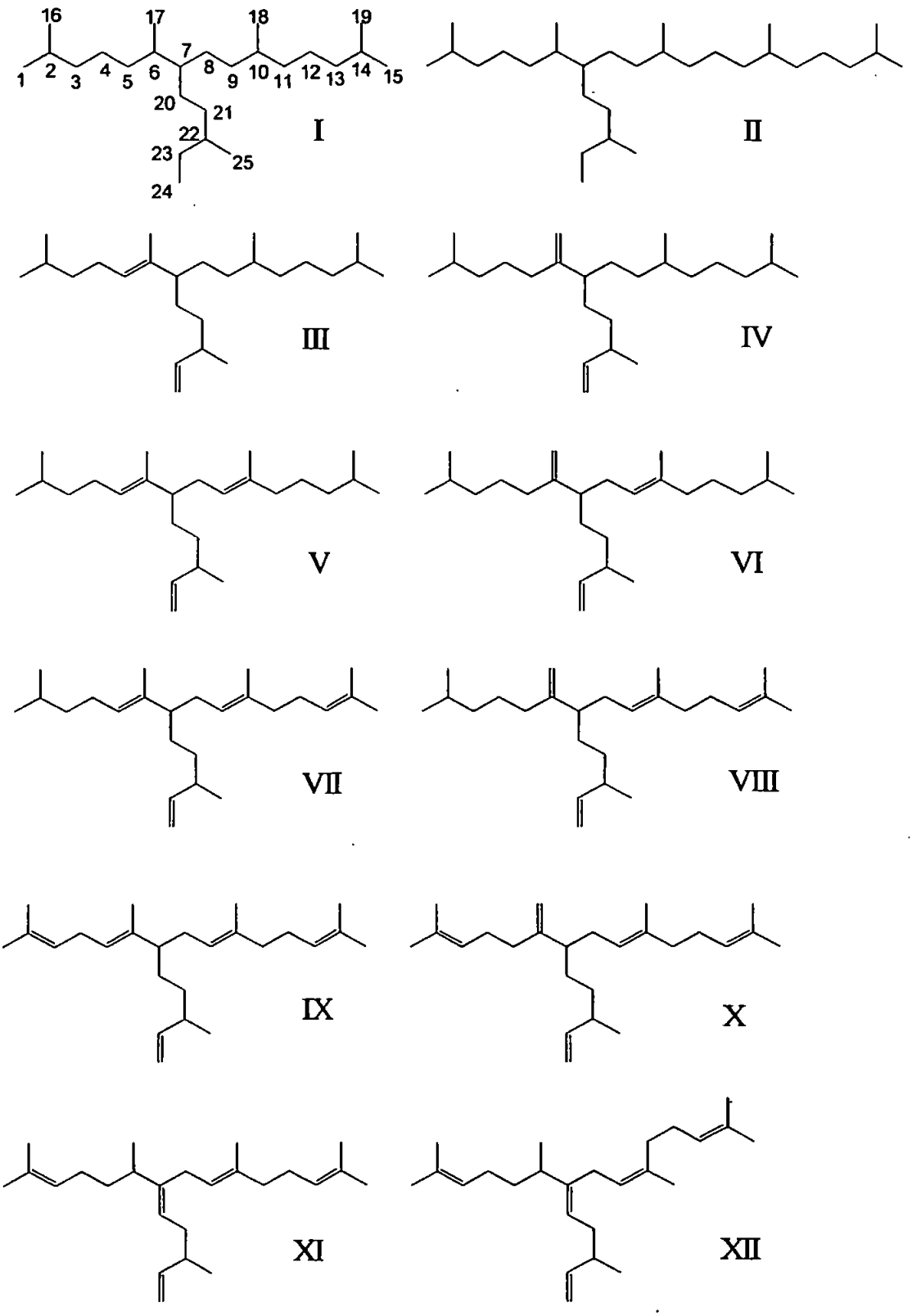


APPENDIX I. Structures of $C_{25}$ and $C_{30}$ HBI parent structures and typical HBI alkenes from sediments and diatoms.

## APPENDIX 2. $^1H$ and $^{13}C$ NMR data for HBIs XIII–XVIII

XIII and XIV : $^1H$ (δ/ppm): 5.74 (ddd, J = 17.1, 10.2, 6.6 Hz, H-23), 5.11 (m, H-9, 20), 4.92 (d, J = 17.1 Hz, H-24), 4.88 (d, J = 10.2 Hz, H-24), 2.62 (m, H-6), 2.56 (m, H-8), 2.13 (m, H-22), 1.97 (m, H-11, 21), 1.69 (s, H-18 (XIII)), 1.54 (s, H-18 (XIV)), 1.52 (m, H-2, 14), 1.28 (m, H-5), 1.20 (m, H-4, 12), 1.14 (m, H-3, 13), 0.93 (d, J = 6.6 Hz, H-17), 0.85, 0.84 (2 × d, J = 6.6 Hz, H-1, 15, 16, 19); $^{13}C$ (δ/ppm): 144.6 (C-23), 143.0 (C-7 (XIII)), 142.8 (C-7 (XIV)), 136.1 (C-10 (XIII)), 136.0 (C-10 (XIV)), 123.7 (C-9 (XIII)), 123.2 (C-9 (XIV)), 122.9 (C-20 (XIII)), 122.7 (C-20 (XIV)), 112.1 (C-24), 40.0 (C-11 (XIV)), 39.3 (C-3), 39.0 (C-13 (XIII)), 38.7 (C-13 (XIV)), 38.2 (C-22), 35.3 (C-5), 34.4 (C-21), 34.3 (C-6), 31.8 (C-11 (XIII)), 29.3 (C-8 (XIV)), 29.0 (C-8 (XIII)), 27.9 (C-2, 14), 25.8 (C-12), 25.7 (C-4), 23.5 (C-18 (XIII)), 22.6 (C-1, 15, 16, 19), 19.6, 19.5 (C-17, 25), 15.7 (C-18 (XIV)).

XV–XVIII: $^1H$ (δ/ppm): 5.73 (ddd, J = 17.1, 10.2, 6.6 Hz, H-23), 5.11 (m, H-3 (XVI, XVIII), 9, 13 (XV, XVII), 20), 4.92 (d, J = 17.1 Hz, H-24), 4.88 (d, J = 10.2 Hz, H-24), 2.62 (m, H-6), 2.56 (m, H-8), 2.13 (m, H-22), 1.99 (m, H-4 (XVI, XVIII), 11, 12 (XV, XVII), 21), 1.53-1.69 (7 × s, H-1,16 (XVI, XVIII), 15, 19 (XV, XVII), 18), 1.52 (m, H-2 (XV, XVII), 14 (XVI, XVIII)), 1.28 (m, H-5), 1.20 (m, H-4 (XV, XVII), 12 (XVI, XVIII)), 1.14 (m, H-3 (XV, XVII), 13 (XVI, XVIII)), 0.95 (m, H-17, 25), 0.86 (m, H-1, 16 (XV, XVII)), 15, 19 (XVI, XVIII)). $^{13}C$ (δ/ppm): 144.6 (C-23), 143.0 (C-7 (XV)), 142.8 (C-7 (XVI)), 142.7 (C-7 (XVII)), 142.5 (C-7 (XVIII)), 136.2, 136.1 (C-10 (XVI, XVIII)), 135.6 (C-10 (XV, XVII)), 131.4 (C-14 (XV)), 131.3 (C-2 (XVI or XVIII)), 131.1 (C-14 (XVII)), (C-2 (XVI or XVIII)), 124.4 (C-13 (XV)), 124.0 (C-9 (XV)), 122.9 (C-20 (XV)), 124.9, 124.5, 123.6, 123.4, 123.0, 122.8, 122.7 (C-9, 13, 20 (XVI–XVIII)), 112.1 (C-24), 40.0 (C-11 (XVIII)), 39.8 (C-11 (XVI)), 39.3 (C-3 (XV, XVII)), 38.9 (C-13 (XVI)), 38.6 (C-13 (XVIII)), 38.2 (C-22), 35.2 (C-5), 34.4 (C-21), 34.3 (C-6 (XV, XVII)), 34.0 (C-6 (XVI, XVIII)), 31.9 (C-11 (XV)), 31.8 (C-11 (XVI)), 29.3, 29.2 (C-8 (XVI–XVIII)), 28.9 (C-8 (XV)), 27.9 (C-2 (XV, XVII)), C-14 (XVI, XVIII)), 26.7 (C-12 (XV, XVII)), 26.4 (C-4 (XVI, XVIII)), 25.8 (C-12 (XVI, XVIII)), 25.7 (C-4 (XV, XVII)), 25.7 (C-1 (XV, XVII)), (C-15 (XVI, XVIII)), 23.5 (C-18 (XV, XVI)), 22.6 (C-1,16 (XV, XVII), C-15,19 (XVI, XVIII)), 19.6, 19.5, 19.4 (C-17, 25 (XV–XVIII)), 17.7, 17.6 (C-16 (XVI, XVIII), C-19 (XV, XVII)), 15.8, 15.7 (C-18 (XVII, XVIII)).

PERGAMON

Phytochemistry 56 (2001) 795–800

PHYTOCHEMISTRY

www.elsevier.com/locate/phytochem

# Tetra-unsaturated sesterterpenoids (Haslenes) from *Haslea ostrearia* and related species

W. Guy Allard [a], Simon T. Belt [a,*], Guillaume Massé [a,b], Raoul Naumann [a], Jean-Michel Robert [b], Steven Rowland [a,*]

[a] *Petroleum and Environmental Geochemistry Group, Department of Environmental Sciences, University of Plymouth, Drake Circus, Plymouth, PL4 8AA, UK*

[b] *ISOMer, Faculté des Sciences et des Techniques, Université de Nantes, 2 rue de la Houssinière, 44072 Nantes, Cedex 3, France*

Accepted 13 October 2000

**Abstract**

The structures and distributions of $C_{25}$ highly branched isoprenoid (HBI) alkenes (Haslenes) have been determined following isolation from cultures of the diatoms *Haslea ostrearia*, *Haslea crucigera*, *Haslea pseudostrearia* and *Haslea saltstonica*. The distributions of the HBIs change between *Haslea* species and also between different cultures of the same species. Large scale culturing of *H. ostrearia* and *H. pseudostrearia* has enabled the structures of three new tetra-unsaturated alkenes to be determined by NMR spectroscopy. The structural relationships between different Haslenes together with the potential significance of the biosynthesis of HBIs by the *Haslea* genus is discussed. 

*Keywords:* *Haslea ostrearia*; *Haslea crucigera*; *Haslea pseudostrearia*; *Haslea saltstonica*; Microalgae; Diatoms; Isoprenoid alkenes; Highly branched isoprenoids; $C_{25}$ alkenes; Non-saponifiable lipids

## 1. Introduction

In a number of recent reports, we have described the structures and distributions of a series of $C_{25}$ highly branched isoprenoid (HBI) hydrocarbons that are present in the diatom *Haslea ostrearia* (Gaillon) Simonsen (Belt et al., 1996; Johns et al., 1999; Wraige et al., 1997, 1999). These compounds (parent structure I; Fig. 1) are ubiquitous in contemporary marine sediments and are often the major hydrocarbons present (for a review, see Rowland and Robson, 1990). Further, by use of axenic cultures, we have demonstrated conclusively that *H. ostrearia* is a primary producer of these lipids (Wraige et al., 1999). In culture, HBIs range in their unsaturation (e.g. III–X) between two and six double bonds, though monoenes (e.g. II) and the parent alkane (I) have also been observed in sediments (Robson and Rowland, 1986). Cultures of *H. ostrearia* are usually dominated by trienes and tetraenes, often as mixtures of geometric and/or diastereoisomers (Belt et al., 1996). To date, the reasons for varying distributions of HBIs in cultures of *H. ostrearia* are not fully understood, though it is apparent that temperature and not salinity is a major controlling influence over unsaturation (Wraige et al., 1998; Rowland et al., 2001). In sediments, it is likely that HBIs undergo isomerisation and cyclisation reactions depending on the degree of unsaturation (Belt et al., 2000a). More recently, two new producers of $C_{25}$ HBI alkenes have been reported (viz. *Rhizosolenia setigera* (Sinninghe Damsté et al., 1999) and *Pleurosigma intermedium* (Belt et al., 2000b,c)). The $C_{25}$ pentaene (IX) found in *R. setigera* is also produced by *H. ostrearia* (Wraige et al., 1997) but the HBIs from *P. intermedium* represent a slightly different structural type (e.g. XI-XII), since these compounds are unsaturated at the major branch point, C-7.

In the present study, we report the presence of HBI alkenes in three previously unexamined *Haslea* species (*Haslea crucigera* (Wm. Smith) Simonsen, *Haslea pseudostrearia* Massé et al. and *Haslea saltstonica* Massé et al.) together with the characterisation of three new HBI tetraenes.

* Corresponding authors. Tel.: +44-1752-233042; fax: +44-1752-233035.

*E-mail address:* sbelt@plymouth.ac.uk (S.T. Belt).

0031-9422/01/$ - see front matter 
PII: S0031-9422(00)00429-5

## 2. Results and discussion

### 2.1. Identification of HBIs in four species of the Haslea genus

The four *Haslea* species that have been cultured and examined for HBIs in this study are *H. ostrearia*, *H. crucigera*, *H. pseudostrearia* and *H. saltstonica*. Each of these species are pennate, benthic diatoms measuring ca. 30–100×6–20 μm. The main structural differences between them have been described elsewhere (Massé et al., 2000). After large scale culture of each *Haslea* species followed by centrifugation, freeze drying and extraction (hexane), GC and GC–MS analysis of the total hexane extracts (THEs) revealed the presence of several HBI alkenes with varying distributions. HBI production from *H. ostrearia* is well known (Volkman et al., 1994; Belt et al., 1996; Johns et al., 1999; Wraige et al., 1997, 1999), but this is the first report of HBIs from other *Haslea* species. Following saponification (KOH/MeOH/$H_2O$) and re-extraction (hexane), the remaining non-saponifiable lipid fractions consisted almost entirely of HBIs and phytol. Fig. 2 shows representative partial total ion current chromatograms (TICs) of these fractions for *H. ostrearia*, *H. crucigera*, *H. pseudostrearia and H. saltstonica* cultures, which clearly illustrates the presence of different HBI distributions in each *Haslea* species. The differences between these distributions are not presumed to be an indicator of each specific *Haslea* species, since analysis of a number of different cultures of *H. ostrearia* reveals a substantial variation in HBI structure(s) (Belt et al., 1996; Johns et al., 1999; Wraige et al., 1997, 1999) and the same may well be true for the other three *Haslea* species studied here. However, our analyses do verify that each species can be considered to be a primary producer of these sesterterpenoid lipids.

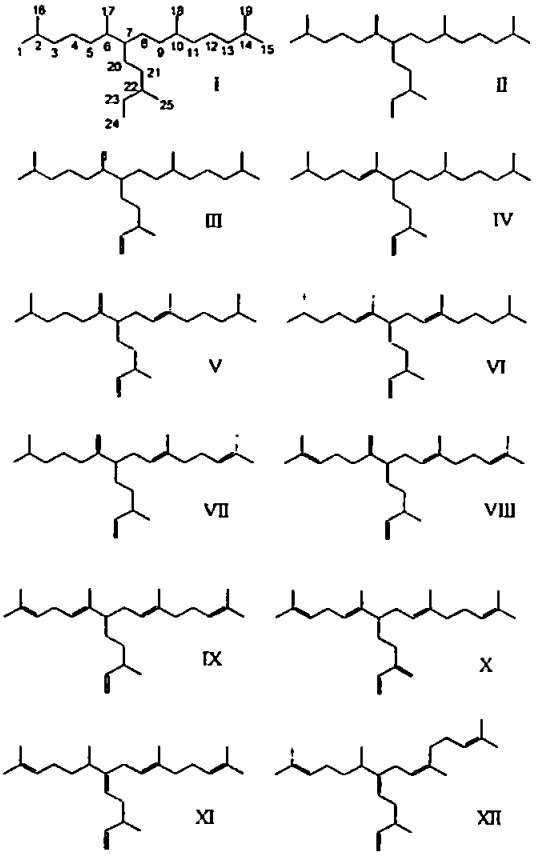


Fig. 1. Structures of $C_{25}$ HBI alkenes previously characterised in sediments and diatoms. The numbering scheme is illustrated for the parent alkane I.

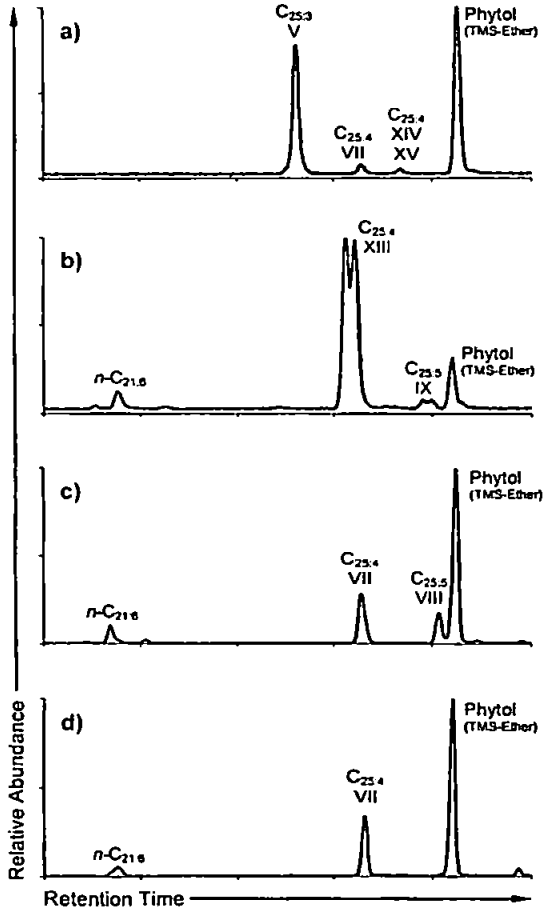


Fig. 2. Representative partial GC (HP-1) total ion current chromatograms (TICs) of non-saponifiable hexane extracts from (a) *Haslea ostrearia*, (b) *Haslea pseudostrearia*, (c) *Haslea crucigera*, and (d) *Haslea saltstonica*.

Closer examination of the TICs reveals that they consist of mixtures of HBIs reported previously in cultures of *H. ostrearia* and new, uncharacterised HBI compounds. Thus, of the three large scale cultures of *H. ostrearia* analysed in this present study, one culture (HO-1; Fig. 2a) was found to contain mainly triene V (ca. 90% of total HBIs) and a trace amount of the tetraene VII characterised from previous cultures (Wraige et al., 1997), together with two previously unreported tetraenes (XIV, XV; see Table 1 for GC RIs). The other two cultures of *H. ostrearia* consisted mainly of HBI triene V with trace quantities of the pseudo-homologues; tetraene (VII) and pentaene (VIII). The new tetraenes found in HO-1 (vide infra) were also present, though their concentrations represented less than 10% of the total HBIs for all three cultures. The single large scale culture of *H. crucigera* was found to yield $C_{25}$ tetraene VII (45%) and pentaene VIII (22%) but no new HBI alkenes were detected (Fig. 2c). Following further fractionation of tetraene VII and pentaene VIII ($SiO_2$/hexane), NMR analysis of these individual components demonstrated that they were present as single stereoisomers rather than mixtures of diastereoisomers even though diastereoisomeric mixtures of HBIs have been observed previously in cultures of *H. ostrearia* (Belt et al., 1996; Johns et al., 1999). Similarly, the bulk culture of *H. saltstonica* yielded only one stereoisomeric $C_{25}$ HBI (Fig. 2d), which corresponded to tetraene VII (Belt et al., 1996). Finally, large scale culture of the second *Haslea* species isolated from the Kingsbridge estuary (UK), *H. pseudostrearia*, contained predominantly a $C_{25}$ HBI alkene (XIII; resolves as 2 GC peaks) that has not been previously characterised, together with a trace of pentaene IX (Fig. 2b).

### 2.2. Characterisation of 2,6,10,14-tetramethyl-9-(3-methylpent-4-enyl)pentadec-2,6,10-triene (XIII)

81 mg of a $C_{25}$ HBI tetraene (94% purity, GC) was isolated from a single large scale culture of *H. pseudostrearia* (Massé et al., 2000) by extraction (hexane), saponification (KOH/MeOH/$H_2O$), re-extraction (hexane) and column chromatography ($SiO_2$/hexane). GC analysis of this compound reveals that it resolves into two peaks on all three phases used (e.g. Fig. 2b) and that the GC RIs for both peaks are different to those obtained for the previously characterised HBI tetraene VII (n.b. diastereomeric HBI VII only resolves into two peaks on DB-WAX; Table 1). In addition, while the mass spectra for the two tetraenes in this fraction are identical to each other, they show differences when compared to ms data obtained for tetraene VII (Fig. 3). In particular, the mass spectrum of tetraene VII exhibits a relatively large number of fragment ions at $m/z > 200$ with the most abundant ion at $m/z$ 259, whereas the same spectral region for XIII is dominated by two ions at $m/z$ 207 and 275. The intensity of ion $m/z$ 95 is also significantly different between the two isomers. Examination of the $^1H$ NMR spectrum obtained for XIII demonstrates the presence of a vinyl moiety ($CH{=}CH_2$), three trisubstituted double bonds, and a 1:1 ratio of isopropyl ($(CH_3)_2CH$) and isoprenyl ($(CH_3)_2C{=}$) groups. The $^{13}C$ NMR spectrum reveals six $CH_3$, eight $CH_2$, seven CH and three quaternary $^{13}C$ resonances which confirms the substitution multiplicity of the double bonds. The appearance of a resonance at ca. 49 ppm confirms that the major branch point of the carbon

Table 1
GC retention indices of four isomeric $C_{25}$ HBI tetraenes obtained from *Haslea ostrearia* and related species

| Tetraene structure | Retention index | | |
|---|---|---|---|
| | HP-1 | HP-5 | DB-WAX |
| VII | 2140 | 2145 | 2232, 2238 |
| XIII | 2134, 2138 | 2143, 2146 | 2221, 2227 |
| XIV | 2157 | 2159 | 2267 |
| XV | 2157 | 2159 | 2277 |

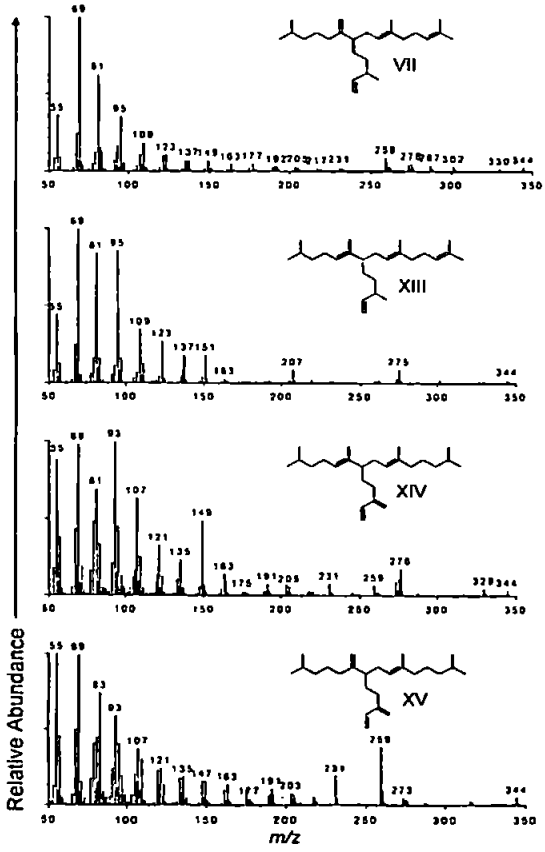


Fig. 3. Mass spectra for 4 isomeric $C_{25}$ HBI tetraenes isolated from cultures of *Haslea ostrearia* and related species.

chain (C-7) is saturated, consistent with other HBI structures from *H. ostrearia* (Belt et al., 1996; Wraige et al., 1997; Johns et al., 1999). Since the presence of a vinyl group and three trisubstituted double bonds are readily identified from the $^{1}H$ and $^{13}C$ NMR data, the four double bonds must be positioned at C23–C24 (vinyl), C5–C6, C9–C10 and either of C2–C3 or C13–C14. Double bonds in both of these latter two positions can be ruled out from the observation of an equal number of isopropyl and isoprenyl groups. In order to determine which end of the carbon chain is unsaturated, the allylic region of the $^{1}H$ NMR spectrum was examined in more detail. Methylene ($CH_2$) protons that are allylic to two double bonds resonate ($\delta$ 2.6–2.8 ppm) to higher frequency compared to those which are monoallylic ($\delta$ 1.8–2.1 ppm). Thus, the chemical shifts for H-4 in pentaene **IX** (Sinninghe Damsté et al., 1999) and hexaene **X** (Wraige et al., 1997) appear at 2.8 and 2.7 ppm, respectively. The $^{1}H$ NMR spectrum of the tetraenes isolated from *H. pseudostrearia* does not have any resonances in this region and integration of the monoallylic region (10H) is consistent with the terminal double bond being in the C13–C14 position. The low frequency chemical shifts for C-17 (11.8 ppm) and C-18 (16.1 ppm) confirm that the stereochemistries for the C5–C6 and C9–C10 double bonds are *E* in both cases. The structure for the $C_{25}$ HBI tetraene can thus be confirmed as **XIII** (Fig. 4).

Finally, since most of the individual resonances in the $^{13}C$ spectrum are split into two peaks, we conclude that the tetraenes exist as a mixture of diastereoisomers, a feature that has been observed for other HBIs from *H. ostrearia* (Belt et al., 1996; Johns et al., 1999). In these cases, C-7 has been shown to have a fixed (but unknown) configuration, with variable stereochemistry at C-22 (Johns et al., 2000). The appearance of two compounds (GC) possessing identical mass spectra (vide infra) can also be explained by the presence of a mixture of diastereoisomers.

### 2.3. Characterisation of 2,6,10,14-tetramethyl-7-(3-methylenepent-4-enyl)pentadec-5,9-diene (XIV) and 2,6,14-trimethyl-10-methylene-9-(3-methylenepent-4-enyl) pentadec-6-diene (XV)

For virtually all cultures of *H. ostrearia* studied, two additional HBI tetraenes could be detected as minor components (< 10% of total HBIs) that had different GC and mass spectral properties to either **VII** or **XIII** (Table 1, Fig. 3). Following repeated fractionation ($SiO_2$/hexane), these two new tetraenes were obtained from several cultures of *H. ostrearia* in sufficient quantities and purity for structural analysis by GC–MS and NMR spectroscopy.

The $^{1}H$ NMR spectra obtained for both compounds contains a resonance due to the vinylic proton H-23 which has a significantly higher frequency chemical shift

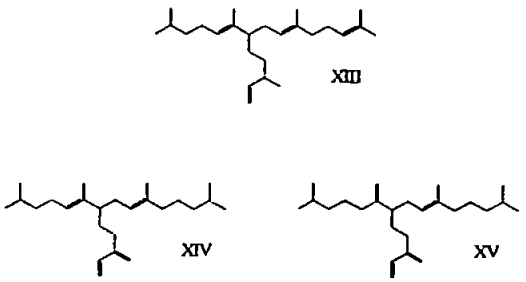


Fig. 4. Structures of new $C_{25}$ HBI tetraenes described in this study.

($\delta$ 6.33 ppm) compared to the analogous resonance observed for **VII** and **XIII**, and appears as a dd due to coupling to H-24$_{cis}$ and H-24$_{trans}$ only. Further methylene (alkene) proton resonances are observed at 4.95 ppm. These observations are consistent with double bonds located at C23–C24 and C22–C25. This arrangement of conjugated double bonds is unusual for HBI alkenes and has only been reported for hexaene **X** which has also been isolated from *H. ostrearia* (Wraige et al., 1997). Additional $^{1}H$ and $^{13}C$ NMR spectral analysis of these two tetraenes confirmed their structures to be **XIV** and **XV** (Fig. 4). HBI **XIV** contains two trisubstituted double bonds while **XV** has one methylene and one trisubstituted double bond. Both compounds are saturated (isopropyl) at each end of the main carbon chain and the stereochemistries of the trisubstituted double bonds (C5–C6 and C9–C10 (**XIV**); C9–C10 (**XV**)) were found to be *E* by analysis of $^{13}C$ data for C-17 and C-18.

The results presented here extend our understanding of the different structural isomers of HBIs biosynthesised by *H. ostrearia*. The generality of HBIs possessing a vinyl moiety together with a double bond in either of the C5–C6 or C6–C17 positions now appears to be fully established. The presence of additional double bonds account for further degrees of unsaturation in the most common tetraenes and pentaenes, though new tetraene structures, with methylenic double bonds in the C22–C25 position have now been determined. Although the reasons for the co-occurrence of individual HBIs are not clear at present, it appears that there are structural relationships between them. Thus, for cultures containing HBIs with different degrees of unsaturation, there is normally a double bond in either the C5–C6 or C6–C17 position (e.g. **V**, **VII** and **VIII**). Similarly, co-occurring isomers also exhibit structural similarities (e.g. **VII** and **XV**).

Our observations are of further significance in that we have shown the biosynthesis of HBIs to be common to four *Haslea* species and this may be the case for the entire genus, though planktonic species such as *Haslea gigantea* and *Haslea wawrikae* (Simonsen, 1974; Von Stosch, 1985) have yet to be analysed. Apart from these taxonomic relationships, the results of these rigorous structural identifications have possible wider implications.

For example, in a geochemical context, by careful comparison with the authenticated algal compounds, the haslenes found in sediments worldwide have recently been shown to be principally isomers with C7–C20, rather than C5–C6 or C6–C17 unsaturation (Belt et al., 2000b,c). The C7–C20 unsaturation is therefore consistent with the positions of sulphur incorporation in the analagous isoprenoid thiophenes found in more ancient sediments and crude oils and which are useful 'biological markers' of ancient algal communities (e.g. Sinninghe Damsté et al., 1989; Kohnen et al., 1990). Finally, the identification of new haslenes is also important in terms of their apparently variable pharmacological activities (Rowland et al., 2001). Some isomers appear to slow the growth of a human lung cancer cell line in vitro, whilst others do not. Examination of the bioactivities of newly discovered isomers is therefore a worthwhile goal of such pharmacological investigations.

## 3. Experimental

### 3.1. Algal cultures

*H. ostrearia* and *H. crucigera* were isolated from the Bay of Bourgneuf (France) while *H. pseudostrearia* and *H. saltstonica* were isolated from the Kingsbridge estuary (Devon, UK). *H. ostrearia* was grown in bulk between April 1991 and June 1998. Large scale cultures (440 l) of each of the other three diatoms were grown in an outdoor facility during September and October 1999 as described previously (Belt et al., 1996).

### 3.2. Isolation and purification of HBIs

Each of the large scale cultures of the four diatoms were centrifuged, freeze dried and extracted (Soxhlet) with hexane to yield total hexane extracts (THEs). The THEs were saponified (KOH/MeOH/$H_2O$) and the non-saponifiable lipids re-extracted into hexane and purified by column chromatography ($SiO_2$/hexane). Fractions containing >90% (GC) of individual HBIs were combined and analysed by $^1H$ and $^{13}C$ NMR spectroscopy. In all cases, the yield of purified HBIs from each culture corresponded to ca. 1 mg per 1 g wet weight (centrifuged algal paste). Small aliquots of each HBI were hydrogenated ($PtO_2.2H_2O$/hexane) to the parent alkane I in order to confirm the carbon skeleton.

### 3.3. NMR spectroscopy

NMR spectra were recorded in $CDCl_3$ using a JEOL EX 270 spectrometer. Chemical shifts ($\delta$) are referenced to residual $CHCl_3$ (7.24 ppm) and $CDCl_3$ (77.0 ppm) for $^1H$ and $^{13}C$ respectively. Resonances marked * indicate the presence of diastereoisomers.

#### 3.3.1. 2,6,10,14-Tetramethyl-9-(3-methylpent-4-enyl) pentadec-2,6,10-triene (XIII)

*3.3.1.1. $^1H$ NMR (270 MHz).* $\delta$ 5.66 (ddd, 1H, J=7, 10.5, 17.5 Hz, H-23), 5.07 (m, 3H, H-5, H-9, H-13), 4.91 (m, 2H, H-24), 2.01 (m, 10H, H-4, H-7, H-8, H-11, H-12, H-22), 1.67 (s, 3H, H-15), 1.59 (s, 3H, H-19), 1.57 (s, 3H, H-18), 1.53 (m, 1H, H-2), 1.45 (s, 3H, H-17), 1.24 (m, 6H, H-3, H-20, H-21), 0.96 (d, 3H, $J$=6.9 Hz, H-25), 0.88 (d, 6H, $J$=6.6 Hz, H-1, H-16).

*3.3.1.2. $^{13}C$ NMR (67.8 MHz).* $\delta$ 145.1, 144.8* (C-23), 136.3 (C-6), 134.8 (C-10), 131.1 (C-14), 126.2, 126.1* (C-5), 124.5 (C-13), 123.5 (C-9), 112.4, 112. 1* (C-24), 49.4, 49.3* (C-7), 39.8 (C-11), 39.1 (C-3), 37.8, 37.7* (C-22), 34.6, 34.5* (C-21), 32.4, 32.3* (C-8), 30.4, 30.3* (C-20), 27.5 (C-2), 26.8 (C-12), 25.7 (C-15), 25.5 (C-4), 22.6 (C-1, C-16), 20.5, 19.9* (C-25), 17.7 (C-19), 16.1 (C-18), 11.8, 11.7* (C-17).

#### 3.3.2. 2,6,10,14-Tetramethyl-7-(3-methylenepent-4-enyl) pentadec-5,9-diene (XIV)

*3.3.2.1. $^1H$ NMR (270 MHz).* $\delta$ 6.33 (dd, $J$=10.7, 17.7 Hz, H-23), 5.20–4.99 (m, H-5, H-9, H-24), 4.95 (br, s, H-25), 2.2–1.9 (m, H-4, H-7, H-8, H-11, H-21), 1.6–1.1 (m, H-2, H-3, H-12, H-13, H-14, H-20), 1.54 (s, H-18), 1.47 (s, H-17), 0.86, 0.84 (2×d, $J$=6.6 Hz, H-1, H-15, H-16, H-19).

*3.3.2.2. $^{13}C$ NMR (67.8 MHz).* $\delta$ 146.9 (C-22), 139.1 (C-23), 135.9 (C-10), 135.4 (C-6), 126.6 (C-5), 123.1 (C-9), 115.4 (C-25), 113.1 (C-24), 49.4 (C-7), 39.9 (C-11), 39.0 (C-3), 38.5 (C-13), 32.2 (C-8), 31.3 (C-21), 29.4 (C-20), 27.9 and 27.5 (C-2, C-14), 25.7 (C-12), 25.5 (C-4), 22.7 and 22.6 (C-1, C-15, C-16, C-19), 16.0 (C-18), 11.9 (C-17).

#### 3.3.3. 2,6,14-Trimethyl-10-methylene-9-(3-methylenepent-4-enyl)pentadec-6-diene (XV)

*3.3.3.1. $^1H$ NMR (270 MHz).* $\delta$ 6.33 (dd, $J$=10.7, 17.7 Hz, H-23), 5.20–4.99 (m, H-9, H-24), 4.95 (br, s, H-25), 4.78 (br, d, H-17a), 4.74 (br, s, H-17b), 2.2–1.9 (m, H-5, H-7, H-8, H-11, H-21), 1.6- 1.1 (m, H-2, H-3, H-4, H-12, H-13, H-14, H-20), 1.54 (s, H-18), 0.86, 0.84 (2×d, $J$=6.6 Hz, H-1, H-15, H-16, H-19).

*3.3.3.2. $^{13}C$ NMR (67.8 MHz).* $\delta$ 152.2 (C-6), 146.8 (C-22), 139.0 (C-23), 135.8 (C-10), 122.9 (C-9), 115.3 (C-25), 113.0 (C-24), 108.9 (C-17), 46.6 (C-7), 39.9 (C-11), 38.9 (C-3), 38.5 (C-13), 33.8 (C-5), 32.8 (C-8), 31.8 (C-21), 29.2 (C-20), 28.0 (C-14), 27.9 (C-2), 25.7 (C-12), 25.5 (C-4), 22.7 and 22.6 (C-1, C-15, C-16, C-19), 16.0 (C-18).

### 3.4. Chromatography

GC–MS was performed using a Hewlett Packard 5890 series II gas chromatograph coupled to a Hewlett Packard 5970 mass selective detector fitted with fused

silica capillary columns (12 m (0.2 mm i.d.) HP-1 and 25 m (0.2 mm i.d.) HP-5 Ultra stationary phases; 15 m (0.32 mm i.d.) DB-WAX stationary phase). Autosplitless injection and helium carrier gas were used. The gas chromatograph oven temperature was programmed from 40 to 300°C at 5°C $min^{-1}$ (HP-1, HP-5) and 40 to 200° at 5°C $min^{-1}$ (DB-WAX) and held at the final temperature for 5–10 min. Mass spectrometer operating conditions were: ion source temperature 250° and 70 eV ionisation energy. Spectra (35–500 Daltons) were collected using Hewlett Packard Chemstation™ software.

## Acknowledgements

We thank the University of Plymouth for research funds and the British Council for an Alliance travel grant.

## References

Belt, S.T., Cooke, D.A., Robert, J.-M., Rowland, S., 1996. Structural characterisation of widespread polyunsturated isoprenoid biomarkers: a $C_{25}$ triene, tetraene and pentaene from the diatom *Haslea ostrearia* Simonsen. Tetrahedron Letters 37, 4755–4758.

Belt, S.T., Allard, W.G., Rintatalo, J., Johns, L.A., van Duin, A.C.T., Rowland, S.J., 2000a. Clay and acid catalysed isomerisation and cyclisation reactions of highly branched isoprenoid (HBI) alkenes: implications for sedimentary reactions and distributions. Geochimica et Cosmochimica Acta 64, 3337–3345.

Belt, S.T., Allard, G., Robert, J.-M., Massé, G., Rowland, S.J., 2000b. Important sedimentary sesterterpenoids from the diatom *Pleurosigma intermedium*. Chemical Communications 501–502.

Belt, S.T., Allard, G., Robert, J.-M., Massé, G., Rowland, S.J., 2000c. Highly branched isoprenoids (HBIs): Identification of the most common and abundant sedimentary isomers. Geochimica et Cosmochimica Acta 64, 3839–3851.

Johns, L., Belt, S.T., Lewis, C.A., Rowland, S., Massé, G., Robert, J.-M., König, W., 2000. Configurations of polyunsaturated sesterterpenoids from the diatom, *Haslea ostrearia*. Phytochemistry 53, 607–611.

Johns, L., Wraige, E.J., Belt, S.T., Lewis, C.A., Massé, G., Robert, J-M., Rowland, S.J., 1999. Identification of $C_{25}$ highly branched isoprenoid (HBI) dienes in Antarctic sediments, sea-ice diatoms and laboratory cultures of diatoms. Organic Geochemistry 30, 1471–1475.

Kohnen, M.E.L., Sinninghe Damsté, J.S., Kock van-Dalen, A.C., ten Haven, H.L., Rullkötter, J., de Leeuw, J.W., 1990. Origin and diagenetic transformations of $C_{25}$ and $C_{30}$ highly branched isoprenoid sulphur: Further evidence for the formation of organically bound sulphur during early diagenesis. Geochimica et Cosmochimica Acta. 54, 3053–3063.

Massé, G., Rincé, Y., Cox, E.J., Allard, G., Belt, S.T. & Rowland, S.J., 2000. *Haslea saltstonica* sp. nov. and *Haslea pseudostrearia* sp. nov., two new marine diatoms from the Kingsbridge estuary, Devon, UK. Comptes rendu de l'Academie des Sciences, in press.

Robson, J.N., Rowland, S.J., 1986. Identification of novel widely distributed sedimentary acyclic sesterterpenoids. Nature 324, 561–563.

Rowland, S.J., Belt, S.T., Wraige, E.J., Massé, G., Roussakis, C., Robert, J.-M., 2001. Effects of temperature on polyunsaturation in cytostatic lipids of *Haslea ostrearia*. Phytochemistry 56, 597–602.

Rowland, S.J., Robson, J.N., 1990. The widespread occurrence of highly branched acyclic $C_{20}$, $C_{25}$ and $C_{30}$ hydrocarbons in recent sediments and biota — a review. Marine Environmental Research 30, 191–216.

Simonsen, S., 1974. The Diatom plankton of the Indian Ocean expedition of R.V. "Meteor". In: Reihe, D. (Ed.), Forschungsergebnisse. Gebrüder Borntraegier, Berlin, pp. 1–66.

Sinninghe Damsté, J.S., van Koert, E.R., Kock-van Dalen, A.C., deLeeuw, J.W., Schenk, P.A., 1989. Characterisation of highly branched isoprenoid thiophenes occurring in sediments and immature crude oils. Organic Geochemistry 15, 555–567.

Sinninghe Damsté, J.S., Schouten, S., Rijpstra, W.I.C., Hopmans, E.C., Peletier, H, Gieskes, W.W.C., Geenevasen, J.A.J., 1999. Structural identification of the $C_{25}$ highly branched isoprenoid pentaene in the marine diatom *Rhizosolenia setigera*. Organic Geochemistry 30, 1581–1583.

Volkman, J.K., Barrett, S.M., Dunstan, G.A., 1994. $C_{25}$ and $C_{30}$ highly branched isoprenoid alkenes in laboratory cultures of two marine diatoms. Organic Geochemistry 21, 407–414.

Von Stosch, H.A., 1985. Some marine diatoms from the Australian region, especially from Port Phillip Bay and tropical North-eastern Australia. Brunonia 8, 293–348.

Wraige, E.J., Belt, S.T., Lewis, C.A., Cooke, D.A., Robert, J.-M., Massé, G., Rowland, S.J., 1997. Variations in structures and distributions of $C_{25}$ highly branched isoprenoid (HBI) alkenes in cultures of the diatom, *Haslea ostrearia* (Simonsen). Organic Geochemistry 27, 497–505.

Wraige, E.J., Belt, S.T., Massé, G., Robert, J.-M., Rowland, S.J., 1998. Variations in distributions of $C_{25}$ highly branched isoprenoid (HBI) alkenes in the diatom, *Haslea ostrearia* : influence of salinity. Organic Geochemistry 28, 855–859.

Wraige, E.J., Johns, L., Belt, S.J., Massé, G., Robert, J.-M., Rowland, S.J., 1999. Highly branched $C_{25}$ isoprenoids in axenic cultures of *Haslea ostrearia*. Phytochemistry 51, 69–73.

PERGAMON

Organic Geochemistry 32 (2001) 1169–1172

Organic Geochemistry

www.elsevier.com/locate/orggeochem

Note

# Identification of a $C_{25}$ highly branched isoprenoid triene in the freshwater diatom *Navicula sclesvicensis*

Simon T. Belt[a,*], Guillaume Massé[a,b], W. Guy Allard[a], Jean-Michel Robert[b], Steven J. Rowland[a]

[a] *Petroleum and Environmental Geochemistry Group, Department of Environmental Sciences, University of Plymouth, Drake Circus, Plymouth, PL4 8AA, Devon, UK*

[b] *ISOMer, Faculté des Sciences et des Techniques, Université de Nantes, 2 Rue de la Houssinière, 44027 Nantes Cedex 3, France*

Received 27 April 2001; accepted 30 July 2001
(returned to author for revision 29 May 2001)

Abstract

The first example of a freshwater diatom species that biosynthesises the widespread organic geochemicals known as highly branched isoprenoids (HBIs) is identified. As a result, diatoms known to produce HBIs now include benthic, planktonic, marine and freshwater species. Laboratory cultures of a number of freshwater diatoms isolated from Swanpool, UK and Paimpont, France were examined for highly branched isoprenoid (HBI) alkenes. A $C_{25}$ HBI triene was identified in *Navicula sclesvicensis*, and characterised using GC–MS, by comparison with an authentic standard.


*Keywords:* HBI; Alkenes; *Navicula sclesvicensis*; Freshwater diatoms; Swanpool; Isoprenoid

## 1. Introduction

$C_{25}$ and $C_{30}$ highly branched isoprenoid (HBI) alkenes are abundant organic geochemicals found in sediments and oils (for a review see Rowland and Robson, 1990). Following the discovery (Volkman et al., 1994; Sinninghe Damsté et al., 1999) that these compounds can be biosynthesised by the marine diatoms *Haslea ostrearia* ($C_{25}$ HBIs) and *Rhizosolenia setigera* ($C_{25}$ or $C_{30}$ HBIs), we and others have reported the structures of many of the $C_{25}$ alkenes from these two species (Belt et al., 1996; Johns et al., 1999; Sinninghe Damsté et al., 1999; Wraige et al., 1997, 1999). More recently, we have elucidated the structures of a number of HBI alkenes obtained from a third species of diatom (viz. *Pleurosigma intermedium*) and shown that these compounds correspond to the most abundant and widespread isomers found in sediments (Belt et al., 2000a,b). Representative structures are shown in Fig. 1 which illustrates some of the most common isomeric forms observed for HBI alkenes.

However, in contrast to the numerous reports of HBI alkenes in marine sediments, there have been relatively few reports of such compounds in lacustrine environments (Rowland and Robson, 1990). This may be due to a reduced number of source organisms present in lakes or simply a paucity of study with regards their hydrocarbon geochemistry. In this report, we describe the detection of the $C_{25}$ triene **III** in the diatom *Navicula sclesvicensis* which was isolated from Swanpool, a freshwater lake in the UK. Analysis of a number of other freshwater species isolated from Swanpool and Paimpont (a freshwater lake in Brittany, France) failed to yield any HBI alkenes in detectable quantities.

## 2. Experimental

### 2.1. Isolation and characterisation of freshwater diatoms

Phytoplankton samples were collected using a 75 μm net from the sub-surface waters of the lakes of Paimpont, Brittany (France) and Swanpool, Cornwall (UK) in September and November 2000, respectively. For both locations, the salinity was below the limit of

* Corresponding author. Fax: +44-1752-233035.
*E-mail address:* sbelt@plymouth.ac.uk (S.T. Belt).

0146-6380/01/$ - see front matter 
PII: S0146-6380(01)00102-4

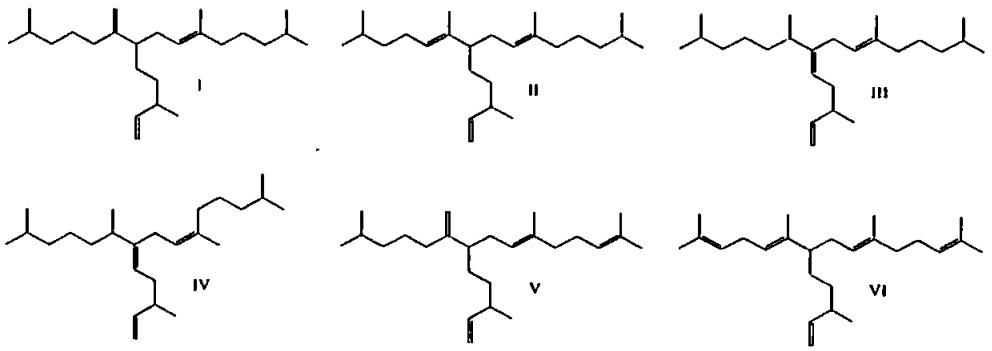


Fig. 1. Representative structures of $C_{25}$ HBI alkenes reported in diatoms and sediments.

detection (<0.1‰). Identification of individual diatom species in the samples was achieved using light and electron microscopy (Hendey, 1974; Massé et al., 2001).

Species isolated were identified as: Swanpool: *Navicula sclesvicensis* (Grunow) Lange-Berthalot (van Heurck, 1885; Germain, 1936, 1981; Lange-Berthalot, 1980); *Navicula gracilis* Ehrenberg and *Synedra tabulata* Agardh (Germain, 1981). Paimpont: *Asterionella Formosa* Hassal, *Melosira italica* (Ehrenberg) Ralfs and *Tabellaria fenestrata* (lygnbye) Kütz (Germain, 1981).

### 2.2. Identification of non-saponifiable lipids

Laboratory scale cultures of all six diatom species were grown in nutrient enriched freshwater CHU 10 medium (Stein, 1973) in 250 ml Erlenmeyer flasks at 15 °C with illumination provided by cool-white fluorescent tubes in a 14/10 h light/dark cycle (100 μmol photons $m^{-2}$ $s^{-1}$). The salinity was <0.1‰ in all cases. After 15 days, cells were harvested, extracted and analyses were made of the non-saponifiable lipid fractions by GC–MS as previously described (see e.g. Wraige et al., 1997, 1999; Johns et al., 1999). Individual compounds were identified on the basis of their retention indices (RIs), mass spectra and/or by co-injection with an authentic standard on HP-1 and Carbowax stationary phases.

## 3. Results and discussion

### 3.1. Identification of $C_{25:3}$ III in N. sclesvicensis

Following laboratory scale culture of *N. sclesvicensis*, the non-saponifiable lipid fractions obtained from this species were analysed by GC and GC–MS. Fig. 2 shows a representative partial total ion current (TIC) chromatogram corresponding to a single culture which illustrates the presence of *n*-$C_{21:6}$, hexadecanoic acid and phytol (characterised as trimethylsilyl ethers) and a further component whose chromatographic properties and mass spectrum ($M^+$ 346) are consistent with a HBI triene. Closer examination of these features suggested that this HBI was triene **III** previously identified in cultures of *P. intermedium* (Belt et al., 2000b). Notably, the RI found for this isomer (RI 2087 $_{HP\text{-}1}$) is lower than that found for either of **I** or **II** which are isomeric trienes found in *H. ostrearia* and related species (Belt et al., 1996; Wraige et al., 1999; Allard et al., 2001), while the mass spectrum contains characteristic ions (and relative intensities) at *m/z* 83, 233 and 261 (Belt et al., 2000b). HBI **III** can be readily distinguished from its geometric isomer **IV** since the latter has a significantly lower RI (RI 2042 $_{HP\text{-}1}$). In order for this assignment to be confirmed, the triene from *N. sclesvicensis* was co-injected with a mixture of authentic **III** and **IV** obtained from a large scale culture of *P. intermedium* (Belt et al., 2000a,b) on two GC phases (HP-1 and Carbowax) and co-elution with **III** was observed in both cases. Thus, the identification of the single HBI found in *N. sclesvicensis* as **III** is established. Ideally culturing of the organism on a larger scale will allow sufficient quantities of this alkene to be obtained for a rigorous identification by NMR spectroscopy (cf. Belt et al., 2000a,b and references therein; Sinninghe Damsté et al., 1999).

Interestingly, only one geometric isomer of the $C_{25}$ triene was detected (viz. *E* at C9-C10) even though both *E* and *Z* isomers (**III** and **IV**) are produced by *P. intermedium* (Belt et al., 2000b). *Pleurosigma intermedium* also biosynthesises $C_{25}$ HBI tetraenes and pentaenes though these too were undetected in the cultures of *N. sclesvicensis* analysed. In addition, we found no evidence for the formation of HBI isomers normally associated with *H. ostrearia* (e.g. **I**, **II**, **V** and **VI**) despite the similarities between the *Navicula* and *Haslea* genera (Simonsen, 1974).

*Navicula sclesvicensis* has been found in many different types of habitat from rivers to slightly brackish waters. It has also been linked with *N. lanceolata*, *N. viridula* (and a variety *rostellata*) to form a distinct group within the *Navicula* genus (Germain, 1981) though these species were not detected in either of Swanpool or Paimpont during the present study.

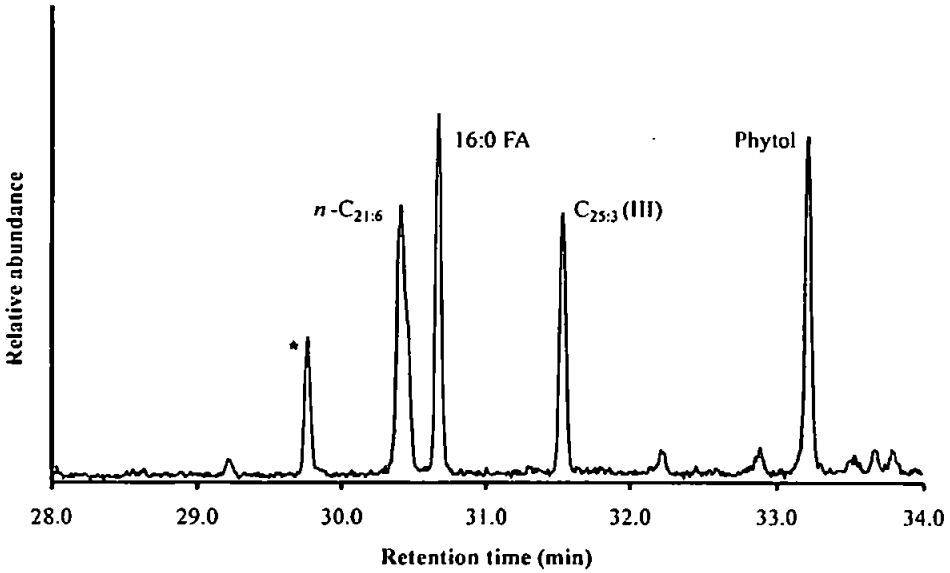


Fig. 2. Partial GC–MS total ion chromatogram of a non-saponifiable lipid fraction obtained from a culture of *Navicula sclesvicensis*. Phytol and hexadecanoic acid (16:0 FA) are present as trimethylsilyl ethers. The peak labelled * is due to an unidentified impurity.

### 3.2. Analysis of other freshwater diatoms

The non-saponifiable lipid fractions for five other species (see Section 2.1) were also examined by GC–MS. *Tabellaria fenestrata* failed to yield any readily characterisable components, while the other four species produced *n*-$C_{21:6}$ and phytol in different relative amounts. In all cases, no peaks due to HBI alkenes including **III** could be detected. Given the presence of the triene **III** in *N. sclesvicensis*, it seemed surprising initially that HBIs were not detected in the related species, *Navicula gracilis*. Indeed, we have recently reported the occurrence of a number of $C_{25}$ HBI alkenes from species within the *Haslea* genus (Allard et al., 2001), and the pseudohomologous $C_{30}$ HBIs have been detected in both *R. setigera* (Volkman et al., 1994, 1998) and *Rhizosolenia fallax* (Massé, personal communication). However, since the *Navicula* genus is distinctly heterogeneous, our observations may not be too surprising and there are other cases where the general trend between a genus and HBI production is not always observed. For example, $C_{25}$ HBIs were absent from cultures containing a *Navicula* species (Volkman et al., 1994) and we have failed to detect HBIs in *Pleurosigma angulatum* and *Haslea wawrikae* (Belt et al., unpublished). In future, it may be of interest to examine the hydrocarbon content of *Navicula* species that are more closely related to *N. sclesvicensis* (vide infra).

Although HBI triene **III** was readily detected in *N. sclesvicensis*, none of the diatoms in the current study yielded $C_{20}$ HBIs despite reports of the co-occurrence of $C_{20}$ and $C_{25}$ alkenes and the parent alkanes in several lakes in the UK (see Rowland and Robson, 1990 and references therein) including Grasmere (Yon, 1981) and Rostherne Mere (Rowland, 1982).

It may be significant that alkene **III** found in *N. sclesvicensis* corresponds to what is probably the most widely occurring isomer found in sediments and biota (see e.g. Belt et al., 2000b for a review). Thus, the source of this compound is not limited to a single species of diatom (viz. *P. intermedium*) and there are probably other diatom producers, including planktonic species, as triene **III** has also been detected in particulate matter in the water column (see e.g. Prahl et al., 1980; Osterroht et al., 1983; Volkman et al., 1983; Albaigés et al., 1984; Bates et al., 1984; Matsueda and Handa, 1986; Wakeham 1990) and *P. intermedium* and *N. sclesvicensis* are both benthic species.

## 4. Conclusions

The $C_{25}$ triene **III**, which is probably the most abundant and widely occurring HBI alkene observed in marine sediments and HBI-producing marine diatoms has now also been identified in the freshwater diatom *N. sclesvicensis*. As a result, the number of diatoms known to be capable of producing HBIs is now known to include benthic, planktonic, marine and freshwater species. This diversification in terms of species undoubtedly contributes to the widespread occurrence of these hydrocarbon alkenes.

**Acknowledgements**

We would like to thank the University of Plymouth, UK and the Region des Pays de la Loire, France for research funds and to the Royal Society of Chemistry, UK, for a JWT Jones Travelling Fellowship to S.T.B.

*Associate Editor*—A.G. Douglas

**References**

Albaigés, J., Grimalt, J., Bayona, J.M., Riseborough, R.W., de Lappe, B., Walker II, W., 1984. Dissolved, particulate and sedimentary hydrocarbons in a deltaic environment. In: Schenk, P. A., de Leeuw, J. W., Lijmbach, G. W. M. (Eds.). Advances in Organic Geochemistry 1983, Pergamon, Oxford. Organic Geochemistry 6, 237–248.

Allard, W.G., Belt, S.T., Massé, G., Naumann, R., Robert, J.-M., Rowland, S., 2001. Tetra-unsaturated sesterterpenoids (Haslenes) from *Haslea ostrearia* and related species. Phytochemistry 56, 795–800.

Bates, T.S., Hamilton, S.E., Cline, J.D., 1984. Vertical transport and sedimentation of hydrocarbons in the central main basin of Puget Sound, Washington. Environmental Science and Technology 18, 299–305.

Belt, S.T., Cooke, D.A., Robert, J.-M., Rowland, S.J., 1996. Structural characterisation of widespread polyunsturated isoprenoid biomarkers: a $C_{25}$ triene, tetraene and pentaene from the diatom *Haslea ostrearia* Simonsen. Tetrahedron Letters 37, 4755–4758.

Belt, S.T., Allard, G., Massé, G., Robert, J.-M., Rowland, S., 2000a. Important sedimentary sesterterpenoids from the diatom *Pleurosigma intermedium*. Chemical Communications 501–502.

Belt, S.T., Allard, W.G., Massé, G., Robert, J.-M., Rowland, S.J., 2000b. Highly branched isoprenoids (HBIs): identification of the most common and abundant sedimentary isomers. Geochimica et Cosmochimica Acta 64, 3839–3851.

Germain, H., 1936. Les lieux de développement et de muliplication des diatomées d'eau douce. Contribution à l'écologie des diatomées. Bullelin des Sciences Naturelles de l'Ouest, Fifth Series, No. 6. Nantes, pp. 1–200.

Germain, H., 1981. Flore des Diatomees: eaux douches et saumatres. pp. 1–444. Paris.

Hendey, N.I., 1974. The permanganate method for cleaning freshly gathered diatoms. Microscopy 32, 423–426.

Johns, L., Wraige, E.J., Belt, S.T., Lewis, C.A., Massé, G., Robert, J.-M., Rowland, S.J., 1999. Identification of $C_{25}$ highly branched isoprenoid (HBI) dienes in Antarctic sediments, sea-ice diatoms and laboratory cultures of diatoms. Organic Geochemistry 30, 1471–1475.

Lange-Bertelot, H., 1980. Zur taxonomischen Revision einiger ökologisch wichtiger *Naviculae lineolatae* Cleve. Die Formenkreise um *Navicula lanceolata*, *N. viridula*, *N. cari*. Cryptogamie Algologie 1, 29–50.

Massé, G., Rincé, Y., Cox, E.J., Allard, G., Belt, S.T., Rowland, S.J., 2001. *Haslea salstonica* sp. nov. and *Haslea pseudostrearia* sp. nov. (Bacillariophyta), two new epibenthic diatoms from the Kingsbridge estuary, United Kingdom. Comptes Rendu Academie des Sciences de la vie/Life Sciences 324, 617–626.

Matsueda, M., Handa, N., 1986. Vertical flux of hydrocarbons as measured in sediment traps in the eastern North Pacific Ocean. Marine Chemistry 20, 179–182.

Osterroht, C., Petrick, G., Wenck, A., 1983. Seasonal variation of particulate hydrocarbons in relation to biological parameters. Marine Chemistry 14, 175–194.

Prahl, F.G., Bennett, T.J., Carpenter, R., 1980. The early diagenesis of aliphatic hydrocarbons and organic matter in sedimentary particles from Dabob Bay, Washington. Geochimica et Cosmochimica Acta 44, 1967–1976.

Rowland, S.J., 1982. Origins and Fate of Sedimentary Acyclic Isoprenoids. PhD thesis, University of Bristol.

Rowland, S.J., Robson, J.N., 1990. The widespread occurrence of highly branched acyclic $C_{20}$, $C_{25}$ and $C_{30}$ hydrocarbons in recent sediments and biota—a review. Marine Environmental Research 30, 191–216.

Simonsen, R., 1974. The diatom plankton of the Indian Ocean expedition of R.V. "Meteor". In: Reihe, D. (Ed.), Forschungsergebnisse. 19. Gebruder Borntraeger, Berlin, pp. 1–66.

Sinninghe Damsté, J.S., Schouten, S., Rijpstra, W.I.C., Hopmans, E.C., Peletier, H., Gieskes, W.W.C., Geenevasen, J.A.J., 1999. Structural identification of the $C_{25}$ highly branched isoprenoid pentaene in the marine diatom *Rhizosolenia setigera*. Organic Geochemistry 30, 1581–1583.

Stein, J. (Ed.), 1973. Handbook of Phycological Methods. Culture Methods and Growth Measurements. Cambridge University Press. pp. 1–448.

van Heurck, H.C., 1885. Synopsis des Diatomées de Belgique, pp. 1–235. Anvers.

Volkman, J.K., Farrington, J.W., Gagosian, R.B., Wakeham, S.G., 1983. Lipid composition of coastal marine sediments from the Peru upwelling region. In: Bjoroy, M. et al. (Eds.), Advances in Organic Geochemistry 1981. Wiley, Chichester, UK, pp. 228–240.

Volkman, J.K., Barratt, S.M., Dunstan, G.A., 1994. $C_{25}$ and $C_{30}$ highly branched isoprenoid alkenes in laboratory cultures of two marine diatoms. Organic Geochemistry 21, 407–414.

Volkman, J.K., Barratt, S.M., Blackburn, S.I., Mansour, M.P., Sikes, E.L., Gelin, F., 1998. Microalgal biomarkers: a review of recent research developments. Organic Geochemistry 29, 1163–1179.

Wakeham, S.G., 1990. Algal and bacterial hydrocarbons in particulate matter and interfacial sediment of the Cariaco Trench. Geochimica et Cosmochimica Acta 54, 1325–1336.

Wraige, E.J., Belt, S.T., Lewis, C.A., Cooke, D.A., Robert, J.-M., Massé, G., Rowland, S.J., 1997. Variations in structures and distributions of $C_{25}$ highly branched isoprenoid (HBI) alkenes in cultures of the diatom, *Haslea ostrearia* (Simonsen). Organic Geochemistry 27, 497–505.

Wraige, E.J., Johns, L., Belt, S.T., Massé, G., Robert, J.-M., Rowland, S., 1999. Highly branched $C_{25}$ isoprenoids in axenic cultures of *Haslea ostrearia*. Phytochemistry 51, 69–73.

Yon, D.A., 1981. Structural, Synthetic and Stereochemical Studies of Sedimentary Isoprenoid Compounds. PhD thesis, University of Bristol.

PERGAMON

Organic Geochemistry 32 (2001) 1271–1275

Organic Geochemistry

www.elsevier.com/locate/orggeochem

Note

# $C_{25}$ highly branched isoprenoid alkenes in planktonic diatoms of the *Pleurosigma* genus

Simon T. Belt[a,*], Guillaume Massé[a,b], W. Guy Allard[a], Jean-Michel Robert[b], Steven J. Rowland[a]

[a] *Petroleum and Environmental Geochemistry Group, Department of Environmental Sciences, University of Plymouth, Drake Circus, Plymouth, PL4 8AA, Devon, UK*

[b] *Faculté des Sciences et des Techniques, Université de Nantes, 2 Rue de la Houssinière, 44027 Nantes Cedex 3, France*

Received 30 July 2001; accepted 20 August 2001
(returned to author for revision 7 August 2001)

**Abstract**

The $C_{25}$ highly branched alkenes which have been widely reported in coastal and deep sea marine sediments and sedimenting particles have to date only been detected in benthic diatoms. Logically, a planktonic organism would be a much more likely source for the HBIs found in deep sea environments. Here we report the structures of $C_{25}$ HBI alkenes isolated from two planktonic diatoms belonging to the *Pleurosigma* genus. The HBI structures have been determined using NMR and mass spectral techniques. The HBIs from *Pleurosigma* sp. were identical to those found in many deep sea marine samples whereas those of *P. planktonicum* consisted of two isomeric tetraenes whose structures are novel and which are reported here for the first time. 

*Keywords:* HBI alkenes; *Pleurosigma planktonicum*; Diatoms; Tetraenes; Plankton

## 1. Introduction

In two recent reports, we described the structures (e.g. Fig. 1) of the most common and abundant sedimentary isomers of $C_{25}$ highly branched isoprenoid (HBI) alkenes, which are widely distributed in recent coastal marine sediments. This was achieved by comparison of the gas chromatographic (GC) and mass spectral (MS) features of the sedimentary compounds which those of $C_{25}$ alkenes isolated from the benthic diatom, *Pleurosigma intermedium* which were characterised by nuclear magnetic resonance (NMR) spectroscopy (Belt et al., 2000a,b).

However, since HBI alkenes have been widely reported from water column particles (e.g. Prahl et al., 1980; Osterroht et al., 1983; Volkman et al., 1983; Albaigés et al., 1984; Bates et al., 1984; Matsueda and Handa, 1986; Wakeham, 1990) from as far afield as Dabob Bay, Washington, USA, the Peru Upwelling zone, the Ebro Delta, Spain, and the eastern North Pacific Ocean, it seems unlikely that benthic diatoms such as *P. intermedium* and *Haslea ostrearia* (Volkman et al., 1994) are a major source of $C_{25}$ HBIs in deep sea marine environments. Whilst *Rhizosolenia setigera* is also a planktonic diatom producer of HBI alkenes, this organism produces either an uncommon $C_{25}$ pentaene (Sinninghe Damsté et al., 1999) or both $C_{25}$ and $C_{30}$ HBIs depending on the particular strain (Rowland et al., in press). Thus, *R. setigera* is probably not the sole source of $C_{25}$ HBIs in the deep sea. We have therefore examined two planktonic diatom species of the *Pleurosigma* genus for HBI alkenes. Significantly, one of these (*Pleurosigma* sp.) produced $C_{25}$ tetraenes and pentaenes identical to those previously found in suspended particles and sediments, whilst another (*Pleurosigma planktonicum*) produced novel and isomeric $C_{25}$ tetraenes.

* Corresponding author. Tel.: +44-1752-233042; fax: +44-1752-233035.
*E-mail address:* sbelt@plymouth.ac.uk (S.T. Belt).

0146-6380/01/$ - see front matter 
PII: S0146-6380(01)00111-5

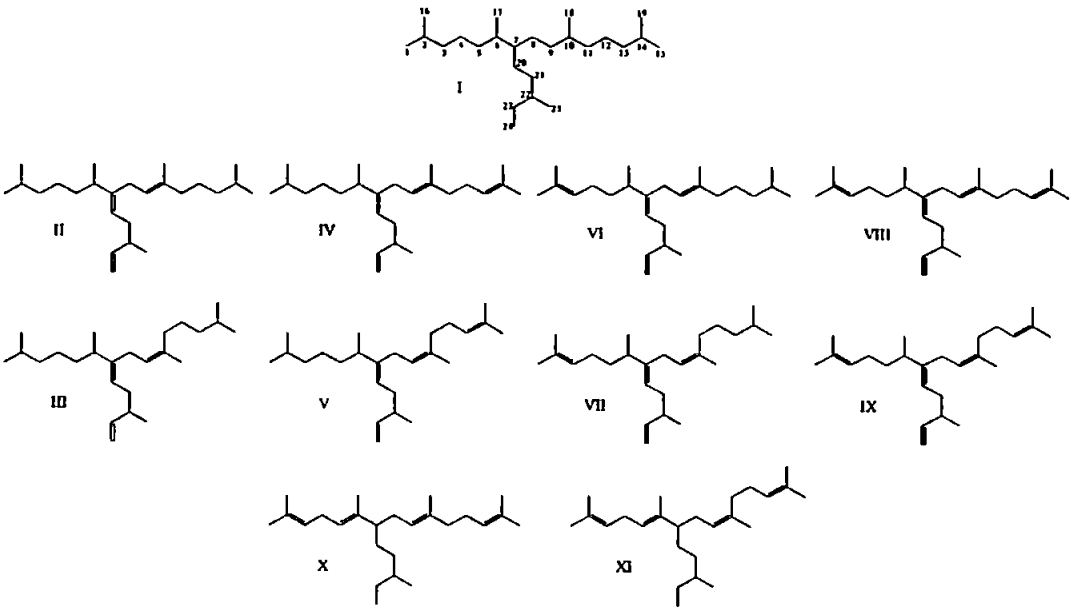


Fig. 1. Structures of $C_{25}$ HBI alkenes described in the present study. The parent alkane $C_{25:0}$ (including numbering scheme) is also shown.

## 2. Experimental

### 2.1. Identification of diatom species

*P. planktonicum* and *Pleurosigma.* sp. were isolated from phytoplankton collected from surface waters at Le Croisic, France (25/03/2000) and characterised using light and electron microscopy (Hendey, 1974). The literature description of *P. planktonicum* is detailed (Simonsen, 1974; Boalch and Harbour, 1977), allowing an unambiguous assignment to be made. For the second species, the extremely delicate striation suggests that it may be *Pleurosigma subhyalinum* (Hustedt and Aleem, 1951). However, since the structural definition of *P. subhyalinum* is rather limited, we prefer to use the designation *Pleurosigma* sp. In any case, from the location of its isolation and primary structural features (sigmoidal valves; oblique striae), we can confidently consider this species to be a planktonic member of the *Pleurosigma* genus.

### 2.2. Identification of $C_{25}$ HBIs

Laboratory (14 °C, 14/10 light/dark light cycle) and large-scale (ambient temperature, light) cultures of each species were grown in seawater enriched with F/2 Guillard medium according to published methods (Wraige et al., 1997). Isolation of cells (end of exponential growth phase; 10–15 days) together with extraction, purification and analysis of the non-saponifiable lipid fractions obtained from each species was as previously described (e.g. Wraige et al., 1997). Individual compounds were identified on the basis of their published GC retention indices (RIs), mass spectra, NMR spectra (see Appendix) and/or by co-injection (GC) with authentic standards on a HP-1 stationary phase. $^{1}H$ and $^{13}C$ NMR analyses were carried out on $CDCl_3$ solutions using a Jeol EX-270 spectrometer.

## 3. Results and discussion

### 3.1. A planktonic source of HBI alkenes

Cultures of *Pleurosigma* sp. contained $C_{25}$ HBIs previously reported in *P. intermedium*. The compounds had identical mass spectra and GC retention indices to those well-characterised isomers. However, the number and relative abundances of the different HBIs was found to change between cultures. Thus, in one culture, pentaenes VIII and IX were abundant, with tetraenes IV–VII as minor components (Fig. 2a), while in a second culture, IV and V were the only detectable tetraenes, and these were in concentrations comparable to those of the pentaenes VIII and IX (Fig. 2b). These differences, together with the absence of the pseudo-structural trienes (II and III), despite the presence of these compounds in cultures of *P. intermedium* (Belt et al., 2000a,b), may be due to subtle phenotypic controls or (in the case of the trienes) simply reflect intra-species

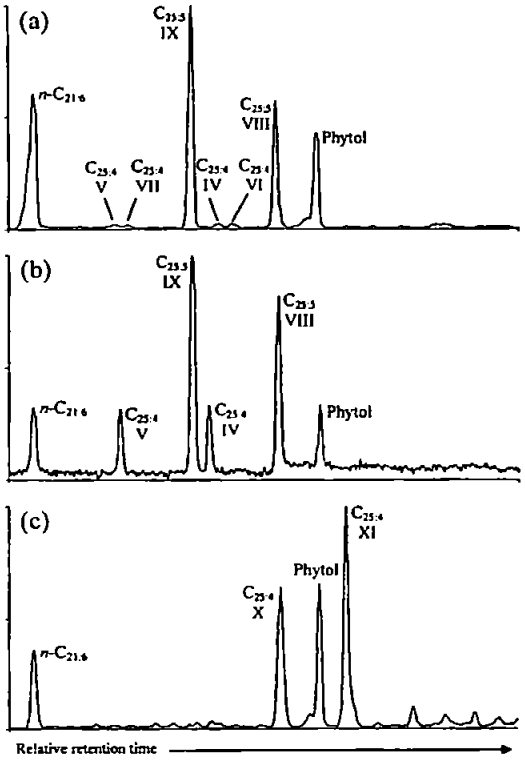


Fig. 2. Partial total ion current (TIC) chromatograms of the non-saponifiable lipid fractions obtained from cultures of (a) and (b) *Pleurosigma* sp; (c) *Pleurosigma planktonicum*. Phytol is present as its TMS ether.

effects. These will require further investigation before e.g. correlations with distributions in the water column or sediments can be made. In any case, it is clear that a planktonic source of widely occurring $C_{25}$ HBI alkenes has been identified.

### 3.2. Novel HBI alkenes in *Pleurosigma planktonicum*

Large scale culture (400 l) of *P. planktonicum*, followed by extraction and purification yielded 6 mg of a mixture of three compounds whose gas chromatographic (RI 2163 and 2198 $_{HP\text{-}1}$) and mass spectral properties ($M^+$ 344) were consistent with the presence of two isomeric $C_{25}$ HBI tetraenes together with a small quantity of $n$-$C_{21:6}$ (Fig. 2c). The mass spectra of the two HBI isomers X and XI (Fig. 3) were indistinguishable indicating a pair of stereoisomers. Although the RI of X (RI 2163 $_{HP\text{-}1}$) was found to be similar to that of pentaene VIII found in *Pleurosigma* sp. and *P. intermedium* (RI 2159 $_{HP\text{-}1}$), the two compounds could be readily distinguished from their mass spectra (Fig. 3; Belt et al., 2000b). Hydrogenation of an aliquot of this mixture ($PtO_2 \cdot 2H_2O$/hexane/$H_2$) resulted in the formation of a compound, identified as the parent hydrocarbon $C_{25:0}$ (I) by comparison of its GC retention index (RI 2110 $_{HP\text{-}1}$) and mass spectrum with that of an authentic standard.

$^1$H NMR analysis of the two HBI tetraenes revealed the presence of tri-substituted double bonds ($\delta$ 5.06 ppm), but surprisingly, the absence of any resonances associated with a vinyl moiety, a structural feature which is common to all other HBI alkenes that have

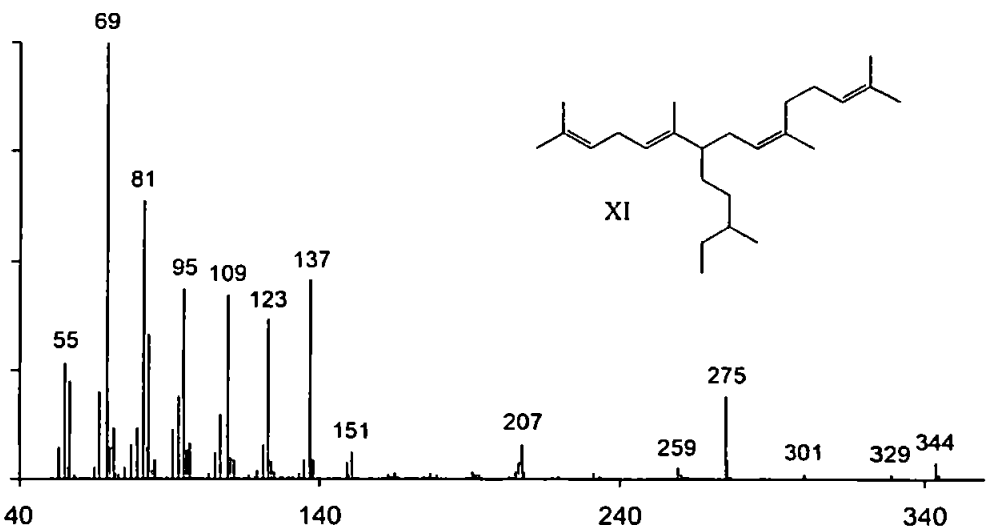


Fig. 3. Mass spectrum of $C_{25}$ HBI tetraene XI (n.b. the spectrum of X is the same as that shown for XI).

been rigorously characterised by NMR spectroscopy (e.g. Belt et al., 1996, 2000a,b; Wraige et al., 1997; Sinninghe Damsté et al., 1999; Allard et al., 2001). $^{13}C$ NMR analysis confirmed this observation with exclusive detection of resonances attributable to tri-substituted alkenes. Further, both $^{1}H$ and $^{13}C$ NMR spectra verified the presence of an ethyl moiety as the terminal group of the main side chain. The absence of isopropyl groups enabled two double bonds to be positioned at C2-C3 and C13-C14 (see I for numbering scheme), while the positions of the other two double bonds could be located by detailed analysis of the NMR spectra and comparison of published data for compounds with related structures.

The appearance of two closely related compounds could be explained by the presence of two geometric isomers (C9–C10), identified by NMR methods described previously (Belt et al., 2000a,b). This included the observation of characteristic resonances ($^{1}H$ and $^{13}C$) associated with (*E* and *Z*) H/C-18. In addition, since the two isomers were present in a ratio ca. 2:1 (*E*:*Z*), the GC elution order was also established (viz. *Z* before *E*). This elution order, together with the difference in RI units between the two isomers ($\Delta RI = 35$), is the same as that found for other HBIs possessing geometric isomerism in the C9-C10 position (Belt et al., 2000a,b). An analogous isomerism is absent for $C_{25}$ HBIs isolated from *Haslea spp.* and *R. setigera* (e.g. Belt et al., 1996; Wraige et al., 1997; Sinninghe Damsté et al., 1999; Allard et al., 2001). Thus, the structures of the two $C_{25}$ HBI tetraenes isolated from *P. planktonicum* have been identified as X and XI.

The geochemical significance of these isomeric tetraenes is unknown at this stage. Although we have been unable to find any reports of these isomers in sediments or in the water column, we note that the unusually high retention indices (for $C_{25}$ HBIs) associated with these compounds (RI 2163 and 2198 $_{HP-1}$) suggests that they may not have been identified as HBIs in previous analyses.

## 4. Conclusions

$C_{25}$ HBI alkenes have been found in two planktonic species of the *Pleurosigma* genus. *P. planktonicum* was found to contain two novel tetraenes whose structures are reported for the first time. In contrast, the HBIs found in a second species, *Pleurosigma* sp., corresponded to some of the most widely occurring isomeric forms reported in deep sea sediments and particles.

## Acknowledgements

We thank the University of Plymouth, UK and the Region des Pays de la Loire, France for research funds and to the Royal Society of Chemistry for a J.W.T. Jones Travelling Fellowship to S.T.B.

*Associate Editor*—A.G. Douglas

## Appendix

$^{1}H$ (270 MHz) and $^{13}C$ (67 MHz) NMR data for X and XI ($CDCl_3$; referenced to residual $CHCl_3$, ($^{1}H$ 7.24 ppm) and $CDCl_3$ ($^{13}C$ 77.0 ppm) respectively).

$^{1}H$: $\delta$ 5.06 (*m*, 4H, H-3,5,9,13), 2.66 (*t*, 2H, $J = 7$ Hz, H-4), 1.99 (*m*, 7H, H-7,8,11,12), 1.67 (*s*, H-1,15,18 (XI)), 1.60, 1.58, 1.55 (C-16,19), 1.54 (*s*, H-18 (X)), 1.46 (*s*, 3H, H-17), 1.04–1.35 (*m*, 7H, H-20,21,22,23), 0.85 (*m*, 6H, H-24,25).

$^{13}C$: $\delta$ 136.7 (C-6 (X)), 136.6 (C-6 (XI)), 135.0 (C-10 (XI)), 134.8 (C-10 (X)), 131. 4 (C-2), 131.2 (C-14), 124.4, 124.3, 124.2 (C-3,5,13), 123.6 (C-9 (X)), 123.5 (C-9 (XI)), 49.4 (C-7 (XI)), 49.2 (C-7 (X)), 39.8 (C-11 (X)), 34.3 (C-22), 34.2 (C-21), 32.4 (C-8 (X)), 32.2 (C-8 (XI)), 31.9 (C-11 (XI)), 30.2 (C-20), 30.0 (C-23), 26.7, 26.8 (C-4,12), 25.6 (C-1,15), 23.4 (C-18 (XI)), 19.1 (C-25), 17.7 (C-16,19), 16.1 (C-18 (X)), 11.9 (C-17 (X)), 11.8 (C-17 (XI)), 11.5 (C-24).

## References

Albaigés, J., Grimalt, J., Bayona, J. M., Risebrough, R., de Lappe, B and Walker II, W. 1984. Dissolved, particulate and sedimentary hydrocarbons in a deltaic environment. In: Schenk, P.A., de Leeuw, J.W., Lijmbach, G.W.M. (Eds.), Advances in Organic Geochemistry 1983. Organic Geochemistry 6, 237-248.

Allard, W.G., Belt, S.T., Massé, G., Naumann, R., Robert, J.-M., Rowland, S., 2001. Tetra-unsaturated sesterterpenoids (Haslenes) from *Haslea ostrearia* and related species. Phytochemistry 56, 795–800.

Bates, T.S., Hamilton, S.E., Cline, J.D., 1984. Vertical transport and sedimentation of hydrocarbons in the central main basin of Puget Sound, Washington. Environmental Science and Technology 18, 299–305.

Belt, S.T., Cooke, D.A., Robert, J.-M., Rowland, S.J., 1996. Structural characterisation of widespread polyunsaturated isoprenoid biomarkers: a $C_{25}$ triene, tetraene and pentaene from the diatom *Haslea ostrearia* Simonsen. Tetrahedron Letters 37, 4755–4758.

Belt, S.T., Allard, G., Massé, G., Robert, J-M., Rowland, S., 2000a. Important sedimentary sesterterpenoids from the diatom *Pleurosigma intermedium*. Chemical Communications 501–502.

Belt, S.T., Allard, W.G., Massé, G., Robert, J.-M., Rowland, S.J., 2000b. Highly branched isoprenoids (HBIs): Identification of the most common and abundant sedimentary isomers. Geochimica et Cosmochimica Acta 64, 3839–3851.

Boalch, G.T., Harbour, D.S., 1977. Observations on the structure of a planktonic *Pleurosigma*. Nova Hedwigia, Beiheft 54, 275–280.

Hendey, N.I., 1974. The permanganate method for cleaning freshly gathered diatoms. Microscopy 32, 423–426.

Hustedt, F., Aleem, A.A., 1951. Littoral diatoms from the Salstone near Plymouth. Journal of the Marine Biological Association, UK 30, 177–196.

Matsueda, M., Handa, N., 1986. Vertical flux of hydrocarbons as measured in sediment traps in the eastern North Pacific Ocean. Marine Chemistry 20, 179–182.

Osterroht, C., Petrick, G., Wenck, A., 1983. Seasonal variation of particulate hydrocarbons in relation to biological parameters. Marine Chemistry 14, 175–194.

Prahl, F.G., Bennett, T.J., Carpenter, R., 1980. The early diagenesis of aliphatic hydrocarbons and organic matter in sedimentary particles from Dabob Bay, Washington. Geochimica et Cosmochimica Acta 44, 1967–1976.

Rowland, S.J., Allard, W.G., Belt, S.T., Massé, G., Robert, J.-M., Blackburn, S, Frampton, D., Revill, A.T., Volkman, J.K. in press. Factors effecting the distributions of polyunsaturated terpenoids in the diatom, *Rhizosolenia setigera*. Phytochemistry.

Simonsen, R., 1974. The Diatom plankton of the Indian Ocean expedition of R.V. "Meteor". In: Reihe, D. (Ed.), Forschungsergebnisse, vol. 19. Gebruder Borntraegier, Berlin, pp. 1–66.

Sinninghe Damsté, J.S., Schouten, S., Rijpstra, W.I.C., Hopmans, E.C., Peletier, H., Gieskes, W.W.C., Geenevasen, J.A.J., 1999. Structural identification of the $C_{25}$ highly branched isoprenoid pentaene in the marine diatom *Rhizosolenia setigera*. Organic Geochemistry 30, 1581–1583.

Volkman, J.K., Farrington, J.W., Gagosian, R.B., Wakeham, S.G., 1983. Lipid composition of coastal marine sediments from the Peru upwelling region. In: Bjorøy, M. et al. (Eds.), Advances in Organic Geochemistry 1981. Wiley, Chichester, UK, pp. 228–240.

Volkman, J.K., Barrett, S.M., Dunstan, G.A., 1994. $C_{25}$ and $C_{30}$ highly branched isoprenoid alkenes in laboratory cultures of two marine diatoms. Organic Geochemistry 21, 407–414.

Wakeham, S.G., 1990. Algal and bacterial hydrocarbons in particulate matter and interfacial sediment of the Cariaco Trench. Geochimica et Cosmochimica Acta 54, 1325–1336.

Wraige, E.J., Belt, S.T., Lewis, C.A., Cooke, D.A., Robert, J.-M., Massé, G., Rowland, S.J., 1997. Variations in structures and distributions of $C_{25}$ highly branched isoprenoid (HBI) alkenes in cultures of the diatom, *Haslea ostrearia* (Simonsen). Organic Geochemistry 27, 497–505.

CHIRALITY 13:415–419 (2001)

# Variable Stereochemistry in Highly Branched Isoprenoids from Diatoms

SIMON T. BELT,[1] W. GUY ALLARD,[1] LESLEY JOHNS,[1] WILFRIED A. KÖNIG,[2] GUILLAUME MASSÉ,[1,3] JEAN-MICHEL ROBERT,[3] AND STEVE ROWLAND[1]

[1]*Department of Environmental Sciences and Plymouth Environmental Research Centre (PERC), University of Plymouth, Drake Circus, UK*

[2]*Institut für Organische Chemie, Universität Hamburg, Hamburg, Germany*

[3]*ISOMer, Faculté de Sciences et des Techniques, Université de Nantes, Nantes, France*

*ABSTRACT* $C_{25}$ highly branched isoprenoid (HBI) alkenes are ubiquitous lipids found in geochemical samples around the globe. The origins of these widespread geochemicals are believed to be restricted to a limited number of diatoms, including *Haslea ostrearia* (and related species), *Rhizosolenia setigera*, and *Pleurosigma intermedium*. The unsaturation of the HBI alkenes ranges from 2–6 in different species and cultures. The number of stereogenic centres is usually limited to two in the HBI alkenes due to double bond positions. The relative and/or absolute configurations for these have been determined for a range of HBI alkenes produced from different diatoms cultured under a number of growth conditions. These determinations have involved a combined spectroscopic and chromatographic analysis using NMR spectroscopy and chiral gas chromatography, respectively. HBIs isolated from *Haslea spp.* belong to a specific structural type which exhibit configurational diastereoisomerism, while those isolated from *P. intermedium* and *R. setigera* represent a different structural type and usually exist as mixtures of geometric isomers only. HBIs are reported from a new species of diatom whose stereochemical properties lie between those found for *Haslea spp.* and *P. intermedium*. *Chirality 13:415–419, 2001.* 

*KEY WORDS:* highly branched isoprenoids; HBIs; diatoms; algae; chiral GC

Pergamon

Tetrahedron Letters 42 (2001) 5583–5585

TETRAHEDRON LETTERS

# Structural characterisation of $C_{30}$ highly branched isoprenoid alkenes (rhizenes) in the marine diatom *Rhizosolenia setigera*

Simon T. Belt,[a,*] W. Guy Allard,[a] Guillaume Massé,[a,b] Jean-Michel Robert[b] and Steven J. Rowland[a]

[a]*Petroleum and Environmental Geochemistry Group, Department of Environmental Sciences, University of Plymouth, Drake Circus, Plymouth PL4 8AA, Devon, UK*

[b]*ISOMer, Faculté des Sciences et des Techniques, Université de Nantes, 2 Rue de la Houssinière, 44027 Nantes Cedex 3, France*

Received 17 April 2001; accepted 14 June 2001

**Abstract**—Highly branched isoprenoid $C_{30}$ penta- and hexaenes have been isolated from the marine diatom *Rhizosolenia setigera* and characterised by NMR spectroscopy. 

$C_{20}$, $C_{25}$ and $C_{30}$ highly branched isoprenoid (HBI) alkenes are widely occurring secondary metabolites that are routinely found in a range of geochemical settings ranging from recent sediments to ancient oils (see Fig. 1 for parent structures).[1] In a number of recent reports, we and others have reported on source organisms for the $C_{25}$ and $C_{30}$ alkenes, though to date, a primary producer for the $C_{20}$ analogues remains elusive.[2–5] Structures of various $C_{25}$ HBIs have been determined using NMR spectroscopy following large scale culture of the source diatoms *Haslea ostrearia* (and related species),[6–12] *Pleurosigma intermedium*[4,5] and *Rhizosolenia setigera*.[3] These compounds exist in a number of isomeric forms exhibiting both geometric and configurational isomerism.[4–6,10,11] In addition, their degrees of unsaturation range from two to six for alkenes isolated from diatoms, while monoenes and the saturated hydrocarbons also exist in sediments and oils.[1] However, there have been no reports on the structures of the pseudo-homologous $C_{30}$ compounds (rhizenes) other than their unsaturation.[2] Here, we describe the structural elucidation of $C_{30}$ HBI penta- and hexaenes ($C_{30:5}$ and $C_{30:6}$) following large scale culture of the marine diatom *R. setigera* (Fig. 2).

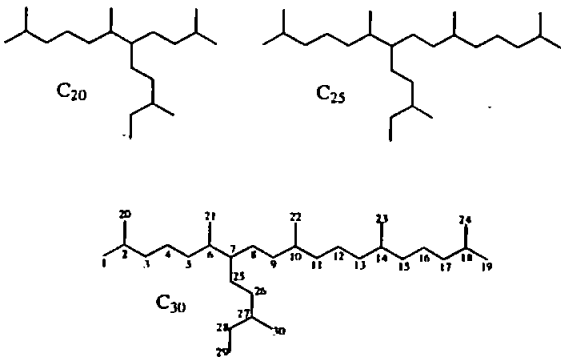


Figure 1. Parent carbon skeletons of $C_{20}$, $C_{25}$ and $C_{30}$ highly branched isoprenoids.

*R. setigera* was isolated from Le Croisic, France and cultured in 4×60 L tanks containing underground saltwater enriched with $NaNO_3$ (8 mg $ml^{-1}$) and Guillard's medium[13] (f/2, 0.2 ml $l^{-1}$) at 16–18°C. After centrifuging, the concentrated biomass was freeze-dried and extracted with hexane to yield a non-polar fraction. This was then saponified with KOH/MeOH to remove triglyceride esters and then re-extracted into hexane. Analysis of this non-saponifiable lipid fraction by GC and GC–MS revealed the presence of heneicosa-3,6,9,12,15,18-hexaene ($n$-$C_{21:6}$) together with two pairs of compounds whose chromatographic (retention indices[14]) and mass spectral properties ($M^+$ 412, 410) were consistent with $C_{30}$ rhizenes possessing five and six double bonds. Separation of these components was achieved using column chromatography ($SiO_2$/hexane) to yield two $C_{30:5}$ (21 mg) and two $C_{30:6}$ (10 mg) alkenes.

*Keywords*: highly branched isoprenoids; alkenes; diatoms; *Rhizosolenia setigera*; NMR spectroscopy; rhizenes.

* Corresponding author. Tel.: +44 (0)1752 233042; fax: +44 (0)1752 233035; e-mail: sbelt@plymouth.ac.uk

0040-4039/01/$ - see front matter 
PII: S0040-4039(01)01063-2

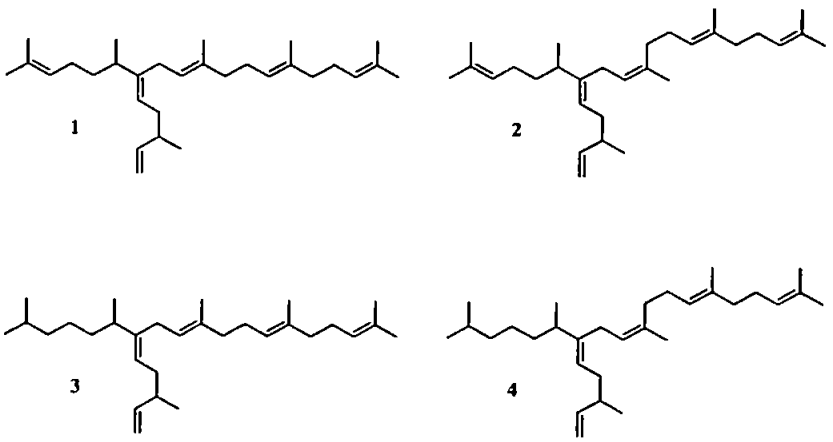


Figure 2. Structures of $C_{30}$ penta- and hexaenes isolated from *R. setigera*.

Examination of the $^1H$, $^{13}C$ and DEPT NMR spectra of the two $C_{30:6}$ HBI alkenes revealed the presence of a vinyl moiety and five tri-substituted double bonds. Two of the tri-substituted double bonds could be located at the terminal positions of the main alkyl chain as resonances due to isopropyl groups were absent. A further double bond could be located at the C-7 branch point (see Fig. 1 for numbering scheme) due to characteristic $^{13}C$ resonances for this quaternary carbon ($\delta$ 142.6 and 142.3 ppm) and the absence of any peak at ca. 45–50 ppm, which is diagnostic when HBI alkene isomers are saturated at this position.[3–12] The remaining two tri-substituted double bonds were positioned at C9–C10 and C13–C14 since the H-8 protons (and only H-8) were found to be di-allylic ($\delta$ 2.6 ppm). No evidence could be found for the presence of positional isomers, a feature which is commonly observed for $C_{25}$ HBI alkenes from *Haslea* sp.[6–12] However, the presence of two hexaenes could be explained in terms of geometric (and not configurational) isomerism. Thus, unique $^1H$ and $^{13}C$ resonances were detected for the methyl group at C-22,[14] indicating that the geometric isomerism exists at C9–C10 in an analogous manner to that observed for the pseudo-homologous $C_{25}$ tri-, tetra- and pentaenes isolated from *P. intermedium*.[4,5] Pairs of resonances with significant differences in frequency could be assigned to C-7, C-8 and C-9,[14] verifying that this isomerism was at C9–C10 rather than at C13–C14. Further, by comparison of the relative intensities of the $^1H$ and $^{13}C$ resonances with those of the peaks corresponding to the two $C_{30:6}$ HBIs in the total ion current (TIC) chromatogram, the GC elution order could be determined (viz. *Z* before *E*), which is the same as that observed for the related $C_{25}$ alkenes.[4,5]

The structures of the co-occurring pentaenes ($C_{30:5}$) were also examined by $^1H$ and $^{13}C$ NMR spectroscopy and not surprisingly many of the spectral features were extremely similar to those found for the $C_{30:6}$ alkenes. Thus, resonances were consistent with a vinyl moiety and four tri-substituted double bonds with one of these occurring at the C7–C25 branch point.[14] *E*/*Z* isomerism was also verified as being present at C9–C10, though somewhat surprisingly the major isomer was found to be *Z* (*Z*/*E* = 1.5 cf. 0.9 for 2/1). The only significant spectral differences consisted of resonances attributable to a single isopropyl group confirming that one end of the main hydrocarbon chain was saturated. Despite the extreme structural similarities and expected spectrosopic features for isomers possessing unsaturation at either end of the principal carbon chain (viz. C2–C3 and C17–C18), an unambiguous assignment could be made by careful examination of the $^{13}C$ spectrum. For example, for the pseudo-homologous $C_{25:3}$, $C_{25:4}$ and $C_{25:5}$ alkenes (eight isomers due to positional and geometric isomerism) the frequency for C-6 is always significantly higher ($\Delta\delta = 0.3$–$0.4$ ppm) when C2–C3 is unsaturated (ca. $\delta$ 34.3 ppm).[4,5] Since C-6 was found to resonate at 34.3 ppm, with the corresponding resonance for the $C_{30}$ hexaenes (which is unsaturated at C2–C3) occurring at 33.9 ppm, C2–C3 must be saturated at this position. An analogous trend was observed for C-7 with chemical shifts to higher frequency when C2–C3 is saturated (irrespective of whether C9–C10 is *E* or *Z*).

The structures of the two pairs of rhizenes ($C_{30:5}$ and $C_{30:6}$) are therefore established as **1**–**4**. The double bond positions and stereochemistry are equivalent to those established for some $C_{25}$ alkenes found in other strains of *R. setigera*[15] and *P. intermedium*.[4,5] Although the biosynthesis or function of the rhizenes is as yet unknown, isotope ratio ($\delta$ $^{13}C$) measurements suggest that they may be derived from different (and temperature dependent) pools of isopentenyl pyrophosphate (IPP) within the cells.[15] Now that the structures of the $C_{30}$ alkenes have been established, their biosynthesis and function can be examined in more detail.

## Acknowledgements

This work was supported by the University of Plymouth for studentships to W.G.A. and G.M., the British Council (ALLIANCE program), the Region des Pays de la Loire, France and the Royal Society of Chemistry, UK for a JWT Jones Travelling Fellowship to S.T.B.

## References

1. Rowland, S. J.; Robson, J. N. *Mar. Environ. Res.* 1990, *30*, 191–216.
2. Volkman, J. K.; Barratt, S. M.; Dunstan, G. A. *Org. Geochem.* 1994, *21*, 407–413.
3. Sinninghe Damsté, J. S.; Schouten, S.; Rijpstra, W. I. C.; Hopmans, E. C.; Peletier, M. H.; Gieskes, W. W. C.; Geenevasen, J. A. J. *Org. Geochem.* 1999, *30*, 95–100.
4. Belt, S. T.; Allard, G.; Robert, J.-M.; Massé, G.; Rowland, S. J. *Chem. Commun.* 2000, 501–502.
5. Belt, S. T.; Allard, G.; Robert, J.-M.; Massé, G.; Rowland, S. J. *Geochim. Cosmochim. Acta* 2000, *64*, 3839–3851.
6. Belt, S. T.; Cooke, D. A.; Robert, J.-M.; Rowland, S. J. *Tetrahedron Lett.* 1996, *37*, 4755–4758.
7. Wraige, E. J.; Belt, S. T.; Lewis, C. A.; Cooke, D. A.; Robert, J.-M.; Massé, G.; Rowland, S. J. *Org. Geochem.* 1997, *27*, 497–505.
8. Wraige, E. J.; Belt, S. T.; Johns, L.; Massé, G.; Robert, J.-M.; Rowland, S. J. *Org. Geochem.* 1998, *28*, 855–859.
9. Wraige, E. J.; Belt, S. T.; Johns, L.; Massé, G.; Robert, J.-M.; Rowland, S. J. *Phytochemistry* 1999, *15*, 69–73.
10. Johns, L.; Wraige, E. J.; Belt, S. T.; Lewis, C. A.; Massé, G.; Robert, J.-M.; Rowland, S. J. *Org. Geochem.* 1999, *30*, 1471–1475.
11. Johns, L.; Belt, S. T.; Lewis, C. A.; Rowland, S. J.; Massé, G.; Robert, J.-M.; König, W. *Phytochemistry* 2000, *53*, 607–611.
12. Allard, W. G.; Belt, S. T.; Massé, G.; Naumann, R.; Robert, J.-M.; Rowland, S. *Phytochemistry* 2001, *56*, 795–800.
13. Guillard, R. R. L. In *Culture of Marine Invertebrate Animals*; Smith, W. L.; Chanley, M. H., Eds. Culture of phytoplankton for feeding marine invertebrates; Plenum Press: New York, 1975; pp. 26–60.
14. Retention indices were measured using HP-1 and HP-5 stationary phases. HP-1: 2596, 1; 2545, 2; 2558, 3; 2505, 4. HP-5: 2617, 1; 2565, 2; 2574, 3; 2519, 4. $^{1}H$ and $^{13}C$ NMR spectra were recorded using a JEOL EX-270 NMR spectrometer in $CDCl_3$ with chemical shifts referenced to residual $CHCl_3$ (7.24 ppm) and $^{13}CDCl_3$ (77.0 ppm), respectively. 1–2: $^{1}H$ ($\delta$/ppm): 5.71 (m, 1H, H-28), 5.07 (m, 5H, H-3,9,13,17,25), 4.92 and 4.88 (2×m, 2H, H-29), 2.60 (m, 3H, 6,8), 1.8–2.2 (m, 13H, H-4,11,12,15,16,26,27), 1.7 (s, H-22, 2), 1.66 (s, 6H, H-1,19), 1.57, 1.54 (2×s, H-20,23,24,22, 1), 1.30 (m, 2H, H-5), 0.95 (m, 6H, H-21,30). $^{13}C$ ($\delta$/ppm): 144.5 (C-28), 142.6 (C-7, 2), 142.3 (C-7, 1), 135.7 (C-10), 135.1 (C-14, 2), 134.9 (C-14, 1), 131.3, 131.2 (C-2,18), 124.9, 124.3, 124.2, 124.1 (C3,13,17), 123.8 (C-9, 2), 123.1 (C-9, 1), 123.0, 122.9 (C-25), 112.2 (C-29), 39.8, 39.7 (C-11, 1,15), 38.22, 38.17 (C-27), 35.1 (C-5), 34.3 (C-26), 33.9 (C-6), 31.8 (C-11, 2), 29.1 (C-8, 1), 28.8 (C-8, 2), 26.7, 26.5, 26.4 (C-4,12,16), 25.7 (C-1,19), 23.5 (C-22, 2), 19.5, 19.4 (C-21,30), 17.68, 17.65 (C-20,24), 15.96, 15.92 (C-23), 15.8 (C-22, 1). 3–4: $^{1}H$ ($\delta$/ppm): 5.73 (m, 1H, H-28), 5.09 (m, 4H, H-9,13,17,25), 4.93 and 4.88 (2×m, 2H, H-29), 2.60 (m, 3H, 6,8), 1.9–2.2 (m, 11H, H-11,12,15,16,26,27), 1.71 (s, H-22, 4), 1.66 (s, 3H, H-19), 1.58, 1.56, 1.53 (3×s, H-23,24,22, 3), 1.50 (m, 1H, H-2), 1.04–1.30 (m, 6H, H-3,4,5), 0.96, 0.94 (2×d, $J$=6.6 Hz, 6H, H-21,30), 0.84 (d, $J$=6.6 Hz, 6H, H-1,20). $^{13}C$ ($\delta$/ppm): 144.6 (C-28), 143.0 (C-7, 4), 142.7 (C-7, 3), 135.6 (C-10), 135.1 (C-14, 4), 134.9 (C-14, 3), 131.3 (C-18), 124.4, 124.3, 124.2 (C-13,17), 124.0 (C-9, 4), 123.3 (C-9, 3), 122.9 (C-25, 4), 122.7 (C-25, 3), 112.1 (C-29), 39.8 (C-11, 3), 39.7 (C-15), 39.3 (C-3), 38.2 (C-27), 35.3 (C-5), 34.4 (C-26), 34.3 (C-6), 31.8 (C-11, 4), 29.2 (C-8, 3), 28.9 (C-8, 4), 27.9 (C-2), 26.8, 26.7, 26.6 (C-12,16), 25.7 (C19), 25.7 (C-4), 23.5 (C-22, 4), 22.6 (C-1,20), 19.6, 19.5 (C-21,30), 17.7 (C-24), 15.9 (C-23), 15.8 (C-22, 3).
15. Rowland, S. J.; Allard, W. G.; Belt, S. T.; Massé, G.; Robert, J.-M.; Blackburn, S.; Frampton, D.; Revill, A. T.; Volkman, J. K. *Phytochemistry* 2001, submitted.

C.R. Acad. Sci. Paris, Sciences de la vie / Life Sciences 324 (2001) 617–626

S0764446901013300/FLA

Plant biology and pathology / Biologie et pathologie végétale

# *Haslea salstonica* sp. nov. and *Haslea pseudostrearia* sp. nov. (Bacillariophyta), two new epibenthic diatoms from the Kingsbridge estuary, United Kingdom

Guillaume Massé[a]*, Yves Rincé[b]*, Eileen J. Cox[c], Guy Allard[a], Simon T. Belt[a], Steve J. Rowland[c]

[a] Petroleum and Environmental Geochemistry Group, Department of Environmental Sciences, University of Plymouth, Drake Circus, Plymouth, Devon PL4 8AA, UK

[b] Laboratoire de biologie marine, ISOMer, université de Nantes, 2, rue de la Houssinière, 44322 Nantes cedex 3, France

[c] Department of Botany, The Natural History Museum, Cromwell Road, London SW7 5BD, UK

Received 17 March 2000; accepted 19 February 2001

Communicated by Lucien Laubier

**Abstract** – Two new diatom species, *Haslea salstonica* and *Haslea pseudostrearia* are described in light and electron microscopy and compared with two well-known members of *Haslea*. Scanning electron microscope observations confirm that the new species belong to the genus *Haslea*. This study extends previous observations on the genus, particularly with respect to the development of a pseudostauros. The characteristic features of the genus are discussed briefly. © 2001 Académie des sciences/Éditions scientifiques et médicales Elsevier SAS

diatoms / *Haslea* / new species / taxonomy / ultrastructure

**Résumé** – ***Haslea salstonica* sp. nov. et *Haslea pseudostrearia* sp. nov. (Bacillariophyta), deux nouvelles diatomées épibenthiques de l'estuaire de Kingsbridge, Royaume-Uni.** Deux nouvelles espèces de diatomées, *Haslea salstonica* et *Haslea pseudostrearia* sont décrites et illustrées au moyen des microscopes optique et électronique. Les observations au microscope électronique à balayage permettent de démontrer l'appartenance de ces deux nouvelles espèces au genre *Haslea*. L'étude de l'ultrastructure du frustule de quatre espèces du genre *Haslea* permet de préciser les observations antérieures notamment concernant les stries médianes transversales et le pseudostauros. © 2001 Académie des sciences/Éditions scientifiques et médicales Elsevier SAS

diatomées / *Haslea* / nouvelles espèces / taxonomie / ultrastructure

## . Version abrégée

L'utilisation des techniques de microscopie électronique pour la description de l'ultrastructure des frustules de diatomées est à l'origine de nombreux changements au sein de la classification des Bacillariophyta notamment au sein du genre *Haslea*. Lors de son inventaire des diatomées planctoniques de l'océan indien, Simonsen a reclassé plusieurs diatomées du genre *Navicula* Bory présentant les mêmes particularités ultrastructurales dans le genre nouveau *Haslea*. Ce genre regroupe actuellement une vingtaine d'espèces

* *Correspondence and reprints.*
*E-mail address:* gmasse@plymouth.ac.uk (G. Massé).

dont l'espèce type est la diatomée *Haslea ostrearia* (Gaillon) Simonsen (toutefois, cette espèce est unique dans sa capacité à synthétiser un pigment surnuméraire bleu–vert).

Dans cet article, nous décrivons l'ultrastructure de la valve de deux nouveaux *Haslea* isolés à la suite d'une campagne de prélèvements du microphytobenthos dans l'estuaire de Kingsbridge près de Salcombe en Grande-Bretagne et nous effectuons une comparaison de ces deux taxons avec deux *Haslea* benthiques issus de la collection de microalgues de notre laboratoire.

*Haslea salstonica* sp. nov. et *Haslea pseudostrearia* sp. nov. proviennent d'un échantillon de sédiment récolté à marée basse le 28 juillet 1999 dans la partie sud de l'estuaire de Kingsbridge. (Devon, Grande-Bretagne). Cet estuaire a fait l'objet d'une campagne d'échantillonnage dans le but de préciser les travaux de Hustedt et Aleem qui font état de la présence de la diatomée *H. ostrearia*. De plus, des lipides, caractéristiques des diatomées appartenant au genre *Haslea* ont été retrouvés en concentration importante dans les sédiments de cet estuaire.

*H. ostrearia* et *Haslea crucigera* (Wm. Smith) Simonsen ont été isolés respectivement en avril et juin 1999 dans un prélèvement effectué dans les claires ostréicoles de la baie de Bourgneuf en France. Les microalgues après isolement sont entretenues sur du milieu ES1/3 Provasoli modifié.

Le matériel a été préparé selon le protocole décrit par Hendey puis rincé à l'eau distillée. Une partie des frustules nettoyés a été montée entre lame et lamelle à l'aide d'Hyrax pour les observations en microscopie optique. Le reste a été déposé sur un support en laiton et recouvert d'une couche d'or/palladium pour les observations en microscopie électronique à balayage (MEB).

En microscopie optique, la cytologie du genre *Haslea* est dominée par la présence de deux plastes en bande, plaqués contre le cingulum. Leur contour parfois irrégulier traduit l'implantation de pyrénoïdes en forme de courtes baguettes.

Lors des observations au MEB, nous avons pu mettre en évidence plusieurs caractéristiques ultrastructurales communes chez les quatre espèces qui les rattachent au genre *Haslea*. En vue externe, on retiendra que les valves sont revêtues de bandes silicifiées parallèles au raphé, l'aire centrale étant réduite voire absente. En vue interne, les stries transapicales toutes perpendiculaires au raphé, et les vimines délimitent des aréoles rectangulaires. Un bourrelet accessoire (côte axiale) accompagne le raphé sur toute la longueur de la valve du côté primaire. La fissure du raphé est tournée vers le côté secondaire de la valve sauf au centre et aux apex. Au centre de la valve, la fissure du raphé est très fine et les pores centraux sont à peine dilatés. Aux apex, le bourrelet s'atténue progressivement et la fissure du raphé se termine en un hélictoglosse. Au centre, sur le côté secondaire de la valve, un bourrelet plus court fait face au bourrelet accessoire. Il est parfois réduit à une ébauche en forme d'épaississement localisé des stries. On peut grouper par deux ces quatre espèces : *Haslea pseudostrearia* avec *H. ostrearia* et *H. salstonica* avec *H. crucigera*. Lors de l'observation de spécimens vivants, abstraction faite d'une importante différence de taille ainsi que d'une absence de coloration bleu–vert des apex, *H. pseudostrearia* apparaît comme une forme proche d'*H. ostrearia*. Elles ont plusieurs caractéristiques ultrastructurales en commun : l'ornementation de la valve est imperceptible en microscopie optique, on note l'absence d'épaississement des virges centrales et on compte environ 36 stries transapicales en 10 µm pour les deux espèces. Cependant, la petite taille des spécimens, une forme sub-capitée, une aire axiale plus large que chez *Haslea ostrearia*, un bourrelet accessoire court et fin mais bien défini au centre sur le côté secondaire et surtout l'absence de marennine chez *H. pseudostrearia* à tous les stades physiologiques et dans des conditions de culture identiques à celles de *H. ostrearia* nous permettent d'affirmer qu'il s'agit de deux taxons distincts. La taille des spécimens, inférieure à celle des autres taxons a été retenue comme un caractère discriminant car si certains spécimens d'*H. ostrearia* de notre algothèque peuvent avoir une taille approximativement égale à celle des valves d'*H. pseudostrearia* après plusieurs mois de culture, tous les frustules de dimension inférieure à 50 µm sont systématiquement déformés.

*H. salstonica* et *H. crucigera* ont, elles aussi, plusieurs caractéristiques ultrastructurales en commun dont l'épaississement des stries médianes des deux côtés du raphé. Dans la littérature, on note cependant que les ensembles aires médianes, stries formant le pseudostauros, peuvent varier. Cardinal, Poulin et Bérard-Therriault présentent un spécimen où seulement deux virges médianes du côté de la côte axiale et un du côté opposé s'épaississent pour former le pseudostauros. Round, Crawford et Mann décrivent un spécimen où trois virges côté primaire et deux à l'opposé s'épaississent pour former le pseudostauros alors que celui que nous décrivons dans cette étude présente trois virges qui s'épaississent de chaque côté. Les stries transapicales sont au nombre de 15 à 17 en 10 µm et les fissures centrales du raphé s'incurvent de la même manière chez les deux espèces. Le contour anguleux des valves et leurs dimensions plus faibles chez *H. salstonica* nous permettent de dire qu'il s'agit d'une espèce distincte d'*H. crucigera*.

## 1. Introduction

Cleve [1] created two sections, *Fusiformes* and *Orthostichae*, within the genus *Navicula* to include species with parallel transverse striae, with pores arranged in longitudinal rows, or forming longitudinal striae respectively. Both had small or indistinct central areas while some of the *Orthostichae* had a stauros-like structure at the centre. Also using light microscopy (LM), Patrick [2] and later Hustedt [3] produced accounts of the genus *Navicula* and accommodated species with very lightly silicified valves, a straight raphe with approximate central pores and transapical striae crossed at right angles by a longitudinal pattern in the subgenus or section *Fusiformes*, respectively. With the help of scanning electron microscopy (SEM), Schrader [4] extended Hustedt's [5] observations on the raphe structure and pointed out the need to create a new genus for Patrick's subgenus on the basis of frustule outline, raphe system and valve striation like *Navicula* cf. *vitrea* Cleve.

This taxonomic revision was achieved with Simonsen's diagnosis of *Haslea* [6]. By means of improved light microscopical techniques, the longitudinal striation intersecting the transapical striae was resolved as apically oriented slits on the outer surface of the valve. All the *Haslea* species observed by Simonsen [6] were gathered from plankton samples and the question could be asked whether these characters were also present in benthic forms.

Robert and Prat [7] and Neuville et al. [8, 9] contributed to the ultrastructural description of *Haslea ostrearia*. Their results confirmed the presence of characters diagnostic for *Haslea* in both pelagic and benthic species. Among benthic species transferred to *Haslea*, *H. crucigera* was shown by SEM [10, 11] to have some additional internal features that are now considered typical of *Haslea*. An accessory rib (axial costa) runs alongside the raphe sternum on one side, overlapping the raphe sternum for part of its length. A shorter rib (central bar) is present on the other side of the central area. In *H. crucigera*, thickening of the central virgae creates a 'false stauros' (pseudostauros).

Von Stosch [12] presented a comparative study of planktonic species of *Haslea* (*H. gigantea* (Hustedt) Simonsen, *H. gigantea* var. *tenuis* von Stosch and *H. wawrikae* (Hustedt)) Simonsen but also referring to benthic species (*H. ostrearia* and *H. crucigera*). He considered additional characters such as apical striae, basal pore membrane of the areolae and among components such as the shape, position and number of plastids to be of systematic interest.

In this paper we describe two new diatoms in the genus *Haslea*. They were isolated from mud samples collected in Kingsbridge estuary (UK). We compare them with two taxonomically well established *Haslea* species that we isolated from comparable benthic substrata and have maintained in culture in our laboratory.

## 2. Materials and methods

### 2.1. Algal cultures

*2.1.1.* Haslea salstonica *sp. nov. and* Haslea pseudostrearia *sp. nov.*

Samples were collected with a sterile syringe from the uppermost 1 cm of mud surface in the south part of the Kingsbridge estuary, Devon (UK). Samples were taken on the 28th July 1999 and preserved in darkness in a cool box. In the laboratory, cells of both diatoms were picked out by means of a mouth pipette under the microscope, transferred to 250-mL erlenmeyer flasks containing 150 ml of ES modified Provasoli's medium [13, 14] and grown under controlled conditions (14 °C, 100 µmol·Photon·$m^{-2}$·$s^{-1}$, 14/10 L/D cycle).

We originally chose the Kingsbridge estuary in order to find a British strain of the diatom *Haslea ostrearia* which had been reported from Great Britain [15] and from this estuary by Hustedt and Aleem in 1951 [16]. We also investigated this area since lipids which are characteristic of *Haslea* spp. [17, 18] have been found there in relatively high concentrations [Belt, personal communication].

*2.1.2. Haslea ostrearia and Haslea crucigera*

These two diatoms were isolated in April and June 1999, respectively, from oyster ponds in the Bay of Bourgneuf, France. We used the same methodology as described for *H. salstonica* and *H. pseudostrearia*. Strains were grown in the same culture medium as *H. salstonica* and *H. pseudostrearia* and under the same conditions.

### 2.2. Microscopy

Material was prepared following Hendey's methodology [19] and then rinsed with distilled water. A portion of the cleaned cells was mounted in Hyrax for LM observation (Olympus Provis). Selected cells were dried onto aluminium stubs and coated with gold/palladium for scanning electron microscopy (JEOL 6400F).

## 3. Results

### 3.1. *Haslea salstonica* Massé, Rincé and Cox

(*Plate I, figures B, G, plate II, figures A–F*)

*3.1.1. Description*

Frustules naviculoid, narrowly rectangular and slightly curved in girdle view. Valves rhombic, 60-65 µm long and 17 µm wide. Two apically elongated chloroplasts lie against each side of the girdle. Raphe straight and central with very small central area. Transapical striae uniseriate and parallel, 17 in 10 µm, with the central two or three virgae thickened to form a pseudostauros. Longitudinal striation not resolvable with light microscopy, even under interference contrast, 25 in 10 µm.

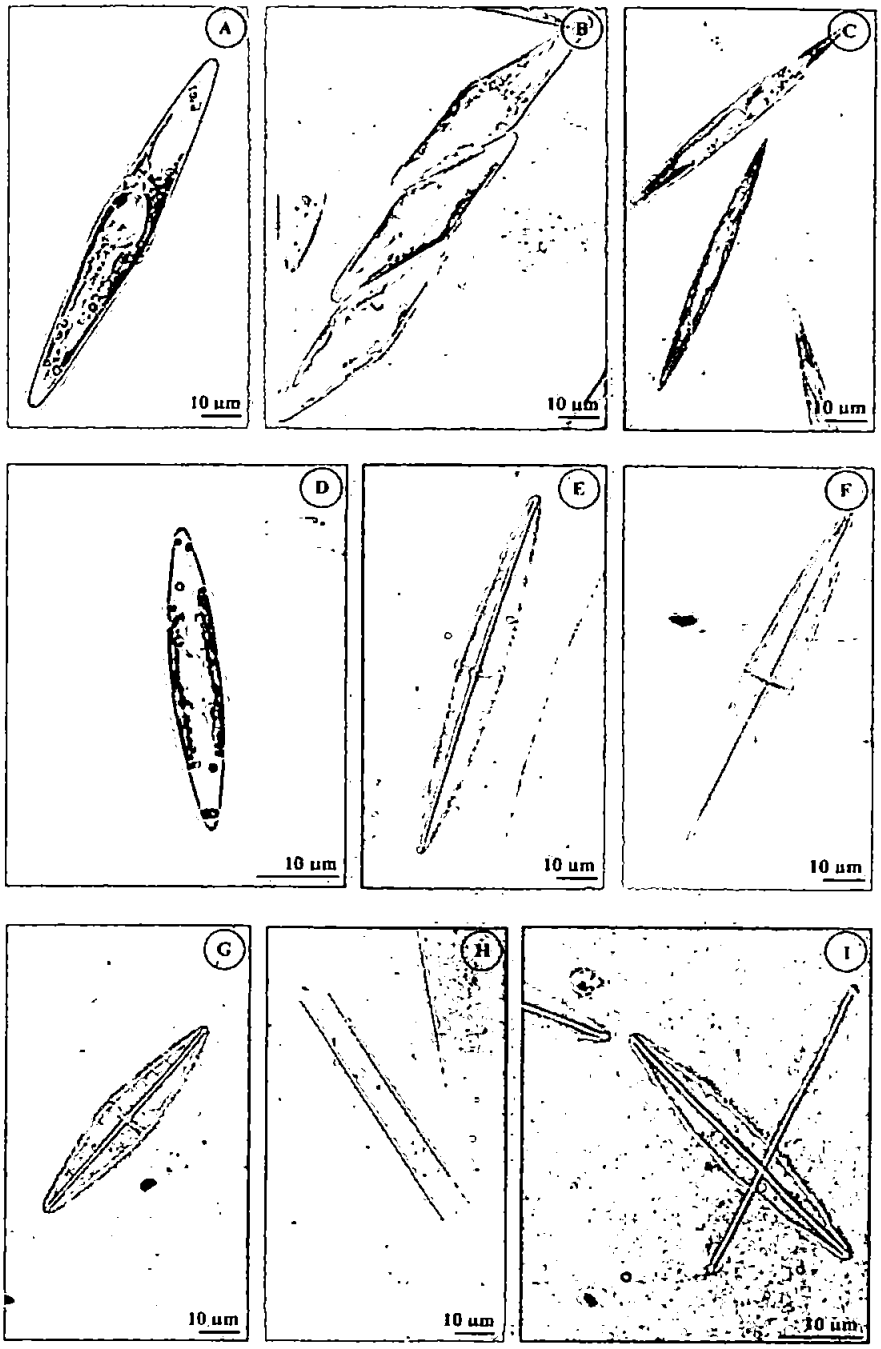


**Plate I.** Light micrographs of four taxa of *Haslea*.
**Figure A.** *Haslea crucigera* showing the two chloroplasts. **Figures E, F.** *Haslea crucigera*, cleaned valves. **Figure B.** *Haslea salstonica* showing the two parietal chloroplasts. **Figure G.** *Haslea salstonica* cleaned valve. **Figure C.** *Haslea ostrearia* showing the two chloroplasts and the blue pigmentation at the poles. **Figure H.** *Haslea ostrearia* cleaned valves. **Figure D.** *Haslea pseudostrearia* showing the two parietal chloroplasts. **Figure I.** *Haslea pseudostrearia* cleaned valves.

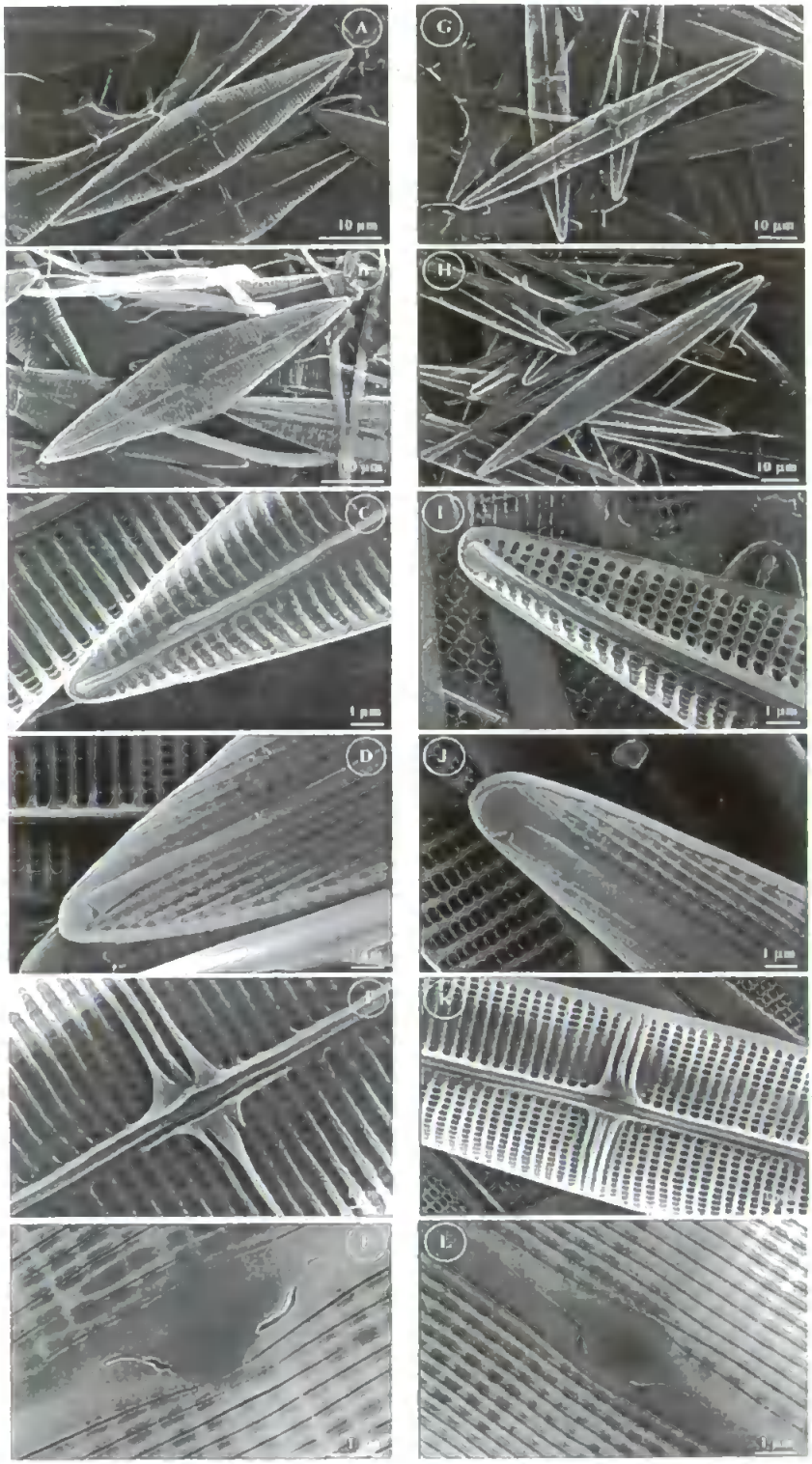


**Plate II.** Scanning electron micrographs of *Haslea salstonica* and *Haslea crucigera*.

**Figures A to F.** *Haslea salstonica*. **A.** Whole valve in internal view. **B.** External view of the whole valve. **C.** Internal view of the apical end of a valve showing the accessory rib ending near the pole and a small helictoglossa. **D.** Apex in external view exhibiting the curved distal raphe fissure and part of the parallel and longitudinal slits abutting the peripheral one. **E.** Centre of the valve showing the pseudostauros consisting of thick virgae, the accessory rib on the primary side of the valve and the short second accessory rib on the secondary side. **F.** Proximal raphe fissure in external view slightly enlarged and curved to the same side of the valve.

**Figures G to L.** *Haslea crucigera*. **G.** Whole valve in internal view. **H.** External view of the whole valve. **I.** Internal view of the apical pole showing the accessory rib ending, the enlargement of the raphe fissure and the helictoglossa. **J.** Apex in external view exhibiting the curved distal raphe fissure and part of the parallel and longitudinal slits abuting the peripheral one. **K.** Centre of the valve showing the pseudostauros consisting of thick virgae, the accessory rib on the primary side of the valve and the short second accessory rib on the secondary side. **L.** Proximal raphe fissure in external view slightly enlarged and curved to the same side of the valve.

External raphe fissure straight, with slightly expanded, unilaterally deflected central endings and polar endings strongly deflected to same side. Internally the raphe fissures open to one side of the raphe sternum for most of their length, except at the centre and near the apices where they end in long helictoglossae. An accessory rib (axial costa) extends throughout most of the valve on the primary side of the raphe sternum, with a shorter rib (central bar) at the centre on the secondary side. The thickenings of the central virgae are continuous with the accessory rib. Areolae quadrate arranged in rows. Longitudinal slits, parallel to the raphe, merging with a peripheral slit near the apices on the outer side of the valve.

*Frustulum chromatophora duo lamininformia, ad utrumque cincturae latus appressa includens. Valvae lineari-angulatae, 60–65 µm longae, 17 µm latae; area centralis minima; striae transapicales circiter 17 in 10 µm, per totam longitudinem raphi perpandiculares; striae longitudinales circiter 25 in 10 µm, per microscopium opticum non visae; pseudostaurum in media parte valvae, 2–3 virgis crassioribus formatum. Raphe recta, axialis, fissures externis rectis, extremis centralibus apicalibusque modice dilatatis et unilateraliter curvatis ad primarium valvae latus; fissurae internae raphis ad raphosterni latus per majorem partem longitudinis aperientes, extremis centralibus simplicibus, rectis proximisque, extremis apicalibus in helictoglossa terminantibus. Raphosternum pulvino accessorio (costa axiali) per quasi totam longitudinem ad primarium valvae latus comitatum; pulvinus minor (costa minor) ad secundarium valvae latus praesens; areolae quadrangulatae in striis perpendicularibus dispositae. Extus, frons valvae rimis longitudinalibus, raphi parallelis, ad apices cum rima peripherali conjugatis ornata.*

*3.1.2. Holotype*

BM 100257, National History Museum, London

*3.1.3. Type locality*

Kingsbridge estuary close to Salcombe on the sand bank at the east of Warham point, UK Marine, intertidal sediments collected in the *Fucus* belt by G. Massé, S. Rowland and S. Belt (July 28, 1999).

*3.1.4. Etymology*

This species is named with reference to the sampling area 'Saltstone', a sand-bank in the middle of the Salcombe estuary. Devon, UK.

*3.1.5. Microscopy*

In LM, cells are free living or adherent, as if in delicate mucilage tubes (*plate I, figure B*) with naviculoid frustules and rhombic valves. Each cell has two, band-like plastids lying against the girdle on each side of the cell (*plate I, figure B*). In cleaned material (*plate I, figure G*) transapical striae are visible throughout the whole valve, crossed by less obvious longitudinal striation. The central 2 or 3 striae on each side of the central area are thickened to form a pseudostauros. The raphe is indistinct except for its central endings which lie in a very small central area.

In SEM, the external valve surface appears to be covered with parallel, longitudinal strips of silica separated by very narrow slits. The strips are tapered at each end where they abut a continuous peripheral slit (*plate II, figure D*). The external raphe system consists of 2 straight branches with central fissures curved in the same direction and the polar fissures sharply deflected to the same side. Internally, the uniseriate rows of square to rectangular areolae are visible (*plate II, figure E*), alternating with thick transapical virgae, crossed at right angles by longitudinal vimines (*plate II, figures C* and *E*). The raphe fissures open laterally (toward the secondary side of the valve) along most of the length of the raphe sternum but are central in the middle of the valve and at the apices (*plate II, figures C* and *E*). The central raphe endings are co-axial and close to each other (1 µm, 2 striae apart) while at the poles they end in a straight helictoglossa (*plate II, figures C* and *E*). An accessory rib is present on the primary side of the valve and slightly overlaps the raphe sternum for part of its length (*plate II, figure C*). The accessory rib merges centrally with 3 thickened virgae, as does a much shorter and less well-defined rib on the secondary side (*plate II, figure E*). These transapical thickenings form a distinct pseudostauros visible in LM (*plate I, figure G*).

### 3.2. *Haslea pseudostrearia* Massé, Rincé and Cox

(*plate I, figures D, I* and *plate III, figures A–F*)

*3.2.1. Description*

Frustules narrowly rectangular and slightly curved in girdle view. Valves lanceolate with sub-acute apices, 37–43 µm long and 6–7 µm wide. Two apically elongated chloroplasts lying against each side of the girdle. Raphe straight and central without a well-defined axial area. Cell wall extremely delicate, longitudinal and transapical striation not visible in light microscopy. Transapical striation 34–36 in 10 µm, longitudinal striation 42 in 10 µm.

External raphe endings straight and slightly expanded at the centre of the valve, strongly deflected to one side at the poles. Internal raphe fissures open to one side of the raphe sternum except at the centre and near the apices. An accessory rib extends besides the raphe sternum throughout most of the valve, on the primary side (*plate III, figures C* and *E*). Internally the areolae are quadrate, arranged in regular rows. Externally, the valve appears covered by longitudinal strips, separated by slits parallel to the raphe and merging with a peripheral slit near the apices.

*Frustulum delicatum (paulo silificatum), chromatophoris duobus, lamininformibus, ad utrumque cincturae latus appressis. Valvae lineari-lanceolatae, 37–43 µm longae, 6–7 µm latae, polis subacutis; area axialis inconspicua; striae transapicales circiter 34–36 in 10 µm, per totam longitudinem valvae raphi perpendiculares et striae longitudinales ciciter 42 in 10 µm, per microscopium opticum non visae. Raphe recta, axialis, fissuris externis rectis,*

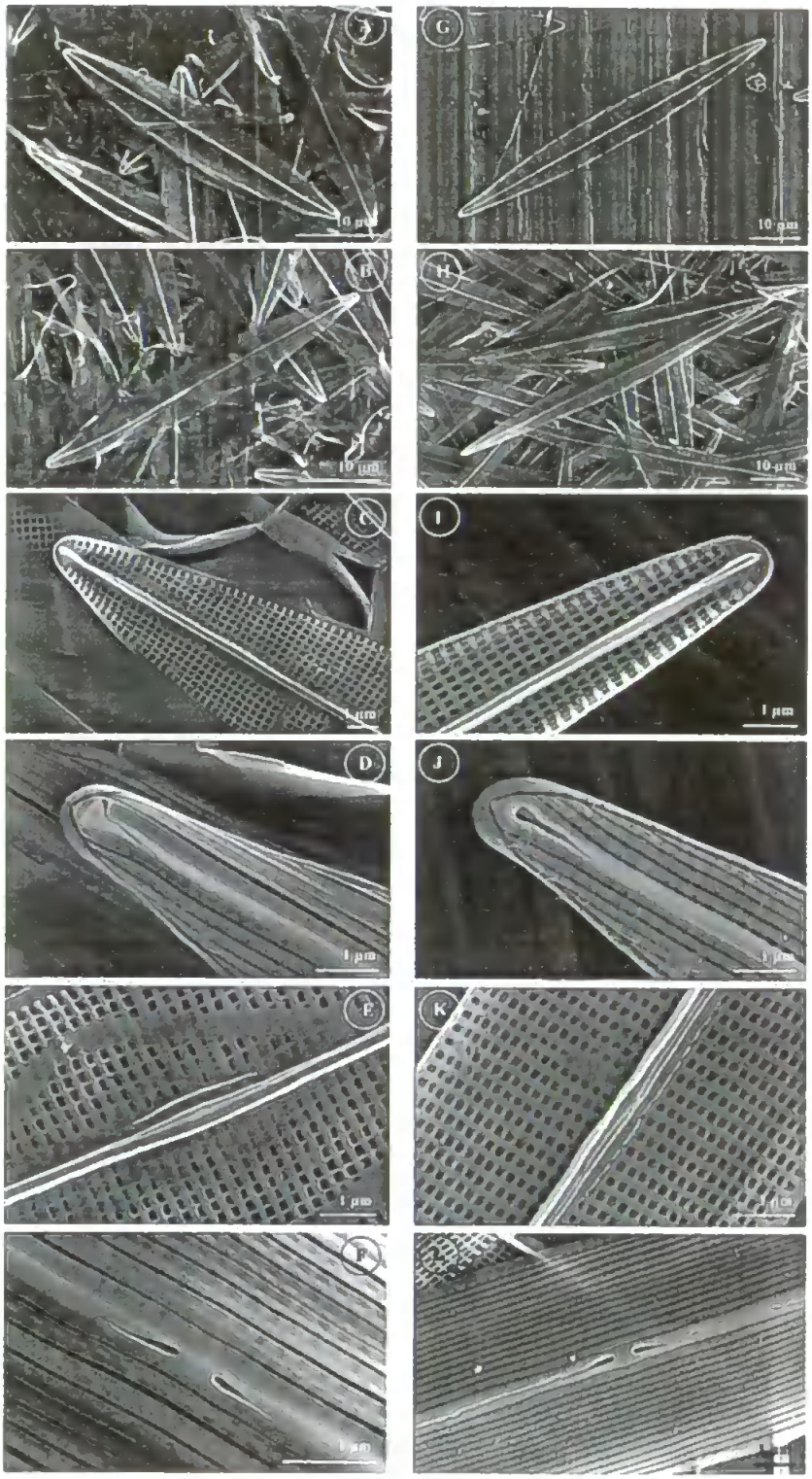


**Plate III.** Scanning electron micrographs of *Haslea pseudostrearia* and *Haslea ostrearia*.

**Figures A to F.** *Haslea pseudostrearia* **A.** Whole valve in internal view. **B.** External view of the whole valve. **C.** Internal view of the apical end of a valve showing the accessory rib ending near the pole and a small helictoglossa. **D.** Apex in external view exhibiting the curved distal raphe fissure and part of the parallel and longitudinal slits abuting the peripheral one. **E.** Centre of the valve showing the accessory ribs. **F.** Proximal raphe fissure in external view straight and slightly enlarged.

**Figures G to L.** *Haslea ostrearia*. **G.** Whole valve in internal view. **H.** External view of the whole valve. **I.** Internal view of the apical end of a valve showing the accessory rib ending near the pole and a small helictoglossa. **J.** Apex in external view exhibiting the straight distal raphe fissure. **K.** Centre of the valve showing the accessory rib. **L.** Proximal raphe fissure in external view straight and slightly enlarged.

*extremis centralibus rectis, modice dilatatis, extremis apicalibus, modice dilatatis, ad primarium valvae latus curvatis; fissurae internae raphis per magnam partem longitudinis ad latum raphosterni aperientes, extremis centralibus simplicibus, rectis, proximisque, extremis apicalibus in helictoglossa terminantibus. Raphosternum pulvino accessorio per quasi totam longitudinem ad primarium valvae latus comitatum; areolae quadrangulatae in striis perpendicularibus dispositae. Extus, frons valvae rimis longitudinalibus, raphi parallelis, ad apices cum rima peripherali conjugatis ornata.*

*3.2.2. Holotype*

BM 100258, National History Museum, London.

*3.2.3. Type locality*

Kingsbridge estuary close to Salcombe on the sand bank at the east of Warham point, UK Marine, intertidal sediments collected in the *Fucus* belt by G. Massé, S. Rowland and S. Belt (July 28, 1999).

*3.2.4. Etymology*

This species is named because of its similarity to *Haslea ostrearia*.

*3.2.5. Microscopy*

Cells are free living (*plate I, figure D*), naviculoid, lanceolate with sub-acute apices. Each cell has two band-like plastids lying against the girdle on each side of the cell. Cleaned valves (*plate I, figure I*) appear hyaline apart from the apically orientated raphe system with indiscernible nodules.

In SEM, the external valve surface appears covered with parallel, longitudinal strips of silica separated by very narrow slits. The strips are tapered at each end where they abut a continuous peripheral slit (*plate III, figure D*). The external raphe system comprises 2 straight branches with terminal fissures slightly expanded but almost straight at the centre and sharply deflected to the same side at the poles (*plate III, figures D* and *F*). Internally, the valve has uniseriate rows of square to rectangular areolae (*plate III, figure E*) separated by very slightly thickened transapical virgae, crossed at right angles by longitudinal vimines (*plate III, figures C* and *E*). The raphe fissures open laterally along most of the raphe sternum except in the middle and at the apices where they open centrally (*plate III, figures C* and *E*). The central raphe endings are co-axial and very close to each other (140 nm apart, 1 stria) while at the poles they end in a straight and short helictoglossa (*plate III, figures C* and *E*). There is no lateral expansion of the raphe sternum into a central nodule. The raphe sternum is flanked by an accessory rib on the primary side of the valve and a short and thin rib on the secondary side (*plate III, figure E*).

### 3.3. *Haslea crucigera* (Wm. Smith) Simonsen

(*plate I, figures A, E, F; plate II, figures G–L*) [3, 11, 20]

Living cells have a slightly curved, narrowly rectangular frustules in girdle view (not shown). The valves are lanceolate to linear-lanceolate, flat, 95–97 µm long and 11–12 µm wide (*plate I, figures A, E,* and *F, plate II, figures G* and *H*). Two band-like plastids lie against the girdle on each side of the cell (*plate I, figure A*). The internal margin of the plastids usually appear slightly undulate due to the presence of small obliquely inserted rod-shaped pyrenoids. In cleaned cells (*plate I, figures E* and *F*), the raphe appears straight and central. Transapical striae (15 in 10 µm) are visible with in LM and are crossed by more delicate longitudinal striae. The central 2 or 3 transapical virgae are thickened forming a pseudostauros.

In SEM, the external valve surface is covered with closely spaced, longitudinal strips of silica separated by narrow slits which merge with a continuous peripheral slit near the apices (*plate II, figure J*). The external raphe fissures are slightly expanded and turned to one side centrally and sharply deflected to the same side at the poles (*plate II, figures J* and *L*). Internally the raphe slits open laterally in the raphe sternum except at the centre where the endings are straight and approximate (1 µm apart / 2 striae width) (*plate II, figure K*) and at the apices where they are slightly expanded in a slightly raised helictoglossa (*plate II, figure I*).

An accessory rib on the primary side of the valve flanges over the raphe sternum and obscures it for much of its length. The internal areola arrangement is similar to the other taxa but with fewer longitudinal striae (20 in 10 µm).

On both sides of the raphe, the 3 central virgae are thickening forming a pseudostauros. The thickened virgae are fused with accessory rib on the primary side of the valve, and with a shorter thinner rib on the secondary side of the valve (*plate II, figure K*). The thickening of the virgae extends further across the valve and is more even in *H. crucigera* than *H. salstonica* (*plate II, figure E*).

### 3.4. *Haslea ostrearia* (Gaillon) Simonsen

(*plate I, figures C, H; plate III, figures G–L*) [3, 7, 8, 9]

When cells are suffering from nutrient depletion [14, 21], light microscopy reveals the characteristic, blue–green cytoplasmic coloration at the cell apices (*plate I, figure C*). Two band-like plastids lie against each girdle. Their extent is variable as a function of the blueing status of the cells [22]. The valves are narrowly lanceolate, flat with sub-acute apices, 68–69 µm long, about 6.5–7.5 µm wide (*plate I, figures C* and *H; plate III, figures G* and *H*). Frustules are narrowly rectangular in girdle view (not shown). In cleaned cells (*plate I, figure H*) the raphe appears straight and central. The valve is extremely delicate and the striae are not visible in LM.

In SEM, the external valve structure is comparable to the previous species, but the external raphe fissures are straight, slightly expanded at both centre and poles (*plate III, figures J* and *L*). Internally the areolation is again as above, but there are 36 transapical striae in 10 µm, and about 53 longitudinal striae in 10 µm (*plate III, figure K*).

Table I. Summary of features of the four *Haslea* spp. investigated.

| | *Haslea salstonica* | *Haslea crucigera* | *Haslea pseudostrearia* | *Haslea ostrearia* |
|---|---|---|---|---|
| length (µm) | 60–65 | 95–97 | 37–43 | 68–69 |
| breadth (µm) | 17 | 11–12 | 6–7 | 6.5–7.6 |
| transapical striae in 10 µm | 15 | 17 | 34–36 | 36 |
| longitudinal striae in 10 µm | 25 | 20 | 42 | 53 |
| central virgae | thickened | thickened | unthickened | unthickened |
| accessory rib | present | present | present | present |
| shorter accessory rib | present | present | present | very slight |
| central raphe endings | deflected | deflected | straight | straight |
| polar raphe endings | deflected | deflected | deflected | straight |

The internal central raphe endings are approximate, less than 200 nm apart (*plate III, figure K*). Although there is well-developed accessory rib on the primary side of the valve (*plate III, figures I* and *K*), there is only a very slight suggestion of a thickening on the secondary side and no thickening of the central virgae.

## 4. Discussion and conclusion

The species described above can be considered in two groups, *Haslea ostrearia* with *H. pseudostrearia*, and *H. crucigera* with *H. salstonica*. A summary of valve features is given in *table I*.

### 4.1. *H. ostrearia* and *H. pseudostrearia*

Observations of both live and cleaned material revealed similarities between these taxa. Both have very delicate, lanceolate valves with about 36 transapical striae in 10 µm. However, *H. pseudostrearia* is smaller, has sub-acute rather than acute apices and a wider axial area than *H. ostrearia*. Some small specimens of *H. ostrearia* have been observed, but cells less than 50 µm long are always warped [23, 24], unlike *H. pseudostrearia*. The absence of blue pigment in living cells of *H. pseudostrearia* compared with *H. ostrearia* under the same growth conditions supports their recognition as distinct taxa.

### 4.2. *H. salstonica* and *H. crucigera*

These taxa share the possession of a pseudostauros formed by a thickening along the central virgae and approximately the same transapical stria density (15–17 in 10 µm). The external raphe fissures are similar, deflected at the centre and poles, while internally there is an accessory rib on the primary side and a short bar on the secondary side of the valve. *Haslea salstonica* is smaller and more rhombic than *H. crucigera*, with more closely spaced longitudinal striae. It can therefore be recognised as a distinct taxon. The development of the pseudostauros may vary in *H. crucigera*. Cardinal, Poulin and Bérard-Therriault [11, *figure 114*] illustrated a specimen with 2 thickened virgae on the primary side and one on the secondary side while Round, Crawford and Mann [25] showed a specimen with 3 thickened virgae on the primary side and 2 on the secondary side forming the pseudostauros. Our specimens have 3 thickened virgae on each side.

Based on this study and recently published investigations of *Haslea* species, several ultrastuctural features now appear to be typical for *Haslea*, and should be incorporated into the generic circumscription. The characteristic external morphology of the valves, appearing to have longitudinal strips of silica over the vimines with intervening forming continuous slits, is largely confined to this genus. It was first reported for *Haslea ostrearia* (the generitype) by Neuville et al. [8, 9] and corroborated by Robert and Prat [7]. Cox [10, 26] has shown that *Haslea crucigera* and another, as yet undescribed, species of *Haslea* are similarly constructed, while von Stosch [12] demonstrated the same construction for three planktonic members of the genus (*H. wawrikae*, *H. gigantea and H. gigantea* var. *tenuis*). Round, Crawford and Mann [25] mention this feature in their description of the genus and it is clearly present in the two new species we describe here. There are a few instances where similar external valve morphology has been observed in members of other genera. Cox [27] has noted that continuous slits can be seen in some *Navicula* species, while external pores may extend over more than one areola in some *Gyrosigma* Hassal species, e.g. *Gyrosigma litorale* (W. Smith) Griffith and Henfrey [28]. More recently this type of pore construction has also been observed in a sigmoid diatom [29]. However, we consider that the possession of continuous external slits over many areolae should be considered one of the diagnostic characters for inclusion in *Haslea*.

In addition to its distinctive areola structure, *Haslea* also has a characteristic combination of raphe features which while confirming its position in the Naviculaceae, nevertheless supports its recognition as a distinct genus. Like other members of the Naviculaceae, *Haslea* has a distinct raphe sternum in which the raphe slits open laterally for most of their length, but are central at their proximal endings, and near the poles where they terminate in elongate helictoglossae. There is a well-defined accessory rib on the primary side of the raphe sternum, which often overlaps the raphe sternum for most of its length. The degree of overlap is species-specific. On the secondary side of the raphe at the centre of the valve there is usually a shorter accessory rib. However, in some species this

feature is barely distinguishable. Externally the raphe fissures are straight for most of their length, slightly expanded at their endings, all endings usually deflected to the same side of the valve. The polar deflections are usually abrupt, the central deflections may be only slight. This contrasts with the external raphe fissures of *Navicula* which are usually hooked at the poles and more or less straight at the centre. In *Gyrosigma* and *Pleurosigma* W. Smith, the raphe endings are simpler deflections, although the ends of each slit are usually opposite deflected in *Gyrosigma*. In *Pleurosigma* the central endings turn to the same side, but polar endings are opposite. The accessory rib configurations in these other genera differ from those in *Haslea*.

Observations on live cells of benthic *Haslea* species [Cox, unpubl.] indicate that cells have two band-like chloroplasts containing numerous, obliquely inserted, small rod-shaped pyrenoids. These often make the inner chloroplast margins slightly irregular. This can also be seen in von Stosch's illustrations of *H. wawrikae* [12, *figure 23*]. Although von Stosch [12] describes *H. gigantea* var. *gigantea* as having small, bacilliform or roundish plastids, he also questions whether this is a function of its growth conditions rather than the typical state because old cultures of *H. wawrikae* could produce numerous small, almost colourless platelets. Further work on the stability of chloroplast form is clearly warranted.

**Acknowledgements.** We would like to thank particularly Pr. Jean Michel Robert for fruitful discussions, Dr. Pierre Compère and Denise Moreau for their help with the Latin diagnosis, the University of Plymouth Microscopy Init and Alain Barreau from the 'service commun de microscopie' from the University of Nantes for their help with SEM photographs. The University of Plymouth funded G. Massé. We are also grateful to Dr. Michel Poulin for the constructive evaluation of the manuscript.

## References

[1] Cleve P.T., Synopsis of the naviculoid diatoms Part 1, Kongliga Svenska Vetenskapsakademiens Handlingar 26 (1894) 1–194.

[2] Patrick R., New subgenera and two new species of the genus *Navicula* (Bacillariophyceae), Notulae Naturae 324 (1959) 1–11.

[3] Hustedt F., Die Kieselagen, in: Rabenhorst L. (Ed.), Kryptogamen-Flora von Deutschland, Österreich und der Schweiz, 1961–1966, 1966.

[4] Schrader H.J., Types of raphe structures in the diatoms, Nova Hedwigia 45 (1973) 195–230.

[5] Hustedt F., Untersuchungen über den Bau der Diatomeen, IV, Ber. Deutsch. Bot. Ges. 46 (1928) 148–157.

[6] Simonsen R., The diatom plankton of the Indian Ocean Expedition of R/V 'Meteor' 1964–1965, 'Meteor' Forschungsergebnisse Reihe D 19 (1974) 1–107.

[7] Robert J.M., Prat D., Ultrastructure de la diatomée *Navicula ostrearia* Bory révélée par le microscope électronique à balayage, C. R. Hebd. Séances Acad. Sci. Ser. D 277 (1973) 1981–1983.

[8] Neuville D., Daste P., Genevès L., Premières données sur l'ultrastructure du frustule de la diatomée *Navicula ostrearia* (Gaillon) Bory, C. R. Hebd. Séances Acad. Sci. Ser. D 273 (1971) 2331–2334.

[9] Neuville D., Daste P., Genèves L., Gasse F., Données complémentaires sur l'organisation ultrastructurale du frustule de la diatomée *Navicula ostrearia* (Gaillon) Bory, C. R. Hebd. Séances Acad. Sci. Ser. D 278 (1974) 2983–2986.

[10] Cox E.J., Raphe structure in naviculoid diatoms as revealed by the scanning electron microscope, Nova Hedwigia 54 (1977) 261–274.

[11] Cardinal A., Poulin M., Bérard-Therriault L., Les diatomées benthiques de substrats durs des eaux marines et saumâtres du Quebec 4. Naviculales, Naviculaceae (à l'exclusion des genres *Navicula*, *Donkinia*, *Gyrosigma* et *Pleurosigma*), Nat. Can. 111 (1984) 369–394.

[12] von Stosch H.A., Some marine diatoms from the Australian region, especially from Port Phillip Bay and tropical north-eastern Australia, Brunonia 8 (1985) 293–348.

[13] Provasoli L., Media and prospects for the cultivation of marine algae, in: Watanabe A., Hattori A. (Eds.), Cultures and Collections of Algae, Proc. U.S., Japan Conf. Hakone, Sept. 1966, Jap. Soc. Plant. Physiol., 1968, pp. 63–75.

[14] Robert J.M., Fertilité des eaux de claires ostréicoles et verdissement: utilisation de l'azote par les diatomées dominantes, thèse de doctorat d'état, université de Nantes, 1983.

[15] Hendey N.I., A preliminary check-list of British marine diatoms, J. Mar. Biol. Assoc. U.K. 33 (1954) 537–560.

[16] Hustedt F., Aleem A.A., Littoral diatoms from Salstone, near Plymouth, J. Mar. Biol. Assoc. U.K. 30 (1951) 177–196.

[17] Volkmann J.K., Barret S.M., Dunstan G.A., $C_{25}$ and $C_{30}$ highly branched isoprenoids alkenes in laboratory cultures of two marine diatoms, Org. Geochem. 21 (3/4) (1994) 407–413.

[18] Rowland S.J., Robson J.N., The widespread occurrence of highly branched acyclic $C_{20}$, $C_{25}$ and $C_{30}$ hydrocarbons in recent sediments and biota – a review, Mar. Environ. Res. 30 (1990) 191–216.

[19] Hendey N.I., The permanganate method for cleaning freshly gathered diatoms, Microscopy 32 (1974) 423–426.

[20] Hendey N.I., Part V. *Bacillariophyceae* (Diatoms), An introductory account of the smaller algae of the British coastal waters, Fisheries Investigations series IV, H.M.S.O., London, 1964.

[21] Robert J.M., Pagès J., Prat D., Applications de la biométrie cytologique à la définition des stades de développement du Navicula ostrearia Bory: incidences de l'évolution pigmentaire sur le verdissement des claires à huîtres, Physiol. Vég. 13 (1975) 225–241.

[22] Nassiri Y., Robert J.M., Rincé Y., Ginsburger-Vogel T., The cytoplasmic fine structure of the diatom *Haslea ostrearia* (Bacillariophyceae) in relation to marennine production, Phycologia 37 (1998) 84–91.

[23] Rouillard I., Optimisation de la production en masse d'*Haslea ostrearia* Simonsen sur une eau souterraine salée: importance de la souche et des conditions de culture; comparaison avec *Skeletonema costatum* (Grev.) Cleve, thèse de doctorat, université de Nantes, 1996.

[24] Robert J.M., Variations biométriques de l'algue *Navicula ostrearia* Bory (diatomée pennée) en culture, Bull. Soc. Phycol. Fr. 23 (1978) 38–44.

[25] Round F.E., Crawford R.M., Mann D.G., The diatoms, Cambridge University Press, Cambridge, 1990.

[26] Cox E.J., Variations in patterns of valve morphogenesis between representatives of six biraphid diatom genera (Bacillariophyceae), J. Phycol. 35 (1999) 1297–1312.

[27] Cox E.J., Studies on the diatom genus Navicula Bory. VIII. Variation in valve morphology in relation to the generic diagnosis based in Navicula tripunctata (O. F. Müller) Bory, Diatom Res. 14 (1999) 207–237.

[28] Cox E.J., Symmetry and valve structure in naviculoid diatoms, Nova Hedwigia 64 (1979) 193–206.

[29] Poulin M., Massé G., Belt S.T., Rincé Y., Robert J.M., Rowland S.J., A striking case of a sigmoid diatom sharing features with *Gyrosigma* and *Haslea*, 16th International Diatom Symposium, Abstract booklet (2000) 118.

SHORT TECHNICAL NOTE

# A simple method for SEM examination of sectioned diatom frustules

G. MASSÉ*†, M. POULIN‡, S. T. BELT†, J. -M. ROBERT*, A. BARREAU§, Y. RINCÉ* & S. J. ROWLAND†

*Laboratoire de Biologie Marine, ISOMer, Université de Nantes, 2 rue de la Houssinière, 44322 Nantes cedex 3, France

†Department of Environmental Sciences, University of Plymouth, Drake Circus, Plymouth, Devon PL4 8AA, U.K.

‡Research Division, Canadian Museum of Nature, PO Box 3443, Station D, Ottawa, Ontario K1P 6P4, Canada

§Service Commun de Microscopie, Université de Nantes, 2 rue de la Houssinière, 44322 Nantes cedex 3, France

Key words. Diatom, scanning electron microscopy, ultrastructure, ultrathin section.

## Summary

We describe an innovative yet straightforward method to obtain high quality thin sections of diatom exoskeletons for observation by scanning electron microscopy (SEM). The use of this new technique allows for clear observations of some ultrastructural valve features, including the raphe, which are generally difficult to observe and describe accurately using transmission electron microscopy analysis of thin sections or SEM of randomly fractured diatom valves. In addition, because this method involves the complete removal of the organic content of the diatom cells, resulting in clean and mostly undisturbed skeletal thin cross-sections, even the intact valvar structures of weak girdle bands can be studied.

## Introduction

Since the beginning of the 18th century when diatoms were first observed with a simple microscope, it is clear that the technological advances in microscopy over the past 300 years have allowed phycologists to characterize diatoms in increasing detail. Thousands of diatoms were described with conventional optical microscopes during the latter part of the 19th century when numerous trans-global scientific expeditions took place. Diatom genera and species were monographed in publications that are still in current use, even though the taxa are mainly illustrated with line drawings (Cleve & Grunow, 1880; Van Heurck, 1880–1885; Grunow, 1884; Cleve, 1894, 1895). During these early investigations diagnoses of diatoms were based on light microscopy (LM), which highlighted the overall shape of valves, the occurrence of hyaline areas, the nature of the raphe fissures and the characteristic ornamentation kf the valve, sometimes with brief considerations of the arrangement of chloroplasts (Mereschkowsky, 1901; 1902–1903).

During the middle part of the 20th century electron microscopy (EM) techniques were developed (Claugher, 1990) and used for the analysis of diatoms (Gaul *et al.*, 1993). Transmission electron microscopy (TEM) contributed important information concerning cytoplasmic organelles and the fine structure of diatom frustules (Stoermer *et al.*, 1964; Drum *et al.*, 1966; Pickett-Heaps *et al.*, 1979a, b; Edgar & Pickett-Heaps, 1984). Despite the high resolution offered by TEM (e.g. 5–10 nm resolution for pore occlusion observations), the introduction of scanning electron microscopy (SEM) has had a more profound impact on diatom taxonomy (Mann, 1981). SEM has allowed phycologists to appreciate the three-dimensional structure of diatom valves and the highly characteristic architecture of the silica shell (Gerloff & Helmcke, 1974; Paddock & Sims, 1990; Round *et al.*, 1990).

However, despite these advances there are still some morphological valvar features, such as the raphe-associated structures, which are extremely difficult to describe accurately using optical microscopy and problematic to study

Correspondence: Guillaume Massé. Tel.: +33 2 51 12 56 57; fax: +33 2 51 12 56 12; e-mail: gmasse@isomer.univ-nantes.fr

with conventional electron microscopy techniques. Such ultrastructural features could potentially provide us with a better understanding of the classification of diatoms. Indeed, features associated with the raphe were studied by Cox (1977, 1999a) and used as taxonomic criteria to improve the classification of some naviculoid diatoms. Cox stressed the importance of taking into consideration all characters related to the raphe system, which is one of the first siliceous elements of the valve to form during morphogenesis (Schmid, 1979; Cox, 1999b). Other authors have reported brief descriptions of such structural features by manually or accidentally breaking the cell walls. However, although this approach can be informative, it is usually time consuming as the position of the fractures cannot be predetermined, and many attempts are necessary to obtain reliable information. In a single study Pocock & Cox (1982) developed a novel resin etching technique to obtain sections of *Rhabdonema arcuatum*, which facilitated examination of the cingulum. Although the accumulated information is undoubtedly important (Schrader, 1973; Cox, 1977; Krammer, 1982; Mann, 1986; Schoeman & Archibald, 1986), it also remains incomplete, because clean fractures of diatom cells are rarely obtained. As a consequence of these limitations such structural features tend to be omitted from present taxonomic studies. To allow a more analytical and comprehensive study of raphe-associated structures to be made, we describe herein an innovative technique to enhance the SEM characterization of diatom specimens in transapical thin sections.

This method, which yields both clean and predominantly undamaged skeletal cross-sections, allows for the study of intact valvar structures, even of weak girdle bands once the organic content has been completely removed. We have tested this method using several pennate diatoms within the genera *Navicula* Bory and *Gyrosigma* Hassall, as well as for some more delicate members of the genus *Haslea* Simonsen.

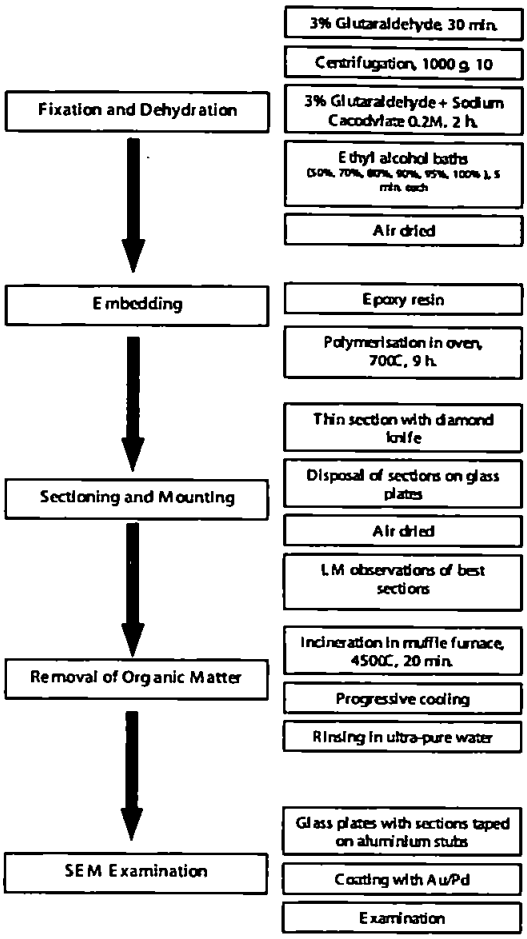


Fig. 1. Step-by-step procedure for the production and analysis of thin cross-sections of diatoms.

## Experimental

Benthic diatoms were collected by sampling the top surface (1–2 cm) of mudflats in the Bay of Bourgneuf, France. In the laboratory, diatoms were isolated under the optical microscope from the soft sediments by manually transferring cells with a pipette to 250 mL Erlenmeyer flasks. Diatom cells were grown in F/2-enriched sea-water (Guillard, 1975) at 14 °C, with an illumination of 100 $\mu$mol $m^{-2}$ $s^{-1}$ provided by cool-white fluorescent tubes (LD 14 : 10 h cycle). Cells were harvested during the exponential growing phase, transferred to 10 mL tubes and centrifuged at 1000 *g* for 10 min to minimize frustule disconnection and apex breakage (Fig. 1).

In order to maintain cell integrity, cells were fixed for 30 min at room temperature in a 3% glutaraldehyde solution prepared with the culture medium as described by Nassiri *et al.* (1998). Fixed cells were then centrifuged (1000 *g*, 10 min), the supernatant removed and the fixation continued for an additional 2 h in a 3% glutaraldehyde solution buffered with sodium cacodylate (0.2 M). Samples were dehydrated for 5 min in each of the serial alcohol baths (50%, 70%, 80%, 90%, 95% and 100%) following the method described by Beninger *et al.* (1995) and embedded in Spurr's epoxy resin (Spurr, 1969; McCully *et al.*, 1980; Reimann *et al.*, 1980) according to the modified technique outlined by Nassiri *et al.* (1998) in order to maximize a suitable orientation of the diatom cells prior to sectioning. The polymerization of the resin was then accelerated by transfer of the embedded capsules to a laboratory oven for 9 h (70 °C).

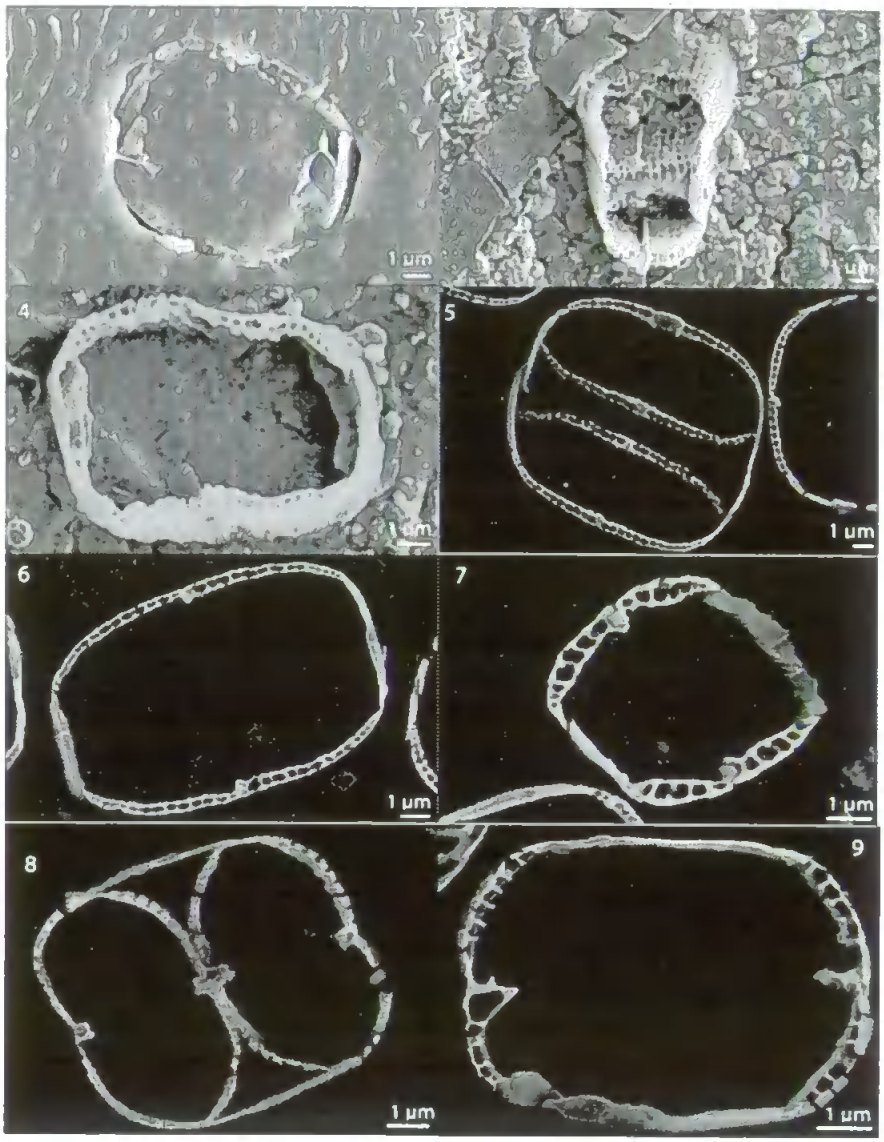


Fig. 2. SEM images of transapical thin sections of diatom valves. Transapical section of a diatom showing mainly the embedding resin with all valvar features obscurred.

Fig. 3. Thin sections of diatoms following the evaporation of the embedding resin. Note the remaining organic matter between the siliceous layers and the cut sections.

Fig. 4. Thin sections of diatoms following the evaporation of the embedding resin. Note the remaining organic matter between the siliceous layers and the cut sections.

Fig. 5. Transapical sections performed with a diamond knife, heated to burn the resin and rinsed to eliminate the residues of organic matter. Cross-section of a cell in division at the valve centre of *Gyrosigma* cf. *limosum*.

Fig. 6. Cross-section through the middle of the valve of *Gyrosigma* cf. *limosum*.

Fig. 7. Cross-section near the valve apex of *Gyrosigma* cf. *limosum*.

Fig. 8. Cross-section of a cell in division at the valve centre of *Navicula ramosissima*.

Fig. 9. Cross-section through the middle of the valve of *Haslea crucigera*.

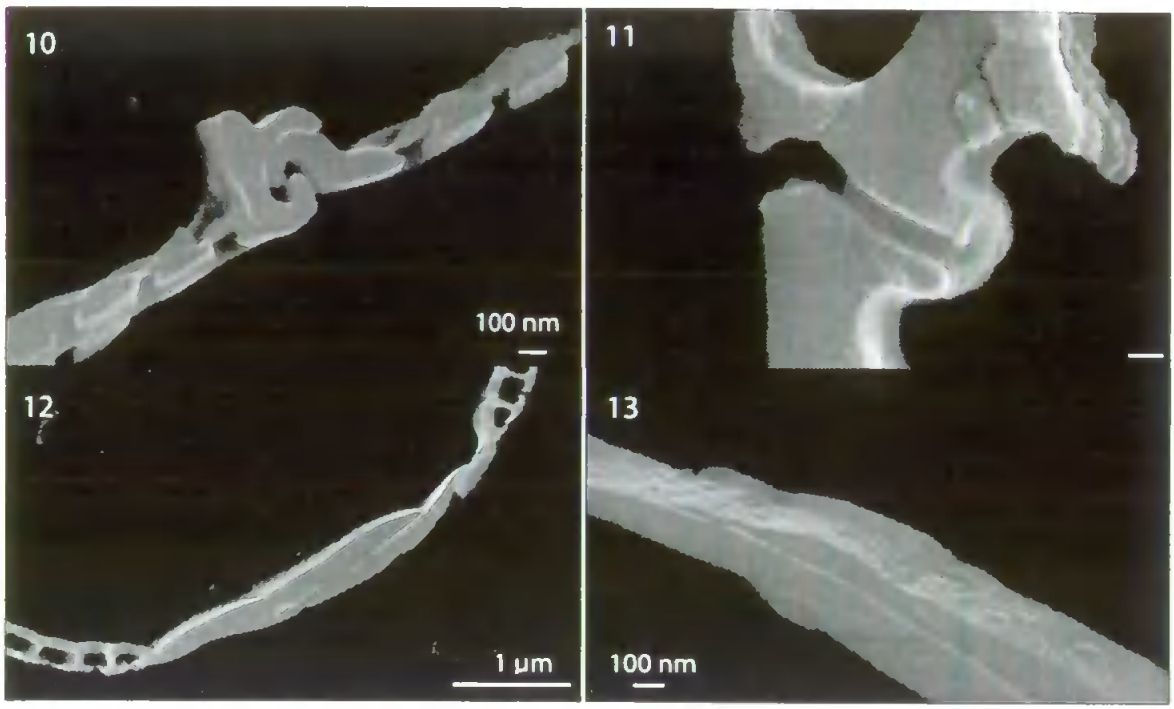


Fig. 10. SEM images of transapical thin sections of diatom valves at high magnification. Sectioning was performed with a diamond knife heated to burn the resin and rinsed to eliminate the residues of organic matter. Cross-section at the valve centre of *Navicula ramosissima* showing details of the C-shaped raphe fissure.
Fig. 11. Cross-section focusing on raphe-associated features at the valve centre of *Gyrosigma* sp.
Fig. 12. Cross-sections of *Gyrosigma* sp. showing details of the cingulum.
Fig. 13. Cross-sections of *Gyrosigma* sp. showing details of the cingulum.

Different types of glass and diamond knives were tested with a Reichert OM-U3 ultramicrotome ( ) in order to obtain thin (250–500 nm) sections. Sections were then picked up with an eyelash, disposed on a circular glass cover slide, air dried and examined in LM. Slides with suitable thin sections were heated in a Pyrolabo WE 01 muffle furnace ( ) (450 ± 10 °C, 20 min) to remove the resin and all of the intracellular organic matter. After a gradual cooling in the furnace (≈1 h), the slides were taped onto another glass plate, which was then placed in a beaker with ultra-pure water with gentle stirring (15 min). The slides were then mounted with carbon tape onto aluminium stubs, coated with Au/Pd and examined in SEM (JEOL 6400F) at an accelerating voltage of 6–8 kV, a 10–15 mm working distance and a tilt angle of 6–10°.

## Results and discussion

In order to establish a satisfactory experimental protocol for obtaining thin sections of sufficient quality suitable for SEM analysis, we made a number of modifications to an elementary method.

Initially, we used glass knives to cut transapical sections of diatoms, which were placed on a glass slide, coated with Au/Pd and examined immediately by SEM. The embedding medium clearly achieved its main fixing function, but we were unable to see the ultrastructure of the diatom valves, because they were completely obscured by the surrounding resin (Fig. 2). The only noticeable feature was a circular outline in the resin, indicating that a section of a diatom valve was present. However, as it is impossible to cut through diatom frustules without using any embedding medium, we had to find a method by which it would be feasible to remove the resin from the diatom shells after sectioning with glass knives, without displacing the valvar and connective pieces. Therefore, our second attempt involved removal of the embedding resin by incinerating the sectioned material on the slide at a minimum of 450 °C (Zoto *et al.*, 1973; Germain, 1981; Ricard, 1987), which should also remove all the intracellular organic matter.

Following this modification, SEM observations revealed that the general morphological outline was conserved without disconnection of the two valves or girdle bands. However, some residues were still visible on sectioned diatoms, particularly between the siliceous layers. In addition, because the appearance of the sections were not 'clean' but ripped (Figs 3 and 4), presumably due to the inferior cutting capability of the glass knife, a further modification was needed.

Thus, the final protocol involved the use of a SPI diamond knife to produce thin cross-sections, incineration to remove most of the organic matter, and finally rinsing these sections with distilled water to eliminate unwanted residues. These modifications resulted in sharp, well-defined thin sections through the diatom shells. When examined in SEM, the transapical sections appeared extremely clear with a perfect cutting plane through the diatom frustules (Figs 5–13). There were no residual traces of the embedding resin or the organic content in the diatom cells and all the skeletal structural features were both well defined and distinct.

By using this technique, the integrity of the valve structures was generally preserved (Figs 5–13). The chambered areolation was quite obvious in *Gyrosigma* cf. *limosum* Sterrenburg & Underwood (Figs 5–7) and *Haslea crucigera* (W. Smith) Simonsen (Fig. 8), as well as the characteristic raphe-associated structures at various locations on *Gyrosigma* valves. In addition, the integrity of the girdle bands between the two valves of the frustules was largely maintained with this method (Figs 5–9). At higher magnification, these valvar features were observed in even greater detail. The raphe-associated structures at the centre of the valves of *Navicula ramosissima* (C.A. Agardh) Cleve and *Gyrosigma* sp. clearly show distinct fissures, including a raphe-sternum and an axial costa (Figs 10 and 11), while the details of the cingulum are well illustrated for *Gyrosigma* sp. (Figs 12 and 13).

In conclusion, the information available via this innovative technique should complement that obtained from conventional SEM methods and therefore contribute to a better definition of the various elements of diatom valves and our understanding of the phylogeny of the diatom genera. Furthermore, because serial cross-sections from a single cell can be obtained, it is also possible to follow the organization of these valvar features along the entire length of the valve (Figs 5–7). Finally, there is also the potential for such a technique to be used comparatively in morphogenetic studies (Figs 5 and 8), which may complement TEM (e.g. Stoermer *et al.*, 1964) or SEM (e.g. Schmid, 1979; Cox, 1999b) observations.

## Acknowledgements

We would like to thank the University of Plymouth, U.K., and the Université de Nantes, France, for financial and logistic support to G.M. We also thank the Canadian Museum of Nature for its financial support to M.P. and to a referee for some extremely useful comments on the manuscript.

## References

Beninger, P.T., Potter, T.M. & St-Jean, S.D. (1995) Paddle cilia fixation artefacts in pallial organ of adult *Mytilus edulis* and *Placopecten megellanicus* (Mollusca: Bivalvia). *Can. J. Zool.* 73, 610–614.

Claugher, D., ed. (1990) *Scanning Electron Microscopy in Taxonomy and Functional Morphology.* Systematics Association Special Volume no. 41. Clarendon Press, Oxford.

Cleve, P.T. (1894) Synopsis of the naviculoid diatoms. Part 1. *K. Svenska Vetensk. Akad. Handl.* 26, 1–194.

Cleve, P.T. (1895) Synopsis of the naviculoid diatoms. Part 2. *K. Svenska Vetensk. Akad. Handl.* 27, 1–235.

Cleve, P.T. & Grunow, A. (1880) Beiträge zur Kenntniss der arctischen Diatomeen. *K. Svenska Vetensk. Akad. Handl.* 17, 1–121.

Cox, E.J. (1977) Raphe structure in naviculoid diatoms as revealed by the scanning electron microscope. *Nova Hedwigia, Beih.* 54, 261–274.

Cox, E.J. (1999a) Studies on the diatom genus *Navicula* Bory. VIII. Variation in valve morphology in relation to the generic diagnosis based on *Navicula tripunctata* (O.F. Müller) Bory. *Diatom Res.* 14, 207–237.

Cox, E.J. (1999b) Variations in patterns of valve morphogenesis between representatives of six biraphid diatom genera (Bacillariophyceae). *J. Phycol.* 35, 1297–1312.

Cox, E.J. & Ross, R. (1981) The striae of pennate diatoms. *Proceedings of the Sixth Symposium on Recent and Fossil Diatoms. Otto Koeltz, Koenigstein* (ed. by R. Ross), pp. 267–278.

Drum, R.W., Pankratz, H.S. & Stoermer, E.F. (1966) Chapter title? *Diatomeenschalen im elektronenmikroskopischen Bild*, Vol. 6 (ed. by J.-G. Helmcke and W. Krieger), pp. 1–25. Publisher, Town?

Edgar, L.A. & Pickett-Heaps, J.D. (1984) Valve morphogenesis in the pennate diatom *Navicula cuspidata*. *J. Phycol.* 20, 47–61.

Gaul, U., Geissler, U., Henderson, M., Mahoney, R. & Reimer, C.W. (1993) Bibliography of the fine-structure of diatom frustules (Bacillariophyceae). *Proc. Acad. Nat. Sci. Phila.* 144, 69–238.

Gerloff, J. & Helmcke, J.-G. (1974) Chapter title? *Diatomeenschalen im elektronenmikroskopischen Bild*, Vol. 8 (ed. by J.-G. Helmcke, W. Krieger and J. Gerloff), pp. 1–34.Publisher, Town?

Germain, H. (1981) *Flore des Diatomées. Eaux Douces et Saumâtres.* Société Nouvelle des Éditons Boubée, Paris.

Grunow, A. (1884) Die Diatomeen von Franz Josefs-Land. *Akad. Wiss. Math.-Naturw. Kl., Danks. Wien.* 48, 53–112.

Guillard, R.R.L. (1975) Culture of phytoplankton for feeding marine invertebrates. *Culture of Marine Invertebrates Animals* (ed. by W. L. Smith and M. H. Chanley, M.H), pp. 26–60. Plenum Press, New York.

Krammer, K. (1982) Observations on the raphe slit of some Bacillariophyceae and ideas on its function. *Arch. Hydrobiol. Supplement*, 63, 177–188.

Mann, D.G. (1981) Sieves and flaps: siliceous minutiae in the pores of raphid diatoms. *Proceedings of the Sixth Symposium on Recent and Fossil Diatoms* (ed. by R. Ross), pp. 279–301. Koeltz Scientific Books, Koenigstein.

Mann, D.G. (1986) Nitzschia, subgenus Nitzschia. (Notes for a Monograph of the Bacillariophyseae, 2). *Proceedings of the Eighth International Diatom Symposium* (ed. by M. Ricard), pp. 215–227. Koeltz Scientific Books, Koenigstein.

McCully, M.E., Goff, L.J. & Adshead, P.C. (1980) Preparation of algae for light microscopy. *Handbook of Phycological Methods. Developmental and Cytological Methods* (ed. by E. Gantt), pp. 263–283. Cambridge University Press, Cambridge.

Mereschkowsky, C. (1901) Études sur l'endochrome des diatomées. *Mém. Acad. Imp. Sci. St.-Pétersb., Sér. VIII, Cl. Phys.-Math.* 11, 1–40.

Mereschkowsky, C. (1902–03) Les types de l'endochrome chez les diatomées. *Scripta Bot. (St.-Pétersb.)*, 21, 1–106(in Russian), 107–193(in French).

Nassiri, Y., Robert, J.-M., Rincé, Y. & Ginsburger-Vogel, T. (1998) The cytoplasmic fine structure of the diatom *Haslea ostrearia* (Bacillariophyceae) in relation to marennine production. *Phycologia*, 37, 84–91.

Paddock, T.B.B. & Sims, P.A. (1990) Micromorphology and evolution of the keels of raphe-bearing diatoms. *Scanning Electron Microscopy in Taxonomy and Functional Morphology* (ed. by D. Claugher), pp. 171–191. Systematics Association Special Volume No. 41. Clarendon Press, Oxford.

Pickett-Heaps, J.D., Tippit, D.H. & Andreozzi, J.A. (1979a) Cell division in the pennate diatom *Pinnularia*. III – The valve and associated cytoplasmic organelles. *Biol. Cell.* 35, 195–198.

Pickett-Heaps, J.D., Tippit, D.H. & Andreozzi, J.A. (1979b) Cell division in the pennate diatom *Pinnularia*. IV –Valve morphogenesis. *Biol. Cell.* 35, 199–206.

Pocock, K.L. & Cox, E.J. (1982) Frustule structure in the diatom *Rhabdonema arcuatum* (Lyngb.) Kütz. *Nova Hedwigia, Beih.* 36, 621–641.

Reimann, B.E.F., Duke, E.L. & Floyd, G.L. (1980) Fixation, embedding, sectioning, and staining of algae for electron microscopy. *Handbook of Phycological Methods. Developmental and Cytological Methods* (ed. by E. Gantt), pp. 285–303. Cambridge University Press, Cambridge.

Ricard, M. (1987) *Diatomophycées*. Vol. 2. Atlas du Phytoplancton Marin (ed by A. Sournia). Centre National de la Recherche Scientifique, Paris.

Round, F.E., Crawford, R.M. & Mann, D.G. (1990) *The Diatoms*. Cambridge University Press, Cambridge.

Schmid, A.-M.M. (1979) The development of structure in the shells of diatoms. *Nova Hedwigia, Beih.* 64, 219–232.

Schoeman, F.R. & Archibald, R.E.M. (1986) *Gyrosigma rautenbachiae* Cholnoky (Bacillariophyceae): its morphology and taxonomy. *Nova Hedwigia*, 43, 129–157.

Schrader, H.-J. (1973) Types of raphe structures in the diatoms. *Nova Hedwigia, Beih.* 45, 195–230.

Spurr, A.R. (1969) A low viscosity epoxy resin embedding medium for electron microscopy. *J. Ultrastruct. Res.* 26, 31–43.

Stoermer, E.F., Pankratz, H.S. & Drum, R.W. (1964) The fine structure of *Mastogloia grevillei* Wm. *Smith. Protoplasma*, 59, 1–13.

Van Heurck, H. (1880–1885) *Synopsis des diatomées de Belgique*. H. Van Heurck, Anvers.

Zoto, G.A., Dillon, D.O. & Schlichting, H.E. (1973) A rapid method for cleaning diatoms for taxonomic and ecological studies. *Phycologia*, 12, 69–70.

*Submitted to European Journal of Phycology*

# MORPHOLOGICAL, BIOCHEMICAL AND MOLECULAR EVIDENCE FOR THE TRANSFER OF *GYROSIGMA NIPKOWII* MEISTER TO THE GENUS *HASLEA* (BACILLARIOPHYTA)

Michel POULIN [a], Guillaume MASSÉ [b c], Simon T. BELT [c], Philippe DELAVAULT [d], Florence ROUSSEAU [e], Jean-Michel ROBERT [b] & Steve J. ROWLAND [c]

[a] Research Division, Canadian Museum of Nature, P.O. Box 3443, Station D, Ottawa, Ontario K1P 6P4, Canada; mpoulin@mus-nature.ca

[b] Laboratoire de Biologie Marine, ISOMer, Université de Nantes, 2 rue de la Houssinière, 44322 Nantes Cedex 3, France

[c] Petroleum and Environmental Geochemistry Group, Department of Environmental Sciences, University of Plymouth, Drake Circus, Plymouth, Devon PL4 8AA, United Kingdom

[d] Groupe de Physiologie et Pathologie Végétales, Université de Nantes, 2 rue de la Houssinière, 44322 Nantes Cedex 3, France

[e] Institut de Systématique, UPMC-MNHN-CNRS FR 1541, Laboratoire de Cryptogamie, 12 rue Buffon, 75005 Paris, France

**ABSTRACT** The genus *Haslea* Simonsen has been erected to accommodate spindle-shaped valves with acute apices, convex margins, straight raphe and approximate central pores, inconspicuous areas, and transapical striae crossed at a right angle by a longitudinal pattern with a slit apically oriented in each areola. Investigations on mudflats from the French Atlantic coast revealed the presence of a sigmoid diatom sharing characteristics with both *Gyrosigma* Hassall and *Haslea*. Following a thorough morphological study in light and scanning electron microscopy in addition to biochemical and molecular analysis, we are proposing the following new combination, *Haslea nipkowii* (Meister) Poulin & Massé. Despite a deviant sigmoidicity, this taxon shows diagnostic features of *Haslea* with longitudinal slits running externally from one pole to the other, all merging with a peripheral slit at the apex, and the presence of small areolae beyond the helictoglossa. Unique to *H. nipkowii* are the unequal T-shaped distal raphe fissures, the overlapping and deflected proximal raphe ends, and the overhanging axial costa on the primary side of the valve. Similarly, this taxon proved to synthesize $C_{25}$ highly branched isoprenoids typical of the genus *Haslea* with a double bond always present between $C_6$ and $C_5$. The molecular analysis performed on 7 species of *Haslea* and 2 sigmoid taxa has established the monophyly of the genus *Haslea* including *H. nipkowii*.

*Key words: Diatoms, Gyrosigma, Haslea, new combination, ultrastructure, HBI, DNA analysis.*

PERGAMON

Phytochemistry 56 (2001) 597–602

PHYTOCHEMISTRY

www.elsevier.com/locate/phytochem

# Effects of temperature on polyunsaturation in cytostatic lipids of *Haslea ostrearia*

S.J. Rowland [a,*], S.T. Belt [a], E.J. Wraige [a,1], G. Massé [a,b], C. Roussakis [b], J.-M. Robert [b]

[a] *Department of Environmental Sciences, University of Plymouth, Drake Circus, Plymouth PL4 8AA, UK*
[b] *ISOMer, Faculté des Sciences et des Techniques, Université de Nantes, 2, Rue de la Houssinière, 44027 Nantes, Cedex 03, France*

Received 8 June 2000; received in revised form 3 October 2000

**Abstract**

Unusual chemicals produced by the 'blue oyster' diatom, *Haslea ostrearia*, include the water-soluble blue pigment marennine and numerous polyunsaturated sesterterpene oils or haslenes. Aqueous extracts of the alga exhibit in vitro and in vivo activities against human lung cancer cells and anti-HIV effects. Here we report that three haslenes also demonstrate in vitro cytostatic action against a human lung cancer cell line. The most active haslene is the most unsaturated and unsaturation in the haslenes increases with increasing algal growth temperature. © 2001 Elsevier Science Ltd. All rights reserved.

*Keywords:* *Haslea ostrearia*; Bacillariophycane; Diatoms; Isoprenoid alkenes; Haslenes; Highly branched isoprenoids; Temperature; Unsaturation; Cancer; Cytostatic

## 1. Introduction

Haslenes are unsaturated $C_{25}$ highly branched isoprenoid (HBI) hydrocarbons which apparently originate from relatively few species of diatomaceous algae (Volkman et al., 1994; Sinninghe Damsté et al., 1999; Belt et al., 2000). Nonetheless, they are widely distributed and sometimes abundant in aquatic environments and, for instance, are found in sediments from the USA, UK and mainland Europe (Robson and Rowland, 1986; Rowland and Robson, 1990) and even Antarctica (Johns et al., 1999), where they are thought to originate from diatoms living on sea-ice (Nichols et al., 1988).

Laboratory culturing experiments under axenic conditions (Wraige et al., 1999) have shown that one biological producer of haslenes is *Haslea ostrearia*, which is a large pennate diatom (Round et al., 1990). Other diatom sources include other *Haslea* species (Massé et al., in press), *Rhizosolenia setigera* (Volkman et al., 1994; Sinninghe Damsté et al., 1999) and *Pleurosigma intermedium* (Belt et al., 2000) although these have yet to be shown to produce haslenes under axenic conditions. The structures and configurations of many of the haslenes from *H. ostrearia* have been established previously by spectroscopic studies (e.g. Belt et al., 1996; Johns et al., 1999; Wraige et al., 1999). Since several haslenes have been obtained pure in milligram to gram quantities, and given the anti-cancer and anti-HIV activities of some other chemicals produced by *H. ostrearia* (Carbonnelle et al., 1999; Bergé et al., 1999), we decided to determine whether the haslenes also exhibited bioactivity.

Activity *was* observed but varied for dienes, trienes and tetraenes. We therefore examined some factors controlling unsaturation (cf. Wraige et al., 1998). Temperature exhibited the major effect, unsaturation increasing with increasing temperature.

## 2. Results and discussion

Milligram quantities of pure hasla-6(17),23-diene (I), 22*R* and 22*RS*-hasla-6(17),9,23-trienes (II) and

* Corresponding author. Tel.: +44-1752-233013; fax: +44-1752-233035.
*E-mail addresses:* s.rowland@plymouth.ac.uk (S.J. Rowland), s.belt@plymouth.ac.uk (S.T. Belt).
[1] Present address: Ecotoxicology and Hazardous Substances National Centre, Environment Agency, Howbery Park, Wallingford, Oxon, OX10 8BD, UK.

0031-9422/01/$ - see front matter 
PII: S0031-9422(00)00434-9

hasla-6(17),9,13,23-tetraene (**III**) were isolated from pastes obtained from large-scale cultures of *H. ostrearia* as reported previously (e.g. Johns et al., 1999; Wraige et al., 1999). We then measured the concentration of each pure haslene in aqueous dimethylsulfoxide solution required to reduce the growth of an evolving, human non-small-cell bronchopulmonary carcinoma cell line (Roussakis et al., 1991) in vitro by 50% in 72 h ($IC_{50}$) compared to untreated controls (Mosmann, 1983). This is a widely accepted preliminary screening measure of in vitro cytotoxic activity (Suffness and Pezzuto, 1991). For comparison with other studies, we also measured the $IC_{50}$ of the tetraene (compound **III**) against a non-evolving murine cancer cell line ($P_{388}$) (Suffness and Pezzuto, 1991). Haslenes with three and four degrees of unsaturation were able to produce an effect (Table 1).

Cytocidal activities of chemicals are not uncommon in in vitro tests of marine natural products (e.g. Patterson et al., 1991) but at some concentrations the haslenes exhibited only anti-proliferative or cytostatic effects on the growth of the NSCLC-N6 cell line without cytocidal activity. That is, the growth of the cancer cells was slowed or halted but the cells were not killed. Further specificity was indicated by an observed effect of the triene on the NSCLC-N6 cell line (Roussakis et al., 1991) whereas there was no such effect on a clone of this line. It would be interesting to isolate larger quantities for more refined in vivo bioactivity tests and particularly to examine the effects of more unsaturated haslenes such as the pentaenes and hexaenes. We therefore investigated the culture conditions necessary for production of polyunsaturates.

Unsaturation in the so-called *normal* (unbranched) lipids of plants, which are principally esters of fatty acids, usually increases with decreasing growth temperature. This is thought to be a protective response to chilling and to involve regulation of properties such as membrane fluidity and stability (reviewed by Quinn et al., 1989). Essentially the principle is that *cis*-double bonds decrease the melting point of a normal lipid and, therefore, organisms living in low temperature environments require more unsaturated *normal* lipids to preserve fluidity. This general inverse relationship with temperature apparently also extends to the *normal* lipids of some algae. Thus lipid unsaturation in the widespread sedimentary *n*-alkenones derived from some prymnesiophyte algae has been widely used as a proxy measure of palaeo-sea surface temperatures for palaeoclimatic studies (e.g. Eglinton et al., 1992). However, there are numerous exceptions to this common relationship where *normal* lipids possess more than two double bonds (e.g. Farkas et al., 2000 and references therein) and neither is it known what the effect of the *trans*-double bonds, which usually occur in acyclic isoprenoids such as haslenes, would have on melting point and fluidity. All haslenes isolated thus far (e.g. Belt et al., 1994) and even the parent saturated haslane (Robson and Rowland, 1986) are oils even at room temperature.

In preliminary experiments with *H. ostrearia* cultures, we noted considerable diversity in haslene distributions as revealed by gas chromatography–mass spectrometry (GC–MS; Wraige et al., 1997). Since salinity appeared to exhibit no appreciable effect on unsaturation (Wraige et al., 1998), we investigated the effect of growth temperature on haslene distributions. Small-scale batch cultures of *H. ostrearia* were grown in the laboratory in replicate in a controlled atmosphere in modified Provosali media at constant salinity and irradiance intensity at temperatures of 5, 15 and 25±0.5°C. A stock of the alga used as inocula for these experiments was grown at 15±1°C for multiple generations. Lipid extracts were obtained by solvent extraction and examined by GC–MS (Johns et al., 1999; Wraige et al., 1999).

Whilst growth from the inoculum was slow to initiate at 5°C, requiring about 10 days to reach the logarithmic phase (Fig. 1a) the only haslenes produced between 10 and 27 days, were the 6(17), 23 and 5, 23 dienes (Figs. 2 and 3, compounds **I** and **IV**) the structural characterizations of which, we have reported previously (e.g. Belt et al., 1994; Johns et al., 1999). A re-equilibration thus occurred from the corresponding triene isomer distributions, which dominated the inoculum grown at 15°C. However, cell growth had not reached the stationary phase by 27 days (ca. 170,000 cell $ml^{-1}$) so we cannot rule out the possibility that more unsaturated haslenes could be produced in later growth, though we consider it unlikely. Indeed, monitoring of a single growth cycle of the alga at 15°C, revealed faster growth than at 5°C, probably partially due to prior acclimation of the stock culture at this temperature and in this case

Table 1
Cytostatic activity of individual haslenes to cell line NSCLC-N6 established from a primary epidermoid carcinoma of human origin (Roussakis et al., 1991) assayed by the methods of Mosmann (1983)

| Haslene | Structure number (Fig. 2) | $IC_{50}$[b] ($\mu g\ ml^{-1}$) | Cancer cell line[a] (in vitro) |
|---|---|---|---|
| Hasla-6(17), 23-diene | I | > 30 (Inactive) | NSCLC-N6 (Human lung) |
| 22*R*-Hasla-6(17), 9,23-triene | II | 13.4 | NSCLC-N6 (Human lung) |
| 22*RS*-Hasla-6(17), 9,23-triene | II | 14.4 | NSCLC-N6 (Human lung) |
| Hasla-6(17),9,13, 23-tetraene | III | 3.8 | NSCLC-N6 (Human lung) |
| Hasla-6(17),9,13, 23-tetraene | III | < 3.3 | $P_{388}$ (Mouse) |

[a] The NSCLC-N6 cell line derives from a human non-small-cell bronchopulmonary carcinoma (moderately differentiated, rarely keratinizing, classified as T2NOMO).

[b] $IC_{50}$ is the concentration of haslene required to reduce the cancer cell concentration by 50% compared to untreated controls after 72 h.

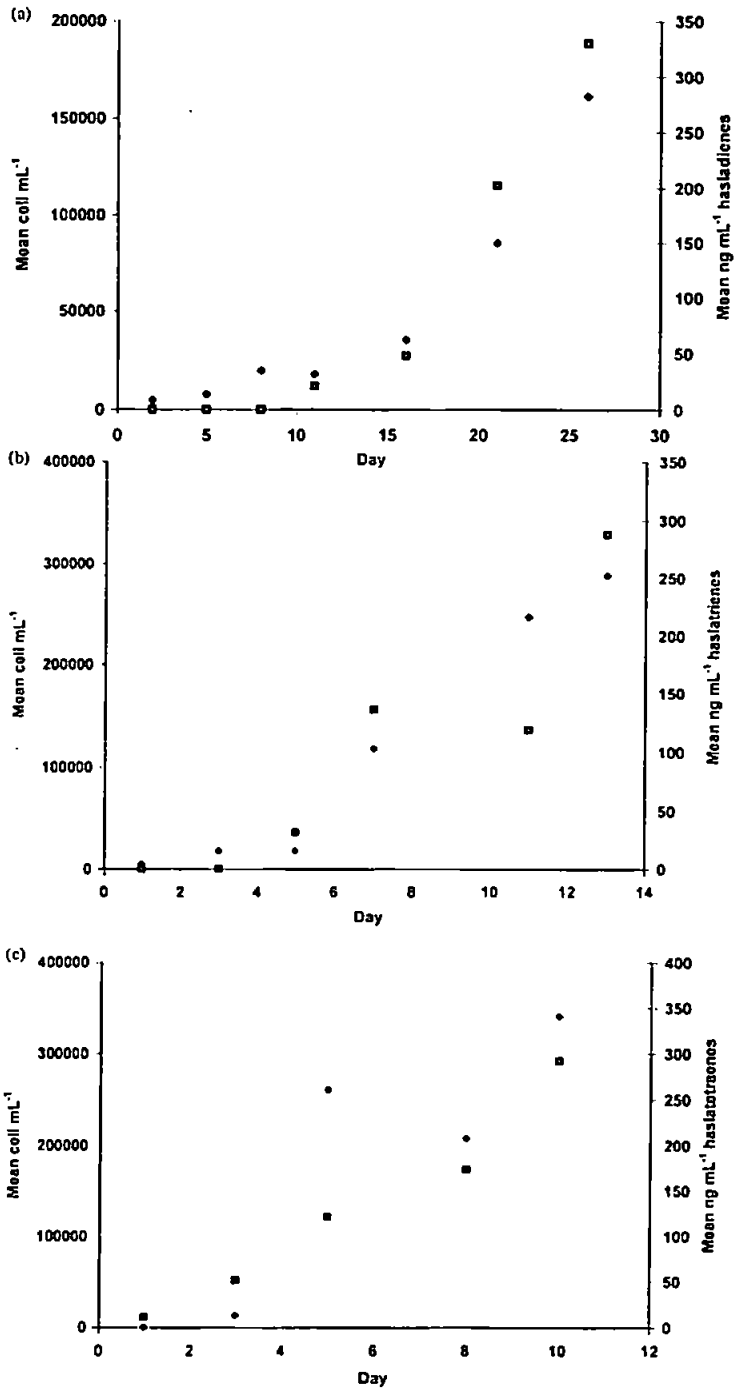


Fig. 1. Mean ($n=4$) cell concentration (◆) and total haslene production (■) in *H. ostrearia* at (a) 5°C (hasla-5,23-diene plus 6(17),23 diene), (b) 15°C (hasla-5,9,23-triene plus 6(17),9,23 triene), (c) 25°C (hasla-5,9,13,23-tetraene plus 6(17),9,13,23 tetraene).

at a cell concentration of ca. 170,000 cell $ml^{-1}$ at day 7 (Fig. 1b), the hasla-trienes (compounds II and V) were dominant (Fig. 3), as they were in the inoculum. Between day 5 and day 11, tetraenes (compounds III and VI) were also detected (Fig. 3). At 25°C, production of successively more polyunsaturated analogues was observed, including production of tetraenes by day 3 and additionally, pentaene production from day 8 (ca. 170,000 cell $ml^{-1}$; Figs. 1c and 3). Thus, there is a significant relationship between culture temperature (and perhaps growth phase) and haslene unsaturation, together with a quite rapid equilibration of haslene distributions with temperature. No such effect was observed on the haslapentaene VII produced by *R. setigera* (Sinninghe Damsté et al., 1999).

Opportunities to examine the effects of phenotypic variables on unsaturation in algal isoprenoids do not often arise. Acyclic isoprenoids (presumably including the haslenes) are initially biosynthesised as polyunsaturated species via isopentenyl diphosphate and dimethylallyl diphosphate, unlike *n*-fatty acids which are mainly desaturated after production (Quinn et al., 1989). Although many algae produce polyunsaturated isoprenoid alkenes such as squalene, lycopene, phytoene and other carotenes, the efficiency of the cyclisation of squalene to sterols and of the desaturation of phytoene to other carotenoids means that significant accumulation of unsaturated hydrocarbons is usually not observed in micro-organisms. Significant amounts of partially saturated squalenes are found in some archaebacteria, such as the anaerobic, thermophilic methanogen, *Methanobacterium thermoautotrophicum* and the variations in unsaturation have been suggested to allow internal proton regulation (Tornabene et al., 1979). However, it has also been argued that the effects of hydrogen flux in the corresponding ether lipids would outweigh those in the hydrocarbons and nothing conclusive is known.

Determination of whether the biosynthesis of the haslenes is *via* the mevalonate or non-mevalonate route may be helpful in elucidating their location and functions (cf. Rohmer et al., 1996).

Culturing of *H. ostrearia* should seemingly be conducted at the higher growth temperatures used herein (e.g. 25°C) if the production of the tetra- and pentaunsaturated haslenes is to be maximised for further bioactivity testing with cancer cells.

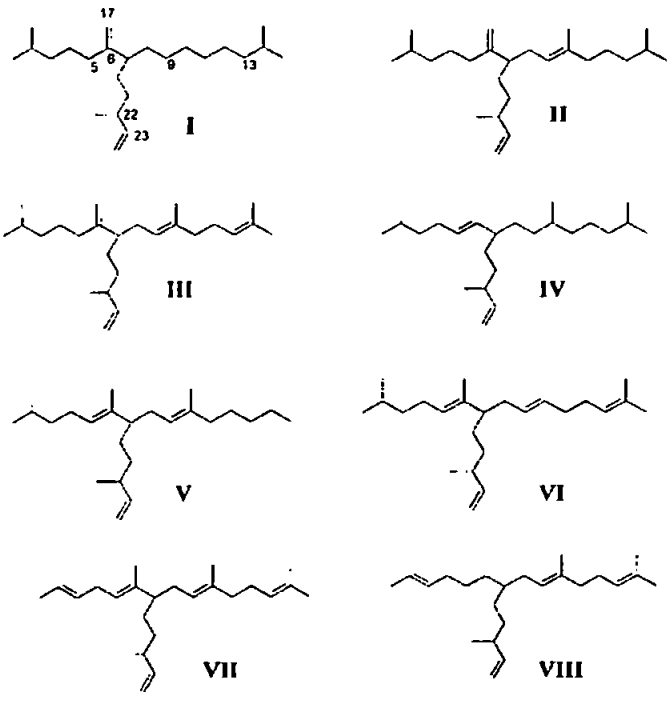


Fig. 2. Structures of haslenes produced by *Haslea ostrearia* at different culture temperatures. Structures were established previously by NMR spectroscopy and other techniques applied to milligram quantities of pure haslenes isolated from larger batch cultures of *H. ostrearia* (e.g. Belt et al., 1994, 1996; Johns et al., 1999; Wraige et al., 1999).

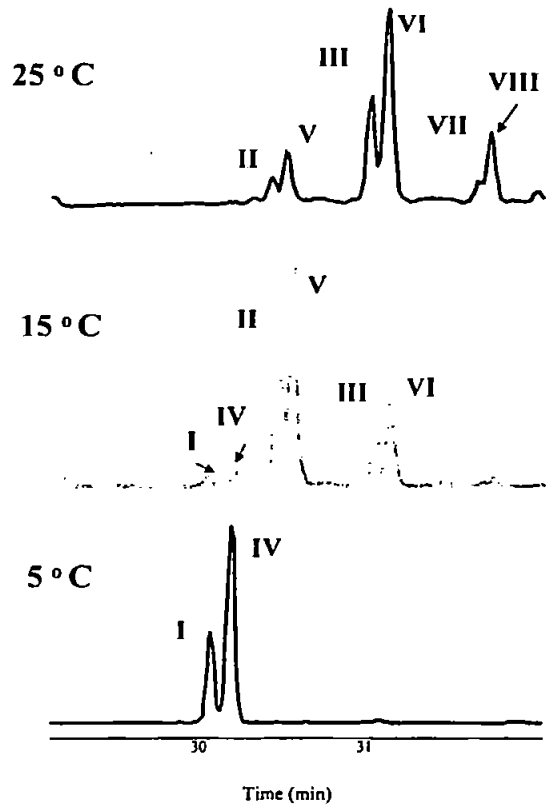


Fig. 3. Partial gas chromatograms illustrating the distributions of haslenes in *H. ostrearia* cultures grown at 5 (day 27), 15 (day 7) and 25°C (day 10). Structures of the haslenes are shown in Fig. 2. Identities were confirmed by comparison of retention indices and mass spectra with authenticated compounds. Gas chromatography–mass spectrometry conditions: HP 5890 GC-MSD 12 m HP- Ultra 1 column, 50–300 at 5°C 40 eV.

## 3. Experimental

### 3.1. Cytostatic tests

The cytostatic activity of individual haslenes (I–III) to cell line NSCLC-N6 established from a primary epidermoid carcinoma of human origin (Roussakis et al., 1991) was assayed by the method of Mosmann (1983). The cells were cultured in RPMI 1640 medium with 5% fetal calf serum, to which was added 100 µl of penicillin, 100 µg streptomycin $ml^{-1}$ and 2 mM glutamine, at 37°C in a 5% $CO_2$ atmosphere.

Experiments were performed in conditions of continuous exposure, in solution in water + 5% dimethylsulphoxide on microtiter plates ($2\times10^5$ cells $ml^{-1}$). Cell growth was estimated by a colorimetric assay based on the conversion of tetrazolium dye (MTT) to a blue formazan product by live mitochondria. Three concentrations were tested in duplicate. Cell growth was estimated at day 0 and day 3 (72 h) and for investigation of cytostatic and anti-proliferative effects also at 24 and 48 h.

### 3.2. Algal cultures

*H. ostrearia* was isolated from oyster ponds of the Baie de Bourgneuf (France). Cultures were grown in quadruplicate in 250 ml Erlenmeyer flasks at 5, 15 and 25°C with illumination provided by cool-white fluorescent tubes in a 14/10 h light/dark cycle. They were incubated in a modified ES 1/3 Provasoli medium at salinities of ca. 32 per mil under 100 µmol photons $m^{-2}$ $s^{-1}$ irradiance. Samples were harvested by filtration. The structures of the haslenes isolated from larger batch cultures were established previously by NMR spectroscopy (e.g. Belt et al., 1994; 1996; Johns et al., 1999; Wraige et al., 1999).

### 3.3. Instrumental

GC–MS was performed using a Hewlett Packard 5890 series II gas chromatograph coupled to a Hewlett Packard 5970 mass selective detector fitted with a 12 m (0.2 mm i.d.) fused silica capillary column (HP-1 Ultra stationary phase). Auto-splitless injection and helium carrier gas were used. The gas chromatograph oven temperature was programmed from 40 to 300°C at 5° $min^{-1}$ and held at the final temperature for 10 min. Mass spectrometer operating conditions were; ion source temperature 250° and 70 eV ionisation energy. Spectra (35–500 Daltons) were collected using Hewlett Packard Chemstation™ software.

## Acknowledgements

We thank the UK Natural Environment Research Council for a ROPA award (1995 scheme) and the British Council for Alliance travel awards.

## References

Belt, S.T., Allard, G., Massé, G., Robert, J.-M., Rowland, S., 2000. Important sedimentary sesterterpenoids from the diatom *Pleurosigma intermedium*. Chemical Communications, 501–502.

Belt, S.T., Cooke, D.A., Hird, S. J., Rowland, S.J., 1994. Structural determination of a highly branched $C_{25}$ sedimentary isoprenoid biomarker by NMR spectroscopy and mass spectrometry. J. Chem. Soc. Chem. Commun. 2077–2078.

Belt, S.T., Cooke, D.A., Robert, J.-M., Rowland, S.J., 1996. Structural characterisation of widespread polyunsaturated isoprenoid biomarkers: A $C_{25}$ triene, tetraene and pentaene from the diatom *Haslea ostrearia* Simonsen. Tetrahedron Letters 37, 4755–4758.

Bergé, J.P., Bougougnon, N., Alban, S., Pojer, F., Billaudel, S., Chermann, J.-C., Robert, J.-M., Franz, G., 1999. Antiviral and anticoagulant activities of a water-soluble fraction of the marine diatom *Haslea ostrearia*. Planta Med. 65, 604–609.

Carbonnelle, D., Pondaven, P., Morancais, M., Massé, G., Bosch, S., Jacquot, C., Braind, G., Robert, J.-M., Roussakis, C., 1999. Antitumor and antiproliferative effects of an aqueous extract from the marine diatom *Haslea ostrearia* (Simonsen) against solid tumors: lung carcinoma (NSCLC-N6), kidney carcinoma (E39) and melanoma (M96) cell lines. Anticancer Res. 19, 621–624.

Eglinton, G., Bradshaw, S.A., Rosell, A., Samthein, M., Pflaumann, U., Tiedemann, R., 1992. Molecular record of secular sea surface temperature changes on 100-year timescales for glacial terminations I, II and IV. Nature 356, 423–426.

Farkas, T., Kitajka, K., Fodor, E., Csengeri, I., Lahdes, E., Yeo, Y.K., Crasznai, Z., Halver, J.E., 2000. Docosahexaenoic acid — containing phospholipid molecular species in brains of vertebrates. Proceedings of National Academy of Sciences 97, 6362–6366.

Johns, L., Wraige, E.J., Belt, S.T., Lewis, C.A., Massé, G., Robert, J.-M., Rowland, S.J., 1999. Identification of a $C_{25}$ highly branched isoprenoid (HBI) diene in Antarctic sediments, sea-ice diatoms and cultured diatoms. Organic Geochemistry 30, 1471–1475.

Massé, G., Rince, Y., Cox, E., Allard, G., Belt, S., Rowland, S., in press. *Haslea saltstonica* sp nov. and *Haslea pseudostrearia* sp. nov., two new diatoms from Salcombe estuary, Devon. Comptes Rend. Acad. Sci.

Mosmann, T., 1983. Rapid colrimetric assay for cellular growth and survival:application to proliferation and cytotoxicity assays. J. Immunol. Methods 65, 55–63.

Nichols, P.D., Volkman, J.K., Palmisano, A.C., Smith, G.A., White, D.C., 1988. Occurrence of an isoprenoid $C_{25}$ diunsaturated alkene and high neutral lipid content in Antarctic sea-ice diatom communities. J. Phycology 24, 90–96.

Patterson, G.M.L., Baldwin, C.L., Bolis, C.M., Caplan, F.R., Karuso, H., Larsen, L.K., Levine, I.A., Moore, R.E., Nelson, C.S., Tschappat, K.D., Tuang, G.D., 1991. Antineoplastic activity of cultured blue-green algae (Cyanophyta). J. Phycology 27, 530.

Quinn, P.J., Joo, F., Vigh, L., 1989. The role of unsaturated lipids in membrane structure and stability. Prog. Biophys. Molec. Biol. 53, 71–103.

Robson, J.N., Rowland, S.J., 1986. Identification of novel, widely-occurring sedimentary sesterterpenoids. Nature 324, 561–563.

Rohmer, R., Seemann, M., Horbach, S., Bringer-Meyer, S., Sahm, H., 1996. Glyceraldehyde 3-phosphate and pyruvate as precursors of isoprenic units in an alternative non-mevalonate pathway for terpenoid biosynthesis. J. Am. Chem. Soc. 118, 2564–2566.

Round, F.E., Crawford, R.M., Mann, D.G., 1990. The Diatoms. Cambridge University Press, Cambridge.

Roussakis, C., Gratas, C., Audouin, A.F., Le Boterff, J., Dabouis, G., Verbist, J.F., 1991. Study of in vitro drug sensitivity on a newly established cell line from a primary bronchial epidermoid carcinoma of human origin (NSCLC-N6). Anticancer Res. 11, 2239.

Rowland, S.J., Robson, J.N., 1990. The widespread occurrence of highly branched acyclic $C_{20}$, $C_{25}$ and $C_{30}$ hydrocarbons in recent sediments: a review. Mar. Environ. Res. 30, 191–216.

Tornabene, T.G., Langworthy, T.A., Holzer, G., Oró, J., 1979. Squalenes, phytanes and other isoprenoids as major neutral lipids of methanogenic and thermoacidophilic "archaebacteria". J. Mol. Evol. 13, 73–83.

Sinninghe Damsté, J.S., Rijpstra, W.I.C., Schouten, S., Peletier, H., van der Maarel, M.J.E.C., Gieskes, W.W.C., 1999. A $C_{25}$ highly branched isoprenoid alkene and $C_{25}$ and $C_{27}$ *n*-polyenes in the marine diatom *Rhizosolenia setigera*. Organic Geochemistry 30, 95–100.

Suffness, M., Pezzuto, J.M., 1991. Assays related to cancer drug discovery. Methods in Plant Biochem. 6, 71–133.

Volkman, J.K., Barrett, S.M., Dunstan, G.A., 1994. $C_{25}$ and $C_{30}$ highly branched isoprenoid alkenes in laboratory cultures of two marine diatoms. Organic Geochemistry 21, 407–414.

Wraige, E.J., Belt, S.T., Lewis, C.A., Cooke, D.A., Robert, J.-M., Massé, G., Rowland, S.J., 1997. Variations in the structures and distributions of $C_{25}$ highly branched isoprenoid (HBI) alkenes in cultures of the diatom, *Haslea ostrearia* (Simonsen). Organic Geochemistry 27, 497–505.

Wraige, E.J., Belt, S.T., Johns, L., Massé, G., Robert, J.-M., Rowland, S.J., 1998. Variations in distributions of $C_{25}$ highly branched isoprenoid (HBI) alkenes in the diatom, *Haslea ostrearia*: influence of salinity. Organic Geochemistry 28, 855–859.

Wraige, E.J., Belt, S.T., Johns, L., Massé, G., Robert, J.-M., Rowland, S.J., 1999. Highly branched $C_{25}$ isoprenoids in axenic cultures of *Haslea ostrearia*. Phytochemistry 51, 69–73.

PERGAMON

Phytochemistry 58 (2001) 717–728

PHYTOCHEMISTRY

www.elsevier.com/locate/phytochem

# Factors influencing the distributions of polyunsaturated terpenoids in the diatom, *Rhizosolenia setigera*

S.J. Rowland[a,*], W.G. Allard[a], S.T. Belt[a], G. Massé[a,b], J.-M. Robert[b], S. Blackburn[c], D. Frampton[c], A.T. Revill[c], J.K. Volkman[c]

[a]*Petroleum and Environmental Geochemistry Group, Department of Environmental Sciences, Plymouth Environmental Research Centre, University of Plymouth, Drake Circus, Plymouth PL4 8AA, UK*

[b]*ISOMer, Faculté des Sciences et des Techniques, Université de Nantes, 2 rue de la Houssinière, 44027 Nantes, Cedex 03, France*

[c]*CSIRO Division of Marine Research, Castray Esplanade, Hobart, Tasmania, Australia*

Received 17 May 2001; received in revised form 10 July 2001

Abstract

Polyunsaturated highly branched isoprenoid (HBI) hydrocarbon distributions of laboratory cultures of five strains of the planktonic diatom *Rhizosolenia setigera* (Brightwell) are shown herein to be highly variable. Some strains produced both haslenes with from three to five double bonds and rhizenes. The haslenes comprised not only Δ5 alkenes but also those with C7(20) unsaturation, including hasla-7(20),9*E*,*Z*, 23-trienes and hasla-7(20),9*E*,*Z*-13, 23-tetraenes. The rhizenes contained C7(25) unsaturation and the vinyl moiety common to all algal haslenes so far characterised. The effects of temperature and salinity on HBI composition, along with isotopic content, were determined in strain CS 389/A. Increase in growth temperature from 18 to 25 °C increased the degree of unsaturation in the haslenes and *E* to *Z* isomerisation in the triene. There was also an increase in unsaturation in the rhizenes at the highest growth temperature, with hexaenes dominant over the pentaenes but in the rhizenes, *Z* to *E* isomerisation increased. Increased salinity from 15 to 35 psu increased cell growth and rhizene production but decreased haslene production. Unsaturation in haslenes was not changed by increased salinity but unsaturation in the rhizenes decreased. These may reflect growth rate differences. The carbon isotopic compositions of the haslenes and rhizenes were similar to that of the major sterol at 18 °C, but the major HBI isomers were 3–4 per mil depleted relative to phytol released by saponification from chlorophyll a. This suggests biosynthesis of HBIs from a different isotopic pool of isopentenyl biphosphate to that from which phytol is biosynthesised. At 25 °C, further isotopic differences were observed. The variables controlling HBI distributions in *R. setigera* are still not fully understood and rationalisation of the environmental controls on the sedimentary distributions of the HBIs from *R. setigera* may only be possible once such factors are established. 

*Keywords:* *Rhizosolenia setigera*; Bacillariophyceae; Microalgae; Diatoms; Isoprenoid alkenes; Highly branched isoprenoids; $C_{30}$ alkenes; Rhizenes; Haslenes

## 1. Introduction

The only highly branched isoprenoid (HBI) hydrocarbons reported to date in the diatom *Rhizosolenia setigera* (Brightwell) are either a $C_{25}$ pentaene (I) or $C_{30}$ alkenes (Volkman et al., 1994, 1998; Sinninghe Damsté et al., 1999a). We have proposed the name 'haslenes' for the HBI $C_{25}$ alkenes (Rowland et al., 2001), because they were first reported (Volkman et al., 1994) from the diatom *Haslea ostrearia* (Simonsen). We now suggest the name 'rhizenes' for the corresponding $C_{30}$ HBIs, as they were first reported from *R. setigera* (Volkman et al., 1994).

The single haslapentaene (I) identified thus far in *R. setigera*, has been characterised by NMR spectroscopy and comparison with data for the same compound in *H. ostrearia* (Wraige et al., 1997; Sinninghe Damsté et al., 1999b) and the double bond positions of four rhizenes have recently been established (Belt et al., 2001). However, the factors controlling the distributions of HBIs in *R. setigera* are at present unknown. These are important since HBIs are quite commonly reported in oceanic sedimenting particles (reviewed in Belt et al., 2000a) where they may be useful indicators of specific diatom inputs. Whilst a number of benthic diatoms are known to produce haslenes (e.g. several *Haslea* spp. and

* Corresponding author. Tel.: +44-1752-233013; fax: +44-1752-233035.

*E-mail address:* s.rowland@plym.ac.edu (S.J. Rowland).

0031-9422/01/$ - see front matter 
PII: S0031-9422(01)00318-1

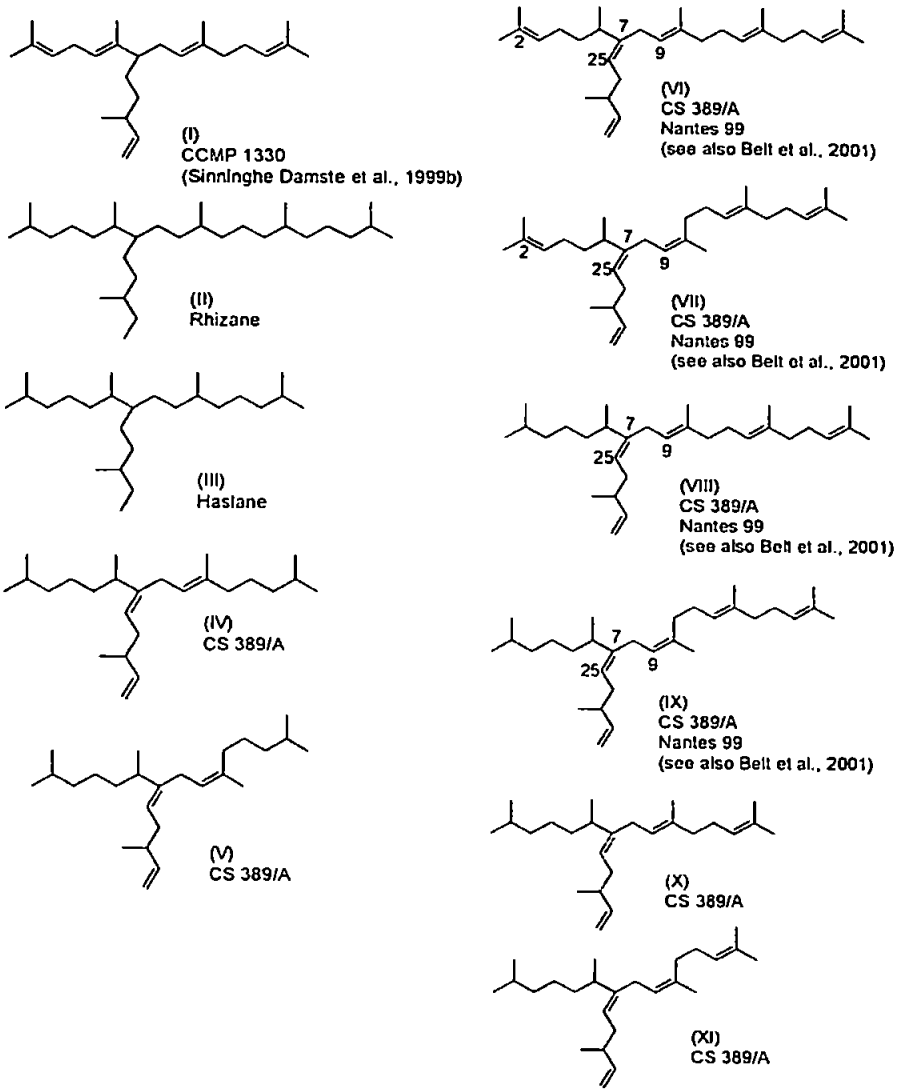


*Pleurosigma intermedium*; Belt et al., 2000a), *R. setigera* is to date the only marine planktonic diatom known to produce either haslene or rhizene HBIs.

The haslenes in estuarine sediments appear to allow resolution of the contributions of the benthic species to the total diatom flux (Cooke et al., 1998) and some haslenes also appear to possess cytostatic effects against human lung cancer cells in vitro (Rowland et al., 2001). It would therefore be interesting to know whether the rhizenes are equally geochemically specific and/or bioactive. Here, we report the haslenes and rhizenes of five strains of *R. setigera* and investigate the effects of growth temperature and salinity on haslene and rhizene production in one strain. Furthermore, we have investigated the effects of these variables on the carbon isotopic composition of the haslenes and rhizenes in this strain. Such data may eventually help to allow the environmental distributions of HBIs in sediments and sedimenting particles to be understood.

## 2. Results and discussion

*R. setigera* (Brightwell) is a common diatom often found in the plankton of coastal and marine waters

(Round et al., 1990). The taxonomy of the genus is however, somewhat uncertain (Round et al., 1990; Volkman et al., 1994, and references therein) and has been revised by Sundström (1986) and also been subject to several other modifications, including the transfer of the only two freshwater *Rhizosolenia* species to a new genus *Urosolenia* (Round et al., 1990).

The HBIs of three strains of *R. setigera* have been reported previously (Volkman et al., 1994, 1998; Sinninghe Damsté et al., 1999a) and, in contrast to the production of haslenes only in the benthic diatom *H. ostrearia*, the HBIs of *R. setigera* varied from rhizenes characterised by GCMS and hydrogenation to the parent rhizane (II) in two Australian strains CS-62 and CS-389/1 grown at 20 and 18.5 °C and 70–80 μE $m^{-2}$ $s^{-1}$ white light and 28 psu salinity (Volkman et al., 1994, 1998), to haslapentaene (I) only, in strain CCMP1330 grown at 4, 12 and 20 °C in North Atlantic seawater (Sinninghe Damsté et al., 1999a). Since the distributions in the previous reports were rather different from one another, we decided to examine further the hydrocarbons of strain CCMP 1330 and four other strains of *R. setigera*.

### 2.1. *R. setigera CS strain 389/A*

#### 2.1.1. *HBI identifications and partial structural characterisation of rhizenes*

A 10 l culture of *R. setigera* was grown from an inoculum obtained from the Huon estuary, Tasmania, Australia. The wet paste obtained after centrifugation was extracted by allowing it to stand in chloroform (24 h). This yielded 220 mg of total chloroform extractable lipids. Microscale hydrogenation (Adam's catalyst) of a small aliquot of the total lipids of a culture grown at 18 °C (35 psu salinity) produced rhizane (II) and haslane (III) as the only HBIs, identified by GCMS and GC retention indices compared to the synthetic alkanes (Robson and Rowland, 1986, 1988). A small amount of an unidentified $C_{30}$ alkane (RI $2543_{HP\text{-}5}$) with two degrees of unsaturation (ca. 10% relative to II) was also present (cf Prahl et al., 1980).

The total chloroform extract was further fractionated by open column chromatography on silica and fractions containing respectively, two $C_{25}$ trienes, three $C_{30}$ pentaenes, and three $C_{30}$ hexaenes (identified by GCMS) obtained by elution with successive volumes of pentane. GCMS, $^1H$ and $^{13}C$ NMR spectroscopy revealed that the $C_{25}$ trienes were identical to those recently identified in *Pleurosigma intermedium* (Belt et al., 2000a) viz. hasla-7(20),9*E*/*Z*,23-trienes (IV and V). Both *E* (major) and *Z* isomers were present. These Δ7(20) haslenes are therefore different to those of *H. ostrearia* and indeed of *R. setigera* strain CCMP 1330 (Sinninghe Damsté et al., 1999a) which contained a Δ5 double bond (I).

The presence of inseparable mixtures of three $C_{30}$ alkenes in each of the pentaene and hexaene fractions precluded full structural characterisations by NMR, but a number of features were nonetheless clear. Namely, the rhizenes all contained a vinyl moiety (Δ28)—present in all haslenes and rhizenes identified in diatoms thus far—a number of trisubstituted double bonds and, consistent with the presence of the haslatrienes (IV and V), Δ7(25) unsaturation ($^1H$ NMR: δ 5.71, 1H, *ddd*, H-28; 4.9, 2H, *m*, H-29; $^{13}C$ NMR DEPT,COSY,COLOC; δ 144.6, C-28; 112, C-29;142, C-7). Full structural characterisation of four of the six alkenes (VI–IX) was possible upon isolation of two pairs of isomers from a further strain of *R. setigera*, Nantes 99 (vide infra; Belt et al., 2001).

Thus, this study has shown that *R. setigera* is able to biosynthesise simultaneously, haslenes *and* rhizenes, whereas previously only one or the other was reported, and that whilst *H. ostrearia* produces haslenes with Δ5 and Δ6(17) double bonds, *P. intermedium* and *R. setigera* apparently produce haslenes with Δ7(20) unsaturation. Interestingly, haslenes and rhizenes have been reported to co-occur in some marine sediments and the present findings raise the possibility that in such cases both may have derived from *R. setigera*.

#### 2.1.2. *Effects of salinity and temperature on HBI distributions*

To investigate the controls on the concentrations and the apparent variability of haslene and rhizene distributions in *R. setigera*, small scale cultures of strain CS 389/A were grown at two salinities (18 °C; 15 and 35 psu) and three temperatures (10,18, 25 °C; 35 psu). Each culture was grown for three growth cycles then a single sample taken from each after the third growth cycle (i.e. four samples) before culturing and harvesting in triplicate after a fourth cycle (i.e. a further 12 samples). This multiple cycle culturing was designed to allow the algae to acclimate somewhat to each set of new culture conditions. Cell concentrations in the fourth growth cycle were monitored by a calibrated fluorescence method (days 0, 2, 4, 6, 7; Fig. 1) and by microscopy (days 0, 7: mean cell counts). Cells were harvested at day 7. Cultures were filtered and filters extracted with chloroform with ultrasonication after addition of *n*-docosane as internal standard for quantification by GCMS. Recovery of the internal standard was 137±17% ($n=12$). Extracts were also saponified, re-extracted into hexane and after silylation the non-saponifiable lipids were examined by GCMS and by GC-isotope ratio monitoring-MS (GC-irm-MS). The absolute concentrations of HBIs ranged from about 5 to 20 pg $cell^{-1}$. The cell concentrations in the day 7 samples were used to estimate these concentrations.

Cell growth was faster at 35 psu salinity than at 15 psu (Fig. 1) and at 35 psu total HBI production (mean 19.4±

0.6 pg cell$^{-1}$) was twice that at 15 psu (10.23±0.57 pg cell$^{-1}$; Fig. 2a). In contrast, haslene production was greatest at the lower salinity (Fig. 2b).

The ratio of rhizenes to haslenes was, however, much higher at 35 psu (Fig. 2c) due to the higher absolute concentrations of rhizenes. Whilst unsaturation in the *E,Z* Δ7(20) haslatrienes (IV, V) was unchanged by salinity (Fig. 3a and b)—as was also the case for the Δ6(17) triene in *H. ostrearia* (Wraige et al., 1998)—unsaturation within the rhizenes was changed and was higher at the lower salinity (Figs. 2d and 3a). Whether these variations can be attributed directly to the differences in salinity, or actually reflect the difference in growth rates, will require further investigation at further, intermediate, salinities.

At 35 psu salinity, *R. setigera* did not grow well after 4 days at 10 °C (Fig. 1) but at 18 and 25 °C growth was good to 7 days (Fig. 1). Variation of growth temperature from 10 to 18 to 25 °C produced a change in the total HBI production, which maximised at 18 °C (19.4 ± 0.6 pg cell$^{-1}$; Fig. 2e). [The mean value at 10 °C (Fig. 2e) should be treated as a maximum since the measurement was based on cell counts determined at 7 days where growth had decreased (Fig. 1).] Thus maximum HBI production in *R. setigera* occurred at 35 psu, 18 °C. This may reflect the conditions to which the strain had become best acclimated in culture previously.

Within the HBIs, maximum haslene production was observed at 25 °C, and there was a steady increase in haslene production with increasing temperature (Fig. 2f). In contrast, rhizene production maximised at 18 °C, leading to a maximum in the rhizene/haslene ratio at this temperature (Fig. 2g).

Unsaturation in the haslenes also varied with temperature; haslatrienes (IV and V) were accompanied by haslatetraenes (X, XI) at 25 °C (Fig. 4c). This variation of the degree of unsaturation in the haslenes of *R. setigera* with growth temperature in strain CS 389/A contrasts with the previous observation of the invariance in the single haslapentaene (I) produced by *R. setigera* strain CCMP 1330 with variation of temperature between 4 and 20 °C (Sinninghe Damste et al., 1999a). However, the degree of unsaturation in the two strains CCMP 1330 vs CS 389/A was quite different (viz. 5 vs 3 and 4 double bonds, respectively) and furthermore, haslenes in the CCMP 1330 strain had a Δ5 double bond whereas those of strain CS 389/A had 7(20) unsaturation. The variation of unsaturation with temperature in this strain is similar to, though less pronounced than, that observed in the Δ5 and Δ6(17) haslenes of *H. ostrearia* which varied from diene production at 5 °C to tetraene and pentaene production at 25 °C (Rowland et al., 2001). Isomerisation of the *E* to *Z* haslene isomers also increased with increasing temperature (Fig. 4).

Strain CS 389/A cultured herein, produced both the haslenes and rhizenes at all temperatures. In contrast, strain CS 389/1 cultured at 18.5 °C, produced only rhizenes (Volkman et al., 1994), suggesting that co-production of haslenes and rhizenes is not a general phenomenon even in *R. setigera* strains from the same

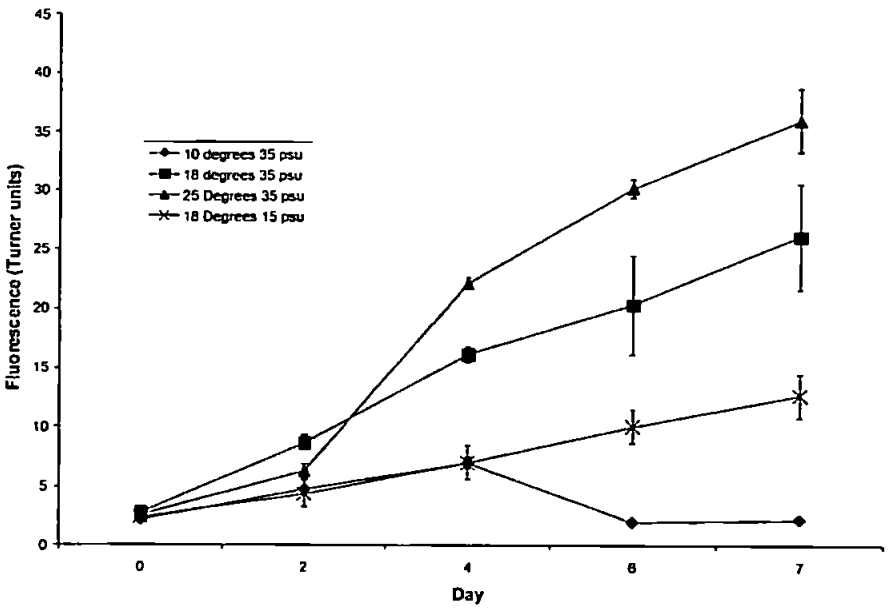


Fig. 1. Growth curves of *Rhizosolenia setigera* strain CS 389/A at 15 and 35 psu, 10, 18 and 25 °C ($n = 3 \pm 1$ standard deviation).

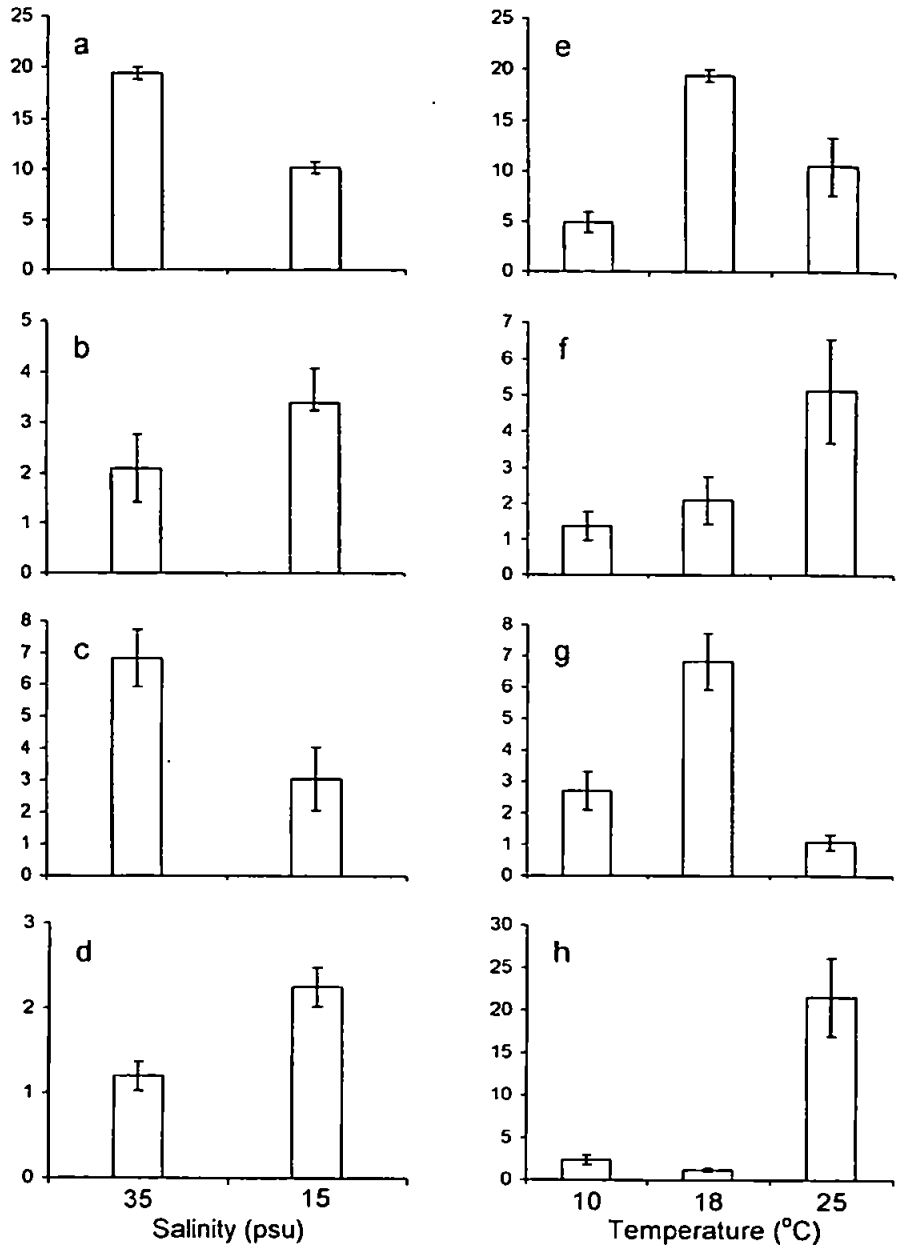


Fig. 2. Histograms illustrating variations of haslene and rhizene production (pg cell$^{-1}$) at different salinities and growth temperatures. Error bars indicate standard deviations of means of triplicate culturing experiments: a and e: total HBI concentrations; b and f: total haslene concentrations; c and g: rhizenes:haslenes ratio; d and h: rhizahexaenes:rhizapentaenes ratio.

general location. Nonetheless, 18 °C was the optimum temperature for rhizene production in strain CS 389/A (Fig. 2g). As with the haslene distributions, the degree of unsaturation in the rhizenes of strain CS 389/A changed reproducibly with temperature; the proportion of hexaenes to pentaenes increasing markedly with an

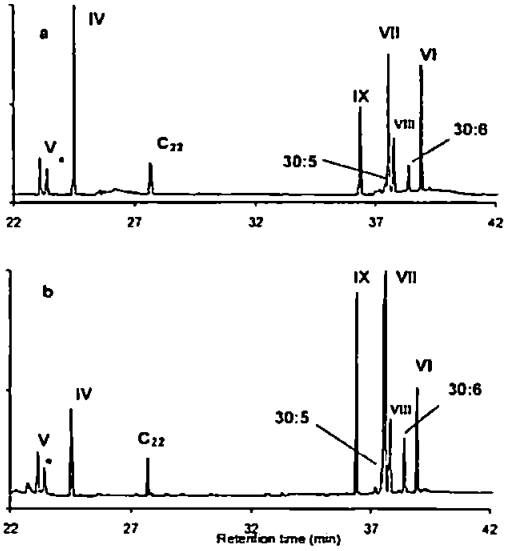


Fig. 3. GCMS total ion current chromatograms of total chloroform extracts of *Rhizosolenia setigera* strain CS 389/A at (a) 15 psu and (b) 35 psu salinity, 18 °C. Roman numerals refer to HBI structures shown in text. $C_{22}$ = *n*-docosane internal standard. * = *n*-Henicosahexaene. 30:5, 30:6 = unknown $C_{30}$ pentaene and hexaene, respectively.

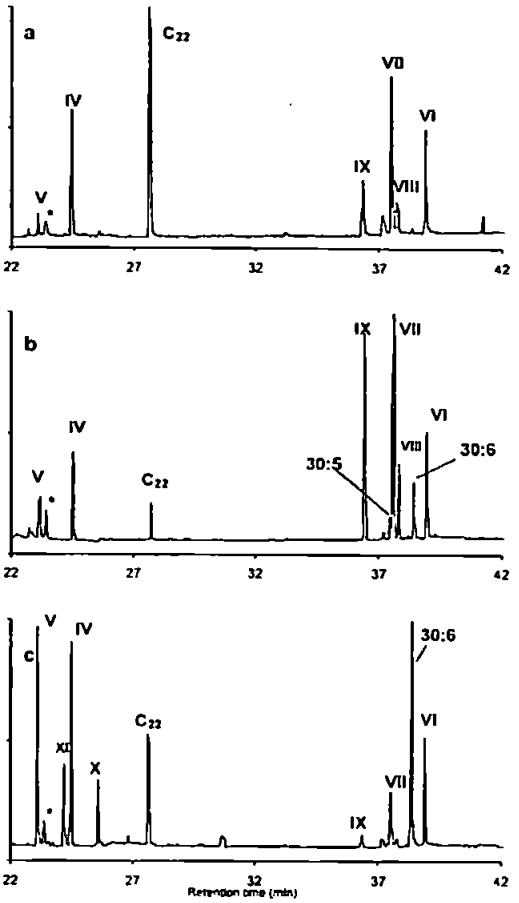


Fig. 4. GCMS total ion current chromatograms of total chloroform extracts of *Rhizosolenia setigera* strain CS 389/A at 35 psu salinity, (a) 10 (b) 18 and (c) 25 °C. Roman numerals refer to HBI structures shown in text. $C_{22}$ = *n*-docosane internal standard. * = *n*-Henicosahexaene. 30:5, 30:6 = unknown $C_{30}$ pentaene and hexaene, respectively.

increase in temperature from 18 to 25 °C (Figs. 2h and 4a–c). Again, this is somewhat similar to the change observed in the Δ5 and Δ6(17) haslenes of *H. ostrearia* (Rowland et al., 2001). However, opposite to the haslenes, Z to E isomerisation occurred in the rhizenes (Fig. 4).

### *2.1.3. Effects of temperature on the isotopic compositions of HBIs*

The $^{13}C/^{12}C$ isotope ratios (in the δ notation relative to PDB standard) of phytol, haslene (IV), five of the six rhizenes and cholest-5, 24-dienol (Barrett et al., 1995) in *R. setigera* CS 389/A grown at 18 and 25 °C were measured by GC-irm-MS. Certified reference materials [*n*-hexadecane (*n*-$C_{16}$), *n*-icosane (*n*-$C_{20}$), *n*-tetracosane (*n*-$C_{24}$) and *n*-dotriacontane (*n*-$C_{32}$)] each of known isotopic composition, were co-chromatographed with each sample during each GC-irm-MS analysis. The isotope value of the *Z*-haslatriene (V) could not be obtained due to insufficient GC resolution from *n*-henicosahexaene. The δ per mil value of each analyte was measured. Then, to allow for within-run instrument drift, differences between the measured and certified values of the nearest eluting *n*-alkane reference were added to the measured value of each analyte to give a range. The means and standard deviations for the ranges obtained in replicate experiments were then calculated and are shown as box and whisker diagrams in Figs. 5 and 6. Thus, any major differences in δ between the individual lipids which emerge are unlikely to be artefactual. The mean within-run variations from the certified values were: [($n = 10$) *n*-$C_{20}$, 0.4 ± 0.3 per mil; *n*-$C_{24}$, 0.3 ± 0.3 per mil; *n*-$C_{32}$, 0.4 ± 0.2 per mil].

At 18 °C, the *E*-haslatriene (IV) was about 3–4 per mil depleted in $^{13}C$ compared to phytol. This applied to both the algae cultured for three generations (Fig. 5a) and the final fourth generation samples (Fig. 5b). At 25 °C the result was the same (Fig. 5a). A previous study showed that haslapentaene (I) in *R. setigera* strain CCMP 1330 grown at 12 °C was 4.5 per mil depleted compared with phytol (Schouten et al., 1998). This is probably not significantly different from the 3–4 per mil determined in the present study.

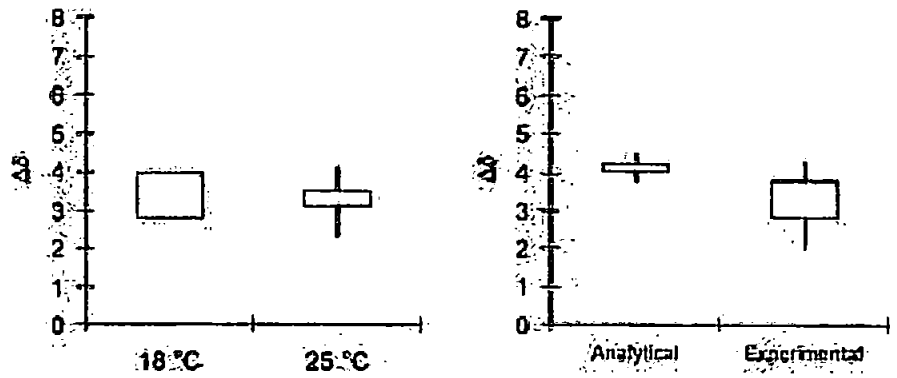


Fig. 5. Bar and whisker diagrams illustrating the influence of growth temperature on the Δδ $^{13}C$ isotope values of hasla −7(20), 9*E*,23-triene (IV) compared with phytol TMSi ether (isotopically corrected) in *Rhizosolenia setigera* CS 389/A. (a). Culture grown for three growth cycles at 18 and 25 °C. Analyses made in duplicate (18 °C) and triplicate (25 °C). (b). Culture grown for four growth cycles at 18 °C in triplicate. The results of triplicate analysis of a single sample ('Analytical') and full experimental triplicate ('Experimental') are shown. The data indicate a 3–4 per mil depletion in $^{13}C$ in IV compared with phytol.

The isotopic compositions of the haslene (Fig. 5) and cholest-5,24-dienol (desmosterol) in the present strain grown at 18 °C, were about equal (Fig. 6f), again as found previously (Schouten et al., 1998). Schouten et al. concluded from these similarities, that (I) was biosynthesised, like the sterol, in the cytosol of the diatom cell and not in the plastid. Our data support the contention that the haslene and the sterol in *R. setigera* CS 389/A were biosynthesised from a similar isotopic pool of isopentenyl diphosphate in the culture grown at 18 °C; perhaps in the cytosol.

At 25 °C, however, the Δδ values of the haslene (ca. 3–4 per mil; Fig. 5a) and the sterol (1–2 per mil; Fig. 6f) were somewhat different; certainly in the 4th generation samples for which the most comprehensive data set was obtained (Figs. 5a and 6f). In fact, the Δδ value of the sterol at both 18 and 25 °C, closely matched the value of the dominant alkene at each temperature (Fig. 6a, d, and f). Thus, at 18 °C, the dominant rhizenes were the *E*-pentaene (Figs. 4b and 6a; IX) and hexaene (Figs. 4b and 6c; VII) and the Δδ values of both these (and the *E*-haslatriene) and the sterol were about 3–4 per mil in the 3rd generation and in the 4th generation samples (Figs. 5a,b and 6a, c, and f). At 25 °C, the dominant alkene was an unknown hexaene (30:6 Figs. 4c and 6d), and whilst there was some spread in the data, the mean range of Δδ values of both this and the sterol were lower than those of the haslene (Fig. 5a) and the other rhizenes.

These data suggest that the biosynthesis of the dominant alkenes and sterol are coupled at both temperatures, probably from an isotopically similar pool of isopentenyl diphosphate.

Interestingly, the Δδ values of some of the individual alkenes varied quite considerably. Thus whilst the values for the $C_{30}$ rhizapentaene (VIII; Fig. 6b) and rhizahexaenes (VII; Fig. 6c; VI; Fig. 6e) were similar to that of the haslenes (ca. 3–4 per mil) at both temperatures, these varied somewhat from those of the unknown hexaene 30:6 (Fig. 6d). (Although there also appeared to be a difference in the Δδ values of the pentaene (IX; Fig. 5a) between 18 and 25 °C (Fig. 6a) this probably reflected the very low abundance of the pentaene at the higher temperature (0.15 ± 0.07 pg cell$^{-1}$; Fig. 4c), which made measurement much less accurate and prone to influences from co-eluting compounds such as bis(2-ethylhexyl)phthalate, a contaminant which was present in the procedural blank and had a similar retention index to the alkene).

Clearly, the isotope studies support our earlier conclusion that biosynthesis of the HBIs in *R. setigera* strain CS 389/A is complex. The following interpretations must therefore be viewed as speculative. Overall the isotopic measurements suggest:

1. Biosynthesis of phytol from an isotopically different pool of IPP to the haslenes, rhizenes and sterol at 18 °C, in the plastid, in agreement with a previous report for a Δ5 haslene in a different *R. setigera* strain.
2. Particularly close coupling of the biosynthesis of the major alkenes and the sterol at both temperatures, but some differences in isotopic fractionation of carbon even within the different $C_{30}$ alkenes, especially between VI,VII and the unknown $C_{30:6}$ (Fig. 5c, d and e) at the highest growth temperature.

We propose, at both 18 and 25 °C, biosynthesis of phytol in the chloroplast from geranyl diphosphate probably via a non-mevalonate route from $CO_2$ as is true of phytol production in some other diatoms (Cvejic and Rohmer, 2000).

At 18 and 25 °C, we envisage biosynthesis of haslenes probably outwith the plastid, either via a mevalonate

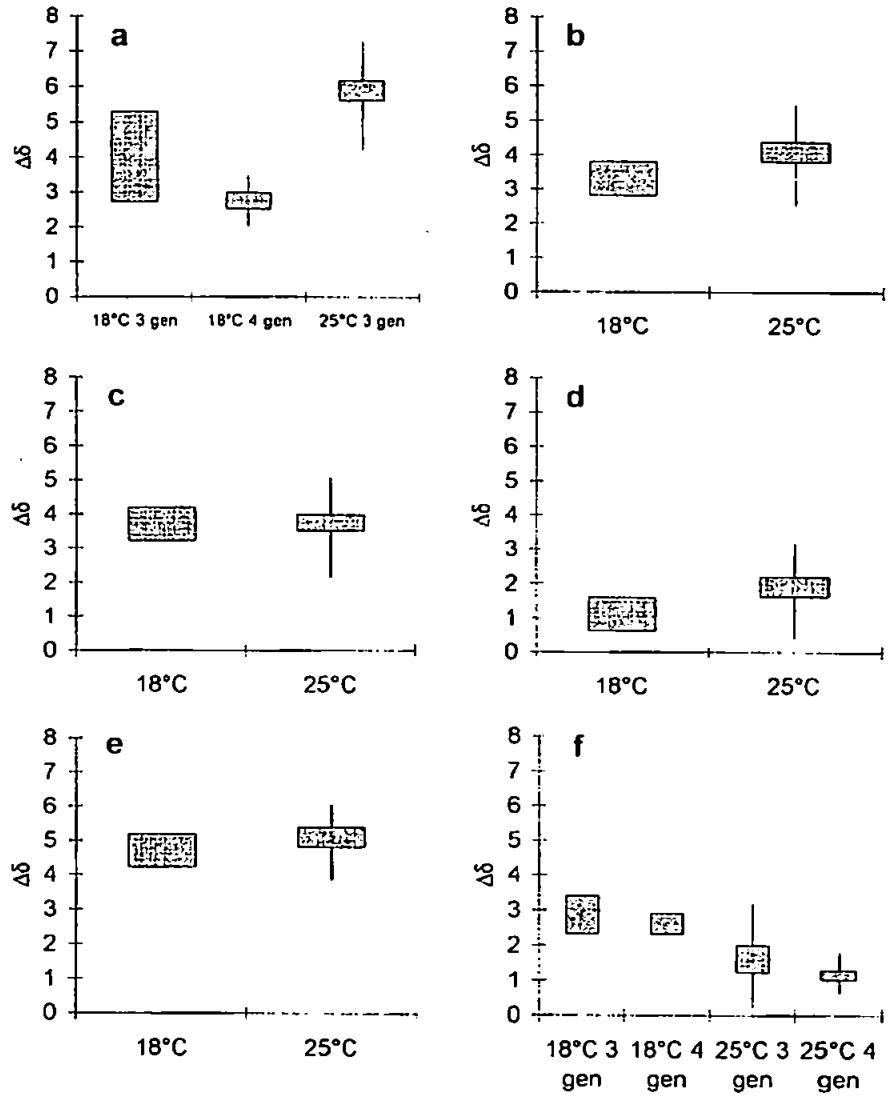


Fig. 6. Bar and whisker diagrams illustrating the influence of growth temperature on the $\Delta\delta^{13}C$ isotope values of alkenes (VII–IX, Unknown 30:6) and cholesta-5,24,-dienol (TMSi ether, isotopically corrected) compared with phytol TMSi ether (isotopically corrected) for *Rhizosolenia setigera* CS 389/A cultures grown for three (3 gen) and four (4 gen) generations at 18 and 25 °C. (a) Rhizapentaene IX; (b) Rhizapentaene VIII; (c) Rhizahexaene VII; (d) unknown $C_{30}$ hexaene 30:6; (e) Rhizahexaene VI; (f) cholest-5,24-dienol.

route leading to isotopic differences in the IPP compared with that used in phytol biosynthesis, or via a non-mevalonate route using an IPP pool which is isotopically distinct from that used in phytol production (cf. Cvejic and Rohmer, 2000). This might involve condensation of geranyl diphosphate (GPP) and a $C_{15}$ isoprenyl moiety (possibly peruviyl diphosphate, PPP). The involvement of PPP rather than farnesyl diphosphate (FPP) might explain coupling to give the C-7 branched HBI structure, rather than coupling of GPP and FPP which would probably lead to a squalene-type structure.

Biosynthesis of many of the rhizenes at 18 and 25 °C (VI, VII, VIII, IX) might be from the same pool of IPP (and hence PPP) as that used for haslene biosynthesis at 18 and 25 °C, but biosynthesis of some $C_{30}$ alkenes (e.g. unknown $C_{30:6}$)—and the sterol at 25 °C, must be from

a somewhat isotopically distinct IPP pool. Given the similarities in the isotopic values of the dominant alkenes and the sterol at both temperatures, we assume alkene synthesis from these IPP pools takes place out with the plastid, even though some terpene secondary metabolites are also believed to be produced in the chloroplast (e.g Cvejic and Rohmer, 2000, and references therein). Production in the cytoplasm is consistent with previous findings that diatoms are able to use different carbon sources in different cell compartments (Cvejic and Rohmer, 2000) and our unpublished findings which indicate that haslenes in *H. ostrearia* are not associated with the fatty acid storage lipids (which are found in the chloroplast).

Whilst more definitive studies of the biosynthetic pathways to the HBIs in *R. setigera* will also require growth of the diatom with isotopically enriched substrates, such as with $^{13}CO_2$ and also studies of the sites of $^{13}C$ incorporation by $^{13}C$ NMR, the GC-irm-MS approach used herein provided useful complementary information and did not require perturbation of algal growth with artificially high substrate concentrations or mixotrophic growth conditions. The results of our studies with isotopically enriched substrates will be published separately.

### 2.2. *R. setigera strain CCMP 1330*

When North Atlantic (off Massachusetts, USA), strain CCMP 1330 was cultured at 4–20 °C previously, it was shown to produce haslapentaene (I) as the only HBI, even when growth temperature was varied. (I) was also the only HBI produced when the same strain was cultured at 15 °C in the present study (Fig. 7a). The HBI was identified by comparison of GC and MS data with authenticated samples from *H. ostrearia* (Wraige et al., 1997) and an aliquot of the previous sample isolated from *R. setigera* (Sinninghe Damsté et al., 1999b). The *n*-alkenes reported previously were also present (Fig. 7a).

### 2.3. *R. setigera strain CCMP 1820*

The HBIs of this strain have not been reported previously but were found herein (Fig. 7b) to comprise haslapentaene (I) as the only HBI in a culture grown at 15 °C . Again, *n*-alkenes were also present (Fig. 7b).

### 2.4. *R. setigera Nantes 1999 and Nantes 2000*

Strains of *R. setigera* isolated from the North Atlantic (off southern Brittany, France) contained, like the Tasmanian strain CS 389/A, both haslenes and rhizenes (Fig. 7c and d) and similar to that strain, the haslenes included trienes (IV and V) with C7(20) unsaturation. The corresponding tetraene [viz. hasla-7(20),9*E*,13, 23-tetraene; X] and traces of the corresponding Δ2 pentaene (cf. Belt et al., 2000b) were also present in this strain grown at 15 °C. All compounds were identified by GCMS retention time and mass spectral comparison with previously authenticated compounds from *P. intermedium* (Belt et al., 2000a,b). The rhizenes present comprised two pentaenes and two hexaenes, both with C7(25) unsaturation (VI–IX) as determined by NMR for strain CS 389/A above. The relative proportions of HBIs, which were very similar in two samples, collected and cultured one year apart, are shown in Fig. 7c and d.

## 3. Experimental

### 3.1. *Algal cultures*

*R. setigera* strain CS 389/A isolated from the Huon estuary, Tasmania, Australia, was grown at 10, 18 or 25 °C, 35 psu, under white light at 80 μE $m^{-2}$ $s^{-1}$ in fE or fE/2-1 medium as described previously for other strains (Volkman et al., 1994, 1998). Both small scale (250 ml Erlenmeyer flasks) and larger scale samples (10 l, 18 °C) were cultured.

*R. setigera* strains isolated from France (Nantes 99 and Nantes 00) were isolated from Le Croisic, France and cultured in 4×60 l tanks containing underground saltwater enriched with $NaNO_3$ (8 mg $ml^{-1}$) and Guillard's medium (f/2, 0.2 ml $l^{-1}$) at 16–18°C and on the smaller scale at 15°C. Samples for hydrocarbon analysis were obtained by centrifugation. Strains CCMP 1330 and 1820 were purchased from the Guillard Collection USA and grown under the same conditions as the French strains above.

### 3.2. *Lipid extraction and alkene isolation*

Alkenes were isolated by extraction of the centrifuged algal paste with chloroform (strain CS 389/A) or hexane, aided by ultrasonication (45 min, Kerry Pulsatron HB172) followed by column chromatogaphy on silica and elution with hexane. Selected samples were saponified by heating (60 °C, 1 h) in methanolic KOH (e.g. Volkman et al., 1998) and derivatised with BSTFA/TMCS (60 °C, 30 min) prior to analyses by GC-MS and GC-irm-MS.

### 3.3. *NMR spectroscopy*

NMR spectroscopy was conducted on a JEOL EX 270 multinuclear ($^1H$, $^{13}C$) 270 MHz spectrometer. Data were recorded on the delta scale (ppm) using the resonances of $CDCl_3$ (7.25 ppm $^1H$, 77.0 ppm $^{13}C$) as internal references.

### 3.4. *Gas chromatography–mass spectrometry*

Derivatised total chloroform extracts (Figs. 3 and 4), non-saponifiable lipids (Fig. 7) or alkene fractions (for

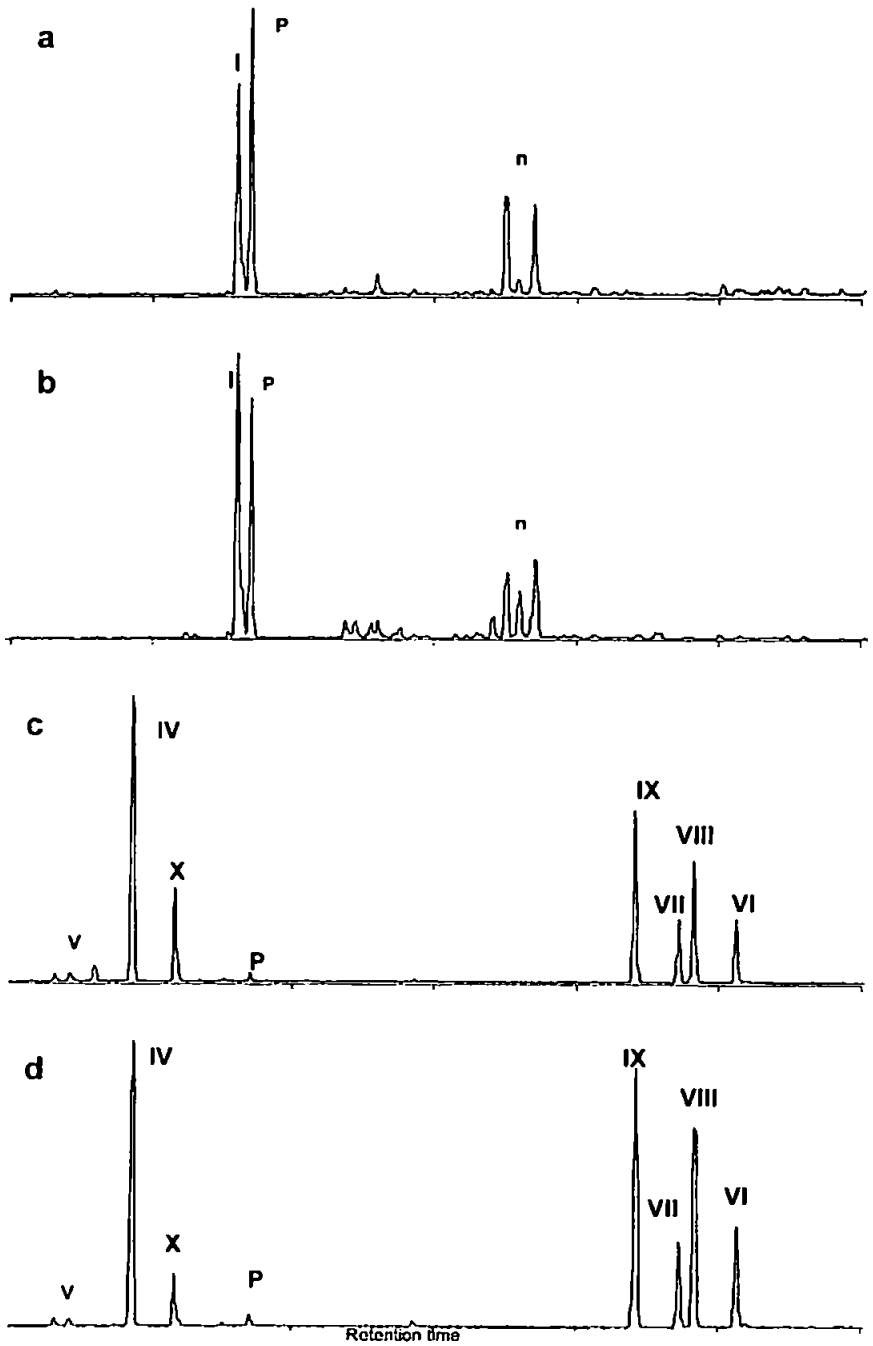


Fig. 7. GCMS total ion current chromatograms of non-saponifiable lipids (TMSi ethers) of *R. setigera* strains CCMP 1330, CCMP 1820, Nantes 99 and Nantes 00. P = phytol, TMSi ether; n = *n*-alkenes. Roman numerals refer to HBI structures shown. (a) *Rhizosolenia setigera* CCMP 1330; (b). *Rhizosolenia setigera* CCMP 1820; (c) *Rhizosolenia setigera* Nantes 1999; (d) *Rhizosolenia setigera* Nantes 2000.

NMR) from strain CS 389/A were examined by gas chromatography–mass spectrometry (GC-MS) performed using a Fisons Instruments MD800 equipped with a Carlo Erba on-column injector. The gas chromatograph was fitted with a 12 m (0.2 mm i.d.) fused silica capillary column (HP-5 Ultra stationary phase). Helium carrier gas was used. The gas chromatograph oven temperature was programmed from 40 to 300 °C at 5 °C $min^{-1}$ and held at the final temperature for 10 min. Mass spectrometer operating conditions were; ion source temperature 250 °C and 70 eV ionisation energy. Spectra (40–650 Daltons) were collected using Fisons Masslab™ software. Alkene fractions from all other strains were examined by gas chromatography-mass spectrometry (GC-MS) performed using a Hewlett Packard 5890 series II gas chromatograph coupled to a Hewlett Packard 5970 mass selective detector fitted with a 12 m (0.2 mm i.d.) fused silica capillary column (HP-1 Ultra stationary phase). Auto-splitless injection and helium carrier gas were used. The gas chromatograph oven temperature was programmed from 40 to 300 °C at 5 °C $min^{-1}$ and held at the final temperature for 10 min. Mass spectrometer operating conditions were; ion source temperature 250 °C and 70 eV ionisation energy. Spectra (35–500 Daltons) were collected using Hewlett Packard Chemstation™ software.

### 3.5. Gas chromatography–isotope ratio monitoring–mass spectrometry

GC-irm-MS was performed with a Finnigan Delta S mass spectrometer essentially as described previously (Merrit et al., 1995). GC conditions were: oven temperature 40–135 °C at 30 °C $min^{-1}$, 135–300 °C at 4 °C $min^{-1}$; 60 m DB-1, helium carrier gas. Isotopic values were determined by integration of the ion currents of $m/z$ 44–46 produced by combustion of chromatographically separated compounds and comparison with $CO_2$ reference gas. Certified reference materials comprising *n*-hexadecane, *n*-icosane, *n*-tetracosane, *n*-dotriacontane and *n*-hexatriacontane of known isotopic composition were co-chromatographed with the algal lipids derivatised with BSTFA/TMCS. Determinations of the haslene were made in full procedural triplicate, including culturing conditions and in analytical triplicate (Fig. 5b). To correct for the isotopic effect of the derivatisation of phytol and cholest-5,24-dienol with BSTFA/TMCS, both free phytol (Aldrich, 97% mixture of *E* and *Z* isomers; *E*-phytol, −28.02 per mil delta notation relative to PDB standard) and a sample of phytol derivatised with each batch of BSTFA/TMCS were examined by GC-irm-MS. The difference in values was used to calculate the isotopic composition of the TMS group using a published method (Jones et al., 1991).

## Acknowledgements

We thank the British Council in Australia and the Royal Society of London for travel awards (S.J.R.) and the British Council for ALLIANCE travel awards (S.T.B., J.-M.R.). We are grateful to Dr. J. Sinninghe Damsté (NIOZ, The Netherlands) for a sample of pentaene (I) isolated previously from *R. setigera* CCMP 1330 (Sinninghe Damsté et al., 1999a,b).

## References

Barrett, S.M., Volkman, J.K., Dunstan, G.A., LeRoi, J.-M., 1995. Sterols of 14 species of marine diatoms (*Bacillariophyta*). J. Phycol. 31, 360–369.

Belt, S.T., Allard, W.G., Massé, G., Robert, J.-M., Rowland, S.J., 2001. Structural characterisation of $C_{30}$ highly branched isoprenoid alkenes (rhizenes) in the marine diatom *Rhizosolenia setigera*. Tetrahedron Lett. 42, 5583–5585.

Belt, S.T., Allard, W.G., Massé, G., Robert, J.-M., Rowland, S.J., 2000a. Highly branched isoprenoids (HBIs): identification of the most common and abundant sedimentary isomers. Geochim. Cosmochim. Acta 64, 3839–3851.

Belt, S.T., Allard, W.G., Rintatalo, J., Johns, L.A., van Duin, A.C.T., Rowland, S.J., 2000b. Clay and acid catalysed isomerisation and cyclisation reactions of highly branched isoprenoid alkenes: implications for sedimentary reactions and distributions. Geochim. Cosmochim. Acta 64, 3337–3345.

Cooke, D.A., Barlow, R., Green, J., Belt, S.T., Rowland, S.J., 1998. Seasonal variations of highly branched isoprenoid hydrocarbons and pigment biomarkers in intertidal sediments of the Tamar estuary, U.K. Mar. Environ. Res. 45, 309–324.

Cvejic, J.H., Rohmer, M., 2000. $CO_2$ as main carbon source for isoprenoid biosynthesis via the mevalonate-independent methylerythritol 4-phosphate route in the marine diatoms *Phaeodactylum tricornutum* and *Nitzschia ovalis*. Phytochemistry 53, 21–28.

Jones, D.M., Carter, J.F., Eglinton, G., Jumeau, E.J., Fenwick, C.S., 1991. Determination of $\delta^{13}C$ values of sedimentary straight chain and cyclic alcohols by gas chromatography/isotope ratio mass spectrometry. Biol. Mass Spectrom. 20, 641–646.

Merrit, D.A., Freeman, K.H., Ricci, M.P., Studley, S.A., Hayes, J.M., 1995. Performance and optimisation of a combustion interface for isotope ratio monitoring gas chromatography/mass spectrometry. Anal. Chem. 67, 2461–2473.

Prahl, F.G., Bennet, J.T., Carpenter, R., 1980. The early diagenesis of aliphatic hydrocarbons and organic matter in sedimentary particles from Dabob Bay, Washington. Geochim. Cosmochim. Acta 44, 1967–1976.

Robson, J.N., Rowland, S.J., 1986. Identification of novel, widely-occurring sedimentary sesterterpenoids. Nature 324, 561–563.

Robson, J.N., Rowland, S.J., 1988. Synthesis of a novel, highly branched, $C_{30}$ sedimentary hydrocarbon. Tetrahedron Lett. 29, 3837–3840.

Round, F.E., Crawford, R.M., Mann, D.G., 1990. The Diatoms. Cambridge University Press, Cambridge, UK.

Rowland, S.J., Belt, S.T., Wraige, E.J., Massé, G., Roussakis, C., Robert, J-M., 2001. Effects of temperature on polyunsaturation in cytostatic lipids of *Haslea ostrearia*. Phytochemistry 56, 597–602.

Schouten, S., Klein Breteler, W.C.M., Blokker, P., Schogt, N., Rijpstra, W.I., Grice, K., Baas, M., Sinninghe Damsté, J.S., 1998. Biosynthetic effects on the stable carbon isotope compositions of algal lipids: implications for deciphering the carbon isotope biomarker record. Geochim. Cosmochim. Acta 62, 1397–1406.

Sinninghe Damsté, J.S., Rijpstra, W.I.C., Schouten, S., Peletier, H., van der Maarel, M.J.E.C., Gieskes, W.W.C., 1999a. A $C_{25}$ highly

branched isoprenoid alkene and $C_{25}$ and $C_{27}$ *n*-alkenes in the marine diatom, *Rhizosolenia setigera*. Org. Geochem. 30, 95–100.

Sinninghe Damsté, J.S., Schouten, S., Rijpstra, W.I.C., Hopmans, E.C., Peletier, H., Gieskes, W.W.C., Geenevasen, J.A.J., 1999b. Structural identification of the $C_{25}$ highly branched isoprenoid pentaene in the marine diatom, *Rhizosolenia setigera*. Org. Geochem. 30, 1581–1583.

Sundström, B.G., 1986. The Marine Genus *Rhizosolenia*. A New Approach to Taxonomy. PhD dissertation, Lund University, Lund, Sweden.

Volkman, J.K., Barrett, S.M., Dunstan, G.A., 1994. $C_{25}$ and $C_{30}$ highly branched isoprenoid alkenes in laboratory cultures of two marine diatoms. Org. Geochem. 21, 407–414.

Volkman, J.K., Barrett, S.M., Blackburn, S.I., Mansour, M.P., Sikes, E.L., Gelin, F., 1998. Microalgal biomarkers: a review of recent research developments. Org. Geochem. 29, 1163–1179.

Wraige, E.J., Belt, S.T., Lewis, C.A., Cooke, D.A., Robert, J.-M., Massé, G., Rowland, S.J., 1997. Variations in structures and distributions of the $C_{25}$ highly branched isoprenoid (HBI) alkenes in cultures of the diatom, *Haslea ostrearia* (Simonsen). Org. Geochem. 27, 97–505.

Wraige, E.J., Belt, S.T., Johns, L., Massé, G., Robert, J.-M., Rowland, S.J., 1998. Variations in structures and distributions of the $C_{25}$ highly branched isoprenoid (HBI) alkenes in cultures of the diatom, *Haslea ostrearia*: influence of salinity. Org. Geochem. 28, 855–859.

PERGAMON

Phytochemistry 59 (2002) 141–148

PHYTOCHEMISTRY

www.elsevier.com/locate/phytochem

# Effects of auxosporulation on distributions of $C_{25}$ and $C_{30}$ isoprenoid alkenes in *Rhizosolenia setigera*

Simon T. Belt[a,*], Guillaume Massé[a,b], W. Guy Allard[a], Jean-Michel Robert[b], Steven J. Rowland[a]

[a] *Petroleum and Environmental Geochemistry Group, Department of Environmental Sciences, University of Plymouth, Drake Circus, Plymouth PL4 8AA, Devon, UK*

[b] *ISOMer, Faculté des Sciences et des Techniques, Université de Nantes, 2 Rue de la Houssinière, 44322 Nantes Cedex 3, France*

Received 12 August 2001; received in revised form 16 October 2001

**Abstract**

The effect of life cycle on the distributions of $C_{25}$ and $C_{30}$ highly branched isoprenoid (HBI) alkene lipids has been investigated for the marine diatom *Rhizosolenia setigera*. The concentrations of the $C_{30}$ compounds are largely independent of the cell volume, though the ratios of the individual isomers possessing five and six double bonds show a dependence on the position of the cell during its life cycle, especially during auxosporulation. In contrast to the $C_{30}$ pseudo-homologues, the $C_{25}$ isomers are not always detected in cultures of *R. setigera*. The biosynthesis of the $C_{25}$ HBIs would appear to result from the onset of auxosporulation, with further changes to their distributions taking place after this phase, including the formation of more unsaturated isomers. The results of this investigation may be used in part to explain the large variations in these lipids reported previously. 

*Keywords:* *Rhizosolenia setigera*; Microalgae; Diatoms; Highly branched isoprenoids; Alkenes; Life cycle; Auxosporulation; HBIs

## 1. Introduction

$C_{25}$ and $C_{30}$ highly branched isoprenoid (HBI) alkenes are unusual secondary metabolites that are derived from diatoms and are commonly used as biological markers in sediments and other geochemical environments (Robson and Rowland, 1986; Rowland and Robson, 1990). Several of the isomeric $C_{25}$ alkenes also possess a cytostatic effect on a human non-small-cell broncopulmonary cell line (NSCLC-N6) (Rowland et al., 2001a). Volkman and co-workers (1994) were the first to determine biological sources of these isoprenoids, namely the marine diatoms *Haslea ostrearia* ($C_{25}$) and *Rhizosolenia setigera* ($C_{30}$). Some representative structures of $C_{25}$ (haslenes) and $C_{30}$ (rhizenes) HBIs are shown in Figs. 1 and 2. Although an account (in terms of structures and distributions) of the $C_{25}$ HBIs produced by *H. ostrearia* would appear to be well defined, the situation with *R. setigera* is less clear. The culture of *R. setigera* investigated by Volkman et al. (1994) was found to contain three $C_{30}$ pentaenes ($C_{30:5}$) and two $C_{30}$ hexaenes ($C_{30:6}$), with no detection of any $C_{25}$ alkenes. In contrast, Sinninghe Damsté et al. (1999a) showed that a strain of *R. setigera* isolated from Vineyard Sound, MA, USA contained only a single $C_{25}$ pentaene in addition to two novel *n*-alkenes, with no $C_{30}$ homologues. The structure of the $C_{25:5}$ in this strain was subsequently shown to be 3, previously found in cultures of *H. ostrearia* (Sinninghe Damsté et al., 1999b). During the course of our own studies, we have observed both $C_{25}$ and $C_{30}$ HBI alkenes within the same cultures of *R. setigera*, together with considerable variations in their distributions (Rowland et al., 2001b). It is of course possible that these differences may be attributable to changes in phenotypic variables employed during the culturing experiments (e.g. light, salinity, temperature, nutrients, etc.) or to the use of different strains of diatoms belonging to the same species. Indeed, we have noted some variation in distributions with temperature and salinity, and also with the origin of the diatom strain. Significantly, however, we have also observed variations in distributions under 'controlled' conditions (constant temperature, salinity, light cycle, etc.) using a

* Corresponding author. Tel.: +44-1752-233042; fax: +44-1752-233035.

*E-mail address:* sbelt@plymouth.ac.uk (S.T. Belt).

0031-9422/02/$ - see front matter 
PII: S0031-9422(01)00444-7

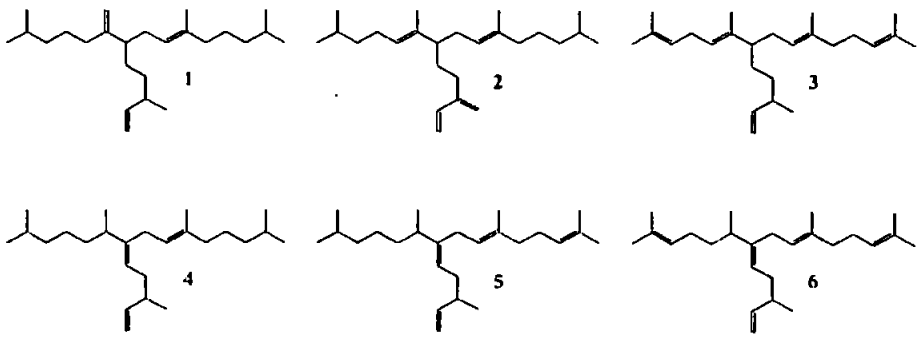


Fig. 1. Representative structures of $C_{25}$ HBI alkenes isolated from various marine diatoms.

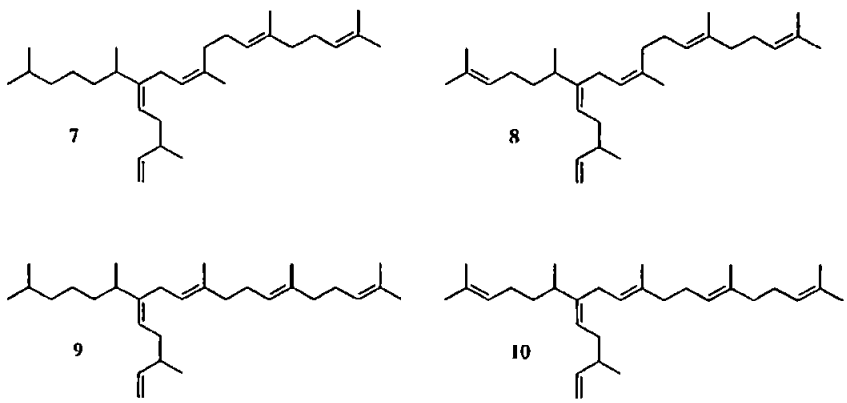


Fig. 2. Structures of $C_{30}$ HBIs isolated from *R. setigera*.

single strain, indicating that other factors are also important (Rowland et al., 2001b). In addition, Sinninghe Damsté and co-workers (2000) have reported that distributions of the HBI $C_{25:5}$ and $C_{25}$ and $C_{27}$ *n*-alkenes produced by *R. setigera* were quite variable for experiments performed at the same temperature.

In this report, we describe an investigation of the distribution of $C_{25}$ and $C_{30}$ HBI alkenes biosynthesised by *R. setigera* as a function of the position of the cells through their life cycle. Our observations reveal a relationship between cell size and HBI content, including a dramatic change in the distribution of alkenes during the regeneration of their original size through a sexual cycle (auxosporulation). This is a necessary phase of the life cycle, since vegetative multiplication, involving the formation of new valves within the parent frustule, results in consequential formation of increasingly smaller cells. After a sufficiently large number of such divisions, a critical point in cell size is reached and sexual reproduction is induced with formation of an auxospore (an expandable zygotic cell). This forms the basis of a new generation of large daughter cells. Since the sexual reproductive phase and auxospore formation is relatively short (ca. 1 week) compared to the total life cycle (as much as several months or years), the observation of such events is more achievable in laboratory cultures (rather than in natural populations) since more homogeneous samples are attainable. Further information relating to diatom life cycles can be found elsewhere (e.g. Round et al., 1990).

## 2. Results and discussion

### 2.1. Distribution of HBIs in RS-1

A strain of *R. setigera* was isolated for the first experiment (RS-1) from Le Croisic, France. From a single cell, an inoculum was obtained (1 month equilibration time) which was used to generate a series of batch cultures corresponding to six consecutive cycles of growth. Following extraction and derivatisation, total ion current

(TIC) chromatograms of the non-saponifiable lipid fractions obtained from each cycle demonstrated the presence of phytol, $n$-$C_{21:6}$ (henicosa-3,6,9,12,15,18-hexaene) and four $C_{30}$ HBI alkenes as the main identifiable components. The $C_{30}$ HBI alkenes, which consisted of two pentaenes ($C_{30:5}$) and two hexaenes ($C_{30:6}$), were identified as isomers 7–10 (Fig. 2) by comparison of their GC and MS properties with authentic compounds (Belt et al., 2001). A small amount of $C_{25}$ triene 4 could also be detected. Fig. 3 shows a partial TIC chromatogram corresponding to cycle 1 which illustrates the relative amounts of these compounds including the $C_{30:5}$ and $C_{30:6}$ isomers. Subsequent cycles resulted in extremely similar chromatograms, though the $C_{25:3}$ observed in cycle 1 could not be detected. For all cycles, the major rhizenes were the pentaene isomers ($C_{30:5}/C_{30:6}$ = 12 ± 1.4).

A summary of the cell dimensions and HBI distributions can be found in Table 1. As expected, cell dimensions

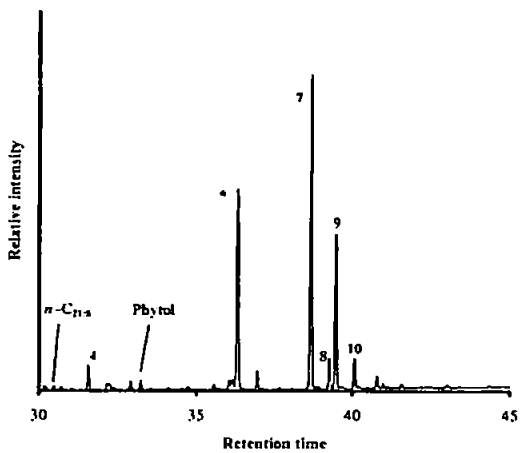


Fig. 3. Partial TIC chromatogram of a non-saponifiable lipid fraction from RS-1 (cycle 1). The peak marked * is due to the internal standard. The peak numbers refer to the $C_{25}$ and $C_{30}$ structure numbers in Figs. 1 and 2.

(mean cell width and volume) decreased slightly with consecutive cycles as a result of cell division. The mean concentration of the $C_{30}$ HBI alkenes (10.7 ± 1.7 pg cell$^{-1}$) is reasonably close to that found by Rowland et al. (2001b) (17.3 pg cell$^{-1}$; 18 °C) but rather higher than that reported by Volkman et al. (1994) (1.6 pg cell$^{-1}$). However, an exact agreement may not be expected due to the differences in culture conditions and/or strains. Perhaps of greater significance is the fact that the mean concentration of HBIs per unit cell volume was found to be essentially invariant throughout the six cycles (Table 1). Although the observation of $C_{30}$ HBI alkenes was in general agreement with those made by Volkman and co-workers (1994), the virtual absence of any $C_{25}$ alkenes seemed surprising since we have previously reported both $C_{25}$ and $C_{30}$ alkenes from *R. setigera* isolated from the same location and cultured under similar experimental conditions (Rowland et al., 2001b). However, in terms of addressing our original aim, we considered that although the six cycles studied in RS-1 certainly represent numerous individual replications or generations, the study may have been limited in terms of a broader range of physiological changes. Since a more comprehensive study involving a whole life cycle, including the sexual regeneration was considered impractical, we decided to concentrate on this last and quite distinct physiological event (viz. auxosporulation). We therefore conducted a second experiment (RS-2) to examine the effect of this sexual reproductive phase on HBI alkene structures and distributions.

### 2.2. Distribution of HBIs in RS-2

In a second experiment (RS-2), a further inoculum was generated from a single *R. setigera* cell, though in contrast to RS-1, the cells were believed to be close to the onset of auxosporulation (ca. 4.7 μm width). Indeed, during the third cycle, auxospores could be detected using light microscopy. Significant numbers of initial or "daughter" cells were seen in cycle 3 (14.0%) with the proportion increasing (61.4%) during cycle 4 (Table 2). By cycles 5 and 6, virtually all cells could be considered

Table 1
Cell dimensions and $C_{25}$ and $C_{30}$ HBI concentrations obtained from six consecutive cycles of a culture of *R. setigera* (RS-1)

| | Biomass (cell ml$^{-1}$) | $n$-$C_{21:6}$ (pg cell$^{-1}$) | Phytol (pg cell$^{-1}$) | Total HBI (pg cell$^{-1}$) | Total $C_{30}$ (pg cell$^{-1}$) | $C_{30:5}$ (pg cell$^{-1}$) | $C_{30:6}$ (pg cell$^{-1}$) | $C_{30:5}/C_{30:6}$ | Mean width (μm) | Mean volume (μm$^3$) | Total HBI (fg μm$^{-3}$) | Total $C_{30}$ (fg μm$^{-3}$) |
|---|---|---|---|---|---|---|---|---|---|---|---|---|
| Cycle 1 | 11 640 | 0.09 | 0.16 | 10.40 | 9.99 | 8.90 | 1.10 | 8.12 | 18.7 | 1309 | 7.9 | 7.6 |
| Cycle 2 | 12 400 | 0.00 | 3.74 | 11.70 | 11.70 | 10.67 | 1.03 | 10.33 | 18.1 | 1279 | 9.1 | 9.1 |
| Cycle 3 | 10 120 | 0.11 | 0.48 | 9.60 | 9.51 | 8.86 | 0.64 | 13.82 | 17.2 | 964 | 10.0 | 9.9 |
| Cycle 4 | 9360 | 0.16 | 4.20 | 13.36 | 13.36 | 12.45 | 0.91 | 13.70 | 16.6 | 1254 | 10.7 | 10.7 |
| Cycle 5 | 10 720 | 0.12 | 0.09 | 9.33 | 9.31 | 8.65 | 0.66 | 13.12 | 15.9 | 1151 | 8.1 | 8.1 |
| Cycle 6 | 14 800 | 0.00 | 2.49 | 10.12 | 10.12 | 9.38 | 0.74 | 12.65 | 15.0 | 1090 | 9.3 | 9.3 |

Table 2
Cell dimensions, populations and $C_{25}$ and $C_{30}$ HBI concentrations obtained for 11 consecutive cycles of a culture of *R. setigera* (RS-2)

| | Biomass | *n*-$C_{21:6}$ | Phytol | Total HBI | Total $C_{25}$ | Total $C_{30}$ | $C_{25}$/$C_{30}$ | $C_{25:3}$ | $C_{25:4}$ | $C_{30:5}$ | $C_{30:6}$ | $C_{30:5}$/$C_{30:6}$ | Daughter cell | Mean volume | Mean volume | Mean volume | Total HBI | Total $C_{25}$ | Total $C_{30}$ |
|---|---|---|---|---|---|---|---|---|---|---|---|---|---|---|---|---|---|---|---|
| | (cell ml$^{-1}$) | (pg cell$^{-1}$) | (pg cell$^{-1}$) | (pg cell$^{-1}$) | (pg cell$^{-1}$) | | (pg cell$^{-1}$) | (pg cell$^{-1}$) | (pg cell$^{-1}$) | (pg cell$^{-1}$) | (pg cell$^{-1}$) | | (% of total cells) | ($\mu m^3$) | mother ($\mu m^3$) | daughter ($\mu m^3$) | (fg $\mu m^{-3}$) | (fg $\mu m^{-3}$) | (fg $\mu m^{-3}$) |
| Cycle 1 | 25440 | 0.00 | 0.00 | 1.87 | 0.03 | 1.85 | 0.02 | 0.03 | 0.00 | 0.89 | 0.96 | 0.93 | 0 | 133 | 133 | - | 14.1 | 0.2 | 13.9 |
| Cycle 2 | 24320 | 0.00 | 0.00 | 2.20 | 0.02 | 2.19 | 0.01 | 0.02 | 0.00 | 1.00 | 1.19 | 0.84 | 0.7 | 116 | 116 | - | 19.0 | 0.1 | 18.9 |
| Cycle 3 | 10560 | 0.00 | 0.00 | 3.88 | 0.00 | 3.88 | 0.00 | 0.00 | 0.00 | 3.02 | 0.87 | 3.48 | 14.0 | 373 | 117 | 1945 | 10.4 | 0.0 | 10.4 |
| Cycle 4 | 5800 | 0.25 | 0.19 | 18.64 | 0.44 | 18.20 | 0.02 | 0.44 | 0.00 | 14.84 | 3.36 | 4.42 | 61.4 | 1379 | 132 | 2164 | 13.5 | 0.3 | 13.2 |
| Cycle 5 | 6480 | 0.55 | 0.37 | 20.70 | 2.40 | 18.30 | 0.13 | 2.06 | 0.34 | 13.45 | 4.85 | 2.78 | 92.6 | 1890 | 128 | 2031 | 11.0 | 1.3 | 9.7 |
| Cycle 6 | 5560 | 0.90 | 0.49 | 25.64 | 4.68 | 20.96 | 0.22 | 3.79 | 0.89 | 15.03 | 5.93 | 2.53 | 100 | 2091 | - | 2091 | 12.3 | 2.2 | 10.0 |
| Cycle 7 | 3070 | 0.74 | 1.05 | 30.51 | 7.45 | 23.06 | 0.32 | 6.04 | 1.41 | 18.04 | 5.02 | 3.59 | 100 | 2288 | - | 2288 | 13.3 | 3.3 | 10.1 |
| Cycle 8 | 4520 | 0.82 | 0.70 | 29.87 | 9.60 | 20.27 | 0.47 | 5.73 | 3.86 | 15.29 | 4.99 | 3.07 | 100 | 2353 | - | 2353 | 12.7 | 4.1 | 8.6 |
| Cycle 9 | 2930 | 1.54 | 1.16 | 47.54 | 17.51 | 30.03 | 0.58 | 10.79 | 6.72 | 22.19 | 7.84 | 2.83 | 100 | 2353 | - | 2353 | 20.2 | 7.4 | 12.8 |
| Cycle 10 | 4140 | 0.98 | 0.62 | 33.20 | 9.53 | 23.68 | 0.40 | 6.13 | 3.40 | 17.40 | 6.27 | 2.77 | 100 | 2359 | - | 2359 | 14.1 | 4.0 | 10.0 |
| Cycle 11 | 3680 | 1.42 | 1.07 | 48.38 | 25.14 | 23.23 | 1.08 | 11.23 | 13.09 | 15.64 | 7.60 | 2.06 | 100 | 2293 | - | 2293 | 21.1 | 11.0 | 10.1 |

to be present as a result of auxosporulation (92.6 and 100% daughter cells, respectively). Cells from a further five cycles were harvested to allow for a further comparison with the results from RS-1. In contrast to the relatively modest volume changes that were observed for cells belonging to consecutive cycles in RS-1 (Table 1), much greater differences were observed as a result of auxosporulation (Table 2; Fig. 4). Thus, mean cell volumes were determined for mother ($125 \pm 8$ $\mu m^3$) and daughter ($2210 \pm 160$ $\mu m^3$) cells using mean cell volumes (total cells) and relative populations (Table 2). Cell volumes for cycles 6–11 were all similar, with little variation from a mean value of $2290 \pm 100$ $\mu m^3$ despite consecutive cell division. Not surprisingly, since cell volumes and growth rates (indicated by the cell concentrations at the end of each exponential phase) are inextricably linked, an inverse relationship was found between these for the pre- and post-auxosporulation phases.

When the non-saponifiable lipid fractions for each cycle were analysed by GC-MS, some differences were observed between cycles and with the results obtained from RS-1 (vide infra). A partial TIC chromatogram from cycle 1 (Fig. 5) indicated the presence of the same $C_{30:5}$ and $C_{30:6}$ HBI alkenes present in RS-1, though phytol and *n*-$C_{21:6}$ were not detected. In addition, there was a trace amount of the $C_{25}$ triene 4 which was mostly absent in the first experiment (RS-1) and there was a greater concentration of the pair of $C_{30}$ hexaenes compared to the pentaenes. Thus, the $C_{30:5}/C_{30:6}$ ratio was 0.93, which compares with a mean ratio of $12 \pm 1.4$ in RS-1. Similar observations were made in cycle 2 (Table 2). During cycle 3, when auxospores and daughter cells were first detected using light microscopy, the small amount of $C_{25:3}$ observed in the first two cycles was absent and the $C_{30}$ pentaenes were the dominant isomers ($C_{30:5}/C_{30:6}$ ratio increased sharply to 3.48). In cycle 4, when over 60% of the culture corresponded to daughter cells, the $C_{30:5}/C_{30:6}$ ratio increased further (4.42). In addition, phytol, *n*-$C_{21:6}$ and the $C_{25}$ triene 4 were also detected and the total concentration of HBIs (pg cell$^{-1}$) increased noticeably (Table 2). This total concentration increased further during cycles 5 and 6-11 (100% daughter cells) though the $C_{25}$ HBI concentrations increased at a greater rate compared with those for the $C_{30}$ HBIs ($C_{25}/C_{30}$ increased from cycles 4 to 11, Table 2). In addition, a $C_{25}$ tetraene (5) was detected during cycle 5 while a $C_{25}$ pentaene (6) was detected in cycle 11. Finally, the $C_{30:5}/C_{30:6}$ ratio underwent further changes, with a gradual reduction between cycles 4 and 11.

The dramatic changes in cell dimensions and concentrations of HBIs (pg cell$^{-1}$) that accompanied auxosporulation (cycles 3–5) prompted us to consider more closely the HBI concentrations on a unit cell volume basis (1 $\mu m^3$). Using this approach, the total concentration of $C_{30}$ HBIs was found to be reasonably constant (Fig. 6a) with a mean value of $12.0 \pm 2.9$ fg $\mu m^{-3}$ fol-

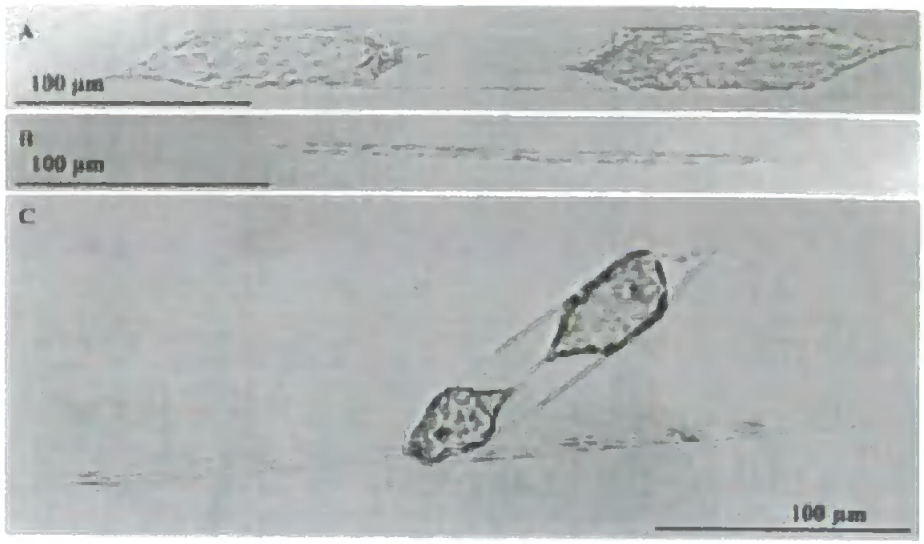


Fig. 4. Photographs of *R. setigera* (RS-2) obtained using light microscopy illustrating the differences in cell dimensions between two daughter cells (A), a single mother cell (B), two evolving daughter cells from their corresponding mother cells (C).

lowing auxosporulation, which compares with that of $9.1 \pm 0.9$ fg $\mu m^{-3}$ obtained for RS-1. However, the ratio of the pentaene and hexaene isomers was affected substantially during the period of auxosporulation, with $C_{30:5}/C_{30:6}$ increasing from 0.84 to 4.42 between cycles 2 and 4. Following auxosporulation, this ratio underwent a gradual decrease (Fig. 6b).

Different changes were observed for the $C_{25}$ HBIs. In contrast to the invariance in the total $C_{30}$ alkene concentrations, we observed an increase in the concentration of the $C_{25}$ HBIs (especially $C_{25:4}$) with cycle number following auxosporulation, and this too was reflected in an increasing $C_{25}/C_{30}$ ratio (Fig. 6c and d). While this trend appeared to be initiated by the onset of auxosporulation, the effects taking place during this phase were not as dramatic as those observed for the $C_{30}$ HBIs (viz. changes in $C_{30:5}/C_{30:6}$ ratio, vide infra). Indeed, consistent changes in the $C_{25}$ HBI concentration took place both during and after auxosporulation, being significant in cultures containing only daughter cells, including the observations of pentaene **6** and tetraene **5** as the major isomer during cycle 11 (Fig. 5).

Thus, we have demonstrated that distributions of $C_{25}$ and $C_{30}$ HBI alkenes biosynthesised by *R. setigera* are strongly dependent on the position of the diatom in its life cycle, with the most noticeable changes taking place as a result of auxosporulation. These observations can be summarised as follows: (1) $C_{30}$ HBIs (rhizenes) are only biosynthesised with five or six degrees of unsaturation. (2) The total rhizene concentrations (measured on a unit volume basis) remain constant during different stages of the life cycle, but the degree of unsaturation ($C_{30:5}/C_{30:6}$ ratio) is highly variable, especially during the period of auxosporulation. (3) $C_{25}$ HBIs (haslenes) are biosynthesised with between three and five degrees of unsaturation. (4) Unlike the rhizene pseudo-homologues, haslenes are not always observed; their production would appear to be mainly stimulated by the onset of auxosporulation, though their concentrations and unsaturation continue to increase after this phase.

While these results can be used in part to explain the large variations in $C_{25}$ and $C_{30}$ HBI distributions observed in other cultures of *R. setigera*, it is not clear at this stage if similar or related effects apply to other lipid classes. Relationships between carbon content or chlorophyll *a* levels as functions of cell dimensions (including volume) have been reported (Mullin et al., 1966; Durbin, 1977), though to our knowledge, such studies have not been carried out on individual lipids. However, it has been reported recently that cell size (amongst other factors) in phytoplankton can contribute to carbon isotope fractionation and therefore cell dimensions and growth rates should be considered if stable carbon isotope compositions of organic material are to be used in determining, e.g. palaeo-[$CO_2$(aq)] levels (Popp et al., 1998). It has also been shown that variations in carbon and hydrogen isotopes of individual compounds within the same and different organisms can occur, and this may result from different and competing biosynthetic pathways, isotopic enrichment in biosynthetic precursors or substrates involved in biosynthesis (e.g. NADPH) (Sessions et al., 1999; Rowland et al., 2001b). Clearly then,

changes in distributions of individual lipids may cause variations in measured isotopic fractionation. The fact that changes in distributions may also be associated with cell dimensions as shown here suggests that the measurement of isotopic fractionation of individual lipids as a function of cell size or dimensions could be highly informative. Such an investigation is currently an area of research in our laboratory.

## 3. Experimental

### 3.1. Isolation and culturing of R. setigera

#### 3.1.1. Experiment 1: RS-1

*R. setigera* was isolated from Le Croisic, France (8/8/2000) using a plankton net (75 μm). In the laboratory, single cells (ca. 20 μm width) were isolated under the microscope and grown in 250 ml Erlenmeyer flasks containing 150 ml F/2 Guillard medium under controlled conditions (14 °C, 100 μmol photons $cm^{-2}$ $s^{-1}$, 14/10 h light/dark cycle). In order to ensure complete equilibration with the culture conditions, cells were replicated several times over a period of 1 month. After this equilibration period, 150 ml of new F/2 medium was inoculated with a concentration of 100 cell $ml^{-1}$ (cycle 1). At the end of the exponential growing phase (11 days), cells were harvested by filtration, with a subsample being used to inoculate a second flask (cycle 2) with the same cell concentration as per cycle 1. This procedure of culturing, harvesting and further inoculation was repeated a further four times to yield a total of six cycles.

For each cycle, cell counting was performed using light microscopy and cell volumes were determined with a Beckman Coulter-Counter.

#### 3.1.2. Experiment 2:RS-2

*R. setigera* (R.s. 99) was isolated from Etel, France (25/03/1999) and cultured using the same general method as described for Experiment 1 with the following exceptions : the cell concentration at the beginning of each cycle was 500 cell $ml^{-1}$ and cells were harvested at the end of each exponential growth phase (ca. 7 days). In addition, single cells were isolated from R.s. 99 which had equilibrated in the laboratory for more than

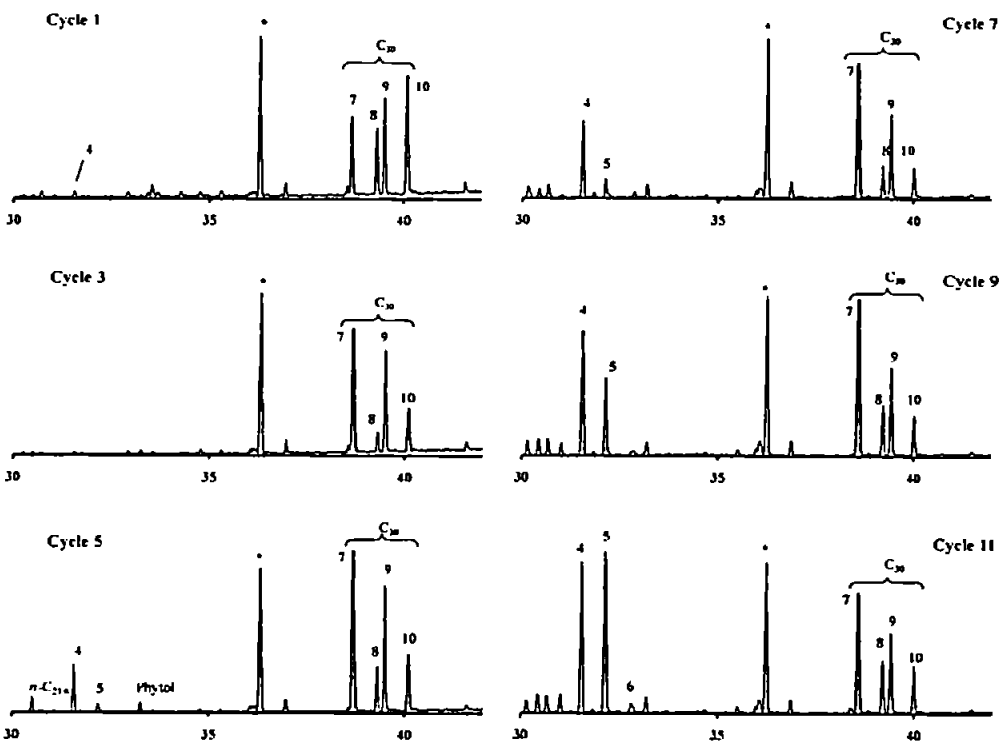


Fig. 5. Partial TIC chromatograms corresponding to alternate cycles of a culture of *R. setigera* (RS-2). The peak marked * is due to the internal standard. The peak numbers refer to the $C_{25}$ and $C_{30}$ structure numbers in Figs. 1 and 2.

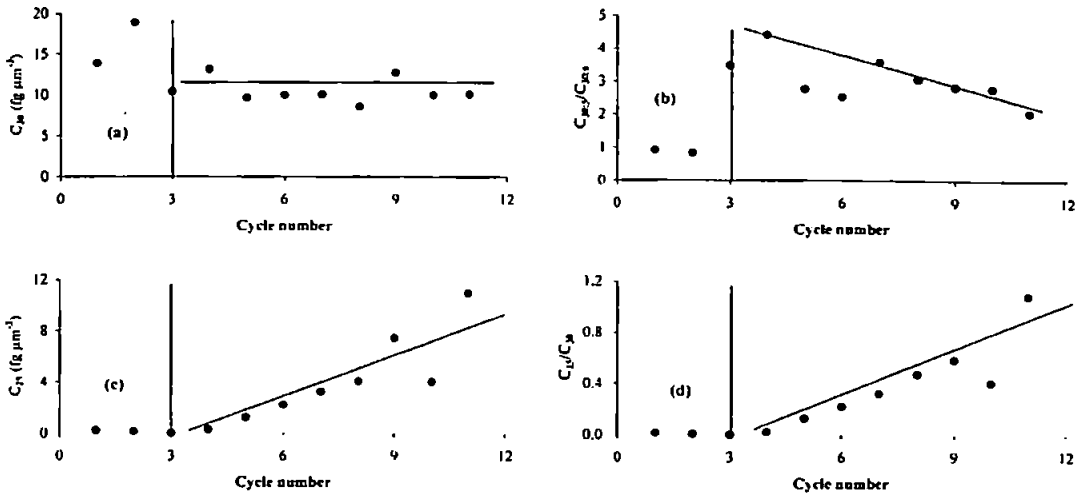


Fig. 6. Concentrations and ratios of $C_{25}$ and $C_{30}$ HBI alkenes as a function of cycle number for *R. setigera* RS-2. The vertical line at cycle 3 denotes the onset of auxosporulation. The horizontal and diagonal lines are trend lines only.

one year. As a result, all of the cells were extremely small (ca. 4 μm width) and believed to be close to the critical size for auxospore formation and the onset of auxosporulation.

### 3.2. Analysis of $C_{25}$ and $C_{30}$ HBIs by GC–MS

Analysis of HBI alkenes was as previously described (Wraige et al., 1997, 1999; Belt et al., 2000a,b). Briefly, cells were filtered at the end of each exponential growth phase and extracted with hexane following addition of an internal standard (7-hexylnonadecane; 1.1 μg filter$^{-1}$). Extracts were saponified (5% (w/w) KOH/80% MeOH/20% $H_2O$) and then re-extracted into hexane, dried and derivatised (BSTFA) to give a non-saponifiable lipid (NSL) fraction. GC–MS analysis of these NSL fractions was performed with a Hewlett Packard 5890 Series II gas chromatograph coupled to a Hewlett Packard Mass Selective Detector (5970 series) fitted with a 12 m (0.2 mm i.d.) fused silica column (HP-1 stationary phase). Auto splitless injection and He carrier gas were used. The gas chromatograph oven temperature was programmed from 40 to 300 °C at 5 °C min$^{-1}$ and held at the final temperature for 10 min. MS operating conditions were: ion source temperature 250 °C and 70 eV ionisation energy. Spectra (50–550 Da) were collected using Chemstation software. Identification of individual compounds was achieved by comparison of retention indices and mass spectra with authentic standards. Systematic errors linked to variations in HBI concentrations from duplicate or replicate determinations are typically 10–15% while random errors associated with, e.g. isomer ratios are less than 5%.

## Acknowledgements

We would like to thank the University of Plymouth and the Region des Pays de la Loire for research funds. S.T.B. acknowledges the Royal Society of Chemistry, UK for a JWT Jones travel award.

## References

Belt, S.T., Allard, G., Massé, G., Robert, J.-M., Rowland, S. 2000a. Important sedimentary sesterterpenoids from the diatom *Pleurosigma intermedium*. Chemical Communications, 501–502.

Belt, S.T., Allard, W.G., Massé, G., Robert, J.-M., Rowland, S.J., 2000b. Highly branched isoprenoids (HBIs): Identification of the most common and abundant sedimentary isomers. Geochimica et Cosmochimica Acta 64, 3839–3851.

Belt, S.T., Allard, W.G., Massé, G., Robert, J.-M., Rowland, S.J., 2001. Structural characterisation of $C_{30}$ highly branched isoprenoid alkenes (rhizenes) in the marine diatom *Rhizosolenia setigera*. Tetrahedron Letters 42, 5583–5585.

Durbin, E.G., 1977. Studies on the autecology of the marine diatom *Thalassiosira nordenskioeldii*. II. The influence of cell size on growth rate, and carbon, nitrogen, chlorophyll *a* and silica content. Journal of Phycology 13, 150–155.

Mullin, M.M., Sloan, P.R., Eppley, R.W., 1966. Relationship between carbon content, cell volume, and area in phytoplankton. Limnology and Oceanography 11, 307–311.

Popp, B.N., Laws, E.A., Bidigare, R.R., Dore, J.E., Hanson, K.L., Wakeham, S.G., 1998. Effect of phytoplankton cell geometry on carbon isotopic fractionation. Geochimica et Cosmochimica Acta 62, 69–77.

Robson, J.N., Rowland, S.J., 1986. Identification of novel widely distributed sedimentary acyclic sesterterpenoids. Nature 324, 561–563.

Round, F.E., Crawford, R.M., Mann, D.G., 1990. The Diatoms. Cambridge University Press, Cambridge.

Rowland, S.J., Robson, J.N., 1990. The widespread occurrence of highly branched acyclic $C_{20}$, $C_{25}$ and $C_{30}$ hydrocarbons in recent sediments and biota—a review. Marine Environmental Research 30, 191–216.

Rowland, S.J., Belt, S.T., Wraige, E.J., Massé, G., Roussakis, C., Robert, J.-M., 2001a. Effects of temperature on polyunsaturation in cytostatic lipids of *Haslea ostrearia*. Phytochemistry 56, 597–602.

Rowland, S.J., Allard, W.G., Belt, S.T., Massé, G., Robert, J.-M., Blackburn, S., Frampton, D., Revill, A.T., Volkman, J.K., 2001b. Factors effecting the distributions of polyunsaturated terpenoids in the diatom, *Rhizosolenia setigera*. Phytochemistry 58, 717–728.

Sessions, A.L., Burgoyne, T.W., Schimmelmann, A., Hayes, J.M., 1999. Fractionation of hydrogen isotopes in lipid biosynthesis. Organic Geochemistry 30, 1193–1200.

Sinninghe Damsté, J.S., Rijpstra, W.I.C., Schouten, S., Peletier, H., van der Maarel, M.J.E.C., Gieskes, W.W.C., 1999a. A $C_{25}$ highly branched isoprenoid alkene and $C_{25}$ and $C_{27}$ *n*-polyenes in the marine diatom *Rhizosolenia setigera*. Organic Geochemistry 30, 95–100.

Sinninghe Damsté, J.S., Schouten, S., Rijpstra, W.I.C., Hopmans, E.C., Peletier, H., Gieskes, W.W.C., Geenevasen, J.A.J., 1999. Structural identification of the $C_{25}$ highly branched isoprenoid pentaene in the marine diatom *Rhizosolenia setigera*. Organic Geochemistry 30, 1581–1583.

Sinninghe Damsté, J.S., Schouten, S., Rijpstra, W.I.C., Hopmans, E.C., Peletier, H., Gieskes, W.W.C., Geenevasen, J.A.J., 2000. Novel polyunsaturated *n*-alkenes in the marine diatom *Rhizosolenia setigera*. European Journal of Biochemistry 267, 5727–5732.

Volkman, J.K., Barratt, S.M., Dunstan, G.A., 1994. $C_{25}$ and $C_{30}$ highly branched isoprenoid alkenes in laboratory cultures of two marine diatoms. Organic Geochemistry 21, 407–414.

Wraige, E.J., Belt, S.T., Lewis, C.A., Cooke, D.A., Robert, J.-M., Massé, G., Rowland, S.J., 1997. Variations in structures and distributions of $C_{25}$ highly branched isoprenoid (HBI) alkenes in cultures of the diatom, *Haslea ostrearia* (Simonsen). Organic Geochemistry 27, 497–505.

Wraige, E.J., Johns, L., Belt, S.T., Massé, G., Robert, J.-M., Rowland, S., 1999. Highly branched $C_{25}$ isoprenoids in axenic cultures of *Haslea ostrearia*. Phytochemistry 51, 69–73.